Averages of b-hadron and c-hadron Properties at the End of 2007

Heavy Flavor Averaging Group (HFAG)*

8 August 2008

Abstract

This article reports world averages for measurements of b-hadron and c-hadron properties obtained by the Heavy Flavor Averaging Group (HFAG) using the results available at the end of 2007. For the averaging, common input parameters used in the various analyses are adjusted (rescaled) to common values, and known correlations are taken into account. The averages include branching fractions, lifetimes, neutral meson mixing parameters, CP violation parameters, and parameters of semileptonic decays.

*The HFAG members involved in producing the averages for the end of 2007 update are: E. Barberio, R. Bernhard, S. Blyth, O. Buchmueller, G. Cavoto, P. Chang, F. Di Lodovico, H. Flaecher, T. Gershon, L. Gibbons, R. Godang, B. Golob, G. Gomez-Ceballos, R. Harr, R. Kowalewski, H. Lacker, C.-J. Lin, D. Lopes-Pegna, V. Lüth, D. Pedrini, B. Petersen, M. Purohit, O. Schneider, C. Schwanda, A. J. Schwartz, J. Smith, A. Snyder, D. Tonelli, S. Tosi, K. Trabelsi, P. Urquijo, R. Van Kooten, C. Voena, and C. Weiser.

Contents

1 Introduction

Flavor dynamics is an important element in understanding the nature of particle physics. The accurate knowledge of properties of heavy flavor hadrons, especially b hadrons, plays an essential role for determination of the Cabibbo-Kobayashi-Maskawa (CKM) matrix [1]. Since asymmetric-energy e^+e^- B factories started their operation, the size of available B meson samples has dramatically increased and the accuracies of measurements have been improved. Tevatron experiments have also provided important results on B and D decays with increased Run II data samples, including confirmation of D^0-$\overline{D}{}^0$ mixing in $D^0 \to K^+\pi^-$ decays.

The Heavy Flavor Averaging Group (HFAG) was formed in 2002 to continue the activities of the LEP Heavy Flavor Steering group [2]. This group was responsible for averages of measurements of b-flavor related quantities. HFAG currently consists of six subgroups:

- the "Lifetime and Mixing" subgroup provides averages for b-hadron lifetimes, b-hadron fractions in $\Upsilon(4S)$ decay and high energy collisions, and various parameters in B^0 and B^0_s oscillations (mixing);
- the "$CP(t)$ and Unitarity Triangle Angles" subgroup provides averages for time-dependent CP asymmetry parameters and angles of the B unitarity triangle;
- the "Semileptonic B Decays" subgroup provides averages for inclusive and exclusive B-decay branching fractions, and estimates of the CKM matrix elements $|V_{cb}|$ and $|V_{ub}|$;
- the "B to Charm Decays" subgroup provides averages of branching fractions for B decays to final states involving open charm mesons or charmonium.
- the "Rare Decays" subgroup provides averages of branching fractions and their asymmetries between B and $\overline{B}$ for charmless mesonic, radiative, leptonic, and baryonic B decays;
- the "Charm Physics" subgroup provides averages of branching fractions for charm decays and averages of D^0-$\overline{D}{}^0$ mixing and direct and indirect CP violation parameters.

The first and third subgroups continue the activities of the LEP working groups with some reorganization (merging four groups into two groups). The second and latter three groups were newly formed to provide averages for results that became available from the B factory experiments (and now from the Fermilab Tevatron experiments). All subgroups consist of representatives and contact persons from *BABAR*, Belle, CDF, CLEO, DØ, and LEP.

This article is an update of the "End of 2006" HFAG preprint [4], and here we report world averages using the results available at the end of 2007. In general we use all publicly available results, including preliminary results presented at conferences; however, we do not use preliminary results that have remained unpublished for an extended period time or for which no publication is planned. Close contacts have been established between representatives from the experiments and members of different subgroups in charge of the averages to ensure that the data are prepared in a form suitable for combinations.

In the case of obtaining a world average for which $\chi^2/\mathrm{dof} > 1$, where dof is the number of degrees of freedom in the average calculation, we do not scale the resulting error (as is presently done by the Particle Data Group [3]). Rather, we examine the systematics of each measurement to better understand them. Unless we find possible systematic discrepancies

between the measurements, we do not apply any additional correction to the calculated error. We provide the confidence level of the fit as an indicator for the consistency of the measurements included in the average. We include a warning message in case some special treatment was necessary to calculate an average, or if an approximation used in the average calculation may not be good enough (*e.g.*, assuming Gaussian errors when the likelihood function indicates non-Gaussian behavior).

Section 2 describes the methodology for calculating averages for various quantities used by HFAG. In the averaging, common input parameters used in the various analyses are adjusted (rescaled) to common values, and, where possible, known correlations are taken into account. Sections 3–8 present world average values from each of the subgroups mentioned above.

The complete listing of averages and plots described in this article are also available on the HFAG web page:

`http://www.slac.stanford.edu/xorg/hfag` and
`http://belle.kek.jp/mirror/hfag` (KEK mirror site).

2 Methodology

The general averaging problem that HFAG faces is to combine information provided by different measurements of the same parameter to obtain our best estimate of the parameter's value and uncertainty. The methodology described here focuses on the problems of combining measurements performed with different systematic assumptions and with potentially-correlated systematic uncertainties. Our methodology relies on the close involvement of the people performing the measurements in the averaging process.

Consider two hypothetical measurements of a parameter x, which might be summarized as

$$x = x_1 \pm \delta x_1 \pm \Delta x_{1,1} \pm \Delta x_{2,1} \ldots$$
$$x = x_2 \pm \delta x_2 \pm \Delta x_{1,2} \pm \Delta x_{2,2} \ldots \ ,$$

where the δx_k are statistical uncertainties, and the $\Delta x_{i,k}$ are contributions to the systematic uncertainty. One popular approach is to combine statistical and systematic uncertainties in quadrature

$$x = x_1 \pm (\delta x_1 \oplus \Delta x_{1,1} \oplus \Delta x_{2,1} \oplus \ldots)$$
$$x = x_2 \pm (\delta x_2 \oplus \Delta x_{1,2} \oplus \Delta x_{2,2} \oplus \ldots)$$

and then perform a weighted average of x_1 and x_2, using their combined uncertainties, as if they were independent. This approach suffers from two potential problems that we attempt to address. First, the values of the x_k may have been obtained using different systematic assumptions. For example, different values of the B^0 lifetime may have been assumed in separate measurements of the oscillation frequency Δm_d. The second potential problem is that some contributions of the systematic uncertainty may be correlated between experiments. For example, separate measurements of Δm_d may both depend on an assumed Monte-Carlo branching fraction used to model a common background.

The problems mentioned above are related since, ideally, any quantity y_i that x_k depends on has a corresponding contribution $\Delta x_{i,k}$ to the systematic error which reflects the uncertainty Δy_i on y_i itself. We assume that this is the case and use the values of y_i and Δy_i assumed

by each measurement explicitly in our averaging (we refer to these values as $y_{i,k}$ and $\Delta y_{i,k}$ below). Furthermore, since we do not lump all the systematics together, we require that each measurement used in an average have a consistent definition of the various contributions to the systematic uncertainty. Different analyses often use different decompositions of their systematic uncertainties, so achieving consistent definitions for any potentially correlated contributions requires close coordination between HFAG and the experiments. In some cases, a group of systematic uncertainties must be lumped to obtain a coarser description that is consistent between measurements. Systematic uncertainties that are uncorrelated with any other sources of uncertainty appearing in an average are lumped with the statistical error, so that the only systematic uncertainties treated explicitly are those that are correlated with at least one other measurement via a consistently-defined external parameter y_i. When asymmetric statistical or systematic uncertainties are quoted, we symmetrize them since our combination method implicitly assumes parabolic likelihoods for each measurement.

The fact that a measurement of x is sensitive to the value of y_i indicates that, in principle, the data used to measure x could equally-well be used for a simultaneous measurement of x and y_i, as illustrated by the large contour in Fig. 1(a) for a hypothetical measurement. However, we often have an external constraint Δy_i on the value of y_i (represented by the horizontal band in Fig. 1(a)) that is more precise than the constraint $\sigma(y_i)$ from our data alone. Ideally, in such cases we would perform a simultaneous fit to x and y_i, including the external constraint, obtaining the filled (x, y) contour and corresponding dashed one-dimensional estimate of x shown in Fig. 1(a). Throughout, we assume that the external constraint Δy_i on y_i is Gaussian.

In practice, the added technical complexity of a constrained fit with extra free parameters is not justified by the small increase in sensitivity, as long as the external constraints Δy_i are sufficiently precise when compared with the sensitivities $\sigma(y_i)$ to each y_i of the data alone. Instead, the usual procedure adopted by the experiments is to perform a baseline fit with all y_i fixed to nominal values $y_{i,0}$, obtaining $x = x_0 \pm \delta x$. This baseline fit neglects the uncertainty due to Δy_i, but this error can be mostly recovered by repeating the fit separately for each external parameter y_i with its value fixed at $y_i = y_{i,0} + \Delta y_i$ to obtain $x = \tilde{x}_{i,0} \pm \delta\tilde{x}$, as illustrated in Fig. 1(b). The absolute shift, $|\tilde{x}_{i,0} - x_0|$, in the central value of x is what the experiments usually quote as their systematic uncertainty Δx_i on x due to the unknown value of y_i. Our procedure requires that we know not only the magnitude of this shift but also its sign. In the limit that the unconstrained data is represented by a parabolic likelihood, the signed shift is given by

$$\Delta x_i = \rho(x, y_i) \frac{\sigma(x)}{\sigma(y_i)} \Delta y_i \ , \tag{1}$$

where $\sigma(x)$ and $\rho(x, y_i)$ are the statistical uncertainty on x and the correlation between x and y_i in the unconstrained data. While our procedure is not equivalent to the constrained fit with extra parameters, it yields (in the limit of a parabolic unconstrained likelihood) a central value x_0 that agrees to $\mathcal{O}(\Delta y_i/\sigma(y_i))^2$ and an uncertainty $\delta x \oplus \Delta x_i$ that agrees to $\mathcal{O}(\Delta y_i/\sigma(y_i))^4$.

In order to combine two or more measurements that share systematics due to the same external parameters y_i, we would ideally perform a constrained simultaneous fit of all data samples to obtain values of x and each y_i, being careful to only apply the constraint on each y_i once. This is not practical since we generally do not have sufficient information to reconstruct the unconstrained likelihoods corresponding to each measurement. Instead, we perform the two-step approximate procedure described below.

Figs. 2(a,b) illustrate two statistically-independent measurements, $x_1 \pm (\delta x_1 \oplus \Delta x_{i,1})$ and $x_2 \pm$

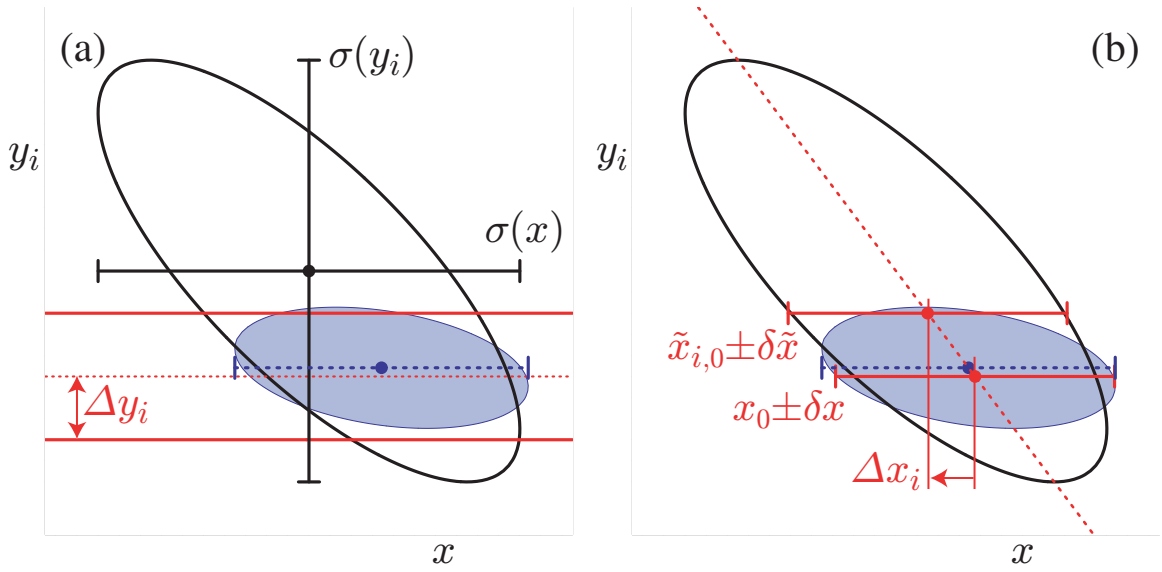

Figure 1: The left-hand plot (a) compares the 68% confidence-level contours of a hypothetical measurement's unconstrained (large ellipse) and constrained (filled ellipse) likelihoods, using the Gaussian constraint on y_i represented by the horizontal band. The solid error bars represent the statistical uncertainties $\sigma(x)$ and $\sigma(y_i)$ of the unconstrained likelihood. The dashed error bar shows the statistical error on x from a constrained simultaneous fit to x and y_i. The right-hand plot (b) illustrates the method described in the text of performing fits to x with y_i fixed at different values. The dashed diagonal line between these fit results has the slope $\rho(x, y_i)\sigma(y_i)/\sigma(x)$ in the limit of a parabolic unconstrained likelihood. The result of the constrained simultaneous fit from (a) is shown as a dashed error bar on x.

$(\delta x_i \oplus \Delta x_{i,2})$, of the same hypothetical quantity x (for simplicity, we only show the contribution of a single correlated systematic due to an external parameter y_i). As our knowledge of the external parameters y_i evolves, it is natural that the different measurements of x will assume different nominal values and ranges for each y_i. The first step of our procedure is to adjust the values of each measurement to reflect the current best knowledge of the values y_i' and ranges $\Delta y_i'$ of the external parameters y_i, as illustrated in Figs. 2(c,b). We adjust the central values x_k and correlated systematic uncertainties $\Delta x_{i,k}$ linearly for each measurement (indexed by k) and each external parameter (indexed by i):

$$x_k' = x_k + \sum_i \frac{\Delta x_{i,k}}{\Delta y_{i,k}} (y_i' - y_{i,k}) \tag{2}$$

$$\Delta x_{i,k}' = \Delta x_{i,k} \cdot \frac{\Delta y_i'}{\Delta y_{i,k}} \, . \tag{3}$$

This procedure is exact in the limit that the unconstrained likelihoods of each measurement is parabolic.

The second step of our procedure is to combine the adjusted measurements, $x_k' \pm (\delta x_k \oplus \Delta x_{k,1}' \oplus \Delta x_{k,2}' \oplus \ldots)$ using the chi-square

$$\chi^2_{\rm comb}(x, y_1, y_2, \ldots) \equiv \sum_k \frac{1}{\delta x_k^2} \left[x_k' - \left(x + \sum_i (y_i - y_i') \frac{\Delta x_{i,k}'}{\Delta y_i'} \right) \right]^2 + \sum_i \left(\frac{y_i - y_i'}{\Delta y_i'} \right)^2 \, , \tag{4}$$

and then minimize this χ^2 to obtain the best values of x and y_i and their uncertainties, as illustrated in Fig. 3. Although this method determines new values for the y_i, we do not report them since the $\Delta x_{i,k}$ reported by each experiment are generally not intended for this purpose (for example, they may represent a conservative upper limit rather than a true reflection of a 68% confidence level).

For comparison, the exact method we would perform if we had the unconstrained likelihoods $\mathcal{L}_k(x, y_1, y_2, \ldots)$ available for each measurement is to minimize the simultaneous constrained likelihood

$$\mathcal{L}_{\rm comb}(x, y_1, y_2, \ldots) \equiv \prod_k \mathcal{L}_k(x, y_1, y_2, \ldots) \prod_i \mathcal{L}_i(y_i) \, , \tag{5}$$

with an independent Gaussian external constraint on each y_i

$$\mathcal{L}_i(y_i) \equiv \exp \left[-\frac{1}{2} \left(\frac{y_i - y_i'}{\Delta y_i'} \right)^2 \right] \, . \tag{6}$$

The results of this exact method are illustrated by the filled ellipses in Figs. 3(a,b) and agree with our method in the limit that each $\mathcal{L}_k$ is parabolic and that each $\Delta y_i' \ll \sigma(y_i)$. In the case of a non-parabolic unconstrained likelihood, experiments would have to provide a description of $\mathcal{L}_k$ itself to allow an improved combination. In the case of $\sigma(y_i) \simeq \Delta y_i'$, experiments are advised to perform a simultaneous measurement of both x and y so that their data will improve the world knowledge about y.

The algorithm described above is used as a default in the averages reported in the following sections. For some cases, somewhat simplified or more complex algorithms are used and noted in the corresponding sections. Some examples for extensions of the standard method for extracting

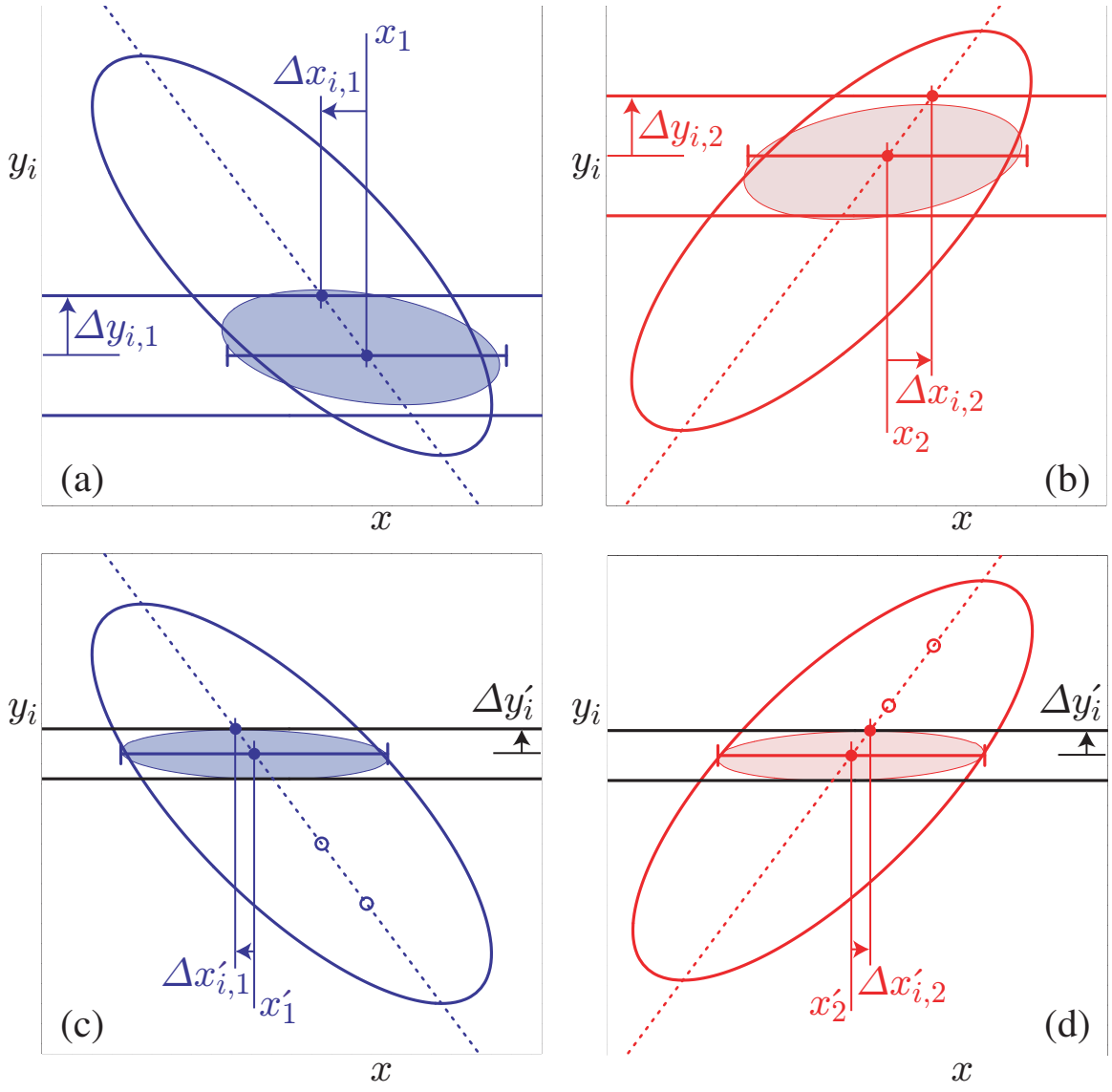

Figure 2: The upper plots (a) and (b) show examples of two individual measurements to be combined. The large ellipses represent their unconstrained likelihoods, and the filled ellipses represent their constrained likelihoods. Horizontal bands indicate the different assumptions about the value and uncertainty of y_i used by each measurement. The error bars show the results of the approximate method described in the text for obtaining x by performing fits with y_i fixed to different values. The lower plots (c) and (d) illustrate the adjustments to accommodate updated and consistent knowledge of y_i as described in the text. Open circles mark the central values of the unadjusted fits to x with y fixed; these determine the dashed line used to obtain the adjusted values.

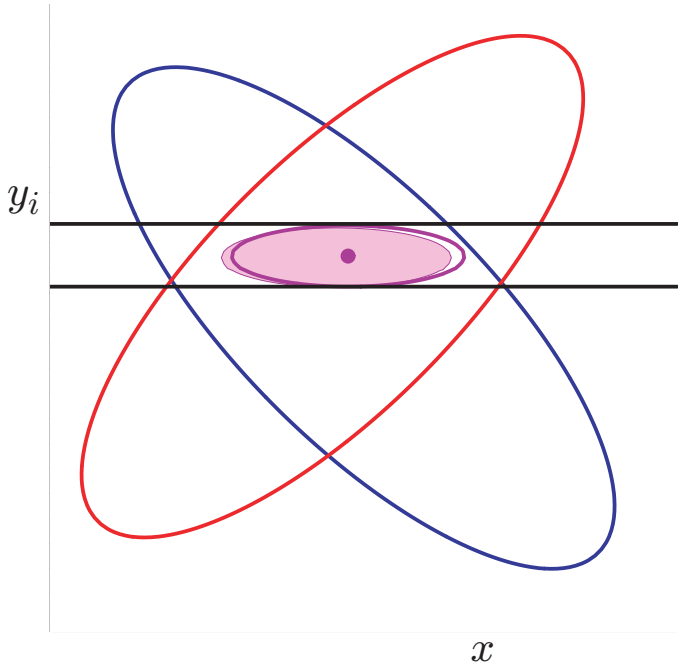

Figure 3: An illustration of the combination of two hypothetical measurements of x using the method described in the text. The ellipses represent the unconstrained likelihoods of each measurement, and the horizontal band represents the latest knowledge about y_i that is used to adjust the individual measurements. The filled small ellipse shows the result of the exact method using $\mathcal{L}_{\rm comb}$, and the hollow small ellipse and dot show the result of the approximate method using $\chi^2_{\rm comb}$.

averages are given here. These include the case where measurement errors depend on the measured value, i.e. are relative errors, unknown correlation coefficients and the breakdown of error sources.

For measurements with Gaussian errors, the usual estimator for the average of a set of measurements is obtained by minimizing the following χ^2:

$$\chi^2(t) = \sum_i^N \frac{(y_i - t)^2}{\sigma_i^2}, \tag{7}$$

where y_i is the measured value for input i and σ_i^2 is the variance of the distribution from which y_i was drawn. The value $\hat{t}$ of t at minimum χ^2 is our estimator for the average. (This discussion is given for independent measurements for the sake of simplicity; the generalization to correlated measurements is straightforward, and has been used when averaging results.) The true σ_i are unknown but typically the error as assigned by the experiment $\sigma_i^{\rm raw}$ is used as an estimator for it. Caution is advised, however, in the case where $\sigma_i^{\rm raw}$ depends on the value measured for y_i. Examples of this include an uncertainty in any multiplicative factor (like an acceptance) that enters the determination of y_i, i.e. the $\sqrt{N}$ dependence of Poisson statistics, where $y_i \propto N$ and $\sigma_i \propto \sqrt{N}$. Failing to account for this type of dependence when averaging leads to a biased average. Biases in the average can be avoided (or at least reduced) by minimizing the following χ^2:

$$\chi^2(t) = \sum_i^N \frac{(y_i - t)^2}{\sigma_i^2(\hat{t})}. \tag{8}$$

In the above $\sigma_i(\hat{t})$ is the uncertainty assigned to input i that includes the assumed dependence of the stated error on the value measured. As an example, consider a pure acceptance error, for which $\sigma_i(\hat{t}) = (\hat{t}/y_i) \times \sigma_i^{\rm raw}$. It is easily verified that solving Eq. 8 leads to the correct behavior, namely

$$\hat{t} = \frac{\sum_i^N y_i^3/(\sigma_i^{\rm raw})^2}{\sum_i^N y_i^2/(\sigma_i^{\rm raw})^2},$$

i.e. weighting by the inverse square of the fractional uncertainty, $\sigma_i^{\rm raw}/y_i$. It is sometimes difficult to assess the dependence of $\sigma_i^{\rm raw}$ on $\hat{t}$ from the errors quoted by experiments.

Another issue that needs careful treatment is the question of correlation among different measurements, e.g. due to using the same theory for calculating acceptances. A common practice is to set the correlation coefficient to unity to indicate full correlation. However, this is not a "conservative" thing to do, and can in fact lead to a significantly underestimated uncertainty on the average. In the absence of better information, the most conservative choice of correlation coefficient between two measurements i and j is the one that maximizes the uncertainty on $\hat{t}$ due to that pair of measurements:

$$\sigma^2_{\hat{t}(i,j)} = \frac{\sigma_i^2\,\sigma_j^2\,(1-\rho_{ij}^2)}{\sigma_i^2 + \sigma_j^2 - 2\,\rho_{ij}\,\sigma_i\,\sigma_j}, \tag{9}$$

namely

$$\rho_{ij} = \min\left(\frac{\sigma_i}{\sigma_j}, \frac{\sigma_j}{\sigma_i}\right), \tag{10}$$

which corresponds to setting $\sigma^2_{\hat{t}(i,j)} = \min(\sigma_i^2, \sigma_j^2)$. Setting $\rho_{ij} = 1$ when $\sigma_i \neq \sigma_j$ can lead to a significant underestimate of the uncertainty on $\hat{t}$, as can be seen from Eq. 9.

Finally, we carefully consider the various sources of error contributing to the overall uncertainty of an average. The overall covariance matrix is constructed from a number of individual sources, e.g. $\mathbf{V} = \mathbf{V_{stat}} + \mathbf{V_{sys}} + \mathbf{V_{th}}$. The variance on the average $\hat{t}$ can be written

$$\sigma^2_{\hat{t}} = \frac{\sum_{i,j} \left(\mathbf{V^{-1}} \left[\mathbf{V_{stat}} + \mathbf{V_{sys}} + \mathbf{V_{th}}\right] \mathbf{V^{-1}}\right)_{ij}}{\left(\sum_{i,j} V_{ij}^{-1}\right)^2} = \sigma^2_{stat} + \sigma^2_{sys} + \sigma^2_{th}. \tag{11}$$

Written in this form, one can readily determine the contribution of each source of uncertainty to the overall uncertainty on the average. This breakdown of the uncertainties is used in the following sections.

Following the prescription described above, the central values and errors are rescaled to a common set of input parameters in the averaging procedures according to the dependency on any of these input parameters. We try to use the most up-to-date values for these common inputs and the same values among the HFAG subgroups. For the parameters whose averages are produced by HFAG, we use the values in the current update cycle. For other external parameters, we use the most recent PDG values [3]. The parameters and values used are listed in each subgroup section.

3 b-hadron production fractions, lifetimes and mixing parameters

Quantities such as b-hadron production fractions, b-hadron lifetimes, and neutral B-meson oscillation frequencies have been studied in the nineties at LEP and SLC (e^+e^- colliders at $\sqrt{s} = m_Z$) as well as at the first version of the Tevatron ($p\overline{p}$ collider at $\sqrt{s} = 1.8$ TeV). Since then precise measurements of the B^0 and B^+ lifetimes, as well as of the B^0 oscillation frequency, have also been performed at the asymmetric B factories, KEKB and PEPII (e^+e^- colliders at $\sqrt{s} = m_{\Upsilon(4S)}$) while measurements related to the other b-hadrons, in particular B_s^0, B_c^+ and Λ_b^0, are being performed at the upgraded Tevatron ($\sqrt{s} = 1.96$ TeV). In most cases, these basic quantities, although interesting by themselves, became necessary ingredients for the more complicated and refined analyses at the asymmetric B factories and at the Tevatron, in particular the time-dependent *CP* asymmetry measurements. It is therefore important that the best experimental values of these quantities continue to be kept up-to-date and improved.

In several cases, the averages presented in this chapter are needed and used as input for the results given in the subsequent chapters. Within this chapter, some averages need the knowledge of other averages in a circular way. This coupling, which appears through the b-hadron fractions whenever inclusive or semi-exclusive measurements have to be considered, has been reduced significantly in the last several years with increasingly precise exclusive measurements becoming available.

In addition to b-hadron fractions, lifetimes and mixing parameters, this chapter also deals with the CP-violating phase β_s, which is the phase difference between the B_s^0 mixing amplitude and the $b \to c\overline{c}s$ decay amplitude. The angle β, which is the equivalent of β_s for the B^0 system, is discussed in Chapter 4.

3.1 b-hadron production fractions

We consider here the relative fractions of the different b-hadron species found in an unbiased sample of weakly-decaying b hadrons produced under some specific conditions. The knowledge of these fractions is useful to characterize the signal composition in inclusive b-hadron analyses, or to predict the background composition in exclusive analyses. Many analyses in B physics need these fractions as input. We distinguish here the following three conditions: $\Upsilon(4S)$ decays, $\Upsilon(5S)$ decays, and high-energy collisions (including Z^0 decays).

3.1.1 b-hadron production fractions in $\Upsilon(4S)$ decays

Only pairs of the two lightest (charged and neutral) B mesons can be produced in $\Upsilon(4S)$ decays, and it is enough to determine the following branching fractions:

$$f^{+-} = \Gamma(\Upsilon(4S) \to B^+B^-)/\Gamma_{\rm tot}(\Upsilon(4S))\,, \tag{12}$$

$$f^{00} = \Gamma(\Upsilon(4S) \to B^0\overline{B}^0)/\Gamma_{\rm tot}(\Upsilon(4S))\,. \tag{13}$$

In practice, most analyses measure their ratio

$$R^{+-/00} = f^{+-}/f^{00} = \Gamma(\Upsilon(4S) \to B^+B^-)/\Gamma(\Upsilon(4S) \to B^0\overline{B}^0)\,, \tag{14}$$

Table 1: Published measurements of the B^+/B^0 production ratio in $\Upsilon(4S)$ decays, together with their average (see text). Systematic uncertainties due to the imperfect knowledge of $\tau(B^+)/\tau(B^0)$ are included. The latest *BABAR* result [10] supersedes the earlier *BABAR* measurements [6, 9].

Experiment and year	Ref.	Decay modes or method	Published value of $R^{+-/00} = f^{+-}/f^{00}$	Assumed value of $\tau(B^+)/\tau(B^0)$
CLEO, 2001	[5]	$J/\psi K^{(*)}$	$1.04 \pm 0.07 \pm 0.04$	1.066 ± 0.024
BABAR, 2002	[6]	$(c\overline{c})K^{(*)}$	$1.10 \pm 0.06 \pm 0.05$	1.062 ± 0.029
CLEO, 2002	[7]	$D^*\ell\nu$	$1.058 \pm 0.084 \pm 0.136$	1.074 ± 0.028
Belle, 2003	[8]	dilepton events	$1.01 \pm 0.03 \pm 0.09$	1.083 ± 0.017
BABAR, 2004	[9]	$J/\psi K$	$1.006 \pm 0.036 \pm 0.031$	1.083 ± 0.017
BABAR, 2005	[10]	$(c\overline{c})K^{(*)}$	$1.06 \pm 0.02 \pm 0.03$	1.086 ± 0.017
Average			1.064 ± 0.029 (tot)	1.073 ± 0.008

which is easier to access experimentally. Since an inclusive (but separate) reconstruction of B^+ and B^0 is difficult, specific exclusive decay modes, $B^+ \to x^+$ and $B^0 \to x^0$, are usually considered to perform a measurement of $R^{+-/00}$, whenever they can be related by isospin symmetry (for example $B^+ \to J/\psi K^+$ and $B^0 \to J/\psi K^0$). Under the assumption that $\Gamma(B^+ \to x^+) = \Gamma(B^0 \to x^0)$, *i.e.* that isospin invariance holds in these B decays, the ratio of the number of reconstructed $B^+ \to x^+$ and $B^0 \to x^0$ mesons is proportional to

$$\frac{f^{+-}\,\mathcal{B}(B^+ \to x^+)}{f^{00}\,\mathcal{B}(B^0 \to x^0)} = \frac{f^{+-}\,\Gamma(B^+ \to x^+)\,\tau(B^+)}{f^{00}\,\Gamma(B^0 \to x^0)\,\tau(B^0)} = \frac{f^{+-}}{f^{00}}\,\frac{\tau(B^+)}{\tau(B^0)}\,, \tag{15}$$

where $\tau(B^+)$ and $\tau(B^0)$ are the B^+ and B^0 lifetimes respectively. Hence the primary quantity measured in these analyses is $R^{+-/00}\,\tau(B^+)/\tau(B^0)$, and the extraction of $R^{+-/00}$ with this method therefore requires the knowledge of the $\tau(B^+)/\tau(B^0)$ lifetime ratio.

The published measurements of $R^{+-/00}$ are listed in Table 1 together with the corresponding assumed values of $\tau(B^+)/\tau(B^0)$. All measurements are based on the above-mentioned method, except the one from Belle, which is a by-product of the B^0 mixing frequency analysis using dilepton events (but note that it also assumes isospin invariance, namely $\Gamma(B^+ \to \ell^+\mathrm{X}) = \Gamma(B^0 \to \ell^+\mathrm{X})$). The latter is therefore treated in a slightly different manner in the following procedure used to combine these measurements:

- each published value of $R^{+-/00}$ from CLEO and *BABAR* is first converted back to the original measurement of $R^{+-/00}\,\tau(B^+)/\tau(B^0)$, using the value of the lifetime ratio assumed in the corresponding analysis;

- a simple weighted average of these original measurements of $R^{+-/00}\,\tau(B^+)/\tau(B^0)$ from CLEO and *BABAR* (which do not depend on the assumed value of the lifetime ratio) is then computed, assuming no statistical or systematic correlations between them;

- the weighted average of $R^{+-/00}\,\tau(B^+)/\tau(B^0)$ is converted into a value of $R^{+-/00}$, using the latest average of the lifetime ratios, $\tau(B^+)/\tau(B^0) = 1.073 \pm 0.008$ (see Sec. 3.2.3);

- the Belle measurement of $R^{+-/00}$ is adjusted to the current values of $\tau(B^0) = 1.530 \pm 0.008$ ps and $\tau(B^+)/\tau(B^0) = 1.073 \pm 0.008$ (see Sec. 3.2.3), using the quoted systematic uncertainties due to these parameters;
- the combined value of $R^{+-/00}$ from CLEO and *BABAR* is averaged with the adjusted value of $R^{+-/00}$ from Belle, assuming a 100% correlation of the systematic uncertainty due to the limited knowledge on $\tau(B^+)/\tau(B^0)$; no other correlation is considered.

The resulting global average,

$$R^{+-/00} = \frac{f^{+-}}{f^{00}} = 1.064 \pm 0.029\,, \tag{16}$$

is consistent with an equal production of charged and neutral B mesons, although only at the 2.2σ level.

On the other hand, the *BABAR* collaboration has performed a direct measurement of the f^{00} fraction using a novel method, which does not rely on isospin symmetry nor requires the knowledge of $\tau(B^+)/\tau(B^0)$. Its analysis, based on a comparison between the number of events where a single $B^0 \to D^{*-}\ell^+\nu$ decay could be reconstructed and the number of events where two such decays could be reconstructed, yields [11]

$$f^{00} = 0.487 \pm 0.010\,(\text{stat}) \pm 0.008\,(\text{syst})\,. \tag{17}$$

The two results of Eqs. (16) and (17) are of very different natures and completely independent of each other. Their product is equal to $f^{+-} = 0.518 \pm 0.019$, while another combination of them gives $f^{+-} + f^{00} = 1.005 \pm 0.030$, compatible with unity. Assuming[1] $f^{+-} + f^{00} = 1$, also consistent with CLEO's observation that the fraction of $\Upsilon(4S)$ decays to $B\overline{B}$ pairs is larger than 0.96 at 95% CL [13], the results of Eqs. (16) and (17) can be averaged (first converting Eq. (16) into a value of $f^{00} = 1/(R^{+-/00} + 1)$) to yield the following more precise estimates:

$$f^{00} = 0.485 \pm 0.006\,, \quad f^{+-} = 1 - f^{00} = 0.515 \pm 0.006\,, \quad \frac{f^{+-}}{f^{00}} = 1.062 \pm 0.025\,. \tag{18}$$

The latter ratio differs from one by 2.4σ.

3.1.2 *b*-hadron production fractions in $\Upsilon(5S)$ decays

Hadronic events produced in e^+e^- collisions at the $\Upsilon(5S)$ energy can be classified into three categories: light-quark continuum events, $b\overline{b}$ continuum events, and $\Upsilon(5S)$ events. The latter two cannot be distinguished and are expected to always produce one of the following final states with a pair of b-flavored mesons: $B\overline{B}$, $B\overline{B}^*$, $B^*\overline{B}$, $B^*\overline{B}^*$, $B\overline{B}\pi$, $B\overline{B}^*\pi$, $B^*\overline{B}\pi$, $B^*\overline{B}^*\pi$, $B\overline{B}\pi\pi$, $B_s^0\overline{B}_s^0$, $B_s^0\overline{B}_s^{0*}$, $B_s^{0*}\overline{B}_s^0$ or $B_s^{0*}\overline{B}_s^{0*}$, where B denotes a B^0 or B^+ meson and $\overline{B}$ denotes a $\overline{B}^0$ or B^- meson. The excited states decay via $B^* \to B\gamma$ and $B_s^{0*} \to B_s^0\gamma$. We define here $f_s(\Upsilon(5S))$ as the fraction of $B_s^{0(*)}\overline{B}_s^{0(*)}$ events over all events with a pair of b-flavored mesons at the $\Upsilon(5S)$ energy:

$$f_s(\Upsilon(5S)) = \frac{\sigma(e^+e^- \to B_s^{0(*)}\overline{B}_s^{0(*)})}{\sigma(e^+e^- \to \Upsilon(5S) \text{ or } b\overline{b}X)} \quad \text{at } \sqrt{s} = m(\Upsilon(5S))\,. \tag{19}$$

Table 2: Published values of $f_s(\Upsilon(5S))$ and their average.

Experiment, year and dataset	Ref.	Decay modes or method	Published value of $f_s(\Upsilon(5S))$
CLEO, 2006, $0.42\,\text{fb}^{-1}$	[14]	$\Upsilon(5S) \to D_s X$	$0.168 \pm 0.026^{+0.067}_{-0.034}$
	[14]	$\Upsilon(5S) \to \phi X$	$0.246 \pm 0.029^{+0.110}_{-0.053}$
	[14]	$\Upsilon(5S) \to B\overline{B}X$	$0.411 \pm 0.100 \pm 0.092$
	[14]	CLEO average of above 3	$0.21^{+0.06}_{-0.03}$
Belle, 2006, $1.86\,\text{fb}^{-1}$	[15]	$\Upsilon(5S) \to D_s X$	$0.179 \pm 0.014 \pm 0.041$
	[15]	$\Upsilon(5S) \to D^0 X$	$0.181 \pm 0.036 \pm 0.075$
	[15]	Belle average of above 2	$0.180 \pm 0.013 \pm 0.032$
Average of all above after adjustments to inputs of Table 3			$0.194 \pm 0.011 \pm 0.027$

Table 3: External inputs on which the $f_s(\Upsilon(5S))$ average is based.

Branching fraction	Value	Explanation and reference
$\mathcal{B}(B \to D_s X) \times \mathcal{B}(D_s \to \phi\pi)$	0.00374 ± 0.00014	derived from [3]
$\mathcal{B}(B_s^0 \to D_s X)$	0.92 ± 0.11	model-dependent estimate [16]
$\mathcal{B}(D_s \to \phi\pi)$	0.045 ± 0.004	[3]
$\mathcal{B}(B \to D^0 X) \times \mathcal{B}(D^0 \to K\pi)$	0.0243 ± 0.0011	derived from [3]
$\mathcal{B}(B_s^0 \to D^0 X)$	0.08 ± 0.07	model-dependent estimate [15, 16]
$\mathcal{B}(D^0 \to K\pi)$	0.0382 ± 0.0007	[3]
$\mathcal{B}(B \to \phi X)$	0.0344 ± 0.0012	world average [3, 14]
$\mathcal{B}(B_s^0 \to \phi X)$	0.161 ± 0.024	model-dependent estimate [14]

The CLEO and Belle collaborations have recently published measurements of several inclusive $\Upsilon(5S)$ branching fractions, $\mathcal{B}(\Upsilon(5S) \to D_s X)$, $\mathcal{B}(\Upsilon(5S) \to \phi X)$, $\mathcal{B}(\Upsilon(5S) \to D^0 X)$, and $\mathcal{B}(\Upsilon(5S) \to B\overline{B}X)$, from which they extract the model-dependent estimates of $f_s(\Upsilon(5S))$ reported in Table 2. This extraction requires the knowledge of several other branching fractions, which are listed in Table 3 together with their most recent values. Before being averaged, the CLEO and Belle results are adjusted to these new external inputs. The world average of $f_s(\Upsilon(5S))$ taking into account all systematic correlations introduced by the use of common external inputs, as well as the experiment-specific correlations due to the estimated number of $b\overline{b}$ events, is

$$f_s(\Upsilon(5S)) = 0.194 \pm 0.029\,. \tag{20}$$

This production of B_s^0 mesons at the $\Upsilon(5S)$ is observed to be dominated by the $B_s^{0*}\overline{B}_s^{0*}$ channel [17, 18], with $\sigma(e^+e^- \to B_s^{0*}\overline{B}_s^{0*})/\sigma(e^+e^- \to B_s^{0(*)}\overline{B}_s^{0(*)}) = (93^{+7}_{-9} \pm 1)\%$ [18].

[1] A few non-$B\overline{B}$ decay modes of the $\Upsilon(4S)$ ($\Upsilon(1S)\pi^+\pi^-$, $\Upsilon(2S)\pi^+\pi^-$, $\Upsilon(1S)\eta$) have been observed with branching fractions of the order of 10^{-4} [12], corresponding to a partial width several times larger than that in the e^+e^- channel. However, this can still be neglected and the assumption $f^{+-} + f^{00} = 1$ remains valid in the present context of the determination of f^{+-} and f^{00}.

3.1.3 *b*-hadron production fractions at high energy

At high energy, all species of weakly-decaying b hadrons can be produced, either directly or in strong and electromagnetic decays of excited b hadrons. We assume here that the fractions of these different species are the same in unbiased samples of high-$p_{\rm T}$ b jets originating from Z^0 decays or from $p\overline{p}$ collisions at the Tevatron. This hypothesis is plausible considering that, in both cases, the last step of the jet hadronization is a non-perturbative QCD process occurring at the scale of $\Lambda_{\rm QCD}$. On the other hand, there is no strong argument to claim that these fractions should be strictly equal, so this assumption should be checked experimentally. Although the available data is not sufficient at this time to perform a significant check, it is expected that more data from Tevatron Run II may improve this situation and allow one to confirm or disprove this assumption with reasonable confidence. Meanwhile, the attitude adopted here is that these fractions are assumed to be equal at all high-energy colliders until demonstrated otherwise by experiment.[2] However, as explained below, the measurements performed at LEP and at the Tevatron show slight discrepancies. Therefore we present two sets of averages: one set including only measurements performed at LEP, and a second set including measurements performed at both LEP and Tevatron.

Contrary to what happens in the charm sector where the fractions of D^+ and D^0 are different, the relative amount of B^+ and B^0 is not affected by the electromagnetic decays of excited B^{+*} and B^{0*} states and strong decays of excited B^{+**} and B^{0**} states. Decays of the type $B_s^{0**} \to B^{(*)}K$ also contribute to the B^+ and B^0 rates, but with the same magnitude if mass effects can be neglected. We therefore assume equal production of B^+ and B^0. We also neglect the production of weakly-decaying states made of several heavy quarks (like B_c^+ and other heavy baryons) which is known to be very small. Hence, for the purpose of determining the b-hadron fractions, we use the constraints

$$f_u = f_d \quad \text{and} \quad f_u + f_d + f_s + f_{\rm baryon} = 1\,, \tag{21}$$

where f_u, f_d, f_s and $f_{\rm baryon}$ are the unbiased fractions of B^+, B^0, B_s^0 and b baryons, respectively.

The LEP experiments have measured $f_s \times \mathcal{B}(B_s^0 \to D_s^- \ell^+ \nu_\ell X)$ [19], $\mathcal{B}(b \to \Lambda_b^0) \times \mathcal{B}(\Lambda_b^0 \to \Lambda_c^+ \ell^- \overline{\nu}_\ell X)$ [20, 21] and $\mathcal{B}(b \to \Xi_b^-) \times \mathcal{B}(\Xi_b^- \to \Xi^- \ell^- \overline{\nu}_\ell X)$ [22, 23][3] from partially reconstructed final states including a lepton, $f_{\rm baryon}$ from protons identified in b events [25], and the production rate of charged b hadrons [26]. The various b-hadron fractions have also been measured at CDF using electron-charm final states [27] and double semileptonic decays with $K^*\mu\mu$ and $\phi\mu\mu$ final states [28]. All these results[4] have been combined following the procedure and assumptions described in [2], to yield $f_u = f_d = 0.402 \pm 0.011$, $f_s = 0.097 \pm 0.016$ and $f_{\rm baryon} = 0.099 \pm 0.020$ under the constraints of Eq. (21). Following the PDG prescription, we have scaled the combined uncertainties on these fractions by 1.2 to account for slight discrepancies in the input data. Repeating the combination using LEP data only, we obtain $f_u = f_d = 0.406 \pm 0.009$, $f_s = 0.087 \pm 0.014$ and $f_{\rm baryon} = 0.100 \pm 0.017$ and find that no scaling factor is necessary. For these combinations other external inputs are used, *e.g.* the branching ratios of B mesons to final states with a D, D^* or D^{**} in semileptonic decays, which are needed to evaluate the fraction of semileptonic B_s^0 decays with a D_s^- in the final state.

[2] It is not unlikely that the b-hadron fractions in low-$p_{\rm T}$ jets at a hadronic machine be different; in particular, beam-remnant effects may enhance the b-baryon production.

[3] The DELPHI result of Ref. [23] is considered to supersede an older one [24].

[4] Recent measurements [29] performed by CDF with Run II data have not been included here.

Table 4: Time-integrated mixing probability $\overline{\chi}$ (defined in Eq. (22)), and fractions of the different b-hadron species in an unbiased sample of weakly-decaying b hadrons, obtained from both direct and mixing measurements. Measurements performed in Z decays are included in both sets of averages.

Quantity		in Z decays	at high energy
Mixing probability	$\overline{\chi}$	0.1259 ± 0.0042	0.1284 ± 0.0069
B^+ or B^0 fraction	$f_u = f_d$	0.403 ± 0.009	0.401 ± 0.011
B_s^0 fraction	f_s	0.101 ± 0.009	0.106 ± 0.012
b baryon fraction	$f_{\rm baryon}$	0.092 ± 0.015	0.093 ± 0.019
Correlation between f_s and $f_u = f_d$		-0.515	-0.475
Correlation between $f_{\rm baryon}$ and $f_u = f_d$		-0.873	-0.836
Correlation between $f_{\rm baryon}$ and f_s		$+0.032$	-0.087

Time-integrated mixing analyses performed with lepton pairs from $b\overline{b}$ events produced at high-energy colliders measure the quantity

$$\overline{\chi} = f'_d \, \chi_d + f'_s \, \chi_s \, , \tag{22}$$

where f'_d and f'_s are the fractions of B^0 and B_s^0 hadrons in a sample of semileptonic b-hadron decays, and where χ_d and χ_s are the B^0 and B_s^0 time-integrated mixing probabilities. Assuming that all b hadrons have the same semileptonic decay width implies $f'_i = f_i R_i$, where $R_i = \tau_i/\tau_b$ is the ratio of the lifetime τ_i of species i to the average b-hadron lifetime $\tau_b = \sum_i f_i \tau_i$. Hence measurements of the mixing probabilities $\overline{\chi}$, χ_d and χ_s can be used to improve our knowledge of f_u, f_d, f_s and $f_{\rm baryon}$. In practice, the above relations yield another determination of f_s obtained from $f_{\rm baryon}$ and mixing information,

$$f_s = \frac{1}{R_s} \frac{(1+r)\overline{\chi} - (1 - f_{\rm baryon} R_{\rm baryon})\chi_d}{(1+r)\chi_s - \chi_d} \, , \tag{23}$$

where $r = R_u/R_d = \tau(B^+)/\tau(B^0)$.

The published measurements of $\overline{\chi}$ performed by the LEP experiments have been combined by the LEP Electroweak Working Group to yield $\overline{\chi} = 0.1259 \pm 0.0042$ [30]. This can be compared with the Tevatron average, $\overline{\chi} = 0.147 \pm 0.011$, obtained from a CDF measurement with Run I data [31] and from a recent DØ measurement with Run II data [32]. The two averages deviate from each other by $1.8\,\sigma$; this could be an indication that the production fractions of b hadrons at the Z peak or at the Tevatron are not the same. Although this discrepancy is not very significant it should be carefully monitored in the future. We choose to combine these two results in a simple weighted average, assuming no correlations, and, following the PDG prescription, we multiply the combined uncertainty by 1.8 to account for the discrepancy. Our world average is then $\overline{\chi} = 0.1284 \pm 0.0069$.

Introducing the $\overline{\chi}$ average in Eq. (23), together with our world average $\chi_d = 0.1881 \pm 0.0023$ (see Eq. (56) of Sec. 3.3.1), the assumption $\chi_s = 1/2$ (justified by Eq. (101) in Sec. 3.3.2), the best knowledge of the lifetimes (see Sec. 3.2) and the estimate of $f_{\rm baryon}$ given above, yields $f_s = 0.119 \pm 0.019$ (or $f_s = 0.112 \pm 0.012$ using only LEP data), an estimate dominated

by the mixing information. Taking into account all known correlations (including the one introduced by $f_{\rm baryon}$), this result is then combined with the set of fractions obtained from direct measurements (given above), to yield the improved estimates of Table 4, still under the constraints of Eq. (21). As can be seen, our knowledge on the mixing parameters substantially reduces the uncertainty on f_s, and this even in the case of the world averages where a rather strong deweighting was introduced in the computation of $\overline{\chi}$. It should be noted that the results are correlated, as indicated in Table 4.

New CDF measurements performed with Run II data, and not included in the above averages, have recently been published [29],

$$\frac{f_u}{f_d} = 1.054 \pm 0.018(\text{stat})\,^{+0.025}_{-0.041}(\text{syst}) \pm 0.058(\mathcal{B})\,, \tag{24}$$

$$\frac{f_s}{f_d+f_u} = 0.160 \pm 0.005(\text{stat})\,^{+0.011}_{-0.010}(\text{syst})\,^{+0.057}_{-0.034}(\mathcal{B})\,, \tag{25}$$

$$\frac{f_{\Lambda_b}}{f_d+f_u} = 0.281 \pm 0.012(\text{stat})\,^{+0.058}_{-0.056}(\text{syst})\,^{+0.128}_{-0.087}(\mathcal{B})\,, \tag{26}$$

where f_{Λ_b} is the fraction of Λ_b in an unbiased sample of weakly-decaying b-hadrons, and where the third quoted error ($\mathcal{B}$) is due to uncertainties on measured branching fractions. According to the authors of Ref. [29], these results on f_u/f_d and $f_s/(f_d+f_u)$ are in agreement with the averages computed from LEP data, but the central value of $f_{\Lambda_b}/(f_d+f_u)$ is twice as large as that of $f_{\rm baryon}/(f_d+f_u)$ measured at LEP, showing a $\sim 2.3\sigma$ discrepancy attributed to a possible momentum dependence of the b-baryon fragmentation.

3.2 *b*-hadron lifetimes

In the spectator model the decay of b-flavored hadrons H_b is governed entirely by the flavor changing $b \to Wq$ transition ($q = c, u$). For this very reason, lifetimes of all b-flavored hadrons are the same in the spectator approximation regardless of the (spectator) quark content of the H_b. In the early 1990's experiments became sophisticated enough to start seeing the differences of the lifetimes among various H_b species. The first theoretical calculations of the spectator quark effects on H_b lifetime emerged only few years earlier.

Currently, most of such calculations are performed in the framework of the Heavy Quark Expansion, HQE. In the HQE, under certain assumptions (most important of which is that of quark-hadron duality), the decay rate of an H_b to an inclusive final state f is expressed as the sum of a series of expectation values of operators of increasing dimension, multiplied by the correspondingly higher powers of $\Lambda_{\rm QCD}/m_b$:

$$\Gamma_{H_b\to f} = |CKM|^2 \sum_n c_n^{(f)} \Big(\frac{\Lambda_{\rm QCD}}{m_b}\Big)^n \langle H_b|O_n|H_b\rangle, \tag{27}$$

where $|CKM|^2$ is the relevant combination of the CKM matrix elements. Coefficients $c_n^{(f)}$ of this expansion, known as Operator Product Expansion [33], can be calculated perturbatively. Hence, the HQE predicts $\Gamma_{H_b\to f}$ in the form of an expansion in both $\Lambda_{\rm QCD}/m_b$ and $\alpha_s(m_b)$. The precision of current experiments makes it mandatory to go to the next-to-leading order in QCD, *i.e.* to include correction of the order of $\alpha_s(m_b)$ to the $c_n^{(f)}$'s. All non-perturbative physics is shifted into the expectation values $\langle H_b|O_n|H_b\rangle$ of operators O_n. These can be calculated using

lattice QCD or QCD sum rules, or can be related to other observables via the HQE [34]. One may reasonably expect that powers of $\Lambda_{\rm QCD}/m_b$ provide enough suppression that only the first few terms of the sum in Eq. (27) matter.

Theoretical predictions are usually made for the ratios of the lifetimes (with $\tau(B^0)$ chosen as the common denominator) rather than for the individual lifetimes, for this allows several uncertainties to cancel. The precision of the current HQE calculations (see Refs. [35–37] for the latest updates) is in some instances already surpassed by the measurements, *e.g.* in the case of $\tau(B^+)/\tau(B^0)$. Also, HQE calculations are not assumption-free. More accurate predictions are a matter of progress in the evaluation of the non-perturbative hadronic matrix elements and verifying the assumptions that the calculations are based upon. However, the HQE, even in its present shape, draws a number of important conclusions, which are in agreement with experimental observations:

- The heavier the mass of the heavy quark the smaller is the variation in the lifetimes among different hadrons containing this quark, which is to say that as $m_b \to \infty$ we retrieve the spectator picture in which the lifetimes of all H_b's are the same. This is well illustrated by the fact that lifetimes are rather similar in the b sector, while they differ by large factors in the c sector ($m_c < m_b$).

- The non-perturbative corrections arise only at the order of $\Lambda^2_{\rm QCD}/m_b^2$, which translates into differences among H_b lifetimes of only a few percent.

- It is only the difference between meson and baryon lifetimes that appears at the $\Lambda^2_{\rm QCD}/m_b^2$ level. The splitting of the meson lifetimes occurs at the $\Lambda^3_{\rm QCD}/m_b^3$ level, yet it is enhanced by a phase space factor $16\pi^2$ with respect to the leading free b decay.

To ensure that certain sources of systematic uncertainty cancel, lifetime analyses are sometimes designed to measure a ratio of lifetimes. However, because of the differences in decay topologies, abundance (or lack thereof) of decays of a certain kind, *etc.*, measurements of the individual lifetimes are more common. In the following section we review the most common types of the lifetime measurements. This discussion is followed by the presentation of the averaging of the various lifetime measurements, each with a brief description of its particularities.

3.2.1 Lifetime measurements, uncertainties and correlations

In most cases lifetime of an H_b is estimated from a flight distance and a $\beta\gamma$ factor which is used to convert the geometrical distance into the proper decay time. Methods of accessing lifetime information can roughly be divided in the following five categories:

1. ***Inclusive (flavor-blind) measurements***. These measurements are aimed at extracting the lifetime from a mixture of b-hadron decays, without distinguishing the decaying species. Often the knowledge of the mixture composition is limited, which makes these measurements experiment-specific. Also, these measurements have to rely on Monte Carlo for estimating the $\beta\gamma$ factor, because the decaying hadrons are not fully reconstructed. On the bright side, these usually are the largest statistics b-hadron lifetime measurements that are accessible to a given experiment, and can, therefore, serve as an important performance benchmark.

2. ***Measurements in semileptonic decays of a specific H_b.*** W from $b \to Wc$ produces $\ell\nu_l$ pair ($\ell = e, \mu$) in about 21% of the cases. Electron or muon from such decays is usually a well-detected signature, which provides for clean and efficient trigger. c quark from $b \to Wc$ transition and the other quark(s) making up the decaying H_b combine into a charm hadron, which is reconstructed in one or more exclusive decay channels. Knowing what this charmed hadron is allows one to separate, at least statistically, different H_b species. The advantage of these measurements is in statistics, which usually is superior to that of the exclusively reconstructed H_b decays. Some of the main disadvantages are related to the difficulty of estimating lepton+charm sample composition and Monte Carlo reliance for the $\beta\gamma$ factor estimate.

3. ***Measurements in exclusively reconstructed hadronic decays.*** These have the advantage of complete reconstruction of decaying H_b, which allows one to infer the decaying species as well as to perform precise measurement of the $\beta\gamma$ factor. Both lead to generally smaller systematic uncertainties than in the above two categories. The downsides are smaller branching ratios, larger combinatoric backgrounds, especially in $H_b \to H_c\pi(\pi\pi)$ and multi-body H_c decays, or in a hadron collider environment with non-trivial underlying event. $H_b \to J/\psi H_s$ are relatively clean and easy to trigger on $J/\psi \to \ell^+\ell^-$, but their branching fraction is only about 1%.

4. ***Measurements at asymmetric B factories.***

   In the $\Upsilon(4S) \to B\overline{B}$ decay, the B mesons (B^+ or B^0) are essentially at rest in the $\Upsilon(4S)$ frame. This makes direct lifetime measurements impossible in experiments at symmetric colliders producing $\Upsilon(4S)$ at rest. At asymmetric B factories the $\Upsilon(4S)$ meson is boosted resulting in B and $\overline{B}$ moving nearly parallel to each other with the same boost. The lifetime is inferred from the distance Δz separating the B and $\overline{B}$ decay vertices along the beam axis and from the $\Upsilon(4S)$ boost known from the beam energies. This boost is equal to $\beta\gamma \approx 0.55$ (0.43) in the *BABAR* (Belle) experiment, resulting in an average B decay length of approximately 250 (190) μm.

   In order to determine the charge of the B mesons in each event, one of the them is fully reconstructed in a semileptonic or hadronic decay mode. The other B is typically not fully reconstructed, only the position of its decay vertex is determined from the remaining tracks in the event. These measurements benefit from large statistics, but suffer from poor proper time resolution, comparable to the B lifetime itself. This resolution is dominated by the uncertainty on the decay vertices, which is typically 50 (100) μm for a fully (partially) reconstructed B meson. With very large future statistics, the resolution and purity could be improved (and hence the systematics reduced) by fully reconstructing both B mesons in the event.

5. ***Direct measurement of lifetime ratios.*** This method has so far been only applied in the measurement of $\tau(B^+)/\tau(B^0)$. The ratio of the lifetimes is extracted from the dependence of the observed relative number of B^+ and B^0 candidates (both reconstructed in semileptonic decays) on the proper decay time.

In some of the latest analyses, measurements of two (*e.g.* $\tau(B^+)$ and $\tau(B^+)/\tau(B^0)$) or three (*e.g.* $\tau(B^+)$, $\tau(B^+)/\tau(B^0)$, and Δm_d) quantities are combined. This introduces correlations

Table 5: Measurements of average b-hadron lifetimes.

Experiment	Method	Data set	τ_b (ps)	Ref.
ALEPH	Dipole	91	$1.511 \pm 0.022 \pm 0.078$	[39]
DELPHI	All track i.p. (2D)	91–92	$1.542 \pm 0.021 \pm 0.045$	[40][a]
DELPHI	Sec. vtx	91–93	$1.582 \pm 0.011 \pm 0.027$	[41][a]
DELPHI	Sec. vtx	94–95	$1.570 \pm 0.005 \pm 0.008$	[42]
L3	Sec. vtx + i.p.	91–94	$1.556 \pm 0.010 \pm 0.017$	[43][b]
OPAL	Sec. vtx	91–94	$1.611 \pm 0.010 \pm 0.027$	[44]
SLD	Sec. vtx	93	$1.564 \pm 0.030 \pm 0.036$	[45]
Average set 1 (b vertex)			1.572 ± 0.009	
ALEPH	Lepton i.p. (3D)	91–93	$1.533 \pm 0.013 \pm 0.022$	[46]
L3	Lepton i.p. (2D)	91–94	$1.544 \pm 0.016 \pm 0.021$	[43][b]
OPAL	Lepton i.p. (2D)	90–91	$1.523 \pm 0.034 \pm 0.038$	[47]
Average set 2 ($b \to \ell$)			1.537 ± 0.020	
CDF1	J/ψ vtx	92–95	$1.533 \pm 0.015^{+0.035}_{-0.031}$	[48]
Average of all above			1.568 ± 0.009	

[a] The combined DELPHI result quoted in [41] is $1.575 \pm 0.010 \pm 0.026$ ps.
[b] The combined L3 result quoted in [43] is $1.549 \pm 0.009 \pm 0.015$ ps.

among measurements. Another source of correlations among the measurements are the systematic effects, which could be common to an experiment or to an analysis technique across the experiments. When calculating the averages, such correlations are taken into account per general procedure, described in Ref. [38].

3.2.2 Inclusive *b*-hadron lifetimes

The inclusive b hadron lifetime is defined as $\tau_b = \sum_i f_i \tau_i$ where τ_i are the individual species lifetimes and f_i are the fractions of the various species present in an unbiased sample of weakly-decaying b hadrons produced at a high-energy collider.[5] This quantity is certainly less fundamental than the lifetimes of the individual species, the latter being much more useful in comparisons of the measurements with the theoretical predictions. Nonetheless, we perform the averaging of the inclusive lifetime measurements for completeness as well as for the reason that they might be of interest as "technical numbers."

In practice, an unbiased measurement of the inclusive lifetime is difficult to achieve, because it would imply an efficiency which is guaranteed to be the same across species. So most of the measurements are biased. In an attempt to group analyses which are expected to select the same mixture of b hadrons, the available results (given in Table 5) are divided into the following three sets:

1. measurements at LEP and SLD that accept any b-hadron decay, based on topological reconstruction (secondary vertex or track impact parameters);

[5] In principle such a quantity could be slightly different in Z decays and a the Tevatron, in case the fractions of b-hadron species are not exactly the same; see the discussion in Sec. 3.1.3.

2. measurements at LEP based on the identification of a lepton from a b decay; and

3. measurements at the Tevatron based on inclusive $H_b \to J/\psi X$ reconstruction, where the J/ψ is fully reconstructed.

The measurements of the first set are generally considered as estimates of τ_b, although the efficiency to reconstruct a secondary vertex most probably depends, in an analysis-specific way, on the number of tracks coming from the vertex, thereby depending on the type of the H_b. Even though these efficiency variations can in principle be accounted for using Monte Carlo simulations (which inevitably contain assumptions on branching fractions), the H_b mixture in that case can remain somewhat ill-defined and could be slightly different among analyses in this set.

On the contrary, the mixtures corresponding to the other two sets of measurements are better defined in the limit where the reconstruction and selection efficiency of a lepton or a J/ψ from an H_b does not depend on the decaying hadron type. These mixtures are given by the production fractions and the inclusive branching fractions for each H_b species to give a lepton or a J/ψ. In particular, under the assumption that all b hadrons have the same semileptonic decay width, the analyses of the second set should measure $\tau(b \to \ell) = (\sum_i f_i \tau_i^2)/(\sum_i f_i \tau_i)$ which is necessarily larger than τ_b if lifetime differences exist. Given the present knowledge on τ_i and f_i, $\tau(b \to \ell) - \tau_b$ is expected to be of the order of 0.01 ps.

Measurements by SLC and LEP experiments are subject to a number of common systematic uncertainties, such as those due to (lack of knowledge of) b and c fragmentation, b and c decay models, $\mathcal{B}(B \to \ell)$, $\mathcal{B}(B \to c \to \ell)$, $\mathcal{B}(c \to \ell)$, τ_c, and H_b decay multiplicity. In the averaging, these systematic uncertainties are assumed to be 100% correlated. The averages for the sets defined above (also given in Table 5) are

$$\tau(b \text{ vertex}) = 1.572 \pm 0.009 \text{ ps}, \quad (28)$$

$$\tau(b \to \ell) = 1.537 \pm 0.020 \text{ ps}, \quad (29)$$

$$\tau(b \to J/\psi) = 1.533^{+0.038}_{-0.034} \text{ ps}, \quad (30)$$

whereas an average of all measurements, ignoring mixture differences, yields 1.568 ± 0.009 ps.

3.2.3 B^0 and B^+ lifetimes and their ratio

After a number of years of dominating these averages the LEP experiments yielded the scene to the asymmetric B factories and the Tevatron experiments. The B factories have been very successful in utilizing their potential – in only a few years of running, *BABAR* and, to a greater extent, Belle, have struck a balance between the statistical and the systematic uncertainties, with both being close to (or even better than) the impressive 1%. In the meanwhile, CDF and DØ have emerged as significant contributors to the field as the Tevatron Run II data flowed in. Both appear to enjoy relatively small systematic effects, and while current statistical uncertainties of their measurements are factors of 2 to 4 larger than those of their B-factory counterparts, both Tevatron experiments stand to increase their samples by almost an order of magnitude.

At present time we are in an interesting position of having three sets of measurements (from LEP/SLC, B factories and the Tevatron) that originate from different environments, obtained using substantially different techniques and are precise enough for incisive comparison.

Table 6: Measurements of the B^0 lifetime.

Experiment	Method	Data set	$\tau(B^0)$ (ps)	Ref.
ALEPH	$D^{(*)}\ell$	91–95	$1.518 \pm 0.053 \pm 0.034$	[49]
ALEPH	Exclusive	91–94	$1.25^{+0.15}_{-0.13} \pm 0.05$	[50]
ALEPH	Partial rec. $\pi^+\pi^-$	91–94	$1.49^{+0.17+0.08}_{-0.15-0.06}$	[50]
DELPHI	$D^{(*)}\ell$	91–93	$1.61^{+0.14}_{-0.13} \pm 0.08$	[51]
DELPHI	Charge sec. vtx	91–93	$1.63 \pm 0.14 \pm 0.13$	[52]
DELPHI	Inclusive $D^*\ell$	91–93	$1.532 \pm 0.041 \pm 0.040$	[53]
DELPHI	Charge sec. vtx	94–95	$1.531 \pm 0.021 \pm 0.031$	[42]
L3	Charge sec. vtx	94–95	$1.52 \pm 0.06 \pm 0.04$	[54]
OPAL	$D^{(*)}\ell$	91–93	$1.53 \pm 0.12 \pm 0.08$	[55]
OPAL	Charge sec. vtx	93–95	$1.523 \pm 0.057 \pm 0.053$	[56]
OPAL	Inclusive $D^*\ell$	91–00	$1.541 \pm 0.028 \pm 0.023$	[57]
SLD	Charge sec. vtx ℓ	93–95	$1.56^{+0.14}_{-0.13} \pm 0.10$	[58][a]
SLD	Charge sec. vtx	93–95	$1.66 \pm 0.08 \pm 0.08$	[58][a]
CDF1	$D^{(*)}\ell$	92–95	$1.474 \pm 0.039^{+0.052}_{-0.051}$	[59]
CDF1	Excl. $J/\psi K^{*0}$	92–95	$1.497 \pm 0.073 \pm 0.032$	[60]
CDF2	Incl. $D^{(*)}\ell$	02–04	$1.473 \pm 0.036 \pm 0.054$	[61][p]
CDF2	Excl. $D^-(3)\pi$	02–04	$1.511 \pm 0.023 \pm 0.013$	[62][p]
CDF2	Excl. $J/\psi K_S$, $J/\psi K^{*0}$	02–06	$1.551 \pm 0.019 \pm 0.011$	[63][p]
DØ	Excl. $J/\psi K^{*0}$	02–05	$1.530 \pm 0.043 \pm 0.023$	[64, 65]
DØ	Excl. $J/\psi K_S$	02–06	$1.501^{+0.078}_{-0.074} \pm 0.050$	[66]
BABAR	Exclusive	99–00	$1.546 \pm 0.032 \pm 0.022$	[67]
BABAR	Inclusive $D^*\ell$	99–01	$1.529 \pm 0.012 \pm 0.029$	[68]
BABAR	Exclusive $D^*\ell$	99–02	$1.523^{+0.024}_{-0.023} \pm 0.022$	[69]
BABAR	Incl. $D^*\pi$, $D^*\rho$	99–01	$1.533 \pm 0.034 \pm 0.038$	[70]
BABAR	Inclusive $D^*\ell$	99–04	$1.504 \pm 0.013^{+0.018}_{-0.013}$	[71]
Belle	Exclusive	00–03	$1.534 \pm 0.008 \pm 0.010$	[72]
Average			1.530 ± 0.008	

[a] The combined SLD result quoted in [58] is $1.64 \pm 0.08 \pm 0.08$ ps.
[p] Preliminary.

The averaging of $\tau(B^+)$, $\tau(B^0)$ and $\tau(B^+)/\tau(B^0)$ measurements is summarized in Tables 6, 7, and 8. For $\tau(B^+)/\tau(B^0)$ we averaged only the measurements of this quantity provided by experiments rather than using all available knowledge, which would have included, for example, $\tau(B^+)$ and $\tau(B^0)$ measurements which did not contribute to any of the ratio measurements.

The following sources of correlated (within experiment/machine) systematic uncertainties have been considered:

- for SLC/LEP measurements – D^{**} branching ratio uncertainties [2], momentum estimation of b mesons from Z^0 decays (b-quark fragmentation parameter $\langle X_E \rangle = 0.702 \pm 0.008$ [2]), B_s^0 and b baryon lifetimes (see Secs. 3.2.4 and 3.2.6), and b-hadron fractions at high energy (see Table 4);

Table 7: Measurements of the B^+ lifetime.

Experiment	Method	Data set	$\tau(B^+)$ (ps)	Ref.
ALEPH	$D^{(*)}\ell$	91–95	$1.648 \pm 0.049 \pm 0.035$	[49]
ALEPH	Exclusive	91–94	$1.58^{+0.21+0.04}_{-0.18-0.03}$	[50]
DELPHI	$D^{(*)}\ell$	91–93	$1.61 \pm 0.16 \pm 0.12$	[51][a]
DELPHI	Charge sec. vtx	91–93	$1.72 \pm 0.08 \pm 0.06$	[52][a]
DELPHI	Charge sec. vtx	94–95	$1.624 \pm 0.014 \pm 0.018$	[42]
L3	Charge sec. vtx	94–95	$1.66 \pm 0.06 \pm 0.03$	[54]
OPAL	$D^{(*)}\ell$	91–93	$1.52 \pm 0.14 \pm 0.09$	[55]
OPAL	Charge sec. vtx	93–95	$1.643 \pm 0.037 \pm 0.025$	[56]
SLD	Charge sec. vtx ℓ	93–95	$1.61^{+0.13}_{-0.12} \pm 0.07$	[58][b]
SLD	Charge sec. vtx	93–95	$1.67 \pm 0.07 \pm 0.06$	[58][b]
CDF1	$D^{(*)}\ell$	92–95	$1.637 \pm 0.058^{+0.045}_{-0.043}$	[59]
CDF1	Excl. $J/\psi K$	92–95	$1.636 \pm 0.058 \pm 0.025$	[60]
CDF2	Excl. $J/\psi K$	02–06	$1.630 \pm 0.016 \pm 0.011$	[63][p]
CDF2	Incl. $D^0\ell$	02–04	$1.653 \pm 0.029^{+0.033}_{-0.031}$	[61][p]
CDF2	Excl. $D^0\pi$	02–04	$1.661 \pm 0.027 \pm 0.013$	[62][p]
BABAR	Exclusive	99–00	$1.673 \pm 0.032 \pm 0.023$	[67]
Belle	Exclusive	00–03	$1.635 \pm 0.011 \pm 0.011$	[72]
Average			1.639 ± 0.009	

[a] The combined DELPHI result quoted in [52] is 1.70 ± 0.09 ps.
[b] The combined SLD result quoted in [58] is $1.66 \pm 0.06 \pm 0.05$ ps.
[p] Preliminary.

- for *BABAR* measurements – alignment, z scale, PEP-II boost, sample composition (where applicable);
- for DØ and CDF Run II measurements – alignment (separately within each experiment).

The resultant averages are:

$$\tau(B^0) = 1.530 \pm 0.008 \text{ ps}, \quad (31)$$

$$\tau(B^+) = 1.639 \pm 0.009 \text{ ps}, \quad (32)$$

$$\tau(B^+)/\tau(B^0) = 1.073 \pm 0.008. \quad (33)$$

3.2.4 B_s^0 lifetime

Similar to the kaon system, neutral B mesons contain short- and long-lived components, since the light (L) and heavy (H) eigenstates, $B_{\rm L}$ and $B_{\rm H}$, differ not only in their masses, but also in their widths with $\Delta\Gamma = \Gamma_{\rm L} - \Gamma_{\rm H}$. In the case of the B_s^0 system, $\Delta\Gamma_s$ can be particularly large. The current theoretical prediction in the Standard Model for the fractional width difference is $\Delta\Gamma_s = 0.096 \pm 0.039$ [74], where $\Gamma_s = (\Gamma_{\rm L} + \Gamma_{\rm H})/2$. Specific measurements of $\Delta\Gamma_s$ and Γ_s are explained in Sec. 3.3.2, but the result for Γ_s is quoted here.

Neglecting *CP* violation in $B_s^0 - \overline{B}_s^0$ mixing, which is expected to be small [74], the B_s^0 mass eigenstates are also *CP* eigenstates. In the Standard Model assuming no *CP* violation in the

Table 8: Measurements of the ratio $\tau(B^+)/\tau(B^0)$.

Experiment	Method	Data set	Ratio $\tau(B^+)/\tau(B^0)$	Ref.
ALEPH	$D^{(*)}\ell$	91–95	$1.085 \pm 0.059 \pm 0.018$	[49]
ALEPH	Exclusive	91–94	$1.27^{+0.23+0.03}_{-0.19-0.02}$	[50]
DELPHI	$D^{(*)}\ell$	91–93	$1.00^{+0.17}_{-0.15} \pm 0.10$	[51]
DELPHI	Charge sec. vtx	91–93	$1.06^{+0.13}_{-0.11} \pm 0.10$	[52]
DELPHI	Charge sec. vtx	94–95	$1.060 \pm 0.021 \pm 0.024$	[42]
L3	Charge sec. vtx	94–95	$1.09 \pm 0.07 \pm 0.03$	[54]
OPAL	$D^{(*)}\ell$	91–93	$0.99 \pm 0.14^{+0.05}_{-0.04}$	[55]
OPAL	Charge sec. vtx	93–95	$1.079 \pm 0.064 \pm 0.041$	[56]
SLD	Charge sec. vtx ℓ	93–95	$1.03^{+0.16}_{-0.14} \pm 0.09$	[58][a]
SLD	Charge sec. vtx	93–95	$1.01^{+0.09}_{-0.08} \pm 0.05$	[58][a]
CDF1	$D^{(*)}\ell$	92–95	$1.110 \pm 0.056^{+0.033}_{-0.030}$	[59]
CDF1	Excl. $J/\psi K$	92–95	$1.093 \pm 0.066 \pm 0.028$	[60]
CDF2	Excl. $J/\psi K^{(*)}$	02–06	$1.051 \pm 0.023 \pm 0.004$	[63][p]
CDF2	Incl. $D\ell$	02–04	$1.123 \pm 0.040^{+0.041}_{-0.039}$	[61][p]
CDF2	Excl. $D\pi$	02–04	$1.10 \pm 0.02 \pm 0.01$	[62][p]
DØ	$D^{*+}\mu$ $D^0\mu$ ratio	02–04	$1.080 \pm 0.016 \pm 0.014$	[73]
BABAR	Exclusive	99–00	$1.082 \pm 0.026 \pm 0.012$	[67]
Belle	Exclusive	00–03	$1.066 \pm 0.008 \pm 0.008$	[72]
Average			1.073 ± 0.008	

[a] The combined SLD result quoted in [58] is $1.01 \pm 0.07 \pm 0.06$.
[p] Preliminary.

B_s^0 system, $\Gamma_{\rm L}$ is the width of the *CP*-even state and $\Gamma_{\rm H}$ the width of the *CP*-odd state. Final states can be decomposed into *CP*-even and *CP*-odd components, each with a different lifetime.

In view of a possibly substantial width difference, and the fact that various decay channels will have different proportions of the $B_{\rm L}$ and $B_{\rm H}$ eigenstates, the straight average of all available B_s^0 lifetime measurements is rather ill-defined. Therefore, the B_s^0 lifetime measurements are broken down into four categories and averaged separately.

- ***Flavor-specific decays***, such as semileptonic $B_s \to D_s\ell\nu$ or $B_s \to D_s\pi$, will have equal fractions of $B_{\rm L}$ and $B_{\rm H}$ at time zero, where $\tau_{\rm L} = 1/\Gamma_{\rm L}$ is expected to be the shorter-lived component and $\tau_{\rm H} = 1/\Gamma_{\rm H}$ expected to be the longer-lived component. A superposition of two exponentials thus results with decay widths $\Gamma_s \pm \Delta\Gamma_s/2$. Fitting to a single exponential one obtains a measure of the flavor-specific lifetime [75]:

$$\tau(B_s^0)_{\rm fs} = \frac{1}{\Gamma_s}\frac{1+\left(\frac{\Delta\Gamma_s}{2\Gamma_s}\right)^2}{1-\left(\frac{\Delta\Gamma_s}{2\Gamma_s}\right)^2}. \tag{34}$$

  As given in Table 9, the flavor-specific B_s^0 lifetime world average is:

$$\tau(B_s^0)_{\rm fs} = 1.456 \pm 0.030 \text{ ps}\,. \tag{35}$$

Table 9: Measurements of the B_s^0 lifetime.

Experiment	Method	Data set	$\tau(B_s^0)$ (ps)	Ref.
ALEPH	$D_s\ell$	91–95	$1.54^{+0.14}_{-0.13} \pm 0.04$	[76]
CDF1	$D_s\ell$	92–96	$1.36 \pm 0.09^{+0.06}_{-0.05}$	[77]
DELPHI	$D_s\ell$	91–95	$1.42^{+0.14}_{-0.13} \pm 0.03$	[78]
OPAL	$D_s\ell$	90–95	$1.50^{+0.16}_{-0.15} \pm 0.04$	[79]
DØ	$D_s\mu$	02–04	$1.398 \pm 0.044^{+0.028}_{-0.025}$	[80]
CDF2	$D_s\pi(X)$	02–06	$1.518 \pm 0.041 \pm 0.025$	[81]^p
CDF2	$D_s\ell$	02–04	$1.381 \pm 0.055^{+0.052}_{-0.046}$	[82]^p
Average of flavor-specific measurements			1.456 ± 0.030	
ALEPH	D_sh	91–95	$1.47 \pm 0.14 \pm 0.08$	[83]
DELPHI	D_sh	91–95	$1.53^{+0.16}_{-0.15} \pm 0.07$	[84]
OPAL	D_s incl.	90–95	$1.72^{+0.20+0.18}_{-0.19-0.17}$	[85]
Average of all above D_s measurements			1.459 ± 0.030	
CDF1	$J/\psi\phi$	92–95	$1.34^{+0.23}_{-0.19} \pm 0.05$	[48]
CDF2	$J/\psi\phi$	02–06	$1.494 \pm 0.054 \pm 0.009$	[63]^p
DØ	$J/\psi\phi$	02–04	$1.444^{+0.098}_{-0.090} \pm 0.02$	[65]
Average of $J/\psi\phi$ measurements			1.477 ± 0.046	

^{p} Preliminary.

This world average will be used later in Sec. 3.3.2 in combination with other measurements to find $\overline{\tau}(B_s^0) = 1/\Gamma_s$ and $\Delta\Gamma_s$.

The following correlated systematic errors were considered: average B lifetime used in backgrounds, B_s^0 decay multiplicity, and branching ratios used to determine backgrounds (*e.g.* $\mathcal{B}(B \to D_sD)$). A knowledge of the multiplicity of B_s^0 decays is important for measurements that partially reconstruct the final state such as $B \to D_sX$ (where X is not a lepton). The boost deduced from Monte Carlo simulation depends on the multiplicity used. Since this is not well known, the multiplicity in the simulation is varied and this range of values observed is taken to be a systematic. Similarly not all the branching ratios for the potential background processes are measured. Where they are available, the PDG values are used for the error estimate. Where no measurements are available estimates can usually be made by using measured branching ratios of related processes and using some reasonable extrapolation.

- ***$B_s^0 \to D_s^+X$ decays***. Included in Table 9 are measurements of lifetimes using samples of B_s^0 decays to D_s plus hadrons, and hence into a less known mixture of *CP*-states. A lifetime weighted this way can still be a useful input for analyses examining such an inclusive sample. These are separated in Table 9 and combined with the semileptonic lifetime to obtain:

$$\tau(B_s^0)_{D_s\mathrm{X}} = 1.459 \pm 0.030 \text{ ps}\,. \tag{36}$$

- ***Fully exclusive $B_s^0 \to J/\psi\phi$ decays*** are expected to be dominated by the *CP*-even state and its lifetime. First measurements of the *CP* mix for this decay mode are outlined

in Sec. 3.3.2. CDF and DØ measurements from this particular mode $B_s^0 \to J/\psi\phi$ are combined into an average given in Table 9. There are no correlations between the measurements for this fully exclusive channel, and the world average for this specific decay is:

$$\tau(B_s^0)_{J/\psi\phi} = 1.477 \pm 0.046 \text{ ps}\,. \tag{37}$$

A caveat is that different experimental acceptances will likely lead to different admixtures of the *CP*-even and *CP*-odd states, and fits to a single exponential may result in inherently different measurements of these quantities.

- ***Fully exclusive $B_s^0 \to K^+K^-$ decays*** are expected to be *CP* even to within 5%, and hence measures the lifetime of the "light" mass eigenstate $\tau_L = 1/\Gamma_L$. The measurement of this lifetime from CDF in Run II [86] is:

$$\tau(B_s^0)_{K^+K^-} = 1.53 \pm 0.18 \pm 0.02\,\text{ps}, \tag{38}$$

and will be used as an input in Sec. 3.3.2 for the average described below.

Finally, as will be shown in Sec. 3.3.2, measurements of $\Delta\Gamma_s$, including separation into *CP*-even and *CP*-odd components, give

$$\overline{\tau}(B_s^0) = 1/\Gamma_s = 1.515^{+0.034}_{-0.034} \text{ ps}\,, \tag{39}$$

and when combined with the flavor-specific lifetime measurements:

$$\overline{\tau}(B_s^0) = 1/\Gamma_s = 1.478^{+0.020}_{-0.022} \text{ ps}\,. \tag{40}$$

3.2.5 B_c^+ lifetime

There are currently three measurements of the lifetime of the B_c^+ meson from CDF [87,88] and DØ [89] using the semileptonic decay mode $B_c^+ \to J/\psi\ell$ and fitting simultaneously to the mass and lifetime using the vertex formed with the leptons from the decay of the J/ψ and the third lepton. Correction factors to estimate the boost due to the missing neutrino are used. In the analysis of the CDF Run I data [87], a mass value of $6.40 \pm 0.39 \pm 0.13$ GeV/c^2 is found by fitting to the tri-lepton invariant mass spectrum. In the CDF and DØ Run II results [88,89], the B_c^+ mass is assumed to be $6285.7 \pm 5.3 \pm 1.2$ MeV/c^2, taken from a CDF result [90]. These mass measurements are consistent within uncertainties, and also consistent with the most recent precision determination from CDF of $6275.6 \pm 2.9 \pm 2.5$ MeV/c^2 [91]. Correlated systematic errors include the impact of the uncertainty of the B_c^+ p_T spectrum on the correction factors, the level of feed-down from $\psi(2S)$, MC modeling of the decay model varying from phase space to the ISGW model, and mass variations. Values of the B_c^+ lifetime are given in Table 10 and the world average is determined to be:

$$\tau(B_c^+) = 0.461 \pm 0.036 \text{ ps}\,. \tag{41}$$

Table 10: Measurements of the B_c^+ lifetime.

Experiment	Method	Data set	$\tau(B_c^+)$ (ps)	Ref.
CDF1	$J/\psi\ell$	92–95	$0.46^{+0.18}_{-0.16} \pm 0.03$	[87]
CDF2	$J/\psi\ell$	02–06	$0.475^{+0.053}_{-0.049} \pm 0.018$	[88]^p
DØ	$J/\psi\mu$	02–06	$0.448^{+0.038}_{-0.036} \pm 0.032$	[89]
Average			0.461 ± 0.036	

^{p} Preliminary.

3.2.6 Λ_b^0 and b-baryon lifetimes

The most precise measurements of the b-baryon lifetime originate from two classes of partially reconstructed decays. In the first class, decays with an exclusively reconstructed Λ_c^+ baryon and a lepton of opposite charge are used. These products are more likely to occur in the decay of Λ_b^0 baryons. In the second class, more inclusive final states with a baryon (p, $\overline{p}$, Λ, or $\overline{\Lambda}$) and a lepton have been used, and these final states can generally arise from any b baryon.

The following sources of correlated systematic uncertainties have been considered: experimental time resolution within a given experiment, b-quark fragmentation distribution into weakly decaying b baryons, Λ_b^0 polarization, decay model, and evaluation of the b-baryon purity in the selected event samples. In computing the averages the central values of the masses are scaled to $M(\Lambda_b^0) = 5620 \pm 2$ MeV/c^2 [92] and $M(b\text{-baryon}) = 5670 \pm 100$ MeV/c^2.

For the semi-inclusive lifetime measurements, the meaning of decay model systematic uncertainties and the correlation of these uncertainties between measurements are not always clear. Uncertainties related to the decay model are dominated by assumptions on the fraction of n-body semileptonic decays. To be conservative it is assumed that these are 100% correlated whenever given as an error. DELPHI varies the fraction of 4-body decays from 0.0 to 0.3. In computing the average, the DELPHI result is corrected to a value of 0.2 ± 0.2 for this fraction.

Furthermore, in computing the average, the semileptonic decay results from LEP are corrected for a polarization of $-0.45^{+0.19}_{-0.17}$ [2] and a Λ_b^0 fragmentation parameter $\langle X_E \rangle = 0.70 \pm 0.03$ [93].

Inputs to the averages are given in Table 11. Note that the CDF $\Lambda_b \to J/\psi\Lambda$ lifetime result [63] is 4.0σ larger than the world average computed excluding this result. It is nonetheless combined with the rest without adjustment of input errors. The world average lifetime of b baryons is then:

$$\langle \tau(b\text{-baryon}) \rangle = 1.311 \pm 0.040 \text{ ps}. \tag{42}$$

Keeping only $\Lambda_c^\pm \ell^\mp$, $\Lambda \ell^- \ell^+$, and fully exclusive final states, as representative of the Λ_b^0 baryon, the following lifetime is obtained:

$$\tau(\Lambda_b^0) = 1.379 \pm 0.051 \text{ ps}. \tag{43}$$

Averaging the measurements based on the $\Xi^\mp \ell^\mp$ final states [22–24] gives a lifetime value for a sample of events containing Ξ_b^0 and Ξ_b^- baryons:

$$\langle \tau(\Xi_b) \rangle = 1.42^{+0.28}_{-0.24} \text{ ps}. \tag{44}$$

Table 11: Measurements of the b-baryon lifetimes.

Experiment	Method	Data set	Lifetime (ps)	Ref.
ALEPH	$\Lambda_c^+\ell$	91–95	$1.18^{+0.13}_{-0.12} \pm 0.03$	[21][a]
ALEPH	$\Lambda\ell^-\ell^+$	91–95	$1.30^{+0.26}_{-0.21} \pm 0.04$	[21][a]
CDF1	$\Lambda_c^+\ell$	91–95	$1.32 \pm 0.15 \pm 0.07$	[94]
CDF2	$J/\psi\Lambda$	02–06	$1.580 \pm 0.077 \pm 0.012$	[63][p]
DØ	$J/\psi\Lambda$	02–06	$1.218^{+0.130}_{-0.115} \pm 0.042$	[66][b]
DØ	$\Lambda_c^+\mu$	02–06	$1.290^{+0.119+0.087}_{-0.110-0.091}$	[95][b]
DELPHI	$\Lambda_c^+\ell$	91–94	$1.11^{+0.19}_{-0.18} \pm 0.05$	[96][c]
OPAL	$\Lambda_c^+\ell$, $\Lambda\ell^-\ell^+$	90–95	$1.29^{+0.24}_{-0.22} \pm 0.06$	[79]
Average of above 8 (Λ_b^0 lifetime)			1.379 ± 0.051	
ALEPH	$\Lambda\ell$	91–95	$1.20 \pm 0.08 \pm 0.06$	[21]
DELPHI	$\Lambda\ell\pi$ vtx	91–94	$1.16 \pm 0.20 \pm 0.08$	[96][c]
DELPHI	$\Lambda\mu$ i.p.	91–94	$1.10^{+0.19}_{-0.17} \pm 0.09$	[97][c]
DELPHI	$p\ell$	91–94	$1.19 \pm 0.14 \pm 0.07$	[96][c]
OPAL	$\Lambda\ell$ i.p.	90–94	$1.21^{+0.15}_{-0.13} \pm 0.10$	[98][d]
OPAL	$\Lambda\ell$ vtx	90–94	$1.15 \pm 0.12 \pm 0.06$	[98][d]
Average of above 14 (b-baryon lifetime)			1.311 ± 0.040	
ALEPH	$\Xi\ell$	90–95	$1.35^{+0.37+0.15}_{-0.28-0.17}$	[22]
DELPHI	$\Xi\ell$	91–93	$1.5^{+0.7}_{-0.4} \pm 0.3$	[24][e]
DELPHI	$\Xi\ell$	92–95	$1.45^{+0.55}_{-0.43} \pm 0.13$	[23][e]
Average of above 3 (Ξ_b lifetime)			$1.42^{+0.28}_{-0.24}$	

[a] The combined ALEPH result quoted in [21] is 1.21 ± 0.11 ps.
[b] The combined DØ result quoted in [95] is $1.251^{+0.102}_{-0.096}$ ps.
[c] The combined DELPHI result quoted in [96] is $1.14 \pm 0.08 \pm 0.04$ ps.
[d] The combined OPAL result quoted in [98] is $1.16 \pm 0.11 \pm 0.06$ ps.
[e] The combined DELPHI result quoted in [23] is $1.48^{+0.40}_{-0.31} \pm 0.12$ ps.
[p] Preliminary.

3.2.7 Summary and comparison with theoretical predictions

Averages of lifetimes of specific b-hadron species are collected in Table 12. As described in Sec. 3.2, Heavy Quark Effective Theory can be employed to explain the hierarchy of $\tau(B_c^+) \ll \tau(\Lambda_b^0) < \overline{\tau}(B_s^0) \approx \tau(B^0) < \tau(B^+)$, and used to predict the ratios between lifetimes. Typical predictions are compared to the measured lifetime ratios in Table 13. A recent prediction of the ratio between the B^+ and B^0 lifetimes, is 1.06 ± 0.02 [36], in good agreement with experiment.

The total widths of the B_s^0 and B^0 mesons are expected to be very close and differ by at most 1% [37, 99]. However, the experimental ratio $\overline{\tau}(B_s^0)/\tau(B^0)$, where $\overline{\tau}(B_s^0) = 1/\Gamma_s$ is obtained from $\Delta\Gamma_s$ and flavour-specific lifetime measurements, appears to be smaller than 1 by (3.4 ± 1.5)%, at deviation with respect to the prediction.

The ratio $\tau(\Lambda_b^0)/\tau(B^0)$ has particularly been the source of theoretical scrutiny since earlier calculations [33,100] predicted a value greater than 0.90, almost two sigma higher than the world average at the time. Many predictions cluster around a most likely central value of 0.94 [101]. More recent calculations of this ratio that include higher-order effects predict a lower ratio

Table 12: Summary of lifetimes of different b-hadron species.

b-hadron species	Measured lifetime
B^+	1.639 ± 0.009 ps
B^0	1.530 ± 0.008 ps
B_s^0 ($\rightarrow$ flavor specific)	1.456 ± 0.030 ps
B_s^0 ($\rightarrow J/\psi\phi$)	1.477 ± 0.046 ps
B_s^0 ($1/\Gamma_s$)	$1.478^{+0.020}_{-0.022}$ ps
B_c^+	0.461 ± 0.036 ps
Λ_b^0	1.379 ± 0.051 ps
Ξ_b mixture	$1.42^{+0.28}_{-0.24}$ ps
b-baryon mixture	1.311 ± 0.040 ps
b-hadron mixture	1.568 ± 0.009 ps

Table 13: Measured ratios of b-hadron lifetimes relative to the B^0 lifetime and ranges predicted by theory [36, 37].

Lifetime ratio	Measured value	Predicted range
$\tau(B^+)/\tau(B^0)$	1.073 ± 0.008	1.04 – 1.08
$\overline{\tau}(B_s^0)/\tau(B^0)^a$	0.966 ± 0.015	0.99 – 1.01
$\tau(\Lambda_b^0)/\tau(B^0)$	0.901 ± 0.034	0.86 – 0.95
$\tau(b\text{-baryon})/\tau(B^0)$	0.857 ± 0.026	0.86 – 0.95

[a] Using $\overline{\tau}(B_s^0) = 1/\Gamma_s = 2/(\Gamma_{\rm L} + \Gamma_{\rm H})$.

between the Λ_b^0 and B^0 lifetimes [36, 37] and reduce this difference. References [36, 37] present probability density functions of their predictions with variation of theoretical inputs, and the indicated ranges in Table 13 are the RMS of the distributions from the most probable values. Again, the CDF measurement of the Λ_b lifetime in the exclusive decay mode $J/\psi\Lambda$ [63] is significantly higher than the world average before inclusion, with a ratio to the $\tau(B^0)$ world average of $\tau(\Lambda_b^0)/\tau(B^0) = 1.042 \pm 0.057$, resulting in continued interest in lifetimes of b baryons.

3.3 Neutral B-meson mixing

The $B^0 - \overline{B}^0$ and $B_s^0 - \overline{B}_s^0$ systems both exhibit the phenomenon of particle-antiparticle mixing. For each of them, there are two mass eigenstates which are linear combinations of the two flavour states, B and $\overline{B}$. The heaviest (lightest) of the these mass states is denoted $B_{\rm H}$ ($B_{\rm L}$), with mass $m_{\rm H}$ ($m_{\rm L}$) and total decay width $\Gamma_{\rm H}$ ($\Gamma_{\rm L}$). We define

$$\Delta m = m_{\rm H} - m_{\rm L}\,, \qquad x = \Delta m/\Gamma\,, \tag{45}$$

$$\Delta\Gamma = \Gamma_{\rm L} - \Gamma_{\rm H}\,, \qquad y = \Delta\Gamma/(2\Gamma)\,, \tag{46}$$

where $\Gamma = (\Gamma_{\rm H} + \Gamma_{\rm L})/2 = 1/\overline{\tau}(B)$ is the average decay width. Δm is positive by definition, and $\Delta\Gamma$ is expected to be positive within the Standard Model.[6]

There are four different time-dependent probabilities describing the case of a neutral B meson produced as a flavour state and decaying to a flavour-specific final state. If CPT is conserved (which will be assumed throughout), they can be written as

$$\left\{\begin{array}{lcl} \mathcal{P}(B \to B) & = & \frac{e^{-\Gamma t}}{2}\left[\cosh\left(\frac{\Delta\Gamma}{2}t\right) + \cos(\Delta m t)\right] \\ \mathcal{P}(B \to \overline{B}) & = & \frac{e^{-\Gamma t}}{2}\left[\cosh\left(\frac{\Delta\Gamma}{2}t\right) - \cos(\Delta m t)\right] \left|\frac{q}{p}\right|^2 \\ \mathcal{P}(\overline{B} \to B) & = & \frac{e^{-\Gamma t}}{2}\left[\cosh\left(\frac{\Delta\Gamma}{2}t\right) - \cos(\Delta m t)\right] \left|\frac{p}{q}\right|^2 \\ \mathcal{P}(\overline{B} \to \overline{B}) & = & \frac{e^{-\Gamma t}}{2}\left[\cosh\left(\frac{\Delta\Gamma}{2}t\right) + \cos(\Delta m t)\right] \end{array}\right. , \tag{47}$$

where t is the proper time of the system (*i.e.* the time interval between the production and the decay in the rest frame of the B meson). At the B factories, only the proper-time difference Δt between the decays of the two neutral B mesons from the $\Upsilon(4S)$ can be determined, but, because the two B mesons evolve coherently (keeping opposite flavours as long as none of them has decayed), the above formulae remain valid if t is replaced with Δt and the production flavour is replaced by the flavour at the time of the decay of the accompanying B meson in a flavour-specific state. As can be seen in the above expressions, the mixing probabilities depend on three mixing observables: Δm, $\Delta\Gamma$, and $|q/p|^2$ which signals CP violation in the mixing if $|q/p|^2 \neq 1$.

In the next sections we review in turn the experimental knowledge on these three parameters, separately for the B^0 meson (Δm_d, $\Delta\Gamma_d$, $|q/p|_d$) and the B^0_s meson (Δm_s, $\Delta\Gamma_s$, $|q/p|_s$).

3.3.1 B^0 mixing parameters

CP violation parameter $|q/p|_d$

Evidence for CP violation in B^0 mixing has been searched for, both with flavor-specific and inclusive B^0 decays, in samples where the initial flavor state is tagged. In the case of semileptonic (or other flavor-specific) decays, where the final state tag is also available, the following asymmetry

$$\mathcal{A}^d_{\rm SL} = \frac{N(\overline{B}^0(t) \to \ell^+\nu_\ell X) - N(B^0(t) \to \ell^-\overline{\nu}_\ell X)}{N(\overline{B}^0(t) \to \ell^+\nu_\ell X) + N(B^0(t) \to \ell^-\overline{\nu}_\ell X)} = \frac{|p/q|^2_d - |q/p|^2_d}{|p/q|^2_d + |q/p|^2_d} \tag{48}$$

has been measured, either in time-integrated analyses at CLEO [102–104], CDF [105, 106] and DØ [32], or in time-dependent analyses at OPAL [107], ALEPH [108], *BABAR* [109–112] and Belle [113]. In the inclusive case, also investigated and published at ALEPH [108] and OPAL [114], no final state tag is used, and the asymmetry [115]

$$\frac{N(B^0(t) \to \text{all}) - N(\overline{B}^0(t) \to \text{all})}{N(B^0(t) \to \text{all}) + N(\overline{B}^0(t) \to \text{all})} \simeq \mathcal{A}^d_{\rm SL}\left[\frac{\Delta m_d}{2\Gamma_d}\sin(\Delta m_d\, t) - \sin^2\left(\frac{\Delta m_d\, t}{2}\right)\right] \tag{49}$$

[6] For reason of symmetry in Eqs. (45) and (46), $\Delta\Gamma$ is sometimes defined with the opposite sign. The definition adopted here, *i.e.* Eq. (46), is the one used by most experimentalists and many phenomenologists in B physics.

must be measured as a function of the proper time to extract information on *CP* violation. In all cases asymmetries compatible with zero have been found, with a precision limited by the available statistics.

A simple average of all measurements performed at B factories [103,104,109,111–113] yields

$$\mathcal{A}^d_{\rm SL} = -0.0047 \pm 0.0046 \tag{50}$$

or, equivalently through Eq. (48),

$$|q/p|_d = 1.0024 \pm 0.0023\,. \tag{51}$$

Analyses performed at higher energy, either at LEP or at the Tevatron, can't separate the contributions from the B^0 and B^0_s mesons. Under the assumption of no *CP* violation in B^0_s mixing, a number of these analyses [32, 107, 108, 114] quote a measurement of $\mathcal{A}^d_{\rm SL}$ or $|q/p|_d$ for the B^0 meson. Combining these results, as well as that of a recent preliminary CDF analysis [106][7], with the above B factory averages leads to

$$\left.\begin{array}{l}\mathcal{A}^d_{\rm SL} = -0.0058 \pm 0.0034 \\ |q/p|_d = 1.0030 \pm 0.0017\end{array}\right\} \quad \text{if } \mathcal{A}^s_{\rm SL} = 0,\ |q/p|_s = 1. \tag{52}$$

These results[8], summarized in Table 14, are compatible with no *CP* violation in the B^0 mixing, an assumption we make for the rest of this section.

Mass and decay width differences Δm_d and $\Delta\Gamma_d$

Many time-dependent B^0–$\overline{B}^0$ oscillation analyses have been performed by the ALEPH, *BABAR*, Belle, CDF, DØ, DELPHI, L3 and OPAL collaborations. The corresponding measurements of Δm_d are summarized in Table 15, where only the most recent results are listed (*i.e.* measurements superseded by more recent ones have been omitted). Although a variety of different techniques have been used, the individual Δm_d results obtained at high-energy colliders have remarkably similar precision. Their average is compatible with the recent and more precise measurements from the asymmetric B factories. The systematic uncertainties are not negligible; they are often dominated by sample composition, mistag probability, or b-hadron lifetime contributions. Before being combined, the measurements are adjusted on the basis of a common set of input values, including the averages of the b-hadron fractions and lifetimes given in this report (see Secs. 3.1 and 3.2). Some measurements are statistically correlated. Systematic correlations arise both from common physics sources (fractions, lifetimes, branching ratios of b hadrons), and from purely experimental or algorithmic effects (efficiency, resolution, flavour tagging, background description). Combining all published measurements listed in Table 15 and accounting for all identified correlations as described in [2] yields $\Delta m_d = 0.508 \pm 0.003 \pm 0.003$ ps^{-1}.

On the other hand, ARGUS and CLEO have published measurements of the time-integrated mixing probability χ_d [102,103,134], which average to $\chi_d = 0.182 \pm 0.015$. Following Ref. [103], the width difference $\Delta\Gamma_d$ could in principle be extracted from the measured value of $\Gamma_d =$

[7] A low-statistics analysis published by CDF using the Run I data [105] has not been included.

[8] Early analyses and (perhaps hence) the PDG use the complex parameter $\epsilon_B = (p-q)/(p+q)$; if *CP* violation in the mixing in small, $\mathcal{A}^d_{\rm SL} \cong 4{\rm Re}(\epsilon_B)/(1+|\epsilon_B|^2)$ and our current averages are ${\rm Re}(\epsilon_B)/(1+|\epsilon_B|^2) = -0.0012 \pm 0.0011$ (B factory measurements only) and -0.0015 ± 0.0008 (all measurements).

Table 14: Measurements of *CP* violation in B^0 mixing and their average in terms of both $\mathcal{A}^d_{\rm SL}$ and $|q/p|_d$. The individual results are listed as quoted in the original publications, or converted[8] to an $\mathcal{A}^d_{\rm SL}$ value. When two errors are quoted, the first one is statistical and the second one systematic. The second group of measurements, performed at high-energy colliders, assume no *CP* violation in B^0_s mixing, *i.e.* $|q/p|_s = 1$.

Exp. & Ref.	Method	Measured $\mathcal{A}^d_{\rm SL}$	Measured $\lvert q/p\rvert_d$
CLEO [103]	partial hadronic rec.	$+0.017 \pm 0.070 \pm 0.014$	
CLEO [104]	dileptons	$+0.013 \pm 0.050 \pm 0.005$	
CLEO [104]	average of above two	$+0.014 \pm 0.041 \pm 0.006$	
BABAR [109]	full hadronic rec.		$1.029 \pm 0.013 \pm 0.011$
BABAR [111]	dileptons		$0.9992 \pm 0.0027 \pm 0.0019$
BABAR [112][p]	part. rec. $D^*\ell\nu$	$-0.0130 \pm 0.0068 \pm 0.0040$	$1.0065 \pm 0.0034 \pm 0.0020$
Belle [113]	dileptons	$-0.0011 \pm 0.0079 \pm 0.0085$	$1.0005 \pm 0.0040 \pm 0.0043$
	Average of 7 above	-0.0047 ± 0.0046 (tot)	1.0024 ± 0.0023 (tot)
OPAL [107]	leptons	$+0.008 \pm 0.028 \pm 0.012$	
OPAL [114]	inclusive (Eq. (49))	$+0.005 \pm 0.055 \pm 0.013$	
ALEPH [108]	leptons	$-0.037 \pm 0.032 \pm 0.007$	
ALEPH [108]	inclusive (Eq. (49))	$+0.016 \pm 0.034 \pm 0.009$	
ALEPH [108]	average of above two	-0.013 ± 0.026 (tot)	
DØ [32]	dimuons	$-0.0092 \pm 0.0044 \pm 0.0032$	
CDF2 [106][p]	dimuons	$+0.0136 \pm 0.0151 \pm 0.0115$	
	Average of 14 above	-0.0058 ± 0.0034 (tot)	1.0030 ± 0.0017 (tot)

[p] Preliminary.

$1/\tau(B^0)$ and the above averages for Δm_d and χ_d (provided that $\Delta\Gamma_d$ has a negligible impact on the Δm_d $\tau(B^0)$ analyses that have assumed $\Delta\Gamma_d = 0$), using the relation

$$\chi_d = \frac{x_d^2 + y_d^2}{2(x_d^2+1)} \quad \text{with} \quad x_d = \frac{\Delta m_d}{\Gamma_d} \quad \text{and} \quad y_d = \frac{\Delta\Gamma_d}{2\Gamma_d}\,. \tag{53}$$

However, direct time-dependent studies provide much stronger constraints: $|\Delta\Gamma_d|/\Gamma_d < 18\%$ at 95% CL from DELPHI [118], and $-6.8\% < \mathrm{sign}(\mathrm{Re}\lambda_{CP})\Delta\Gamma_d/\Gamma_d < 8.4\%$ at 90% CL from *BABAR* [109], where $\lambda_{CP} = (q/p)_d(\overline{A}_{CP}/A_{CP})$ is defined for a *CP*-even final state (the sensitivity to the overall sign of $\mathrm{sign}(\mathrm{Re}\lambda_{CP})\Delta\Gamma_d/\Gamma_d$ comes from the use of B^0 decays to *CP* final states). Combining these two results after adjustment to $1/\Gamma_d = \tau(B^0) = 1.530 \pm 0.008$ ps yields

$$\mathrm{sign}(\mathrm{Re}\lambda_{CP})\Delta\Gamma_d/\Gamma_d = 0.009 \pm 0.037\,. \tag{54}$$

The sign of $\mathrm{Re}\lambda_{CP}$ is not measured, but expected to be positive from the global fits of the Unitarity Triangle within the Standard Model.

Assuming $\Delta\Gamma_d = 0$ and using $1/\Gamma_d = \tau(B^0) = 1.530 \pm 0.008$ ps, the Δm_d and χ_d results are combined through Eq. (53) to yield the world average

$$\Delta m_d = 0.507 \pm 0.004 \text{ ps}^{-1}\,, \tag{55}$$

Table 15: Time-dependent measurements included in the Δm_d average. The results obtained from multi-dimensional fits involving also the B^0 (and B^+) lifetimes as free parameter(s) [69, 71, 72] have been converted into one-dimensional measurements of Δm_d. All the measurements have then been adjusted to a common set of physics parameters before being combined. The CDF results from Run II are preliminary.

Experiment and Ref.	Method rec.	Method tag	Δm_d in ps^{-1} before adjustment	Δm_d in ps^{-1} after adjustment
ALEPH [116]	ℓ	$Q_{\rm jet}$	0.404±0.045±0.027	
ALEPH [116]	ℓ	ℓ	0.452±0.039±0.044	
ALEPH [116]	above two combined		0.422±0.032±0.026	$0.439\pm0.032\ ^{+0.020}_{-0.019}$
ALEPH [116]	D^*	$\ell, Q_{\rm jet}$	0.482±0.044±0.024	0.482±0.044±0.024
DELPHI [117]	ℓ	$Q_{\rm jet}$	0.493±0.042±0.027	0.502±0.042±0.024
DELPHI [117]	$\pi^*\ell$	$Q_{\rm jet}$	0.499±0.053±0.015	0.501±0.053±0.015
DELPHI [117]	ℓ	ℓ	0.480±0.040±0.051	$0.498\pm0.040\ ^{+0.042}_{-0.041}$
DELPHI [117]	D^*	$Q_{\rm jet}$	0.523±0.072±0.043	0.518±0.072±0.043
DELPHI [118]	vtx	comb	0.531±0.025±0.007	0.529±0.025±0.006
L3 [119]	ℓ	ℓ	0.458±0.046±0.032	0.467±0.046±0.028
L3 [119]	ℓ	$Q_{\rm jet}$	0.427±0.044±0.044	0.437±0.044±0.042
L3 [119]	ℓ	ℓ(IP)	0.462±0.063±0.053	$0.474\pm0.063\ ^{+0.045}_{-0.044}$
OPAL [120]	ℓ	ℓ	$0.430\pm0.043\ ^{+0.028}_{-0.030}$	$0.462\pm0.043\ ^{+0.017}_{-0.016}$
OPAL [121]	ℓ	$Q_{\rm jet}$	$0.444\pm0.029\ ^{+0.020}_{-0.017}$	$0.471\pm0.029\ ^{+0.014}_{-0.013}$
OPAL [122]	$D^*\ell$	$Q_{\rm jet}$	0.539±0.060±0.024	0.544±0.060±0.023
OPAL [122]	D^*	ℓ	$0.567\pm0.089\ ^{+0.029}_{-0.023}$	$0.570\pm0.089\ ^{+0.028}_{-0.022}$
OPAL [123]	$\pi^*\ell$	$Q_{\rm jet}$	0.497±0.024±0.025	0.495±0.024±0.025
CDF1 [124]	$D\ell$	SST	$0.471\ ^{+0.078}_{-0.068}\ ^{+0.033}_{-0.034}$	$0.471\ ^{+0.078}_{-0.068}\ ^{+0.033}_{-0.034}$
CDF1 [125]	μ	μ	0.503±0.064±0.071	0.514±0.064±0.070
CDF1 [126]	ℓ	$\ell, Q_{\rm jet}$	0.500±0.052±0.043	0.539±0.052±0.036
CDF1 [127]	$D^*\ell$	ℓ	$0.516\pm0.099\ ^{+0.029}_{-0.035}$	$0.522\pm0.099\ ^{+0.028}_{-0.035}$
CDF2 [128]	$D^{(*)}\ell$	OST	0.509±0.010±0.016	0.509±0.010±0.016
CDF2 [129]	B^0	comb	0.536±0.028±0.006	0.536±0.028±0.006
DØ [130]	$D^{(*)}\mu$	OST	0.506±0.020±0.016	0.506±0.020±0.016
BABAR [131]	B^0	ℓ, K, NN	0.516±0.016±0.010	0.519±0.016±0.008
BABAR [132]	ℓ	ℓ	0.493±0.012±0.009	0.489±0.012±0.006
BABAR [71]	$D^*\ell\nu$(part)	ℓ	0.511±0.007±0.007	0.513±0.007±0.007
BABAR [69]	$D^*\ell\nu$	ℓ, K, NN	0.492±0.018±0.014	0.491±0.018±0.013
Belle [133]	$D^*\pi$(part)	ℓ	0.509±0.017±0.020	0.512±0.017±0.019
Belle [8]	ℓ	ℓ	0.503±0.008±0.010	0.506±0.008±0.009
Belle [72]	$B^0, D^*\ell\nu$	comb	0.511±0.005±0.006	0.511±0.005±0.006
World average (all above measurements included):				0.508±0.003±0.003
– ALEPH, DELPHI, L3, OPAL and CDF1 only:				0.495±0.010±0.009
– Above measurements of *BABAR* and Belle only:				0.508±0.003±0.003

Table 16: Simultaneous measurements of Δm_d and $\tau(B^0)$, and their average. The Belle analysis also measures $\tau(B^+)$ at the same time, but it is converted here into a two-dimensional measurement of Δm_d and $\tau(B^0)$, for an assumed value of $\tau(B^+)$. The first quoted error on the measurements is statistical and the second one systematic; in the case of adjusted measurements, the latter includes a contribution obtained from the variation of $\tau(B^+)$ or $\tau(B^+)/\tau(B^0)$ in the indicated range. Units are ps^{-1} for Δm_d and ps for lifetimes. The three different values of $\rho(\Delta m_d, \tau(B^0))$ correspond to the statistical, systematic and total correlation coefficients between the adjusted measurements of Δm_d and $\tau(B^0)$.

Exp. & Ref.	Measured Δm_d	Measured $\tau(B^0)$	Measured $\tau(B^+)$	Assumed $\tau(B^+)$
BABAR [69]	$0.492\pm0.018\pm0.013$	$1.523\pm0.024\pm0.022$	—	$(1.083 \pm 0.017)\tau(B^0)$
BABAR [71]	$0.511\pm0.007\ ^{+0.007}_{-0.006}$	$1.504\pm0.013\ ^{+0.018}_{-0.013}$	—	1.671 ± 0.018
Belle [72]	$0.511\pm0.005\pm0.006$	$1.534\pm0.008\pm0.010$	$1.635\pm0.011\pm0.011$	—
	Adjusted Δm_d	Adjusted $\tau(B^0)$	$\rho(\Delta m_d, B^0)$	Assumed $\tau(B^+)$
BABAR [69]	$0.492\pm0.018\pm0.013$	$1.524\pm0.025\pm0.022$	$-0.22\ +0.74\ +0.16$	$(1.073\pm0.008)\tau(B^0)$
BABAR [71]	$0.512\pm0.007\pm0.007$	$1.506\pm0.013\pm0.018$	$+0.01\ -0.85\ -0.48$	1.639 ± 0.009
Belle [72]	$0.510\pm0.007\pm0.005$	$1.535\pm0.009\pm0.009$	$-0.27\ -0.08\ -0.19$	1.639 ± 0.009
Average	$0.509\pm0.005\pm0.003$	$1.527\pm0.007\pm0.007$	$-0.19\ -0.29\ -0.23$	1.639 ± 0.009

or, equivalently,

$$x_d = 0.777 \pm 0.008 \quad \text{and} \quad \chi_d = 0.1881 \pm 0.0023\,. \tag{56}$$

Figure 4 compares the Δm_d values obtained by the different experiments.

The B^0 mixing averages given in Eqs. (55) and (56) and the b-hadron fractions of Table 4 have been obtained in a fully consistent way, taking into account the fact that the fractions are computed using the χ_d value of Eq. (56) and that many individual measurements of Δm_d at high energy depend on the assumed values for the b-hadron fractions. Furthermore, this set of averages is consistent with the lifetime averages of Sec. 3.2.

It should be noted that the most recent (and precise) analyses at the asymmetric B factories measure Δm_d as a result of a multi-dimensional fit. Two *BABAR* analyses [69,71], based on fully and partially reconstructed $B^0 \to D^*\ell\nu$ decays respectively, extract simultaneously Δm_d and $\tau(B^0)$ while the latest Belle analysis [72], based on fully reconstructed hadronic B^0 decays and $B^0 \to D^*\ell\nu$ decays, extracts simultaneously Δm_d, $\tau(B^0)$ and $\tau(B^+)$. The measurements of Δm_d and $\tau(B^0)$ of these three analyses are displayed in Table 16 and in Fig. 5. Their two-dimensional average, taking into account all statistical and systematic correlations, and expressed at $\tau(B^+) = 1.639 \pm 0.009$ ps, is

$$\left.\begin{array}{r} \Delta m_d = 0.509 \pm 0.006\ \mathrm{ps}^{-1} \\ \tau(B^0) = 1.527 \pm 0.010\ \mathrm{ps} \end{array}\right\} \text{ with a total correlation of } -0.23. \tag{57}$$

3.3.2 B_s^0 mixing parameters

CP violation parameter $|q/p|_s$

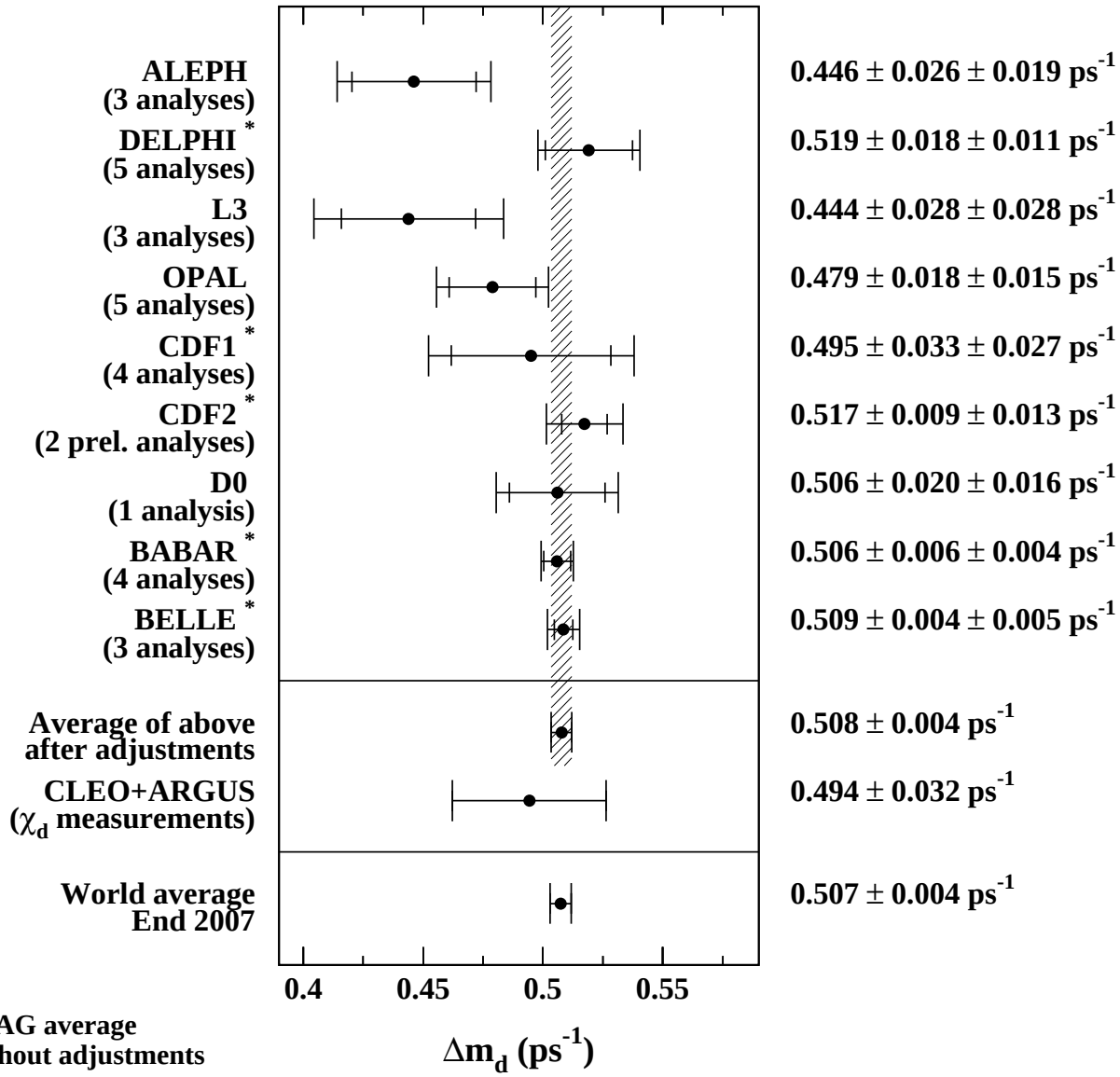

Figure 4: The B^0–$\overline{B}^0$ oscillation frequency Δm_d as measured by the different experiments. The averages quoted for ALEPH, L3 and OPAL are taken from the original publications, while the ones for DELPHI, CDF, *BABAR*, and Belle have been computed from the individual results listed in Table 15 without performing any adjustments. The time-integrated measurements of χ_d from the symmetric B factory experiments ARGUS and CLEO have been converted to a Δm_d value using $\tau(B^0) = 1.530 \pm 0.008$ ps. The two global averages have been obtained after adjustments of all the individual Δm_d results of Table 15 (see text).

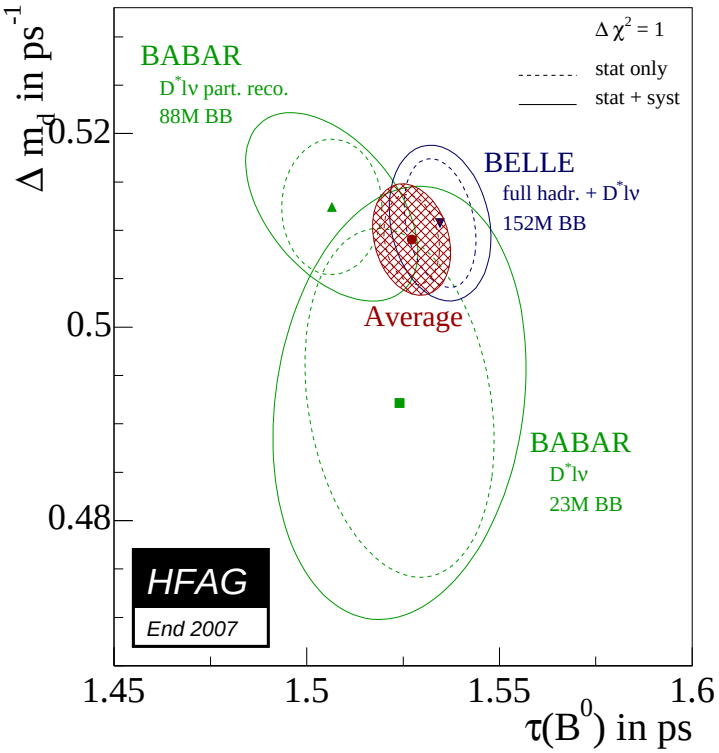

Figure 5: Simultaneous measurements of Δm_d and $\tau(B^0)$ [69, 71, 72], after adjustment to a common set of parameters (see text). Statistical and total uncertainties are represented as dashed and solid contours respectively. The average of the three measurements is indicated by a hatched ellipse.

Constraints on a combination of $|q/p|_d$ and $|q/p|_s$ (or equivalently $\mathcal{A}^d_{\rm SL}$ and $\mathcal{A}^s_{\rm SL}$) have been explicitly quoted by the Tevatron experiments, using inclusive semileptonic decays of b hadrons:

$$\frac{1}{4}\left(f'_d\,\chi_d\mathcal{A}^d_{\rm SL} + f'_s\,\chi_s\mathcal{A}^s_{\rm SL}\right) = +0.0015 \pm 0.0038({\rm stat}) \pm 0.0020({\rm syst}) \qquad \text{CDF1 [105]}\,, \quad (58)$$

$$\frac{f'_d Z_d\mathcal{A}^d_{\rm SL} + f'_s Z_s\mathcal{A}^s_{\rm SL}}{f'_d Z_d + f'_s Z_s} = +0.0080 \pm 0.0090({\rm stat}) \pm 0.0068({\rm syst}) \qquad \text{CDF2 [106]}\,, \quad (59)$$

$$\frac{1}{4}\left(\mathcal{A}^d_{\rm SL} + \mathcal{A}^s_{\rm SL}\frac{f'_s\chi_s}{f'_d\chi_d}\right) = -0.0023 \pm 0.0011({\rm stat}) \pm 0.0008({\rm syst}) \qquad \text{DØ [32]}\,, \quad (60)$$

where[9] $Z_q = 1/(1-y_q^2) - 1/(1+x_q^2) = 2\chi_q/(1-y_q^2)$, $q = d, s$. In addition a first direct determination of $\mathcal{A}^s_{\rm SL}$ and hence $|q/p|_s$ has been obtained by DØ by measuring the charge asymmetry of $B^0_s \to D_s\mu\nu$ decays:

$$\mathcal{A}^s_{\rm SL} = +0.0245 \pm 0.0193({\rm stat}) \pm 0.0035({\rm syst}) \qquad \text{DØ [136]}\,. \quad (61)$$

Given the average $\mathcal{A}^d_{\rm SL} = -0.0047 \pm 0.0046$ of Eq. (50), obtained from results at B factories, as well as other averages presented in this chapter for the quantities appearing in Eqs. (58),

[9] In Ref. [135], the DØ result [32] was reinterpreted by replacing χ_s/χ_d with Z_s/Z_d. For simplicity, and since this has anyway a negligible numerical effect on our combined result of Eq. (62), we follow the same interpretation and set $\chi_q = Z_q/2$ in Eqs. (58) and (60). We also set $f'_q = f_q$.

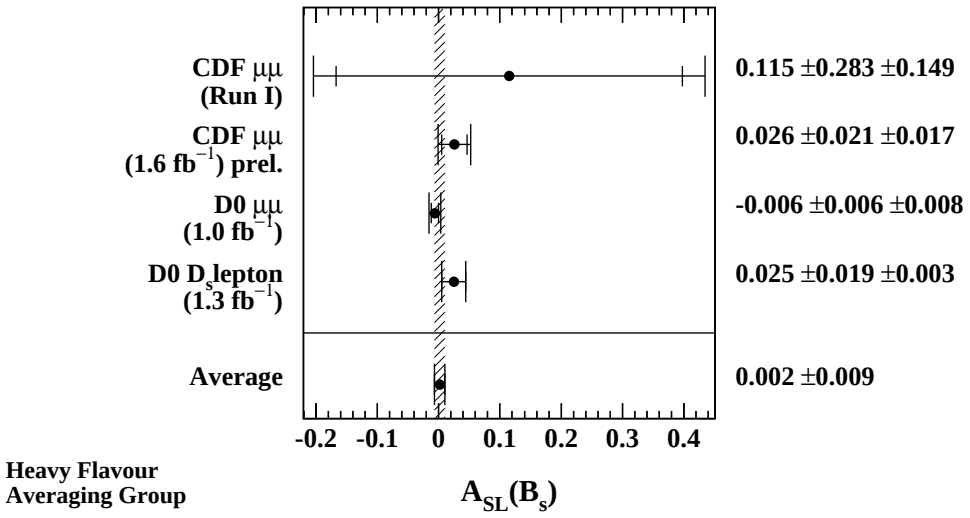

Figure 6: Measurements of $\mathcal{A}^s_{\rm SL}$, derived from CDF [105, 106] and DØ [32, 136] analyses and ajusted to the latest averages of $\mathcal{A}^d_{\rm SL}$, b-hadron fractions and mixing parameters. The combined value of $\mathcal{A}^s_{\rm SL}$ is also shown.

(59), and (60), these four results are turned into measurements of $\mathcal{A}^s_{\rm SL}$ (displayed in Fig. 6) and combined to yield

$$\mathcal{A}^s_{\rm SL} = +0.0016 \pm 0.0054(\text{stat}) \pm 0.0066(\text{syst}) = +0.0016 \pm 0.0085 \tag{62}$$

or, equivalently through Eq. (48),

$$|q/p|_s = 0.9992 \pm 0.0027(\text{stat}) \pm 0.0033(\text{syst}) = 0.9992 \pm 0.0042\,. \tag{63}$$

The quoted systematic errors include experimental systematics as well as the correlated dependence on external parameters. These results are compatible with no CP violation in B^0_s mixing, an assumption made in almost all of the results described below.

Decay width difference $\Delta\Gamma_s$

Definitions and an introduction to $\Delta\Gamma_s$ can also be found in Sec. 3.2.4. Neglecting CP violation, the mass eigenstates are also CP eigenstates, with the short-lived state being CP-even and the long-lived one being CP-odd. Information on $\Delta\Gamma_s$ can be obtained by studying the proper time distribution of untagged data samples enriched in B^0_s mesons [75]. In the case of an inclusive B^0_s selection [54] or a semileptonic B^0_s decay selection [77, 78, 80], both the short- and long-lived components are present, and the proper time distribution is a superposition of two exponentials with decay constants $\Gamma_s \pm \Delta\Gamma_s/2$. In principle, this provides sensitivity to both Γ_s and $(\Delta\Gamma_s/\Gamma_s)^2$. Ignoring $\Delta\Gamma_s$ and fitting for a single exponential leads to an estimate of Γ_s with a relative bias proportional to $(\Delta\Gamma_s/\Gamma_s)^2$. An alternative approach, which is directly sensitive to first order in $\Delta\Gamma_s/\Gamma_s$, is to determine the lifetime of B^0_s candidates decaying to CP eigenstates; measurements exist for $B^0_s \to J/\psi\phi$ [48, 63, 65] and $B^0_s \to D_s^{(*)+} D_s^{(*)-}$, discussed

Table 17: Experimental constraints on $\Delta\Gamma_s/\Gamma_s$ from lifetime analyses, assuming no (or very small SM) *CP* violation. The upper limits, which have been obtained by the working group, are quoted at the 95% CL.

Experiment	Method	$\Delta\Gamma_s/\Gamma_s$	Ref.
L3	lifetime of inclusive b-sample	< 0.67	[54]
DELPHI	$\overline{B}_s \to D_s^+ \ell^- \overline{\nu_\ell} X$, lifetime	< 0.46	[78]
DELPHI	$\overline{B}_s \to D_s^+$ hadron, lifetime	< 0.69	[84]
CDF1	$B_s^0 \to J/\psi\phi$, lifetime	$0.33^{+0.45}_{-0.42}$	[48]
		$\Delta\Gamma_s$	
CDF2	$B_s^0 \to J/\psi\phi$, time-dependent angular analysis	$0.076^{+0.059}_{-0.063} \pm 0.006$ ps^{-1}	[138]
DØ	$B_s^0 \to J/\psi\phi$, time-dependent angular analysis	0.14 ± 0.07 ps^{-1}	[140]

later, which are mostly *CP*-even states [137]. However, more recent time-dependent angular analyses of $B_s^0 \to J/\psi\phi$ allow the simultaneous extraction of $\Delta\Gamma_s$ and the *CP*-even and *CP*-odd amplitudes [138–140]. Flavor tagging the B_s^0 (or $\overline{B}_s^0$) that subsequently decays to $J/\psi\phi$ allows for a more effective extraction of the weak mixing phase as discussed later. The CDF analysis [138] that does not employ flavor tagging under the assumption of no *CP* violation provides a better measurement of $\Delta\Gamma_s$ and is used here, while the CDF analysis [139] that does use flavor tagging is used as an input for determining an average weak mixing phase in the next subsection. The DØ flavor-tagged $B_s^0 \to J/\psi\phi$ analysis [140] gives separate results both assuming the very small SM value of mixing-induced CP violation in the B_s^0 system (effectively zero compared to current experimental resolution), and also allowing for large CP violation.

Measurements quoting $\Delta\Gamma_s$ results from lifetime analyses are listed in Table 17 under the hypothesis of no (or very small SM) *CP* violation. There is significant correlation between $\Delta\Gamma_s$ and $1/\Gamma_s$. In order to combine these measurements, the two-dimensional log-likelihood for each measurement in the $(1/\Gamma_s,\, \Delta\Gamma_s)$ plane is summed and the total normalized with respect to its minimum. The one-sigma contour (corresponding to 0.5 units of log-likelihood greater than the minimum) and 95% contour are found. Inputs as indicated in Table 17 were used in the combination, with the exception of the L3 [54] result since the likelihood in this case was not available.

Results of the combination are shown as the one-sigma contour labeled "Direct" in both plots of Fig. 7. Transformation of variables from $(1/\Gamma_s,\, \Delta\Gamma_s)$ space to other pairs of variables such as $(1/\Gamma_s,\, \Delta\Gamma_s/\Gamma_s)$ and $(\tau_{\rm L} = 1/\Gamma_{\rm L},\, \tau_{\rm H} = 1/\Gamma_{\rm H})$ are also made. The resulting one-sigma contour for the latter is shown in Fig. 7(b).

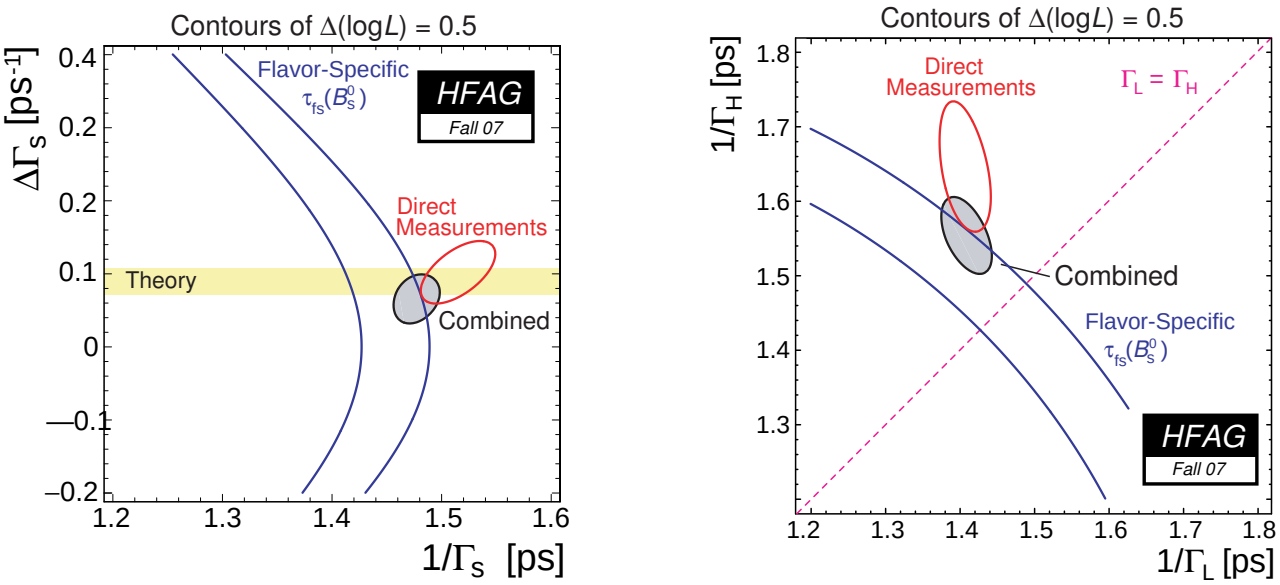

Figure 7: $\Delta\Gamma_s$ combination results with one-sigma contours ($\Delta \log \mathcal{L} = 0.5$) shown for (a) $\Delta\Gamma_s$ versus $\overline{\tau}(B_s^0) = 1/\Gamma_s$ and (b) $\tau_{\rm H} = 1/\Gamma_{\rm H}$ versus $\tau_{\rm L} = 1/\Gamma_{\rm L}$. The red contours labeled "Direct" are the result of the combination of most measurements of Table 17, the blue bands are the one-sigma contours due to the world average of flavor-specific B_s^0 lifetime measurements, and the shaded region the combination constraints described in the text. In (b), the diagonal dashed line indicates $\Gamma_{\rm L} = \Gamma_{\rm H}$, *i.e.*, where $\Delta\Gamma_s = 0$.

Numerical results of the combination of the described inputs of Table 17 are:

$$\Delta\Gamma_s/\Gamma_s \in [+0.024, +0.290] \text{ at } 95\% \text{ CL}\,, \tag{64}$$

$$\Delta\Gamma_s/\Gamma_s = +0.154^{+0.067}_{-0.065}\,, \tag{65}$$

$$\Delta\Gamma_s \in [+0.016, +0.192]\ \text{ps}^{-1} \text{ at } 95\% \text{ CL}\,, \tag{66}$$

$$\Delta\Gamma_s = +0.102^{+0.043}_{-0.043}\ \text{ps}^{-1}\,, \tag{67}$$

$$\overline{\tau}(B_s^0) = 1/\Gamma_s = 1.515^{+0.034}_{-0.034}\ \text{ps}\,, \tag{68}$$

$$1/\Gamma_{\rm L} = \tau_{\rm short} = 1.407^{+0.035}_{-0.034}\ \text{ps}\,, \tag{69}$$

$$1/\Gamma_{\rm H} = \tau_{\rm long} = 1.642^{+0.091}_{+0.083}\ \text{ps}\,. \tag{70}$$

Flavor-specific lifetime measurements are of an equal mix of *CP*-even and *CP*-odd states at time zero, and if a single exponential function is used in the likelihood lifetime fit of such a sample [75],

$$\tau(B_s^0)_{\rm fs} = \frac{1}{\Gamma_s}\frac{1+\left(\frac{\Delta\Gamma_s}{2\Gamma_s}\right)^2}{1-\left(\frac{\Delta\Gamma_s}{2\Gamma_s}\right)^2}\,. \tag{71}$$

Using the world average flavor-specific lifetime[10] of Sec. 3.2.4 the one-sigma blue bands shown in

[10]The world average of all B_s^0 lifetime measurements using flavour-specific final states is 1.456 ± 0.030 ps; however, for the purpose of the $\Delta\Gamma_s$ extraction, we remove from this average one DELPHI analysis [78] that is already included in the set of "direct measurements" and obtain 1.458 ± 0.031 ps, shown as the blue bands on the two plots of Fig. 7.

Table 18: Measurements of $\mathcal{B}(B_s^0 \to D_s^{(*)+} D_s^{(*)-})$.

Experiment	Method	Value	Ref.
Belle	B_s^0-pair production at $\Upsilon(5S)$	< 0.257 at 90% CL	[18][a]
ALEPH	ϕ-ϕ correlations	$0.077 \pm 0.034^{+0.038}_{-0.026}$	[142][b]
DØ	$D_s \to \phi\pi$, $D_s \to \phi\mu\nu$	$0.039^{+0.019+0.016}_{-0.017-0.015}$	[143]
Average		0.046 ± 0.022	

[a] This limit is for $B_s^0 \to D_s^{*+} D_s^{*-}$.
[b] Recalculated using the PDG 2006 value of $\mathcal{B}(D_s \to \phi\pi)$.

Fig. 7 are obtained. Higher-order corrections were checked to be negligible in the combination.

As described earlier, $B_s^0 \to K^+K^-$ decays can be used to measure the lifetime of the "light" mass eigenstate $\tau_L = 1/\Gamma_L = \tau(B_s^0)_{K^+K^-} = 1.53 \pm 0.18 \pm 0.02\,\text{ps}$ [86], and this additional constraint is included in the combination shown in Fig. 7.

When the flavor-specific lifetime measurements and τ_L measurements are combined with the measurements of Table 17, the shaded regions of Fig. 7 are obtained, with numerical results:

$$\Delta\Gamma_s/\Gamma_s \in [-0.003, +0.191] \text{ at } 95\% \text{ CL}\,, \tag{72}$$
$$\Delta\Gamma_s/\Gamma_s = +0.099^{+0.048}_{-0.053}\,, \tag{73}$$
$$\Delta\Gamma_s \in [-0.002, +0.130]\ \text{ps}^{-1} \text{ at } 95\% \text{ CL}\,, \tag{74}$$
$$\Delta\Gamma_s = +0.067^{+0.031}_{-0.035}\ \text{ps}^{-1}\,, \tag{75}$$
$$\overline{\tau}(B_s^0) = 1/\Gamma_s = 1.478^{+0.020}_{-0.022}\ \text{ps}\,, \tag{76}$$
$$1/\Gamma_{\rm L} = \tau_{\rm short} = 1.408^{+0.035}_{-0.033}\ \text{ps}\,, \tag{77}$$
$$1/\Gamma_{\rm H} = \tau_{\rm long} = 1.554^{+0.051}_{+0.053}\ \text{ps}\,. \tag{78}$$

These results can be compared with the theoretical prediction of $\Delta\Gamma_s = 0.096 \pm 0.039\ \text{ps}^{-1}$ (or $\Delta\Gamma_s = 0.088 \pm 0.017\ \text{ps}^{-1}$ if there is no new physics in Δm_s) [74].

Measurements of $\mathcal{B}(B_s^0 \to D_s^{(*)+} D_s^{(*)-})$ can also be sensitive to $\Delta\Gamma_s$. The decay $B_s^0 \to D_s^+ D_s^-$ is into a final state that is purely *CP* even. Under various theoretical assumptions [137], the inclusive decay into this plus the excited states $B_s^0 \to D_s^{(*)+} D_s^{(*)-}$ is also *CP* even to within 5%, and $B_s^0 \to D_s^{(*)+} D_s^{(*)-}$ saturates $\Gamma_s^{CP\,\text{even}}$. Under these assumptions, for no *CP* violation, we have:

$$\Delta\Gamma_s/\Gamma_s \approx \frac{2\mathcal{B}(B_s^0 \to D_s^{(*)+} D_s^{(*)-})}{1 - \mathcal{B}(B_s^0 \to D_s^{(*)+} D_s^{(*)-})}\,. \tag{79}$$

However, there are concerns [141] that the assumptions needed for the above are overly restrictive and that the inclusive branching ratio may be *CP* even to only 30%. Due to this uncertainty, extracted values of $\Delta\Gamma_s/\Gamma_s$ from this branching ratio are not included in the overall combination but are only extracted here to compare with the world average result.

Measurements for the branching fraction for this decay channel are shown in Table 18. Using their average value of 0.046 ± 0.022 with Eq. (79) yields

$$\Delta\Gamma_s/\Gamma_s = +0.096 \pm 0.048\,, \tag{80}$$

consistent with the value given in Eq. (73), but with the above caveat. CDF has also measured the exclusive branching fraction $\mathcal{B}(B_s^0 \to D_s^+ D_s^-) = (9.4^{+4.4}_{-4.2}) \times 10^{-3}$ [144], and they use this to set a lower bound of $\Delta\Gamma_s^{CP}/\Gamma_s \geq 0.012$ at 95% CL (since on its own it does not saturate the CP-even states).

Weak phase in B_s^0 mixing

In general there will be a *CP*-violating weak phase difference:

$$\phi_s = \arg\left[-M_{12}/\Gamma_{12}\right], \tag{81}$$

where M_{12} and Γ_{12} are the off-diagonal elements of the mass and decay matrices of the B_s^0-$\overline{B}_s^0$ system. This is related to the observed $\Delta\Gamma_s$ through the relation:

$$\Delta\Gamma_s = 2|\Gamma_{12}|\cos\phi_s. \tag{82}$$

The SM prediction for this phase is tiny, $\phi_s^{\rm SM} = 0.004$ [145]; however, new physics in B_s^0 mixing could change this observed phase to

$$\phi_s = \phi_s^{\rm SM} + \phi_s^{\rm NP}. \tag{83}$$

The relative phase between the B_s^0 mixing amplitude and that of specific $b \to c\bar{c}s$ quark transitions such as for B_s^0 or $\overline{B}_s^0 \to J/\psi\phi$ in the SM is [145, 146]:

$$2\beta_s^{SM} = 2\arg\left[-\left(V_{ts}V_{tb}^*\right)/\left(V_{cs}V_{cb}^*\right)\right] = 0.037 \pm 0.002 \approx 0.04. \tag{84}$$

This angle is analogous to the β angle in the usual CKM unitarity triangle aside from the negative sign (resulting in a positive angle in the SM). The same additional contribution due to new physics would show up in this observed phase [145], i.e.:

$$2\beta_s = 2\beta_s^{\rm SM} - \phi_s^{\rm NP}. \tag{85}$$

The current experimental precision does not allow these small *CP*-violating phases $\phi_s^{\rm SM}$ and $\beta_s^{\rm SM}$ to be resolved, and for large new physics effect, we can approximate $\phi_s \approx -2\beta_s \approx \phi_s^{\rm NP}$, i.e., a significantly large observed phase would indicate new physics.

For non-zero $|\Gamma_{12}|$, analysis of the time-dependent decay $B_s^0 \to J/\psi\phi$ can measure the weak phase. Including information on the B_s^0 flavor at production time via flavor tagging improves precision and also resolves the sign ambiguity on the weak phase angle for a given $\Delta\Gamma_s$. Both CDF [139] and DØ [140] have performed such analyses and measure the same observed phase that we denote $\phi_s^{J/\psi\phi} = -2\beta_s^{J/\psi\phi}$ to reflect the different conventions of the experiments.

Under the assumption of non-zero $\phi_s^{J/\psi\phi}$, in addition to the result listed in Table 17, the DØ collaboration [140] has also made simultaneous fits allowing $\phi_s^{J/\psi\phi}$ to float while weakly constraining the strong phases, δ_i to find:

$$\Delta\Gamma_s = +0.19 \pm 0.07^{+0.02}_{-0.01}\ {\rm ps}^{-1}, \tag{86}$$

$$\overline{\tau}(B_s^0) = 1/\Gamma_s = 1.52 \pm 0.06\ {\rm ps}, \tag{87}$$

$$\phi_s^{J/\psi\phi} = -0.57^{+0.24+0.07}_{-0.30-0.02}. \tag{88}$$

If the SM value of $\phi_s^{J/\psi\phi} = -0.04$ is assumed, a probability of 6.6% to obtain a value of $\phi_s^{J/\psi\phi}$ lower than -0.57 is found.

The CDF analysis [139] reports confidence regions in the two-dimensional space of $2\beta_s^{J/\psi\phi}$ and $\Delta\Gamma_s$. They present a Feldman-Cousins confidence interval of $2\beta_s^{J/\psi\phi}$ where $\Delta\Gamma_s$ is treated as a nuisance parameter:

$$2\beta_s^{J/\psi\phi} = -\phi_s^{J/\psi\phi} \in [0.32, 2.82] \text{ at } 95\% \text{ CL}. \tag{89}$$

Note that only a confidence range is quoted and a point estimate is not given since biases were observed in the analysis. Assuming the SM predictions for $2\beta_s$ and $\Delta\Gamma_s$, they find that the probability of a deviation as large as the level of the observed data is 15%.

Given the consistency of these two measurements of the weak phase, as well as their deviations from the SM, there is interest in combining the results and using in global fits, e.g., see Ref. [147]. To allow a combination on equal footing, the DØ collaboration has redone their fits [148] allowing strong phase values, δ_i, to float as in the CDF analysis. Ensemble studies to test confidence level coverage were performed by both collaborations and used to adjust likelihood values to correspond to the usual Gaussian confidence levels. Two-dimensional likelihoods were combined with the result shown in Fig. 8(a). After the combination, consistency of the best fit values for $\phi_s^{J/\psi\phi} = -2\beta_s^{J/\psi\phi}$ with SM predictions is at the level of 2.2σ, with numerical results for the two solutions given below. Despite possible biases in the CDF input, point estimates are still presented and the confidence level regions are straight projections onto the $\Delta\Gamma_s$ or phase angle axes.

$$\begin{aligned}
\Delta\Gamma_s &= +0.154^{+0.054}_{-0.070}\ \text{ps}^{-1} \text{ or } -0.154^{+0.070}_{-0.054}\ \text{ps}^{-1}\,, && (90)\\
&\in [+0.036, +0.264] \cup [-0.264, -0.036]\ \text{ps}^{-1} \text{ at } 90\%\ \text{CL}\,, && (91)\\
\phi_s^{J/\psi\phi} = -2\beta_s^{J/\psi\phi} &= -0.77^{+0.29}_{-0.37} \text{ or } -2.36^{+0.37}_{-0.29}\,, && (92)\\
&\in [-1.47, -0.29] \cup [-2.85, -1.65] \text{ at } 90\%\ \text{CL}\,. && (93)
\end{aligned}$$

Further constraints were applied to the above sum of the CDF and DØ likelihoods, i.e., to the flavor-specific B_s^0 lifetime world average of Eq. (35) through Eq. (71) and to the world average B_s^0 semileptonic asymmetry of Eq. (62) through [149]:

$$\mathcal{A}_{\text{SL}}^s = \frac{\Delta\Gamma_s}{\Delta m_s} \tan\phi_s. \tag{94}$$

Confidence level regions following these constraints are shown in Fig. 8(b) including the region delineated by new physics traced by the relation of Eq. (82). Numerical results for the two solutions are:

$$\begin{aligned}
\Delta\Gamma_s &= +0.054^{+0.060}_{-0.033}\ \text{ps}^{-1} \text{ or } -0.054^{+0.033}_{-0.060}\ \text{ps}^{-1}\,, && (95)\\
&\in [-0.148, +0.148]\ \text{ps}^{-1} \text{ at } 90\%\ \text{CL}\,, && (96)\\
\phi_s^{J/\psi\phi} = -2\beta_s^{J/\psi\phi} &= -0.76^{+0.37}_{-0.33} \text{ or } -2.37^{+0.33}_{-0.37}\,, && (97)\\
&\in [-1.26, -0.13] \cup [-3.00, -1.88] \text{ at } 90\%\ \text{CL}\,. && (98)
\end{aligned}$$

with a consistency of the best fit values with SM predictions of $2\beta_s$ at the level of 2.4σ.

Mass difference Δm_s

B_s^0 oscillations have been observed for the first time in 2006 by the CDF collaboration [150], based on samples of flavour-tagged hadronic and semileptonic B_s^0 decays (in flavour-specific

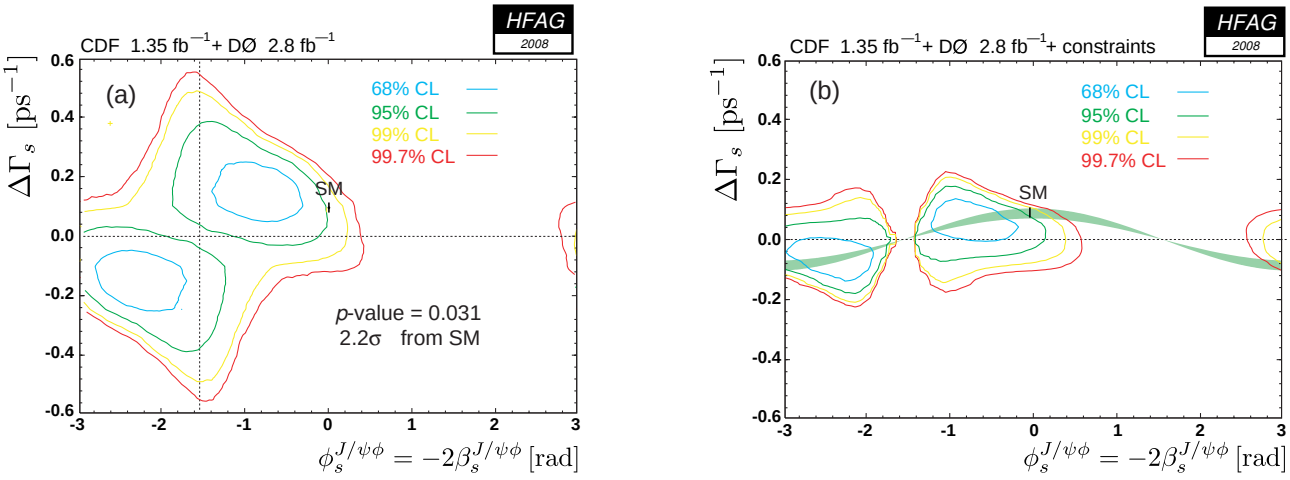

Figure 8: (a) Confidence regions in B_s^0 width difference $\Delta\Gamma_s$ and weak phase angle $\phi_s^{J/\psi\phi} = -2\beta_s^{J/\psi\phi}$ from combined CDF and DØ likelihoods determined in flavor-tagged $B_s^0 \to J/\psi\phi$ time-dependent angular analyses [139, 148] compared to the SM value of $-2\beta_s^{SM}$; (b) after adding constraints from the world average flavor-specific B_s^0 lifetime and B_s^0 semileptonic asymmetry, $\mathcal{A}_{\rm SL}^s$. The region allowed in new physics models given by $\Delta\Gamma_s = 2|\Gamma_{12}|\cos\phi_s$ is also shown (light green band).

final states), partially or fully reconstructed in 1 fb^{-1} of data collected during Tevatron's Run II. From the proper-time dependence of these B_s^0 candidates, CDF observe B_s^0 oscillations with a significance of at least 5σ and measure $\Delta m_s = 17.77 \pm 0.10 \pm 0.07$ ps^{-1} [150]. More recently, the DØ collaboration has obtained with 2.4 fb^{-1} an independent $\sim 3\sigma$ preliminary evidence for B_s^0 oscillations; combining all their results [151] they obtain $\Delta m_s = 18.53 \pm 0.93 \pm 0.30$ ps^{-1} [152]. To a good approximation, both the CDF and DØ results have Gaussian errors, and the world average value of Δm_s can be obtained as a simple weighted average:

$$\Delta m_s = 17.78 \pm 0.12 \text{ ps}^{-1} . \tag{99}$$

Multiplying this result with the mean B_s^0 lifetime of Eq. (76), $1/\Gamma_s = 1.478^{+0.020}_{-0.022}$ ps, yields

$$x_s = \frac{\Delta m_s}{\Gamma_s} = 26.3 \pm 0.4 . \tag{100}$$

With $2y_s = \Delta\Gamma_s/\Gamma_s = +0.099^{+0.048}_{-0.053}$ (see Eq. (73)) and under the assumption of no CP violation in B_s^0 mixing, this corresponds to

$$\chi_s = \frac{x_s^2 + y_s^2}{2(x_s^2+1)} = 0.49928 \pm 0.00002 . \tag{101}$$

The ratio of the B^0 and B_s^0 oscillation frequencies, obtained from Eqs. (55) and (99),

$$\frac{\Delta m_d}{\Delta m_s} = 0.0285 \pm 0.0003 , \tag{102}$$

can be used to extract the following ratio of CKM matrix elements,

$$\left|\frac{V_{td}}{V_{ts}}\right| = \xi \sqrt{\frac{\Delta m_d}{\Delta m_s}\frac{m(B_s^0)}{m(B^0)}} = 0.2061 \pm 0.0011^{+0.0080}_{-0.0060} , \tag{103}$$

where the first quoted error is from experimental uncertainties (with the masses $m(B_s^0)$ and $m(B^0)$ taken from [3]), and where the second quoted error is from theoretical uncertainties in the estimation of the SU(3) flavor-symmetry breaking factor $\xi = 1.210^{+0.047}_{-0.035}$ obtained from lattice QCD calculations [153].

B_s^0 mesons were known to mix since many years. Indeed the time-integrated measurements of $\overline{\chi}$ (see Sec. 3.1.3), when compared to our knowledge of χ_d and the b-hadron fractions, indicated that B_s^0 mixing was large, with a value of χ_s close to its maximal possible value of 1/2. However, the time dependence of this mixing could not be observed until recently, mainly because of lack of proper-time resolution to resolve the small period of the B_s^0 oscillations.

The statistical significance $\mathcal{S}$ of a B_s^0 oscillation signal can be approximated as [154]

$$\mathcal{S} \approx \sqrt{\frac{N}{2}}\, f_{\rm sig}\,(1-2w)\,\exp\left(-\left(\Delta m_s \sigma_t\right)^2/2\right), \tag{104}$$

where N is the number of selected and tagged B_s^0 candidates, $f_{\rm sig}$ is the fraction of B_s^0 signal in the selected and tagged sample, w is the total mistag probability, and σ_t is the resolution on proper time. As can be seen, the quantity $\mathcal{S}$ decreases very quickly as Δm_s increases: this dependence is controlled by σ_t, which is therefore the most critical parameter for Δm_s analyses. The method widely used for B_s^0 oscillation searches consists of measuring a B_s^0 oscillation amplitude $\mathcal{A}$ at several different test values of Δm_s, using a maximum likelihood fit based on the functions of Eq. (47) where the cosine terms have been multiplied by $\mathcal{A}$. One expects $\mathcal{A} = 1$ at the true value of Δm_s and $\mathcal{A} = 0$ at a test value of Δm_s (far) below the true value. To a good approximation, the statistical uncertainty on $\mathcal{A}$ is Gaussian and equal to $1/\mathcal{S}$ [154]. In any analysis, a particular value of Δm_s can be excluded at 95% CL if $\mathcal{A} + 1.645\,\sigma_{\mathcal{A}} < 1$, where $\sigma_{\mathcal{A}}$ is the total uncertainty on $\mathcal{A}$. Because of the proper time resolution, the quantity $\sigma_{\mathcal{A}}(\Delta m_s)$ is an increasing function of Δm_s (see Eq. (104) which merely models $1/\sigma_{\mathcal{A}}(\Delta m_s)$ in an analysis limited by the available statistics). Therefore, if the true value of Δm_s were infinitely large, one expects to be able to exclude all values of Δm_s up to $\Delta m_s^{\rm sens}$, where $\Delta m_s^{\rm sens}$, called here the sensitivity of the analysis, is defined by $1.645\,\sigma_{\mathcal{A}}(\Delta m_s^{\rm sens}) = 1$.

Figure 9 shows the measured B_s^0 amplitude as a function of Δm_s, as obtained by CDF (top) and DØ (middle) using Run II data. The recent DØ evidence of a B_s^0 oscillation signal is consistent with the 2006 observation by CDF. A large number of B_s^0 oscillation searches, already based on the amplitude method, had been performed previously by ALEPH [155], CDF (Run I) [156], DELPHI [78, 84, 118, 157], OPAL [158, 159] and SLD [160–162] (we omit references to searches that have been superseded by more recent ones). All the results published by these experiments (between 1997 and 2004) have been combined by averaging the measured amplitudes $\mathcal{A}$ at each test value of Δm_s. The individual results have been adjusted to common physics inputs, and all known correlations have been accounted for; in the case of the inclusive (lepton) analyses, performed at LEP and SLC, the sensitivities (*i.e.* the statistical uncertainties on $\mathcal{A}$), which depend directly through Eq. (104) on the assumed fraction $f_{\rm sig} \sim f_s$ of B_s^0 mesons in an unbiased sample of weakly-decaying b hadrons, have also been rescaled to the LEP average $f_s = 0.101 \pm 0.009$. The resulting average amplitude spectrum, completely dominated by the $e^+e^- \to Z$ experiments, is displayed as the bottom plot of Fig. 9. Although no significant signal is seen, it is interesting to note the hint in the region 15–20 ps^{-1}, consistent with the recent results from the Tevatron.

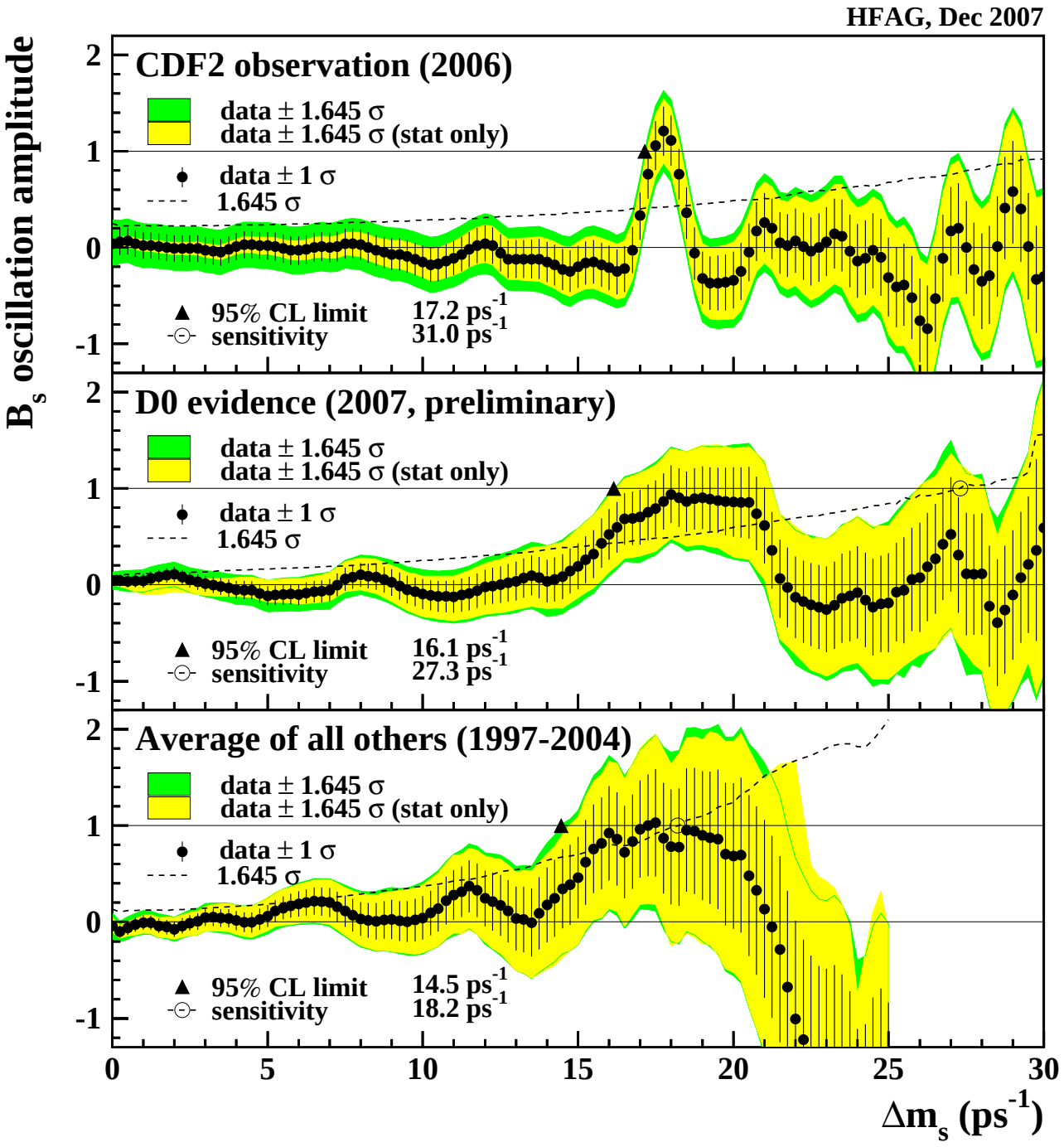

Figure 9: B_s^0 oscillation amplitude as a function of Δm_s. Top: CDF result based on Run II data, published in 2006 [150]. Middle: Average of all preliminary DØ results available at the end of 2007 [151]. Bottom: Average of all ALEPH [155], DELPHI [78, 84, 118, 157], OPAL [158, 159], SLD [160, 161], and CDF Run I [156] results published between 1997 and 2004. Statistical uncertainties dominate. Neighboring points are statistically correlated.

4 Measurements related to Unitarity Triangle angles

The charge of the "$CP(t)$ and Unitarity Triangle angles" group is to provide averages of measurements from time-dependent asymmetry analyses, and other quantities that are related to the angles of the Unitarity Triangle (UT). In cases where considerable theoretical input is required to extract the fundamental quantities, no attempt is made to do so at this stage. However, straightforward interpretations of the averages are given, where possible.

In Sec. 4.1 a brief introduction to the relevant phenomenology is given. In Sec. 4.2 an attempt is made to clarify the various different notations in use. In Sec. 4.3 the common inputs to which experimental results are rescaled in the averaging procedure are listed. We also briefly introduce the treatment of experimental errors. In the remainder of this section, the experimental results and their averages are given, divided into subsections based on the underlying quark-level decays.

4.1 Introduction

The Standard Model Cabibbo-Kobayashi-Maskawa (CKM) quark mixing matrix V must be unitary. A 3×3 unitary matrix has four free parameters,[11] and these are conventionally written by the product of three (complex) rotation matrices [253], where the rotations are characterized by the Euler angles θ_{12}, θ_{13} and θ_{23}, which are the mixing angles between the generations, and one overall phase δ,

$$V = \begin{pmatrix} V_{ud} & V_{us} & V_{ub} \\ V_{cd} & V_{cs} & V_{cb} \\ V_{td} & V_{ts} & V_{tb} \end{pmatrix} = \begin{pmatrix} c_{12}c_{13} & s_{12}c_{13} & s_{13}e^{-i\delta} \\ -s_{12}c_{23} - c_{12}s_{23}s_{13}e^{i\delta} & c_{12}c_{23} - s_{12}s_{23}s_{13}e^{i\delta} & s_{23}c_{13} \\ s_{12}s_{23} - c_{12}c_{23}s_{13}e^{i\delta} & -c_{12}s_{23} - s_{12}c_{23}s_{13}e^{i\delta} & c_{23}c_{13} \end{pmatrix} \quad (105)$$

where $c_{ij} = \cos\theta_{ij}$, $s_{ij} = \sin\theta_{ij}$ for $i < j = 1, 2, 3$.

Following the observation of a hierarchy between the different matrix elements, the Wolfenstein parameterization [254] is an expansion of V in terms of the four real parameters λ (the expansion parameter), A, ρ and η. Defining to all orders in λ [255]

$$\begin{aligned} s_{12} &\equiv \lambda, \\ s_{23} &\equiv A\lambda^2, \\ s_{13}e^{-i\delta} &\equiv A\lambda^3(\rho - i\eta), \end{aligned} \quad (106)$$

and inserting these into the representation of Eq. (105), unitarity of the CKM matrix is achieved to all orders. A Taylor expansion of V leads to the familiar approximation

$$V = \begin{pmatrix} 1 - \lambda^2/2 & \lambda & A\lambda^3(\rho - i\eta) \\ -\lambda & 1 - \lambda^2/2 & A\lambda^2 \\ A\lambda^3(1 - \rho - i\eta) & -A\lambda^2 & 1 \end{pmatrix} + \mathcal{O}\left(\lambda^4\right) . \quad (107)$$

At order λ^5, the obtained CKM matrix in this extended Wolfenstein parametrization is:

$$V = \begin{pmatrix} 1 - \frac{1}{2}\lambda^2 - \frac{1}{8}\lambda^4 & \lambda & A\lambda^3(\rho - i\eta) \\ -\lambda + \frac{1}{2}A^2\lambda^5\left[1 - 2(\rho + i\eta)\right] & 1 - \frac{1}{2}\lambda^2 - \frac{1}{8}\lambda^4(1 + 4A^2) & A\lambda^2 \\ A\lambda^3\left[1 - (1 - \frac{1}{2}\lambda^2)(\rho + i\eta)\right] & -A\lambda^2 + \frac{1}{2}A\lambda^4\left[1 - 2(\rho + i\eta)\right] & 1 - \frac{1}{2}A^2\lambda^4 \end{pmatrix} + \mathcal{O}\left(\lambda^6\right) . \quad (108)$$

[11] In the general case there are nine free parameters, but five of these are absorbed into unobservable quark phases.

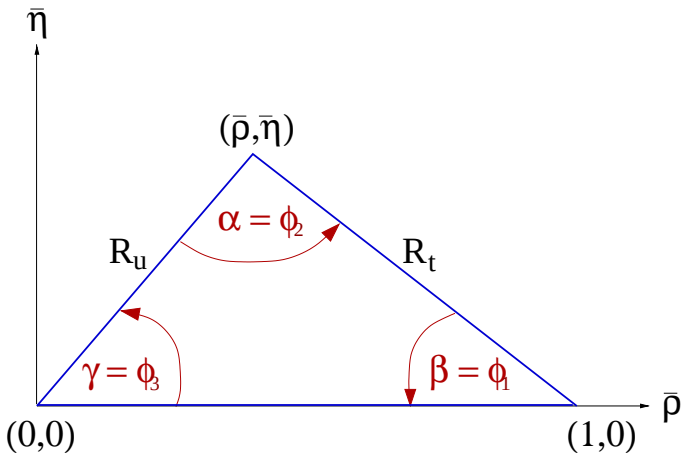

Figure 10: The Unitarity Triangle.

The non-zero imaginary part of the CKM matrix, which is the origin of *CP* violation in the Standard Model, is encapsulated in a non-zero value of η.

The unitarity relation $V^\dagger V = 1$ results in a total of nine expressions, that can be written as $\sum_{i=u,c,t} V_{ij}^* V_{ik} = \delta_{jk}$, where δ_{jk} is the Kronecker symbol. Of the off-diagonal expressions ($j \neq k$), three can be transformed into the other three leaving six relations, in which three complex numbers sum to zero, which therefore can be expressed as triangles in the complex plane. More details about unitarity triangles can be found in [256–258].

One of these relations,

$$V_{ud}V_{ub}^* + V_{cd}V_{cb}^* + V_{td}V_{tb}^* = 0, \tag{109}$$

is of particular importance to the B system, being specifically related to flavour changing neutral current $b \to d$ transitions. The three terms in Eq. (109) are of the same order ($\mathcal{O}(\lambda^3)$), and this relation is commonly known as the Unitarity Triangle. For presentational purposes, it is convenient to rescale the triangle by $(V_{cd}V_{cb}^*)^{-1}$, as shown in Fig. 10.

Two popular naming conventions for the UT angles exist in the literature:

$$\alpha \equiv \phi_2 = \arg\left[-\frac{V_{td}V_{tb}^*}{V_{ud}V_{ub}^*}\right], \quad \beta \equiv \phi_1 = \arg\left[-\frac{V_{cd}V_{cb}^*}{V_{td}V_{tb}^*}\right], \quad \gamma \equiv \phi_3 = \arg\left[-\frac{V_{ud}V_{ub}^*}{V_{cd}V_{cb}^*}\right]. \tag{110}$$

In this document the (α, β, γ) set is used.[12] The sides R_u and R_t of the Unitarity Triangle (the third side being normalized to unity) are given by

$$R_u = \left|\frac{V_{ud}V_{ub}^*}{V_{cd}V_{cb}^*}\right| = \sqrt{\overline{\rho}^2 + \overline{\eta}^2}, \quad R_t = \left|\frac{V_{td}V_{tb}^*}{V_{cd}V_{cb}^*}\right| = \sqrt{(1-\overline{\rho})^2 + \overline{\eta}^2}. \tag{111}$$

where $\overline{\rho}$ and $\overline{\eta}$ define the apex of the Unitarity Triangle [255]

$$\overline{\rho} + i\overline{\eta} \equiv -\frac{V_{ud}V_{ub}^*}{V_{cd}V_{cb}^*} \equiv 1 + \frac{V_{td}V_{tb}^*}{V_{cd}V_{cb}^*} = \frac{\sqrt{1-\lambda^2}\,(\rho + i\eta)}{\sqrt{1 - A^2\lambda^4} + \sqrt{1-\lambda^2}A^2\lambda^4(\rho + i\eta)} \tag{112}$$

[12] The relevant unitarity triangle for the B_s^0 system is obtained by replacing $d \leftrightarrow s$ in Eq. 109. Definitions of the set of angles $(\alpha_s, \beta_s, \gamma_s)$ can be obtained using equivalant relations to those of Eq. 110, for example $\beta_s = \arg\left[-(V_{cs}V_{cb}^*)/(V_{ts}V_{tb}^*)\right]$. This definition gives a value of β_s that is negative in the Standard Model, so that the sign is often flipped in the literature.

The exact relation between (ρ,η) and $(\overline{\rho},\overline{\eta})$ is

$$\rho + i\eta \;=\; \frac{\sqrt{1-A^2\lambda^4}(\overline{\rho}+i\overline{\eta})}{\sqrt{1-\lambda^2}\,[1-A^2\lambda^4(\overline{\rho}+i\overline{\eta})]}\,. \tag{113}$$

By expanding in powers of λ, several useful approximate expressions can be obtained, including

$$\overline{\rho} = \rho(1-\frac{1}{2}\lambda^2)+\mathcal{O}(\lambda^4)\,, \quad \overline{\eta} = \eta(1-\frac{1}{2}\lambda^2)+\mathcal{O}(\lambda^4)\,, \quad V_{td} = A\lambda^3(1-\overline{\rho}-i\overline{\eta})+\mathcal{O}(\lambda^6)\,. \tag{114}$$

4.2 Notations

Several different notations for *CP* violation parameters are commonly used. This section reviews those found in the experimental literature, in the hope of reducing the potential for confusion, and to define the frame that is used for the averages.

In some cases, when B mesons decay into multibody final states via broad resonances (ρ, K^*, *etc.*), the experimental analyses ignore the effects of interference between the overlapping structures. This is referred to as the quasi-two-body (Q2B) approximation in the following.

4.2.1 *CP* asymmetries

The *CP* asymmetry is defined as the difference between the rate involving a b quark and that involving a $\overline{b}$ quark, divided by the sum. For example, the partial rate (or charge) asymmetry for a charged B decay would be given as

$$\mathcal{A}_f \;\equiv\; \frac{\Gamma(B^-\to f)-\Gamma(B^+\to \overline{f})}{\Gamma(B^-\to f)+\Gamma(B^+\to \overline{f})}. \tag{115}$$

4.2.2 Time-dependent *CP* asymmetries in decays to *CP* eigenstates

If the amplitudes for B^0 and $\overline{B}^0$ to decay to a final state f, which is a *CP* eigenstate with eigenvalue η_f, are given by A_f and $\overline{A}_f$, respectively, then the decay distributions for neutral B mesons, with known flavour at time $\Delta t = 0$, are given by

$$\Gamma_{\overline{B}^0\to f}(\Delta t) \;=\; \frac{e^{-|\Delta t|/\tau(B^0)}}{4\tau(B^0)}\left[1+\frac{2\,\mathrm{Im}(\lambda_f)}{1+|\lambda_f|^2}\sin(\Delta m\Delta t)-\frac{1-|\lambda_f|^2}{1+|\lambda_f|^2}\cos(\Delta m\Delta t)\right], \tag{116}$$

$$\Gamma_{B^0\to f}(\Delta t) \;=\; \frac{e^{-|\Delta t|/\tau(B^0)}}{4\tau(B^0)}\left[1-\frac{2\,\mathrm{Im}(\lambda_f)}{1+|\lambda_f|^2}\sin(\Delta m\Delta t)+\frac{1-|\lambda_f|^2}{1+|\lambda_f|^2}\cos(\Delta m\Delta t)\right]. \tag{117}$$

Here $\lambda_f = \frac{q}{p}\frac{\overline{A}_f}{A_f}$ contains terms related to B^0–$\overline{B}^0$ mixing and to the decay amplitude (the eigenstates of the effective Hamiltonian in the $B^0\overline{B}^0$ system are $|B_\pm\rangle = p\,|B^0\rangle \pm q\,|\overline{B}^0\rangle$). This formulation assumes *CPT* invariance, and neglects possible lifetime differences (between the eigenstates of the effective Hamiltonian; see Section 3.3 where the mass difference Δm is also defined) in the neutral B meson system. The case where non-zero lifetime differences are taken into account is discussed in Section 4.2.6. The time-dependent *CP* asymmetry, again defined as

the difference between the rate involving a b quark and that involving a $\overline{b}$ quark, is then given by

$$\mathcal{A}_f\,(\Delta t) \;\equiv\; \frac{\Gamma_{\overline{B}^0\to f}(\Delta t) - \Gamma_{B^0\to f}(\Delta t)}{\Gamma_{\overline{B}^0\to f}(\Delta t) + \Gamma_{B^0\to f}(\Delta t)} \;=\; \frac{2\,\mathrm{Im}(\lambda_f)}{1+|\lambda_f|^2}\sin(\Delta m\Delta t) - \frac{1-|\lambda_f|^2}{1+|\lambda_f|^2}\cos(\Delta m\Delta t). \quad (118)$$

While the coefficient of the $\sin(\Delta m\Delta t)$ term in Eq. (118) is everywhere[13] denoted S_f:

$$S_f \;\equiv\; \frac{2\,\mathrm{Im}(\lambda_f)}{1+|\lambda_f|^2}, \quad (119)$$

different notations are in use for the coefficient of the $\cos(\Delta m\Delta t)$ term:

$$C_f \;\equiv\; -A_f \;\equiv\; \frac{1-|\lambda_f|^2}{1+|\lambda_f|^2}. \quad (120)$$

The C notation is used by the *BABAR* collaboration (see *e.g.* [261]), and also in this document. The A notation is used by the Belle collaboration (see *e.g.* [262]).

Neglecting effects due to *CP* violation in mixing (by taking $|q/p| = 1$), if the decay amplitude contains terms with a single weak (*i.e.*, *CP* violating) phase then $|\lambda_f| = 1$ and one finds $S_f = -\eta_f \sin(\phi_{\rm mix}+\phi_{\rm dec})$, $C_f = 0$, where $\phi_{\rm mix} = \arg(q/p)$ and $\phi_{\rm dec} = \arg(\overline{A}_f/A_f)$. Note that the B^0–$\overline{B}^0$ mixing phase $\phi_{\rm mix} \approx 2\beta$ in the Standard Model (in the usual phase convention) [259,260].

If amplitudes with different weak phases contribute to the decay, no clean interpretation of S_f is possible. If the decay amplitudes have in addition different *CP* conserving strong phases, then $|\lambda_f| \neq 1$ and no clean interpretation is possible. The coefficient of the cosine term becomes non-zero, indicating direct *CP* violation. The sign of A_f as defined above is consistent with that of $\mathcal{A}_f$ in Eq. (115).

Frequently, we are interested in combining measurements governed by similar or identical short-distance physics, but with different final states (*e.g.*, $B^0 \to J/\psi\,K^0_S$ and $B^0 \to J/\psi\,K^0_L$). In this case, we remove the dependence on the *CP* eigenvalue of the final state by quoting $-\eta S_f$. In cases where the final state is not a *CP* eigenstate but has an effective *CP* content (see below), the reported $-\eta S$ is corrected by the effective *CP*.

4.2.3 Time-dependent *CP* asymmetries in decays to vector-vector final states

Consider B decays to states consisting of two spin-1 particles, such as $J/\psi\,K^{*0}(\to K^0_S\pi^0)$, $D^{*+}D^{*-}$ and $\rho^+\rho^-$, which are eigenstates of charge conjugation but not of parity.[14] In fact, for such a system, there are three possible final states; in the helicity basis these can be written h_{-1}, h_0, h_{+1}. The h_0 state is an eigenstate of parity, and hence of *CP*; however, *CP* transforms $h_{+1} \leftrightarrow h_{-1}$ (up to an unobservable phase). In the transversity basis, these states are transformed into $h_\parallel = (h_{+1}+h_{-1})/2$ and $h_\perp = (h_{+1}-h_{-1})/2$. In this basis all three states are *CP* eigenstates, and $h_\perp$ has the opposite *CP* to the others.

The amplitudes to these states are usually given by $A_{0,\perp,\parallel}$ (here we use a normalization such that $|A_0|^2 + |A_\perp|^2 + |A_\parallel|^2 = 1$). Then the effective *CP* of the vector-vector state is known

[13] Occasionally one also finds Eq. (118) written as $\mathcal{A}_f\,(\Delta t) = \mathcal{A}_f^{\rm mix}\sin(\Delta m\Delta t) + \mathcal{A}_f^{\rm dir}\cos(\Delta m\Delta t)$, or similar.

[14] This is not true of all vector-vector final states, *e.g.*, $D^{*\pm}\rho^\mp$ is clearly not an eigenstate of charge conjugation.

if $|A_\perp|^2$ is measured. An alternative strategy is to measure just the longitudinally polarized component, $|A_0|^2$ (sometimes denoted by $f_{\rm long}$), which allows a limit to be set on the effective *CP* since $|A_\perp|^2 \leq |A_\perp|^2 + |A_\parallel|^2 = 1 - |A_0|^2$. The most complete treatment for neutral B decays to vector-vector final states is time-dependent angular analysis (also known as time-dependent transversity analysis). In such an analysis, the interference between the *CP*-even and *CP*-odd states provides additional sensitivity to the weak and strong phases involved.

In most analyses of time-dependent *CP* asymmetries in decays to vector-vector final states carried out to date, an assumption has been made that each helicity (or transversity) amplitude has the same weak phase. This is a good approximation for decays that are dominated by amplitudes with a single weak phase, such $B^0 \to J/\psi K^{*0}$, and is a reasonable approximation in any mode for which only very limited statistics are available. However, for modes that have contributions from amplitudes with different weak phases, the relative size of these contributions can be different for each helicity (or transversity) amplitude, and therefore the time-dependent *CP* asymmetry parameters can also differ. The most generic analysis, suitable for modes with sufficient statistics, would allow for this effect; an intermediate analysis can allow different parameters for the *CP*-even and *CP*-odd components. Such an analysis has been carried out by *BABAR* for the decay $B^0 \to D^{*+}D^{*-}$ [329].

4.2.4 Time-dependent asymmetries: self-conjugate multiparticle final states

Amplitudes for neutral B decays into self-conjugate multiparticle final states such as $\pi^+\pi^-\pi^0$, $K^+K^-K^0_S$, $J/\psi\pi^+\pi^-$ or $D\pi^0$ with $D \to K^0_S\pi^+\pi^-$ may be written in terms of *CP*-even and *CP*-odd amplitudes. As above, the interference between these terms provides additional sensitivity to the weak and strong phases involved in the decay, and the time-dependence depends on both the sine and cosine of the weak phase difference. In order to perform unbinned maximum likelihood fits, and thereby extract as much information as possible from the distributions, it is necessary to select a model for the multiparticle decay, and therefore the results acquire some model dependence (binned, model independent methods are also possible, though are not as statistically powerful). The number of observables depends on the final state (and on the model used); the key feature is that as long as there are regions where both *CP*-even and *CP*-odd amplitudes contribute, the interference terms will be sensitive to the cosine of the weak phase difference. Therefore, these measurements allow distinction between multiple solutions for, *e.g.*, the four values of β from the measurement of $\sin(2\beta)$.

We now consider the various notations which have been used in experimental studies of time-dependent asymmetries in decays to self-conjugate multiparticle final states.

$B^0 \to D^{(*)}h^0$ with $D \to K^0_S\pi^+\pi^-$

The states $D\pi^0$, $D^*\pi^0$, $D\eta$, $D^*\eta$, $D\omega$ are collectively denoted $D^{(*)}h^0$. When the D decay model is fixed, fits to the time-dependent decay distributions can be performed to extract the weak phase difference. However, it is experimentally advantageous to use the sine and cosine of this phase as fit parameters, since these behave as essentially independent parameters, with low correlations and (potentially) rather different uncertainties. A parameter representing direct *CP* violation in the B decay can also be floated. For consistency with other analyses, this could be chosen to be C_f, but could equally well be $|\lambda_f|$, or other possibilities.

Belle performed an analysis of these channels with $\sin(2\phi_1)$ and $\cos(2\phi_1)$ as free parameters [291]. *BABAR* have performed an analysis floating also $|\lambda_f|$ [292] (and, of course, replacing

$\phi_1 \Leftrightarrow \beta$).

$B^0 \to D^{*+}D^{*-}K^0_S$

The hadronic structure of the $B^0 \to D^{*+}D^{*-}K^0_S$ decay is not sufficiently well understood to perform a full time-dependent Dalitz plot analysis. Instead, following Browder *et al.* [277], *BABAR* [278] divide the Dalitz plane in two: $m(D^{*+}K^0_S)^2 > m(D^{*-}K^0_S)^2$ ($\eta_y = +1$) and $m(D^{*+}K^0_S)^2 < m(D^{*-}K^0_S)^2$ ($\eta_y = -1$); and then fit to a decay time distribution with asymmetry given by

$$\mathcal{A}_f\,(\Delta t) = \eta_y \frac{J_c}{J_0}\cos(\Delta m \Delta t) - \left[\frac{2J_{s1}}{J_0}\sin(2\beta) + \eta_y \frac{2J_{s2}}{J_0}\cos(2\beta)\right]\sin(\Delta m \Delta t)\,. \tag{121}$$

A similar analysis has also been carried out by Belle [279]. The measured values are $\frac{J_c}{J_0}$, $\frac{2J_{s1}}{J_0}\sin(2\beta)$ and $\frac{2J_{s2}}{J_0}\cos(2\beta)$, where the parameters J_0, J_c, J_{s1} and J_{s2} are the integrals over the half Dalitz plane $m(D^{*+}K^0_S)^2 < m(D^{*-}K^0_S)^2$ of the functions $|a|^2 + |\overline{a}|^2$, $|a|^2 - |\overline{a}|^2$, $\mathrm{Re}(\overline{a}a^*)$ and $\mathrm{Im}(\overline{a}a^*)$ respectively, where a and $\overline{a}$ are the decay amplitudes of $B^0 \to D^{*+}D^{*-}K^0_S$ and $\overline{B}^0 \to D^{*+}D^{*-}K^0_S$ respectively. The parameter J_{s2} (and hence J_{s2}/J_0) is predicted to be positive; with this assumption is it possible to determine the sign of $\cos(2\beta)$.

$B^0 \to K^+K^-K^0$

Studies of $B^0 \to K^+K^-K^0$ [311] and of the related decay $B^+ \to K^+K^-K^+$ [321,322], show that the decay is dominated by components from the intermediate K^+K^- resonances $\phi(1020)$, $f_0(980)$, a poorly understood scalar structure that peaks near $m(K^+K^-) \sim 1550$ MeV/c^2 and is denoted $X_0(1550)$, as well as a large nonresonant contribution. There is also a contribution from χ_{c0}.

The full time-dependent Dalitz plot analysis allows the complex amplitudes of each contributing term to be determined from data, including *CP* violation effects (*i.e.* allowing the complex amplitude for the B^0 decay to be independent from that for $\overline{B}^0$ decay), although one amplitude must be fixed to give a reference point. There are several choices for parametrization of the complex amplitudes (*e.g.* real and imaginary part, or magnitude and phase). Similarly, there are various approaches to include *CP* violation effects. Note that positive definite parameters such as magnitudes are disfavoured in certain circumstances (they inevitably lead to biases for small values). In order to compare results between analyses, it is useful for each experiment to present results in terms of the parameters that can be measured in a Q2B analysis (such as $\mathcal{A}_f$, S_f, C_f, $\sin(2\beta^{\rm eff})$, $\cos(2\beta^{\rm eff})$, *etc.*)

In the *BABAR* analysis of $B^0 \to K^+K^-K^0$ [311], the complex amplitude for each resonant contribution is written as

$$A_f = c_f(1+b_f)e^{i(\phi_f+\delta_f)}\,, \quad \overline{A}_f = c_f(1-b_f)e^{i(\phi_f-\delta_f)}\,, \tag{122}$$

where b_f and δ_f introduce *CP* violation in the magnitude and phase respectively. [The weak phase in B^0–$\overline{B}^0$ mixing (2β) also appears in the full formula for the time-dependent decay distribution.] The Q2B direct *CP* violation parameter is directly related to b_f

$$\mathcal{A}_f = \frac{-2b_f}{1+b_f^2}\,. \tag{123}$$

BABAR present results for c_f, ϕ_f, $\mathcal{A}_f$ and $\beta^{\rm eff}$ for each resonant contribution, as well as averaged values of $\mathcal{A}_f$ and $\beta^{\rm eff}$ for the entire $K^+K^-K^0$ Dalitz plot.

$B^0 \to \pi^+\pi^- K^0_S$

Studies of $B^0 \to \pi^+\pi^- K^0_S$ [316,323] and of the related decay $B^+ \to \pi^+\pi^- K^+$ [321,324] show that the decay is dominated by components from intermediate resonances in the $K\pi$ ($K^*(892)$, $K^*_0(1430)$) and $\pi\pi$ ($\rho(770)$, $f_0(980)$, $f_2(1270)$) spectra, together with a poorly understood scalar structure that peaks near $m(\pi\pi) \sim 1300$ MeV/c^2 and is denoted $f_X(1300)$ (that could be identified as either the $f_0(1370)$ or $f_0(1500)$), and a large nonresonant component. There is also a contribution from χ_{c0}.

The full time-dependent Dalitz plot analysis allows the complex amplitudes of each contributing term to be determined from data, including *CP* violation effects. In the *BABAR* analysis [316], the magnitude and phase of each component (for both B^0 and $\overline{B}^0$ decays) are measured relative to $B^0 \to f_0(980)K^0_S$. These results are translated into quasi-two-body parameters such as $2\beta^{\rm eff}_f$, S_f, C_f for each *CP* eigenstate f, and direct *CP* asymmetries for each flavour-specific state. Relative phase differences between resonant terms are also extracted.

$B^0 \to \pi^+\pi^-\pi^0$

The $B^0 \to \pi^+\pi^-\pi^0$ decay is dominated by intermediate ρ resonances. Though it is possible, as above, to determine directly the complex amplitudes for each component, an alternative approach, suggested by Quinn and Silva [345], has been used by both *BABAR* [354] and Belle [355, 356]. The amplitudes for B^0 and $\overline{B}^0$ to $\pi^+\pi^-\pi^0$ are written

$$A_{3\pi} = f_+ A_+ + f_- A_- + f_0 A_0 \ , \quad \overline{A}_{3\pi} = f_+ \overline{A}_+ + f_- \overline{A}_- + f_0 \overline{A}_0 \tag{124}$$

respectively. A_+, A_- and A_0 represent the complex decay amplitudes for $B^0 \to \rho^+\pi^-$, $B^0 \to \rho^-\pi^+$ and $B^0 \to \rho^0\pi^0$ while $\overline{A}_+$, $\overline{A}_-$ and $\overline{A}_0$ represent those for $\overline{B}^0 \to \rho^+\pi^-$, $\overline{B}^0 \to \rho^-\pi^+$ and $\overline{B}^0 \to \rho^0\pi^0$ respectively. f_+, f_- and f_0 incorporate kinematical and dynamical factors and depend on the Dalitz plot coordinates. The full time-dependent decay distribution can then be written in terms of 27 free parameters, one for each coefficient of the form factor bilinears, as listed in Table 19. These parameters are often referred to as "the Us and Is", and can be expressed in terms of A_+, A_-, A_0, $\overline{A}_+$, $\overline{A}_-$ and $\overline{A}_0$. If the full set of parameters is determined, together with their correlations, other parameters, such as weak and strong phases, direct *CP* violation parameters, *etc.*, can be subsequently extracted. Note that one of the parameters (typically U^+_+) is often fixed to unity to provide a reference point; this does not affect the analysis.

4.2.5 Time-dependent *CP* asymmetries in decays to non-*CP* eigenstates

Consider a non-*CP* eigenstate f, and its conjugate $\overline{f}$. For neutral B decays to these final states, there are four amplitudes to consider: those for B^0 to decay to f and $\overline{f}$ (A_f and $A_{\overline{f}}$, respectively), and the equivalents for $\overline{B}^0$ ($\overline{A}_f$ and $\overline{A}_{\overline{f}}$). If *CP* is conserved in the decay, then $A_f = \overline{A}_{\overline{f}}$ and $A_{\overline{f}} = \overline{A}_f$.

The time-dependent decay distributions can be written in many different ways. Here, we follow Sec. 4.2.2 and define $\lambda_f = \frac{q}{p}\frac{\overline{A}_f}{A_f}$ and $\lambda_{\overline{f}} = \frac{q}{p}\frac{\overline{A}_{\overline{f}}}{A_{\overline{f}}}$. The time-dependent *CP* asymmetries

Parameter	Description
U_+^+	Coefficient of $\lvert f_+\rvert^2$
U_0^+	Coefficient of $\lvert f_0\rvert^2$
U_-^+	Coefficient of $\lvert f_-\rvert^2$
U_0^-	Coefficient of $\lvert f_0\rvert^2 \cos(\Delta m \Delta t)$
U_-^-	Coefficient of $\lvert f_-\rvert^2 \cos(\Delta m \Delta t)$
U_+^-	Coefficient of $\lvert f_+\rvert^2 \cos(\Delta m \Delta t)$
I_0	Coefficient of $\lvert f_0\rvert^2 \sin(\Delta m \Delta t)$
I_-	Coefficient of $\lvert f_-\rvert^2 \sin(\Delta m \Delta t)$
I_+	Coefficient of $\lvert f_+\rvert^2 \sin(\Delta m \Delta t)$
$U_{+-}^{+,\mathrm{Im}}$	Coefficient of $\mathrm{Im}[f_+ f_-^*]$
$U_{+-}^{+,\mathrm{Re}}$	Coefficient of $\mathrm{Re}[f_+ f_-^*]$
$U_{+-}^{-,\mathrm{Im}}$	Coefficient of $\mathrm{Im}[f_+ f_-^*] \cos(\Delta m \Delta t)$
$U_{+-}^{-,\mathrm{Re}}$	Coefficient of $\mathrm{Re}[f_+ f_-^*] \cos(\Delta m \Delta t)$
I_{+-}^{Im}	Coefficient of $\mathrm{Im}[f_+ f_-^*] \sin(\Delta m \Delta t)$
I_{+-}^{Re}	Coefficient of $\mathrm{Re}[f_+ f_-^*] \sin(\Delta m \Delta t)$
$U_{+0}^{+,\mathrm{Im}}$	Coefficient of $\mathrm{Im}[f_+ f_0^*]$
$U_{+0}^{+,\mathrm{Re}}$	Coefficient of $\mathrm{Re}[f_+ f_0^*]$
$U_{+0}^{-,\mathrm{Im}}$	Coefficient of $\mathrm{Im}[f_+ f_0^*] \cos(\Delta m \Delta t)$
$U_{+0}^{-,\mathrm{Re}}$	Coefficient of $\mathrm{Re}[f_+ f_0^*] \cos(\Delta m \Delta t)$
I_{+0}^{Im}	Coefficient of $\mathrm{Im}[f_+ f_0^*] \sin(\Delta m \Delta t)$
I_{+0}^{Re}	Coefficient of $\mathrm{Re}[f_+ f_0^*] \sin(\Delta m \Delta t)$
$U_{-0}^{+,\mathrm{Im}}$	Coefficient of $\mathrm{Im}[f_- f_0^*]$
$U_{-0}^{+,\mathrm{Re}}$	Coefficient of $\mathrm{Re}[f_- f_0^*]$
$U_{-0}^{-,\mathrm{Im}}$	Coefficient of $\mathrm{Im}[f_- f_0^*] \cos(\Delta m \Delta t)$
$U_{-0}^{-,\mathrm{Re}}$	Coefficient of $\mathrm{Re}[f_- f_0^*] \cos(\Delta m \Delta t)$
I_{-0}^{Im}	Coefficient of $\mathrm{Im}[f_- f_0^*] \sin(\Delta m \Delta t)$
I_{-0}^{Re}	Coefficient of $\mathrm{Re}[f_- f_0^*] \sin(\Delta m \Delta t)$

Table 19: Definitions of the U and I coefficients. Modified from [354].

then follow Eq. (118):

$$\mathcal{A}_f(\Delta t) \equiv \frac{\Gamma_{\overline{B}^0 \to f}(\Delta t) - \Gamma_{B^0 \to f}(\Delta t)}{\Gamma_{\overline{B}^0 \to f}(\Delta t) + \Gamma_{B^0 \to f}(\Delta t)} = S_f \sin(\Delta m \Delta t) - C_f \cos(\Delta m \Delta t), \quad (125)$$

$$\mathcal{A}_{\overline{f}}(\Delta t) \equiv \frac{\Gamma_{\overline{B}^0 \to \overline{f}}(\Delta t) - \Gamma_{B^0 \to \overline{f}}(\Delta t)}{\Gamma_{\overline{B}^0 \to \overline{f}}(\Delta t) + \Gamma_{B^0 \to \overline{f}}(\Delta t)} = S_{\overline{f}} \sin(\Delta m \Delta t) - C_{\overline{f}} \cos(\Delta m \Delta t), \quad (126)$$

with the definitions of the parameters C_f, S_f, $C_{\overline{f}}$ and $S_{\overline{f}}$, following Eqs. (119) and (120).

The time-dependent decay rates are given by

$$\Gamma_{\overline{B}^0\to f}(\Delta t) = \frac{e^{-|\Delta t|/\tau(B^0)}}{8\tau(B^0)}(1+\langle\mathcal{A}_{f\overline{f}}\rangle)\left\{1+S_f\sin(\Delta m\Delta t)-C_f\cos(\Delta m\Delta t)\right\}, \quad (127)$$

$$\Gamma_{B^0\to f}(\Delta t) = \frac{e^{-|\Delta t|/\tau(B^0)}}{8\tau(B^0)}(1+\langle\mathcal{A}_{f\overline{f}}\rangle)\left\{1-S_f\sin(\Delta m\Delta t)+C_f\cos(\Delta m\Delta t)\right\}, \quad (128)$$

$$\Gamma_{\overline{B}^0\to \overline{f}}(\Delta t) = \frac{e^{-|\Delta t|/\tau(B^0)}}{8\tau(B^0)}(1-\langle\mathcal{A}_{f\overline{f}}\rangle)\left\{1+S_{\overline{f}}\sin(\Delta m\Delta t)-C_{\overline{f}}\cos(\Delta m\Delta t)\right\}, \quad (129)$$

$$\Gamma_{B^0\to \overline{f}}(\Delta t) = \frac{e^{-|\Delta t|/\tau(B^0)}}{8\tau(B^0)}(1-\langle\mathcal{A}_{f\overline{f}}\rangle)\left\{1-S_{\overline{f}}\sin(\Delta m\Delta t)+C_{\overline{f}}\cos(\Delta m\Delta t)\right\}, \quad (130)$$

where the time-independent parameter $\langle\mathcal{A}_{f\overline{f}}\rangle$ represents an overall asymmetry in the production of the f and $\overline{f}$ final states,[15]

$$\langle\mathcal{A}_{f\overline{f}}\rangle = \frac{\left(|A_f|^2+\left|\overline{A}_f\right|^2\right)-\left(\left|A_{\overline{f}}\right|^2+\left|\overline{A}_{\overline{f}}\right|^2\right)}{\left(|A_f|^2+\left|\overline{A}_f\right|^2\right)+\left(\left|A_{\overline{f}}\right|^2+\left|\overline{A}_{\overline{f}}\right|^2\right)}. \quad (131)$$

Assuming $|q/p|=1$, the parameters C_f and $C_{\overline{f}}$ can also be written in terms of the decay amplitudes as follows:

$$C_f = \frac{|A_f|^2-\left|\overline{A}_f\right|^2}{|A_f|^2+\left|\overline{A}_f\right|^2} \quad \text{and} \quad C_{\overline{f}} = \frac{\left|A_{\overline{f}}\right|^2-\left|\overline{A}_{\overline{f}}\right|^2}{\left|A_{\overline{f}}\right|^2+\left|\overline{A}_{\overline{f}}\right|^2}, \quad (132)$$

giving asymmetries in the decay amplitudes of B^0 and $\overline{B}^0$ to the final states f and $\overline{f}$ respectively. In this notation, the direct CP invariance conditions are $\langle\mathcal{A}_{f\overline{f}}\rangle = 0$ and $C_f = -C_{\overline{f}}$. Note that C_f and $C_{\overline{f}}$ are typically non-zero; *e.g.*, for a flavour-specific final state, $\overline{A}_f = A_{\overline{f}} = 0$ ($A_f = \overline{A}_{\overline{f}} = 0$), they take the values $C_f = -C_{\overline{f}} = 1$ ($C_f = -C_{\overline{f}} = -1$).

The coefficients of the sine terms contain information about the weak phase. In the case that each decay amplitude contains only a single weak phase (*i.e.*, no direct CP violation), these terms can be written

$$S_f = \frac{-2\,|A_f|\left|\overline{A}_f\right|\sin(\phi_{\rm mix}+\phi_{\rm dec}-\delta_f)}{|A_f|^2+\left|\overline{A}_f\right|^2} \quad \text{and} \quad S_{\overline{f}} = \frac{-2\left|A_{\overline{f}}\right|\left|\overline{A}_{\overline{f}}\right|\sin(\phi_{\rm mix}+\phi_{\rm dec}+\delta_f)}{\left|A_{\overline{f}}\right|^2+\left|\overline{A}_{\overline{f}}\right|^2}, \quad (133)$$

where δ_f is the strong phase difference between the decay amplitudes. If there is no CP violation, the condition $S_f = -S_{\overline{f}}$ holds. If decay amplitudes with different weak and strong phases contribute, no clean interpretation of S_f and $S_{\overline{f}}$ is possible.

Since two of the CP invariance conditions are $C_f = -C_{\overline{f}}$ and $S_f = -S_{\overline{f}}$, there is motivation for a rotation of the parameters:

$$S_{f\overline{f}} = \frac{S_f+S_{\overline{f}}}{2}, \quad \Delta S_{f\overline{f}} = \frac{S_f-S_{\overline{f}}}{2}, \quad C_{f\overline{f}} = \frac{C_f+C_{\overline{f}}}{2}, \quad \Delta C_{f\overline{f}} = \frac{C_f-C_{\overline{f}}}{2}. \quad (134)$$

[15] This parameter is often denoted $\mathcal{A}_f$ (or $\mathcal{A}_{CP}$), but here we avoid this notation to prevent confusion with the time-dependent CP asymmetry.

With these parameters, the *CP* invariance conditions become $S_{f\overline{f}} = 0$ and $C_{f\overline{f}} = 0$. The parameter $\Delta C_{f\overline{f}}$ gives a measure of the "flavour-specificity" of the decay: $\Delta C_{f\overline{f}} = \pm 1$ corresponds to a completely flavour-specific decay, in which no interference between decays with and without mixing can occur, while $\Delta C_{f\overline{f}} = 0$ results in maximum sensitivity to mixing-induced *CP* violation. The parameter $\Delta S_{f\overline{f}}$ is related to the strong phase difference between the decay amplitudes of B^0 to f and to $\overline{f}$. We note that the observables of Eq. (134) exhibit experimental correlations (typically of $\sim 20\%$, depending on the tagging purity, and other effects) between $S_{f\overline{f}}$ and $\Delta S_{f\overline{f}}$, and between $C_{f\overline{f}}$ and $\Delta C_{f\overline{f}}$. On the other hand, the final state specific observables of Eq. (125) tend to have low correlations.

Alternatively, if we recall that the *CP* invariance conditions at the decay amplitude level are $A_f = \overline{A}_{\overline{f}}$ and $A_{\overline{f}} = \overline{A}_f$, we are led to consider the parameters [271]

$$\mathcal{A}_{f\overline{f}} = \frac{\left|\overline{A}_{\overline{f}}\right|^2 - |A_f|^2}{\left|\overline{A}_{\overline{f}}\right|^2 + |A_f|^2} \quad \text{and} \quad \mathcal{A}_{\overline{f}f} = \frac{\left|\overline{A}_f\right|^2 - \left|A_{\overline{f}}\right|^2}{\left|\overline{A}_f\right|^2 + \left|A_{\overline{f}}\right|^2}. \tag{135}$$

These are sometimes considered more physically intuitive parameters since they characterize direct *CP* violation in decays with particular topologies. For example, in the case of $B^0 \to \rho^\pm\pi^\mp$ (choosing $f = \rho^+\pi^-$ and $\overline{f} = \rho^-\pi^+$), $\mathcal{A}_{f\overline{f}}$ (also denoted $\mathcal{A}_{\rho\pi}^{+-}$) parameterizes direct *CP* violation in decays in which the produced ρ meson does not contain the spectator quark, while $\mathcal{A}_{\overline{f}f}$ (also denoted $\mathcal{A}_{\rho\pi}^{-+}$) parameterizes direct *CP* violation in decays in which it does. Note that we have again followed the sign convention that the asymmetry is the difference between the rate involving a b quark and that involving a $\overline{b}$ quark, *cf.* Eq. (115). Of course, these parameters are not independent of the other sets of parameters given above, and can be written

$$\mathcal{A}_{f\overline{f}} = -\frac{\langle\mathcal{A}_{f\overline{f}}\rangle + C_{f\overline{f}} + \langle\mathcal{A}_{f\overline{f}}\rangle\Delta C_{f\overline{f}}}{1 + \Delta C_{f\overline{f}} + \langle\mathcal{A}_{f\overline{f}}\rangle C_{f\overline{f}}} \quad \text{and} \quad \mathcal{A}_{\overline{f}f} = \frac{-\langle\mathcal{A}_{f\overline{f}}\rangle + C_{f\overline{f}} + \langle\mathcal{A}_{f\overline{f}}\rangle\Delta C_{f\overline{f}}}{-1 + \Delta C_{f\overline{f}} + \langle\mathcal{A}_{f\overline{f}}\rangle C_{f\overline{f}}}. \tag{136}$$

They usually exhibit strong correlations.

We now consider the various notations which have been used in experimental studies of time-dependent *CP* asymmetries in decays to non-*CP* eigenstates.

$B^0 \to D^{*\pm}D^\mp$

The above set of parameters ($\langle\mathcal{A}_{f\overline{f}}\rangle$, C_f, S_f, $C_{\overline{f}}$, $S_{\overline{f}}$), has been used by both *BABAR* [327] and Belle [331] in the $D^{*\pm}D^\mp$ system ($f = D^{*+}D^-$, $\overline{f} = D^{*-}D^+$). However, slightly different names for the parameters are used: *BABAR* uses ($\mathcal{A}$, C_{+-}, S_{+-}, C_{-+}, S_{-+}); Belle uses ($\mathcal{A}$, C_+, S_+, C_-, S_-). In this document, we follow the notation used by *BABAR*.

$B^0 \to \rho^\pm\pi^\mp$

In the $\rho^\pm\pi^\mp$ system, the ($\langle\mathcal{A}_{f\overline{f}}\rangle$, $C_{f\overline{f}}$, $S_{f\overline{f}}$, $\Delta C_{f\overline{f}}$, $\Delta S_{f\overline{f}}$) set of parameters has been used originally by *BABAR* [352] and Belle [353], in the Q2B approximation; the exact names[16] used in this case are ($\mathcal{A}_{CP}^{\rho\pi}, C_{\rho\pi}, S_{\rho\pi}, \Delta C_{\rho\pi}, \Delta S_{\rho\pi}$), and these names are also used in this document.

Since $\rho^\pm\pi^\mp$ is reconstructed in the final state $\pi^+\pi^-\pi^0$, the interference between the ρ resonances can provide additional information about the phases (see Sec. 4.2.4). Both *BABAR* [354] and Belle [355, 356] have performed time-dependent Dalitz plot analyses, from which the weak

[16] *BABAR* has used the notations $A_{CP}^{\rho\pi}$ [352] and $\mathcal{A}_{\rho\pi}$ [354] in place of $\mathcal{A}_{CP}^{\rho\pi}$.

phase α is directly extracted. In such an analysis, the measured Q2B parameters are also naturally corrected for interference effects. See Sec. 4.2.4.

$B^0 \to D^{\pm}\pi^{\mp}, D^{*\pm}\pi^{\mp}, D^{\pm}\rho^{\mp}$

Time-dependent *CP* analyses have also been performed for the final states $D^{\pm}\pi^{\mp}$, $D^{*\pm}\pi^{\mp}$ and $D^{\pm}\rho^{\mp}$. In these theoretically clean cases, no penguin contributions are possible, so there is no direct *CP* violation. Furthermore, due to the smallness of the ratio of the magnitudes of the suppressed ($b \to u$) and favoured ($b \to c$) amplitudes (denoted R_f), to a very good approximation, $C_f = -C_{\overline{f}} = 1$ (using $f = D^{(*)-}h^+$, $\overline{f} = D^{(*)+}h^-$ $h = \pi, \rho$), and the coefficients of the sine terms are given by

$$S_f = -2R_f \sin(\phi_{\rm mix} + \phi_{\rm dec} - \delta_f) \quad \text{and} \quad S_{\overline{f}} = -2R_f \sin(\phi_{\rm mix} + \phi_{\rm dec} + \delta_f). \tag{137}$$

Thus weak phase information can be cleanly obtained from measurements of S_f and $S_{\overline{f}}$, although external information on at least one of R_f or δ_f is necessary. (Note that $\phi_{\rm mix} + \phi_{\rm dec} = 2\beta + \gamma$ for all the decay modes in question, while R_f and δ_f depend on the decay mode.)

Again, different notations have been used in the literature. *BABAR* [361, 363] defines the time-dependent probability function by

$$f^{\pm}(\eta, \Delta t) = \frac{e^{-|\Delta t|/\tau}}{4\tau}\left[1 \mp S_\zeta \sin(\Delta m \Delta t) \mp \eta C_\zeta \cos(\Delta m \Delta t)\right], \tag{138}$$

where the upper (lower) sign corresponds to the tagging meson being a B^0 ($\overline{B}^0$). [Note here that a tagging B^0 ($\overline{B}^0$) corresponds to $-S_\zeta$ ($+S_\zeta$).] The parameters η and ζ take the values $+1$ and $+$ (-1 and $-$) when the final state is, *e.g.*, $D^-\pi^+$ ($D^+\pi^-$). However, in the fit, the substitutions $C_\zeta = 1$ and $S_\zeta = a \mp \eta b_i - \eta c_i$ are made.[17] [Note that, neglecting b terms, $S_+ = a - c$ and $S_- = a + c$, so that $a = (S_+ + S_-)/2$, $c = (S_- - S_+)/2$, in analogy to the parameters of Eq. (134).] The subscript i denotes the tagging category. These are motivated by the possibility of *CP* violation on the tag side [366], which is absent for semileptonic B decays (mostly lepton tags). The parameter a is not affected by tag side *CP* violation. The parameter b only depends on tag side *CP* violation parameters and is not directly useful for determining UT angles. A clean interpretation of the c parameter is only possible for lepton-tagged events, so the *BABAR* measurements report c measured with those events only.

The parameters used by Belle in the analysis using partially reconstructed B decays [364], are similar to the S_ζ parameters defined above. However, in the Belle convention, a tagging B^0 corresponds to a $+$ sign in front of the sine coefficient; furthermore the correspondence between the super/subscript and the final state is opposite, so that $S_\pm$ (*BABAR*) $= -S^\mp$ (Belle). In this analysis, only lepton tags are used, so there is no effect from tag side *CP* violation. In the Belle analysis using fully reconstructed B decays [365], this effect is measured and taken into account using $D^* l\nu$ decays; in neither Belle analysis are the a, b and c parameters used. In the latter case, the measured parameters are $2R_{D^{(*)}\pi}\sin(2\phi_1 + \phi_3 \pm \delta_{D^{(*)}\pi})$; the definition is such that $S^\pm$ (Belle) $= -2R_{D^*\pi}\sin(2\phi_1 + \phi_3 \pm \delta_{D^*\pi})$. However, the definition includes an angular momentum factor $(-1)^L$ [367], and so for the results in the $D\pi$ system, there is an additional factor of -1 in the conversion.

Explicitly, the conversion then reads as given in Table 20, where we have neglected the b_i terms used by *BABAR* (which are zero in the absence of tag side *CP* violation). For the averages

[17] The subscript i denotes tagging category.

Table 20: Conversion between the various notations used for *CP* violation parameters in the $D^{\pm}\pi^{\mp}$, $D^{*\pm}\pi^{\mp}$ and $D^{\pm}\rho^{\mp}$ systems. The b_i terms used by *BABAR* have been neglected. Recall that $(\alpha, \beta, \gamma) = (\phi_2, \phi_1, \phi_3)$.

	BABAR	Belle partial rec.	Belle full rec.
$S_{D^+\pi^-}$	$-S_- = -(a + c_i)$	N/A	$2R_{D\pi}\sin(2\phi_1 + \phi_3 + \delta_{D\pi})$
$S_{D^-\pi^+}$	$-S_+ = -(a - c_i)$	N/A	$2R_{D\pi}\sin(2\phi_1 + \phi_3 - \delta_{D\pi})$
$S_{D^{*+}\pi^-}$	$-S_- = -(a + c_i)$	S^+	$-2R_{D^*\pi}\sin(2\phi_1 + \phi_3 + \delta_{D^*\pi})$
$S_{D^{*-}\pi^+}$	$-S_+ = -(a - c_i)$	S^-	$-2R_{D^*\pi}\sin(2\phi_1 + \phi_3 - \delta_{D^*\pi})$
$S_{D^+\rho^-}$	$-S_- = -(a + c_i)$	N/A	N/A
$S_{D^-\rho^+}$	$-S_+ = -(a - c_i)$	N/A	N/A

Table 21: Translations used to convert the parameters measured by Belle to the parameters used for averaging in this document. The angular momentum factor L is -1 for $D^*\pi$ and $+1$ for $D\pi$. Recall that $(\alpha, \beta, \gamma) = (\phi_2, \phi_1, \phi_3)$.

	$D^*\pi$ partial rec.	$D^{(*)}\pi$ full rec.
a	$-(S^+ + S^-)$	$\frac{1}{2}(-1)^{L+1}\left(2R_{D^{(*)}\pi}\sin(2\phi_1 + \phi_3 + \delta_{D^{(*)}\pi}) + 2R_{D^{(*)}\pi}\sin(2\phi_1 + \phi_3 - \delta_{D^{(*)}\pi})\right)$
c	$-(S^+ - S^-)$	$\frac{1}{2}(-1)^{L+1}\left(2R_{D^{(*)}\pi}\sin(2\phi_1 + \phi_3 + \delta_{D^{(*)}\pi}) - 2R_{D^{(*)}\pi}\sin(2\phi_1 + \phi_3 - \delta_{D^{(*)}\pi})\right)$

in this document, we use the a and c parameters, and give the explicit translations used in Table 21. It is to be fervently hoped that the experiments will converge on a common notation in future.

Time-dependent asymmetries in radiative B decays

As a special case of decays to non-*CP* eigenstates, let us consider radiative B decays. Here, the emitted photon has a distinct helicity, which is in principle observable, but in practice is not usually measured. Thus the measured time-dependent decay rates are given by [334, 335]

$$\begin{aligned}\Gamma_{\overline{B}^0\to X\gamma}(\Delta t) &= \Gamma_{\overline{B}^0\to X\gamma_L}(\Delta t) + \Gamma_{\overline{B}^0\to X\gamma_R}(\Delta t) \qquad (139)\\ &= \frac{e^{-|\Delta t|/\tau(B^0)}}{4\tau(B^0)}\left\{1 + (S_L + S_R)\sin(\Delta m\Delta t) - (C_L + C_R)\cos(\Delta m\Delta t)\right\},\\ \Gamma_{B^0\to X\gamma}(\Delta t) &= \Gamma_{B^0\to X\gamma_L}(\Delta t) + \Gamma_{B^0\to X\gamma_R}(\Delta t) \qquad (140)\\ &= \frac{e^{-|\Delta t|/\tau(B^0)}}{4\tau(B^0)}\left\{1 - (S_L + S_R)\sin(\Delta m\Delta t) + (C_L + C_R)\cos(\Delta m\Delta t)\right\},\end{aligned}$$

where in place of the subscripts f and $\overline{f}$ we have used L and R to indicate the photon helicity. In order for interference between decays with and without B^0-$\overline{B}^0$ mixing to occur, the X system must not be flavour-specific, *e.g.*, in case of $B^0 \to K^{*0}\gamma$, the final state must be $K^0_S\pi^0\gamma$. The sign of the sine term depends on the C eigenvalue of the X system. At leading order, the photons from $b \to q\gamma$ ($\overline{b} \to \overline{q}\gamma$) are predominantly left (right) polarized, with corrections of order of m_q/m_b, thus interference effects are suppressed. Higher order effects can lead to corrections of order $\Lambda_{\rm QCD}/m_b$ [336, 337], though explicit calculations indicate such corrections are small for

exclusive final states [338,339]. The predicted smallness of the S terms in the Standard Model results in sensitivity to new physics contributions.

4.2.6 Time-dependent *CP* asymmetries in the B_s System

A complete analysis of the time-dependent decay rates of neutral B mesons must also take into account the lifetime difference between the eigenstates of the effective Hamiltonian, denoted by $\Delta\Gamma$. This is particularly important in the B_s system, since non-negligible values of $\Delta\Gamma_s$ are expected (see Section 3.3 for the latest experimental constraints). Neglecting *CP* violation in mixing, the relevant replacements for Eqs. 116 & 117 are [280]

$$\Gamma_{\overline{B}_s\to f}(\Delta t) = \mathcal{N}\frac{e^{-|\Delta t|/\tau(B_s^0)}}{4\tau(B_s^0)}\Big[\cosh(\tfrac{\Delta\Gamma\Delta t}{2})+ \frac{2\,\mathrm{Im}(\lambda_f)}{1+|\lambda_f|^2}\sin(\Delta m\Delta t) - \frac{1-|\lambda_f|^2}{1+|\lambda_f|^2}\cos(\Delta m\Delta t) - \frac{2\,\mathrm{Re}(\lambda_f)}{1+|\lambda_f|^2}\sinh(\tfrac{\Delta\Gamma\Delta t}{2})\Big], \tag{141}$$

and

$$\Gamma_{B_s^0\to f}(\Delta t) = \mathcal{N}\frac{e^{-|\Delta t|/\tau(B_s^0)}}{4\tau(B_s^0)}\Big[\cosh(\tfrac{\Delta\Gamma\Delta t}{2})- \frac{2\,\mathrm{Im}(\lambda_f)}{1+|\lambda_f|^2}\sin(\Delta m\Delta t) + \frac{1-|\lambda_f|^2}{1+|\lambda_f|^2}\cos(\Delta m\Delta t) - \frac{2\,\mathrm{Re}(\lambda_f)}{1+|\lambda_f|^2}\sinh(\tfrac{\Delta\Gamma\Delta t}{2})\Big]. \tag{142}$$

To be consistent with our earlier notation,[18] we write here the coefficient of the sinh term as

$$A_f^{\Delta\Gamma} = -\frac{2\,\mathrm{Re}(\lambda_f)}{1+|\lambda_f|^2}\,. \tag{143}$$

A complete, tagged, time-dependent analysis of *CP* asymmetries in B_s decays to a *CP* eigenstate f can thus obtain the parameters S_f, C_f and $A_f^{\Delta\Gamma}$. Note that

$$(S_f)^2 + (C_f)^2 + \left(A_f^{\Delta\Gamma}\right)^2 = 1\,. \tag{144}$$

Since these parameters have sensitivity to both $\mathrm{Im}(\lambda_f)$ and $\mathrm{Re}(\lambda_f)$, alternative choices of parametrization, including those directly involving *CP* violating phases (such as β_s), are possible. These can also be adopted for vector-vector final states.

The *untagged* time-dependent decay rate is given by

$$\Gamma_{\overline{B}_s\to f}(\Delta t) + \Gamma_{B_s^0\to f}(\Delta t) = \mathcal{N}\frac{e^{-|\Delta t|/\tau(B_s^0)}}{2\tau(B_s^0)}\Big[\cosh(\frac{\Delta\Gamma\Delta t}{2}) - \frac{2\,\mathrm{Re}(\lambda_f)}{1+|\lambda_f|^2}\sinh(\frac{\Delta\Gamma\Delta t}{2})\Big]\,. \tag{145}$$

With the requirement $\int_{-\infty}^{+\infty}\Gamma_{\overline{B}_s\to f}(\Delta t) + \Gamma_{B_s^0\to f}(\Delta t)d(\Delta t) = 1$, the normalization factor $\mathcal{N}$ is fixed to $1-(\frac{\Delta\Gamma}{2\Gamma})^2$. Note that an untagged time-dependent analysis can probe λ_f, through $\mathrm{Re}(\lambda_f)$, when $\Delta\Gamma \neq 0$. The tagged analysis is, of course, more sensitive.

Other expressions can be similarly modified to take into account non-zero lifetime differences. Note that when the final state contains a mixture of *CP*-even and *CP*-odd states (as, for example, for vector-vector or multibody self-conjugate states), that $\mathrm{Re}(\lambda_f)$ contains terms proportional to both the sine and cosine of the weak phase difference, albeit with rather different sensitivities.

[18] As ever, alternative and conflicting notations appear in the literature. One popular alternative notation for this parameter is $\mathcal{A}_{\Delta\Gamma}$. Particular care must be taken over the signs.

4.2.7 Asymmetries in $B \to D^{(*)}K^{(*)}$ decays

CP asymmetries in $B \to D^{(*)}K^{(*)}$ decays are sensitive to γ. The neutral $D^{(*)}$ meson produced is an admixture of $D^{(*)0}$ (produced by a $b \to c$ transition) and $\overline{D}^{(*)0}$ (produced by a colour-suppressed $b \to u$ transition) states. If the final state is chosen so that both $D^{(*)0}$ and $\overline{D}^{(*)0}$ can contribute, the two amplitudes interfere, and the resulting observables are sensitive to γ, the relative weak phase between the two B decay amplitudes [368]. Various methods have been proposed to exploit this interference, including those where the neutral D meson is reconstructed as a *CP* eigenstate (GLW) [369, 370], in a suppressed final state (ADS) [371, 372], or in a self-conjugate three-body final state, such as $K^0_S\pi^+\pi^-$ (Dalitz) [373, 374]. It should be emphasised that while each method differs in the choice of D decay, they are all sensitive to the same parameters of the B decay, and can be considered as variations of the same technique.

Consider the case of $B^\mp \to DK^\mp$, with D decaying to a final state f, which is accessible to both D^0 and $\overline{D}^0$. We can write the decay rates for B^- and B^+ ($\Gamma_\mp$), the charge averaged rate ($\Gamma = (\Gamma_- + \Gamma_+)/2$) and the charge asymmetry ($\mathcal{A} = (\Gamma_- - \Gamma_+)/(\Gamma_- + \Gamma_+)$, see Eq. (115)) as

$$\Gamma_\mp \propto r_B^2 + r_D^2 + 2r_B r_D \cos(\delta_B + \delta_D \mp \gamma), \tag{146}$$

$$\Gamma \propto r_B^2 + r_D^2 + 2r_B r_D \cos(\delta_B + \delta_D)\cos(\gamma), \tag{147}$$

$$\mathcal{A} = \frac{2r_B r_D \sin(\delta_B + \delta_D)\sin(\gamma)}{r_B^2 + r_D^2 + 2r_B r_D \cos(\delta_B + \delta_D)\cos(\gamma)}, \tag{148}$$

where the ratio of B decay amplitudes[19] is usually defined to be less than one,

$$r_B = \frac{\left|A\left(B^- \to \overline{D}^0 K^-\right)\right|}{\left|A\left(B^- \to D^0 K^-\right)\right|}, \tag{149}$$

and the ratio of D decay amplitudes is correspondingly defined by

$$r_D = \frac{\left|A\left(D^0 \to f\right)\right|}{\left|A\left(\overline{D}^0 \to f\right)\right|}. \tag{150}$$

The strong phase differences between the B and D decay amplitudes are given by δ_B and δ_D, respectively. The values of r_D and δ_D depend on the final state f: for the GLW analysis, $r_D = 1$ and δ_D is trivial (either zero or π), in the Dalitz plot analysis r_D and δ_D vary across the Dalitz plot, and depend on the D decay model used, for the ADS analysis, the values of r_D and δ_D are not trivial.

Note that, for given values of r_B and r_D, the maximum size of $\mathcal{A}$ (at $\sin(\delta_B + \delta_D) = 1$) is $2r_B r_D \sin(\gamma) / (r_B^2 + r_D^2)$. Thus even for D decay modes with small r_D, large asymmetries, and hence sensitivity to γ, may occur for B decay modes with similar values of r_B. For this reason, the ADS analysis of the decay $B^\mp \to D\pi^\mp$ is also of interest.

In the GLW analysis, the measured quantities are the partial rate asymmetry, and the charge averaged rate, which are measured both for *CP*-even and *CP*-odd D decays. For the latter, it is experimentally convenient to measure a double ratio,

$$R_{CP} = \frac{\Gamma\left(B^- \to D_{CP}K^-\right) / \Gamma\left(B^- \to D^0 K^-\right)}{\Gamma\left(B^- \to D_{CP}\pi^-\right) / \Gamma\left(B^- \to D^0 \pi^-\right)} \tag{151}$$

[19] Note that here we use the notation r_B to denote the ratio of B decay amplitudes, whereas in Sec. 4.2.5 we used, *e.g.*, $R_{D\pi}$, for a rather similar quantity. The reason is that here we need to be concerned also with D decay amplitudes, and so it is convenient to use the subscript to denote the decaying particle. Hopefully, using r in place of R will help reduce potential confusion.

that is normalized both to the rate for the favoured $D^0 \to K^-\pi^+$ decay, and to the equivalent quantities for $B^- \to D\pi^-$ decays (charge conjugate modes are implicitly included in Eq. (151)). In this way the constant of proportionality drops out of Eq. (147).

For the ADS analysis, using a suppressed $D \to f$ decay, the measured quantities are again the partial rate asymmetry, and the charge averaged rate. In this case it is sufficient to measure the rate in a single ratio (normalized to the favoured $D \to \overline{f}$ decay) since detection systematics cancel naturally; the observed quantity is then

$$R_{\rm ADS} = \frac{\Gamma\left(B^- \to [f]_D K^-\right)}{\Gamma\left(B^- \to \left[\overline{f}\right]_D K^-\right)}. \tag{152}$$

In the ADS analysis, there are an additional two unknowns (r_D and δ_D) compared to the GLW case. However, the value of r_D can be measured using decays of D mesons of known flavour.

In the Dalitz plot analysis, once a model is assumed for the D decay, which gives the values of r_D and δ_D across the Dalitz plot, it is possible to perform a simultaneous fit to the B^+ and B^- samples and directly extract γ, r_B and δ_B. However, the uncertainties on the phases depend approximately inversely on r_B. Furthermore, r_B is positive definite (and small), and therefore tends to be overestimated, which can lead to an underestimation of the uncertainty. Some statistical treatment is necessary to correct for this bias. An alternative approach is to extract from the data the "Cartesian" variables

$$(x_\pm, y_\pm) = \left({\rm Re}(r_B e^{i(\delta_B \pm \gamma)}), {\rm Im}(r_B e^{i(\delta_B \pm \gamma)})\right) = (r_B \cos(\delta_B \pm \gamma), r_B \sin(\delta_B \pm \gamma)) \,. \tag{153}$$

These are (a) approximately statistically uncorrelated and (b) almost Gaussian. The pairs of variables $(x_\pm, y_\pm)$ can be extracted from independent fits of the $B^\pm$ data samples. Use of these variables makes the combination of results much simpler.

However, if the Dalitz plot is effectively dominated by one CP state, there will be additional sensitivity to γ in the numbers of events in the $B^\pm$ data samples. This can be taken into account in various ways. One possibility is to extract GLW-like variables in addition to the $(x_\pm, y_\pm)$ parameters. An alternative proceeds by defining $z_\pm = x_\pm + iy_\pm$ and $x_0 = -\int {\rm Re}\left[f(s_1,s_2)f^*(s_2,s_1)\right] ds_1 ds_2$, where s_1, s_2 are the coordinates of invariant mass squared that define the Dalitz plot and f is the complex amplitude for D decay as a function of the Dalitz plot coordinates.[20] The fitted parameters $(\rho^\pm, \theta^\pm)$ are then defined by

$$\rho^\pm e^{i\theta^\pm} = z_\pm - x_0 \,. \tag{154}$$

Note that the yields of $B^\pm$ decays are proportional to $1 + (\rho^\pm)^2 - (x_0)^2$. This choice of variables has been used by *BABAR* in the analysis of $B^\mp \to DK^\mp$ with $D \to \pi^+\pi^-\pi^0$ [391]; for this D decay, $x_0 = 0.850$.

The relations between the measured quantities and the underlying parameters are summarized in Table 22. Note carefully that the hadronic factors r_B and δ_B are different, in general, for each B decay mode.

4.3 Common inputs and error treatment

The common inputs used for rescaling are listed in Table 23. The B^0 lifetime ($\tau(B^0)$) and mixing parameter (Δm_d) averages are provided by the HFAG Lifetimes and Oscillations subgroup

[20] The x_0 parameter is closely related to the c_i parameters of the model dependent Dalitz plot analysis [373, 375, 376], and the coherence factor of inclusive ADS-type analyses [377], integrated over the entire Dalitz plot.

Table 22: Summary of relations between measured and physical parameters in GLW, ADS and Dalitz analyses of $B \to D^{(*)}K^{(*)}$.

GLW analysis	
$R_{CP\pm}$	$1 + r_B^2 \pm 2r_B \cos(\delta_B)\cos(\gamma)$
$A_{CP\pm}$	$\pm 2r_B \sin(\delta_B)\sin(\gamma)\,/R_{CP\pm}$
ADS analysis	
$R_{\rm ADS}$	$r_B^2 + r_D^2 + 2r_B r_D \cos(\delta_B+\delta_D)\cos(\gamma)$
$A_{\rm ADS}$	$2r_B r_D \sin(\delta_B+\delta_D)\sin(\gamma)\,/R_{\rm ADS}$
Dalitz analysis ($D \to K^0_S\pi^+\pi^-$)	
$x_\pm$	$r_B \cos(\delta_B \pm \gamma)$
$y_\pm$	$r_B \sin(\delta_B \pm \gamma)$
Dalitz analysis ($D \to \pi^+\pi^-\pi^0$)	
$\rho^\pm$	$\lvert z_\pm - x_0\rvert$
$\theta^\pm$	$\tan^{-1}(\mathrm{Im}(z_\pm)/(\mathrm{Re}(z_\pm) - x_0))$

(Sec. 3). The fraction of the perpendicularly polarized component ($|A_\perp|^2$) in $B \to J/\psi\, K^*(892)$ decays, which determines the *CP* composition, is averaged from results by *BABAR* [263] and Belle [264]. See also HFAG B to Charm Decay Parameters subgroup (Sec. 6).

At present, we only rescale to a common set of input parameters for modes with reasonably small statistical errors ($b \to c\bar{c}s$ transitions). Correlated systematic errors are taken into account in these modes as well. For all other modes, the effect of such a procedure is currently negligible.

Table 23: Common inputs used in calculating the averages.

$\tau(B^0)$ (ps)	1.527 ± 0.008
Δm_d (ps^{-1})	0.508 ± 0.004
$\lvert A_\perp\rvert^2\,(J/\psi\, K^*)$	0.219 ± 0.009

As explained in Sec. 1, we do not apply a rescaling factor on the error of an average that has $\chi^2/\mathrm{dof} > 1$ (unlike the procedure currently used by the PDG [3]). We provide a confidence level of the fit so that one can know the consistency of the measurements included in the average, and attach comments in case some care needs to be taken in the interpretation. Note that, in general, results obtained from data samples with low statistics will exhibit some non-Gaussian behaviour. We average measurements with asymmetric errors using the PDG [3] prescription. In cases where several measurements are correlated (*e.g.* S_f and C_f in measurements of time-dependent *CP* violation in B decays to a particular *CP* eigenstate) we take these into account in the averaging procedure if the uncertainties are sufficiently Gaussian. For measurements where one error is given, it represents the total error, where statistical and systematic uncertainties have been added in quadrature. If two errors are given, the first is statistical and the second systematic. If more than two errors are given, the origin of the additional uncertainty will be explained in the text.

4.4 Time-dependent asymmetries in $b \to c\bar{c}s$ transitions

4.4.1 Time-dependent *CP* asymmetries in $b \to c\bar{c}s$ decays to *CP* eigenstates

In the Standard Model, the time-dependent parameters for $b \to c\bar{c}s$ transitions are predicted to be: $S_{b\to c\bar{c}s} = -\eta \sin(2\beta)$, $C_{b\to c\bar{c}s} = 0$ to very good accuracy. The averages for $-\eta S_{b\to c\bar{c}s}$ and $C_{b\to c\bar{c}s}$ are provided in Table 24. The averages for $-\eta S_{b\to c\bar{c}s}$ are shown in Fig. 11.

Both *BABAR* and Belle have used the $\eta = -1$ modes $J/\psi K^0_S$, $\psi(2S)K^0_S$, $\chi_{c1}K^0_S$ and $\eta_c K^0_S$, as well as $J/\psi K^0_L$, which has $\eta = +1$ and $J/\psi K^{*0}(892)$, which is found to have η close to $+1$ based on the measurement of $|A_\perp|$ (see Sec. 4.3). ALEPH, OPAL and CDF used only the $J/\psi K^0_S$ final state. In the latest result from Belle [266], only $J/\psi K^0_S$ and $J/\psi K^0_L$ are used, while results from $\psi(2S)K^0_S$ have been presented separately [267]. A breakdown of results in each charmonium-kaon final state is given in Table 25.

Table 24: $S_{b\to c\bar{c}s}$ and $C_{b\to c\bar{c}s}$.

Experiment		$N(B\overline{B})$	$-\eta S_{b\to c\bar{c}s}$	$C_{b\to c\bar{c}s}$
BABAR	[265]	384M	$0.714 \pm 0.032 \pm 0.018$	$0.049 \pm 0.022 \pm 0.017$
Belle $J/\psi K^0$	[266]	535M	$0.642 \pm 0.031 \pm 0.017$	$-0.018 \pm 0.021 \pm 0.014$
Belle $\psi(2S)K^0_S$	[267]	657M	$0.718 \pm 0.090 \pm 0.033$	$-0.039 \pm 0.069 \pm 0.049$
B factory average			0.680 ± 0.025	0.012 ± 0.020
Confidence level			0.33	0.10
ALEPH	[268]	–	$0.84\,^{+0.82}_{-1.04} \pm 0.16$	–
OPAL	[269]	–	$3.2\,^{+1.8}_{-2.0} \pm 0.5$	–
CDF	[270]	–	$0.79\,^{+0.41}_{-0.44}$	–
Average			0.681 ± 0.025	0.012 ± 0.020

It should be noted that, while the uncertainty in the average for $-\eta S_{b\to c\bar{c}s}$ is still limited by statistics, that for $C_{b\to c\bar{c}s}$ is close to being dominated by systematics. This occurs due to the possible effect of tag side interference on the $C_{b\to c\bar{c}s}$ measurement, an effect which is correlated between the different experiments. Understanding of this effect may continue to improve in future, allowing the uncertainty to reduce.

From the average for $-\eta S_{b\to c\bar{c}s}$ above, we obtain the following solutions for β (in $[0, \pi]$):

$$\beta = (21.5 \pm 1.0)^\circ \quad \text{or} \quad \beta = (68.5 \pm 1.0)^\circ \tag{155}$$

In radians, these values are $\beta = (0.38 \pm 0.02)$, $\beta = (1.20 \pm 0.02)$.

This result gives a precise constraint on the $(\overline{\rho}, \overline{\eta})$ plane, as shown in Fig. 11. The measurement is in remarkable agreement with other constraints from *CP* conserving quantities, and with *CP* violation in the kaon system, in the form of the parameter ϵ_K. Such comparisons have been performed by various phenomenological groups, such as CKMfitter [271] and UTFit [272].

4.4.2 Time-dependent transversity analysis of $B^0 \to J/\psi K^{*0}$

B meson decays to the vector-vector final state $J/\psi K^{*0}$ are also mediated by the $b \to c\bar{c}s$ transition. When a final state which is not flavour-specific ($K^{*0} \to K^0_S\pi^0$) is used, a time-dependent transversity analysis can be performed allowing sensitivity to both $\sin(2\beta)$ and

Table 25: Breakdown of B factory results on $S_{b\to c\bar{c}s}$ and $C_{b\to c\bar{c}s}$.

Mode		$N(B\overline{B})$	$-\eta S_{b\to c\bar{c}s}$	$C_{b\to c\bar{c}s}$
			BABAR	
$J/\psi K^0_S$	[265]	384M	$0.686 \pm 0.039 \pm 0.015$	$0.051 \pm 0.027 \pm 0.015$
$J/\psi K^0_L$	[265]	384M	$0.735 \pm 0.074 \pm 0.067$	$-0.063 \pm 0.062 \pm 0.030$
$\boldsymbol{J/\psi K^0}$	[265]	384M	$0.697 \pm 0.035 \pm 0.016$	$0.035 \pm 0.025 \pm 0.018$
$\psi(2S)K^0_S$	[265]	384M	$0.947 \pm 0.112 \pm 0.062$	$0.142 \pm 0.079 \pm 0.047$
$\chi_{c1}K^0_S$	[265]	384M	$0.759 \pm 0.170 \pm 0.037$	$0.339 \pm 0.102 \pm 0.104$
$\eta_c K^0_S$	[265]	384M	$0.778 \pm 0.195 \pm 0.093$	$0.053 \pm 0.141 \pm 0.037$
$J/\psi\, K^{*0}(892)$	[265]	384M	$0.477 \pm 0.271 \pm 0.155$	$0.047 \pm 0.083 \pm 0.026$
All	[265]	384M	$0.714 \pm 0.032 \pm 0.018$	$0.049 \pm 0.022 \pm 0.017$
			Belle	
$J/\psi K^0_S$	[266]	535M	$0.643 \pm 0.038_{\rm stat}$	$0.001 \pm 0.028_{\rm stat}$
$J/\psi K^0_L$	[266]	535M	$0.641 \pm 0.057_{\rm stat}$	$-0.045 \pm 0.033_{\rm stat}$
$\boldsymbol{J/\psi K^0}$	[266]	535M	$0.642 \pm 0.031 \pm 0.017$	$-0.018 \pm 0.021 \pm 0.014$
$\psi(2{\rm S})K^0_S$	[267]	657M	$0.718 \pm 0.090 \pm 0.033$	$-0.039 \pm 0.069 \pm 0.049$
All	[267]	–	$0.650 \pm 0.029 \pm 0.015$	–
$\boldsymbol{J/\psi K^0}$ **average**			0.668 ± 0.026	0.002 ± 0.021
$\boldsymbol{\psi(2S)K^0}$ **average**			0.802 ± 0.077	0.032 ± 0.068

$\cos(2\beta)$ [273]. Such analyses have been performed by both B factory experiments. In principle, the strong phases between the transversity amplitudes are not uniquely determined by such an analysis, leading to a discrete ambiguity in the sign of $\cos(2\beta)$. The *BABAR* collaboration resolves this ambiguity using the known variation [274] of the P-wave phase (fast) relative to the S-wave phase (slow) with the invariant mass of the $K\pi$ system in the vicinity of the $K^*(892)$ resonance. The result is in agreement with the prediction from s quark helicity conservation, and corresponds to Solution II defined by Suzuki [275]. We use this phase convention for the averages given in Table 26.

Table 26: Averages from $B^0 \to J/\psi K^{*0}$ transversity analyses.

Experiment		$N(B\overline{B})$	$\sin 2\beta$	$\cos 2\beta$	Correlation
BABAR	[276]	88M	$-0.10 \pm 0.57 \pm 0.14$	$3.32^{+0.76}_{-0.96} \pm 0.27$	-0.37
Belle	[264]	275M	$0.24 \pm 0.31 \pm 0.05$	$0.56 \pm 0.79 \pm 0.11$	0.22
Average			0.16 ± 0.28	1.64 ± 0.62	uncorrelated averages
Confidence level			0.61 (0.5σ)	0.03 (2.2σ)	

At present the results are dominated by large and non-Gaussian statistical errors, and exhibit significant correlations. We perform uncorrelated averages, the interpretation of which has to be done with the greatest care. Nonetheless, it is clear that $\cos(2\beta) > 0$ is preferred by the experimental data in $J/\psi K^*$. [*BABAR* [276] find a confidence level for $\cos(2\beta) > 0$ of 89%.]

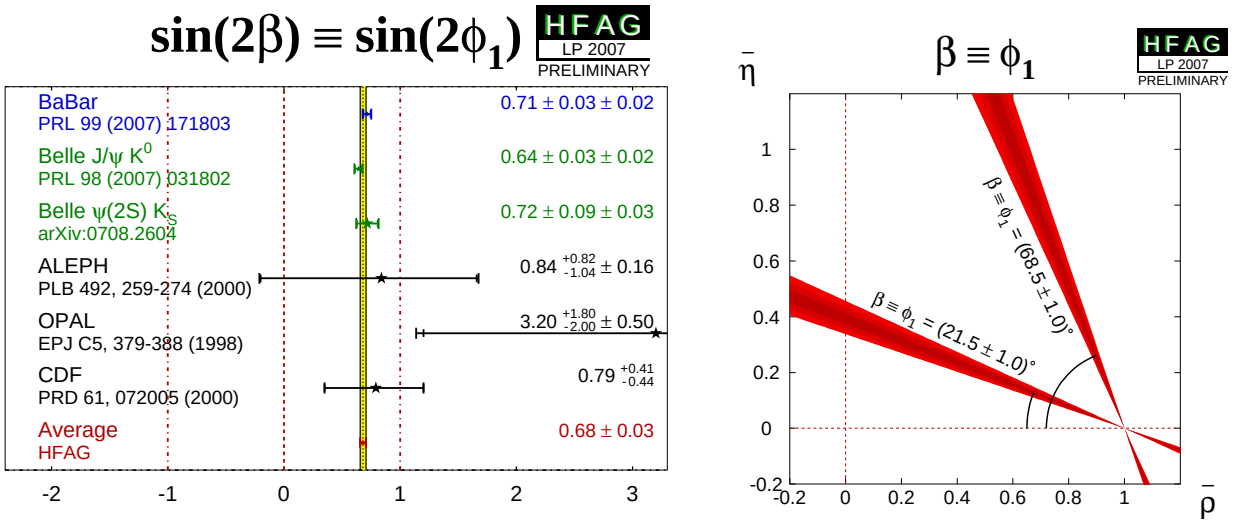

Figure 11: (Left) Average of measurements of $S_{b\to c\bar{c}s}$. (Right) Constraints on the $(\overline{\rho},\overline{\eta})$ plane, obtained from the average of $-\eta S_{b\to c\bar{c}s}$ and Eq. 155.

4.4.3 Time-dependent *CP* asymmetries in $B^0 \to D^{*+}D^{*-}K^0_s$ decays

Both *BABAR* [278] and Belle [279] have performed time-dependent analyses of the $B^0 \to D^{*+}D^{*-}K^0_S$ decay, to obtain information on the sign of $\cos(2\beta)$. More information can be found in Sec. 4.2.4. The results are shown in Table 27, and Fig. 12.

Table 27: Results from time-dependent analysis of $B^0 \to D^{*+}D^{*-}K^0_S$.

Experiment		$N(B\overline{B})$	$\frac{J_c}{J_0}$	$\frac{2J_{s1}}{J_0}\sin(2\beta)$	$\frac{2J_{s2}}{J_0}\cos(2\beta)$
BABAR	[278]	230M	$0.76 \pm 0.18 \pm 0.07$	$0.10 \pm 0.24 \pm 0.06$	$0.38 \pm 0.24 \pm 0.05$
Belle	[279]	449M	$0.60\,^{+0.25}_{-0.28} \pm 0.08$	$-0.17 \pm 0.42 \pm 0.09$	$-0.23\,^{+0.43}_{-0.41} \pm 0.13$
Average			0.71 ± 0.16	0.03 ± 0.21	0.24 ± 0.22
Confidence level			0.63 (0.5σ)	0.59 (0.5σ)	0.23 (1.2σ)

From the above result and the assumption that $J_{s2} > 0$, *BABAR* infer that $\cos(2\beta) > 0$ at the 94% confidence level.

4.4.4 Time-dependent analysis of $B^0_s \to J/\psi\phi$

As described in Sec. 4.2.6, time-dependent analysis of $B^0_s \to J/\psi\phi$ probes the *CP* violating phase of B^0_s–$\overline{B}_s$ oscillations, ϕ_s. Within the Standard Model, this parameter is predicted to be small.[21]

[21] We make the approximation $\phi_s = 2\beta_s$, where $\phi_s \equiv \arg[-M_{12}/\Gamma_{12}]$ and $2\beta_s \equiv 2\arg[-(V_{ts}V^*_{tb})/(V_{cs}V^*_{cb})]$ (see Section 4.1). This is a reasonable approximation since, although the equality does not hold in the Standard Model [281], both are much smaller than the current experimental resolution, whereas new physics contributions add a phase $\phi_{\rm NP}$ to ϕ_s and subtract the same phase from $2\beta_s$, so that the approximation remains valid.

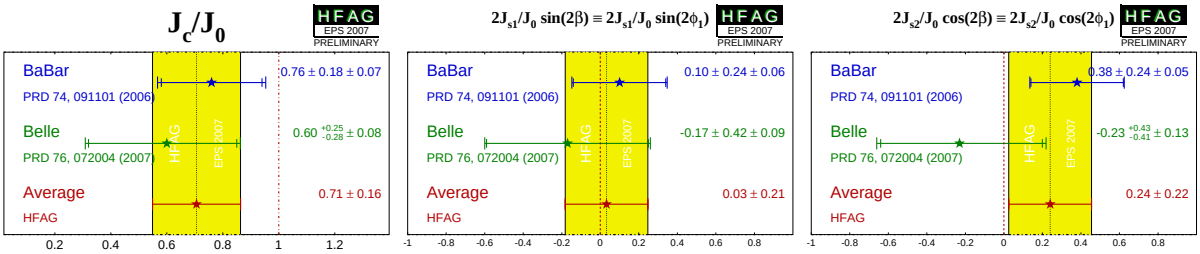

Figure 12: Averages of (left) (J_c/J_0), (middle) $(2J_{s1}/J_0)\sin(2\beta)$ and (right) $(2J_{s2}/J_0)\cos(2\beta)$ from time-dependent analyses of $B^0 \to D^{*+}D^{*-}K^0_S$ decays.

Both CDF [282] and DØ [283] have performed full tagged, time-dependent angular analyses of $B^0_s \to J/\psi\phi$ decays, superceding their previous untagged results [284, 285].

Both experiments perform analyses that take into account the correlations between the average B^0_s lifetime $\tau(B^0_s)$, $\Delta\Gamma_s$, ϕ_s, the magnitude of the perpendicularly polarized component $A_\perp$, the difference in the fractions of the two CP-even components $|A_0|^2 - |A|^2_\parallel$, and the strong phases associated with the two CP-even components δ_0 and $\delta_\parallel$. The CDF analysis [282] uses 1.35 fb^1 of data. The likelihood function is found to have a highly non-Gaussian shape, so that central values and uncertainties are not presented. The DØ analysis [283] uses 2.8 fb^1 of data, and constrains the strong phase differences to take equivalent values to those measured in $B^0 \to J/\psi K^*$ [263], up to an uncertainty of $\pi/5$ that allows for SU(3) breaking effects.

The results are given in Table 28 below. See also HFAG Lifetimes and Oscillations, Sec. 3.

Table 28: Results from time-dependent analysis of $B^0_s \to J/\psi\phi$.

Experiment	$\tau(B^0_s)$	$\Delta\Gamma$	ϕ_s	$A_\perp$	$\lvert A_0\rvert^2 - \lvert A\rvert^2_\parallel$
DØ [283]	$1.52 \pm 0.06 \pm 0.01$	$0.19 \pm 0.07\,^{+0.02}_{-0.01}$	$-0.57\,^{+0.24\ +0.07}_{-0.30\ -0.02}$	$0.41 \pm 0.04\,^{+0.01}_{-0.02}$	$0.34 \pm 0.05 \pm 0.03$

Note the implicit convention above is that $|A_\perp|^2 + |A_0|^2 + |A_\parallel|^2 = 1$, and the strong phases are measured relative to that of the $A_\perp$ component (which is set to zero). The polarization components are defined at time $t = 0$, *i.e.* at the production (primary) vertex of the B^0_s. Note also that there is an ambiguity in the result for ϕ_s.

Constraints on ϕ_s

- CDF [282] present a confidence region in the ϕ_s–$\Delta\Gamma_s$ plane, from which they obtain $\phi_s \in [-2.82, -0.32]$ at the 68% confidence level. The consistency with the Standard Model expectation for $(\phi_s, \Delta\Gamma_s)$ is 15%.
- DØ [283] obtain a 90% CL allowed interval $\phi_s \in [-1.20, +0.06]$.
- The UTFit group have performed a preliminary average of the above two results.

For more details, see the HFAG Lifetimes and Oscillations group, Sec. 3.

4.5 Time-dependent *CP* asymmetries in colour-suppressed $b \to c\overline{u}d$ transitions

Decays of B mesons to final states such as $D\pi^0$ are governed by $b \to c\overline{u}d$ transitions. If the final state is a *CP* eigenstate, *e.g.* $D_{CP}\pi^0$, the usual time-dependence formulae are recovered, with the sine coefficient sensitive to $\sin(2\beta)$. Since there is no penguin contribution to these decays, there is even less associated theoretical uncertainty than for $b \to c\overline{c}s$ decays like $B \to J/\psi\, K^0_S$. Such measurements therefore allow to test the Standard Model prediction that the *CP* violation parameters in $b \to c\overline{u}d$ transitions are the same as those in $b \to c\overline{c}s$ [286].

Note that there is an additional contribution from CKM suppressed $b \to u\overline{c}d$ decays. The effect of this contribution is small, and can be taken into account in the analysis [287, 288].

Results of such an analysis are available from *BABAR* [289]. The decays $B^0 \to D\pi^0$, $B^0 \to D\eta$, $B^0 \to D\omega$, $B^0 \to D^*\pi^0$ and $B^0 \to D^*\eta$ are used. The daughter decay $D^* \to D\pi^0$ is used. The *CP*-even D decay to K^+K^- is used for all decay modes, with the *CP*-odd D decay to $K^0_S\omega$ also used in $B^0 \to D^{(*)}\pi^0$ and the additional *CP*-odd D decay to $K^0_S\pi^0$ also used in $B^0 \to D\omega$. Results are presented separately for *CP*-even and *CP*-odd $D^{(*)}$ decays (denoted $D^{(*)}_+h^0$ and $D^{(*)}_-h^0$ respectively), and for both combined, with the different *CP* factors accounted for (denoted $D^{(*)}_{CP}h^0$). The results are summarized in Table 29.

Table 29: Results from analyses of $B^0 \to D^{(*)}h^0$, $D \to CP$ eigenstates decays.

Experiment		$N(B\overline{B})$	S_{CP}	C_{CP}	Correlation
			$D^{(*)}_+h^0$		
BABAR	[289]	383M	$-0.65 \pm 0.26 \pm 0.06$	$-0.33 \pm 0.19 \pm 0.04$	0.04
			$D^{(*)}_-h^0$		
BABAR	[289]	383M	$-0.46 \pm 0.46 \pm 0.13$	$-0.03 \pm 0.28 \pm 0.07$	-0.14
			$D^{(*)}_{CP}h^0$		
BABAR	[289]	383M	$-0.56 \pm 0.23 \pm 0.05$	$-0.23 \pm 0.16 \pm 0.04$	-0.02

When multibody D decays, such as $D \to K^0_S\pi^+\pi^-$ are used, a time-dependent analysis of the Dalitz plot of the neutral D decay allows a direct determination of the weak phase: 2β. (Equivalently, both $\sin(2\beta)$ and $\cos(2\beta)$ can be measured.) This information allows to resolve the ambiguity in the measurement of 2β from $\sin(2\beta)$ [290].

Results of such analyses are available from both Belle [291] and *BABAR* [292]. The decays $B \to D\pi^0$, $B \to D\eta$, $B \to D\omega$, $B \to D^*\pi^0$ and $B \to D^*\eta$ are used. [This collection of states is denoted by $D^{(*)}h^0$.] The daughter decays are $D^* \to D\pi^0$ and $D \to K^0_S\pi^+\pi^-$. The results are shown in Table 30, and Fig. 13. Note that *BABAR* quote uncertainties due to the D decay model separately from other systematic errors, while Belle do not.

Again, it is clear that the data prefer $\cos(2\beta) > 0$. Indeed, Belle [291] determine the sign of $\cos(2\phi_1)$ to be positive at 98.3% confidence level, while *BABAR* [292] favour the solution of β with $\cos(2\beta) > 0$ at 87% confidence level. Note, however, that the Belle measurement has strongly non-Gaussian behaviour. Therefore, we perform uncorrelated averages, from which any interpretation has to be done with the greatest care.

Table 30: Averages from $B^0 \to D^{(*)}h^0$, $D \to K_S\pi^+\pi^-$ analyses.

Experiment	$N(B\overline{B})$	$\sin 2\beta$	$\cos 2\beta$	$\lvert\lambda\rvert$
BABAR [292]	383M	$0.29 \pm 0.34 \pm 0.03 \pm 0.05$	$0.42 \pm 0.49 \pm 0.09 \pm 0.13$	$1.01 \pm 0.08 \pm 0.02$
Belle [291]	386M	$0.78 \pm 0.44 \pm 0.22$	$1.87\ ^{+0.40\ +0.22}_{-0.53\ -0.32}$	–
Average		0.45 ± 0.28	1.01 ± 0.40	1.01 ± 0.08
Confidence level		0.59 (0.5σ)	0.12 (1.6σ)	–

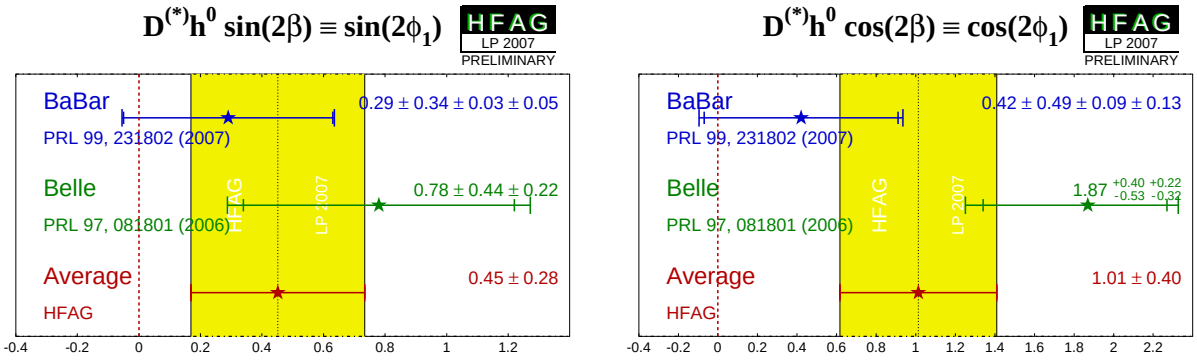

Figure 13: Averages of (left) $\sin(2\beta)$ and (right) $\cos(2\beta)$ measured in colour-suppressed $b \to c\overline{u}d$ transitions.

4.6 Time-dependent *CP* asymmetries in charmless $b \to q\overline{q}s$ transitions

The flavour changing neutral current $b \to s$ penguin can be mediated by any up-type quark in the loop, and hence the amplitude can be written as

$$\begin{aligned} A_{b\to s} &= F_u V_{ub}V_{us}^* + F_c V_{cb}V_{cs}^* + F_t V_{tb}V_{ts}^* \\ &= (F_u - F_c)V_{ub}V_{us}^* + (F_t - F_c)V_{tb}V_{ts}^* \\ &= \mathcal{O}(\lambda^4) + \mathcal{O}(\lambda^2) \end{aligned} \quad (156)$$

using the unitarity of the CKM matrix. Therefore, in the Standard Model, this amplitude is dominated by $V_{tb}V_{ts}^*$, and to within a few degrees ($\delta\beta \lesssim 2^\circ$ for $\beta \approx 20^\circ$) the time-dependent parameters can be written[22] $S_{b\to q\overline{q}s} \approx -\eta \sin(2\beta)$, $C_{b\to q\overline{q}s} \approx 0$, assuming $b \to s$ penguin contributions only ($q = u, d, s$).

Due to the large virtual mass scales occurring in the penguin loops, additional diagrams from physics beyond the Standard Model, with heavy particles in the loops, may contribute. In general, these contributions will affect the values of $S_{b\to q\overline{q}s}$ and $C_{b\to q\overline{q}s}$. A discrepancy between the values of $S_{b\to c\overline{c}s}$ and $S_{b\to q\overline{q}s}$ can therefore provide a clean indication of new physics [286, 293–295].

However, there is an additional consideration to take into account. The above argument assumes only the $b \to s$ penguin contributes to the $b \to q\overline{q}s$ transition. For $q = s$ this is a good assumption, which neglects only rescattering effects. However, for $q = u$ there is a colour-suppressed $b \to u$ tree diagram (of order $\mathcal{O}(\lambda^4)$), which has a different weak (and possibly strong) phase. In the case $q = d$, any light neutral meson that is formed from $d\overline{d}$ also has a $u\overline{u}$ component, and so again there is "tree pollution". The B^0 decays to $\pi^0 K_S^0$, ρ^0 K_S^0 and ωK_S^0 belong to this category. The mesons f_0 and η' are expected to have predominant $s\overline{s}$ parts, which reduces the relative size of the possible tree pollution. If the inclusive decay $B^0 \to K^+K^-K^0$ (excluding ϕK^0) is dominated by a nonresonant three-body transition, an OZI-rule suppressed tree-level diagram can occur through insertion of an $s\overline{s}$ pair. The corresponding penguin-type transition proceeds via insertion of a $u\overline{u}$ pair, which is expected to be favored over the $s\overline{s}$ insertion by fragmentation models. Neglecting rescattering, the final state $K^0\overline{K}^0K^0$ (reconstructed as $K_S^0K_S^0K_S^0$) has no tree pollution [296]. Various estimates, using different theoretical approaches, of the values of $\Delta S = S_{b\to q\overline{q}s} - S_{b\to c\overline{c}s}$ exist in the literature [297–310]. In general, there is agreement that the modes ϕK^0, $\eta' K^0$ and $K^0\overline{K}^0K^0$ are the cleanest, with values of $|\Delta S|$ at or below the few percent level (ΔS is usually positive).

4.6.1 Time-dependent *CP* asymmetries: $b \to q\overline{q}s$ decays to *CP* eigenstates

The averages for $-\eta S_{b\to q\overline{q}s}$ and $C_{b\to q\overline{q}s}$ can be found in Table 31, and are shown in Figs. 14, 15 and 16. Results from both *BABAR* and Belle are averaged for the modes ϕK^0, $\eta' K^0$, $f_0 K^0$ and $K^+K^-K^0$ (K^0 indicates that both K_S^0 and K_L^0 are used, although Belle use neither $f_0 K_L^0$ nor $K^+K^-K_L^0$), $K_S^0K_S^0K_S^0$, $\pi^0 K_S^0$, ωK_S^0 and $\pi^0\pi^0 K_S^0$. *BABAR* also has results for the mode $\rho^0 K_S^0$. Of these, ϕK_S^0, $\eta' K_S^0$, $\pi^0 K_S^0$, ωK_S^0 and $\rho^0 K_S^0$ have *CP* eigenvalue $\eta = -1$, while ϕK_L^0, $\eta' K_L^0$, $f_0 K_S^0$, $\pi^0\pi^0 K_S^0$ and $K_S^0K_S^0K_S^0$ have $\eta = +1$.

[22] The presence of a small ($\mathcal{O}(\lambda^2)$) weak phase in the dominant amplitude of the s penguin decays introduces a phase shift given by $S_{b\to q\overline{q}s} = -\eta \sin(2\beta) \cdot (1 + \Delta)$. Using the CKMfitter results for the Wolfenstein parameters [271], one finds: $\Delta \simeq 0.033$, which corresponds to a shift of 2β of $+2.1$ degrees. Nonperturbative contributions can alter this result.

The final state $K^+K^-K^0$ (contributions from ϕK^0 are implicitly excluded) is not a *CP* eigenstate. However, it can be treated as a quasi-two-body decay, with the *CP* composition determined using either an isospin argument (used by Belle to determine a *CP*-even fraction of $0.93 \pm 0.09 \pm 0.05$ [315]) or a moments analysis (previously used by *BABAR* to find a *CP*-even fractions of $0.89 \pm 0.08 \pm 0.06$ in $K^+K^-K^0_S$ [320]). Note that uncertainty in the *CP* composition of the final state leads to a third source of uncertainty on the Belle results for $-\eta S_{K^+K^-K^0}$.

BABAR have performed time-dependent Dalitz plot analyses of $B^0 \to K^+K^-K^0$ and $B^0 \to \pi^+\pi^-K^0_S$ (see subsection 4.6.2). Their results for ϕK^0 and $K^+K^-K^0$ are determined from the $B^0 \to K^+K^-K^0$ analysis, the latter taken from the inclusive "high-mass" ($m_{K^+K^-} > 1.1$ GeV/c^2) region (this approach automatically corrects for the *CP* composition of the final state). *BABAR* results for $\rho^0 K^0_S$ are taken from the $B^0 \to \pi^+\pi^-K^0_S$ analysis, and their results for f_0K^0 are a combination of results from the both time-dependent Dalitz plot analyses ($-\eta S_{b\to q\bar{q}s} = 0.25 \pm 0.26 \pm 0.10$, $C_{b\to q\bar{q}s} = -0.41 \pm 0.23 \pm 0.07$ from $B^0 \to f_0K^0$ with $f_0 \to K^+K^-$ [311]; $-\eta S_{b\to q\bar{q}s} = 0.94\,^{+0.02}_{-0.07}\,^{+0.03}_{-0.05} \pm 0.02$, $C_{b\to q\bar{q}s} = 0.35 \pm 0.27 \pm 0.07 \pm 0.04$ from $B^0 \to f_0K^0$ with $f_0 \to \pi^+\pi^-$ [316]).

It must be noted that Q2B parameters extracted from Dalitz plot analyses are constrained to lie within the physical boundary ($S^2_{CP} + C^2_{CP} < 1$) and consequenty the obtained errors are highly non-Gaussian when the central value is close to the boundary. This is particularly evident in the *BABAR* results for $B^0 \to f_0K^0$ with $f_0 \to \pi^+\pi^-$ [316]. These results must be treated with extreme caution.

As explained above, each of the modes listed in Table 31 has different uncertainties within the Standard Model, and so each may have a different value of $-\eta S_{b\to q\bar{q}s}$. Therefore, there is no strong motivation to make a combined average over the different modes. We refer to such an average as a "naïve s-penguin average." It is naïve not only because of the neglect of the theoretical uncertainty, but also since possible correlations of systematic effects between different modes are neglected. In spite of these caveats, there remains substantial interest in the value of this quantity, and therefore it is given here: $\langle -\eta S_{b\to q\bar{q}s}\rangle = 0.64 \pm 0.04$, with confidence level 0.008 (2.7σ). This value is in very good agreement with the average $-\eta S_{b\to c\bar{c}s}$ given in Sec. 4.4.1. However, this result is strongly effected by the highly non-Gaussian errors of the *BABAR* result for $B^0 \to f_0K^0$ with $f_0 \to \pi^+\pi^-$ [316], which is only marginally consistent with *BABAR* result for $B^0 \to f_0K^0$ with $f_0 \to K^+K^-$ [311] and the Belle result for $B^0 \to f_0K^0$ with $f_0 \to \pi^+\pi^-$ (treated as a Q2B decay) [315]. If the naïve s-penguin average is recalculated without this result, we find $\langle -\eta S_{b\to q\bar{q}s}\rangle = 0.56 \pm 0.05$, with confidence level 0.25 (1.1σ). Again treating the uncertainties as Gaussian and neglecting correlations, this value is found to be 2.2σ below the average $-\eta S_{b\to c\bar{c}s}$ given in Sec. 4.4.1.

(The average for $C_{b\to q\bar{q}s}$ is $\langle C_{b\to q\bar{q}s}\rangle = -0.01 \pm 0.04$ with confidence level 0.54 (0.6σ). This result is not strongly effected by the inclusion of the *BABAR* result for $B^0 \to f_0K^0$ with $f_0 \to \pi^+\pi^-$.)

We emphasise again that we do not advocate the use of these averages, and that the values should be treated with *extreme caution*, if at all.

From Table 31 it may be noted that the average for $-\eta S_{b\to q\bar{q}s}$ in $\eta' K^0$ (0.61 ± 0.07), is now more than 5σ away from zero, so that *CP* violation in this mode is well established. Amongst other modes, *CP* violation effects in both f_0K^0 and $K^+K^-K^0$ appear to be established – *BABAR* have claimed 5.1σ observation of *CP* violation in $B^0 \to K^+K^-K^0$ [311] and 4.3σ evidence of *CP* violation in $B^0 \to f_0K^0_S$ with $f_0 \to \pi^+\pi^-$ [316]. Due to possible non-Gaussian errors in these results it may be prudent to defer any strong conclusions on the numerical significance

of the averages. There is no evidence (above 2σ) for direct *CP* violation in any $b \to q\overline{q}s$ mode.

4.6.2 Time-dependent Dalitz plot analyses: $B^0 \to K^+K^-K^0$ and $B^0 \to \pi^+\pi^-K^0_S$

As mentioned in Sec. 4.2.4 and above, *BABAR* have performed time-dependent Dalitz plot analysis of $B^0 \to K^+K^-K^0$ [311] and $B^0 \to \pi^+\pi^-K^0_S$ [314] decays. The results are summarized in Tabs. 32 and 33. For $B^0 \to K^+K^-K^0$, results are presented in terms of the effective weak phase (from mixing and decay) difference $\beta^{\rm eff}$ and the direct *CP* violation parameter $\mathcal{A}$ ($\mathcal{A} = -C$) for each of the resonant contributions ϕK^0 and f_0K^0, together with averaged values of those parameters (taking *CP* properties into account) over the entire high-mass ($m_{K^+K^-} > 1.1$ GeV/c^2) region of the Dalitz plot. For $B^0 \to \pi^+\pi^-K^0_S$, results for $2\beta^{\rm eff}$ are presented in Tab. 33. Results on flavour specific amplitudes that contribute to the Dalitz plot (such as $K^{*+}\pi^-$) are averaged by the HFAG Rare Decays subgroup (Sec. 7).

From the results in Tab. 33, *BABAR* infer that the trigonometric reflection at $\pi/2 - \beta^{\rm eff}$ in $B^0 \to K^+K^-K^0$, which is inconsistent with the Standard Model expectation, is disfavoured at 4.6σ.

Table 31: Averages of $-\eta S_{b\to q\bar{q}s}$ and $C_{b\to q\bar{q}s}$.

Experiment		$N(B\overline{B})$	$-\eta S_{b\to q\bar{q}s}$	$C_{b\to q\bar{q}s}$	Correlation
			ϕK^0		
BABAR	[311]	383M	$0.21 \pm 0.26 \pm 0.11$	$0.08 \pm 0.18 \pm 0.04$	–
Belle	[266]	535M	$0.50 \pm 0.21 \pm 0.06$	$-0.07 \pm 0.15 \pm 0.05$	0.05
Average			0.39 ± 0.17	-0.01 ± 0.12	0.03
Confidence level			0.59 (0.5σ)		
			$\eta' K^0$		
BABAR	[312]	384M	$0.58 \pm 0.10 \pm 0.03$	$-0.16 \pm 0.07 \pm 0.03$	0.03
Belle	[266]	535M	$0.64 \pm 0.10 \pm 0.04$	$0.01 \pm 0.07 \pm 0.05$	0.09
Average			0.61 ± 0.07	-0.09 ± 0.06	0.04
Confidence level			0.32 (1.0σ)		
			$K^0_S K^0_S K^0_S$		
BABAR	[313]	384M	$0.71 \pm 0.24 \pm 0.04$	$0.02 \pm 0.21 \pm 0.05$	-0.14
Belle	[266]	535M	$0.30 \pm 0.32 \pm 0.08$	$-0.31 \pm 0.20 \pm 0.07$	–
Average			0.58 ± 0.20	-0.14 ± 0.15	-0.08
Confidence level			0.31 (1.0σ)		
			$\pi^0 K^0_S$		
BABAR	[314]	383M	$0.40 \pm 0.23 \pm 0.03$	$0.24 \pm 0.15 \pm 0.03$	-0.07
Belle	[315]	535M	$0.33 \pm 0.35 \pm 0.08$	$0.05 \pm 0.14 \pm 0.05$	-0.08
Average			0.38 ± 0.19	0.14 ± 0.11	-0.07
Confidence level			0.66 (0.5σ)		
			$\rho^0 K^0_S$		
BABAR	[316]	383M	$0.61\,^{+0.22}_{-0.24} \pm 0.09 \pm 0.08$	$0.02 \pm 0.27 \pm 0.08 \pm 0.06$	–
Average			$0.61\,^{+0.25}_{-0.27}$	0.02 ± 0.29	–
			ωK^0_S		
BABAR	[317]	347M	$0.62\,^{+0.25}_{-0.30} \pm 0.02$	$-0.43\,^{+0.25}_{-0.23} \pm 0.03$	–
Belle	[315]	535M	$0.11 \pm 0.46 \pm 0.07$	$0.09 \pm 0.29 \pm 0.06$	–
Average			0.48 ± 0.24	-0.21 ± 0.19	–
Confidence level			0.35 (0.9σ)	0.18 (1.3σ)	
			$f_0 K^0$		
BABAR	[311, 316]	–	0.90 ± 0.07	-0.01 ± 0.18	–
Belle	[315]	535M	$0.18 \pm 0.23 \pm 0.11$	$0.15 \pm 0.15 \pm 0.07$	-0.01
Average			0.85 ± 0.07	0.08 ± 0.12	-0.00
Confidence level			0.02 (2.3σ)		
			$\pi^0\pi^0 K^0_S$		
BABAR	[318]	227M	$-0.72 \pm 0.71 \pm 0.08$	$0.23 \pm 0.52 \pm 0.13$	-0.02
Belle	[319]	657M	$-0.43 \pm 0.49 \pm 0.09$	$0.17 \pm 0.24 \pm 0.06$	0.09
Average			-0.52 ± 0.41	0.18 ± 0.22	0.06
Confidence level			0.94 (0.1σ)		
			$K^+K^-K^0$		
BABAR	[311]	383M	$0.76 \pm 0.11\,^{+0.07}_{-0.04}$	$0.05 \pm 0.10 \pm 0.06$	–
Belle	[315]	535M	$0.68 \pm 0.15 \pm 0.03\,^{+0.21}_{-0.13}$	$0.09 \pm 0.10 \pm 0.05$	–
Average			0.73 ± 0.10	0.07 ± 0.08	–
Confidence level			0.67 (0.4σ)	0.82 (0.2σ)	

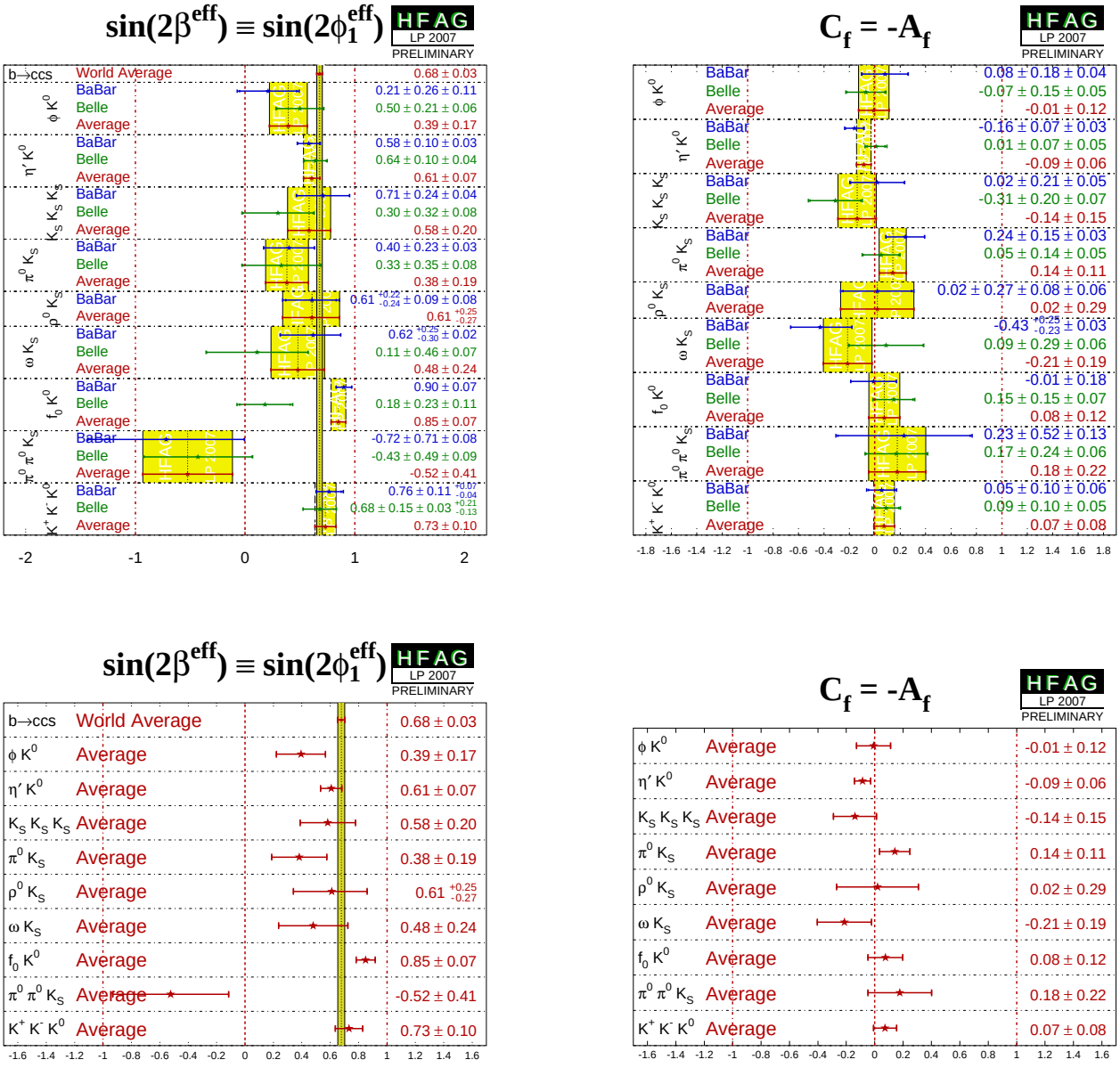

Figure 14: (Top) Averages of (left) $-\eta S_{b\to q\bar{q}s}$ and (right) $C_{b\to q\bar{q}s}$. The $-\eta S_{b\to q\bar{q}s}$ figure compares the results to the world average for $-\eta S_{b\to c\bar{c}s}$ (see Section 4.4.1). (Bottom) Same, but only averages for each mode are shown. More figures are available from the HFAG web pages.

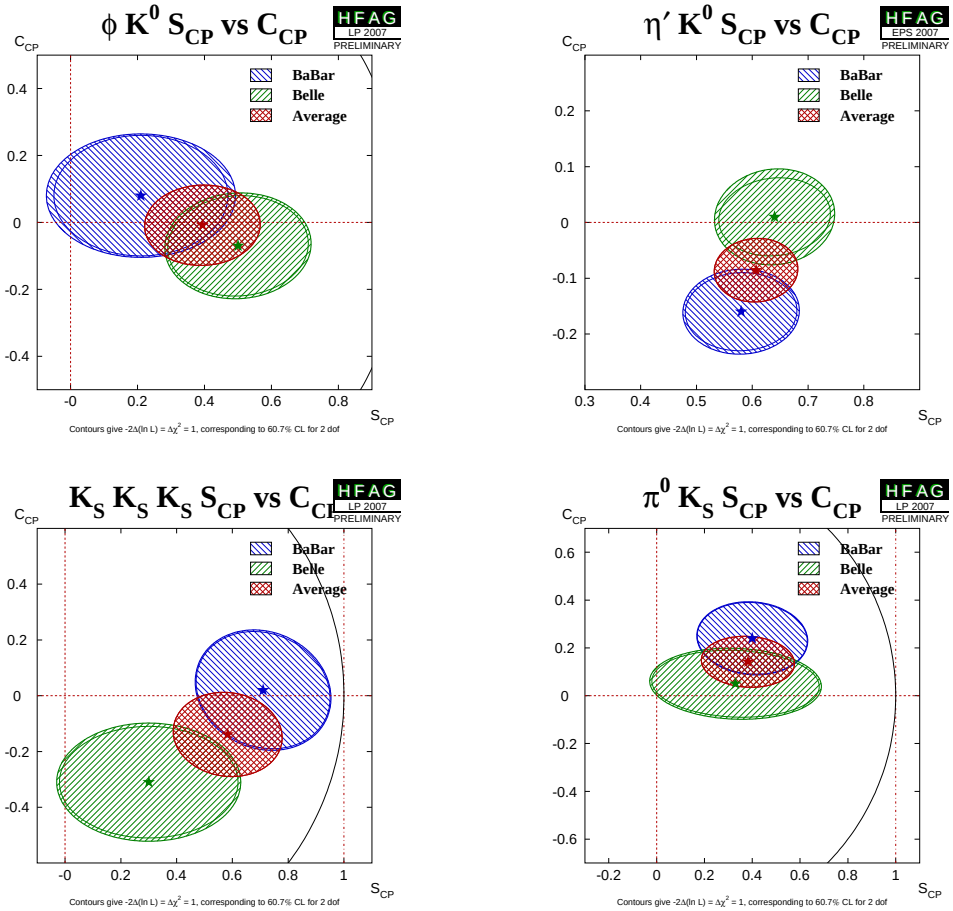

Figure 15: Averages of four $b \to q\overline{q}s$ dominated channels, for which correlated averages are performed, in the S_{CP} *vs.* C_{CP} plane, where S_{CP} has been corrected by the CP eigenvalue to give $\sin(2\beta^{\rm eff})$. (Top left) $B^0 \to \phi K^0$, (top right) $B^0 \to \eta' K^0$, (bottom left) $B^0 \to K^0_S K^0_S K^0_S$, (bottom right) $B^0 \to \pi^0 K^0_S$. More figures are available from the HFAG web pages.

Table 32: Results from time-dependent Dalitz plot analysis of the $B^0 \to K^+K^-K^0$ decay.

Experiment	$N(B\overline{B})$	ϕK^0		$f_0 K^0$	
		$\beta^{\rm eff}$	$\mathcal{A}$	$\beta^{\rm eff}$	$\mathcal{A}$
BABAR [311]	383M	$0.11 \pm 0.14 \pm 0.06$	$-0.08 \pm 0.18 \pm 0.14$	$0.14 \pm 0.15 \pm 0.05$	$0.41 \pm 0.23 \pm 0.07$

Experiment	$N(B\overline{B})$	$K^+K^-K^0$	
		$\beta^{\rm eff}$	$\mathcal{A}$
BABAR [311]	383M	$0.436 \pm 0.087\,^{+0.055}_{-0.031}$	$-0.054 \pm 0.102 \pm 0.060$

Table 33: Results from time-dependent Dalitz plot analysis of the $B^0 \to \pi^+\pi^-K^0$ decay.

Experiment	$N(B\overline{B})$	$2\beta^{\rm eff}$ $(f_0 K^0_S)$	$2\beta^{\rm eff}$ $(\rho^0 K^0_S)$
BABAR [314]	383M	$(89\,^{+22}_{-20} \pm 5 \pm 8)^\circ$	$(37\,^{+19}_{-17} \pm 5 \pm 6)^\circ$

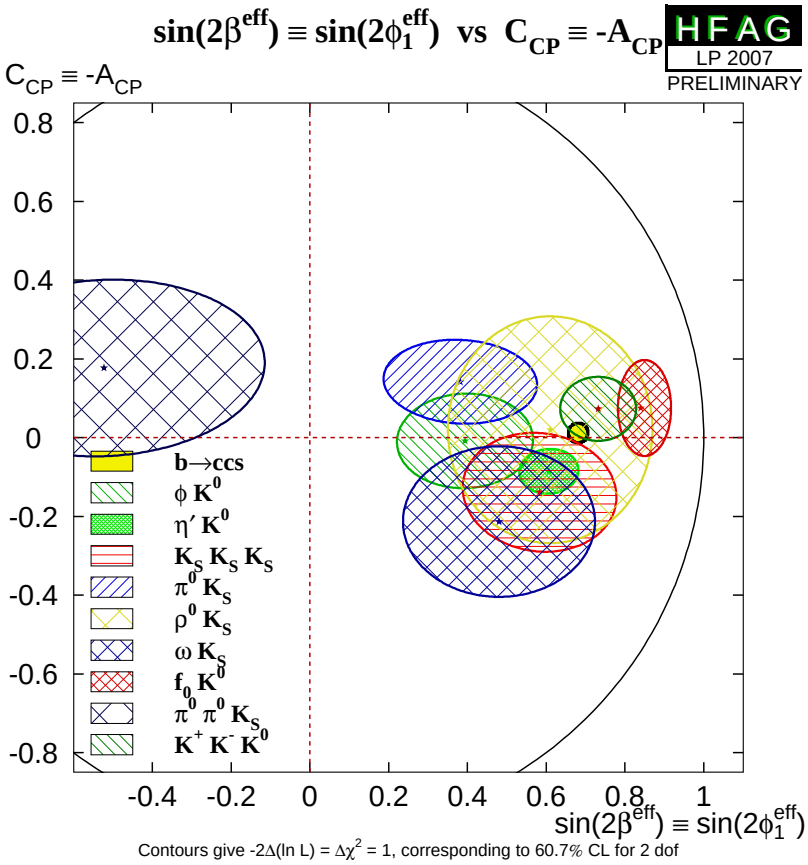

Figure 16: Compilation of constraints in the $-\eta S_{b\to q\bar{q}s}$ *vs.* $C_{b\to q\bar{q}s}$ plane.

4.7 Time-dependent *CP* asymmetries in $b \to c\bar{c}d$ transitions

The transition $b \to c\bar{c}d$ can occur via either a $b \to c$ tree or a $b \to d$ penguin amplitude. Similarly to Eq. (156), the amplitude for the $b \to d$ penguin can be written

$$\begin{aligned} A_{b\to d} &= F_u V_{ub}V_{ud}^* + F_c V_{cb}V_{cd}^* + F_t V_{tb}V_{td}^* \\ &= (F_u - F_c)V_{ub}V_{ud}^* + (F_t - F_c)V_{tb}V_{td}^* \\ &= \mathcal{O}(\lambda^3) + \mathcal{O}(\lambda^3). \end{aligned} \tag{157}$$

From this it can be seen that the $b \to d$ penguin amplitude contains terms with different weak phases at the same order of CKM suppression.

In the above, we have followed Eq. (156) by eliminating the F_c term using unitarity. However, we could equally well write

$$\begin{aligned} A_{b\to d} &= (F_u - F_t)V_{ub}V_{ud}^* + (F_c - F_t)V_{cb}V_{cd}^*, \\ &= (F_c - F_u)V_{cb}V_{cd}^* + (F_t - F_u)V_{tb}V_{td}^*. \end{aligned} \tag{158}$$

Since the $b \to c\bar{c}d$ tree amplitude has the weak phase of $V_{cb}V_{cd}^*$, either of the above expressions allow the penguin to be decomposed into parts with weak phases the same and different to the tree amplitude (the relative weak phase can be chosen to be either β or γ). However, if the tree amplitude dominates, there is little sensitivity to any phase other than that from B^0–$\overline{B}^0$ mixing.

The $b \to c\bar{c}d$ transitions can be investigated with studies of various different final states. Results are available from both *BABAR* and Belle using the final states $J/\psi\pi^0$, D^+D^-, $D^{*+}D^{*-}$ and $D^{*\pm}D^{\mp}$, the averages of these results are given in Table 34. The results using the *CP* eigenstate ($\eta = +1$) modes $J/\psi\pi^0$ and D^+D^- are shown in Fig. 17 and Fig. 18 respectively, with two-dimensional constraints shown in Fig. 19.

The vector-vector mode $D^{*+}D^{*-}$ is found to be dominated by the *CP*-even longitudinally polarized component; *BABAR* measures a *CP*-odd fraction of $0.143 \pm 0.034 \pm 0.008$ [329] while Belle measures a *CP*-odd fraction of $0.19 \pm 0.08 \pm 0.01$ [330] (here we do not average these fractions and rescale the inputs, however the average is almost independent of the treatment). *BABAR* allows the *CP*-odd fraction (actually, the transversely polarized fraction, $R_\perp$, which is equivalent) to float in the fit, so that its uncertainty is automatically incorporated into the statistical error. Belle quotes a third uncertainty due to the polarization. *BABAR* have also performed an additional fit in which the *CP*-even and *CP*-odd components are allowed to have different *CP* violation parameters S and C. These results are included in Table 34. Results using $D^{*+}D^{*-}$ are shown in Fig. 20.

For the non-*CP* eigenstate mode $D^{*\pm}D^{\mp}$ *BABAR* uses fully reconstructed events while Belle combines both fully and partially reconstructed samples. At present we perform uncorrelated averages of the parameters in the $D^{*\pm}D^{\mp}$ system.

In the absence of the penguin contribution (tree dominance), the time-dependent parameters would be given by $S_{b\to c\bar{c}d} = -\eta\sin(2\beta)$, $C_{b\to c\bar{c}d} = 0$, $S_{+-} = \sin(2\beta + \delta)$, $S_{-+} = \sin(2\beta - \delta)$, $C_{+-} = -C_{-+}$ and $\mathcal{A} = 0$, where δ is the strong phase difference between the $D^{*+}D^-$ and $D^{*-}D^+$ decay amplitudes. In the presence of the penguin contribution, there is no clean interpretation in terms of CKM parameters, however direct *CP* violation may be observed as any of $C_{b\to c\bar{c}d} \neq 0$, $C_{+-} \neq -C_{-+}$ or $A_{+-} \neq 0$.

The averages for the $b \to c\bar{c}d$ modes are shown in Figs. 21 and 22. Results are consistent with tree dominance, and with the Standard Model, though the Belle results in $B^0 \to D^+D^-$ [328]

Table 34: Averages for the $b \to c\overline{c}d$ modes, $B^0 \to J/\psi\pi^0$, D^+D^-, $D^{*+}D^{*-}$ and $D^{*\pm}D^{\mp}$.

Experiment	$N(B\overline{B})$	S_{CP}	C_{CP}	Correlation
		$J/\psi\pi^0$		
BABAR [325]	232M	$-0.68 \pm 0.30 \pm 0.04$	$-0.21 \pm 0.26 \pm 0.06$	0.08
Belle [326]	535M	$-0.65 \pm 0.21 \pm 0.05$	$-0.08 \pm 0.16 \pm 0.05$	-0.10
Average		-0.65 ± 0.18	-0.12 ± 0.14	-0.04
Confidence level		0.92 (0.1σ)		
		D^+D^-		
BABAR [327]	364M	$-0.54 \pm 0.34 \pm 0.06$	$0.11 \pm 0.22 \pm 0.07$	-0.17
Belle [328]	535M	$-1.13 \pm 0.37 \pm 0.09$	$-0.91 \pm 0.23 \pm 0.06$	-0.04
Average		-0.75 ± 0.26	-0.37 ± 0.17	-0.10
Confidence level		0.003 (3.0σ)		
		$D^{*+}D^{*-}$		
BABAR [329]	383M	$-0.66 \pm 0.19 \pm 0.04$	$-0.02 \pm 0.11 \pm 0.02$	-0.04
Belle [330]	152M	$-0.75 \pm 0.56 \pm 0.10 \pm 0.06$	$0.26 \pm 0.26 \pm 0.05 \pm 0.01$	–
Average		-0.67 ± 0.18	0.02 ± 0.10	-0.03
Confidence level		0.62 (0.5σ)		

Experiment	$N(B\overline{B})$	S_{CP+}	C_{CP+}	S_{CP-}	C_{CP-}
			$D^{*+}D^{*-}$		
BABAR [329]	383M	$-0.72 \pm 0.19 \pm 0.05$	$-0.05 \pm 0.14 \pm 0.02$	$-1.83 \pm 1.04 \pm 0.23$	$0.23 \pm 0.67 \pm 0.10$

Experiment	$N(B\overline{B})$	S_{+-}	C_{+-}	S_{-+}	C_{-+}	$\mathcal{A}$
			$D^{*\pm}D^{\mp}$			
BABAR [327]	364M	$-0.79 \pm 0.21 \pm 0.06$	$0.18 \pm 0.15 \pm 0.04$	$-0.44 \pm 0.22 \pm 0.06$	$0.23 \pm 0.15 \pm 0.04$	$0.12 \pm 0.06 \pm 0.02$
Belle [331]	152M	$-0.55 \pm 0.39 \pm 0.12$	$-0.37 \pm 0.22 \pm 0.06$	$-0.96 \pm 0.43 \pm 0.12$	$0.23 \pm 0.25 \pm 0.06$	$0.07 \pm 0.08 \pm 0.04$
Average		-0.74 ± 0.19	0.01 ± 0.13	-0.55 ± 0.20	0.23 ± 0.13	0.10 ± 0.05
Confidence level		0.60 (0.5σ)	0.05 (2.0σ)	0.30 (1.0σ)	1.00 (0.0σ)	0.65 (0.5σ)

show an indication of direct *CP* violation, and hence a non-zero penguin contribution. The average of $S_{b\to c\overline{c}d}$ in both $J/\psi\pi^0$ and $D^{*+}D^{*-}$ final states are about 3σ from zero; however, due to the large uncertainty and possible non-Gaussian effects, any strong conclusion should be deferred.

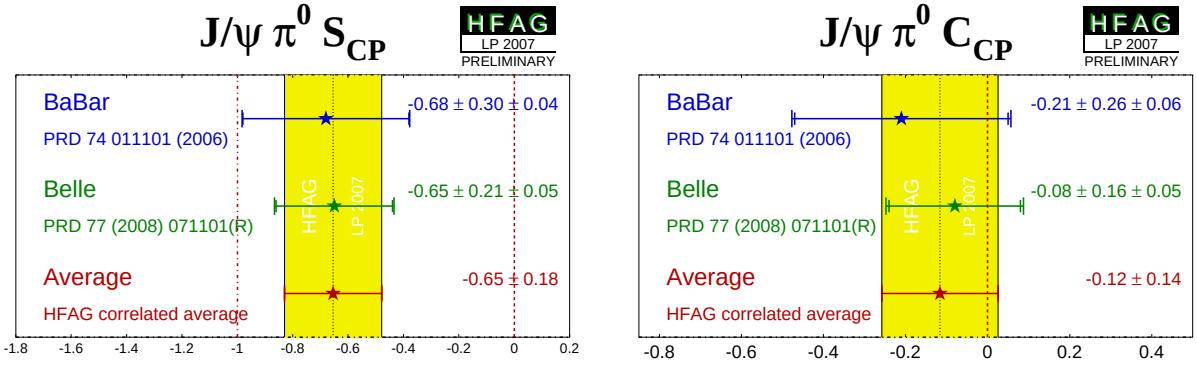

Figure 17: Averages of (left) $S_{b\to c\bar{c}d}$ and (right) $C_{b\to c\bar{c}d}$ for the mode $B^0 \to J/\psi\pi^0$.

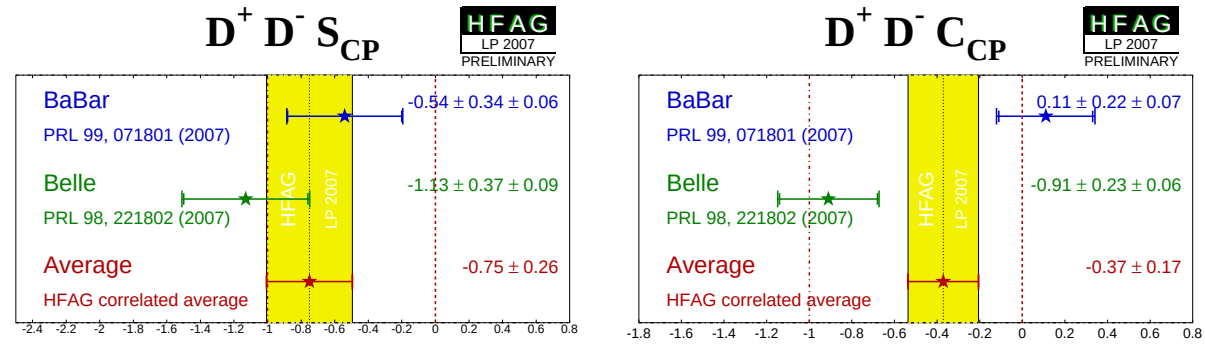

Figure 18: Averages of (left) $S_{b\to c\bar{c}d}$ and (right) $C_{b\to c\bar{c}d}$ for the mode $B^0 \to D^+D^-$.

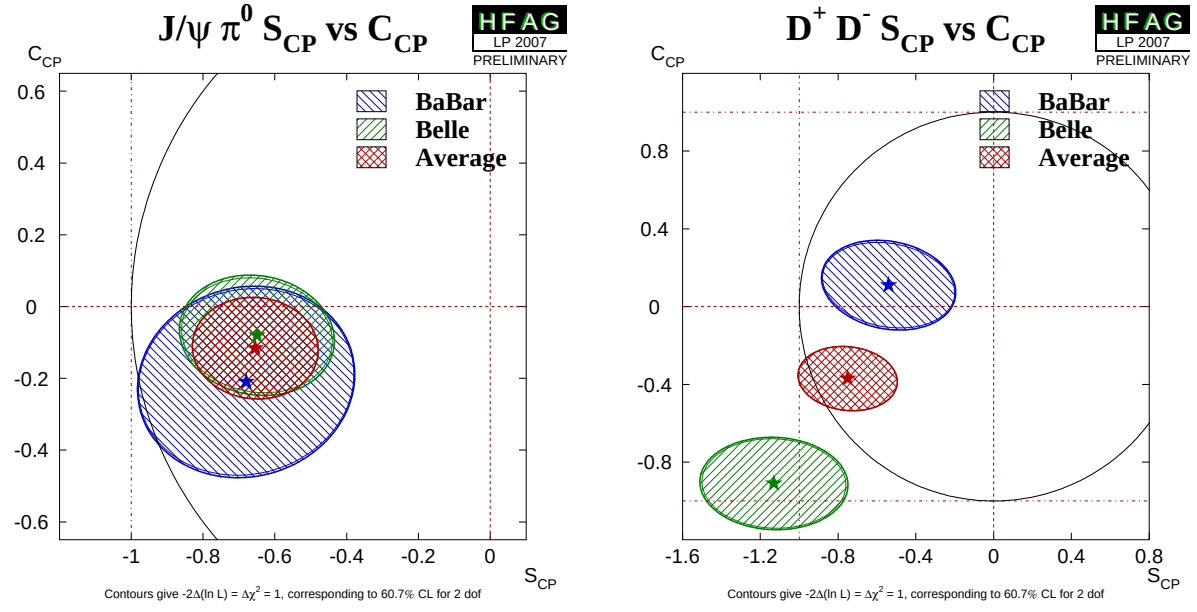

Figure 19: Averages of two $b \to c\bar{c}d$ dominated channels, for which correlated averages are performed, in the S_{CP} *vs.* C_{CP} plane. (Left) $B^0 \to J/\psi\pi^0$ and (right) $B^0 \to D^+D^-$.

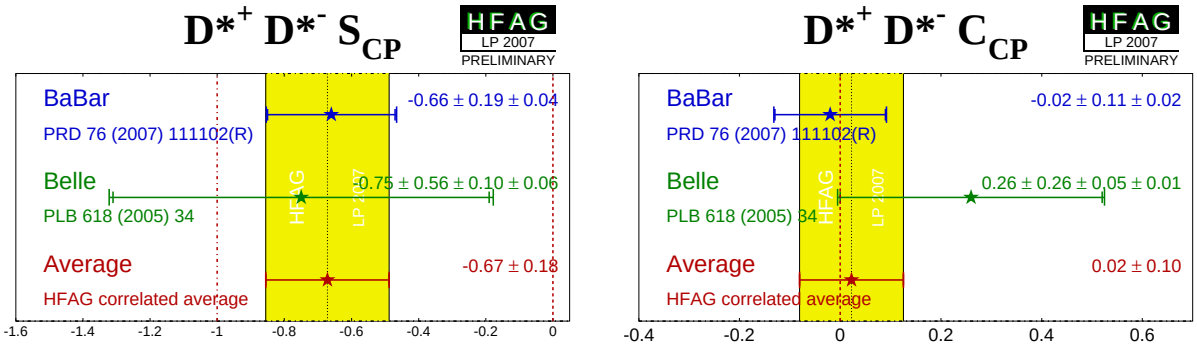

Figure 20: Averages of (left) $S_{b\to c\bar{c}d}$ and (right) $C_{b\to c\bar{c}d}$ for the mode $B^0 \to D^{*+}D^{*-}$.

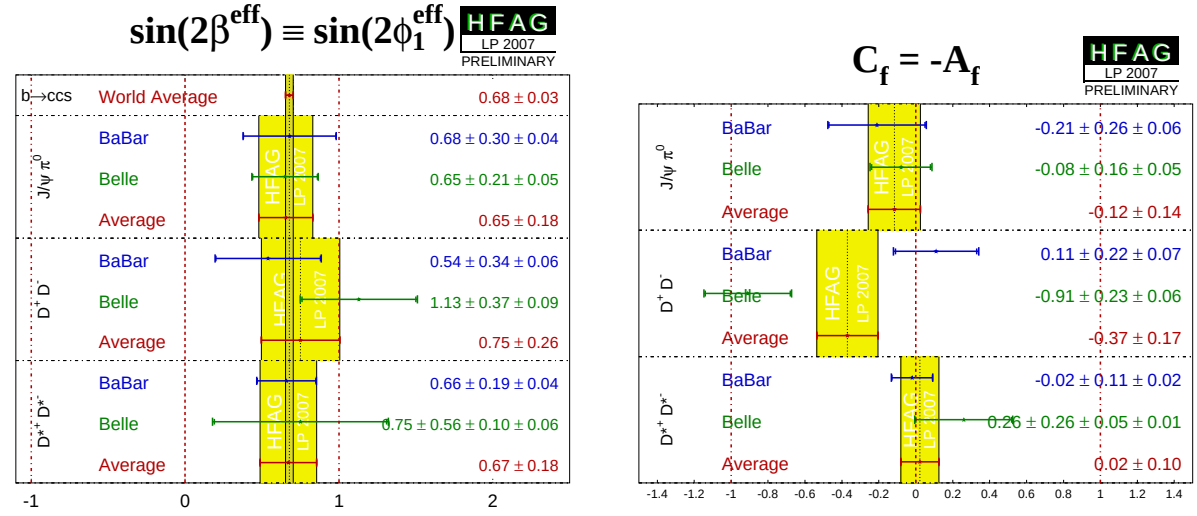

Figure 21: Averages of (left) $-\eta S_{b\to c\bar{c}d}$ and (right) $C_{b\to c\bar{c}d}$. The $-\eta S_{b\to q\bar{q}s}$ figure compares the results to the world average for $-\eta S_{b\to c\bar{c}s}$ (see Section 4.4.1).

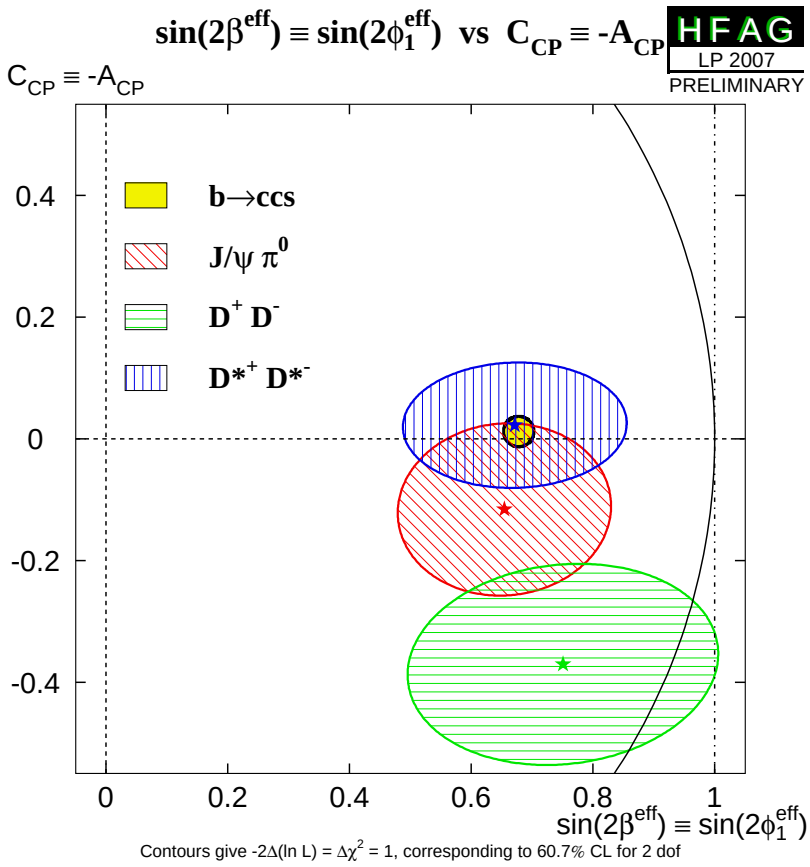

Figure 22: Compilation of constraints in the $-\eta S_{b\to c\bar{c}d}$ *vs.* $C_{b\to c\bar{c}d}$ plane.

4.8 Time-dependent *CP* asymmetries in $b \to q\bar{q}d$ transitions

Decays such as $B^0 \to K^0_S K^0_S$ are pure $b \to q\bar{q}d$ penguin transitions. As shown in Eq. 157, this diagram has different contributing weak phases, and therefore the observables are sensitive to the difference (which can be chosen to be either β or γ). Note that if the contribution with the top quark in the loop dominates, the weak phase from the decay amplitudes should cancel that from mixing, so that no *CP* violation (neither mixing-induced nor direct) occurs. Non-zero contributions from loops with intermediate up and charm quarks can result in both types of effect (as usual, a strong phase difference is required for direct *CP* violation to occur).

Both *BABAR* [332] and Belle [333] have performed time-dependent analyses of $B^0 \to K^0_S K^0_S$. The results are shown in Table 35 and Fig. 23.

Table 35: Results for $B^0 \to K^0_S K^0_S$.

Experiment		$N(B\overline{B})$	S_{CP}	C_{CP}	Correlation
BABAR	[332]	350M	$-1.28\,^{+0.80}_{-0.73}\,^{+0.11}_{-0.16}$	$-0.40 \pm 0.41 \pm 0.06$	-0.32
Belle	[333]	657M	$-0.38\,^{+0.69}_{-0.77} \pm 0.09$	$0.38 \pm 0.38 \pm 0.05$	0.48
Average			-1.08 ± 0.49	-0.06 ± 0.26	0.14
Confidence level			0.29 (1.1σ)		

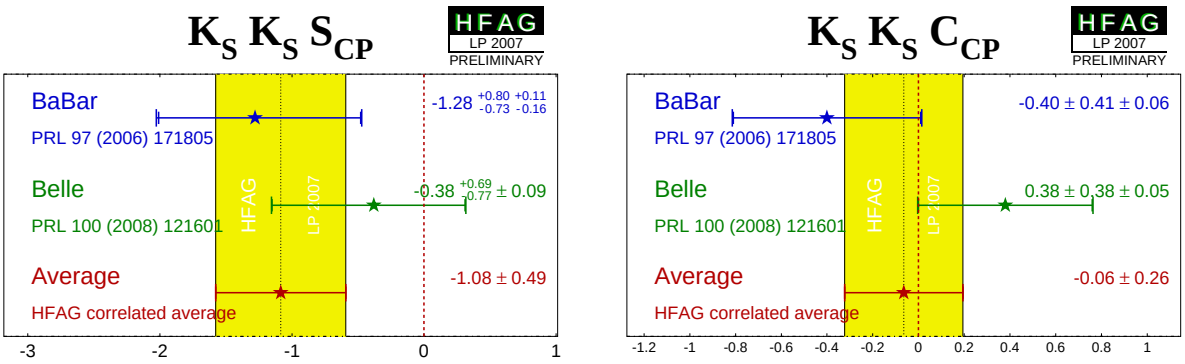

Figure 23: Averages of (left) $S_{b\to q\bar{q}d}$ and (right) $C_{b\to q\bar{q}d}$ for the mode $B^0 \to K^0_S K^0_S$.

4.9 Time-dependent asymmetries in $b \to s\gamma$ transitions

The radiative decays $b \to s\gamma$ produce photons which are highly polarized in the Standard Model. The decays $B^0 \to F\gamma$ and $\overline{B}^0 \to F\gamma$ produce photons with opposite helicities, and since the polarization is, in principle, observable, these final states cannot interfere. The finite mass of the s quark introduces small corrections to the limit of maximum polarization, but any large mixing induced *CP* violation would be a signal for new physics. Since a single weak phase dominates the $b \to s\gamma$ transition in the Standard Model, the cosine term is also expected to be small.

Atwood *et al.* [335] have shown that an inclusive analysis with respect to $K^0_S\pi^0\gamma$ can be performed, since the properties of the decay amplitudes are independent of the angular momentum of the $K^0_S\pi^0$ system. However, if non-dipole operators contribute significantly to the amplitudes, then the Standard Model mixing-induced *CP* violation could be larger than the naïve expectation $S \simeq -2(m_s/m_b)\sin(2\beta)$ [336,337]. In this case, the *CP* parameters may vary over the $K^0_S\pi^0\gamma$ Dalitz plot, for example as a function of the $K^0_S\pi^0$ invariant mass. Explicit calculations indicate such corrections are small for exclusive final states [338, 339].

With the above in mind, we quote two averages: one for $K^*(892)$ candidates only, and the other one for the inclusive $K^0_S\pi^0\gamma$ decay (including the $K^*(892)$). If the Standard Model dipole operator is dominant, both should give the same quantities (the latter naturally with smaller statistical error). If not, care needs to be taken in interpretation of the inclusive parameters, while the results on the $K^*(892)$ resonance remain relatively clean. Results from *BABAR* and Belle are used for both averages; both experiments use the invariant mass range $0.60\ \text{GeV}/c^2 < M_{K^0_S\pi^0} < 1.80\ \text{GeV}/c^2$ in the inclusive analysis. Note that these averages include an update from *BABAR* [340] on the $K^*\gamma$ parameters but not on the $K^0_S\pi^0\gamma$ parameters, so that the former are measured more precisely than the latter.

Table 36: Averages for $b \to s\gamma$ modes.

Experiment		$N(B\overline{B})$	$S_{CP}(b \to s\gamma)$	$C_{CP}(b \to s\gamma)$	Correlation
			$K^*(892)\gamma$		
BABAR	[340]	431M	$-0.08 \pm 0.31 \pm 0.05$	$-0.15 \pm 0.17 \pm 0.03$	0.05
Belle	[341]	535M	$-0.32\,^{+0.36}_{-0.33} \pm 0.05$	$0.20 \pm 0.24 \pm 0.05$	0.08
Average			-0.19 ± 0.23	-0.03 ± 0.14	0.06
Confidence level			0.43 (0.8σ)		
			$K^0_S\pi^0\gamma$ (including $K^*(892)\gamma$)		
BABAR	[342]	232M	-0.06 ± 0.37	-0.48 ± 0.22	0.05
Belle	[341]	535M	$-0.10 \pm 0.31 \pm 0.07$	$0.20 \pm 0.20 \pm 0.06$	0.08
Average			-0.09 ± 0.24	-0.12 ± 0.15	0.06
Confidence level			0.08 (1.8σ)		

The results are shown in Table 36, and in Figs. 24 and 25. No significant *CP* violation results are seen; the results are consistent with the Standard Model and with other measurements in the $b \to s\gamma$ system (see Sec. 7).

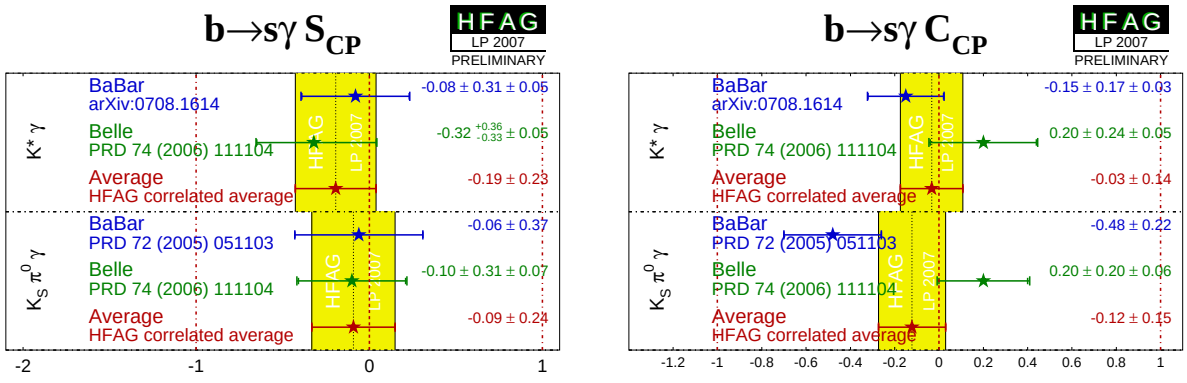

Figure 24: Averages of (left) $S_{b\to s\gamma}$ and (right) $C_{b\to s\gamma}$. Recall that the data for $K^*\gamma$ is a subset of that for $K^0_S\pi^0\gamma$.

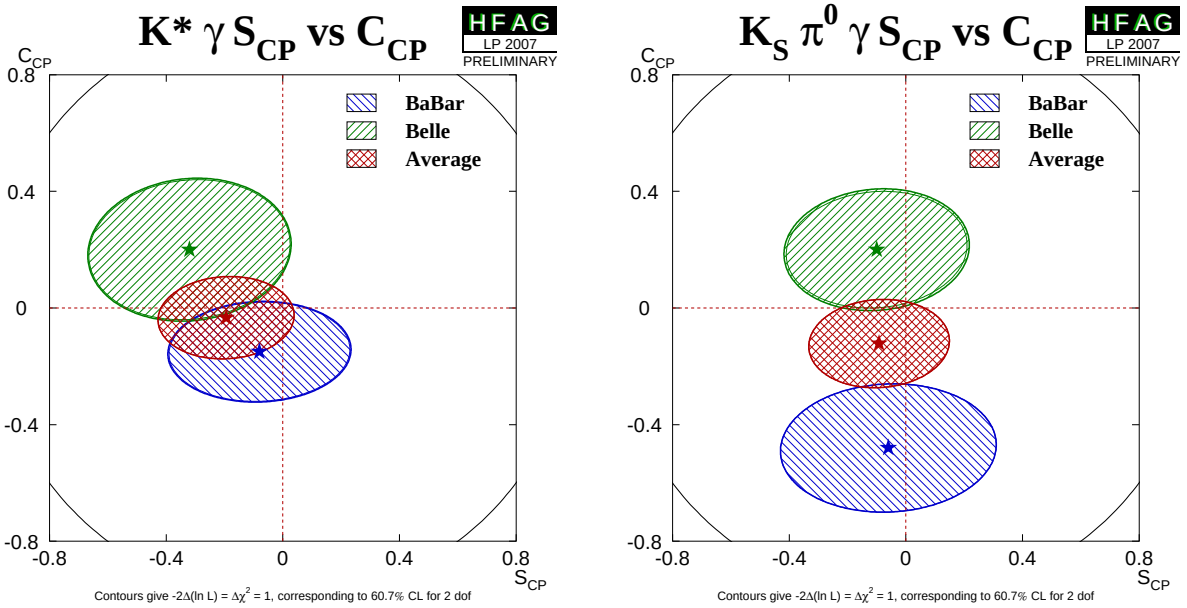

Figure 25: Averages of $b \to s\gamma$ dominated channels, for which correlated averages are performed, in the S_{CP} *vs.* C_{CP} plane. (Left) $B^0 \to K^*\gamma$ and (right) $B^0 \to K^0_S\pi^0\gamma$ (including $K^*\gamma$).

4.10 Time-dependent asymmetries in $b \to d\gamma$ transitions

The formalism for the radiative decays $b \to d\gamma$ is much the same as that for $b \to s\gamma$ discussed above. Assuming dominance of the top quark in the loop, the weak phase in decay should cancel with that from mixing, so that the mixing-induced CP violation parameter S_{CP} should be very small. Corrections due to the finite light quark mass are smaller compared to $b \to s\gamma$, since $m_d < m_s$, and although QCD corrections may still play a role, they cannot significantly affect the prediction $S_{b\to d\gamma} \simeq 0$. Large direction CP violation effects could, however, be seen through a non-zero value of $C_{b\to d\gamma}$, since the top loop is not the only contribution.

Results using the mode $B^0 \to \rho^0\gamma$ are available from Belle and are shown in Table 37.

Table 37: Averages for $B^0 \to \rho^0\gamma$.

Experiment		$N(B\overline{B})$	S_{CP}	C_{CP}	Correlation
Belle	[343]	657M	$-0.83 \pm 0.65 \pm 0.18$	$0.44 \pm 0.49 \pm 0.14$	-0.08

4.11 Time-dependent *CP* asymmetries in $b \to u\overline{u}d$ transitions

The $b \to u\overline{u}d$ transition can be mediated by either a $b \to u$ tree amplitude or a $b \to d$ penguin amplitude. These transitions can be investigated using the time dependence of B^0 decays to final states containing light mesons. Results are available from both *BABAR* and Belle for the *CP* eigenstate ($\eta = +1$) $\pi^+\pi^-$ final state and for the vector-vector final state $\rho^+\rho^-$, which is found to be dominated by the *CP*-even longitudinally polarized component (*BABAR* measure $f_{\rm long} = 0.992 \pm 0.024\,^{+0.026}_{-0.013}$ [348] while Belle measure $f_{\rm long} = 0.941\,^{+0.034}_{-0.040} \pm 0.030$ [349]). *BABAR* have also performed a time-dependent analysis of the vector-vector final state $\rho^0\rho^0$ [351], in which they measure $f_{\rm long} = 0.70 \pm 0.14 \pm 0.05$, and furthermore have also performed a time-dependent analysis of the $B^0 \to a_1^\pm\pi^\mp$ decay [357]. These results, and averages, are listed in Table 38. The averages for $\pi^+\pi^-$ are shown in Fig. 26, and those for $\rho^+\rho^-$ are shown in Fig. 27, with the averages in the S_{CP} *vs.* C_{CP} plane shown in Fig. 28.

Table 38: Averages for $b \to u\overline{u}d$ modes.

Experiment		$N(B\overline{B})$	S_{CP}	C_{CP}	Correlation
			$\pi^+\pi^-$		
BABAR	[346]	383M	$-0.60 \pm 0.11 \pm 0.03$	$-0.21 \pm 0.09 \pm 0.02$	-0.07
Belle	[347]	535M	$-0.61 \pm 0.10 \pm 0.04$	$-0.55 \pm 0.08 \pm 0.05$	-0.15
Average			-0.61 ± 0.08	-0.38 ± 0.07	-0.09
Confidence level			0.034 (2.1σ)		
			$\rho^+\rho^-$		
BABAR	[348]	387M	$-0.17 \pm 0.20\,^{+0.05}_{-0.06}$	$0.01 \pm 0.15 \pm 0.06$	-0.04
Belle	[350]	535M	$0.19 \pm 0.30 \pm 0.07$	$-0.16 \pm 0.21 \pm 0.07$	0.10
Average			-0.05 ± 0.17	-0.06 ± 0.13	0.01
Confidence level			0.50 (0.7σ)		
			$\rho^0\rho^0$		
BABAR	[351]	427M	$0.5 \pm 0.9 \pm 0.2$	$0.4 \pm 0.9 \pm 0.2$	–

Experiment		$N(B\overline{B})$	A_{CP}	C	S	ΔC	ΔS
				$a_1^\pm\pi^\mp$			
BABAR	[357]	384M	$-0.07 \pm 0.07 \pm 0.02$	$-0.10 \pm 0.15 \pm 0.09$	$0.37 \pm 0.21 \pm 0.07$	$0.26 \pm 0.15 \pm 0.07$	$-0.14 \pm 0.21 \pm 0.06$

If the penguin contribution is negligible, the time-dependent parameters for $B^0 \to \pi^+\pi^-$ and $B^0 \to \rho^+\rho^-$ are given by $S_{b\to u\overline{u}d} = \eta \sin(2\alpha)$ and $C_{b\to u\overline{u}d} = 0$. In the presence of the penguin contribution, direct *CP* violation may arise, and there is no straightforward interpretation of $S_{b\to u\overline{u}d}$ and $C_{b\to u\overline{u}d}$. An isospin analysis [358] can be used to disentangle the contributions and extract α.

For the non-*CP* eigenstate $\rho^\pm\pi^\mp$, both *BABAR* [354] and Belle [355, 356] have performed time-dependent Dalitz plot (DP) analyses of the $\pi^+\pi^-\pi^0$ final state [344]; such analyses allow direct measurements of the phases. Both experiments have measured the U and I parameters discussed in Sec. 4.2.4 and defined in Table 19. We have performed a full correlated average of these parameters, the results of which are summarized in Fig. 29.

Both experiments have also extracted the Q2B parameters. We have performed a full correlated average of these parameters, which is equivalent to determining the values from the

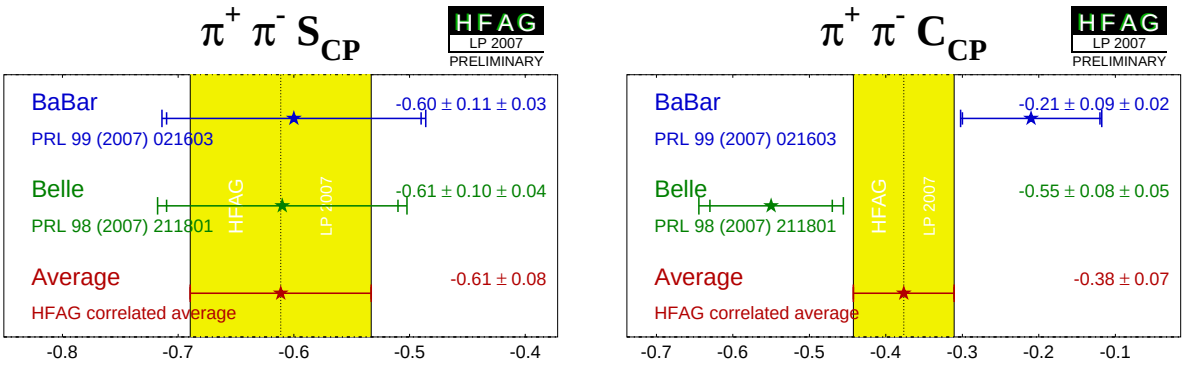

Figure 26: Averages of (left) $S_{b\to u\bar{u}d}$ and (right) $C_{b\to u\bar{u}d}$ for the mode $B^0 \to \pi^+\pi^-$.

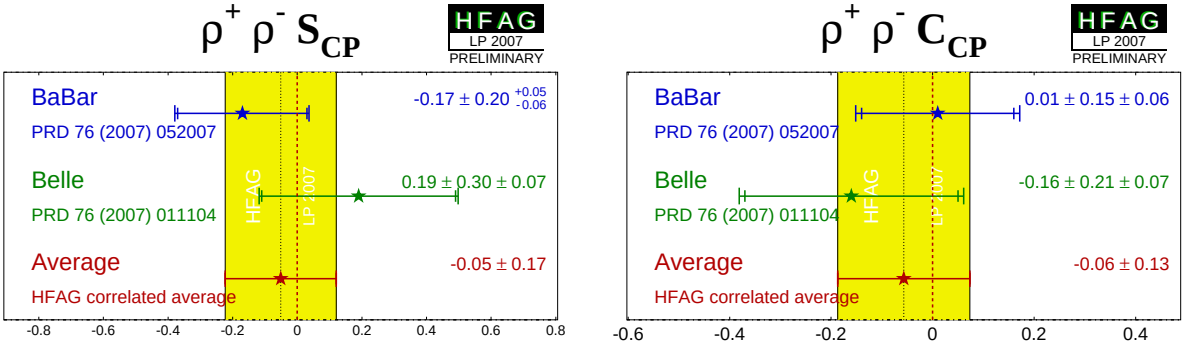

Figure 27: Averages of (left) $S_{b\to u\bar{u}d}$ and (right) $C_{b\to u\bar{u}d}$ for the mode $B^0 \to \rho^+\rho^-$.

averaged U and I parameters. The results are shown in Table. 39. Averages of the $B^0 \to \rho^0\pi^0$ Q2B parameters are shown in Figs. 30 and 31.

With the notation described in Sec. 4.2 (Eq. (134)), the time-dependent parameters for the Q2B $B^0 \to \rho^\pm\pi^\mp$ analysis are, neglecting penguin contributions, given by

$$S_{\rho\pi} = \sqrt{1-\left(\frac{\Delta C}{2}\right)^2}\sin(2\alpha)\cos(\delta)\ , \quad \Delta S_{\rho\pi} = \sqrt{1-\left(\frac{\Delta C}{2}\right)^2}\cos(2\alpha)\sin(\delta) \qquad (159)$$

and $C_{\rho\pi} = \mathcal{A}_{CP}^{\rho\pi} = 0$, where $\delta = \arg(A_{-+}A_{+-}^*)$ is the strong phase difference between the $\rho^-\pi^+$ and $\rho^+\pi^-$ decay amplitudes. In the presence of the penguin contribution, there is no straightforward interpretation of the Q2B observables in the $B^0 \to \rho^\pm\pi^\mp$ system in terms of CKM parameters. However direct CP violation may arise, resulting in either or both of $C_{\rho\pi} \neq 0$ and $\mathcal{A}_{CP}^{\rho\pi} \neq 0$. Equivalently, direct CP violation may be seen by either of the decay-type-specific observables $\mathcal{A}_{\rho\pi}^{+-}$ and $\mathcal{A}_{\rho\pi}^{-+}$, defined in Eq. (135), deviating from zero. Results and averages for these parameters are also given in Table 39. Averages of the direct CP violation effect in $B^0 \to \rho^\pm\pi^\mp$ are shown in Fig. 32, both in $\mathcal{A}_{CP}^{\rho\pi}$ *vs.* $C_{\rho\pi}$ space and in $\mathcal{A}_{\rho\pi}^{-+}$ *vs.* $\mathcal{A}_{\rho\pi}^{+-}$ space.

Some difference is seen between the *BABAR* and Belle measurements in the $\pi^+\pi^-$ system. The confidence level of the average is 0.034, which corresponds to a 2.1σ discrepancy. Since there is no evidence of systematic problems in either analysis, we do not rescale the errors of

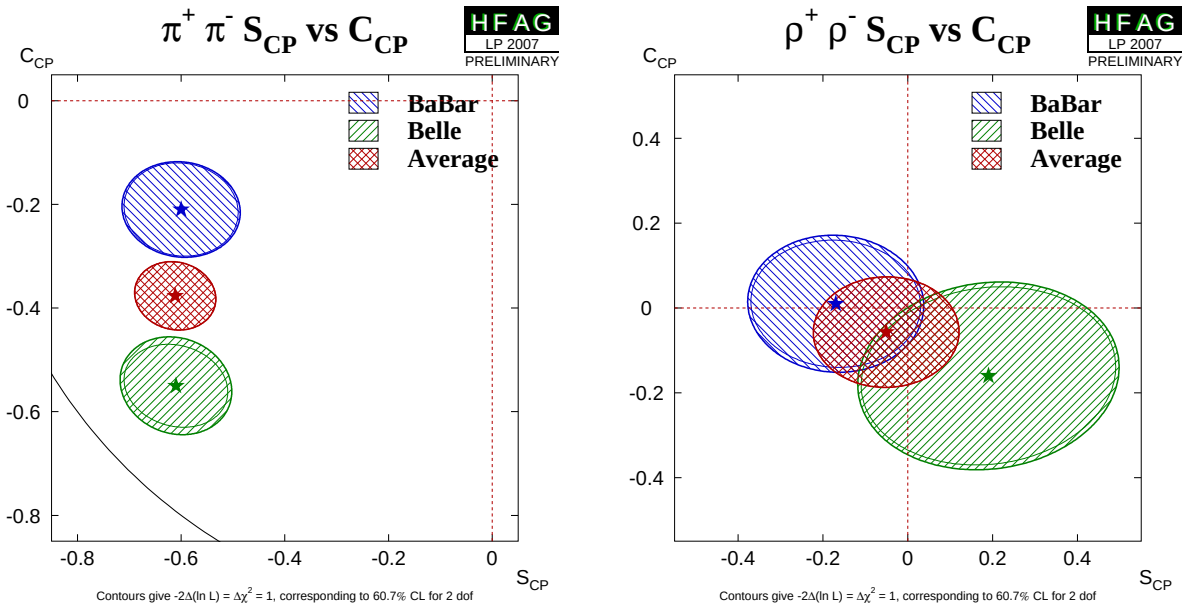

Figure 28: Averages of $b \to u\overline{u}d$ dominated channels, for which correlated averages are performed, in the S_{CP} *vs.* C_{CP} plane. (Left) $B^0 \to \pi^+\pi^-$ and (right) $B^0 \to \rho^+\rho^-$.

the averages. The averages for $S_{b\to u\overline{u}d}$ and $C_{b\to u\overline{u}d}$ in $B^0 \to \pi^+\pi^-$ are both more than 5σ away from zero, suggesting that both mixing-induced and direct *CP* violation are well-established in this channel. Nonetheless, due to the possible discrepancy mentioned above, a slightly cautious interpretation should be made with regard to the significance of direct *CP* violation.

In $B^0 \to \rho^\pm\pi^\mp$, however, both experiments see an indication of direct *CP* violation in the $\mathcal{A}_{CP}^{\rho\pi}$ parameter (as seen in Fig. 32). The average is more than 3σ from zero, providing evidence of direct *CP* violation in this channel.

Constraints on α

The precision of the measured *CP* violation parameters in $b \to u\overline{u}d$ transitions allows constraints to be set on the UT angle α. Constraints have been obtained with various methods:

- Both *BABAR* [360] and Belle [347] have performed isospin analyses in the $\pi\pi$ system. Belle exclude $9^\circ < \phi_2 < 81^\circ$ at the 95.4% C.L. while *BABAR* give a confidence level interpretation for α, exclude the range $25^\circ < \alpha < 66^\circ$ at the 90% C.L., and find the solution consistent with the Standard Model to be $\alpha = (96^{+10}_{-6})^\circ$. In both cases, only solutions in 0°–180° are considered.

- Both experiments have also performed isospin analyses in the $\rho\rho$ system. *BABAR* [348] find $\alpha \in [73.1, 117.0]^\circ$ at 68% C.L. while Belle [350] obtain $54^\circ < \phi_2 < 113^\circ$ at 90% confidence level. The largest contribution to the uncertainty is due to the possible penguin contribution, limited by the knowledge of the $B^0 \to \rho^0\rho^0$ branching fraction and is correlated between the measurements. In the *BABAR* [351] study of $B^0 \to \rho^0\rho^0$, a constraint of $|\alpha - \alpha^{\rm eff}| < 14.5^\circ$ (16.5°) is obtained at 68% (90%) CL. The solution at $\alpha - \alpha^{\rm eff} = +11.3^\circ$ is preferred.

- The time-dependent Dalitz plot analysis of the $B^0 \to \pi^+\pi^-\pi^0$ decay allows a determi-

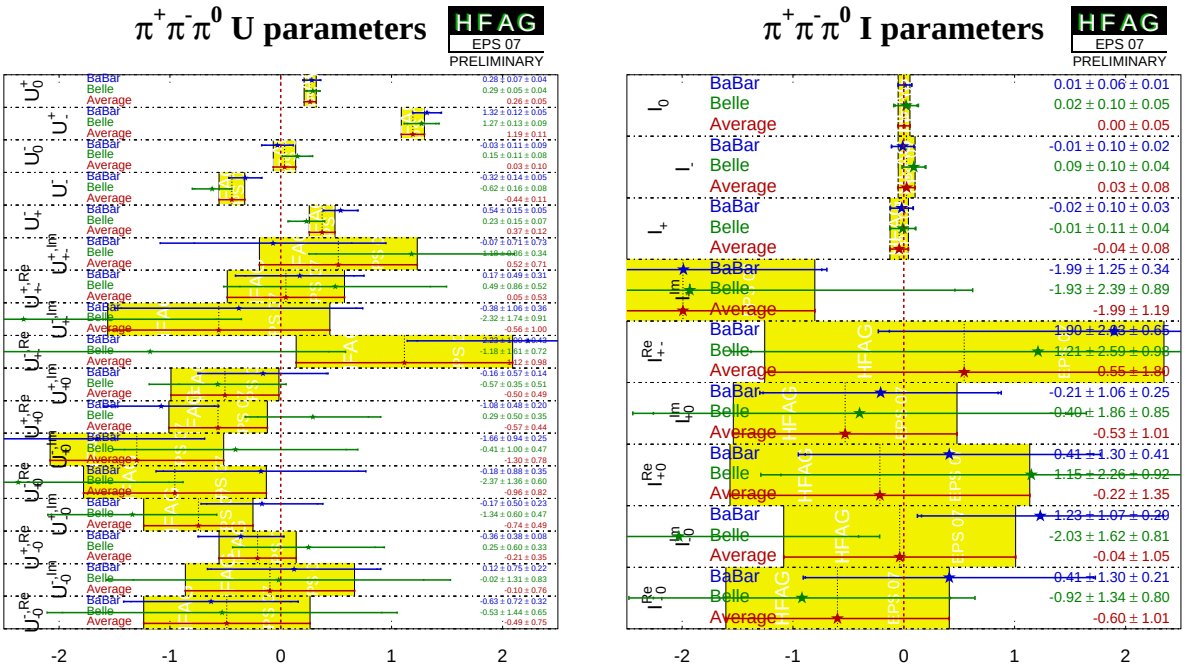

Figure 29: Summary of the U and I parameters measured in the time-dependent $B^0 \to \pi^+\pi^-\pi^0$ Dalitz plot analysis.

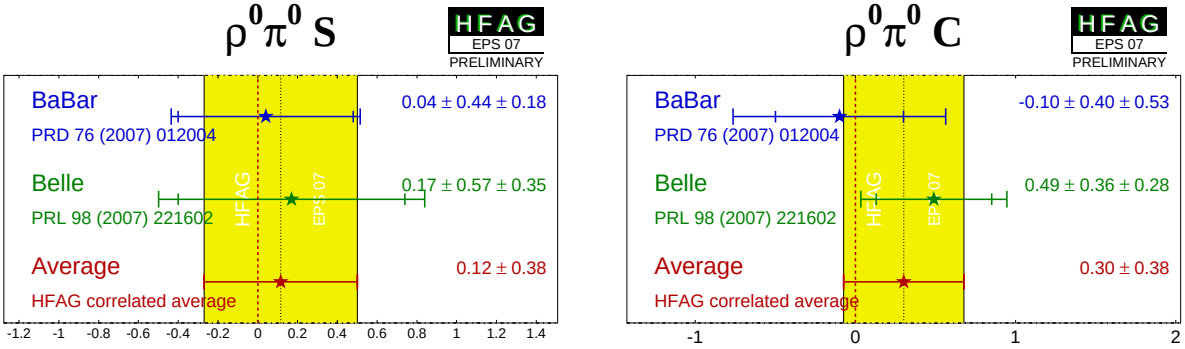

Figure 30: Averages of (left) $S_{b\to u\overline{u}d}$ and (right) $C_{b\to u\overline{u}d}$ for the mode $B^0 \to \rho^0\pi^0$.

nation of α without input from any other channels. *BABAR* [354] obtain the constraint $75^\circ < \alpha < 152^\circ$ at 68% C.L. Belle [355, 356] have performed a similar analysis, and in addition have included information from the SU(2) partners of $B \to \rho\pi$, which can be used to constrain α via an isospin pentagon relation [359]. With this analysis, Belle obtain the tighter constraint $\phi_2 = (83\,^{+12}_{-23})^\circ$ (where the errors correspond to 1σ, *i.e.* 68.3% confidence level).

- Each experiment has obtained a value of α from combining its results in the different $b \to u\overline{u}d$ modes (with some input also from HFAG). These values have appeared in talks, but not in publications, and are not listed here.

Table 39: Averages of quasi-two-body parameters extracted from time-dependent Dalitz plot analysis of $B^0 \to \pi^+\pi^-\pi^0$.

Experiment	$N(B\overline{B})$	$\mathcal{A}_{CP}^{\rho\pi}$	$C_{\rho\pi}$	$S_{\rho\pi}$	$\Delta C_{\rho\pi}$	$\Delta S_{\rho\pi}$
BABAR [354]	375M	$-0.14 \pm 0.05 \pm 0.02$	$0.15 \pm 0.09 \pm 0.05$	$-0.03 \pm 0.11 \pm 0.04$	$0.39 \pm 0.09 \pm 0.09$	$-0.01 \pm 0.14 \pm 0.06$
Belle [355, 356]	449M	$-0.12 \pm 0.05 \pm 0.04$	$-0.13 \pm 0.09 \pm 0.05$	$0.06 \pm 0.13 \pm 0.05$	$0.36 \pm 0.10 \pm 0.05$	$-0.08 \pm 0.13 \pm 0.05$
Average		-0.13 ± 0.04	0.01 ± 0.07	0.01 ± 0.09	0.37 ± 0.08	-0.04 ± 0.10
Confidence level				0.52 (0.6σ)		

Experiment	$N(B\overline{B})$	$\mathcal{A}_{\rho\pi}^{-+}$	$\mathcal{A}_{\rho\pi}^{+-}$	Correlation
BABAR [354]	375M	$-0.37\,^{+0.16}_{-0.10} \pm 0.09$	$0.03 \pm 0.07 \pm 0.04$	0.62
Belle [355, 356]	449M	$0.08 \pm 0.16 \pm 0.11$	$0.21 \pm 0.08 \pm 0.04$	0.47
Average		-0.18 ± 0.12	0.11 ± 0.06	0.40
Confidence level			0.14 (1.5σ)	

Experiment	$N(B\overline{B})$	$C_{\rho^0\pi^0}$	$S_{\rho^0\pi^0}$	Correlation
BABAR [354]	375M	$-0.10 \pm 0.40 \pm 0.53$	$0.04 \pm 0.44 \pm 0.18$	0.35
Belle [355, 356]	449M	$0.49 \pm 0.36 \pm 0.28$	$0.17 \pm 0.57 \pm 0.35$	0.08
Average		0.30 ± 0.38	0.12 ± 0.38	0.12
Confidence level			0.76 (0.3σ)	

- The CKMfitter [271] and UTFit [272] groups use the measurements from Belle and *BABAR* given above with other branching fractions and *CP* asymmetries in $B \to \pi\pi$, $\rho\pi$ and $\rho\rho$ modes, to perform isospin analyses for each system, and to make combined constraints on α.

Note that methods based on isospin symmetry make extensive use of measurements of branching fractions and direct *CP* asymmetries, as averaged by the HFAG Rare Decays subgroup (Sec. 7). Note also that each method suffers from discrete ambiguities in the solutions. The model assumption in the $B^0 \to \pi^+\pi^-\pi^0$ analysis allows to resolve some of the multiple solutions, and results in a single preferred value for α in $[0, \pi]$. All the above measurements correspond to the choice that is in agreement with the global CKM fit.

At present we make no attempt to provide an HFAG average for α. More details on procedures to calculate a best fit value for α can be found in Refs. [271, 272].

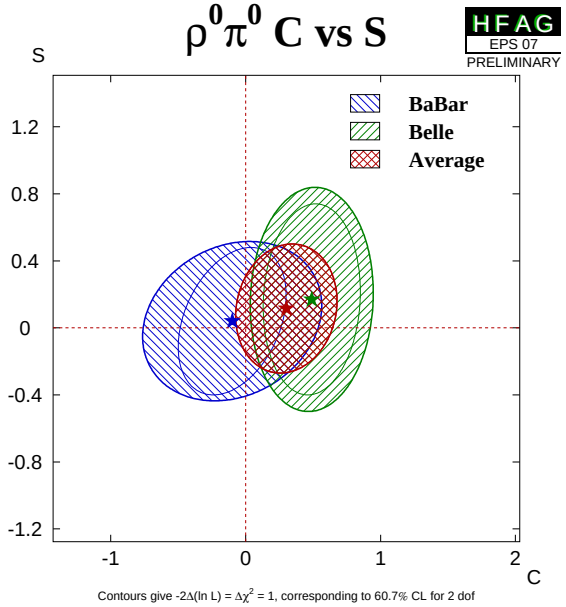

Figure 31: Averages of $b \to u\overline{u}d$ dominated channels, for the mode $B^0 \to \rho^0\pi^0$ in the S_{CP} *vs.* C_{CP} plane.

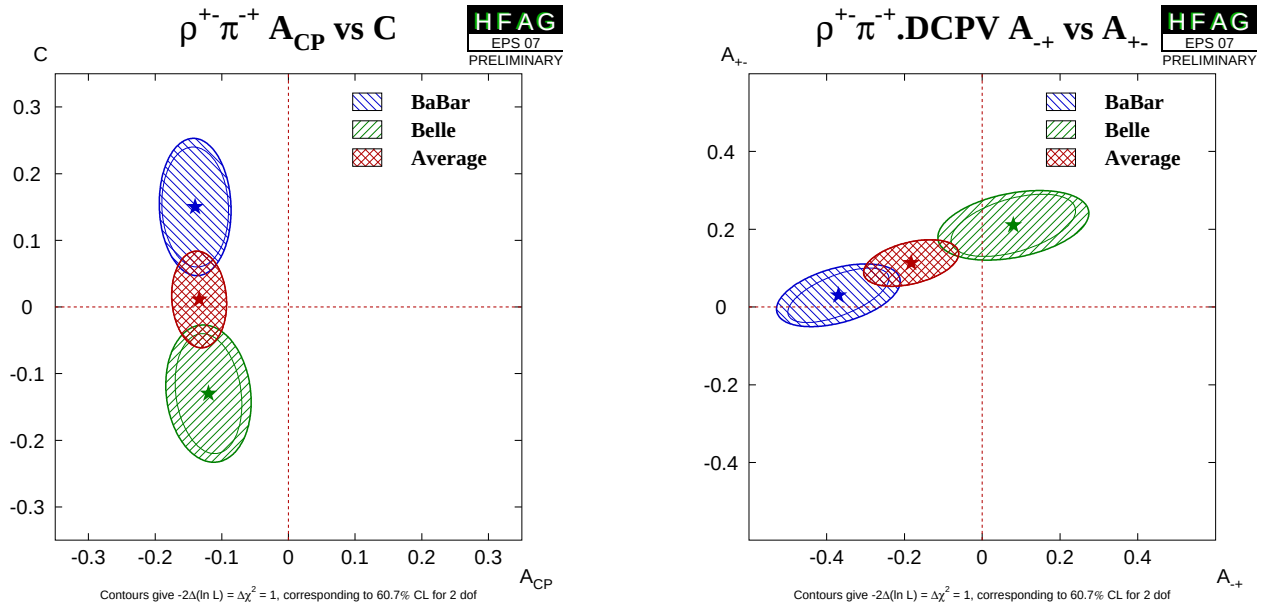

Figure 32: Direct CP violation in $B^0 \to \rho^{\pm}\pi^{\mp}$. (Left) $\mathcal{A}_{CP}^{\rho\pi}$ *vs.* $C_{\rho\pi}$ space, (right) $\mathcal{A}_{\rho\pi}^{-+}$ *vs.* $\mathcal{A}_{\rho\pi}^{+-}$ space.

4.12 Time-dependent *CP* asymmetries in $b \to c\bar{u}d/u\bar{c}d$ transitions

Non-*CP* eigenstates such as $D^{\pm}\pi^{\mp}$, $D^{*\pm}\pi^{\mp}$ and $D^{\pm}\rho^{\mp}$ can be produced in decays of B^0 mesons either via Cabibbo favoured ($b \to c$) or doubly Cabibbo suppressed ($b \to u$) tree amplitudes. Since no penguin contribution is possible, these modes are theoretically clean. The ratio of the magnitudes of the suppressed and favoured amplitudes, R, is sufficiently small (predicted to be about 0.02), that terms of $\mathcal{O}(R^2)$ can be neglected, and the sine terms give sensitivity to the combination of UT angles $2\beta + \gamma$.

As described in Sec. 4.2.5, the averages are given in terms of parameters a and c. *CP* violation would appear as $a \neq 0$. Results are available from both *BABAR* and Belle in the modes $D^{\pm}\pi^{\mp}$ and $D^{*\pm}\pi^{\mp}$; for the latter mode both experiments have used both full and partial reconstruction techniques. (*BABAR* have provided separate results with each technique, while Belle have in addition provided a combined result.) Results are also available from *BABAR* using $D^{\pm}\rho^{\mp}$. These results, and their averages, are listed in Table 40, and are shown in Fig. 33. The constraints in c *vs.* a space for the $D\pi$ and $D^*\pi$ modes are shown in Fig. 34. It is notable that the average value of a from $D^*\pi$ is more than 3σ from zero, providing evidence of *CP* violation in this channel.

Table 40: Averages for $b \to c\bar{u}d/u\bar{c}d$ modes. Note that the "Belle (combined)" result for $D^{*\pm}\pi^{\mp}$ is a combination of the "Belle (full rec.)" and "Belle (partial rec.)" results.

Experiment		$N(B\overline{B})$	a	c
			$D^{\pm}\pi^{\mp}$	
BABAR (full rec.)	[361]	232M	$-0.010 \pm 0.023 \pm 0.007$	$-0.033 \pm 0.042 \pm 0.012$
Belle (full rec.)	[362]	386M	$-0.050 \pm 0.021 \pm 0.012$	$-0.019 \pm 0.021 \pm 0.012$
Average			-0.030 ± 0.017	-0.022 ± 0.021
Confidence level			0.24 (1.2σ)	0.78 (0.3σ)
			$D^{*\pm}\pi^{\mp}$	
BABAR (full rec.)	[361]	232M	$-0.040 \pm 0.023 \pm 0.010$	$0.049 \pm 0.042 \pm 0.015$
BABAR (partial rec.)	[363]	232M	$-0.034 \pm 0.014 \pm 0.009$	$-0.019 \pm 0.022 \pm 0.013$
Belle (full rec.)	[362]	386M	$-0.039 \pm 0.020 \pm 0.013$	$-0.011 \pm 0.020 \pm 0.013$
Belle (partial rec.)	[362]	386M	$-0.041 \pm 0.019 \pm 0.017$	$-0.007 \pm 0.019 \pm 0.017$
Belle (combined)	[362]	386M	$-0.040 \pm 0.014 \pm 0.011$	$-0.009 \pm 0.014 \pm 0.011$
Average			-0.037 ± 0.011	-0.006 ± 0.014
Confidence level			0.96 (0.0σ)	0.41 (0.8σ)
			$D^{\pm}\rho^{\mp}$	
BABAR (full rec.)	[361]	232M	$-0.024 \pm 0.031 \pm 0.009$	$-0.098 \pm 0.055 \pm 0.018$

For each of $D\pi$, $D^*\pi$ and $D\rho$, there are two measurements (a and c, or S^+ and S^-) which depend on three unknowns (R, δ and $2\beta + \gamma$), of which two are different for each decay mode. Therefore, there is not enough information to solve directly for $2\beta + \gamma$. However, for each choice of R and $2\beta + \gamma$, one can find the value of δ that allows a and c to be closest to their measured values, and calculate the distance in terms of numbers of standard deviations. (We currently neglect experimental correlations in this analysis.) These values of $N(\sigma)_{\rm min}$ can then be plotted as a function of R and $2\beta + \gamma$ (and can trivially be converted to confidence levels).

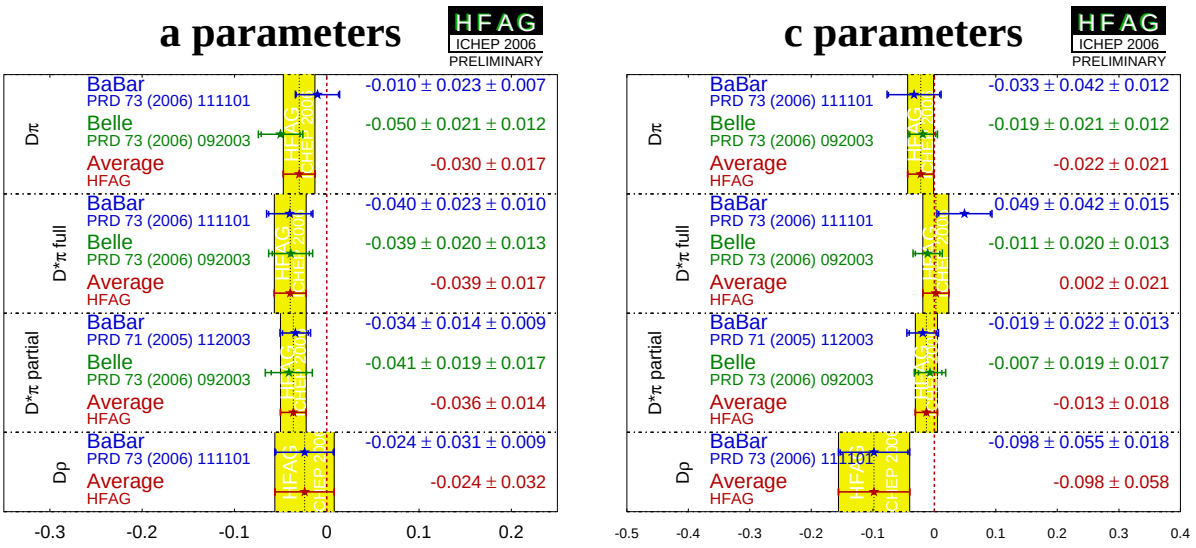

Figure 33: Averages for $b \to c\overline{u}d/u\overline{c}d$ modes.

These plots are given for the $D\pi$ and $D^*\pi$ modes in Figure 34; the uncertainties in the $D\rho$ mode are currently too large to give any meaningful constraint.

The constraints can be tightened if one is willing to use theoretical input on the values of R and/or δ. One popular choice is the use of SU(3) symmetry to obtain R by relating the suppressed decay mode to B decays involving D_s mesons. More details can be found in Refs. [271, 272].

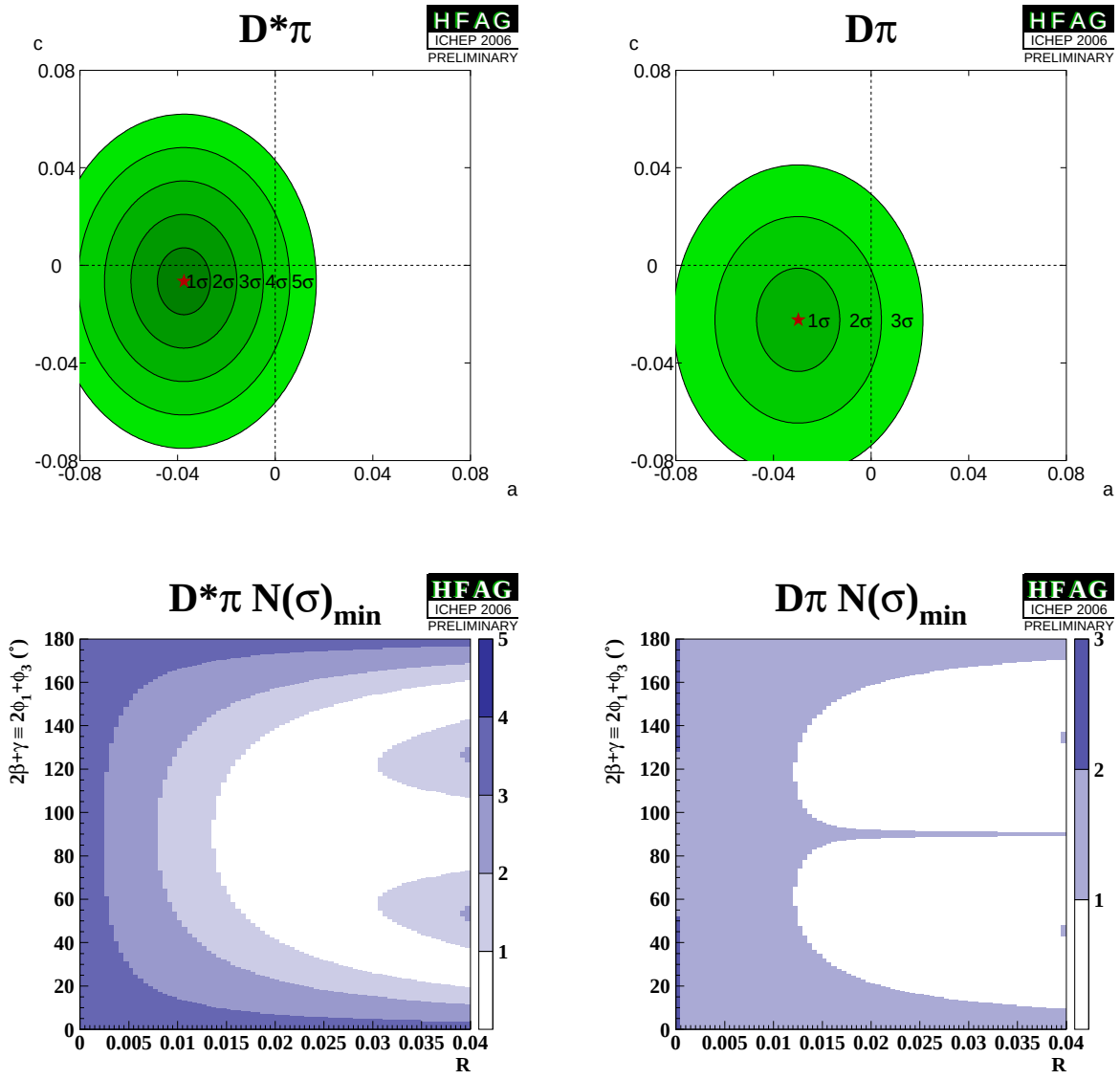

Figure 34: Results from $b \to c\bar{u}d/u\bar{c}d$ modes. (Top) Constraints in c *vs.* a space. (Bottom) Constraints in $2\beta + \gamma$ *vs.* R space. (Left) $D^*\pi$ and (right) $D\pi$ modes.

4.13 Rates and asymmetries in $B^{\mp} \to D^{(*)}K^{(*)\mp}$ decays

As explained in Sec. 4.2.7, rates and asymmetries in $B^{\mp} \to D^{(*)}K^{(*)\mp}$ decays are sensitive to γ. Various methods using different $D^{(*)}$ final states exist.

4.13.1 D decays to CP eigenstates

Results are available from both *BABAR* and Belle on GLW analyses in the decay modes $B^{\mp} \to DK^{\mp}$, $B^{\mp} \to D^*K^{\mp}$ and $B^{\mp} \to DK^{*\mp}$. Both experiments use the CP-even D decay final states K^+K^- and $\pi^+\pi^-$ in all three modes; both experiments also use only the $D^* \to D\pi^0$ decay, which gives $CP(D^*) = CP(D)$. For CP-odd D decay final states, Belle uses $K^0_S\pi^0$, $K^0_S\eta$ and $K^0_S\phi$ in all three analyses, and also use $K^0_S\omega$ in $DK^{\mp}$ and $D^*K^{\mp}$ analyses. *BABAR* uses $K^0_S\pi^0$ only for $DK^{\mp}$ analysis; for $DK^{*\mp}$ analysis they also use $K^0_S\phi$ and $K^0_S\omega$ (and assign an asymmetric systematic error due to CP-even pollution in these CP-odd channels [381]). The results and averages are given in Table 41 and shown in Fig. 35.

Table 41: Averages from GLW analyses of $b \to c\overline{u}s/u\overline{c}s$ modes.

Experiment	$N(B\overline{B})$	A_{CP+}	A_{CP-}	R_{CP+}	R_{CP-}
			$D_{CP}K^-$		
BABAR [379]	382M	$0.35 \pm 0.09 \pm 0.05$	$-0.19 \pm 0.12 \pm 0.02$	$1.07 \pm 0.10 \pm 0.04$	$0.81 \pm 0.10 \pm 0.05$
Belle [380]	275M	$0.06 \pm 0.14 \pm 0.05$	$-0.12 \pm 0.14 \pm 0.05$	$1.13 \pm 0.16 \pm 0.08$	$1.17 \pm 0.14 \pm 0.14$
Average		0.26 ± 0.08	-0.16 ± 0.09	1.09 ± 0.09	0.90 ± 0.10
Confidence level		0.11 (1.6σ)	0.72 (0.4σ)	0.77 (0.3σ)	0.11 (1.6σ)
			$D^*_{CP}K^-$		
BABAR [381]	123M	$-0.10 \pm 0.23^{+0.03}_{-0.04}$	–	$1.06 \pm 0.26^{+0.10}_{-0.09}$	–
Belle [380]	275M	$-0.20 \pm 0.22 \pm 0.04$	$0.13 \pm 0.30 \pm 0.08$	$1.41 \pm 0.25 \pm 0.06$	$1.15 \pm 0.31 \pm 0.12$
Average		-0.15 ± 0.16	0.13 ± 0.31	1.25 ± 0.19	1.15 ± 0.33
Confidence level		0.76 (0.3σ)	–	0.36 (0.9σ)	–
			$\mathcal{D}_{CP}K^{*-}$		
BABAR [382]	232M	$-0.08 \pm 0.19 \pm 0.08$	$-0.26 \pm 0.40 \pm 0.12$	$1.96 \pm 0.40 \pm 0.11$	$0.65 \pm 0.26 \pm 0.08$

4.13.2 D decays to suppressed final states

For ADS analysis, both *BABAR* and Belle have studied the mode $B^{\mp} \to DK^{\mp}$; Belle has also studied $B^{\mp} \to D\pi^{\mp}$ and *BABAR* has also analyzed the $B^{\mp} \to D^*K^{\mp}$ and $B^{\mp} \to DK^{*\mp}$ modes ($D^* \to D\pi^0$ and $D^* \to D\gamma$ are studied separately; $K^{*\mp}$ is reconstructed as $K^0_S\pi^{\mp}$). In all cases the suppressed decay $D \to K^+\pi^-$ has been used. *BABAR* also has results using $B^{\mp} \to DK^{\mp}$ with $D \to K^+\pi^-\pi^0$. The results and averages are given in Table 42 and shown in Fig. 36. Note that although no clear signals for these modes have yet been seen, the central values are given. In $B^- \to D^*K^-$ decays there is an effective shift of π in the strong phase difference between the cases that the D^* is reconstructed as $D\pi^0$ and $D\gamma$ [378]. As a consequence, the different D^* decay modes are treated separately.

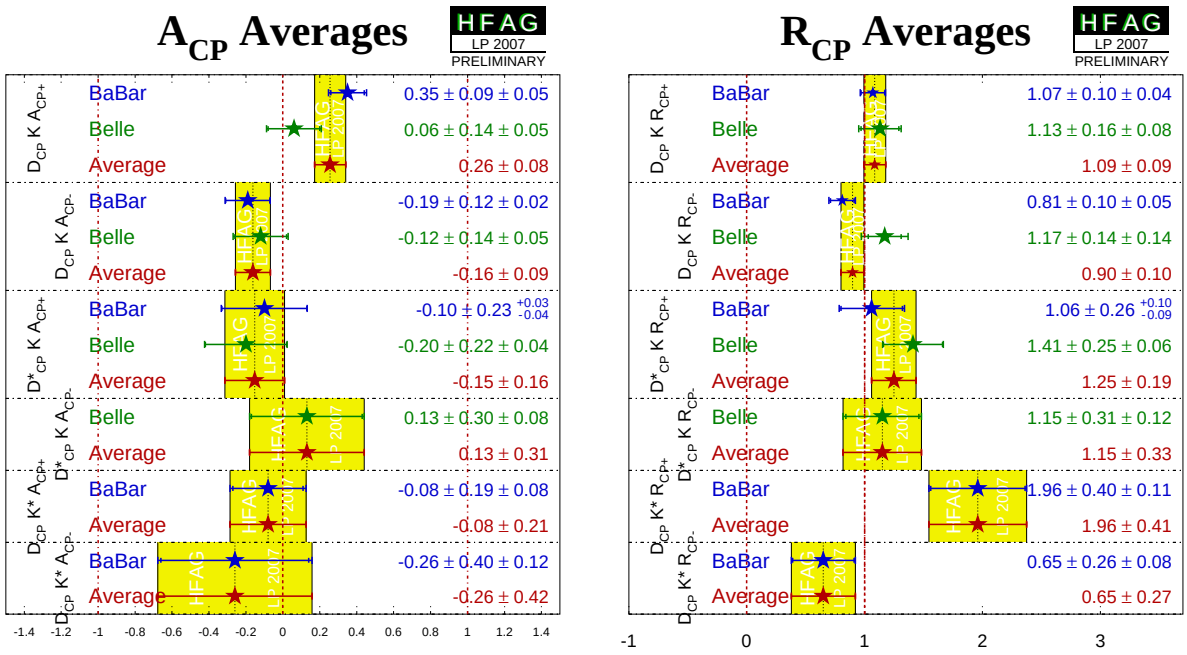

Figure 35: Averages of A_{CP} and R_{CP} from GLW analyses.

4.13.3 *D* decays to multiparticle self-conjugate final states

For the Dalitz plot analysis, both *BABAR* [388] and Belle [389] have studied the modes $B^{\mp} \to DK^{\mp}$, $B^{\mp} \to D^*K^{\mp}$ and $B^{\mp} \to DK^{*\mp}$. For $B^{\mp} \to D^*K^{\mp}$, Belle has used only $D^* \to D\pi^0$, while *BABAR* has used both D^* decay modes and taken the effective shift in the strong phase difference into account. In all cases the decay $D \to K^0_S\pi^+\pi^-$ has been used. *BABAR* has also performed an analysis of $B^{\mp} \to DK^{\mp}$ with $D \to \pi^+\pi^-\pi^0$ [391]. Results and averages are given in Table 43. The third error on each measurement is due to D decay model uncertainty.

The parameters measured in the analyses are explained in Sec. 4.2.7. Both *BABAR* and Belle have measured the "Cartesian" $(x_{\pm}, y_{\pm})$ variables, and perform frequentist statistical procedures, to convert these into measurements of γ, r_B and δ_B. In the $B^{\mp} \to DK^{\mp}$ with $D \to \pi^+\pi^-\pi^0$ analysis, the parameters $(\rho^{\pm}, \theta^{\pm})$ are used instead.

Both experiments reconstruct $K^{*\mp}$ as $K^0_S\pi^{\mp}$, but the treatment of possible nonresonant $K^0_S\pi^{\mp}$ differs: Belle assign an additional model uncertainty, while *BABAR* use a reparametrization suggested by Gronau [387]. The parameters r_B and δ_B are replaced with effective parameters κr_s and δ_s; no attempt is made to extract the true hadronic parameters of the $B^{\mp} \to DK^{*\mp}$ decay.

We perform averages using the following procedure, which is based on a set of reasonable, though imperfect, assumptions.

- It is assumed that effects due to the different D decay models used by the two experiments are negligible. Therefore, we do not rescale the results to a common model.
- It is further assumed that the model uncertainty is 100% correlated between experiments, and therefore this source of error is not used in the averaging procedure.

Table 42: Averages from ADS analyses of $b \to c\overline{u}s/u\overline{c}s$ and $b \to c\overline{u}d/u\overline{c}d$ modes.

Experiment		$N(B\overline{B})$	$A_{\rm ADS}$	$R_{\rm ADS}$
		DK^-, $D \to K^+\pi^-$		
BABAR	[383]	232M	–	$0.013\,^{+0.011}_{-0.009}$
Belle	[384]	386M	–	$0.000 \pm 0.008 \pm 0.001$
Average			–	0.006 ± 0.006
Confidence level			–	0.29 (1.1σ)
		D^*K^-, $D^* \to D\pi^0$, $D \to K^+\pi^-$		
BABAR	[383]	232M	–	$-0.002\,^{+0.010}_{-0.006}$
		D^*K^-, $D^* \to D\gamma$, $D \to K^+\pi^-$		
BABAR	[383]	232M	–	$0.011\,^{+0.018}_{-0.013}$
		DK^{*-}, $D \to K^+\pi^-$, $K^{*-} \to K^0_S\pi^-$		
BABAR	[385]	232M	$-0.22 \pm 0.61 \pm 0.17$	$0.046 \pm 0.031 \pm 0.008$
		DK^-, $D \to K^+\pi^-\pi^0$		
BABAR	[386]	226M	–	$0.012 \pm 0.012 \pm 0.009$
		$D\pi^-$, $D \to K^+\pi^-$		
Belle	[384]	386M	$0.10 \pm 0.22 \pm 0.06$	$0.0035\,^{+0.0008}_{-0.0007} \pm 0.0003$

- We include in the average the effect of correlations within each experiments set of measurements.
- At present it is unclear how to assign an average model uncertainty. We have not attempted to do so. Our average includes only statistical and systematic error. An unknown amount of model uncertainty should be added to the final error.
- We follow the suggestion of Gronau [387] in making the DK^* averages. Explicitly, we assume that the selection of $K^{*\pm} \to K^0_S\pi^\pm$ is the same in both experiments (so that κ, r_s and δ_s are the same), and drop the additional source of model uncertainty assigned by Belle due to possible nonresonant decays.
- We do not consider common systematic errors, other than the D decay model.

Constraints on γ

The measurements of $(x_\pm, y_\pm)$ can be used to obtain constraints on γ, as well as the hadronic parameters r_B and δ_B. Both *BABAR* [388] and Belle [389] have done so using a frequentist procedure (there are some differences in the details of the techniques used).

- *BABAR* obtain $\gamma = (92 \pm 41 \pm 11 \pm 12)^\circ$ from $DK^\pm$ and $D^*K^\pm$
- Belle obtain $\phi_3 = (53\,^{+15}_{-18} \pm 3 \pm 9)^\circ$ from $DK^\pm$, $D^*K^\pm$ and $DK^{*\pm}$
- The experiments also obtain values for the hadronic parameters.
  In $DK^\pm$
  BABAR obtain $r_B(DK^\pm) < 0.140(1\sigma)$ and $\delta_B(DK^\pm) = (118 \pm 63 \pm 19 \pm 36)^\circ$
  Belle obtain $r_B(DK^\pm) = 0.16 \pm 0.05 \pm 0.01 \pm 0.05$ and $\delta_B(DK^\pm) = (146\,^{+19}_{-20} \pm 3 \pm 23)^\circ$.

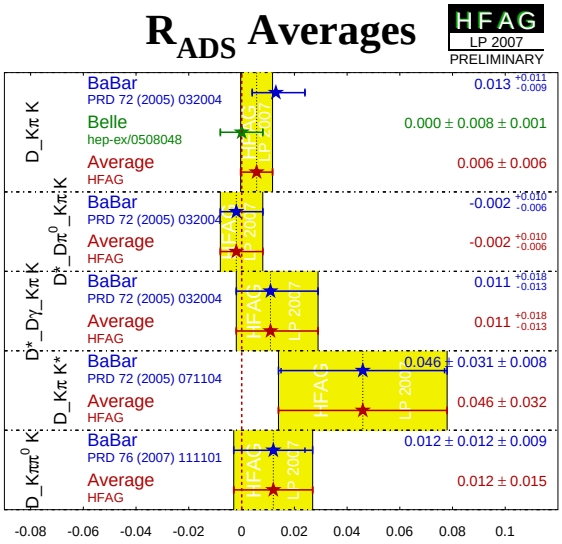

Figure 36: Averages of $R_{\rm ADS}$.

Table 43: Averages from Dalitz plot analyses of $b \to c\bar{u}s/u\bar{c}s$ modes. Note that the uncertainities assigned to the averages do not include model errors.

Experiment	$N(B\overline{B})$	x_+	y_+	x_-	y_-
		DK^-, $D \to K^0_S\pi^+\pi^-$			
BABAR [388]	347M	$-0.072 \pm 0.056 \pm 0.014 \pm 0.029$	$-0.033 \pm 0.066 \pm 0.007 \pm 0.018$	$0.041 \pm 0.059 \pm 0.018 \pm 0.011$	$0.056 \pm 0.071 \pm 0.007 \pm 0.023$
Belle [389]	386M	$-0.135^{+0.069}_{-0.070} \pm 0.017 \pm 0.051$	$-0.085^{+0.090}_{-0.086} \pm 0.009 \pm 0.066$	$0.025^{+0.072}_{-0.080} \pm 0.013 \pm 0.068$	$0.170^{+0.093}_{-0.117} \pm 0.016 \pm 0.049$
Average		-0.097 ± 0.045	-0.051 ± 0.053	0.045 ± 0.047	0.093 ± 0.058
Confidence level			0.83 (0.2σ)		
		D^*K^-, $D^* \to D\pi^0$ or $D\gamma$, $D \to K^0_S\pi^+\pi^-$			
BABAR [388]	347M	$0.084 \pm 0.088 \pm 0.015 \pm 0.018$	$0.096 \pm 0.111 \pm 0.032 \pm 0.017$	$-0.106 \pm 0.091 \pm 0.020 \pm 0.009$	$-0.019 \pm 0.096 \pm 0.022 \pm 0.016$
Belle [389]	386M	$0.032^{+0.120}_{-0.116} \pm 0.004 \pm 0.049$	$0.008^{+0.137}_{-0.136} \pm 0.011 \pm 0.074$	$-0.128^{+0.167}_{-0.146} \pm 0.023 \pm 0.071$	$-0.339^{+0.172}_{-0.158} \pm 0.027 \pm 0.053$
Average		0.067 ± 0.071	0.061 ± 0.088	-0.110 ± 0.080	-0.101 ± 0.085
Confidence level			0.52 (0.6σ)		
		DK^{*-}, $D \to K^0_S\pi^+\pi^-$			
BABAR [390]	227M	$-0.070 \pm 0.230 \pm 0.130 \pm 0.030$	$-0.010 \pm 0.320 \pm 0.180 \pm 0.050$	$-0.200 \pm 0.200 \pm 0.110 \pm 0.030$	$0.260 \pm 0.300 \pm 0.160 \pm 0.030$
Belle [389]	386M	$-0.105^{+0.177}_{-0.167} \pm 0.006 \pm 0.088$	$-0.004^{+0.164}_{-0.156} \pm 0.013 \pm 0.095$	$-0.784^{+0.249}_{-0.295} \pm 0.029 \pm 0.097$	$-0.281^{+0.440}_{-0.335} \pm 0.046 \pm 0.086$
Average		-0.094 ± 0.144	-0.007 ± 0.146	-0.480 ± 0.173	-0.056 ± 0.253
Confidence level			0.33 (1.0σ)		
Experiment	$N(B\overline{B})$	ρ^+	θ^+	ρ^-	θ^-
			DK^-, $D \to \pi^+\pi^-\pi^0$		
BABAR [391]	324M	$0.75 \pm 0.11 \pm 0.04$	$147 \pm 23 \pm 1$	$0.72 \pm 0.11 \pm 0.04$	$173 \pm 42 \pm 2$

In $D^*K^\pm$
BABAR obtain $0.017 < r_B(D^*K^\pm) < 0.203$ and $\delta_B(D^*K^\pm) = (298 \pm 59 \pm 18 \pm 10)^\circ$
Belle obtain $r_B(D^*K^\pm) = 0.18^{+0.11}_{-0.10} \pm 0.01 \pm 0.05$ and $\delta_B(D^*K^\pm) = (302^{+34}_{-35} \pm 6 \pm 23)^\circ$.
In $DK^{*\pm}$
Belle obtain $r_B(DK^{*\pm}) = 0.56^{+0.22}_{-0.16} \pm 0.04 \pm 0.08$ and $\delta_B(DK^{*\pm}) = (243^{+20}_{-23} \pm 3 \pm 50)^\circ$.
BABAR do not obtain a constraint on the hadronic parameters in $DK^{*\pm}$ due to the reparametrization described above.

- Improved constraints can be achieved combining the information from $B^\pm \to DK^\pm$ analysis with different D decay modes. The experiments have not yet published such results,

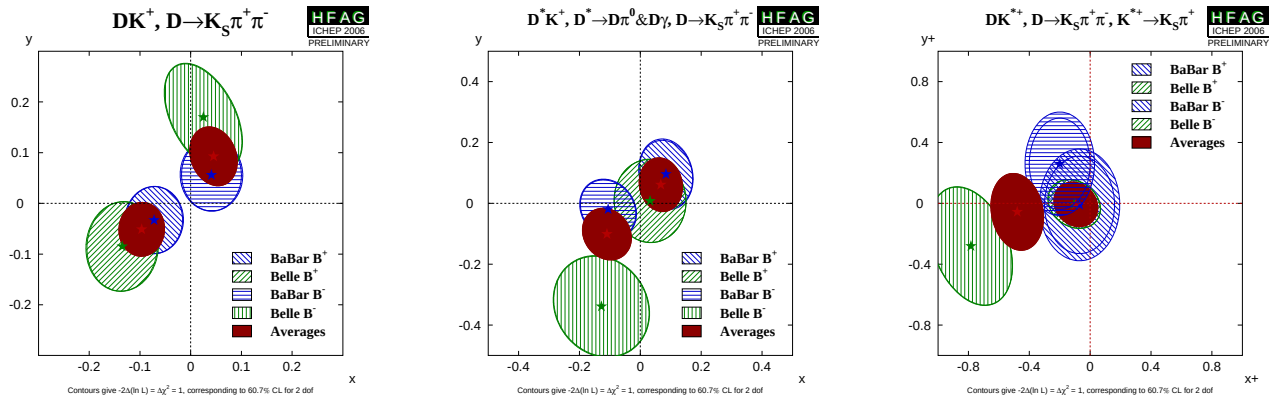

Figure 37: Contours in the $(x_\pm, y_\pm)$ from $B^\mp \to D^{(*)}K^{(*)\pm}$. (Left) $B^\mp \to DK^\mp$, (middle) $B^\mp \to D^*K^\mp$, (right) $B^\mp \to DK^{*\mp}$. Note that the uncertainities assigned to the averages given in these plots do not include model errors.

and none are listed here.

- The CKMfitter [271] and UTFit [272] groups use the measurements from Belle and *BABAR* given above to make combined constraints on γ.
- In the *BABAR* analysis of $B^\mp \to DK^\mp$ with $D \to \pi^+\pi^-\pi^0$ [391], a constraint of $-30° < \gamma < 76°$ is obtained at the 68% confidence level.

At present we make no attempt to provide an HFAG average for γ. More details on procedures to calculate a best fit value for γ can be found in Refs. [271, 272].

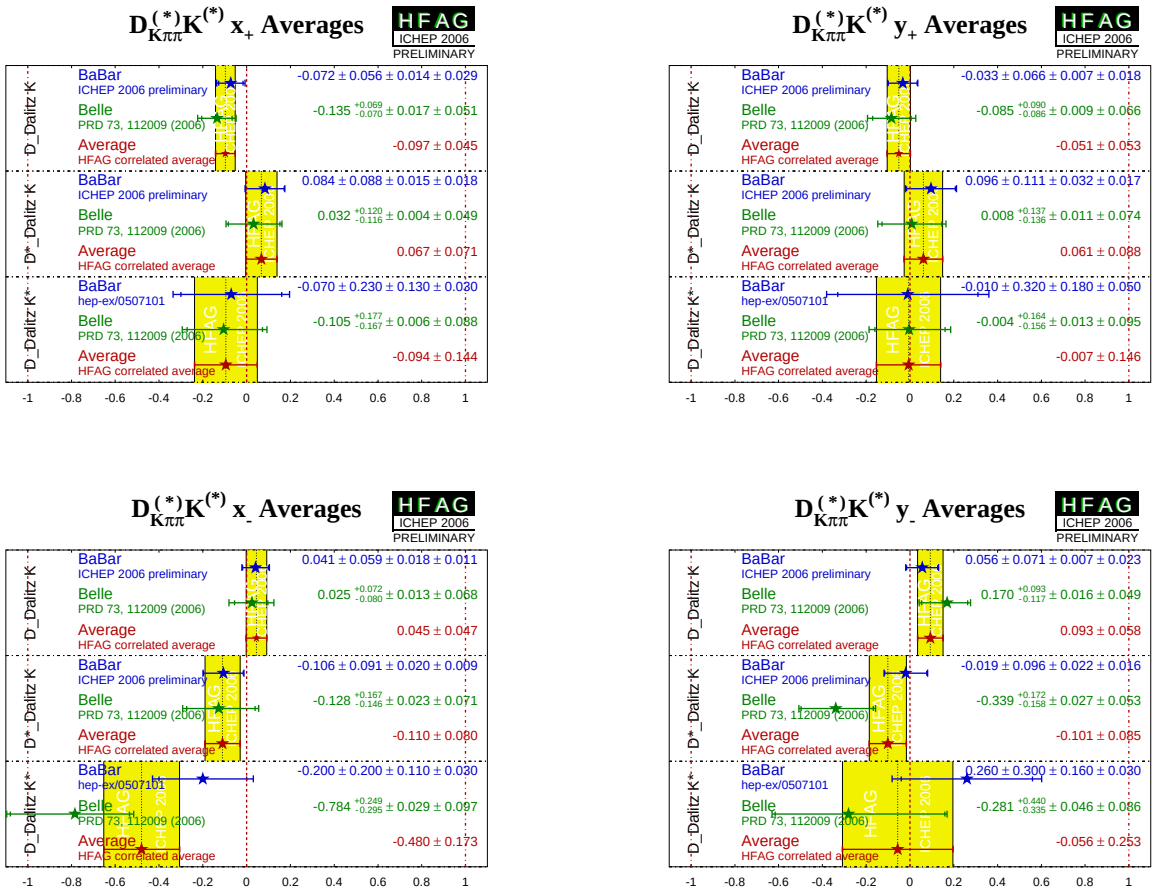

Figure 38: Averages of $(x_\pm, y_\pm)$ from $B^\mp \to D^{(*)}K^{(*)\pm}$. (Top left) x_+, (top right) y_+, (bottom left) x_-, (bottom right) y_-. Note that the uncertainities assigned to the averages given in these plots do not include model errors.

5 Semileptonic B decays

Measurements of semileptonic B-meson decays are an important tool to study the magnitude of the CKM matrix elements $|V_{cb}|$ and $|V_{ub}|$, the Heavy Quark parameters (e.g. b and c–quark masses), QCD form factors, QCD dynamics, new physics, etc.

In the following, we provide averages of exclusive and inclusive branching fractions, the product of $|V_{cb}|$ and the form factor normalisation $F(1)$ and $G(1)$ for $B^0 \to D^{*-}\ell^+\nu$ and $B^0 \to D^-\ell^+\nu$ decays, respectively, and $|V_{ub}|$ as determined from inclusive and exclusive measurements of $B \to X_u\ell^+\nu_\ell$ decays. We will compute Heavy Quark parameters and extract QCD form factors for $B^0 \to D^{*-}\ell^+\nu$ decays. Throughout this section, charge conjugate states are implicitly included, unless otherwise indicated.

Brief descriptions of all parameters and analyses (published or preliminary) relevant for the determination of the combined results are given. The descriptions are based on the information available on the web page at

`http://www.slac.stanford.edu/xorg/hfag/semi/EndOfYear07`

A description of the technique employed for calculating averages was presented in the previous update [4]. Asymmetric errors have been introduced in the current averages for $B \to X_u\ell^+\nu_\ell$ decays to take into account theoretical asymmetric errors.

We thank U. Aglietti, I. Bigi, G. Ferrera, P. Gambino, E. Gardi, P. Giordano, Z. Ligeti, M. Neubert, G. Ricciardi, and N. Uraltsev for useful discussions and for providing the theory codes.

5.1 Common set of input parameters

In the combination of the published results, the central values and errors are rescaled to a common set of input parameters, summarized in Table 44 and provided in the file `common.param` (accessible from the web-page). All measurements with a dependence on any of these parameters are rescaled to the central values given in Table 44, and their errors are recalculated based on the errors provided in the column "Excursion". The detailed dependence for each measurement is contained in files (provided by the experiments) accessible from the web-page. In the following tables, both the published and rescaled results are presented. Some of the (older) measurements are subject to considerables adjustments due to the rescaling.

5.2 Exclusive CKM-favored decays

Averages are provided for the branching fractions $\mathcal{B}(B \to \overline{D}\ell^+\nu_\ell)$ and $\mathcal{B}(B \to \overline{D}^*\ell^+\nu_\ell)$. For the $\overline{D}^{(*)}\pi$ excited states, averages are computed for the inclusive branching fractions $\mathcal{B}(B \to \overline{D}^{(*)}\pi\ell^+\nu_\ell)$, and for the product $\mathcal{B}(B^+ \to \overline{D}_1^0(D^{*-}\pi^+)\ell^+\nu_\ell) \times \mathcal{B}(\overline{D}_1^0 \to D^{*-}\pi^+)$ and $\mathcal{B}(B^+ \to \overline{D}_2^0(D^{*-}\pi^+)\ell^+\nu_\ell) \times \mathcal{B}(\overline{D}_2^0 \to D^{*-}\pi^+)$. In addition, averages are provided for $F(1)|V_{cb}|$ vs ρ^2, where $F(1)$ and ρ^2 are the normalization and slope of the form factor at zero recoil in $B^0 \to D^{*-}\ell^+\nu$ decays, and for the corresponding quantities $G(1)|V_{cb}|$ vs ρ^2 in $B^0 \to D^-\ell^+\nu$ decays.

5.2.1 $B \to \overline{D}\ell^+\nu_\ell$

The average branching fraction $\mathcal{B}(B \to \overline{D}\ell^+\nu_\ell)$ is determined by the combination of the results provided in Table 45 and 46, for $B^0 \to D^-\ell^+\nu_\ell$ and $B^+ \to \overline{D}^0\ell^+\nu_\ell$, respectively. The branching

Table 44: Common input parameters for the combination of semileptonic B decays. Most of the parameters are taken from Ref. [3]. This table is encoded in the file `common.param`. The units are picoseconds for lifetimes and percentage for branching fractions.

Parameter	Assumed Value	Excursion	Description
rb	21.629	± 0.066	R_b
bdst	1.27	± 0.021	$\mathcal{B}(B \to \overline{D}^* \tau \nu)$
bdsd	1.62	± 0.040	$\mathcal{B}(B \to \overline{D}^* D)$
bdst2	0.65	± 0.013	$\mathcal{B}(b \to \overline{D}^* \tau)$ (OPAL incl)
bdsd2	4.2	± 1.5	$\mathcal{B}(b \to \overline{D}^* D)$ (OPAL incl)
bdsd3	0.87	$^{+0.23}_{-0.19}$	$\mathcal{B}(b \to \overline{D}^* D)$ (DELPHI incl)
xe	0.702	± 0.008	B fragmentation: $\langle E_B \rangle / E_{\rm beam}$
bdsi	17.3	± 2.0	$\mathcal{B}(b \to D^{*+}$ incl)
cdsi	22.6	± 1.4	$\mathcal{B}(c \to D^{*+}$ incl)
bpi0gg	98.798	± 0.032	$\mathcal{B}(\pi^0 \to \gamma\gamma)$
tb0	1.530	± 0.008	$\tau(B^0)$
tbplus	1.639	± 0.009	$\tau(B^+)$
tbps	1.456	± 0.030	$\tau(B_s^0)$
fbd	40.3	± 0.9	B^0 fraction at $\sqrt{s} = m_{Z^0}$
fbs	10.1	± 0.9	B_s^0 fraction at $\sqrt{s} = m_{Z^0}$
fbar	9.2	± 1.5	Baryon fraction at $\sqrt{s} = m_{Z^0}$
dst	67.7	± 0.5	$\mathcal{B}(D^{*+} \to D^0 \pi^+)$
dkpp	9.22	± 0.21	$\mathcal{B}(D^+ \to K^- \pi^+ \pi^+)$
dkp	3.84	± 0.06	$\mathcal{B}(D^0 \to K^- \pi^+)$
dkpzp	13.7	± 0.6	$\mathcal{B}(D^0 \to K^- \pi^+ \pi^0)$
dkppp	8.00	$^{+0.25}_{-0.22}$	$\mathcal{B}(D^0 \to K^- \pi^+ \pi^+ \pi^-)$
dkzpp	2.89	± 0.20	$\mathcal{B}(D^0 \to K^0 \pi^+ \pi^-)$
dkln	6.83	± 0.15	$\mathcal{B}(D^0 \to K^- \ell^+ \nu)$
dkk	0.388	± 0.009	$\mathcal{B}(D^0 \to K^- K^+)$
dkx	1.100	± 0.025	$K^- \pi^+ X$ rates
dkox	0.47	± 0.04	$\mathcal{B}(D^0 \to K^0 X)$
dnlx	6.53	± 0.17	$\mathcal{B}(D^0 \to X \ell \nu)$
dkpcl	61.9	± 2.9	$\mathcal{B}(\overline{D}^{*0} \to D^0 \pi^0)$
dssR	0.64	± 0.11	$\mathcal{B}(b \to D^{**} \ell \overline{\nu}) \times \mathcal{B}(D^{**} \to D^{*+} X)$
fb0	48.5	± 0.6	$f^{00} = \mathcal{B}(\Upsilon(4S) \to B^0 \overline{B}^0)$
fpp00	1.062	± 0.025	f^{++}/f^{00} ratio $\mathcal{B}(\Upsilon(4S) \to B^+ B^-)$ over $\mathcal{B}(\Upsilon(4S) \to B^0 \overline{B}^0)$
chid	0.1881	± 0.0023	χ_d, time-integrated probability for B^0 mixing
chi	0.0912	± 0.0016	$\chi = \chi_d \times (f^{00}/100)$

fractions are obtained from the integral over the measured differential decay rates, apart for the *BABAR* results, for which the semileptonic B signal yields are extracted from a fit to the missing mass squared in a sample of fully reconstructed $B\overline{B}$ events.

Figure 39 shows the measurements and the resulting average.

Table 45: Average of the branching fraction $\mathcal{B}(B^0 \to D^- \ell^+ \nu)$ and individual results.

Experiment	$\mathcal{B}(B^0 \to D^- \ell^+ \nu)[\%]$ (rescaled)	$\mathcal{B}(B^0 \to D^- \ell^+ \nu)[\%]$ (published)
ALEPH [165]	$2.25 \pm 0.18_{\rm stat} \pm 0.36_{\rm syst}$	$2.35 \pm 0.18_{\rm stat} \pm 0.44_{\rm syst}$
CLEO [166]	$2.10 \pm 0.13_{\rm stat} \pm 0.15_{\rm syst}$	$2.20 \pm 0.13_{\rm stat} \pm 0.18_{\rm syst}$
Belle [167]	$2.09 \pm 0.12_{\rm stat} \pm 0.39_{\rm syst}$	$2.13 \pm 0.12_{\rm stat} \pm 0.41_{\rm syst}$
BABAR [168]	$2.21 \pm 0.11_{\rm stat} \pm 0.12_{\rm syst}$	$2.22 \pm 0.11_{\rm stat} \pm 0.12_{\rm syst}$
Average	$\mathbf{2.17 \pm 0.12}$	$\boldsymbol{\chi^2/\mathrm{dof} = 0.3/3}$ (CL=**96%**)

Table 46: Average of the branching fraction $\mathcal{B}(B^+ \to \overline{D}^0 \ell^+ \nu_\ell)$ and individual results.

Experiment	$\mathcal{B}(B^+ \to \overline{D}^0 \ell^+ \nu_\ell)[\%]$ (rescaled)	$\mathcal{B}(B^+ \to \overline{D}^0 \ell^+ \nu_\ell)[\%]$ (published)
CLEO [166]	$2.23 \pm 0.13_{\rm stat} \pm 0.17_{\rm syst}$	$2.21 \pm 0.13_{\rm stat} \pm 0.19_{\rm syst}$
CLEO [169]	$1.68 \pm 0.6_{\rm stat} \pm 0.21_{\rm syst}$	$1.6 \pm 0.6_{\rm stat} \pm 0.3_{\rm syst}$
BABAR [168]	$2.32 \pm 0.09_{\rm stat} \pm 0.09_{\rm syst}$	$2.33 \pm 0.09_{\rm stat} \pm 0.09_{\rm syst}$
Average	$\mathbf{2.28 \pm 0.11}$	$\boldsymbol{\chi^2/\mathrm{dof} = 0.97/2}$ (CL=**60%**)

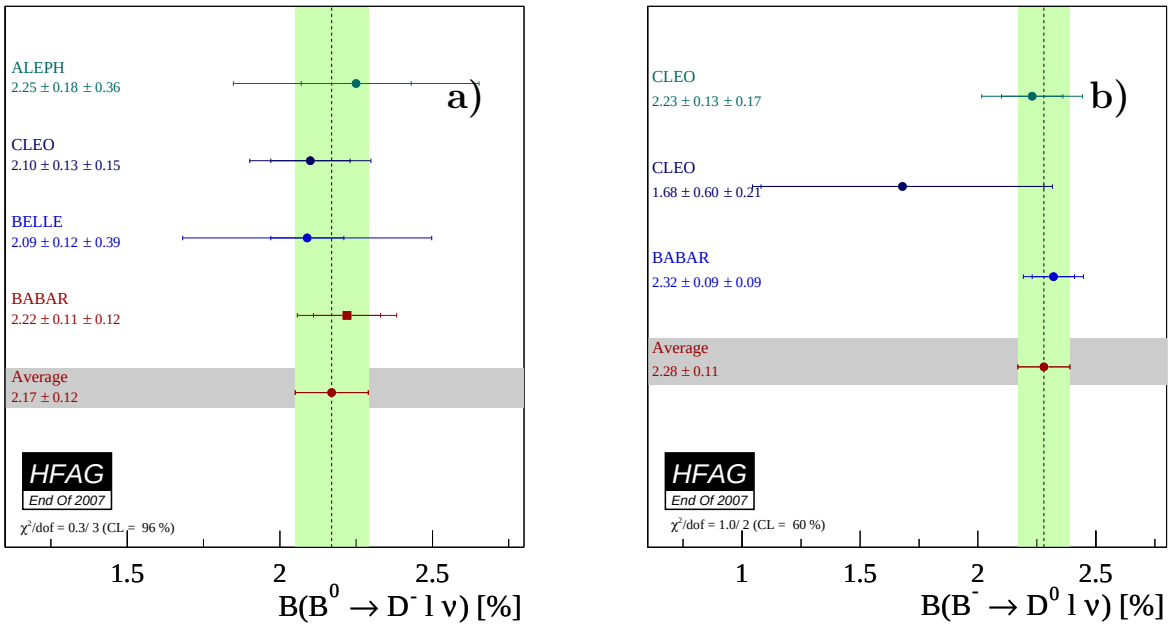

Figure 39: Average branching fraction of exclusive semileptonic B decays (a) $B^0 \to D^- \ell^+ \nu_\ell$ and (b) $B^+ \to \overline{D}^0 \ell^+ \nu_\ell$ and individual results.

The average for $G(1)|V_{cb}|$ is determined by the two-dimensional combination of the results provided in Table 47. Figure 40 (a) provides a one-dimensional projection for illustrative purposes, and figure 40 (b) shows the average $G(1)|V_{cb}|$ and the measurements included in the average.

Table 47: Average of $G(1)|V_{cb}|$ determined in the decay $B^0 \to D^- \ell^+ \nu$ and individual results. The fit for the average has $\chi^2/\mathrm{dof} = 0.3/4$. The total correlation between the average $G(1)|V_{cb}|$ and ρ^2 is 0.93.

Experiment	$G(1)\|V_{cb}\|[10^{-3}]$ (rescaled) $G(1)\|V_{cb}\|[10^{-3}]$ (published)	ρ^2 (rescaled) ρ^2 (published)
ALEPH [165]	$38.8 \pm 11.8_{\mathrm{stat}} \pm 6.2_{\mathrm{syst}}$ $31.1 \pm 9.9_{\mathrm{stat}} \pm 8.6_{\mathrm{syst}}$	$0.95 \pm 0.98_{\mathrm{stat}} \pm 0.36_{\mathrm{syst}}$ $0.70 \pm 0.98_{\mathrm{stat}} \pm 0.50_{\mathrm{syst}}$
CLEO [166]	$44.8 \pm 5.9_{\mathrm{stat}} \pm 3.45_{\mathrm{syst}}$ $44.8 \pm 6.1_{\mathrm{stat}} \pm 3.7_{\mathrm{syst}}$	$1.27 \pm 0.25_{\mathrm{stat}} \pm 0.14_{\mathrm{syst}}$ $1.30 \pm 0.27_{\mathrm{stat}} \pm 0.14_{\mathrm{syst}}$
Belle [167]	$40.07 \pm 4.4_{\mathrm{stat}} \pm 5.14_{\mathrm{syst}}$ $41.1 \pm 4.4_{\mathrm{stat}} \pm 5.1_{\mathrm{syst}}$	$1.12 \pm 0.22_{\mathrm{stat}} \pm 0.14_{\mathrm{syst}}$ $1.12 \pm 0.22_{\mathrm{stat}} \pm 0.14_{\mathrm{syst}}$
Average	$\mathbf{42.3 \pm 4.5}$	$\mathbf{1.17 \pm 0.18}$

For a determination of $|V_{cb}|$, the form factor at zero recoil $G(1)$ needs to be computed. A possible choice is $G(1) = 1.074 \pm 0.018_{\mathrm{stat}} \pm 0.016_{\mathrm{syst}}$ [177], resulting, once corrected by a factor 1.007 for QED effect, in

$$|V_{cb}| = (39.1 \pm 4.2_{\mathrm{exp}} \pm 0.9_{\mathrm{theo}}) \times 10^{-3},$$

where the errors are from experiment and theory, respectively.

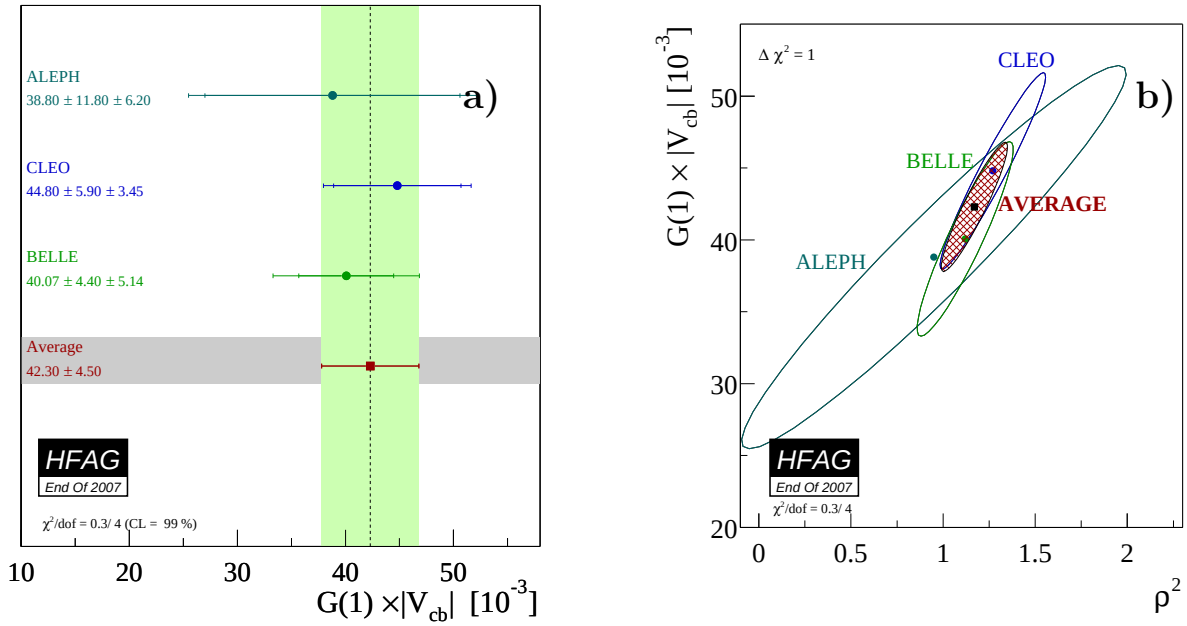

Figure 40: (a)$G(1)|V_{cb}|$ average and rescaled measurements of exclusive $B^0 \to D^- \ell^+ \nu$ decays determined in a two-dimensional fit. (b) $G(1)|V_{cb}|$ vs. ρ^2 error ellipses corresponding to $\Delta\chi^2 = 1$.

5.2.2 $B \to \overline{D}^{*}\ell^{+}\nu_{\ell}$

The average branching fraction $\mathcal{B}(B \to \overline{D}^{*}\ell^{+}\nu_{\ell})$ is determined by the combination of the results provided in Table 48 and 49, for $B^0 \to D^{*-}\ell^{+}\nu_{\ell}$ and $B^{+} \to \overline{D}^{*0}\ell^{+}\nu_{\ell}$, respectively. Advances have also been made in the determination of $|V_{cb}|$ from exclusive $B \to \overline{D}^{*}\ell^{+}\nu_{\ell}$ decays with substantially improved measurements of the form factor ratios R_1 and R_2.

Table 48: Average branching fraction $B^0 \to \overline{D}^{*+}\ell^{+}\nu_{\ell}$ and individual results, where "excl" and "partial reco" refer to full and partial reconstruction of the $B^0 \to \overline{D}^{*+}\ell^{+}\nu_{\ell}$ decay, respectively.

Experiment		$B^0 \to \overline{D}^{*+}\ell^{+}\nu_{\ell}[\%]$ (rescaled)	$B^0 \to \overline{D}^{*+}\ell^{+}\nu_{\ell}[\%]$ (published)
ALEPH (excl)	[165]	$5.60 \pm 0.26_{\rm stat} \pm 0.21_{\rm syst}$	$5.53 \pm 0.26_{\rm stat} \pm 0.52_{\rm syst}$
OPAL (excl)	[170]	$5.22 \pm 0.20_{\rm stat} \pm 0.40_{\rm syst}$	$5.11 \pm 0.20_{\rm stat} \pm 0.49_{\rm syst}$
OPAL (partial reco)	[170]	$5.63 \pm 0.27_{\rm stat} \pm 0.43_{\rm syst}$	$5.92 \pm 0.28_{\rm stat} \pm 0.68_{\rm syst}$
DELPHI (partial reco)	[171]	$5.01 \pm 0.15_{\rm stat} \pm 0.18_{\rm syst}$	$4.70 \pm 0.14_{\rm stat}\ ^{+0.36}_{-0.31}\ _{\rm syst}$
Belle (excl)	[172]	$4.80 \pm 0.25_{\rm stat} \pm 0.19_{\rm syst}$	$4.60 \pm 0.24_{\rm stat} \pm 0.42_{\rm syst}$
CLEO (excl)	[173]	$6.10 \pm 0.19_{\rm stat} \pm 0.20_{\rm syst}$	$6.09 \pm 0.19_{\rm stat} \pm 0.40_{\rm syst}$
DELPHI (excl)	[174]	$5.60 \pm 0.19_{\rm stat} \pm 0.34_{\rm syst}$	$5.90 \pm 0.20_{\rm stat} \pm 0.50_{\rm syst}$
BABAR (excl)	[175]	$4.62 \pm 0.04_{\rm stat} \pm 0.13_{\rm syst}$	$4.69 \pm 0.04_{\rm stat} \pm 0.34_{\rm syst}$
BABAR (tagged)	[168]	$5.44 \pm 0.16_{\rm stat} \pm 0.10_{\rm syst}$	$5.49 \pm 0.16_{\rm stat} \pm 0.25_{\rm syst}$
Average		$\mathbf{5.16 \pm 0.11}$	$\boldsymbol{\chi^2/\mathrm{dof} = 34.1/9}$ (CL=$\mathbf{8^{-5}}$)

Table 49: Average of the branching fraction $B^0 \to \overline{D}^{*+}\ell^{+}\nu_{\ell}$ and individual results.

Experiment		$B^0 \to \overline{D}^{*+}\ell^{+}\nu_{\ell}[\%]$ (rescaled)	$B^0 \to \overline{D}^{*+}\ell^{+}\nu_{\ell}[\%]$ (published)
ARGUS	[176]	$6.53 \pm 1.60_{\rm stat} \pm 0.56_{\rm syst}$	$6.6 \pm 1.6_{\rm stat} \pm 1.5_{\rm syst}$
CLEO	[173]	$6.64 \pm 0.2_{\rm stat} \pm 0.40_{\rm syst}$	$6.50 \pm 0.20_{\rm stat} \pm 0.43_{\rm syst}$
BABAR	[168]	$5.78 \pm 0.15_{\rm stat} \pm 0.30_{\rm syst}$	$5.83 \pm 0.15_{\rm stat} \pm 0.30_{\rm syst}$
Average		$\mathbf{6.09 \pm 0.29}$	$\boldsymbol{\chi^2/\mathrm{dof} = 3.7/2}$ (CL=$\mathbf{17\%}$)

For the $\mathcal{B}(B^{+} \to \overline{D}^{*0}\ell^{+}\nu_{\ell})$, the average is performed as for the $B \to \overline{D}\ell^{+}\nu_{\ell}$ modes, by scaling the different measurements to a common set of input parameters. For the $\mathcal{B}(B^0 \to D^{*-}\ell^{+}\nu_{\ell})$, the average is performed using a global χ^2 fit built incorporating all the experimental determinations of $F(1)|V_{cb}|$, the slope parameter ρ^2 and the other form-factor parameters R_1 and R_2. Statistical correlations between measurements from the same experiment are taken into account. The form-factor parametrization derived by Caprini, Lellouch and Neubert [178] is used.

The χ^2 minimization gives values for the form-factor parameters equal to $R_1 = 1.356 \pm 0.066$ and $R_2 = 0.851 \pm 0.039$. The errors contain both the common and the experiment dependent systematic uncertainties. With respect to the original measurements by CLEO [179], $R_1 = 1.18 \pm 0.30 \pm 0.12$ and $R_2 = 0.71 \pm 0.22 \pm 0.07$, the accuracy on the form-factor parameters R_1 and R_2 given by the global χ^2 minimization has been considerably improved due to a

recent measurement by *BABAR* [175], with results that are consistent with the earlier ones, but considerably more precise.

The values extracted from the fit for $F(1)|V_{cb}|$ and the form-factor parameters are used to obtain the $\mathcal{B}(B^0 \to D^{*-}\ell^+\nu_\ell)$ branching fractions by computing the integral over the measured differential decay rates. The $\mathcal{B}(B^0 \to D^{*-}\ell^+\nu_\ell)$ average is computed from these inputs, apart from the *BABAR* result [168], for which the semileptonic B signal yields are extracted from a fit to the missing mass squared in a sample of fully reconstructed $B\overline{B}$ events. This measurement is rescaled to the common set of input parameters, and then averaged with the other ones, neglecting at this stage remaining correlations. Figure 41 shows the measurements and the resulting average for the $\mathcal{B}(B \to \overline{D}^*\ell^+\nu_\ell)$.

The average for $F(1)|V_{cb}|$ is determined by the two-dimensional combination of the results provided by the global χ^2 minimization described above: the corresponding values are reported in Table 50. This allows the correlation between $F(1)|V_{cb}|$ and ρ^2 to be maintained. Figure 42(a) provides a one-dimensional projection for illustrative purposes. Figure 42(b) shows the average $F(1)|V_{cb}|$ and the measurements included in the average. The largest systematic errors correlated between measurements are due to uncertainties on: the ratio of production cross-sections $\sigma_{b\bar{b}}/\sigma_{\rm had}$, the branching fractions $\mathcal{B}(D^0 \to K^-\pi^+)$ and $\mathcal{B}(D^0 \to K^-\pi^+\pi^0)$, the correlated background from D^{**}, and the D^* form factor ratios R_1 and R_2. Moreover, contributions from R_b and the B^0 fraction at $\sqrt{s} = m_{Z^0}$ are taken into account for the measurements from the LEP experiments. Together these uncertainties account for about two thirds of the systematic error. In all the measurements the total systematic errors are reduced with respect to the published values because the values and uncertainties for parameters on which these measurements depend, for example R_1 and R_2, have since been better determined.

For a determination of $|V_{cb}|$, the form factor at zero recoil $F(1)$ needs to be computed. A possible choice is $F(1) = 0.924 \pm 0.012_{\rm stat} \pm 0.019_{\rm syst}$ [180], which takes into account the QED correction(+0.7%), resulting in

$$|V_{cb}| = (38.8 \pm 0.6_{\rm exp} \pm 0.9_{\rm theo}) \times 10^{-3},$$

where the errors are from experiment and theory, respectively.

5.2.3 $B \to \overline{D}^{(*)}\pi\ell^+\nu_\ell$

The average inclusive branching fractions for $B \to \overline{D}^*\pi\ell^+\nu_\ell$ decays , where no constrain is applied to the hadronic $D^{(*)}\pi$ system, are determined by the combination of the results provided in Tables 51 - 54 for $B^0 \to \overline{D}^0\pi^-\ell^+\nu_\ell$, $B^0 \to \overline{D}^{*0}\pi^-\ell^+\nu_\ell$, $B^+ \to D^-\pi^+\ell^+\nu_\ell$, and $B^+ \to D^{*-}\pi^+\ell^+\nu_\ell$, respectively. The measurements included in the average are scaled to a consistent set of input parameters and their errors, see Section 5.1.

For both the *BABAR* and Belle results, the B semileptonic signal yields are extracted from a fit to the missing mass squared in a sample of fully reconstructed $B\overline{B}$ events.

Figure 43 illustrates the measurements and the resulting average.

5.2.4 $B \to \overline{D}^{**}\ell^+\nu_\ell$

Averages are perfomed also for B semileptonic decays into narrow orbitally-excited D states, namely the $D_1(2420)$ and $D_2^*(2460)$ [3]. Due to the unknown $D_{1,2}$ branching fractions, the

Table 50: Average of $F(1)|V_{cb}|$ determined in the decay $\overline{B}^0 \to D^{*+}\ell^-\overline{\nu}$ and individual results, where "excl" and "partial reco" refer to full and partial reconstruction of the $\overline{B}^0 \to D^{*+}\ell^-\overline{\nu}$ decay, respectively. The fit for the average has $\chi^2/\mathrm{dof} = 33.9/17$ (CL=1%). The total correlation between the average $F(1)|V_{cb}|$ and ρ^2 is 0.24.

Experiment	$F(1)\|V_{cb}\|[10^{-3}]$ (rescaled) $F(1)\|V_{cb}\|[10^{-3}]$ (published)	ρ^2 (rescaled) ρ^2 (published)
ALEPH (excl) [165]	$32.0 \pm 1.8_{\rm stat} \pm 1.3_{\rm syst}$ $31.9 \pm 1.8_{\rm stat} \pm 1.9_{\rm syst}$	$0.49 \pm 0.20_{\rm stat} \pm 0.09_{\rm syst}$ $0.37 \pm 0.26_{\rm stat} \pm 0.14_{\rm syst}$
OPAL (excl) [170]	$37.2 \pm 1.6_{\rm stat} \pm 1.5_{\rm syst}$ $36.8 \pm 1.6_{\rm stat} \pm 2.0_{\rm syst}$	$1.24 \pm 0.20_{\rm stat} \pm 0.14_{\rm syst}$ $1.31 \pm 0.21_{\rm stat} \pm 0.16_{\rm syst}$
OPAL (partial reco) [170]	$37.6 \pm 1.2_{\rm stat} \pm 2.4_{\rm syst}$ $37.5 \pm 1.2_{\rm stat} \pm 2.5_{\rm syst}$	$1.13 \pm 0.13_{\rm stat} \pm 0.27_{\rm syst}$ $1.12 \pm 0.14_{\rm stat} \pm 0.29_{\rm syst}$
DELPHI (partial reco) [171]	$35.9 \pm 1.4_{\rm stat} \pm 2.3_{\rm syst}$ $35.5 \pm 1.4_{\rm stat}\ ^{+2.3}_{-2.4{\rm syst}}$	$1.18 \pm 0.13_{\rm stat} \pm 0.25_{\rm syst}$ $1.34 \pm 0.14_{\rm stat}\ ^{+0.24}_{-0.22{\rm syst}}$
Belle (excl) [172]	$34.9 \pm 2.0_{\rm stat} \pm 1.8_{\rm syst}$ $35.8 \pm 1.9_{\rm stat} \pm 1.9_{\rm syst}$	$1.15 \pm 0.15_{\rm stat} \pm 0.10_{\rm syst}$ $1.45 \pm 0.16_{\rm stat} \pm 0.20_{\rm syst}$
CLEO (excl) [173]	$41.6 \pm 1.3_{\rm stat} \pm 1.8_{\rm syst}$ $43.1 \pm 1.3_{\rm stat} \pm 1.8_{\rm syst}$	$1.37 \pm 0.09_{\rm stat} \pm 0.20_{\rm syst}$ $1.61 \pm 0.09_{\rm stat} \pm 0.21_{\rm syst}$
DELPHI (excl) [174]	$36.6 \pm 1.8_{\rm stat} \pm 1.9_{\rm syst}$ $39.2 \pm 1.8_{\rm stat} \pm 2.3_{\rm syst}$	$1.04 \pm 0.14_{\rm stat} \pm 0.15_{\rm syst}$ $1.32 \pm 0.15_{\rm stat} \pm 0.33_{\rm syst}$
BABAR (excl) [175]	$34.2 \pm 0.3_{\rm stat} \pm 1.1_{\rm syst}$ $34.7 \pm 0.3_{\rm stat} \pm 1.1_{\rm syst}$	$1.18 \pm 0.05_{\rm stat} \pm 0.03_{\rm syst}$ $1.18 \pm 0.05_{\rm stat} \pm 0.03_{\rm syst}$
Average	$\mathbf{36.14 \pm 0.55}$	$\mathbf{1.17 \pm 0.05}$

Table 51: Average of the branching fraction $B^0 \to \overline{D}^0\pi^-\ell^+\nu_\ell$ and individual results.

Experiment	$\mathcal{B}(B^0 \to \overline{D}^0\pi^-\ell^+\overline{\nu}_\ell)[\%]$ (rescaled)	$\mathcal{B}(B^0 \to \overline{D}^0\pi^-\ell^+\nu_\ell)[\%]$ (published)
Belle [181]	$0.43 \pm 0.07_{\rm stat} \pm 0.05_{\rm syst}$	$0.42 \pm 0.07_{\rm stat} \pm 0.06_{\rm syst}$
BABAR [168]	$0.43 \pm 0.08_{\rm stat} \pm 0.03_{\rm syst}$	$0.43 \pm 0.08_{\rm stat} \pm 0.03_{\rm syst}$
Average	$\mathbf{0.43 \pm 0.06}$	$\boldsymbol{\chi^2/\mathrm{dof} = 0.001}$ (CL=**99%**)

Table 52: Average of the branching fraction $B^0 \to \overline{D}^{*0}\pi^-\ell^+\nu_\ell$ and individual results.

Experiment	$\mathcal{B}(B^0 \to \overline{D}^{*0}\pi^-\ell^+\nu_\ell)[\%]$ (rescaled)	$\mathcal{B}(B^0 \to \overline{D}^{*0}\pi^-\ell^+\nu_\ell)[\%]$ (published)
Belle [181]	$0.57 \pm 0.21_{\rm stat} \pm 0.07_{\rm syst}$	$0.56 \pm 0.21_{\rm stat} \pm 0.08_{\rm syst}$
BABAR [168]	$0.48 \pm 0.08_{\rm stat} \pm 0.04_{\rm syst}$	$0.48 \pm 0.08_{\rm stat} \pm 0.04_{\rm syst}$
Average	$\mathbf{0.49 \pm 0.08}$	$\boldsymbol{\chi^2/\mathrm{dof} = 0.15}$ (CL=**70%**)

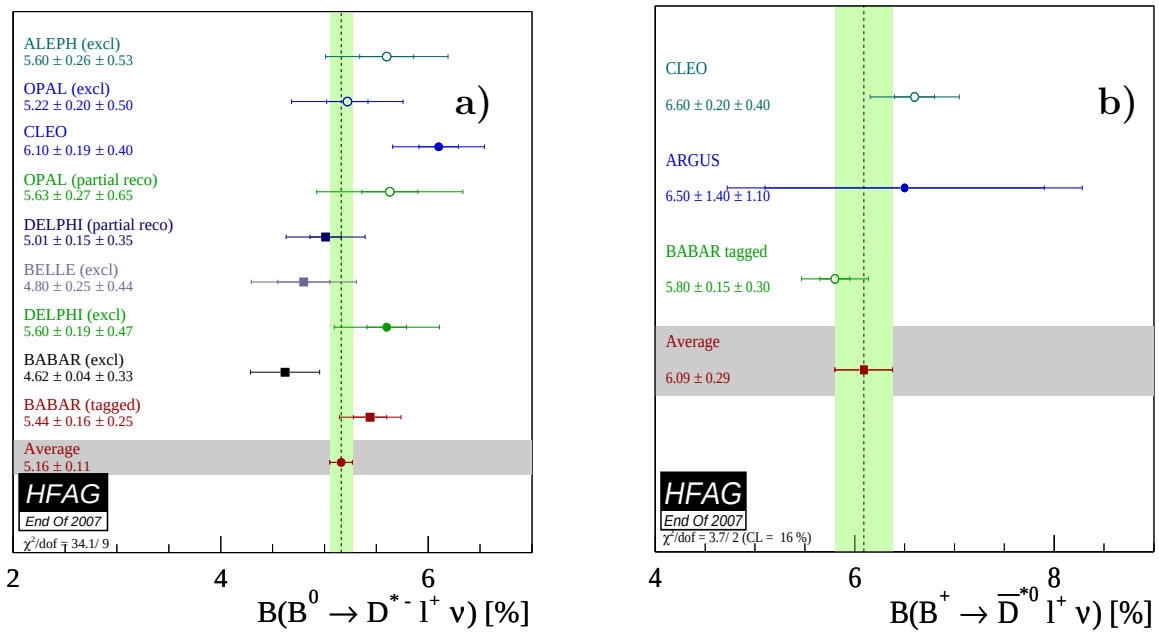

Figure 41: Average branching fraction of exclusive semileptonic B decays (a) $B^0 \to D^{*-}\ell^+\nu_\ell$ and (b) $B^+ \to \overline{D}^{*0}\ell^+\nu_\ell$ and individual results. For Aleph and Delphi, the measurements of $B^0 \to D^{*-}\ell^+\nu$ decays have been done both with inclusive ("partial reco") and exclusive ("excl") analyses based on a partial and full reconstruction of the $B^0 \to D^{*-}\ell^+\nu$ decay, respectively.

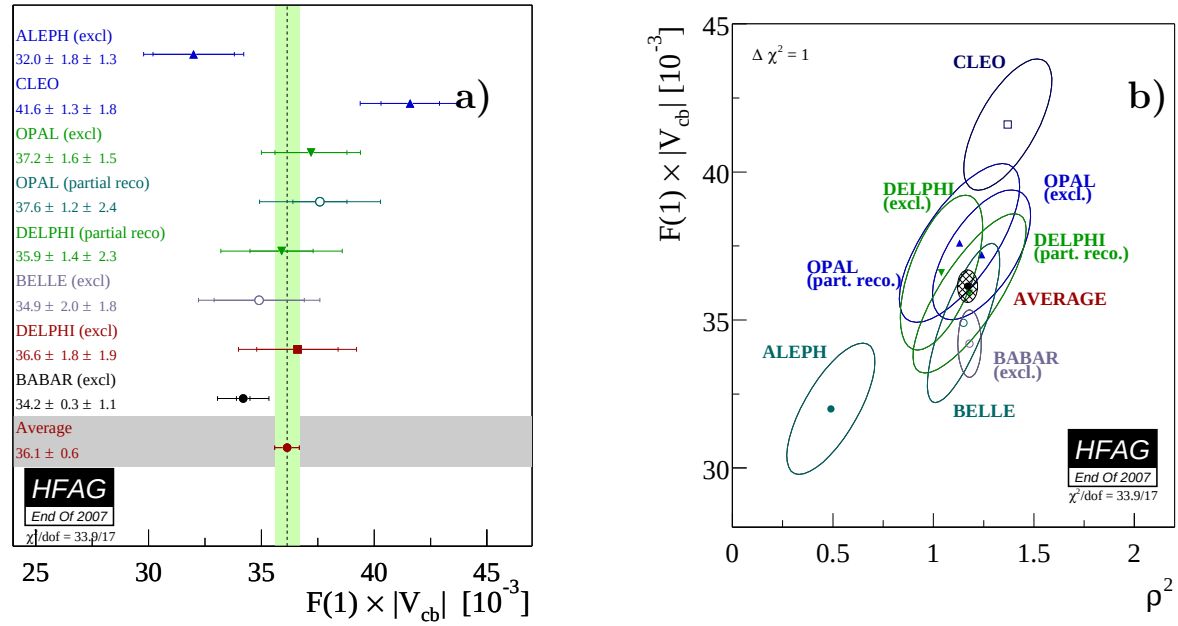

Figure 42: (a) $F(1)|V_{cb}|$ average and rescaled measurements of the exclusive $B^0 \to D^{*-}\ell^+\nu$ decays determined in a two-dimensional fit, where "excl" and "partial reco" refer to full and partial reconstruction. (b) $F(1)|V_{cb}|$ vs. ρ^2 error ellipse for $\Delta\chi^2 = 1$ (CL=39%).

averages have been computed for the product of branching fractions. The average are de-

Table 53: Average of the branching fraction $B^+ \to D^- \pi^+ \ell^+ \nu_\ell$ and individual results.

Experiment	$\mathcal{B}(B^+ \to D^- \pi^+ \ell^+ \nu_\ell)[\%]$ (rescaled)	$\mathcal{B}(B^+ \to D^- \pi^+ \ell^+ \overline{\nu}_\ell)[\%]$ (published)
Belle [181]	$0.42 \pm 0.04_{\rm stat} \pm 0.05_{\rm syst}$	$0.40 \pm 0.04_{\rm stat} \pm 0.06_{\rm syst}$
BABAR [168]	$0.42 \pm 0.06_{\rm stat} \pm 0.03_{\rm syst}$	$0.42 \pm 0.06_{\rm stat} \pm 0.03_{\rm syst}$
Average	$\mathbf{0.42 \pm 0.05}$	$\boldsymbol{\chi^2/\mathrm{dof} = 0.001}$ (CL=**98%**)

Table 54: Average of the branching fraction $B^+ \to D^{*-} \pi^+ \ell^+ \nu_\ell$ and individual results.

Experiment	$\mathcal{B}(B^+ \to D^{*-} \pi^+ \ell^+ \nu_\ell)[\%]$ (rescaled)	$\mathcal{B}(B^+ \to D^{*-} \pi^+ \ell^+ \nu_\ell)[\%]$ (published)
Belle [181]	$0.68 \pm 0.08_{\rm stat} \pm 0.07_{\rm syst}$	$0.64 \pm 0.08_{\rm stat} \pm 0.09_{\rm syst}$
BABAR [168]	$0.59 \pm 0.05_{\rm stat} \pm 0.04_{\rm syst}$	$0.59 \pm 0.05_{\rm stat} \pm 0.04_{\rm syst}$
Average	$\mathbf{0.61 \pm 0.05}$	$\boldsymbol{\chi^2/\mathrm{dof} = 0.5}$ (CL=**49%**)

termined from the combination of the results provided in Tables 55 and 56 for $\mathcal{B}(B^+ \to \overline{D}_1^0(D^{*-}\pi^+)\ell^+\nu_\ell) \times \mathcal{B}(\overline{D}_1^0 \to D^{*-}\pi^+)$ and $\mathcal{B}(B^+ \to \overline{D}_2^0(D^{*-}\pi^+)\ell^+\nu_\ell) \times \mathcal{B}(\overline{D}_2^0 \to D^{*-}\pi^+)$, respectively. The measurements included in the average are scaled to a consistent set of input parameters and their errors, see Section 5.1.

For both the B-factory and the LEP and Tevatron results, the B semileptonic signal yields are extracted from a fit to the invariant mass distribution of the $D^{*-}\pi^+$ system. Except CLEO and Belle results, the measurements are for the final state $B \to \overline{D}_2(D^{*-}\pi^+)X\ell^+\nu_\ell$. Figure 43 shows the measurements and the resulting average.

Table 55: Average of the branching fraction $\mathcal{B}(B^+ \to \overline{D}_1^0(D^{*-}\pi^+)\ell^+\nu_\ell) \times \mathcal{B}(\overline{D}_1^0 \to D^{*-}\pi^+))$ and individual results.

Experiment	$\mathcal{B}(B^+ \to \overline{D}_1^0(D^{*-}\pi^+)\ell^+\nu_\ell))[\%]$ (rescaled)	$\mathcal{B}(B^+ \to \overline{D}_1^0(D^{*-}\pi^+)\ell^+\nu_\ell))[\%]$ (published)
ALEPH [182]	$0.45 \pm 0.10_{\rm stat} \pm 0.07_{\rm syst}$	$0.47 \pm 0.098_{\rm stat} \pm 0.074_{\rm syst}$
OPAL [183]	$0.60 \pm 0.21_{\rm stat} \pm 0.10_{\rm syst}$	$0.698 \pm 0.21_{\rm stat} \pm 0.10_{\rm syst}$
CLEO [184]	$0.35 \pm 0.08_{\rm stat} \pm 0.06_{\rm syst}$	$0.373 \pm 0.085_{\rm stat} \pm 0.057_{\rm syst}$
D0 [185]	$0.22 \pm 0.02_{\rm stat} \pm 0.04_{\rm syst}$	$0.219 \pm 0.018_{\rm stat} \pm 0.035_{\rm syst}$
Belle [181]	$0.44 \pm 0.07_{\rm stat} \pm 0.06_{\rm syst}$	$0.42 \pm 0.07_{\rm stat} \pm 0.07_{\rm syst}$
Average	$\mathbf{0.24 \pm 0.04}$	$\boldsymbol{\chi^2/\mathrm{dof} = 12/4}$ (CL=**2%**)

5.3 Inclusive CKM-favored decays

5.3.1 Inclusive Semileptonic Branching Fraction for $B \to X\ell^+\nu_\ell$

The branching fraction for inclusive decays $B \to X\ell^+\nu_\ell$ is presented, where B corresponds to both B^0 and B^+. We use measurements that require the momentum of the prompt charged

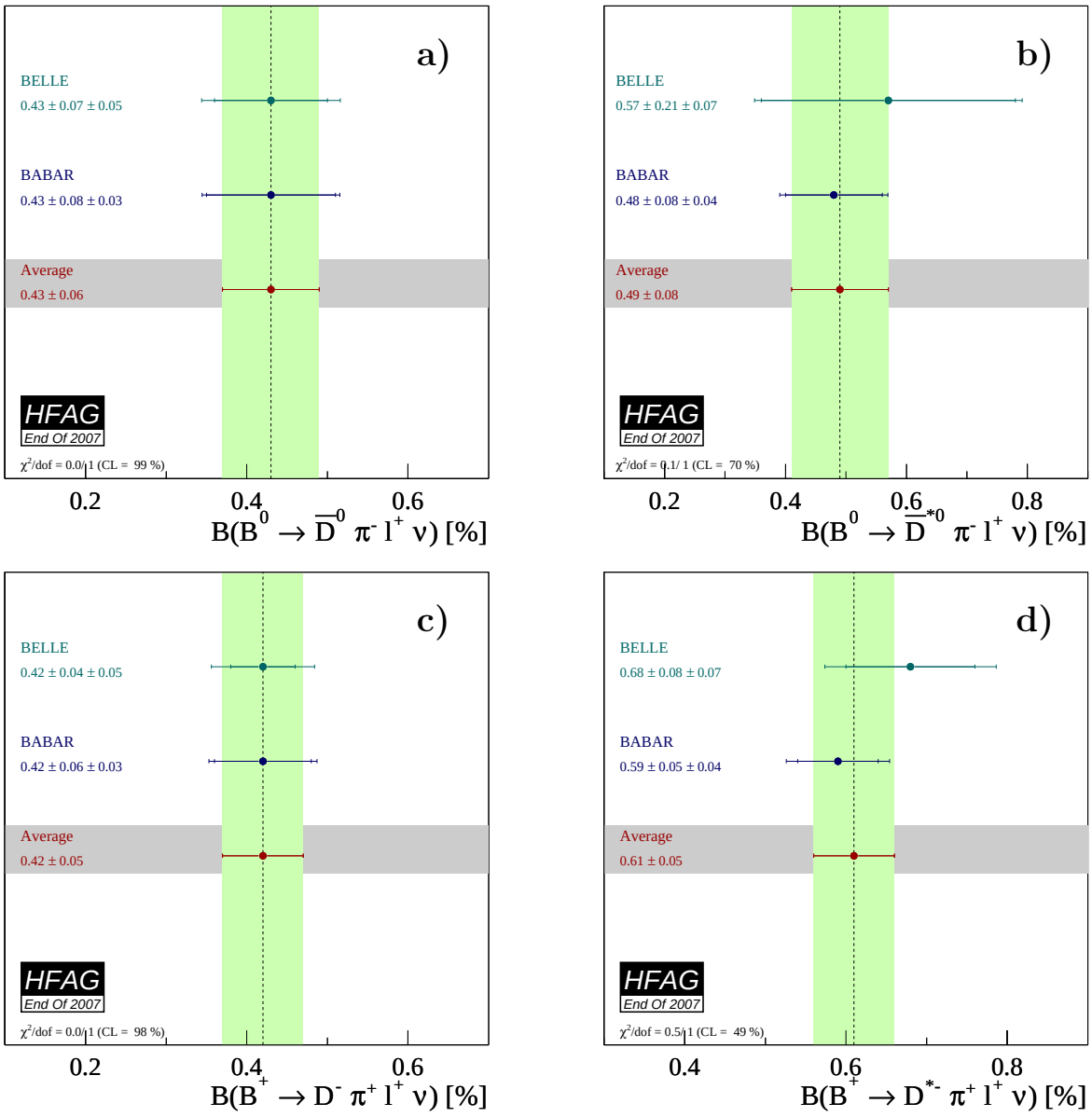

Figure 43: Average branching fraction of exclusive semileptonic B decays (a) $B^0 \to \overline{D}^0 \pi^- \ell^+ \nu_\ell$, (b) $B^0 \to \overline{D}^{*0} \pi^- \ell^+ \nu_\ell$, (c) $B^+ \to D^- \pi^+ \ell^+ \nu_\ell$, and (d) $B^+ \to D^{*-} \pi^+ \ell^+ \nu_\ell$. The corresponding individual results are also shown.

lepton ($p_{\rm cms}$) to be greater than 0.6 GeV/c, as measured in the rest frame of either the B-meson or $\Upsilon(4S)$ [23]. The measurements and average are given in Table 57 and plotted in Figure 45. We determine the branching fraction over the full lepton spectrum using an extrapolation factor derived from a global fit [192] employed to extract HQET parameters in the kinetic scheme [193–195] from measured moments of inclusive distributions (see section 5.3.5). The global fit minimizes the dependence on the measurements used in this average. The extrapolation factor is $1.0495 \pm 0.0005 \pm 0.0010$, where the first error represent the experimental and

[23]The difference in reference frames has a negligible impact.

Table 56: Average of the branching fraction $\mathcal{B}(B^+ \to \overline{D}{}^0_2(D^{*-}\pi^+)\ell^+\nu_\ell) \times \mathcal{B}(\overline{D}{}^0_2 \to D^{*-}\pi^+))$ and individual results.

Experiment	$\mathcal{B}(B^- \to D^0_2(D^{*+}\pi^-)\ell^-\overline{\nu}_\ell))[\%]$ (rescaled)	$\mathcal{B}(B^- \to D^0_2(D^{*+}\pi^-)\ell^-\overline{\nu}_\ell))[\%]$ (published)
CLEO [184]	$0.06 \pm 0.07_{\rm stat} \pm 0.01_{\rm syst}$	$0.059 \pm 0.066_{\rm stat} \pm 0.011_{\rm syst}$
D0 [185]	$0.09 \pm 0.02_{\rm stat} \pm 0.02_{\rm syst}$	$0.088 \pm 0.018_{\rm stat} \pm 0.020_{\rm syst}$
Belle [181]	$0.19 \pm 0.06_{\rm stat} \pm 0.03_{\rm syst}$	$0.18 \pm 0.06_{\rm stat} \pm 0.03_{\rm syst}$
Average	$\mathbf{0.09 \pm 0.025}$	$\boldsymbol{\chi^2/\mathrm{dof} = 2.8/2}$ (CL=**25%**)

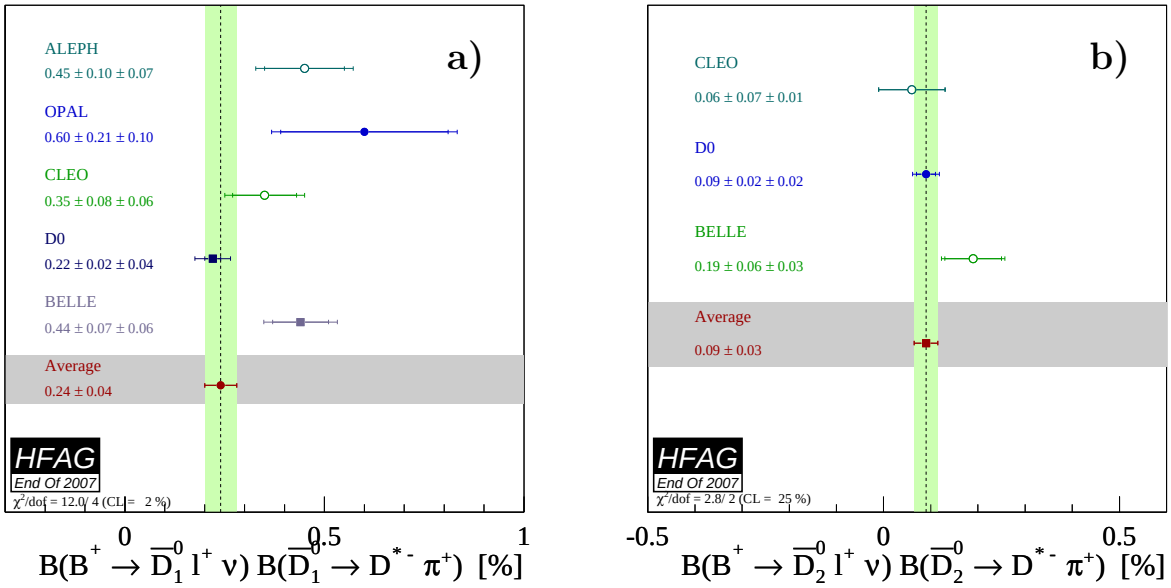

Figure 44: Average of the product of branching fraction (a) $\mathcal{B}(B^+ \to \overline{D}{}^0_1(D^{*-}\pi^+)\ell^+\nu_\ell) \times \mathcal{B}(\overline{D}{}^0_1 \to D^{*-}\pi^+)$ and (b) $\mathcal{B}(B^+ \to \overline{D}{}^0_2(D^{*-}\pi^+)\ell^+\nu_\ell) \times \mathcal{B}(\overline{D}{}^0_2 \to D^{*-}\pi^+)$ The corresponding individual results are also shown.

theoretical uncertainties obtained from the global fit. The second error refers to an additional theoretical uncertainty on the ratio $\Gamma_{\rm sl}(0.6)/\Gamma_{\rm sl}(0.0)$ of 0.1%, on the recommendation of the authors of the fit. The resultant full branching fraction is $\mathcal{B}(B \to X\ell^+\nu_\ell) = (10.74 \pm 0.16)\%$.

5.3.2 Ratio of $\mathcal{B}(B^+ \to X\ell^+\nu_\ell)$ to $\mathcal{B}(B^0 \to X\ell^+\nu_\ell)$

The total width of semileptonic B-meson decays is expected to be the same for both neutral and charged B mesons. Therefore the ratio of the branching fractions, R_{+0}, should be equivalent to the ratio of the B-meson lifetimes τ_{B+}/τ_{B^0}, where

$$R_{+0} = \frac{\mathcal{B}(B^+ \to X\ell^+\nu_\ell)}{\mathcal{B}(B^0 \to X\ell^+\nu_\ell)}.$$

Table 57: Average of the partial semileptonic branching fractions $\mathcal{B}(B \to X\ell^+\nu_\ell)(p_{\rm cms} > 0.6\,{\rm GeV/c})$ and the full branching fraction extrapolated from the average. In parentheses we identify the type of tag used to identify $B\overline{B}$ events: e-tag and ℓ-tag refer to measurements with events tagged by an electron and either an electron or muon, respectively, $B_{\rm reco}$-tag refers to analyses with events tagged by a fully reconstructed hadronic B decay.

Experiment		$\mathcal{B}(B \to X\ell^+\nu_\ell)[\%]$ (rescaled) $(p_{\rm cms} > 0.6\,{\rm GeV/c})$	$\mathcal{B}(B \to X\ell^+\nu_\ell)[\%]$ (published) $(p_{\rm cms} > 0.6\,{\rm GeV/c})$
ARGUS (e-tag)	[186]	$9.15 \pm 0.50 \pm 0.33$	$9.10 \pm 0.50 \pm 0.40$
Belle (ℓ-tag)	[187]	$10.30 \pm 0.11 \pm 0.46$	$10.24 \pm 0.11 \pm 0.46$
CLEO (e-tag)	[188]	$10.23 \pm 0.08 \pm 0.22$	$10.21 \pm 0.08 \pm 0.22$
BABAR (e-tag)	[189]	$10.37 \pm 0.06 \pm 0.23$	$10.36 \pm 0.06 \pm 0.23$
BABAR (B_{reco}-tag)	[190]	$10.03 \pm 0.19 \pm 0.33$	$10.03 \pm 0.19 \pm 0.33$
Belle (B_{reco}-tag)	[191]	$10.28 \pm 0.18 \pm 0.24$	$10.28 \pm 0.18 \pm 0.24$
Average at $(p_{\rm cms} > 0.6\,{\rm GeV/c})$		$\mathbf{10.23 \pm 0.15}$	$\boldsymbol{\chi^2/{\rm dof} = 4.2/5}$ (CL=**52%**)
$\mathcal{B}_{tot}(B^0/B^+ \to X\ell\nu_\ell)$ (%)		$\mathbf{10.74 \pm 0.16}$	

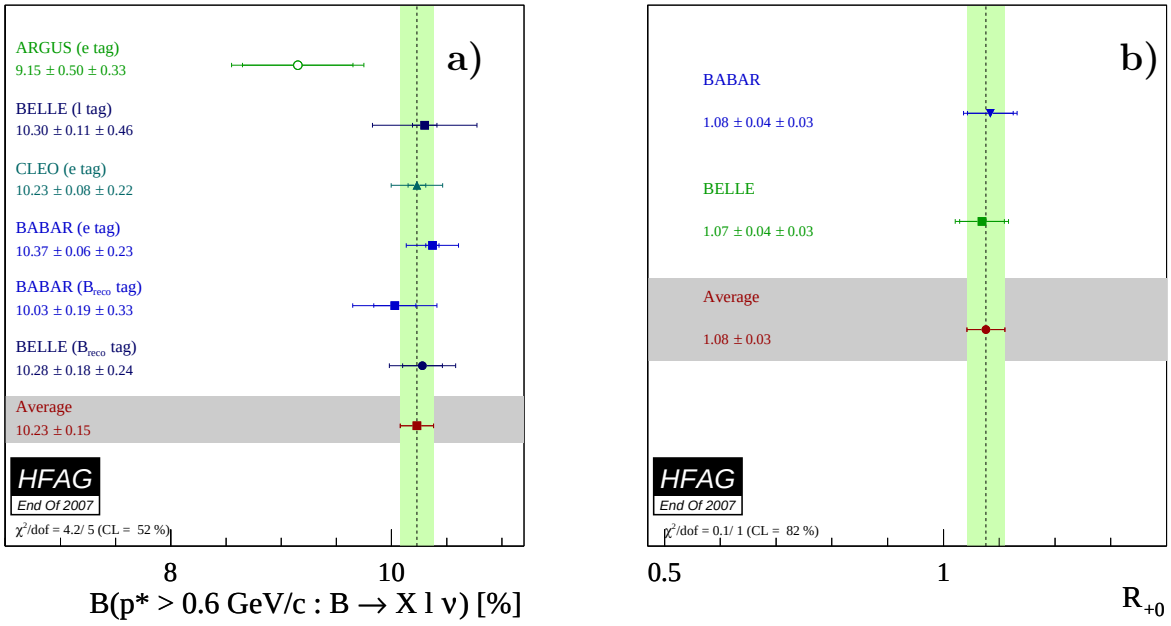

Figure 45: (a) Measurements of $\mathcal{B}(B \to X\ell^+\nu_\ell)$ and their average. (b) Measurements of the ratio of the branching fractions R_{+0} and their average.

Recently, both *BABAR* and Belle reported precise measurements of R_{+0}, using a "$B_{\rm reco}$"-tagged sample. The measurements and average are listed in Table 58 and plotted in Figure 45. The average, 1.076 ± 0.034, is in agreement with the ratio of lifetimes, 1.073 ± 0.008 (this preprint).

Table 58: Individual measurements and average of the ratio of the branching fractions R_{+0}.

Experiment	R_{+0}
BABAR [190]	$1.084 \pm 0.041 \pm 0.025$
Belle [191]	$1.069 \pm 0.040 \pm 0.026$
Average	$\mathbf{1.076 \pm 0.034}$ $\boldsymbol{\chi^2/\text{dof} = 0.05/1}$ **CL=82%**

5.3.3 Branching Fractions for $B^+ \to X\ell^+\nu_\ell$

We provide averages of the branching fractions of $B^+ \to X\ell^+\nu_\ell$ and $B^0 \to X^-\ell^+\nu_\ell$ separately, using the available measurements at the $\Upsilon(4S)$. We include the measurements from CLEO [196, 197] and ARGUS [198], as well as the latest measurements made by Belle and *BABAR* that utilise the full reconstruction B-meson tag [190, 191]. In those cases, we extrapolate from the partial to full branching fraction using a factor derived from a global fit [192], as in section 5.3.1. In contrast to the B admixture average, averages are made of the full branching fraction since CLEO and ARGUS do not present partial branching fractions. The measurements and averages are given in Tables 59 and 60 and plotted in Figure 46 for $B^+ \to X^0\ell^+\nu_\ell$ and $B^0 \to X^-\ell^+\nu_\ell$, respectively.

Table 59: Individual measurements and average of the total semileptonic branching fraction $\mathcal{B}(B^+ \to X^0\ell^+\nu_\ell)$. "$\ell$-tag" and "$B_{reco}$-tag" indicate analysis experimental technique. No rescaling is applied.

Experiment	$\mathcal{B}_{tot}(B^+ \to X^0\ell^+\nu_\ell)[\%]$
CLEO (ℓ-tag) [196]	$10.25 \pm 0.57 \pm 0.66$
BABAR (B_{reco}-tag) [190]	$10.90 \pm 0.27 \pm 0.39$
Belle (B_{reco}-tag) [191]	$11.17 \pm 0.25 \pm 0.28$
Average	$\mathbf{10.99 \pm 0.28}$ $\boldsymbol{\chi^2/\text{dof} = 1.0/2}$ **CL=61%**

5.3.4 $|V_{cb}|$ Determined from $B \to X\ell^+\nu_\ell$

The magnitude of the CKM matrix $|V_{cb}|$ can be determined from the branching fraction of inclusive charmed semileptonic B-meson decays $B \to X\ell^+\nu_\ell$ and with parameters that describe the motion of the b-quark in the B-meson. These parameters, within the framework of the Heavy Quark Expansion (HQE), include the b-quark mass, m_b. Phenomenology of these decays is reviewed in many papers [199]. In practice $|V_{cb}|$, m_b, and other parameters are determined simultaneously from a *global* fit to measured moments of inclusive leptons spectrum, the hadron mass spectrum in semileptonic decays, and the inclusive photon spectrum in radiative B–meson penguin decays. The moments are measured as a function of a minimum lepton of photon

Table 60: Individual measurements and average of the total semileptonic branching fraction $\mathcal{B}(B^0 \to X^- \ell^+ \nu)$. "partial-tag" and "$B_{reco}$-tag" indicate analysis experimental technique. No rescaling is applied.

Experiment		$\mathcal{B}_{tot}(B^0 \to X^- \ell^+ \nu)[\%]$
CLEO (partial-tag)	[197]	$9.9 \pm 3.0 \pm 0.9$
ARGUS (partial-tag)	[198]	$9.3 \pm 1.1 \pm 1.5$
CLEO (partial-tag)	[196]	$10.78 \pm 0.60 \pm 0.69$
BABAR (B_{reco}-tag)	[190]	$10.14 \pm 0.28 \pm 0.33$
Belle (B_{reco}-tag)	[191]	$10.46 \pm 0.30 \pm 0.23$
Average		$\mathbf{10.33 \pm 0.28}$ $\boldsymbol{\chi^2/\mathrm{dof} = 0.9/4}$ **CL= 92%**

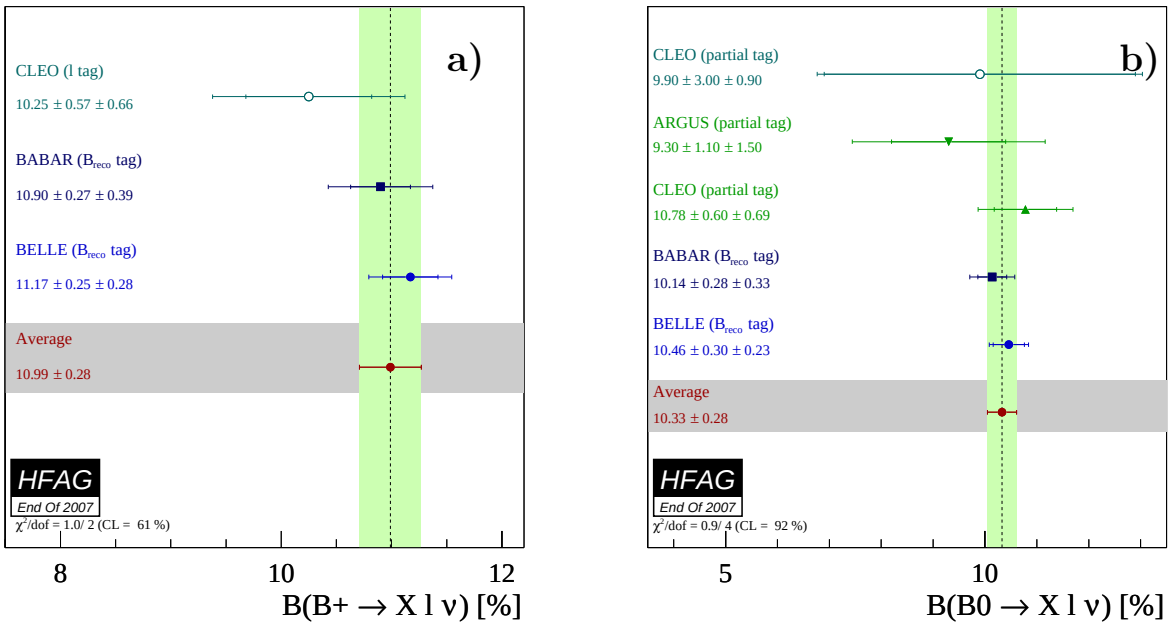

Figure 46: (a) Measurements of the total semileptonic branching fraction $\mathcal{B}(B^+ \to X \ell^+ \nu_\ell)$ and their average. (b) Individual measurements and average of the total semileptonic branching fraction $\mathcal{B}(B^0 \to X^- \ell^+ \nu)$. "$\ell$-tag", "partial-tag" and "B_{reco}-tag" indicate the event tag used in different analyses.

energy. To date three types of global fits have been performed; they differ in the choice of scheme, either *pole*, "1S" or *kinetic*, which are characterized by different definitions of the b-quark mass m_b. However, fits in the *pole* scheme are disfavoured due to the poor convergence of series expansions in that scheme. In the following, we present the most up-to-date fits, which are performed in the *kinetic* and "1S" schemes. They are based on a common set of measurements.

5.3.5 HQE fit in the kinetic scheme

This fit to the moment measurements relies on HQE calculations in the kinetic scheme presented in Refs. [193–195], including lower energy dependent perturbative corrections to the hadron moments [200–202]. The inclusive spectral moments of $B \to X_c \ell^+ \nu_\ell$ decays have been calculated in the kinetic scheme up to $\mathcal{O}(1/m_b^3)$ and $\mathcal{O}(1/(\alpha_s^2))$. The theoretical expressions for the truncated moments are given in terms of HQE parameters, and coefficients determined by theory, which are functions of the lower energy cut. As μ_G^2 and ρ_{LS}^3 can be estimated from the $B^* - B$ mass splitting and heavy-quark sum rules, respectively, we impose Gaussian error constraints of $\mu_G^2 = 0.35 \pm 0.07\text{GeV}^2$ and $\rho_{LS}^3 = -0.15 \pm 0.10\text{GeV}^3$ on these parameters as advocated in Ref. [193]. The total of free parameters is then eight. The result of the combined fit of the HQEs to all moment measurements from *BABAR* [189, 203–205], Belle [206–208], CDF [209], CLEO [210, 211] and DELPHI [212] is shown in Table 61. To asses the consistency of the calculations and the measurements for the two different decay processes, $B \to X_c \ell^+ \nu_\ell$ and $B \to X_s \gamma$, we have carried out separate fits to $B \to X_c \ell^+ \nu_\ell$ moments and to photon moments only.

The fit to $B \to X_c \ell^+ \nu_\ell$ moments only results in:

$$\begin{aligned} |V_{cb}| &= 41.68 \pm 0.39_{\text{fit}} \pm 0.58_{\Gamma_{SL}} \times 10^{-3}\,, \\ m_b &= 4.677 \pm 0.053_{\text{fit}}\text{GeV}\,, \\ m_c &= 1.285 \pm 0.078_{\text{fit}}\text{GeV}\,, \\ \mu_\pi^2 &= 0.387 \pm 0.039_{\text{fit}}\text{GeV}^2\,. \end{aligned}$$

From the fit to $B \to X_s \gamma$ moments only we obtain:

$$\begin{aligned} m_b &= 4.56^{+0.08}_{-0.14}\text{GeV}\,, \\ \mu_\pi^2 &= 0.44^{+0.30}_{-0.17}\text{GeV}^2\,. \end{aligned}$$

A comparison of results from the combined fit with those obtained from fits to $B \to X_c \ell^+ \nu_\ell$ and $B \to X_s \gamma$ moments separately can be found in Figure 47 where the $\Delta\chi^2 = 1$ contours for the fit results are shown in the $(m_b, |V_{cb}|)$ and (m_b, μ_π^2) planes. However, as they are not sensitive to all the heavy quark parameters, all but m_b and μ_π^2 are fixed to the result obtained from the combined fit. It can be seen that the inclusion of the photon energy moments adds additional sensitivity to the b-quark mass m_b. The values for the b–quark mass m_b and μ_π^2 from the two fits agree within 1.3σ and 0.3σ, respectively.

It is of interest to compare the extracted b–quark mass in the kinetic scheme with other determinations in the commonly used $\overline{\text{MS}}$ scheme. The translation between the kinetic and $\overline{\text{MS}}$ masses to two loop accuracy and including the BLM part of the α_s^3 corrections [195] leads to

$$\overline{m_b}(\overline{m_b}) = 4.22 \pm 0.04\,\text{GeV}.$$

5.3.6 Global Fits in the $1S$ scheme

An independent fit in the $1S$ scheme is performed with the same set of measured lepton energy, hadron mass and photon energy moments as in section 5.3.5.

Table 61: Results for the combined fit to all moments with experimental and theoretical uncertainties. For $|V_{cb}|$ we add an additional theoretical error stemming from the uncertainty in the expansion for $\Gamma_{\rm SL}$ of 1.4%. Below the fit results the correlation matrix is shown.

	OPE FIT RESULT: χ^2/N_{dof} =39.1/62							
$B \to X_c\ell^+\nu_\ell$ + $B \to X_s\gamma$	$\lvert V_{cb}\rvert$ ($\times 10^{-3}$)	m_b (GeV)	m_c (GeV)	μ_π^2 (GeV^2)	ρ_D^3 (GeV^3)	μ_G^2 (GeV^2)	ρ_{LS}^3 (GeV^3)	$BR_{c\ell^+\nu_\ell}$ (%)
RESULT	41.91	4.613	1.187	0.408	0.191	0.261	-0.195	10.64
Δ exp	0.19	0.022	0.033	0.017	0.008	0.019	0.052	0.09
Δ HQE	0.28	0.027	0.040	0.031	0.019	0.035	0.068	0.07
$\Delta\ \Gamma_{\rm SL}$	0.59							
$\lvert V_{cb}\rvert$	1.000	-0.450	-0.315	0.495	0.311	-0.275	0.070	0.674
m_b		1.000	0.962	-0.525	-0.225	-0.226	-0.211	0.121
m_c			1.000	-0.536	-0.310	-0.448	-0.100	0.152
μ_π^2				1.000	0.750	0.230	0.071	0.126
ρ_D^3					1.000	0.185	-0.507	0.123
μ_G^2						1.000	-0.034	-0.160
ρ_{LS}^3							1.000	-0.070
$BR_{c\ell^+\nu_\ell}$								1.000

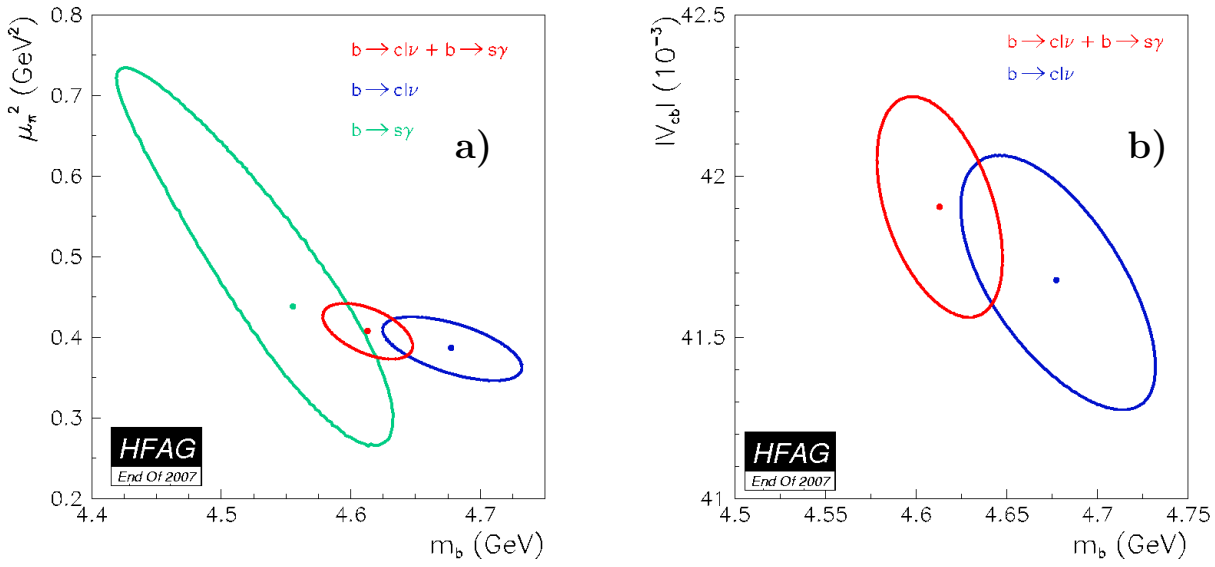

Figure 47: Comparison of scenarios from fits in the kinetic mass scheme. Figure (a) shows the $\Delta\chi^2 = 1$ contour in the (m_b,μ_π^2) plane for the combined fit to all moments (red), the fit to hadron and lepton moments only (blue) and the fit to photon moments only (green). Figure (b) shows the results for the combined fit (red) and the fit to hadron and lepton moments only (blue) in the (m_b,$|V_{cb}|$) plane.

The inclusive spectral moments of $B \to X_c\ell\nu$ decays are derived up to $\mathcal{O}(1/m_b^3)$ in Ref. [214]. The theoretical expressions for the truncated moments are given in terms of HQE parameters, and coefficients determined by theory, which are functions of the lower lepton energy threshold $E_{\rm min}$. The non-perturbative corrections are parametrized by the parameters, $\overline{\Lambda}^{1S}$ ($\mathcal{O}(m_b)$), λ_1 and λ_2 ($\mathcal{O}(1/m_b^2)$), and τ_1, τ_2, τ_3, τ_4, ρ_1 and ρ_2 ($\mathcal{O}(1/m_b^3)$). One of the higher order parameters, τ_4 is set to zero, and from available constraints, *e.g.* $B^* - B$ mass splitting, $\lambda_2 = 0.1227 - 0.0145\lambda_1$ and $\rho_2 = 0.1361 + \tau_2$, following the prescription in Ref. [214].

A total of seven parameters are then determined. We performed the 1S fit following the method described in Ref. [215]. Measurements with higher cutoff energies (*i.e.* electron energy and hadron mass moments with $E_{\rm min} > 1.5$ GeV and photon energy moments with $E_{\rm min} > 2$ GeV) are not used to determine the HQE parameters, as theoretical predictions are not considered reliable in this region. Finally, points where correlations with neighbouring points are too high have also been excluded.

The following results are obtained for the parameters in the fit to the full $B \to X_c\ell^+\nu_\ell$ and $B \to X_s\gamma$ data set (χ^2/n.d.f.= 25.3/63):

$$\begin{aligned} |V_{cb}| &= (41.78 \pm 0.30 \pm 0.08) \times 10^{-3} \ , \\ m_b^{\rm 1S} &= (4.701 \pm 0.030)\ {\rm GeV}/c^2 \ , \ \text{and} \\ \lambda_1 &= (-0.313 \pm 0.025)\ {\rm GeV}^2 \ . \end{aligned}$$

The corresponding fit parameter correlations are given in Table 62. The consistency between the fit results for the two different decay processes, $B \to X_c\ell^+\nu_\ell$ and $B \to X_s\gamma$, is assessed by

	$\lvert V_{cb}\rvert$	m_b^{1S}	λ_1
$\lvert V_{cb}\rvert$	1.000	−0.379	−0.232
m_b^{1S}		1.000	0.852
λ_1			1.000

Table 62: Correlation coefficients of the parameters in the 1S fit.

performing the fit with and without the inclusion of the photon moments. The fit to only the $B \to X_c \ell \overline{\nu}$ moments results in (χ^2/n.d.f.= 22.7/63):

$$\begin{aligned} |V_{cb}| &= (41.56 \pm 0.39 \pm 0.08) \times 10^{-3} \ , \\ m_b^{1S} &= (4.751 \pm 0.058) \ \mathrm{GeV}/c^2 \ , \ \text{and} \\ \lambda_1 &= (-0.274 \pm 0.047) \ \mathrm{GeV}^2 \ . \end{aligned}$$

The first error is from the fit including experimental and theory errors, and the second error (on $|V_{cb}|$ only) is due to the uncertainty on the average B lifetime. The precision on $|V_{cb}|$ is of order 1%. The $\Delta\chi^2 = 1$ fit contour plots in the (m_b,λ_1) and (m_b,$|V_{cb}|$) planes are shown in Figure 48. All fit results are preliminary.

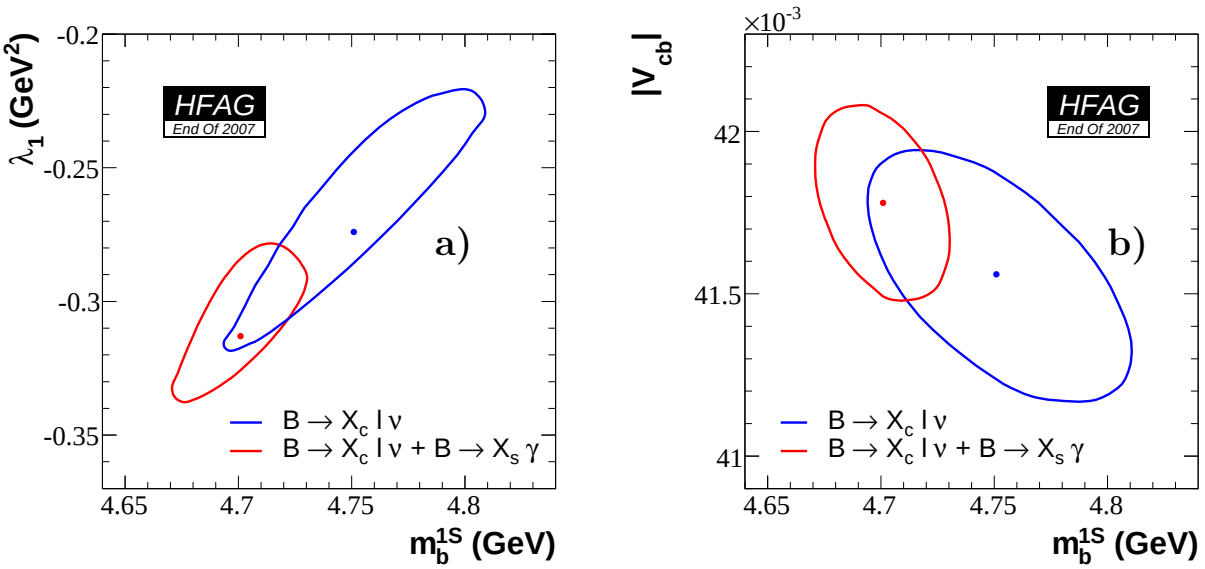

Figure 48: Comparison of scenarios from fits in the 1S mass scheme. Figure (a) shows the $\Delta\chi^2$ = 1 contour in the (m_b,λ_1) plane for the combined fit to all moments (red), the fit to hadron and lepton moments only (blue). Figure (b) shows the results for the combined fit (red) and the fit to hadron and lepton moments only (blue) in the (m_b,$|V_{cb}|$) plane.

5.4 Exclusive CKM-suppressed decays

In this section, we list results on exclusive semileptonic branching fractions and determinations of $|V_{ub}|$ based on $B \to \pi\ell^+\nu_\ell$ decays. A new measurement of the exclusive decay $B \to \pi\ell^+\nu_\ell$ from CLEO was presented in 2007 [216]. Come previous preliminary results from the other Collaborations were finalized. The measurements are based on two different event selections: tagged events, in which the second B meson in the event is fully reconstructed in either a hadronic decay ("B_{reco}") or in a CKM-favored semileptonic decay ("SL"); and untagged events, in which case the selection infers the momentum of the undetected neutrino from the measurement of the sum of the momenta of all detected particles and the knowledge of the initial state. The results for the full and partial branching fraction are given in Table 63 and shown in Figure 49 (a).

When averaging these results, systematic uncertainties due to external inputs, e.g., form factor shapes and background estimates from the modeling of $B \to X_c\ell^+\nu_\ell$ and $B \to X_u\ell^+\nu_\ell$ decays, are treated as fully correlated. Uncertainties due to experimental reconstruction effects are treated as fully correlated among measurements from a given experiment.

Table 63: Summary of exclusive determinations of $\mathcal{B}(B \to \pi\ell^+\nu_\ell)$. The errors quoted correspond to statistical and systematic uncertainties, respectively. Measured branching fractions for $B^+ \to \pi^0\ell^+\nu_\ell$ have been multiplied by $2 \times \tau_{B^0}/\tau_{B^+}$ [3] in accordance with isospin symmetry. The labels "B_{reco}" and "SL" tags refer to the type of B decay tag used in a measurement, and "untagged" refers to an untagged measurement. Concerning Ref. [220], only the measurement in the full q^2 is presented.

	$\mathcal{B}[10^{-4}]$	$\mathcal{B}(q^2 > 16\,\mathrm{GeV}^2/c^2)[10^{-4}]$	$\mathcal{B}(q^2 < 16\,\mathrm{GeV}^2/c^2)[10^{-4}]$
CLEO π^+, π^0 [216]	$1.37 \pm 0.15 \pm 0.11$	$0.41 \pm 0.08 \pm 0.04$	$0.96 \pm 0.13 \pm 0.10$
BABAR π^+ [217]	$1.46 \pm 0.07 \pm 0.08$	$0.38 \pm 0.04 \pm 0.03$	$1.09 \pm 0.06 \pm 0.07$
Average of untagged	$\mathbf{1.43 \pm 0.07 \pm 0.08}$	$\mathbf{0.39 \pm 0.04 \pm 0.04}$	$\mathbf{1.05 \pm 0.06 \pm 0.07}$
BELLE SL π^+ [218]	$1.38 \pm 0.19 \pm 0.14$	$0.36 \pm 0.10 \pm 0.04$	$1.02 \pm 0.16 \pm 0.11$
BELLE SL π^0 [218]	$1.45 \pm 0.26 \pm 0.15$	$0.38 \pm 0.15 \pm 0.04$	$1.07 \pm 0.23 \pm 0.11$
BABAR SL π^+ [219]	$1.12 \pm 0.25 \pm 0.10$	$0.29 \pm 0.15 \pm 0.04$	$0.83 \pm 0.22 \pm 0.08$
BABAR SL π^0 [219]	$1.37 \pm 0.34 \pm 0.15$	$0.19 \pm 0.23 \pm 0.08$	$1.18 \pm 0.30 \pm 0.12$
BABAR B_{reco} π^+ [219]	$1.07 \pm 0.27 \pm 0.15$	$0.65 \pm 0.20 \pm 0.13$	$0.42 \pm 0.18 \pm 0.05$
BABAR B_{reco} π^0 [219]	$1.54 \pm 0.41 \pm 0.21$	$0.49 \pm 0.23 \pm 0.11$	$1.05 \pm 0.36 \pm 0.15$
BELLE B_{reco} π^+ [220]	$1.49 \pm 0.26 \pm 0.06$	n/a	n/a
BELLE B_{reco} π^0 [220]	$1.62 \pm 0.32 \pm 0.11$	n/a	n/a
Average of tagged	$\mathbf{1.35 \pm 0.10 \pm 0.07}$	$\mathbf{0.36 \pm 0.06 \pm 0.03}$	$\mathbf{0.83 \pm 0.09 \pm 0.06}$
Average	$\mathbf{1.40 \pm 0.06 \pm 0.06}$	$\mathbf{0.38 \pm 0.03 \pm 0.03}$	$\mathbf{0.95 \pm 0.05 \pm 0.05}$

The determination of $|V_{ub}|$ from the $B \to \pi\ell^+\nu_\ell$ decays is shown in Table 64, and uses the average branching fraction given in Table 63. Two theoretical approaches are used: QCD sum rules [221] and Lattice QCD (unquenched [177, 222] and quenched [223]). Lattice calculations of the Form Factors (FF) are limited to small hadron momenta, i.e. large q^2, while calculations based on light cone sum rules are restricted to small q^2. More precise calculations of the FF, in particular their normalization, are needed to reduce the overall uncertainties.

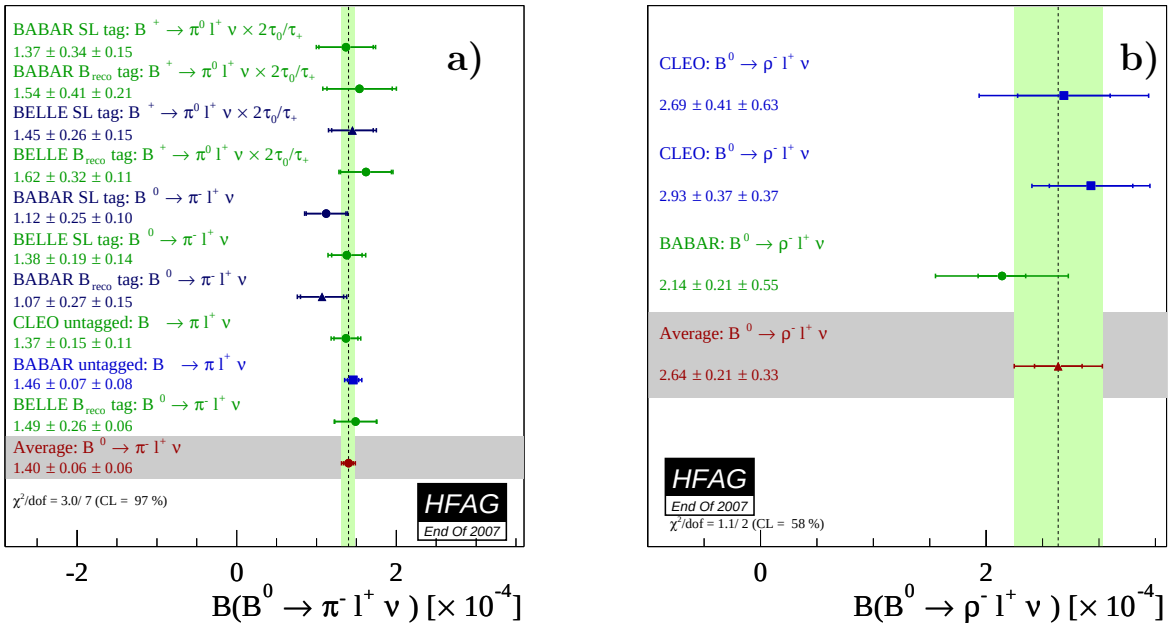

Figure 49: (a) Summary of exclusive determinations of $\mathcal{B}(B \to \pi\ell^+\nu_\ell)$ and their average. Measured branching fractions for $B \to \pi^0\ell^+\nu_\ell$ have been multiplied by $2 \times \tau_{B^0}/\tau_{B^+}$ [3] in accordance with isospin symmetry. The labels "B_{reco}" and "SL" refer to type of B decay tag used in a measurement. "untagged" refers to an untagged measurement. (b) Summary of exclusive determinations of $\mathcal{B}(B \to \rho\ell^+\nu_\ell)$ and their average.

We present for the first time also branching fractions for $B \to \rho\ell^+\nu_\ell$ decays in Table 5.4 and Figure 49 (b). The determination of $|V_{ub}|$ from these other channels looks less promising than for $B \to \pi\ell^+\nu_\ell$, primarily because there is limited theoretical information on the normalization and shape of the form factors, thus at the moment it is not extracted.

Branching fractions for other $B \to X_u\ell^+\nu_\ell$ decays are given in Table 66.

5.5 Inclusive CKM-suppressed decays

The large background from $B \to X_c\ell^+\nu_\ell$ decays is the chief experimental limitation in determinations of $|V_{ub}|$. Cuts designed to reject this background limit the acceptance for $B \to X_u\ell^+\nu_\ell$ decays. The calculation of partial rates for these restricted acceptances is more complicated and requires substantial theoretical machinery. In this update, we had added several new theoretical calculations to extract $|V_{ub}|$. We do not advocate the use of one method over another. The authors for the different calculations have provided codes to compute the partial rates in limited regions of phase space covered by the measurements.

For the averages we performed, the systematic errors associated with the modeling of $B \to X_c\ell^+\nu_\ell$ and $B \to X_u\ell^+\nu_\ell$ decays and the theoretical uncertainties are taken as fully correlated among all measurements. Reconstruction-related uncertainties are taken as fully correlated within a given experiment. From the three results published each by *BABAR* and Belle [227,228], only one is used in the average, because the three measurements are all based on the same dataset and are highly correlated. Specifically, we use the M_X analysis result for the averages. As a consequence, the experimental results have negligible statistical correlations. To make

Table 64: Determinations of $|V_{ub}|$ based on the average total and partial $\overline{B} \to \pi^- \ell^+ \nu_\ell$ decay branching fraction stated in Table 63. The first uncertainty is experimental, and the second is from theory. The full or partial branching fractions are used as indicated. Acronysms for the calculations refer to either the method (LCSR) or the collaboration working on it (HPQCD, FNAL, APE).

Method	$\lvert V_{ub}\rvert[10^{-3}]$
LCSR, full q^2 [221]	$3.41 \pm 0.11^{+0.67}_{-0.42}$
LCSR, $q^2 < 16\,\mathrm{GeV}^2/c^2$ [221]	$3.38 \pm 0.13^{+0.56}_{-0.37}$
HPQCD, full q^2 [222]	$3.11 \pm 0.10^{+0.73}_{-0.43}$
HPQCD, $q^2 > 16\,\mathrm{GeV}^2/c^2$ [222]	$3.47 \pm 0.20^{+0.60}_{-0.39}$
FNAL, full q^2 [177]	$3.80 \pm 0.12^{+0.88}_{-0.52}$
FNAL, $q^2 > 16\,\mathrm{GeV}^2/c^2$ [177]	$3.69 \pm 0.21^{+0.64}_{-0.42}$
APE, full q^2 [223]	$3.59 \pm 0.11^{+1.11}_{-0.57}$
APE, $q^2 > 16\,\mathrm{GeV}^2/c^2$ [223]	$3.72 \pm 0.21^{+1.43}_{-0.66}$

Table 65: Summary of exclusive determinations of $\mathcal{B}(B \to \rho \ell^+ \nu_\ell)$. The errors quoted correspond to statistical and systematic uncertainties, respectively.

	$\mathcal{B}[10^{-4}]$
CLEO ρ^+ [216]	$2.69 \pm 0.41 \pm 0.63$
CLEO ρ^+ [216]	$2.93 \pm 0.37 \pm 0.37$
BABAR ρ^+ [224]	$2.14 \pm 0.21 \pm 0.55$
Average	$\mathbf{2.64 \pm 0.21 \pm 0.33}$

Table 66: Summary of branching fractions to $\mathcal{B}(B \to X \ell^+ \nu_\ell)$ decays other than $B \to \pi \ell^+ \nu_\ell$ and $B \to \rho \ell^+ \nu_\ell$. The errors quoted correspond to statistical and systematic uncertainties, respectively. Where a third uncertainty is quoted, it corresponds to uncertainties from form factor shapes.

Experiment	Mode	$\mathcal{B}[10^{-4}]$
BELLE [225]	$B^+ \to \omega \ell^+ \nu_\ell$	$1.3 \pm 0.4 \pm 0.2 \pm 0.3$
CLEO [216]	$B^+ \to \eta \ell^+ \nu_\ell$	$0.84 \pm 0.31 \pm 0.16 \pm 0.09$
BABAR [226]	$B^+ \to \eta \ell^+ \nu_\ell$	$0.84 \pm 0.27 \pm 0.21$
BABAR [226]	$B^+ \to \eta' \ell^+ \nu_\ell$	$0.33 \pm 0.60 \pm 0.30$

use of the theoretical calculations of Ref. [229], we restrict the kinematic range in M_X and q^2, thereby reducing the size of the data sample significantly, but also the theoretical uncertainty, as stated by the authors [229]. The dependence of the quoted error on the measured value for each source of error is taken into account in the calculation of the averages. Measurements of partial branching fractions for $B \to X_u \ell^+ \nu_\ell$ transitions from $\Upsilon(4S)$ decays, together with the corresponding accepted region, are given in Table 67. The signal yields for all the measurements

shown in Table 67 are not rescaled to common input values of the B meson lifetime (see table 44) and the semileptonic width [3].

It has been first suggested by Neubert [230] and later detailed by Leibovich, Low, and Rothstein (LLR) [231] and Lange, Neubert and Paz (LNP) [232], that the uncertainty of the leading shape functions can be eliminated by comparing inclusive rates for $B \to X_u \ell^+ \nu_\ell$ decays with the inclusive photon spectrum in $B \to X_s \gamma$, based on the assumption that the shape functions for transitions to light quarks, u or s, are the same to first order. However, shape function uncertainties are only eliminated at the leading order and they still enter via the signal models used for the determination of efficiency. For completeness, we provide a comparison of the results using calculations with reduced dependence on the shape function, as just introduced, with our averages using different theoretical approaches. Results are presented by *BABAR* in Ref. [233] using the LLR prescription. More recently, V.B.Golubev, V.G.Luth and Yu.I.Skovpen (Ref. [234]) extracted $|V_{ub}|$ from the endpoint spectrum of $B \to X_u \ell^+ \nu_\ell$ from *BABAR* [235], using several theoretical approaches with reduced dependence on the shape function. In both cases, the photon energy spectrum in the rest frame of the B-meson by *BABAR* [204] has been used.

Table 67: Summary of inclusive determinations of partial branching fractions for $B \to X_u \ell^+ \nu_\ell$ decays. The errors quoted on $\Delta\mathcal{B}$ correspond to statistical and systematic uncertainties. The P_+ analysis is actually not used in the current averages since it is stringly correlated with the M_X analysis. The $s_{\rm h}^{\rm max}$ variable is described in Refs. [237, 238].

Measurement	Accepted region	$\Delta\mathcal{B}[10^{-4}]$
CLEO [236]	$E_e > 2.1\,\text{GeV}$	$3.3 \pm 0.2 \pm 0.7$
BABAR [238]	$E_e > 2.0\,\text{GeV}$, $s_{\rm h}^{\rm max} < 3.5\,\text{GeV}^2$	$4.4 \pm 0.4 \pm 0.4$
BABAR [235]	$E_e > 2.0\,\text{GeV}$	$5.7 \pm 0.4 \pm 0.5$
BELLE [239]	$E_e > 1.9\,\text{GeV}$	$8.5 \pm 0.4 \pm 1.5$
BABAR [227]	$M_X < 1.7\,\text{GeV}/c^2, q^2 > 8\,\text{GeV}^2/c^2$	$8.1 \pm 0.8 \pm 0.7$
BELLE [240]	$M_X < 1.7\,\text{GeV}/c^2, q^2 > 8\,\text{GeV}^2/c^2$	$7.4 \pm 0.9 \pm 1.3$
BELLE [228]	$M_X < 1.7\,\text{GeV}/c^2, q^2 > 8\,\text{GeV}^2/c^2$	$8.4 \pm 0.8 \pm 0.4$
BABAR [227]	$P_+ < 0.66\,\text{GeV}$	$9.4 \pm 1.0 \pm 0.8$
BELLE [228]	$P_+ < 0.66\,\text{GeV}$	$11.0 \pm 1.0 \pm 1.6$
BABAR [227]	$M_X < 1.55\,\text{GeV}/c^2$	$11.7 \pm 0.9 \pm 0.7$
BELLE [228]	$M_X < 1.7\,\text{GeV}/c^2$	$12.3 \pm 1.1 \pm 1.2$

5.5.1 BLNP

Bosch, Lange, Neubert and Paz (BLNP) [241–245] provide theoretical expressions for the triple differential decay rate for $B \to X_u \ell^+ \nu_\ell$ events, incorporating all known contributions, whilst smoothly interpolating between the "shape-function region" of large hadronic energy and small invariant mass, and the "OPE region" in which all hadronic kinematical variables scale with the b-quark mass. BLNP assign uncertainties to the b-quark mass which enters through the leading shape function, to sub-leading shape function forms, to possible weak annihilation contribution, and to matching scales. The extracted values of $|V_{ub}|$ for each measurement along with their average are given in Table 68 and illustrated in Figure 50. The total uncertainty is $^{+8.8}_{-7.7}\%$ and is due to: statistics ($^{+2.0}_{-2.0}\%$), detector ($^{+2.3}_{-2.2}\%$), $B \to X_c \ell^+ \nu_\ell$ model ($^{+1.3}_{-1.2}\%$), $B \to$

$X_u\ell^+\nu_\ell$ model ($^{+1.4}_{-1.4}$%), heavy quark parameters ($^{+7.0}_{-5.8}$%), SF functional form ($^{+0.5}_{-0.5}$%), sub-leading shape functions ($^{+0.7}_{-0.7}$%), BLNP theory: matching scales μ, μ_i, μ_h ($^{+3.6}_{-3.3}$%), and weak annihilation ($^{+1.3}_{-1.3}$%). The error on the HQE parameters (b-quark mass and μ_π^2) is the source of the largest uncertainty, while the uncertainty assigned for the matching scales is a close second.

Table 68: Summary of input parameters used by the different theory calculations, corresponding inclusive determinations of $|V_{ub}|$ and their average. The errors quoted on $|V_{ub}|$ correspond to experimental and theoretical uncertainties, respectively. Note that only the M_X analysis is used for Refs. [227, 228], as the other analyses are highly correlated.

	BLNP	DGE	GGOU	ADFR	BLL
Input parameters					
scheme	SF	$\overline{MS}$	kinetic	$\overline{MS}$	$1S$
Ref.	see Sect. 5.3.5 (only $b \to c\ell\nu$ moments)	Ref. [3]	see Sect. 5.3.5 ($b \to c\ell\nu + b \to s\gamma$ moments)	Ref. [3]	see Sect. 5.3.6
m_b (GeV)	$4.707\ ^{+0.059}_{-0.053}$	4.20 ± 0.07	$4.613\ ^{+0.022}_{-0.027}$	4.20 ± 0.07	4.70 ± 0.03
μ_π^2 (GeV^2)	$0.216\ ^{+0.054}_{-0.076}$	-	$0.408\ ^{+0.017}_{-0.031}$	-	-
Ref.	$\|V_{ub}\|$ values				
E_e [236]	$3.52 \pm 0.41^{+0.38}_{-0.32}$	$3.85 \pm 0.45^{+0.28}_{-0.27}$	$3.70 \pm 0.43^{+0.25}_{-0.39}$	$3.47 \pm 0.20^{+0.25}_{-0.26}$	-
M_X, q^2 [240]	$3.98 \pm 0.42^{+0.34}_{-0.28}$	$4.43 \pm 0.47^{+0.23}_{-0.21}$	$4.15 \pm 0.44^{+0.33}_{-0.34}$	$3.93 \pm 0.42^{+0.25}_{-0.26}$	$3.71 \pm 0.50^{+0.35}_{-0.35}$
E_e [239]	$4.36 \pm 0.41^{+0.36}_{-0.30}$	$4.81 \pm 0.45^{+0.22}_{-0.21}$	$4.55 \pm 0.42^{+0.22}_{-0.31}$	$3.18 \pm 0.16^{+0.23}_{-0.24}$	-
E_e [235]	$3.90 \pm 0.22^{+0.35}_{-0.30}$	$4.30 \pm 0.29^{+0.25}_{-0.24}$	$4.07 \pm 0.23^{+0.23}_{-0.33}$	$3.44 \pm 0.14^{+0.25}_{-0.26}$	-
$E_e, s_{\rm h}^{\rm max}$ [238]	$3.95 \pm 0.27^{+0.42}_{-0.36}$	$4.42 \pm 0.30^{+0.37}_{-0.36}$	-	$3.87 \pm 0.26^{+0.26}_{-0.26}$	$4.71 \pm 0.50^{+0.35}_{-0.35}$
M_X [228]	$3.66 \pm 0.24^{+0.29}_{-0.24}$	$4.29 \pm 0.28^{+0.27}_{-0.24}$	$3.89 \pm 0.26^{+0.19}_{-0.22}$	$3.91 \pm 0.26^{+0.26}_{-0.27}$	-
M_X [227]	$3.73 \pm 0.18^{+0.33}_{-0.28}$	$4.55 \pm 0.22^{+0.30}_{-0.29}$	$4.01 \pm 0.19^{+0.26}_{-0.29}$	$4.01 \pm 0.20^{+0.27}_{-0.28}$	-
M_X, q^2 [227]	-	-	-	-	$4.92 \pm 0.32^{+0.36}_{-0.36}$
M_X, q^2 [228]	-	-	-	-	$5.01 \pm 0.39^{+0.37}_{-0.37}$
Average	$3.98 \pm 0.14^{+0.32}_{-0.27}$	$4.47 \pm 0.16^{+0.25}_{-0.26}$	$3.94 \pm 0.15^{+0.20}_{-0.23}$	$3.78 \pm 0.13^{+0.24}_{-0.24}$	$4.91 \pm 0.24^{+0.38}_{-0.38}$

5.5.2 DGE

J.R. Andersen and E. Gardi (Dressed Gluon Exponentiation, DGE) [246] provide a framework where the on-shell b-quark calculation, converted into hadronic variables, is directly used as an approximation to the meson decay spectrum without the use of a leading-power non-perturbative function (or, in other words, a shape function). The on-shell mass of the b-quark within the B-meson (m_b) is required as input. The extracted values of $|V_{ub}|$ for each measurement along with their average are given in Table 68 and illustrated in Figure 51. The total error is $^{+6.8}_{-6.9}$%, whose breakdown is: statistics ($^{+1.9}_{-1.9}$%), detector ($^{+2.4}_{-2.3}$%), $B \to X_c\ell^+\nu_\ell$ model ($^{+1.8}_{-1.7}$%), $B \to X_u\ell^+\nu_\ell$ model ($^{+1.1}_{-1.1}$%), spectral fraction (m_b) ($^{+3.0}_{-3.3}$%), strong coupling α_s ($^{+0.7}_{-0.8}$%), total semileptonic width (m_b) ($^{+3.0}_{-3.0}$%), weak annihilation ($^{+1.9}_{-1.9}$%), DGE theory: matching scales ($^{+3.2}_{-3.1}$%). The largest contribution to the total error is due to the effect of the uncertainty on m_b on the prediction of the event rate, closely followed by the specific theory error on overall DGE and the total semileptonic decay width.

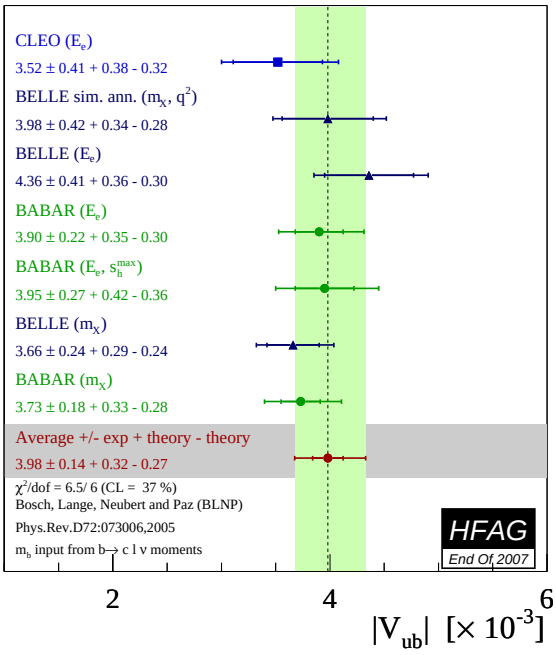

Figure 50: Measurements of $|V_{ub}|$ from inclusive semileptonic decays and their average based on the BLNP prescription. "E_e", "M_X", "(M_X, q^2)" and "(E_e, s_h^{max})" indicate the distributions and cuts used for the measurement of the partial decay rates.

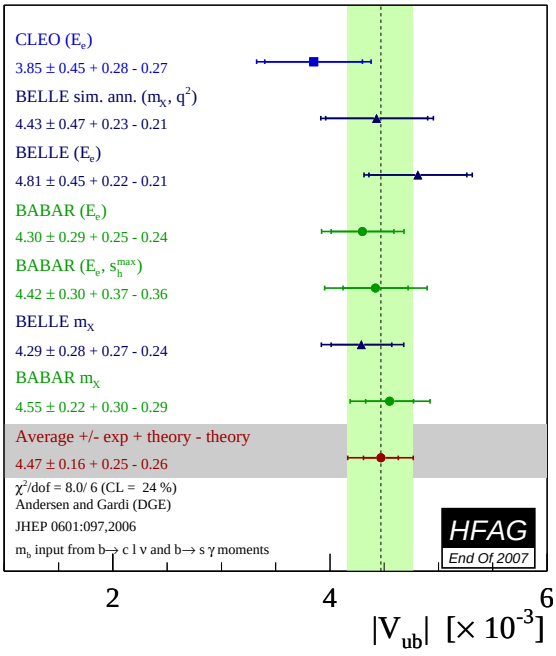

Figure 51: Measurements of $|V_{ub}|$ from inclusive semileptonic decays and their average based on the DGE prescription. "E_e", "M_X", "(M_X, q^2)" and "(E_e, s_h^{max})" indicate the analysis type.

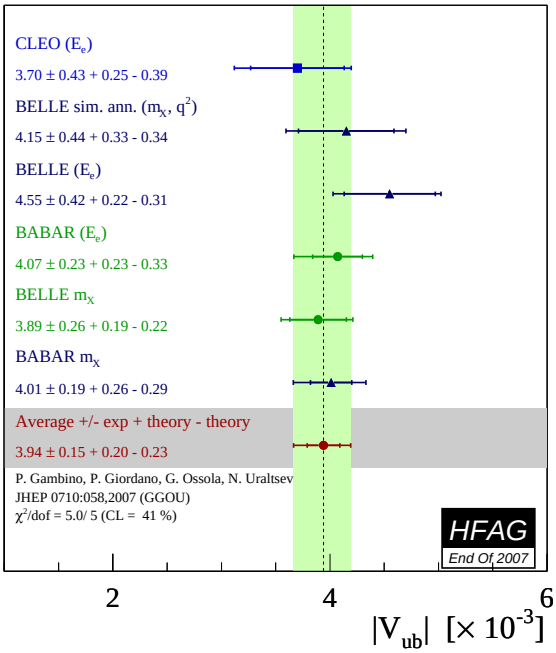

Figure 52: Measurements of $|V_{ub}|$ from inclusive semileptonic decays and their average based on the GGOU prescription. "E_e", "M_X", "(M_X, q^2)" and "(E_e, s_h^{max})" indicate the analysis type.

5.5.3 GGOU

Gambino, Giordano, Ossola and Uraltsev (GGOU) [247] compute the triple differential decay rates of $B \to X_u \ell^+ \nu_\ell$, including all perturbative and non–perturbative effects through $O(\alpha_s^2 \beta_0)$ and $O(1/m_b^3)$. The Fermi motion is parameterized in terms of a single light–cone function for each structure function and for any value of q^2, accounting for all subleading effects. The calculations are performed in the kinetic scheme, a framework characterized by a Wilsonian treatment with a hard cutoff $\mu \sim 1$ GeV. At present, GGOU have not included calculations for the "(E_e, s_h^{max})" analysis, but this addition is planned. The extracted values of $|V_{ub}|$ for each measurement along with their average are given in Table 68 and illustrated in Figure 52. The total error is $^{+6.3}_{-7.0}\%$ whose breakdown is: statistics ($^{+2.1}_{-2.3}\%$), detector ($^{+2.2}_{-2.2}\%$), $B \to X_c \ell^+ \nu_\ell$ model ($^{+1.5}_{-1.2}\%$), $B \to X_u \ell^+ \nu_\ell$ model ($^{+1.4}_{-1.6}\%$), α_s, m_b and other non–perturbative parameters ($^{+3.9}_{-3.8}\%$), higher order perturbative and non–perturbative corrections ($^{+1.8}_{-1.7}\%$), modelling of the q^2 tail and choice of the scale q^{2*} ($^{+2.5}_{-2.7}\%$), weak annihilations matrix element ($^{+0}_{-3.1}\%$), functional form of the distribution functions ($^{+1.3}_{-0.6}\%$), The leading uncertainties on $|V_{ub}|$ are both from theory, and are due to perturbative and non–perturbative parameters and the modelling of the q^2 tail and choice of the scale q^{2*}.

5.5.4 ADFR

Aglietti, Di Lodovico, Ferrera and Ricciardi (ADFR) [248] use a new approach to extract $|V_{ub}|$, which makes use of the ratio of the $B \to X_c \ell^+ \nu_\ell$ and $B \to X_u \ell^+ \nu_\ell$ widths. The normalized triple differential decay rate for $B \to X_u \ell^+ \nu_\ell$ [249–252] is calculated with a model based on (i) soft–gluon resummation to next–to–next–leading order and (ii) an effective QCD coupling without

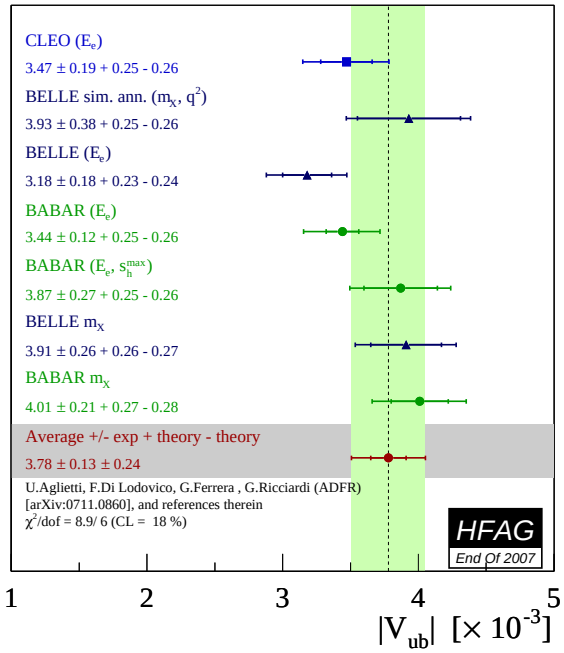

Figure 53: Measurements of $|V_{ub}|$ from inclusive semileptonic decays and their average based on the ADFR prescription. "E_e", "M_X", "(M_X, q^2)" and "(E_e, s_h^{max})" indicate the analysis type.

Landau pole. This coupling is constructed by means of an extrapolation to low energy of the high–energy behaviour of the standard coupling. More technically, an analyticity principle is used. The lower cut on the electron energy for the endpoint analyses is 2.3 GeV [249]. The extracted values of $|V_{ub}|$ for each measurement along with their average are given in Table 68 and illustrated in Figure 53. The total error is $^{+7.2}_{-7.2}\%$ whose breakdown is: statistics ($^{+1.8}_{-1.9}\%$), detector ($^{+2.3}_{-2.3}\%$), $B \to X_c \ell^+ \nu_\ell$ model ($^{+1.2}_{-1.3}\%$), $B \to X_u \ell^+ \nu_\ell$ model ($^{+1.3}_{-1.4}\%$), α_s ($^{+2.0}_{-2.0}\%$), $|V_{cb}|$ ($^{+1.4}_{-1.4}\%$), m_b ($^{+1.0}_{-1.0}\%$), m_c ($^{+4.5}_{-4.3}\%$), semileptonic branching fraction ($^{+0.9}_{-1.0}\%$), theory model ($^{+3.5}_{-3.5}\%$). The leading uncertainties, both from theory, are due to the m_c mass and the theory model.

5.5.5 BLL

Bauer, Ligeti, and Luke (BLL) [229] give a HQET-based prescription that advocates combined cuts on the dilepton invariant mass, q^2, and hadronic mass, m_X, to minimise the overall uncertainty on $|V_{ub}|$. In their reckoning a cut on m_X only, although most efficient at preserving phase space ($\sim$80%), makes the calculation of the partial rate untenable due to uncalculable corrections to the b-quark distribution function or shape function. These corrections are suppressed if events in the low q^2 region are removed. The cut combination used in measurements is $M_x < 1.7$ GeV/c^2 and $q^2 > 8$ GeV$^2/c^2$. The extracted values of $|V_{ub}|$ for each measurement along with their average are given in Table 68 and illustrated in Figure 54. The total error is $^{+9.0}_{-9.0}\%$ whose breakdown is: statistics ($^{+3.2}_{-3.2}\%$), detector ($^{+3.8}_{-3.8}\%$), $B \to X_c \ell^+ \nu_\ell$ model ($^{+1.3}_{-1.3}\%$), $B \to X_u \ell^+ \nu_\ell$ model ($^{+2.1}_{-2.1}\%$), spectral fraction (m_b) ($^{+3.0}_{-3.0}\%$), perturbative : strong coupling α_s ($^{+3.0}_{-3.0}\%$), residual shape function ($^{+4.5}_{-4.5}\%$), third order terms in the OPE ($^{+4.0}_{-4.0}\%$), The leading uncertainties, both from theory, are due to residual shape function effects and third order terms in the OPE expansion. The leading experimental uncertainty is due to statistics.

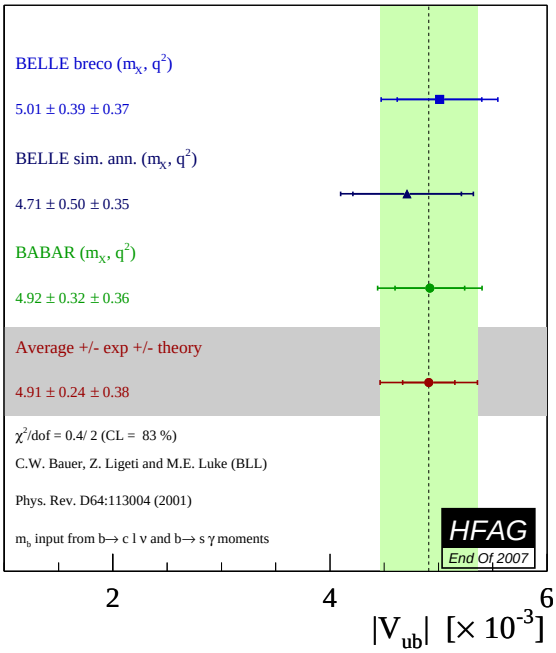

Figure 54: Measurements of $|V_{ub}|$ from inclusive semileptonic decays and their average in the BLL prescription. "(M_X, q^2)" indicates the analysis type.

5.5.6 Summary

A summary of the averages presented in several different frameworks and results by V.B.Golubev, V.G.Luth and Yu.I.Skovpen [234], based on prescriptions by LLR [231] and LNP [232] to reduce the leading shape function uncertainties are presented in Table 69. A value judgement based on a direct comparison should be avoided at the moment, experimental and theoretical uncertainties play out differently between the schemes and the theoretical assumptions for the theory calculations are different.

Table 69: Summary of inclusive determinations of $|V_{ub}|$. The errors quoted on $|V_{ub}|$ correspond to experimental and theoretical uncertainties, except for the last two measurements where the errors are due to the *BABAR* endpoint analysis, the *BABAR* $b \to s\gamma$ analysis [233], the theoretical errors and V_{ts} for the last averages.

Framework	$\lvert V_{ub}\rvert[10^{-3}]$
BLNP	$3.98 \pm 0.14^{+0.32}_{-0.27}$
DGE	$4.47 \pm 0.16^{+0.25}_{-0.26}$
GGOU	$3.94 \pm 0.15^{+0.20}_{-0.23}$
ADFR	$3.78 \pm 0.13^{+0.24}_{-0.24}$
BLL (m_X/q^2 only)	$4.91 \pm 0.24 \pm 0.38$
LLR (*BABAR*) [233]	$4.92 \pm 0.32 \pm 0.36$
LLR (*BABAR*) [234]	$4.28 \pm 0.29 \pm 0.29 \pm 0.26 \pm 0.28$
LNP (*BABAR*) [234]	$4.40 \pm 0.30 \pm 0.41 \pm 0.23$

6 B-decays to charmed hadrons

This section reports the updated contribution to the HFAG report from the "$B \to$ charm" group[24]. The mandate of the group is to compile measurements and perform averages of all available quantities related to B decays to charmed particles, excluding CP related quantities. To date the group has analyzed a total of 492 measurements reported in 148 papers, principally branching fractions. The group aims to organize and present the copious information on B decays to charmed particles obtained from a combined sample of about two billion B mesons from the BABAR, Belle and CDF Collaborations.

This huge sample of B mesons allows to measure decays to states with open or hidden charm content with unprecedented precision. Branching fractions for rare B-meson decays or decay chains of a few 10^{-7} are being measured with statistical uncertainties typically below 30%, and new decay chains can be accessed with branching fractions down to 10^{-8}. Results for more common decay chains, with branching fractions around 10^{-4}, are becoming precision measurements, with uncertainties typically at the 3% level. Some decays have been observed for the first time, for example $B^0 \to J/\psi\eta$ or $B^- \to \Lambda_c^- p$, with a branching fraction of $(9.6 \pm 1.8) \times 10^{-6}$ and $(2.1^{+1.2}_{-0.9}) \times 10^{-5}$, respectively.

The large sample of B mesons allows to greatly improve our understanding of recently discovered new states with either hidden or open charm content, such as the $X(3872)$, the $D_{sJ}^{*-}(2317)$ and $D_{sJ}^{-}(2460)$ mesons. Measurements with many different final states for these particles are reported, allowing to shed more light on their nature. The $D^0\overline{D}^{*0}(2007)$ decay of the $X(3872)$ has been observed for the first time. Using the branching fraction products $\mathcal{B}(B^- \to X(3872)K^-) \times \mathcal{B}(X(3872) \to f)$, a hierarchy can be established between the decay modes f: these branching fraction products are found to be $(1.67 \pm 0.59) \times 10^{-4}$, $(0.12 \pm 0.02) \times 10^{-4}$, and $(0.022 \pm 0.005) \times 10^{-4}$, for $D^0\overline{D}^{*0}(2007)$, $J/\psi\pi^+\pi^-$ and $J/\psi\gamma$, respectively. This is an important piece of information to discriminate between various interpretations for the $X(3872)$ state.

The measurements are classified according to the decaying particle: Charged B, Neutral B or Miscellaneous; the decay products and the type of quantity: branching fraction, product of branching fractions, ratio of branching fractions or other quantities. For the decay product classification the below precedence order is used to ensure that each measurement appears in only one category.

- new particles
- strange D mesons
- baryons
- J/ψ
- charmonium other than J/ψ
- multiple D, D^* or D^{**} mesons
- a single D^* or D^{**} meson
- a single D meson
- other particles

[24]The HFAG/BtoCharm group was formed in the spring of 2005; it performs its work using an XML database backed web application.

Within each table the measurements are color coded according to the publication status and age. Table 70 provides a key to the color scheme and categories used. When viewing the tables with most pdf viewers every number, label and average provides hyperlinks to the corresponding reference and individual quantity web pages on the HFAG/BtoCharm group website http://hfag.phys.ntu.edu.tw. The links provided in the captions of the table lead to the corresponding compilation pages. Both the individual and compilation webpages provide a graphical view of the results, in a variety of formats.

Tables 71 to 111 provide either limits at 90% confidence level or measurements with statistical and systematic uncertainties and in some cases a third error corresponding to correlated systematics. For details on the meanings of the uncertainties and access to the references click on the numbers to visit the corresponding web pages. Where there are multiple determinations of the same quantity by one experiment the table footnotes act to distinguish the methods or datasets used; such cases are visually highlighted in the table by presenting the measurements on the lines beneath the quantity label. Where both limits and measured values of a quantity are available the limits are presented in the tables but are not used in the determination of the average. Where only limits are available the most stringent is presented in the Average column of the tables. Where available the PDG 2006 result is also presented.

Table 70: Key to the colors used to classify the results presented in tables 71 to 111. When viewing these tables in a pdf viewer each number, label and average provides a hyperlink to the corresponding online version provided by the charm subgroup website http://hfag.phys.ntu.edu.tw/b2charm/. Where an experiment has multiple determinations of a single quantity they are distinguished by the table footnotes.

Class	Definition
waiting	Results without a preprint available
pubhot	Results published during or after 2007
prehot	Preprint released during or after 2007
pub	Results published after or during 2006
pre	Preprint released after or during 2006
pubold	Results published before 2006
preold	Preprint released before 2006
error	Incomplete information to classify
superceeded	Results superceeded by more recent measurements from the same experiment
inactive	Results in the process of being entered into the database
noquo	Results without quotes

Table 71: Branching fractions of charged B modes producing new particles in units of 10^{-3}, upper limits are at 90% CL. The latest version is available at: http://hfag.phys.ntu.edu.tw/b2charm/00101.html

Mode	PDG 2006	Belle	*BABAR*	CDF	Average
$X(3872)K^-$	< 0.32		< 0.32		< 0.32
$D_{sJ}^-(2460)D^0$			$4.3 \pm 1.6 \pm 1.3$		4.3 ± 2.1
$D_{sJ}^-(2460)D^{*0}(2007)$			$11.2 \pm 2.6 \pm 2.0$		11.2 ± 3.3

Table 72: Product branching fractions of charged B modes producing new particles in units of 10^{-4}, upper limits are at 90% CL. The latest version is available at: http://hfag.phys.ntu.edu.tw/b2charm/00101.html

Mode	PDG 2006	Belle	*BABAR*	CDF	Average
$K^-X(3872)[\gamma J/\psi(1S)]$		$0.0180 \pm 0.0060 \pm 0.0010$	$0.033 \pm 0.010 \pm 0.003$		$\mathbf{0.022 \pm 0.005}$
$K^-X(3872)[J/\psi(1S)\eta]$	< 0.077		< 0.077		< 0.077
$K^-X(3872)[\pi^+\pi^- J/\psi(1S)]$	0.11 ± 0.02	$0.13 \pm 0.02 \pm 0.01$	$0.101 \pm 0.025 \pm 0.010$		0.12 ± 0.02
$K^-Y(3940)[J/\psi(1S)\gamma]$			< 0.140		$\mathbf{< 0.140}$
$K^-Y(4260)[J/\psi(1S)\pi^+\pi^-]$	< 0.29		$0.20 \pm 0.07 \pm 0.02$		0.20 ± 0.07
$\overline{K}^0X^-(3872)[J/\psi(1S)\pi^-\pi^0]$	< 0.22		< 0.22		< 0.22
$K^-X(3872)[D^+D^-]$	< 0.40	< 0.40			< 0.40
$K^-Y(3940)[J/\psi(1S)\omega(782)]$			$0.49 \pm 0.10 \pm 0.05$		$\mathbf{0.49 \pm 0.11}$
$K^-X(3872)[D^0\overline{D}^0]$	< 0.60	< 0.60			< 0.60
$K^-X(3872)[D^0\overline{D}^0\pi^0]$	< 0.60	< 0.60			< 0.60
$K^-X(3872)[\overline{D}^{*0}(2007)D^0]$			$1.67 \pm 0.36 \pm 0.47$		$\mathbf{1.67 \pm 0.59}$
$D^0D_{sJ}^-(2460)[D_s^-\pi^+\pi^-]$	< 2.2	< 2.2			< 2.2
$D^0D_{sJ}^-(2460)[D_s^-\pi^0]$	< 2.7	< 2.7			< 2.7
$D^0D_{sJ}^-(2460)[D_s^-\gamma]$	4.7 ± 1.3	$5.6 \pm^{1.6}_{1.5} \pm 1.7$	$6.00 \pm 2.00 \pm 1.00 \pm^{2.00}_{1.00}$		$5.8 \pm^{1.7}_{1.9}$
$D^0D_{sJ}^*(2317)^-[D_s^{*-}\gamma]$	< 7.6	< 7.6			< 7.6
$D^{*0}(2007)D_{sJ}^*(2317)^-[D_s^-\pi^0]$	9.0 ± 7.0		$9.0 \pm 6.0 \pm 2.0 \pm^{3.0}_{2.0}$		$9.0 \pm^{7.0}_{6.6}$
$D^0D_{sJ}^*(2317)^-[D_s^-\pi^0]$	7.4 ± 2.1	$8.1 \pm^{3.0}_{2.7} \pm 2.4$	$10.00 \pm 3.00 \pm 1.00 \pm^{4.00}_{2.00}$		$8.9 \pm^{2.7}_{3.2}$
$D^0D_{sJ}^-(2460)[D_s^{*-}\gamma]$	< 9.8	< 9.8			< 9.8
$D^{*0}(2007)D_{sJ}^-(2460)[D_s^-\gamma]$	14.0 ± 7.0		$14.0 \pm 4.0 \pm 3.0 \pm^{5.0}_{3.0}$		$14.0 \pm^{7.1}_{5.8}$
$D^0D_{sJ}^-(2460)[D_s^{*-}\pi^0]$	14.0 ± 6.0	$11.9 \pm^{6.1}_{4.9} \pm 3.6$	$27.0 \pm 7.0 \pm 5.0 \pm^{9.0}_{6.0}$		$15.0 \pm^{5.3}_{5.8}$
$D^{*0}(2007)D_{sJ}^-(2460)[D_s^{*-}\pi^0]$	76 ± 33		$76 \pm 17 \pm 18 \pm^{26}_{16}$		$76 \pm^{36}_{29}$

Table 73: Branching fractions of charged B modes producing strange D mesons in units of 10^{-4}, upper limits are at 90% CL. The latest version is available at: http://hfag.phys.ntu.edu.tw/b2charm/00102.html

Mode	PDG 2006	Belle	*BABAR*	CDF	Average
$D_s^- \phi(1020)$	< 0.019		< 0.019		< 0.019
$D_s^+ K^- K^-$			$0.110 \pm 0.040 \pm 0.020 \pm 0.003$		$\mathbf{0.11 \pm 0.04}$
$D_s^{*-} \phi(1020)$	< 0.120		< 0.120		< 0.120
$D_s^{*+} K^- K^-$			< 0.150		$\mathbf{< 0.150}$
$D_s^- \pi^0$	< 1.70				$\mathbf{0.15 \pm 0.05}$
			$0.15 \pm^{0.05}_{0.04} \pm 0.01 \pm 0.02$ [1]		
			< 0.28 [2]		
$D_s^{*+} K^- \pi^-$	< 9.8				$\mathbf{1.67 \pm 0.39}$
			$1.84 \pm 0.19 \pm 0.40 \pm 0.06$ [3b]		
			$1.67 \pm 0.16 \pm 0.35 \pm 0.05$ [4b]		
$D_s^+ K^- \pi^-$	< 7.0				$\mathbf{1.86 \pm 0.24}$
		$1.77 \pm 0.12 \pm 0.16 \pm 0.23$	$1.88 \pm 0.13 \pm 0.41 \pm 0.06$ [3a]		
			$2.02 \pm 0.13 \pm 0.38 \pm 0.06$ [4a]		
$D_s^- D^0$	109 ± 27	$85.2 \pm^{3.9}_{3.8}$	$133 \pm 18 \pm 32$		$\mathbf{85.7 \pm^{3.8}_{3.9}}$
$D_s^{*-} D^0$	72 ± 26		$93 \pm 18 \pm 19$		93 ± 26
$D_s^- D^{*0}(2007)$	100 ± 40		$121 \pm 23 \pm 20$		121 ± 30
$D_s^{*-} D^{*0}(2007)$	220 ± 70		$170 \pm 26 \pm 24$		170 ± 35

[1] Evidence for the Rare Decay $B^+ \to D_s^+ \pi^0$ (232M $B\overline{B}$ pairs) ; $\overline{B}^- \to D_s^- \pi^0$
[2] Search for $B^- \to D_s^- \pi^0$ (internal document) (124M $B\overline{B}$ pairs) ; $B^- \to D_s^- \pi^0$
[3] Observation of the decays $B^- \to D_s^{(*)+} K^- \pi^-$ (324M $B\overline{B}$ pairs) ; [3a] $B^- \to D_s^+ K^- \pi^-$; [3b] $B^- \to D_s^{*+} K^- \pi^-$
[4] Observation of the decays $B^- \to D_s^{(*)+} K^- \pi^-$ and $\overline{B}^0 \to D_s^+ K_s^0 \pi^-$ and Search for $\overline{B}^0 \to D_s^{*+} K_s^0 \pi^-$ and $B^- \to D_s^{(*)+} K^- K^-$ (383M $B\overline{B}$ pairs) ; [4a] $B^- \to D_s^+ K^- \pi^-$; [4b] $B^- \to D_s^{*+} K^- \pi^-$

Table 74: Product branching fractions of charged B modes producing strange D mesons in units of 10^{-4}, upper limits are at 90% CL. The latest version is available at: http://hfag.phys.ntu.edu.tw/b2charm/00102.html

Mode	PDG 2006	Belle	*BABAR*	CDF	Average
$D^0 D_{s1}^-(2536)[\overline{D}^{*0}(2007) K^-]$			$2.16 \pm 0.52 \pm 0.45$		$\mathbf{2.16 \pm 0.69}$
$D^0 D_{s1}^-(2536)[D^{*-}(2010) \overline{K}^0]$			$2.30 \pm 0.98 \pm 0.43$		$\mathbf{2.3 \pm 1.1}$
$D^{*0}(2007) D_s^-[\phi(1020)\pi^-]$	4.4 ± 1.7		$2.95 \pm 0.65 \pm 0.36$		2.95 ± 0.74
$D_s^{*-} D^0[D_s^- \to \phi(1020)\pi^-]$	3.2 ± 1.1		$3.13 \pm 1.19 \pm 0.58$		3.1 ± 1.3
$D^0 D_s^-[\phi(1020)\pi^-]$	4.80 ± 1.00		$4.00 \pm 0.61 \pm 0.61$		4.00 ± 0.86
$\overline{D}^{*0}(2007) D_{s1}^-(2536)[\overline{D}^{*0}(2007) K^-]$			$5.5 \pm 1.2 \pm 1.0$		$\mathbf{5.5 \pm 1.6}$
$D_s^{*-} D^{*0}(2007)[D_s^- \to \phi(1020)\pi^-]$	9.7 ± 2.8		$8.6 \pm 1.5 \pm 1.1$		8.6 ± 1.9
$D^{*0}(2007) D_{s1}^-(2536)[D^{*-}(2010) \overline{K}^0]$			< 10.7		$\mathbf{< 10.7}$

Table 75: Branching fractions of charged B modes producing baryons in units of 10^{-5}, upper limits are at 90% CL. The latest version is available at: http://hfag.phys.ntu.edu.tw/b2charm/00103.html

Mode	PDG 2006	Belle	*BABAR*	CDF	Average
$J/\psi(1S)\Sigma^0\overline{p}$	< 1.10	< 1.10			$\mathbf{< 1.10}$
$J/\psi(1S)\Lambda\overline{p}$	1.18 ± 0.31	$1.16 \pm 0.28 \pm^{0.18}_{0.23}$	$1.16 \pm^{0.74}_{0.53} \pm^{0.42}_{0.18}$		$\mathbf{1.16 \pm 0.31}$
$D^{*+}(2010)p\overline{p}$		< 1.50			< 1.50
$D^+p\overline{p}$		< 1.50			< 1.50
$\Sigma_c^{*0}\overline{p}$	< 4.6	< 4.6			< 4.6
$\Sigma_c^0\overline{p}$	< 8.0	< 9.3			< 9.3
$\Lambda_c^+\overline{p}\pi^-$	21.0 ± 7.0	$18.7 \pm^{4.3}_{4.0} \pm 2.8 \pm 4.9$	$35.3 \pm 1.8 \pm 3.1 \pm 9.2$		$24.2 \pm^{5.6}_{5.7}$
$\Lambda_c^+\Lambda_c^-K^-$		$65.0 \pm^{10.0}_{9.0} \pm 11.0 \pm 34.0$			$\mathbf{65 \pm 37}$

Table 76: Product branching fractions of charged B modes producing baryons in units of 10^{-5}, upper limits are at 90% CL. The latest version is available at: http://hfag.phys.ntu.edu.tw/b2charm/00103.html

Mode	PDG 2006	Belle	*BABAR*	CDF	Average
$K^-\eta_c(1S)[\Lambda\overline{\Lambda}]$		$0.095 \pm^{0.025}_{0.022} \pm^{0.008}_{0.011}$			$\mathbf{0.10 \pm 0.03}$
$K^-\eta_c(1S)[p\overline{p}]$	0.12 ± 0.04	$0.14 \pm 0.01 \pm^{0.02}_{0.02}$	$0.18 \pm^{0.03}_{0.02} \pm 0.02$		$\mathbf{0.15 \pm 0.02}$
$K^-J/\psi(1S)[\Lambda\overline{\Lambda}]$		$0.20 \pm^{0.03}_{0.03} \pm 0.03$			$\mathbf{0.20 \pm 0.05}$
$K^-J/\psi(1S)[p\overline{p}]$	0.22 ± 0.01	$0.22 \pm 0.01 \pm 0.01$	$0.22 \pm 0.02 \pm 0.01$		$\mathbf{0.22 \pm 0.01}$
$\Lambda_c^-\Xi_c^0[\Xi^-\pi^+]$		$4.80 \pm^{1.00}_{0.90} \pm 1.10 \pm 1.20$			$\mathbf{4.8 \pm 1.9}$

Table 77: Ratios of branching fractions of charged B modes producing baryons in units of 10^0, upper limits are at 90% CL. The latest version is available at: http://hfag.phys.ntu.edu.tw/b2charm/00103.html

Mode	PDG 2006	Belle	*BABAR*	CDF	Average
$\frac{\mathcal{B}(B^-\to\Lambda_c^+\overline{p}\pi^-)}{\mathcal{B}(\overline{B}^0\to\Lambda_c^+\overline{p})}$			$16.4 \pm 2.9 \pm 1.3$		16.4 ± 3.2

Table 78: Branching fractions of charged B modes producing $J/\psi(1S)$ in units of 10^{-4}, upper limits are at 90% CL. The latest version is available at: http://hfag.phys.ntu.edu.tw/b2charm/00104.html

Mode	PDG 2006	Belle	*BABAR*	CDF	Average
$\pi^-\pi^0 J/\psi(1S)$			< 0.073		$\mathbf{< 0.073}$
$J/\psi(1S)D^0\pi^-$	< 0.25	< 0.25	< 0.52		< 0.25
$J/\psi(1S)\phi(1020)K^-$	0.52 ± 0.17		$0.44 \pm 0.14 \pm 0.05 \pm 0.01$		0.44 ± 0.15
$J/\psi(1S)\pi^-$	0.49 ± 0.06	$0.38 \pm 0.06 \pm 0.03$	$0.54 \pm 0.04 \pm 0.02$		0.48 ± 0.04
$\rho^-(770)J/\psi(1S)$			$0.50 \pm 0.07 \pm 0.03$		$\mathbf{0.50 \pm 0.08}$
$J/\psi(1S)\eta K^-$	1.08 ± 0.33		$1.08 \pm 0.23 \pm 0.24 \pm 0.03$		1.08 ± 0.33
$J/\psi(1S)D^-$	< 1.20		< 1.20		< 1.20
$J/\psi(1S)\omega(782)K^-$			$3.50 \pm 0.20 \pm 0.40$		$\mathbf{3.50 \pm 0.45}$
$J/\psi(1S)K^-$	10.08 ± 0.35				10.26 ± 0.37
		$10.10 \pm 0.20 \pm 0.70 \pm 0.20$	$10.61 \pm 0.15 \pm 0.44 \pm 0.18$ [1]		
			$10.10 \pm 0.90 \pm 0.60$ [2]		
			$8.10 \pm 1.30 \pm 0.70$ [3]		
$J/\psi(1S)K^-\pi^+\pi^-$	10.7 ± 1.9		$11.60 \pm 0.70 \pm 0.90$	$6.9 \pm 1.8 \pm 1.2$	10.6 ± 1.0
$J/\psi(1S)K^{*-}(892)$	14.10 ± 0.80	$12.80 \pm 0.70 \pm 1.40 \pm 0.20$	$14.54 \pm 0.47 \pm 0.94 \pm 0.25$	$15.8 \pm 4.7 \pm 2.7$	14.03 ± 0.88
$J/\psi(1S)K_1^-(1270)$	18.0 ± 5.2	$18.0 \pm 3.4 \pm 3.0 \pm 2.5$			18.0 ± 5.2

[1] MEASUREMENT OF BRANCHING FRACTIONS AND CHARGE ASYMMETRIES FOR EXCLUSIVE B DECAYS TO CHARMONIUM (124M $B\overline{B}$ pairs) ; $B^- \to J/\psi K^-$ with J/ψ to leptons
[2] MEASUREMENT OF THE $B^+ \to p\overline{p}K^+$ BRANCHING FRACTION AND STUDY OF THE DECAY DYNAMICS (232M $B\overline{B}$ pairs) ; $B^- \to J/\psi K^-$ with $J/\psi \to p\overline{p}$
[3] Measurements of the absolute branching fractions of $B^\pm \to K^\pm X_{c\overline{c}}$ (231.8M $B\overline{B}$ pairs) ; $B^- \to J/\psi K^-$ (inclusive)

Table 79: Product branching fractions of charged B modes producing $J/\psi(1S)$ in units of 10^{-4}, upper limits are at 90% CL. The latest version is available at: http://hfag.phys.ntu.edu.tw/b2charm/00104.html

Mode	PDG 2006	Belle	*BABAR*	CDF	Average
$K^- h_c(1P)[J/\psi(1S)\pi^+\pi^-]$	< 0.034		< 0.034		< 0.034

Table 80: Ratios of branching fractions of charged B modes producing $J/\psi(1S)$ in units of 10^0, upper limits are at 90% CL. The latest version is available at: http://hfag.phys.ntu.edu.tw/b2charm/00104.html

Mode	PDG 2006	Belle	*BABAR*	CDF	Average
$\frac{\mathcal{B}(B^-\to J/\psi(1S)\pi^-)}{\mathcal{B}(B^-\to J/\psi(1S)K^-)}$	0.049 ± 0.006				$\mathbf{0.052 \pm 0.004}$
			$0.054 \pm 0.004 \pm 0.001$	$0.0500 \pm^{0.0190}_{0.0170} \pm 0.0010$ [1]	
				$0.049 \pm 0.008 \pm 0.002$ [2]	
$\frac{\mathcal{B}(B^-\to J/\psi(1S)K_1^-(1400))}{\mathcal{B}(B^-\to J/\psi(1S)K_1^-(1270))}$	< 0.30	< 0.30			< 0.30
$\frac{\mathcal{B}(B^-\to \chi_{c0}(1P)K^-)}{\mathcal{B}(B^-\to J/\psi(1S)K^-)}$	0.60 ± 0.20	$0.60 \pm^{0.21}_{0.18} \pm 0.05 \pm 0.08$			$0.60 \pm^{0.23}_{0.20}$
$\frac{\mathcal{B}(B^-\to \eta_c(1S)K^-)}{\mathcal{B}(B^-\to J/\psi(1S)K^-)}$	1.33 ± 0.44				1.12 ± 0.20
			$1.28 \pm 0.10 \pm 0.38$ [3]		
			$1.06 \pm 0.23 \pm 0.04$ [4]		
$\frac{\mathcal{B}(B^-\to J/\psi(1S)K^{*-}(892))}{\mathcal{B}(B^-\to J/\psi(1S)K^-)}$	1.39 ± 0.09		$1.37 \pm 0.05 \pm 0.08$	$1.92 \pm 0.60 \pm 0.17$	1.38 ± 0.09
$\frac{\mathcal{B}(B^-\to J/\psi(1S)K_1^-(1270))}{\mathcal{B}(B^-\to J/\psi(1S)K^-)}$		$1.80 \pm 0.34 \pm 0.34$			1.80 ± 0.48

[1] Measurement of the Branching Fraction $B(B^+ \to J/\psi\pi^+)$ and Search for $B^{c+} \to J/\psi\pi^+$
[1] Measurement of the Branching Fraction $B(B^+ \to J/\psi\pi^+)$ and Search for $B^{c+} \to J/\psi\pi^+$
[2] Measurement of the Ratio of Branching Fractions B(B – J/psi Pi)/B(B – J/psi K) ; Br(B–J/psiPi)/Br(B–J/psi K)
[3] Branching Fraction Measurements of $B \to \eta_c K$ Decays (86.1M $B\overline{B}$ pairs) ; Ratio $B^- \to \eta_c K^-$ to $B^- \to J/\psi K^-$ with $\eta_c \to K\overline{K}\pi$
[4] Measurements of the absolute branching fractions of $B^\pm \to K^\pm X_{c\overline{c}}$ (231.8M $B\overline{B}$ pairs) ; Ratio $B^- \to \eta_c K^-$ to $B^- \to J/\psi K^-$ (inclusive analysis)

Table 81: Branching fractions of charged B modes producing charmonium other than $J/\psi(1S)$ in units of 10^{-4}, upper limits are at 90% CL. The latest version is available at: http://hfag.phys.ntu.edu.tw/b2charm/00105.html

Mode	PDG 2006	Belle	*BABAR*	CDF	Average
$h_c(1P)K^-$		< 0.038			$\mathbf{< 0.038}$
$\chi_{c2}(1P)K^{*-}(892)$	< 0.120		< 0.120		< 0.120
$\chi_{c1}(1P)\pi^-$		$0.22 \pm 0.04 \pm 0.03$			$\mathbf{0.22 \pm 0.05}$
$\chi_{c2}(1P)K^-$	< 0.29		< 0.30		< 0.30
$\chi_{c0}(1P)\pi^-$			< 0.61		< 0.61
$\chi_{c0}(1P)K^-$	1.60 ± 0.50				$\mathbf{1.88 \pm 0.30}$
		$6.00 \pm^{2.10}_{1.80} \pm 0.70 \pm 0.90$	2.70 ± 0.70 [2]		
			$1.84 \pm 0.32 \pm 0.14 \pm 0.28$ [3]		
			$1.34 \pm 0.45 \pm 0.15 \pm 0.14$ [1]		
			< 1.80 [6d]		
$\eta_c(2S)K^-$	3.4 ± 1.8		$3.40 \pm 1.80 \pm 0.30$		3.4 ± 1.8
$\chi_{c1}(1P)K^{*-}(892)$	3.60 ± 0.90	$4.10 \pm 0.60 \pm 0.90$	$2.94 \pm 0.95 \pm 0.93 \pm 0.31$		$\mathbf{3.65 \pm 0.85}$
$\psi(3770)K^-$	4.9 ± 1.3	$4.80 \pm 1.10 \pm 0.70$	$3.50 \pm 2.50 \pm 0.30$		4.5 ± 1.2
$\chi_{c1}(1P)K^-$	5.30 ± 0.70				$\mathbf{5.01 \pm 0.37}$
		$4.50 \pm 0.20 \pm 0.70$	$8.00 \pm 1.40 \pm 0.70$ [6b]	$15.5 \pm 5.4 \pm 2.0$	
			$4.90 \pm 0.20 \pm 0.40$ [4]		
$\psi(2S)K^-$	6.48 ± 0.35				6.32 ± 0.37
		6.90 ± 0.60	$6.17 \pm 0.32 \pm 0.38 \pm 0.23$ [5]	$5.50 \pm 1.00 \pm 0.60$	
			$4.90 \pm 1.60 \pm 0.40$ [6a]		
$\psi(2S)K^{*-}(892)$	6.7 ± 1.4	$8.13 \pm 0.77 \pm 0.89$	$5.92 \pm 0.85 \pm 0.86 \pm 0.22$		7.07 ± 0.85
$\eta_c(1S)K^-$	9.1 ± 1.3				9.8 ± 1.3
		$12.50 \pm 1.40 \pm^{1.00}_{1.20} \pm 3.80$	$12.90 \pm 0.90 \pm 1.30 \pm 3.60$ [8]		
			$13.8 \pm^{2.3}_{1.5} \pm 1.5 \pm 4.2$ [7]		
			8.7 ± 1.5 [6c]		
$\eta_c(1S)K^{*-}(892)$			$12.1 \pm^{4.3}_{3.5} \pm^{3.4}_{2.8} \pm^{5.4}_{2.8}$		$\mathbf{12.1 \pm^{7.7}_{5.3}}$
$\chi_{c0}(1P)K^{*-}(892)$	< 29		< 29		< 29

[1] Dalitz-plot analysis of the decays $B^\pm \to K^\pm\pi^\mp\pi^\pm$ (226M $B\overline{B}$ pairs) ; $B^- \to \chi_{c0}K^-$ with $\chi_{c0} \to \pi^+\pi^-$ (Dalitz analysis)
[2] MEASUREMENT OF THE BRANCHING FRACTION FOR $B^\pm \to \chi_{c0}K^\pm$. (88.9M $B\overline{B}$ pairs) ; $B^- \to \chi_{c0}K^-$ with $\chi_{c0} \to K^+K^-, \pi^+\pi^-$
[3] Dalitz plot analysis of the decay $B^\pm \to K^\pm K^\pm K^\mp$ (226M $B\overline{B}$ pairs) ; $B^\pm \to K^\pm\chi_{c0}$, with $chi_c0 \to K^+K^-$ (Dalitz analysis)
[4] Search for $B \to X(3872)K$, $X(3872) \to J/\psi\gamma$ (287M $B\overline{B}$ pairs) ; $B^- \to \chi_{c1}K^-$ with χ_{c1} to $J/\psi\gamma$
[5] MEASUREMENT OF BRANCHING FRACTIONS AND CHARGE ASYMMETRIES FOR EXCLUSIVE B DECAYS TO CHARMONIUM (124M $B\overline{B}$ pairs) ; $B^- \to \psi(2S)K^-$ with $\psi(2S)$ to leptons
[6] Measurements of the absolute branching fractions of $B^\pm \to K^\pm X_{c\overline{c}}$ (231.8M $B\overline{B}$ pairs) ; [6a] $B^- \to \psi(2S)K^-$ (inclusive) ; [6b] $B^- \to \chi_{c1}K^-$ (inclusive) ; [6c] $B^- \to \eta_c K^-$ (inclusive) ; [6d] $B^- \to \chi_{c0}K^-$ (inclusive)
[7] MEASUREMENT OF THE $B^+ \to p\overline{p}K^+$ BRANCHING FRACTION AND STUDY OF THE DECAY DYNAMICS (232M $B\overline{B}$ pairs) ; $B^- \to \eta_c K^-$ with $\eta_c \to p\overline{p}$
[8] Branching Fraction Measurements of $B \to \eta_c K$ Decays (86.1M $B\overline{B}$ pairs) ; $B^- \to \eta_c K^-$ with $\eta_c \to K\overline{K}\pi$

Table 82: Product branching fractions of charged B modes producing charmonium other than $J/\psi(1S)$ in units of 10^{-4}, upper limits are at 90% CL. The latest version is available at: http://hfag.phys.ntu.edu.tw/b2charm/00105.html

Mode	PDG 2006	Belle	*BABAR*	CDF	Average
$K^-\psi(3770)[D^+D^-]$			$0.84 \pm 0.32 \pm 0.21$		$\mathbf{0.84 \pm 0.38}$
$K^-\psi(3770)[D^0\overline{D}^0]$			$1.41 \pm 0.30 \pm 0.22$		$\mathbf{1.41 \pm 0.37}$

Table 83: Ratios of branching fractions of charged B modes producing charmonium other than $J/\psi(1S)$ in units of 10^{-1}, upper limits are at 90% CL. The latest version is available at: http://hfag.phys.ntu.edu.tw/b2charm/00105.html

Mode	PDG 2006	Belle	*BABAR*	CDF	Average
$\frac{\mathcal{B}(B^-\to\chi_{c1}(1P)\pi^-)}{\mathcal{B}(B^-\to\chi_{c1}(1P)K^-)}$		$0.43 \pm 0.08 \pm 0.03$			$\mathbf{0.43 \pm 0.09}$
$\frac{\mathcal{B}(B^-\to h_c(1P)K^-)\times\mathcal{B}(h_c(1P)\to\eta_c(1S)\gamma)}{\mathcal{B}(B^-\to\eta_c(1S)K^-)}$			< 0.58		$\mathbf{< 0.58}$
$\frac{\mathcal{B}(B^-\to\chi_{c1}(1P)K^{*-}(892))}{\mathcal{B}(B^-\to\chi_{c1}(1P)K^-)}$	5.1 ± 2.3		$5.1 \pm 1.7 \pm 1.6$		5.1 ± 2.3
$\frac{\mathcal{B}(B^-\to\psi(2S)K^{*-}(892))}{\mathcal{B}(B^-\to\psi(2S)K^-)}$	9.6 ± 1.7		$9.60 \pm 1.50 \pm 0.90$		9.6 ± 1.7

Table 84: Branching fractions of charged B modes producing multiple D, D^* or D^{**} mesons in units of 10^{-3}, upper limits are at 90% CL. The latest version is available at: http://hfag.phys.ntu.edu.tw/b2charm/00106.html

Mode	PDG 2006	Belle	*BABAR*	CDF	Average
$D^0\overline{D}^0\pi^0K^-$		$0.11 \pm 0.03 \pm^{0.02}_{0.03}$			$\mathbf{0.11 \pm 0.04}$
$D^0D^{*-}(2010)$	0.46 ± 0.09	$0.46 \pm 0.07 \pm 0.06$	$0.36 \pm 0.05 \pm 0.04$		0.39 ± 0.05
D^-D^0	0.48 ± 0.10				$\mathbf{0.41 \pm 0.04}$
		$0.38 \pm 0.03 \pm 0.04$ [2]	$0.38 \pm 0.06 \pm 0.04 \pm 0.03$		
		$0.56 \pm 0.08 \pm 0.06$ [1]			
$D^+D^-K^-$	< 0.40	< 0.90	< 0.40		< 0.40
$D^+D^{*-}(2010)K^-$	< 0.70		< 0.70		< 0.70
$D^{*0}(2007)D^{*-}(2010)$	< 11.0		$0.81 \pm 0.12 \pm 0.11 \pm 0.06$		0.81 ± 0.17
$D^0\overline{D}^0K^-$	1.37 ± 0.32	$1.17 \pm 0.21 \pm 0.15$	$1.90 \pm 0.30 \pm 0.30$		1.37 ± 0.22
$D^{*+}(2010)D^-K^-$	1.50 ± 0.40		$1.50 \pm 0.30 \pm 0.20$		1.50 ± 0.36
$D^{*-}(2010)D^{*+}(2010)K^-$	< 1.80		< 1.80		< 1.80
$D^0D^-\overline{K}^0$	< 2.8		< 2.8		< 2.8
$D^{*0}(2007)\overline{D}^0K^-$	< 3.8		< 3.8		< 3.8
$D^0\overline{D}^{*0}(2007)K^-$	4.70 ± 1.00		$4.70 \pm 0.70 \pm 0.70$		4.70 ± 0.99
$D^0D^{*-}(2010)\overline{K}^0$	5.2 ± 1.2		$5.20 \pm^{1.00}_{0.90} \pm 0.70$		$5.2 \pm^{1.2}_{1.1}$
$\overline{D}^{*0}(2007)D^{*0}(2007)K^-$	5.3 ± 1.6		$5.30 \pm^{1.10}_{1.00} \pm 1.20$		5.3 ± 1.6
$D^{*0}(2007)D^-\overline{K}^0$	< 6.1		< 6.1		< 6.1
$D^{*0}(2007)D^{*-}(2010)\overline{K}^0$	7.8 ± 2.6		$7.8 \pm^{2.3}_{2.1} \pm 1.4$		$7.8 \pm^{2.7}_{2.5}$

[1] Observation of $B^0 \to D^+D^-$, $B^- \to D^0D^-$ and $B^- \to D^0D^{*-}$ decays (152M $B\overline{B}$ pairs)
[2] Measurement of B+ - D+ D0bar branching fraction and charge asymmetry and search for B0 - D0 D0bar (656.7M $B\overline{B}$ pairs)

Table 85: Product branching fractions of charged B modes producing multiple D, D^* or D^{**} mesons in units of 10^{-4}, upper limits are at 90% CL. The latest version is available at: http://hfag.phys.ntu.edu.tw/b2charm/00106.html

Mode	PDG 2006	Belle	*BABAR*	CDF	Average
$\pi^- D_1^0(2420)[D^{*0}(2007)\pi^-\pi^+]$	< 0.060	< 0.060			< 0.060
$\pi^- D_2^{*0}(2460)[D^{*0}(2007)\pi^-\pi^+]$	< 0.22	< 0.22			< 0.22
$\pi^- D_2^{*0}(2460)[D^{*+}(2010)\pi^-]$	1.80 ± 0.50	$1.80 \pm 0.30 \pm 0.30 \pm 0.20$	$1.80 \pm 0.30 \pm 0.50$		1.80 ± 0.36
$\pi^- D_1^0(2420)[D^0\pi^-\pi^+]$	1.90 ± 0.60	$1.85 \pm 0.29 \pm 0.35 \pm^{0.00}_{0.46}$			$1.85 \pm^{0.45}_{0.65}$
$\pi^- D_2^{*0}(2460)[D^+\pi^-]$	3.40 ± 0.80	$3.40 \pm 0.30 \pm 0.60 \pm 0.40$	$2.90 \pm 0.20 \pm 0.50$		3.06 ± 0.44
$\pi^- D_1^0(H)[D^{*+}(2010)\pi^-]$		$5.00 \pm 0.40 \pm 1.00 \pm 0.40$			5.0 ± 1.1
$\pi^- D_0^{*0}[D^+\pi^-]$		$6.10 \pm 0.60 \pm 0.90 \pm 1.60$			6.1 ± 1.9
$\pi^- D_1^0(2420)[D^{*+}(2010)\pi^-]$	6.8 ± 1.5	$6.80 \pm 0.70 \pm 1.30 \pm 0.30$	$5.90 \pm 0.30 \pm 1.10$		6.23 ± 0.91

Table 86: Ratios of branching fractions of charged B modes producing multiple D, D^* or D^{**} mesons in units of 10^0, upper limits are at 90% CL. The latest version is available at: http://hfag.phys.ntu.edu.tw/b2charm/00106.html

Mode	PDG 2006	Belle	*BABAR*	CDF	Average
$\frac{\mathcal{B}(B^-\to D^0K^-)}{\mathcal{B}(B^-\to D^0\pi^-)}$	0.083 ± 0.010	$0.077 \pm 0.005 \pm 0.006$	$0.083 \pm 0.003 \pm 0.002$	$0.065 \pm 0.007 \pm 0.004$	$\mathbf{0.079 \pm 0.003}$
$\frac{\mathcal{B}(B^-\to D^{*0}(2007)K^-)}{\mathcal{B}(B^-\to D^{*0}(2007)\pi^-)}$	0.08 ± 0.02	$0.078 \pm 0.019 \pm 0.009$	$0.081 \pm 0.004 \pm^{0.004}_{0.003}$		0.081 ± 0.005
$\frac{\mathcal{B}(B^-\to D_2^{*0}(2460)\pi^-)}{\mathcal{B}(B^-\to D_1^0(2420)\pi^-)}$			$0.80 \pm 0.07 \pm 0.16$		0.80 ± 0.17
$\frac{\mathcal{B}(B^-\to D^{*0}(2007)\pi^-)}{\mathcal{B}(B^-\to D^0\pi^-)}$			$1.14 \pm 0.07 \pm 0.04$		$\mathbf{1.14 \pm 0.08}$
$\frac{\mathcal{B}(B^-\to D^{**+}\pi^-)}{\mathcal{B}(B^-\to D^0\pi^-)}$			$1.22 \pm 0.13 \pm 0.23$		$\mathbf{1.22 \pm 0.26}$
$\frac{\mathcal{B}(B^-\to D^0\pi^-)}{\mathcal{B}(\overline{B}^0\to D^+\pi^-)}$				$1.97 \pm 0.10 \pm 0.21$	1.97 ± 0.23

Table 87: Branching fractions of charged B modes producing a single D^* or D^{**} meson in units of 10^{-4}, upper limits are at 90% CL. The latest version is available at: http://hfag.phys.ntu.edu.tw/b2charm/00107.html

Mode	PDG 2006	Belle	*BABAR*	CDF	Average
$D^{*-}(2010)\pi^0$	< 1.70	< 0.030			$\mathbf{< 0.030}$
$D^{*-}(2010)\overline{K}^0$	< 0.090		< 0.090		< 0.090
$D^{*0}(2007)K^-$	3.70 ± 0.40	$3.59 \pm 0.87 \pm 0.41 \pm 0.31$			3.6 ± 1.0
$D^{*0}(2007)K^{*-}(892)$	8.1 ± 1.4		$8.30 \pm 1.10 \pm 0.96 \pm 0.27$		8.3 ± 1.5
$D^{*0}(2007)K^-K^0$	< 10.6	< 10.6			< 10.6
$D^{*+}(2010)\pi^-\pi^-$	13.5 ± 2.2	$12.50 \pm 0.80 \pm 2.20$	$12.20 \pm 0.50 \pm 1.80$		12.3 ± 1.5
$D^{*0}(2007)K^-K^{*0}(892)$	15.0 ± 4.0	$15.3 \pm 3.1 \pm 2.9$			15.3 ± 4.2
$D^{*+}(2010)\pi^-\pi^+\pi^-\pi^-$	26.0 ± 4.0	$25.6 \pm 2.6 \pm 3.3$			25.6 ± 4.2
$D^{*0}(2007)\pi^-$	46.0 ± 4.0				$\mathbf{52.8 \pm 2.8}$
			$55.20 \pm 1.70 \pm 4.20 \pm 0.20$ [1]		
			$51.3 \pm 2.2 \pm 2.8$ [2]		
$D^{**+}\pi^-$			$55.0 \pm 5.2 \pm 10.4$		$\mathbf{55 \pm 12}$
$D^{*0}(2007)\pi^-\pi^+\pi^-\pi^+\pi^-$		$56.7 \pm 9.1 \pm 8.5$			57 ± 12
$D^{*0}(2007)\pi^-\pi^+\pi^-$	103 ± 12	$105.5 \pm 4.7 \pm 12.9$			106 ± 14

[1] Branching fraction measurements and isospin analyses for $\overline{B} \to D^{(*)}\pi^-$ decays (65M $B\overline{B}$ pairs) ; $B^- \to D^{*0}\pi^-$

[2] Measurement of the Absolute Branching Fractions $B \to D^{(*,**)}\pi$ with a Missing Mass method (231M $B\overline{B}$ pairs) ; $B^- \to D^{*0}\pi^-$

Table 88: Branching fractions of charged B modes producing a single D meson in units of 10^{-4}, upper limits are at 90% CL. The latest version is available at: http://hfag.phys.ntu.edu.tw/b2charm/00108.html

Mode	PDG 2006	Belle	*BABAR*	CDF	Average
$D^-\overline{K}^0$	< 0.050		< 0.050		< 0.050
D^0K^-	4.08 ± 0.24	$3.83 \pm 0.25 \pm 0.30 \pm 0.22$			3.83 ± 0.45
$D^0K^{*-}(892)$	6.30 ± 0.80				5.29 ± 0.45
			$5.29 \pm 0.30 \pm 0.34$ [1]		
			$6.30 \pm 0.70 \pm 0.50$ [2]		
$D^0K^-K^0$	5.5 ± 1.6	$5.50 \pm 1.40 \pm 0.80$			5.5 ± 1.6
$D^0K^-K^{*0}(892)$	7.5 ± 1.7	$7.5 \pm 1.3 \pm 1.1$			7.5 ± 1.7
$D^+\pi^-\pi^-$	10.2 ± 1.6	$10.20 \pm 0.40 \pm 1.50$	$8.70 \pm 0.40 \pm 1.30$		9.4 ± 1.0
$D^0\pi^-$	49.2 ± 2.0				$\mathbf{47.5 \pm 1.9}$
			$49.00 \pm 0.70 \pm 2.20 \pm 0.06$ [3]		
			$44.9 \pm 2.1 \pm 2.3$ [4]		

[1] Measurement of the $B^- \to D^0K^{*-}$ branching fraction (232M $B\overline{B}$ pairs) ; Measurement of of the $B^- \to D^0K^{*-}$ branching fraction
[2] Measurement of the Branching Fraction for $B^- \to D^0K^{*-}$ (86M $B\overline{B}$ pairs) ; $B^- \to D^0K^{*-}$
[3] Branching fraction measurements and isospin analyses for $\overline{B} \to D^{(*)}\pi^-$ decays (65M $B\overline{B}$ pairs) ; $B^- \to D^0\pi^-$
[4] Measurement of the Absolute Branching Fractions $B \to D^{(*,**)}\pi$ with a Missing Mass method (231M $B\overline{B}$ pairs) ; $B^- \to D^0\pi^-$

Table 89: Branching fractions of neutral B modes producing new particles in units of 10^{-3}, upper limits are at 90% CL. The latest version is available at: http://hfag.phys.ntu.edu.tw/b2charm/00201.html

Mode	PDG 2006	Belle	*BABAR*	CDF	Average
$X^+(3872)K^-$	< 0.50		< 0.50		< 0.50
$D_{sJ}^-(2460)D^+$			$2.60 \pm 1.50 \pm 0.70$		2.6 ± 1.7
$D_{sJ}^-(2460)D^{*+}(2010)$			$8.8 \pm 2.0 \pm 1.4$		8.8 ± 2.4

Table 90: Product branching fractions of neutral B modes producing new particles in units of 10^{-4}, upper limits are at 90% CL. The latest version is available at: http://hfag.phys.ntu.edu.tw/b2charm/00201.html

Mode	PDG 2006	Belle	*BABAR*	CDF	Average
$\pi^+ D_{sJ}^-(2460)[D_s^-\gamma]$	< 0.040	< 0.040			< 0.040
$\overline{K}^0 X(3872)[J/\psi(1S)\pi^+\pi^-]$	< 0.103		$0.051 \pm 0.028 \pm 0.007$		0.05 ± 0.03
$K^- X^+(3872)[J/\psi(1S)\pi^+\pi^0]$	< 0.054		< 0.054		< 0.054
$K^- D_{sJ}^+(2460)[D_s^+\gamma]$	< 0.094	< 0.086			< 0.086
$\overline{K}^0 Y(3940)[J/\psi(1S)\omega(782)]$			$0.15 \pm^{0.14}_{0.12} \pm 0.02$		$\mathbf{0.15 \pm 0.13}$
$\pi^+ D_{sJ}^*(2317)^-[D_s^-\pi^0]$	< 0.25	< 0.25			< 0.25
$K^- D_{sJ}^*(2317)^+[D_s^+\pi^0]$	0.43 ± 0.15	$0.44 \pm 0.08 \pm 0.06 \pm 0.11$			0.44 ± 0.15
$D^+ D_{sJ}^-(2460)[D_s^-\pi^+\pi^-]$	< 2.00	< 2.00			< 2.00
$D^+ D_{sJ}^-(2460)[D_s^-\pi^0]$	< 3.6	< 3.6			< 3.6
$\overline{K}^0 X(3872)[\overline{D}^{*0}(2007)D^0]$			< 4.4		$\mathbf{< 4.4}$
$D^+ D_{sJ}^-(2460)[D_s^{*-}\gamma]$	< 6.0	< 6.0			< 6.0
$D^+ D_{sJ}^-(2460)[D_s^-\gamma]$	6.6 ± 1.7	$8.2 \pm^{2.2}_{1.9} \pm 2.5$	$8.00 \pm 2.00 \pm 1.00 \pm^{3.00}_{2.00}$		$8.1 \pm^{2.2}_{2.5}$
$D^+ D_{sJ}^*(2317)^-[D_s^{*-}\gamma]$	< 9.5	< 9.5			< 9.5
$D^+ D_{sJ}^*(2317)^-[D_s^-\pi^0]$	9.7 ± 3.7	$8.6 \pm^{3.3}_{2.6} \pm 2.6$	$18.0 \pm 4.0 \pm 3.0 \pm^{6.0}_{4.0}$		$10.4 \pm^{3.2}_{3.5}$
$D^{*+}(2010) D_{sJ}^*(2317)^-[D_s^-\pi^0]$	15.0 ± 6.0		$15.0 \pm 4.0 \pm 2.0 \pm^{5.0}_{3.0}$		$15.0 \pm^{6.7}_{5.4}$
$D^{*+}(2010) D_{sJ}^-(2460)[D_s^-\gamma]$	23.0 ± 8.0		$23.0 \pm 3.0 \pm 3.0 \pm^{8.0}_{5.0}$		$23.0 \pm^{9.1}_{6.6}$
$D^+ D_{sJ}^-(2460)[D_s^{*-}\pi^0]$	20.0 ± 5.0	$22.7 \pm^{7.3}_{6.2} \pm 6.8$	$28.0 \pm 8.0 \pm 5.0 \pm^{10.0}_{6.0}$		$24.6 \pm^{7.2}_{8.2}$
$D^{*+}(2010) D_{sJ}^-(2460)[D_s^{*-}\pi^0]$	55 ± 23		$55.0 \pm 12.0 \pm 10.0 \pm^{19.0}_{12.0}$		$55 \pm^{25}_{20}$

Table 91: Ratios of branching fractions of neutral B modes producing new particles in units of 10^0, upper limits are at 90% CL. The latest version is available at: http://hfag.phys.ntu.edu.tw/b2charm/00201.html

Mode	PDG 2006	Belle	*BABAR*	CDF	Average
$\frac{\mathcal{B}(\overline{B}^0 \to X(3872)\overline{K}^0)}{\mathcal{B}(B^- \to X(3872)K^-)}$			$0.50 \pm 0.30 \pm 0.05$		0.50 ± 0.30

Table 92: Branching fractions of neutral B modes producing strange D mesons in units of 10^{-3}, upper limits are at 90% CL. The latest version is available at: http://hfag.phys.ntu.edu.tw/b2charm/00202.html

Mode	PDG 2006	Belle	*BABAR*	CDF	Average
$D_s^- \pi^+$	0.022 ± 0.007				0.014 ± 0.003
		$0.024 \pm^{0.010}_{0.008} \pm 0.004 \pm 0.006$	$0.032 \pm 0.009 \pm 0.007 \pm 0.008$ [2d]		
			$0.013 \pm 0.003 \pm 0.001 \pm 0.002$ [1d]		
$D_s^- a_0^+(980)$			< 0.019		< 0.019
$D_s^- \rho^+(770)$	< 0.60		< 0.019		< 0.019
$D_s^{*+} K^-$	< 0.025				0.020 ± 0.006
			$0.020 \pm 0.005 \pm 0.003 \pm 0.003$ [1c]		
			< 0.025 [2c]		
$D_s^+ K^-$	0.031 ± 0.008				0.027 ± 0.005
		$0.046 \pm^{0.012}_{0.011} \pm 0.006 \pm 0.012$	$0.032 \pm 0.010 \pm 0.007 \pm 0.008$ [2b]		
			$0.025 \pm 0.004 \pm 0.002 \pm 0.003$ [1b]		
$D_s^{*-} \pi^+$	< 0.041				0.028 ± 0.008
			$0.028 \pm 0.006 \pm 0.004 \pm 0.003$ [1a]		
			< 0.041 [2a]		
$D_s^+ \Lambda \overline{p}$					**0.031 ± 0.008**
		$0.029 \pm 0.007 \pm 0.005 \pm 0.004$ [3]			
		$0.036 \pm 0.009 \pm 0.006 \pm 0.009$ [4]			
$D_s^{*-} a_0^+(980)$			< 0.036		< 0.036
$D_s^+ K_S^0 \pi^-$			$0.055 \pm 0.013 \pm 0.010 \pm 0.002$		**0.06 ± 0.02**
$D_s^{*+} K^0 \pi^-$			< 0.055		**< 0.055**
$D_s^- D_s^+$	< 0.100				**< 0.036**
		< 0.200 [5]	< 0.100		
		< 0.036 [6]			
$D_s^- D_s^{*+}$	< 0.130		< 0.130		< 0.130
$D_s^- a_2^+(1320)$			< 0.190		< 0.190
$D_s^{*-} a_2^+(1320)$			< 0.200		< 0.200
$D_s^{*+} D_s^{*-}$	< 0.24		< 0.24		< 0.24
$D_s^{*-} D^+$	8.6 ± 3.4		$6.7 \pm 2.0 \pm 1.1$		6.7 ± 2.3
$D_s^- D^+$	6.5 ± 2.1				**7.67 ± 0.82**
		$7.42 \pm 0.23 \pm 1.36$ [5]	$9.0 \pm 1.8 \pm 1.4$		
		$7.50 \pm 0.20 \pm 0.80 \pm 0.80$ [6]			
$D_s^- D^{*+}(2010)$	8.8 ± 1.6				6.8 ± 1.6
			$5.70 \pm 1.60 \pm 0.90$ [8a]		
			$10.3 \pm 1.4 \pm 1.3 \pm 2.6$ [7a]		
$D_s^{*-} D^{*+}(2010)$	17.9 ± 1.6				18.2 ± 1.6
			$18.80 \pm 0.90 \pm 1.60 \pm 0.60$ [9]		
			$16.5 \pm 2.3 \pm 1.9$ [8b]		
			$19.7 \pm 1.5 \pm 3.0 \pm 4.9$ [7b]		
$D_{s1}^-(2536) D^{*+}(2010)$			$92.00 \pm 24.00 \pm 1.00$		**92 ± 24**

[1] Observation of Decays $\overline{B}^0 \to D_s^{-(*)} \pi^+$ and $\overline{B}^0 \to D_s^{+(*)} K^-$ (230M $B\overline{B}$ pairs) ; [1a] $\overline{B}^0 \to D_s^{*-} \pi^+$; [1b] $\overline{B}^0 \to D_s^+ K^-$; [1c] $\overline{B}^0 \to D_s^{*+} K^-$; [1d] $\overline{B}^0 \to D_s^- \pi^+$

[2] A study of the rare decays $\overline{B}^0 \to D_s^{-(*)} \pi^+$ and $\overline{B}^0 \to D_s^{+(*)} K^-$ (84.3M $B\overline{B}$ pairs) ; [2a] $\overline{B}^0 \to D_s^{*-} \pi^+$; [2b] $\overline{B}^0 \to D_s^+ K^-$; [2c] $\overline{B}^0 \to D_s^{*+} K^-$; [2d] $\overline{B}^0 \to D_s^- \pi^+$

[3] Observation of B0bar - Ds+ Lambda pbar decay (449M $B\overline{B}$ pairs)

[4] Observation of B0bar to Ds+ Lambda pbar (447M $B\overline{B}$ pairs)

[5] Improved measurement of $\overline{B}^0 \to D_s^- D^+$ and search for $\overline{B}0 \to D_s^+ D_s^-$ at Belle

[6] Improved measurement of B0bar - Ds-D+ and search for B0bar - Ds+Ds- (449M $B\overline{B}$ pairs)

[7] Measurement of $\overline{B}^0 \to D_s^{(*)} D^*$ Branching Fractions and $D_s^* D^*$ Polarization with a Partial Reconstruction technique (22.7M $B\overline{B}$ pairs) ; [7a] $\overline{B}^0 \to D_s^- D^{*+}$; [7b] $\overline{B}^0 \to D_s^{*-} D^{*+}$

[8] Study of $\overline{B} \to D^{(*)+,-} X^-$ and $\overline{B} \to D_s^{(*)-} X^{+,0}$ decays and measurement of D_s^- and $D_{sJ}^-(2460)$ absolute branching fractions (230M $B\overline{B}$ pairs) ; [8a] $\overline{B}^0 \to D_s^- D^{*+}$; [8b] $\overline{B}^0 \to D_s^{*-} D^{*+}$)

[9] Measurement of the $\overline{B}^0 \to D_s^{*-} D^+$ and $D_s^+ \to \phi \pi^+$ branching fractions (123M $B\overline{B}$ pairs) ; $\overline{B}^0 \to D_s^{*-} D^{*+}$

Table 93: Product branching fractions of neutral B modes producing strange D mesons in units of 10^{-4}, upper limits are at 90% CL. The latest version is available at: http://hfag.phys.ntu.edu.tw/b2charm/00202.html

Mode	PDG 2006	Belle	*BABAR*	CDF	Average
$D^+D_s^-[\pi^-\phi(1020)[K^+K^-]]$	1.41 ± 0.41	$1.47 \pm 0.05 \pm 0.21$			1.47 ± 0.22
$D^+D_{s1}^-(2536)[K^-\overline{D}^{*0}(2007)]$			$1.71 \pm 0.48 \pm 0.32$		$\mathbf{1.71 \pm 0.58}$
$D^+D_{s1}^-(2536)[D^{*-}(2010)\overline{K}^0]$			$2.61 \pm 1.03 \pm 0.31$		$\mathbf{2.6 \pm 1.1}$
$D^+D_s^-[\phi(1020)\pi^-]$	2.90 ± 0.80		$2.67 \pm 0.61 \pm 0.47$		2.67 ± 0.77
$D^{*+}(2010)D_{s1}^-(2536)[\overline{D}^{*0}(2007)K^+]$			$3.32 \pm 0.88 \pm 0.66$		$\mathbf{3.3 \pm 1.1}$
$D_s^{*-}D^+[D_s^- \to \phi(1020)\pi^-]$	3.8 ± 1.4		$4.14 \pm 1.19 \pm 0.94$		4.1 ± 1.5
$D^{*+}(2010)D_{s1}^-(2536)[D^{*-}(2010)\overline{K}^0]$			$5.00 \pm 1.51 \pm 0.67$		$\mathbf{5.0 \pm 1.7}$
$D^{*+}(2010)D_s^-[\phi(1020)\pi^-]$	3.90 ± 0.50		$5.11 \pm 0.94 \pm 0.72$		5.1 ± 1.2
$D^{*-}(2010)D_{s1}^+(2536)[D^{*+}(2010)K_S^0]$		< 6.0			$\mathbf{< 6.0}$
$D_s^{*-}D^{*+}(2010)[D_s^- \to \phi(1020)\pi^-]$	7.9 ± 1.3		$12.2 \pm 2.2 \pm 2.2$		12.2 ± 3.1

Table 94: Ratios of branching fractions of neutral B modes producing strange D mesons in units of 10^0, upper limits are at 90% CL. The latest version is available at: http://hfag.phys.ntu.edu.tw/b2charm/00202.html

Mode	PDG 2006	Belle	*BABAR*	CDF	Average
$\frac{\mathcal{B}(\overline{B}^0 \to D_s^{*-}D^+)}{\mathcal{B}(\overline{B}^0 \to D_s^-D^+)}$				$0.90 \pm 0.20 \pm 0.10$	0.90 ± 0.22
$\frac{\mathcal{B}(\overline{B}^0 \to D_s^-D^{*+}(2010))}{\mathcal{B}(\overline{B}^0 \to D_s^-D^+)}$				$1.50 \pm 0.40 \pm 0.10$	1.50 ± 0.41
$\frac{\mathcal{B}(\overline{B}^0 \to D_s^-D^+)}{\mathcal{B}(\overline{B}^0 \to D^+\pi^+\pi^-\pi^-)}$				$1.99 \pm 0.13 \pm 0.11 \pm 0.45$	1.99 ± 0.48
$\frac{\mathcal{B}(\overline{B}^0 \to D_s^{*-}D^{*+}(2010))}{\mathcal{B}(\overline{B}^0 \to D_s^-D^+)}$				$2.60 \pm 0.50 \pm 0.20$	2.60 ± 0.54

Table 95: Branching fractions of neutral B modes producing baryons in units of 10^{-5}, upper limits are at 90% CL. The latest version is available at: http://hfag.phys.ntu.edu.tw/b2charm/00203.html

Mode	PDG 2006	Belle	*BABAR*	CDF	Average
$J/\psi(1S)\overline{p}p$	< 0.083	< 0.083	< 0.190		$\mathbf{< 0.083}$
$\Lambda_c^- p$			$2.10 \pm^{0.67}_{0.55} \pm^{0.67}_{0.62} \pm^{0.77}_{0.46}$		$\mathbf{2.1 \pm^{1.2}_{0.9}}$
$\Lambda_c^+ \overline{p}$	2.20 ± 0.80	$2.19 \pm^{0.56}_{0.49} \pm 0.32 \pm 0.57$	$2.15 \pm 0.36 \pm 0.13 \pm 0.56$		2.17 ± 0.53
$\Lambda_c^+ \Lambda_c^-$		< 5.7			$\mathbf{< 5.7}$
$\Sigma_c^{*0} \overline{p}\pi^+$	< 12.1				$\mathbf{< 3.3}$
		< 12.1 [1]			
		< 3.3 [2]			
$D^{*0}(2007)p\overline{p}$					11.1 ± 1.3
		$12.0 \pm^{3.3}_{2.9} \pm 2.1$	$6.70 \pm 2.10 \pm 0.82 \pm 0.36$ [3d]		
			$11.00 \pm 1.00 \pm 0.90$ [4d]		
$D^0 p\overline{p}$					11.39 ± 0.91
		$11.8 \pm 1.5 \pm 1.6$	$12.40 \pm 1.40 \pm 1.16 \pm 0.30$ [3c]		
			$11.30 \pm 0.60 \pm 0.80$ [4c]		
$\Sigma_c^{*++} \overline{p}\pi^-$	16.0 ± 7.0				$\mathbf{12.9 \pm^{3.3}_{3.4}}$
		$16.3 \pm^{5.7}_{5.1} \pm 2.8 \pm 4.2$ [1]			
		$12.0 \pm 1.0 \pm 2.0 \pm 3.0$ [2]			
$\Sigma_c^0 \overline{p}\pi^+$	10.0 ± 8.0				$\mathbf{14.0 \pm 4.9}$
		$14.0 \pm 2.0 \pm 2.0 \pm 4.0$ [2]			
		< 15.9 [1]			
$\Sigma_c^{++} \overline{p}\pi^-$	28.0 ± 9.0				$\mathbf{21.8 \pm^{5.1}_{5.2}}$
		$23.8 \pm^{6.3}_{5.5} \pm 4.1 \pm 6.2$ [1]			
		$21.0 \pm 2.0 \pm 3.0 \pm 5.0$ [2a]			
$D^+ p\overline{p}\pi^-$					33.8 ± 3.2
			$38.00 \pm 3.50 \pm 4.50 \pm 0.95$ [3a]		
			$33.8 \pm 1.4 \pm 2.9$ [4a]		
$D^{*+}(2010)p\overline{p}\pi^-$	65 ± 16				48.1 ± 4.9
			$56.1 \pm 5.9 \pm 6.4 \pm 3.6$ [3b]		
			$48.1 \pm 2.2 \pm 4.4$ [4b]		
$\Lambda_c^+ \Lambda_c^- \overline{K}^0$		$79 \pm^{29}_{23} \pm 12 \pm 41$			$\mathbf{79 \pm^{52}_{49}}$
$\Lambda_c^+ \overline{p}\pi^+\pi^-$	130 ± 40	$110 \pm^{12}_{12} \pm 19 \pm 29$			110 ± 37

[1] STUDY OF EXCLUSIVE B DECAYS TO CHARMED BARYONS AT BELLE. (31.7M $B\overline{B}$ pairs)

[2] Study of the charmed baryonic decays $\overline{B}^0 \to \Sigma_c^{++} \overline{p}\pi^-$ and $\overline{B}^0 \to \Sigma_c^0 \overline{p}\pi^+$ (386M $B\overline{B}$ pairs) ; [2a] B0bar to Sigmac(2455)++ pbar pi

[3] Measurement of the Branching Fraction for the decays $\overline{B}^0 \to D^{*+} p\overline{p}\pi^-$, $\overline{B}^0 \to D^+ p\overline{p}\pi^-$, $\overline{B}^0 \to \overline{D}^{*0} p\overline{p}$, $\overline{B}^0 \to \overline{D}^0 p\overline{p}$ (124M $B\overline{B}$ pairs) ; [3a] $\overline{B}^0 \to D^+ p\overline{p}\pi^-$; [3b] $\overline{B}^0 \to D^{*+} p\overline{p}\pi^-$; [3c] $\overline{B}^0 \to \overline{D}^0 p\overline{p}$; [3d] $\overline{B}^0 \to \overline{D}^{*0} p\overline{p}$

[4] Measurements of the Decays $B^0 \to \overline{D}^0 p\overline{p}$, $B^0 \to \overline{D}^{*0} p\overline{p}$, $B^0 \to D^- p\overline{p}\pi + -$, and $B^0 \to D^- p\overline{p}\pi^+$ (232M $B\overline{B}$ pairs) ; [4a] $\overline{B}^0 \to D^+ p\overline{p}\pi^-$; [4b] $\overline{B}^0 \to D^{*+} p\overline{p}\pi^-$; [4c] $\overline{B}^0 \to \overline{D}^0 p\overline{p}$; [4d] $\overline{B}^0 \to \overline{D}^{*0} p\overline{p}$

Table 96: Product branching fractions of neutral B modes producing baryons in units of 10^{-5}, upper limits are at 90% CL. The latest version is available at: http://hfag.phys.ntu.edu.tw/b2charm/00203.html

Mode	PDG 2006	Belle	*BABAR*	CDF	Average
$\Lambda_c^- \Xi_c^+ [\Xi^- \pi^+ \pi^+]$		$9.3 \pm^{3.7}_{2.8} \pm 1.9 \pm 2.4$			$\mathbf{9.3 \pm^{4.8}_{4.1}}$

Table 97: Branching fractions of neutral B modes producing $J/\psi(1S)$ in units of 10^{-4}, upper limits are at 90% CL. The latest version is available at: http://hfag.phys.ntu.edu.tw/b2charm/00204.html

Mode	PDG 2006	Belle	*BABAR*	CDF	Average
$J/\psi(1S)\gamma$	< 0.016		< 0.016		< 0.016
$J/\psi(1S)\phi(1020)$	< 0.092		< 0.090		< 0.090
$J/\psi(1S)\eta$	< 0.27	$0.096 \pm 0.017 \pm 0.007$	< 0.27		$\mathbf{0.10 \pm 0.02}$
$J/\psi(1S)f_2(1270)$					$\mathbf{0.10 \pm 0.04}$
		$0.10 \pm 0.04 \pm 0.02$ [2]	< 0.046		
		< 0.049 [1]			
$J/\psi(1S)D^0$	< 0.130	< 0.200	< 0.130		< 0.130
$J/\psi(1S)\pi^0$	0.22 ± 0.04	$0.23 \pm 0.05 \pm 0.02$	$0.19 \pm 0.02 \pm 0.02$		$\mathbf{0.20 \pm 0.02}$
$J/\psi(1S)\pi^+\pi^-$	0.46 ± 0.09				$\mathbf{0.22 \pm 0.04}$
		$0.22 \pm 0.03 \pm 0.02$ [1]	< 0.120		
		< 0.100 [2]			
$J/\psi(1S)\rho^0(770)$	0.16 ± 0.07				$\mathbf{0.23 \pm 0.02}$
		$0.28 \pm 0.03 \pm 0.03$ [2]	$0.27 \pm 0.03 \pm 0.02$		
		$0.19 \pm 0.02 \pm 0.02$ [1]			
$J/\psi(1S)\eta'(958)$	< 0.63		< 0.63		< 0.63
$J/\psi(1S)\eta K_S^0$	0.80 ± 0.40		$0.84 \pm 0.26 \pm 0.27 \pm 0.02$		0.84 ± 0.38
$J/\psi(1S)\phi(1020)\overline{K}^0$	0.94 ± 0.26		$1.02 \pm 0.38 \pm 0.10 \pm 0.02$		1.02 ± 0.39
$J/\psi(1S)\omega(782)\overline{K}^0$			$3.00 \pm 0.60 \pm 0.30$		$\mathbf{3.00 \pm 0.67}$
$J/\psi(1S)\overline{K}^0\rho^0(770)$	5.4 ± 3.0			$5.40 \pm 2.90 \pm 0.90$	5.4 ± 3.0
$J/\psi(1S)\overline{K}^{*0}(892)\pi^+\pi^-$	6.6 ± 2.2			$6.6 \pm 1.9 \pm 1.1$	6.6 ± 2.2
$J/\psi(1S)K^{*-}(892)\pi^+$	8.0 ± 4.0			$7.7 \pm 4.1 \pm 1.3$	7.7 ± 4.3
$J/\psi(1S)\overline{K}^0$	8.72 ± 0.33	$7.90 \pm 0.40 \pm 0.90 \pm 0.10$	$8.69 \pm 0.22 \pm 0.26 \pm 0.15$	$11.5 \pm 2.3 \pm 1.7$	8.63 ± 0.35
$J/\psi(1S)\overline{K}^0\pi^+\pi^-$	10.0 ± 4.0			$10.3 \pm 3.3 \pm 1.5$	10.3 ± 3.6
$J/\psi(1S)\overline{K}_1^0(1270)$	13.0 ± 5.0	$13.0 \pm 3.4 \pm 2.5 \pm 1.8$			13.0 ± 4.6
$J/\psi(1S)\overline{K}^{*0}(892)$	13.30 ± 0.60	$12.90 \pm 0.50 \pm 1.30 \pm 0.20$	$13.09 \pm 0.26 \pm 0.74 \pm 0.22$	$17.4 \pm 2.0 \pm 1.8$	13.32 ± 0.68

[1] Study of $B^0 \to J/\psi\pi^+\pi^-$ decays with 449 million $B\overline{B}$ pairs at Belle (449M $B\overline{B}$ pairs)
[2] MEASUREMENT OF BRANCHING FRACTIONS IN B0 — J/PSI PI+ PI- DECAY. (152M $B\overline{B}$ pairs)

Table 98: Ratios of branching fractions of neutral B modes producing $J/\psi(1S)$ in units of 10^0, upper limits are at 90% CL. The latest version is available at: http://hfag.phys.ntu.edu.tw/b2charm/00204.html

Mode	PDG 2006	Belle	*BABAR*	CDF	Average
$\frac{\mathcal{B}(\overline{B}^0\to J/\psi(1S)\overline{K}_1^0(1270))}{\mathcal{B}(B^-\to J/\psi(1S)K^-)}$		$1.30 \pm 0.34 \pm 0.28$			1.30 ± 0.44
$\frac{\mathcal{B}(\overline{B}^0\to \eta_c(1S)\overline{K}^0)}{\mathcal{B}(\overline{B}^0\to J/\psi(1S)\overline{K}^0)}$	1.39 ± 0.49		$1.34 \pm 0.19 \pm 0.13 \pm 0.38$		1.34 ± 0.44
$\frac{\mathcal{B}(\overline{B}^0\to J/\psi(1S)\overline{K}^{*0}(892))}{\mathcal{B}(\overline{B}^0\to J/\psi(1S)\overline{K}^0)}$	1.50 ± 0.09		$1.51 \pm 0.05 \pm 0.08$	$1.39 \pm 0.36 \pm 0.10$	1.50 ± 0.09

Table 99: Miscellaneous quantities of neutral B modes producing $J/\psi(1S)$ in units of 10^0, upper limits are at 90% CL. The latest version is available at: http://hfag.phys.ntu.edu.tw/b2charm/00204.html

Mode	PDG 2006	Belle	*BABAR*	CDF	Average
$\frac{\lvert\mathcal{A}_0\rvert^2(\overline{B}^0\to J/\psi(1S)K^{*0}(892))}{\lvert\mathcal{A}_0\rvert^2(B^0\to J/\psi(1S)K^{*0}(892))}$			< 0.26		< 0.26
$\frac{\lvert\mathcal{A}_0\rvert^2(B^0\to J/\psi(1S)\overline{K}^{*0}(892))}{\lvert\mathcal{A}_0\rvert^2(\overline{B}^0\to J/\psi(1S)\overline{K}^{*0}(892))}$			< 0.32		< 0.32

Table 100: Branching fractions of neutral B modes producing charmonium other than $J/\psi(1S)$ in units of 10^{-3}, upper limits are at 90% CL. The latest version is available at: http://hfag.phys.ntu.edu.tw/b2charm/00205.html

Mode	PDG 2006	Belle	*BABAR*	CDF	Average
$\chi_{c2}(1P)\overline{K}^{*0}(892)$	< 0.036		< 0.036		< 0.036
$\chi_{c2}(1P)\overline{K}^{0}$	< 0.026		< 0.041		< 0.041
$\chi_{c1}(1P)\overline{K}^{*0}(892)$	0.32 ± 0.06	$0.31 \pm 0.03 \pm 0.07$	$0.33 \pm 0.04 \pm 0.05 \pm 0.03$		$\mathbf{0.32 \pm 0.05}$
$\chi_{c1}(1P)\overline{K}^{0}$	0.39 ± 0.04	$0.35 \pm 0.03 \pm 0.05$	$0.45 \pm 0.04 \pm 0.02 \pm 0.05$		$\mathbf{0.40 \pm 0.04}$
$\psi(2S)\overline{K}^{0}$	0.62 ± 0.06	0.67 ± 0.11	$0.65 \pm 0.06 \pm 0.04 \pm 0.02$		0.65 ± 0.07
$\psi(2S)\overline{K}^{*0}(892)$	0.72 ± 0.08	$0.72 \pm 0.04 \pm 0.06$	$0.65 \pm 0.06 \pm 0.09 \pm 0.02$	$0.90 \pm 0.22 \pm 0.09$	0.71 ± 0.06
$\eta_c(1S)\overline{K}^{*0}(892)$	1.60 ± 0.70				$\mathbf{0.67 \pm 0.13}$
		$1.62 \pm 0.32 \pm^{0.24}_{0.34} \pm 0.50$	$0.61 \pm 0.08 \pm 0.11$ [1]		
			$0.80 \pm^{0.21}_{0.19} \pm 0.13 \pm^{0.35}_{0.19}$ [3b]		
$\chi_{c0}(1P)\overline{K}^{*0}(892)$	< 0.77		< 0.77		< 0.77
$\eta_c(1S)\overline{K}^{0}$	0.99 ± 0.19				$\mathbf{0.87 \pm 0.19}$
		$1.23 \pm 0.23 \pm^{0.12}_{0.16} \pm 0.38$	$1.14 \pm 0.15 \pm 0.12 \pm 0.32$ [2]		
			$0.64 \pm^{0.22}_{0.20} \pm 0.04 \pm^{0.28}_{0.15}$ [3a]		
$\chi_{c0}(1P)\overline{K}^{0}$	< 0.50		< 1.24		< 1.24

[1] A study of B-meson decays to $\eta_c K^*$ and $\eta_c \gamma K^{(*)}$ (384M $B\overline{B}$ pairs) ; betackstar0
[2] Branching Fraction Measurements of $B \to \eta_c K$ Decays (86.1M $B\overline{B}$ pairs)
[3] Evidence for the $B^0 \to p\overline{p}K^{*0}$ and $B^+ \to \eta_c K^{*+}$ decays and Study of the Decay Dynamics of B Meson Decays into $p\overline{p}h$ Final States. (232M $B\overline{B}$ pairs) ; [3a] betackzero ; [3b] betackstarzppbar

Table 101: Product branching fractions of neutral B modes producing charmonium other than $J/\psi(1S)$ in units of 10^{-4}, upper limits are at 90% CL. The latest version is available at: http://hfag.phys.ntu.edu.tw/b2charm/00205.html

Mode	PDG 2006	Belle	*BABAR*	CDF	Average
$\overline{K}^{0}\psi(3770)[D^0\overline{D}^0]$			< 1.23		$\mathbf{< 1.23}$
$\overline{K}^{0}\psi(3770)[D^+D^-]$			< 1.88		$\mathbf{< 1.88}$
$\overline{K}^{*0}(892)h_c(1P)[\eta_c(1S)\gamma]$			< 2.4		$\mathbf{< 2.4}$

Table 102: Ratios of branching fractions of neutral B modes producing charmonium other than $J/\psi(1S)$ in units of 10^0, upper limits are at 90% CL. The latest version is available at: http://hfag.phys.ntu.edu.tw/b2charm/00205.html

Mode	PDG 2006	Belle	*BABAR*	CDF	Average
$\frac{\mathcal{B}(\overline{B}^0\to h_c(1P)\overline{K}^{*0}(892))\times\mathcal{B}(h_c(1P)\to\eta_c(1S)\gamma)}{\mathcal{B}(B^-\to\eta_c(1S)K^-)}$			< 0.26		$\mathbf{< 0.26}$
$\frac{\mathcal{B}(\overline{B}^0\to h_c(1P)\overline{K}^{*0}(892))\times\mathcal{B}(h_c(1P)\to\eta_c(1S)\gamma)}{\mathcal{B}(\overline{B}^0\to\eta_c(1S)\overline{K}^{*0}(892))}$			< 0.39		$\mathbf{< 0.39}$
$\frac{\mathcal{B}(\overline{B}^0\to\eta_c(1S)\overline{K}^{*0}(892))}{\mathcal{B}(B^-\to\eta_c(1S)K^-)}$			$0.67 \pm 0.09 \pm 0.07$		$\mathbf{0.67 \pm 0.11}$
$\frac{\mathcal{B}(\overline{B}^0\to\chi_{c1}(1P)\overline{K}^{*0}(892))}{\mathcal{B}(\overline{B}^0\to\chi_{c1}(1P)\overline{K}^0)}$	0.72 ± 0.16		$0.72 \pm 0.11 \pm 0.12$		0.72 ± 0.16
$\frac{\mathcal{B}(\overline{B}^0\to\eta_c(1S)\overline{K}^0)}{\mathcal{B}(B^-\to\eta_c(1S)K^-)}$			$0.87 \pm 0.13 \pm 0.07$		0.87 ± 0.15
$\frac{\mathcal{B}(\overline{B}^0\to\psi(2S)\overline{K}^{*0}(892))}{\mathcal{B}(\overline{B}^0\to\psi(2S)\overline{K}^0)}$	1.00 ± 0.17		$1.00 \pm 0.14 \pm 0.09$		1.00 ± 0.17
$\frac{\mathcal{B}(\overline{B}^0\to\eta_c(1S)\overline{K}^{*0}(892))}{\mathcal{B}(\overline{B}^0\to\eta_c(1S)\overline{K}^0)}$	1.30 ± 0.40	$1.33 \pm 0.36 \pm^{0.24}_{0.33}$			$1.33 \pm^{0.43}_{0.49}$

Table 103: Branching fractions of neutral B modes producing multiple D, D^* or D^{**} mesons in units of 10^{-3}, upper limits are at 90% CL. The latest version is available at: http://hfag.phys.ntu.edu.tw/b2charm/00206.html

Mode	PDG 2006	Belle	*BABAR*	CDF	Average
$D^0\overline{D}^0$		< 0.042	< 0.060		$\mathbf{< 0.042}$
$D^{*0}(2007)\overline{D}^{*0}(2007)$	< 27		< 0.090		< 0.090
$D^0\overline{D}^0\pi^0\overline{K}^0$		$0.17 \pm 0.07 \pm^{0.03}_{0.05}$			$\mathbf{0.17 \pm 0.08}$
D^+D^-	0.19 ± 0.06				$\mathbf{0.22 \pm 0.02}$
		$0.20 \pm 0.02 \pm 0.02$ [1]	$0.28 \pm 0.04 \pm 0.03 \pm 0.04$		
		$0.32 \pm 0.06 \pm 0.05$ [2]			
$D^0\overline{D}^{*0}(2007)$			< 0.29		< 0.29
$D^{*-}(2010)D^+$	< 0.63	$1.17 \pm 0.26 \pm^{0.20}_{0.24} \pm 0.08$	$0.57 \pm 0.07 \pm 0.06 \pm 0.04$		0.62 ± 0.09
$D^{*+}(2010)D^{*-}(2010)$	0.83 ± 0.11				0.81 ± 0.08
		$0.81 \pm 0.08 \pm 0.11$	$0.81 \pm 0.06 \pm 0.09 \pm 0.05$ [3]		
			$0.83 \pm 0.16 \pm 0.12$ [4]		
$D^{*+}(2010)D^-$	< 0.63		$0.88 \pm 0.10 \pm 0.11 \pm 0.06$		0.88 ± 0.16
$D^0\overline{D}^0\overline{K}^0$	< 1.40		< 1.40		< 1.40
$D^+D^-\overline{K}^0$	< 1.70		< 1.70		< 1.70
$D^+\overline{D}^0K^-$	1.70 ± 0.40		$1.70 \pm 0.30 \pm 0.30$		1.70 ± 0.42
$D^{*+}(2010)\overline{D}^0K^-$	3.10 ± 0.60		$3.10 \pm^{0.40}_{0.30} \pm 0.40$		$3.10 \pm^{0.57}_{0.50}$
$D^0\overline{D}^{*0}(2007)\overline{K}^0$	< 3.7		< 3.7		< 3.7
$D^{*+}(2010)D^{*-}(2010)K^0_S$		$3.40 \pm 0.40 \pm 0.70$	$4.40 \pm 0.40 \pm 0.70 \pm 0.04$		$\mathbf{3.90 \pm 0.57}$
$D^+\overline{D}^{*0}(2007)K^-$	4.60 ± 1.00		$4.60 \pm 0.70 \pm 0.70$		4.60 ± 0.99
$D^{*+}(2010)D^-\overline{K}^0$	6.5 ± 1.6		$6.50 \pm 1.20 \pm 1.00$		6.5 ± 1.6
$D^{*0}(2007)\overline{D}^{*0}(2007)\overline{K}^0$	< 6.6		< 6.6		< 6.6
$D^{*-}(2010)D^{*+}(2010)\overline{K}^0$	8.8 ± 1.9		$8.8 \pm^{1.5}_{1.4} \pm 1.3$		$8.8 \pm^{2.0}_{1.9}$
$D^{*+}(2010)\overline{D}^{*0}(2007)K^-$	11.8 ± 2.0		$11.80 \pm 1.00 \pm 1.70$		11.8 ± 2.0

[1] Evidence for CP Violation in B0 - D+D- Decays (535M $B\overline{B}$ pairs)
[2] Observation of $B^0 \to D^+D^-$, $B^- \to D^0D^-$ and $B^- \to D^0D^{*-}$ decays (152M $B\overline{B}$ pairs)
[3] Measurement of Branching Fraction and CP-violating charge asymmetried for B meson decays to $D^{(*)}D^{(*)}$ and implications for the CKM angle γ (232M $B\overline{B}$ pairs) ; $\overline{B}^0 \to D^{*+}D^{*-}$
[4] Measurement of the branching fraction and CP content for the decay B^0 to D^*D^* (23M $B\overline{B}$ pairs) ; $\overline{B}^0 \to D^{*-}D^{*+}$

Table 104: Product branching fractions of neutral B modes producing multiple D, D^* or D^{**} mesons in units of 10^{-4}, upper limits are at 90% CL. The latest version is available at: http://hfag.phys.ntu.edu.tw/b2charm/00206.html

Mode	PDG 2006	Belle	*BABAR*	CDF	Average
$K^- D_2^{*+}(2460)[D^0\pi^+]$	0.18 ± 0.05		$0.18 \pm 0.04 \pm 0.03$		0.18 ± 0.05
$\pi^- D_2^{*+}(2460)[D^{*+}(2010)\pi^-\pi^+]$	< 0.24	< 0.24			< 0.24
$\pi^- D_1^{+}(2420)[D^{*+}(2010)\pi^-\pi^+]$	< 0.33	< 0.33			< 0.33
$\pi^- D_1^{+}(H)[D^{*0}(2007)\pi^+]$		< 0.70			< 0.70
$\pi^- D_1^{+}(2420)[D^{+}\pi^-\pi^+]$	0.89 ± 0.29	$0.89 \pm 0.15 \pm 0.17 \pm^{0.00}_{0.26}$			$0.89 \pm^{0.23}_{0.34}$
$\pi^- D_0^{*+}[D^0\pi^+]$		< 1.20			< 1.20
$\pi^- D_2^{*+}(2460)[D^{*0}(2007)\pi^+]$		$2.45 \pm 0.42 \pm^{0.35}_{0.45} \pm^{0.39}_{0.17}$			$2.45 \pm^{0.67}_{0.64}$
$\pi^- D_2^{*+}(2460)[D^{0}\pi^+]$		$3.08 \pm 0.33 \pm 0.09 \pm^{0.15}_{0.02}$			$3.08 \pm^{0.37}_{0.34}$
$\pi^- D_1^{+}(2420)[D^{*0}(2007)\pi^+]$		$3.68 \pm 0.60 \pm^{0.71}_{0.40} \pm^{0.65}_{0.30}$			$3.68 \pm^{1.13}_{0.78}$
$\omega(782) D_1^{0}(H)[D^{*+}(2010)\pi^-]$			$4.10 \pm 1.20 \pm 1.00 \pm 0.40$		4.1 ± 1.6

Table 105: Ratios of branching fractions of neutral B modes producing multiple D, D^* or D^{**} mesons in units of 10^0, upper limits are at 90% CL. The latest version is available at: http://hfag.phys.ntu.edu.tw/b2charm/00206.html

Mode	PDG 2006	Belle	*BABAR*	CDF	Average
$\frac{\mathcal{B}(\overline{B}^0 \to D^+ K^-)}{\mathcal{B}(\overline{B}^0 \to D^+ \pi^-)}$	0.07 ± 0.02	$0.068 \pm 0.015 \pm 0.007$			0.07 ± 0.02
$\frac{\mathcal{B}(\overline{B}^0 \to D^{*+}(2010) K^-)}{\mathcal{B}(\overline{B}^0 \to D^{*+}(2010) \pi^-)}$	0.07 ± 0.02	$0.074 \pm 0.015 \pm 0.006$	$0.078 \pm 0.003 \pm 0.003$		0.077 ± 0.004
$\frac{\mathcal{B}(\overline{B}^0 \to D^{**0} \pi^-)}{\mathcal{B}(\overline{B}^0 \to D^+ \pi^-)}$			$0.77 \pm 0.22 \pm 0.29$		$\mathbf{0.77 \pm 0.36}$
$\frac{\mathcal{B}(\overline{B}^0 \to D^{*+}(2010) \pi^-)}{\mathcal{B}(\overline{B}^0 \to D^+ \pi^-)}$			$0.99 \pm 0.11 \pm 0.08$		$\mathbf{0.99 \pm 0.14}$
$\frac{\mathcal{B}(\overline{B}^0 \to D^0 \rho^0(770))}{\mathcal{B}(\overline{B}^0 \to D^0 \omega(782))}$		1.60 ± 0.80			1.60 ± 0.80
$\frac{\mathcal{B}(\overline{B}^0 \to D^+ \mu^- \overline{\nu}_\mu)}{\mathcal{B}(\overline{B}^0 \to D^+ \pi^-)}$				$9.80 \pm 1.00 \pm 0.60 \pm 1.20$	9.8 ± 1.7
$\frac{\mathcal{B}(\overline{B}^0 \to D^{*+}(2010) \mu^- \overline{\nu}_\mu)}{\mathcal{B}(\overline{B}^0 \to D^{*+}(2010) \pi^-)}$				$17.70 \pm 2.30 \pm 0.60 \pm 1.20$	17.7 ± 2.7

Table 106: Branching fractions of neutral B modes producing a single D^* or D^{**} meson in units of 10^{-4}, upper limits are at 90% CL. The latest version is available at: http://hfag.phys.ntu.edu.tw/b2charm/00207.html

Mode	PDG 2006	Belle	*BABAR*	CDF	Average
$D^{*0}(2007)\overline{K}^0$	< 0.66				0.36 ± 0.12
		< 0.66	$0.45 \pm 0.19 \pm 0.05$ [2]		
			$0.36 \pm 0.12 \pm 0.03$ [1]		
$\overline{D}^{*0}(2007)\overline{K}^{*0}(892)$	< 0.40	< 0.40			< 0.40
$D^{*0}(2007)\overline{K}^{*0}(892)$	< 0.69	< 0.69			< 0.69
$D^{*0}(2007)\eta'(958)$	1.23 ± 0.35	$1.21 \pm 0.34 \pm 0.22$	< 2.6		1.21 ± 0.40
$D^{*0}(2007)\pi^0$	2.70 ± 0.50	$1.39 \pm 0.18 \pm 0.26$	$2.90 \pm 0.40 \pm 0.46 \pm 0.19$		$\mathbf{1.69 \pm 0.28}$
$D^{*0}(2007)\eta$	2.60 ± 0.60	$1.40 \pm 0.28 \pm 0.26$	$2.60 \pm 0.40 \pm 0.37 \pm 0.16$		$\mathbf{1.77 \pm 0.32}$
$f_2(1270)D^{*0}(2007)$		$1.86 \pm 0.65 \pm 0.60 \pm^{0.80}_{0.52}$			$1.9 \pm^{1.2}_{1.0}$
$D^{*+}(2010)K^-$	2.14 ± 0.20	$2.04 \pm 0.41 \pm 0.17 \pm 0.16$			2.04 ± 0.47
$D^{*0}(2007)\omega(782)$	4.2 ± 1.1	$2.29 \pm 0.39 \pm 0.40$	$4.20 \pm 0.70 \pm 0.86 \pm 0.27$		$\mathbf{2.66 \pm 0.50}$
$D^{*+}(2010)K^0\pi^-$	3.00 ± 0.80		$3.00 \pm 0.70 \pm 0.22 \pm 0.20$		3.00 ± 0.76
$D^{*+}(2010)K^{*-}(892)$	3.30 ± 0.60		$3.20 \pm 0.60 \pm 0.27 \pm 0.12$		3.20 ± 0.67
$D^{*0}(2007)\rho^0(770)$	< 5.1				3.73 ± 0.99
		$3.73 \pm 0.87 \pm 0.46 \pm^{0.18}_{0.08}$ [4]			
		< 5.1 [3]			
$D^{*+}(2010)K^-K^0$	< 4.7	< 4.7			< 4.7
$D^{*0}(2007)\pi^+\pi^-$	6.2 ± 2.2				9.0 ± 1.4
		$6.2 \pm 1.2 \pm 1.8$ [3]			
		$10.90 \pm 0.80 \pm 1.60$ [4]			
$D^{*+}(2010)K^-K^{*0}(892)$	12.9 ± 3.3	$12.9 \pm 2.2 \pm 2.5$			12.9 ± 3.3
$D^{**0}\pi^-$			$23.4 \pm 6.5 \pm 8.8$		$\mathbf{23 \pm 11}$
$D^{*0}(2007)\pi^-\pi^+\pi^-\pi^+$	27.0 ± 5.0	$26.0 \pm 4.7 \pm 3.7$			26.0 ± 6.0
$D^{*+}(2010)\pi^-$	27.6 ± 2.1				$\mathbf{26.2 \pm 1.3}$
		$23.00 \pm 0.60 \pm 1.90$	$27.90 \pm 0.80 \pm 1.70 \pm 0.05$ [6]		
			$29.9 \pm 2.3 \pm 2.4$ [5]		
$D^{*+}(2010)\omega(782)\pi^-$			$28.8 \pm 2.1 \pm 2.8 \pm 1.4$		28.8 ± 3.8
$D^{*+}(2010)\pi^-\pi^+\pi^-\pi^+\pi^-$		$47.2 \pm 5.9 \pm 7.1$			47.2 ± 9.2
$D^{*+}(2010)\pi^-\pi^+\pi^-$	76 ± 18	$68.1 \pm 2.3 \pm 7.2$			68.1 ± 7.6

[1] A study of the $\overline{B}^0 \to D^{(*)0}K^{(*)0}$ decays (226M $B\overline{B}$ pairs) ; $\overline{B}^0 \to D^{*0}\overline{K}^0$
[2] A study of the $\overline{B}^0 \to D^{(*)0}K^{(*)0}$ decays (124M $B\overline{B}$ pairs) ; $B \to D^{*0}\overline{K}^0$
[3] Study of $\overline{B}^0 \to D^{(*)0}\pi^+\pi^-$ Decays (31.3M $B\overline{B}$ pairs)
[4] Study of $\overline{B}^0 \to D^{(*)0}\pi^+\pi^-$ decays ; Dalitz fit analysis (152M $B\overline{B}$ pairs)
[5] Measurement of the Absolute Branching Fractions $B \to D^{(*,**)}\pi$ with a Missing Mass method (231M $B\overline{B}$ pairs) ; $\overline{B}^0 \to D^{*+}\pi^-$
[6] Branching fraction measurements and isospin analyses for $\overline{B} \to D^{(*)}\pi^-$ decays (65M $B\overline{B}$ pairs) ; $\overline{B}^0 \to D^{*+}\pi^-$

Table 107: Branching fractions of neutral B modes producing a single D meson in units of 10^{-4}, upper limits are at 90% CL. The latest version is available at: http://hfag.phys.ntu.edu.tw/b2charm/00208.html

Mode	PDG 2006	Belle	*BABAR*	CDF	Average
$\overline{D}^0\overline{K}^{*0}(892)$	< 0.180				< 0.110
		< 0.180	< 0.41 [2c]		
			< 0.110 [1c]		
$\overline{D}^0 K^-\pi^+$	< 0.190		< 0.190		< 0.190
$D^0\overline{K}^{*0}(892)$	0.53 ± 0.08				0.42 ± 0.06
		$0.48 \pm^{0.11}_{0.10} \pm 0.05$	$0.62 \pm 0.14 \pm 0.06$ [2b]		
			$0.40 \pm 0.07 \pm 0.03$ [1b]		
$D^0\overline{K}^0$	0.50 ± 0.14				0.52 ± 0.07
		$0.50 \pm^{0.13}_{0.12} \pm 0.06$	$0.62 \pm 0.12 \pm 0.04$ [2a]		
			$0.53 \pm 0.07 \pm 0.03$ [1a]		
$D^0 K^-\pi^+$	0.88 ± 0.17		$0.88 \pm 0.15 \pm 0.09$		0.88 ± 0.17
$D^0\eta'(958)$	1.25 ± 0.23	$1.14 \pm 0.20 \pm^{0.10}_{0.13}$	$1.70 \pm 0.40 \pm 0.18 \pm 0.10$		1.26 ± 0.21
$f_2(1270)D^0$		$1.95 \pm 0.34 \pm 0.38 \pm^{0.32}_{0.02}$			$1.95 \pm^{0.60}_{0.51}$
$D^0\eta$	2.20 ± 0.50	$1.77 \pm 0.16 \pm 0.21$	$2.50 \pm 0.20 \pm 0.29 \pm 0.11$		$\mathbf{2.02 \pm 0.21}$
D^+K^-	2.00 ± 0.60	$2.04 \pm 0.45 \pm 0.21 \pm 0.27$			2.04 ± 0.57
$D^0\omega(782)$	2.50 ± 0.60	$2.37 \pm 0.23 \pm 0.28$	$3.00 \pm 0.30 \pm 0.38 \pm 0.13$		$\mathbf{2.59 \pm 0.29}$
$D^0\pi^0$	2.91 ± 0.28	$2.25 \pm 0.14 \pm 0.35$	$2.90 \pm 0.20 \pm 0.27 \pm 0.13$		$\mathbf{2.59 \pm 0.26}$
$D^0\rho^0(770)$	2.9 ± 1.1				$2.91 \pm^{0.58}_{0.40}$
		$2.90 \pm 1.00 \pm 0.40$ [3]			
		$2.91 \pm 0.28 \pm 0.33 \pm^{0.08}_{0.54}$ [4]			
$D^+K^-K^0$	< 3.1	< 3.1			< 3.1
$D^+K^{*-}(892)$	4.50 ± 0.70		$4.60 \pm 0.60 \pm 0.47 \pm 0.16$		4.60 ± 0.78
$D^+K^0\pi^-$	4.90 ± 0.90		$4.90 \pm 0.70 \pm 0.38 \pm 0.32$		4.90 ± 0.86
$D^+K^-K^{*0}(892)$	8.8 ± 1.9	$8.8 \pm 1.1 \pm 1.5$			8.8 ± 1.9
$D^0\pi^+\pi^-$	8.0 ± 1.6				9.78 ± 0.95
		$8.00 \pm 0.60 \pm 1.50$ [3]			
		$10.70 \pm 0.60 \pm 1.00$ [4]			
$D^+\pi^-$	34.0 ± 9.0				$\mathbf{26.5 \pm 1.5}$
			$25.50 \pm 0.50 \pm 1.60 \pm 0.10$ [6]		
			$30.3 \pm 2.3 \pm 2.3$ [5]		

[1] A study of the $\overline{B}^0 \to D^{(*)0}K^{(*)0}$ decays (226M $B\overline{B}$ pairs) ; [1a] $\overline{B}^0 \to D^0\overline{K}^0$; [1b] $\overline{B}^0 \to D^0\overline{K}^{*0}$; [1c] $\overline{B}^0 \to \overline{D}^0\overline{K}^{*0}$

[2] A study of the $\overline{B}^0 \to D^{(*)0}K^{(*)0}$ decays (124M $B\overline{B}$ pairs) ; [2a] $B \to D^0\overline{K}^0$; [2b] $\overline{B}^0 \to D^0K^{*0}$; [2c] $\overline{B}^0 \to \overline{D}^0\overline{K}^{*0}$

[3] Study of $\overline{B}^0 \to D^{(*)0}\pi^+\pi^-$ Decays (31.3M $B\overline{B}$ pairs)

[4] Study of $\overline{B}^0 \to D^{(*)0}\pi^+\pi^-$ decays ; Dalitz fit analysis (152M $B\overline{B}$ pairs)

[5] Measurement of the Absolute Branching Fractions $B \to D^{(*,**)}\pi$ with a Missing Mass method (231M $B\overline{B}$ pairs) ; $\overline{B}^0 \to D^+\pi^-$

[6] Branching fraction measurements and isospin analyses for $\overline{B} \to D^{(*)}\pi^-$ decays (65M $B\overline{B}$ pairs) ; $\overline{B}^0 \to D^+\pi^-$

Table 108: Product branching fractions of neutral B modes producing a single D meson in units of 10^{-5}, upper limits are at 90% CL. The latest version is available at: http://hfag.phys.ntu.edu.tw/b2charm/00208.html

Mode	PDG 2006	Belle	*BABAR*	CDF	Average
$D^0\overline{K}^{*0}(892)[K^-\pi^+]$			$3.80 \pm 0.60 \pm 0.40$		3.80 ± 0.72

Table 109: Branching fractions of miscellaneous modes producing charmed particles in units of 10^{-3}, upper limits are at 90% CL. The latest version is available at: http://hfag.phys.ntu.edu.tw/b2charm/00300.html

Mode	PDG 2006	Belle	*BABAR*	CDF	Average
$\mathcal{B}(B \to D^0\overline{D}^0\pi^0 K)$		$0.13 \pm 0.03 \pm^{0.02}_{0.04}$			**0.13 ± 0.04**
$\mathcal{B}(\overline{\Lambda}_b^0 \to J/\psi(1S)\overline{\Lambda})$	0.47 ± 0.28			$0.47 \pm 0.21 \pm 0.19$	0.47 ± 0.28
$\mathcal{B}(\overline{D}^0 \to D^{*0}(2007)D^-)$			$0.63 \pm 0.14 \pm 0.08 \pm 0.06$		0.63 ± 0.17
$\mathcal{B}(\overline{B}_s^0 \to J/\psi(1S)\phi(1020))$	0.93 ± 0.33			$0.93 \pm 0.28 \pm 0.17$	0.93 ± 0.33

Table 110: Product branching fractions of miscellaneous modes producing charmed particles in units of 10^{-5}, upper limits are at 90% CL. The latest version is available at: http://hfag.phys.ntu.edu.tw/b2charm/00300.html

Mode	PDG 2006	Belle	*BABAR*	CDF	Average
$\mathcal{B}(B \to KY(3940)[\omega(782)J/\psi(1S)])$	7.1 ± 3.4	$7.1 \pm 1.3 \pm 3.1$			7.1 ± 3.4

Table 111: Ratios of branching fractions of miscellaneous modes producing charmed particles in units of 10^0, upper limits are at 90% CL. The latest version is available at: http://hfag.phys.ntu.edu.tw/b2charm/00300.html

Mode	PDG 2006	Belle	*BABAR*	CDF	Average
$\frac{\mathcal{B}(\overline{B}_s^0 \to D_s^+ K^-)}{\mathcal{B}(\overline{B}_s^0 \to D_s^+ \pi^-)}$				$0.107 \pm 0.019 \pm 0.008$	**0.11 ± 0.02**
$\frac{\mathcal{B}(\overline{B}_s^0 \to \psi(2S)\phi(1020))}{\mathcal{B}(\overline{B}_s^0 \to J/\psi(1S)\phi(1020))}$				$0.52 \pm 0.13 \pm 0.07$	0.52 ± 0.15
$\frac{\mathcal{B}(\overline{B}_s^0 \to D_s^+ \pi^+ \pi^- \pi^-)}{\mathcal{B}(\overline{B}^0 \to D^+ \pi^+ \pi^- \pi^-)}$				$1.05 \pm 0.10 \pm 0.22$	1.05 ± 0.24
$\frac{\mathcal{B}(\overline{B}_s^0 \to D_s^+ \pi^-)}{\mathcal{B}(\overline{B}^0 \to D^+ \pi^-)}$				$1.13 \pm 0.08 \pm 0.05 \pm 0.15$	1.13 ± 0.18
$\frac{\mathcal{B}(\overline{B}_s^0 \to D_s^- D_s^+)}{\mathcal{B}(\overline{B}^0 \to D_s^- D^+)}$				$1.67 \pm 0.41 \pm 0.12 \pm 0.46$	1.67 ± 0.63
$\frac{\mathcal{B}(\overline{\Lambda}_b^0 \to \Lambda_c^- \pi^+)}{\mathcal{B}(\overline{B}^0 \to D^+ \pi^-)}$				$3.30 \pm 0.30 \pm 0.40 \pm 1.10$	3.3 ± 1.2
$\frac{\mathcal{B}(\overline{\Lambda}_b^0 \to \Lambda_c^- \mu^+ \nu_\mu)}{\mathcal{B}(\overline{\Lambda}_b^0 \to \Lambda_c^- \pi^+)}$				$20.00 \pm 3.00 \pm 1.20 \pm^{0.90}_{2.20}$	$20.0 \pm^{3.4}_{3.9}$

Table 112: Miscellaneous quantities of miscellaneous modes producing charmed particles in units of 10^0, upper limits are at 90% CL. The latest version is available at: http://hfag.phys.ntu.edu.tw/b2charm/00300.html

Mode	PDG 2006	Belle	*BABAR*	CDF	Average
$\delta_\parallel(B \to J/\psi(1S)K^*)$		$-2.887 \pm 0.090 \pm 0.008$	$-2.93 \pm 0.08 \pm 0.04$		$\mathbf{-2.91 \pm 0.06}$
$\delta_\parallel(B \to \psi(2S)K^*)$			$-2.80 \pm 0.40 \pm 0.10$		$\mathbf{-2.80 \pm 0.41}$
$\delta_\parallel(B \to \chi_{c1}(1P)K^*)$			$0.00 \pm 0.30 \pm 0.10$		$\mathbf{0.00 \pm 0.32}$
$\lvert\mathcal{A}_\perp\rvert^2(B \to \chi_{c1}(1P)K^*)$			$0.03 \pm 0.04 \pm 0.02$		$\mathbf{0.03 \pm 0.04}$
$\lvert\mathcal{A}_\parallel\rvert^2(B \to \chi_{c1}(1P)K^*)$			$0.20 \pm 0.07 \pm 0.04$		$\mathbf{0.20 \pm 0.08}$
$\lvert\mathcal{A}_\perp\rvert^2(B \to J/\psi(1S)K^*)$		$0.195 \pm 0.012 \pm 0.008$	$0.233 \pm 0.010 \pm 0.005$		$\mathbf{0.219 \pm 0.009}$
$\lvert\mathcal{A}_\parallel\rvert^2(B \to J/\psi(1S)K^*)$		$0.231 \pm 0.012 \pm 0.008$	$0.211 \pm 0.010 \pm 0.006$		$\mathbf{0.219 \pm 0.009}$
$\lvert\mathcal{A}_\parallel\rvert^2(B \to \psi(2S)K^*)$			$0.22 \pm 0.06 \pm 0.02$		$\mathbf{0.22 \pm 0.06}$
$\lvert\mathcal{A}_\perp\rvert^2(B \to \psi(2S)K^*)$			$0.30 \pm 0.06 \pm 0.02$		$\mathbf{0.30 \pm 0.06}$
$\lvert\mathcal{A}_0\rvert^2(B \to \psi(2S)K^*)$			$0.48 \pm 0.05 \pm 0.02$		$\mathbf{0.48 \pm 0.05}$
$\lvert\mathcal{A}_0\rvert^2(B \to J/\psi(1S)K^*)$		$0.574 \pm 0.012 \pm 0.009$	$0.556 \pm 0.009 \pm 0.010$		$\mathbf{0.56 \pm 0.01}$
$\lvert\mathcal{A}_0\rvert^2(B \to \chi_{c1}(1P)K^*)$			$0.77 \pm 0.07 \pm 0.04$		$\mathbf{0.77 \pm 0.08}$
$\delta_\perp(B \to \psi(2S)K^*)$			$2.80 \pm 0.30 \pm 0.10$		$\mathbf{2.80 \pm 0.32}$
$\delta_\perp(B \to J/\psi(1S)K^*)$		$2.938 \pm 0.064 \pm 0.010$	$2.91 \pm 0.05 \pm 0.03$		$\mathbf{2.92 \pm 0.04}$

7 B decays to charmless final states

The aim of this section is to provide the branching fractions and the partial rate asymmetries (A_{CP}) of charmless B decays. The asymmetry is defined as $A_{CP} = \frac{N_{\overline{B}} - N_B}{N_{\overline{B}} + N_B}$, where $N_{\overline{B}}$ and N_B are respectively number of $\overline{B}^0/B^-$ and B^0/B^+ decaying into a specific final state. Four different B decay categories are considered: charmless mesonic, baryonic, radiative and leptonic. Measurements supported with written documents are accepted in the averages; written documents could be journal papers, conference contributed papers, preprints or conference proceedings. Results from A_{CP} measurements obtained from time dependent analyses are listed and described in Sec. 4. Measurements of charmful baryonic B decays, which were included in our previous averages [4], are now shown in Section 7, which deals with B decays to charm.

So far all branching fractions assume equal production of charged and neutral B pairs. The best measurements to date show that this is still a good approximation (see Sec. 3). For branching fractions, we provide either averages or the most stringent 90% confidence level upper limits. If one or more experiments have measurements with $>4\sigma$ for a decay channel, all available central values for that channel are used in the averaging. We also give central values and errors for cases where the significance of the average value is at least 3σ, even if no single measurement is above 4σ. Since a few decay modes are sensitive to the contribution of new physics and the current experimental upper limits are not far from the Standard Model expectation, we provide the combined upper limits or averages in these cases. Their upper limits can be estimated assuming that the errors are Gaussian. For A_{CP} we provide averages in all cases.

Our averaging is performed by maximizing the likelihood, $\mathcal{L} = \prod_i \mathcal{P}_i(x)$, where $\mathcal{P}_i$ is the probability density function (PDF) of the ith measurement, and x is the branching fraction or A_{CP}. The PDF is modeled by an asymmetric Gaussian function with the measured central value as its mean and the quadratic sum of the statistical and systematic errors as the standard deviations. The experimental uncertainties are considered to be uncorrelated with each other when the averaging is performed. No error scaling is applied when the fit χ^2 is greater than 1 since we believe that tends to overestimate the errors except in cases of extreme disagreement (we have no such cases). One exception to consider the correlated systematic errors is the inclusive $B \to X_s\gamma$ mode, which is sensitive to physics beyond the Standard Model. In this update, we have included new measurements from both Belle and BaBar to perform the average. The detail is described in Sec. 7.3.

At present, we have measurements of more than 350 decay modes, reported in more than 200 papers. Because the number of references is so large, we do not include them with the tables shown here but the full set of references is available quickly from active gifs at the "Winter 2008" link on the rare web page: `http://www.slac.stanford.edu/xorg/hfag/rare/index.html`. Finally many new measurements on the scalar-tensor and vector-tensor decays and direct CP asymmetry on $B_s^0 \to K^+\pi^-$ are included for the first time.

7.1 Mesonic charmless decays

Table 113: Branching fractions (BF) of charmless mesonic B^+ decays with kaons (in units of $\times 10^6$)). Upper limits are at 90% CL. Values in red (blue) are new published (preliminary) results since PDG2006 [as of April 15, 2008].

RPP#	Mode	PDG2006 Avg.	BABAR	Belle	CLEO	CDF	New avg.
182	$K^0\pi^+$	24.1 ± 1.7	$23.9 \pm 1.1 \pm 1.0$	$22.8^{+0.8}_{-0.7} \pm 1.3$	$18.8^{+3.7+2.1}_{-3.3-1.8}$		23.1 ± 1.0
183	$K^+\pi^0$	12.1 ± 0.8	$13.6 \pm 0.6 \pm 0.7$	$12.4 \pm 0.5 \pm 0.6$	$12.9^{+2.4+1.2}_{-2.2-1.1}$		12.9 ± 0.6
184	$\eta' K^+$	70.5 ± 3.5	$70.0 \pm 1.5 \pm 2.8$	$69.2 \pm 2.2 \pm 3.7$	$80^{+10}_{-9} \pm 7$		70.2 ± 2.5
185	$\eta' K^{*+}$	< 14	$4.9^{+1.9}_{-1.7} \pm 0.8$	< 2.9	$11.1^{+12.7}_{-8.0}$		$4.9^{+2.1}_{-1.9}$
186	ηK^+	2.6 ± 0.6	$3.7 \pm 0.4 \pm 0.1$	$1.9 \pm 0.3^{+0.2}_{-0.1}$	$2.2^{+2.8}_{-2.2}$		2.7 ± 0.3
187	ηK^{*+}	26 ± 4	$18.9 \pm 1.8 \pm 1.3$	$19.3^{+2.0}_{-1.9} \pm 1.5$	$26.4^{+9.6}_{-8.2} \pm 3.3$		19.3 ± 1.6
–	$\eta K_0^{*+}(1430)$	New	$15.8 \pm 2.2 \pm 2.2$				15.8 ± 3.1
–	$\eta K_2^{*+}(1430)$	New	$9.1 \pm 2.7 \pm 1.4$				9.1 ± 3.0
188	ωK^+	5.1 ± 0.7	$6.3 \pm 0.5 \pm 0.3$	$8.1 \pm 0.6 \pm 0.6$	$3.2^{+2.4}_{-1.9} \pm 0.8$		6.7 ± 0.5
189	ωK^{*+}	< 7.4	< 3.4		< 87		< 3.4
190	$a_0^+(980)K^0$ †	< 3.9	< 3.9				< 3.9
191	$a_0^0(980)K^+$ †	< 2.5	< 2.5				< 2.5
192	$K^{*0}\pi^+$	11.6 ± 1.9	$10.8 \pm 0.6^{+1.1}_{-1.3}$	$9.7 \pm 0.6^{+0.8}_{-0.9}$	$7.6^{+3.5}_{-3.0} \pm 1.6$		10.0 ± 0.8
193	$K^{*+}\pi^0$	6.9 ± 2.4	$6.9 \pm 2.0 \pm 1.3$		$7.1^{+11.4}_{-7.1} \pm 1.0$		6.9 ± 2.3
194	$K^+\pi^+\pi^-$	56 ± 9	$54.4 \pm 1.1 \pm 4.6$	$48.8 \pm 1.1 \pm 3.6$			51.0 ± 3.0
195	$K^+\pi^+\pi^-(NR)$	$3.1^{+1.0}_{-0.8}$	$9.3 \pm 1.0^{+6.8}_{-1.2}$	$16.9 \pm 1.3^{+1.7}_{-1.6}$	< 28		16.3 ± 2.0
196	$f_0(980)K^+$ †	8.9 ± 1.0	$10.3 \pm 0.5^{+2.0}_{-1.3}$	$8.8 \pm 0.8^{+0.9}_{-1.8}$			9.5 ± 0.9
197	$f_2(1270)K^+$	< 2.3	$0.88 \pm 0.26^{+0.26}_{-0.21}$	$1.33 \pm 0.30^{+0.23}_{-0.34}$			$1.06^{+0.28}_{-0.29}$
198	$f_0(1370)K^+$ †	< 10.7	< 10.7				< 10.7
199	$\rho^0(1450)K^+$	< 11.7	< 11.7				< 11.7
200	$f_0(1500)K^+$ †	< 4.4	$0.73 \pm 0.21 \pm 0.47$				0.73 ± 0.52
201	$f_2'(1525)K^+$ †	< 3.4	< 3.4	< 4.9			< 3.4
202	$K^+\rho^0$	$5.0^{+0.7}_{-0.8}$	$3.56 \pm 0.45^{+0.57}_{-0.46}$	$3.89 \pm 0.47^{+0.43}_{-0.41}$	$8.4^{+4.0}_{-3.4} \pm 1.8$		$3.81^{+0.48}_{-0.46}$
203	$K_0^{*0}(1430)\pi^+$	38 ± 5	$32.0 \pm 1.2^{+10.8}_{-6.0}$	$51.6 \pm 1.7^{+7.0}_{-7.4}$			$45.2^{+6.2}_{-6.3}$
204	$K_2^{*0}(1430)\pi^+$	< 6.9	$5.6 \pm 1.2^{+1.8}_{-0.8}$	< 6.9			$5.6^{+2.2}_{-1.4}$
205	$K^{*0}(1410)\pi^+$	< 45		< 45			< 45
206	$K^{*0}(1680)\pi^+$	< 12	< 15	< 12			< 12
207	$K^-\pi^+\pi^+$	< 1.8	< 1.8	< 4.5			< 1.8
210	$K^0\pi^+\pi^0$	< 66			< 66		< 66
211	$K^0\rho^+$	< 48	$8.0^{+1.4}_{-1.3} \pm 0.6$		< 48		$8.0^{+1.5}_{-1.4}$
–	$K^{*+}\pi^+\pi^-$	New	$75.3 \pm 6.0 \pm 8.1$				75.3 ± 10.1
213	$K^{*+}\rho^0$	11 ± 4	< 6.1		< 74		< 6.1
–	$K^{*+}f_0(980)$ †	New	$5.2 \pm 1.2 \pm 0.5$				5.2 ± 1.3
–	$a_1^+K^0$	New	$34.9 \pm 5.0 \pm 4.4$				34.9 ± 6.7
–	$b_1^0K^+$	New	$9.1 \pm 1.7 \pm 1.0$				9.1 ± 2.0
214	$K^{*0}\rho^+$	8.9 ± 2.1	$9.6 \pm 1.7 \pm 1.5$	$8.9 \pm 1.7 \pm 1.2$			9.2 ± 1.5
215	$K^{*+}\overline{K^{*0}}$	< 71			< 71		< 71
218	$K^+\overline{K^0}$	1.20 ± 0.32	$1.61 \pm 0.44 \pm 0.09$	$1.22^{+0.33+0.13}_{-0.28-0.16}$	< 3.3		$1.36^{+0.29}_{-0.27}$
219	$K^+\overline{K^0}\pi^0$	< 24			< 24		< 24
220	$K^+K_SK_S$	11.5 ± 1.3	$10.7 \pm 1.2 \pm 1.0$	$13.4 \pm 1.9 \pm 1.5$			11.5 ± 1.3
221	$K_SK_S\pi^+$	< 3.2		< 3.2			< 3.2
222	$K^+K^-\pi^+$	< 6.3	$5.0 \pm 0.5 \pm 0.5$	< 13			5.0 ± 0.7
224	$K^+K^+\pi^-$	< 1.3	< 1.3	< 2.4			< 1.3
226	$\overline{K^{*0}}K^+$	< 5.3	< 1.1		< 5.3		< 1.1
–	$\overline{K_0^{*0}}(1430)K^+$	New	< 2.2				< 2.2
228	$K^+K^-K^+$	30.1 ± 1.9	$33.5 \pm 0.9 \pm 1.6$	$30.6 \pm 1.2 \pm 2.3$			32.5 ± 1.5
229	ϕK^+	9.0 ± 0.8	$8.4 \pm 0.7 \pm 0.7$	$9.60 \pm 0.92^{+1.05}_{-0.84}$	$5.5^{+2.1}_{-1.8} \pm 0.6$	$7.6 \pm 1.3 \pm 0.6$	8.30 ± 0.65
231	a_2K^+†	< 1.1		< 1.1			< 1.1
233	$\phi(1680)K^+$†	< 0.8		< 0.8			< 0.8
235	$K^{*+}K^+K^-$	< 1600	$36.2 \pm 3.3 \pm 3.6$				36.2 ± 4.9
236	ϕK^{*+}	9.6 ± 3.0	$11.2 \pm 1.0 \pm 0.9$	$6.7^{+2.1+0.7}_{-1.9-1.0}$	$10.6^{+6.4+1.8}_{-4.9-1.6}$		10.0 ± 1.1
–	$\eta(1405)K^+$†	New	< 1.2				< 1.2
–	$\eta(1475)K^+$†	New	$13.8^{+1.8+1.0}_{-1.7-0.6}$				$13.8^{+2.1}_{-1.8}$
–	$\phi(1680)K^+$†	New	< 3.4				< 3.4
–	$f_1(1285)K^+$	New	< 2.0				< 2.0
–	$\eta(1295)K^+$†	New	< 4.0				< 4.0
–	$f_1(1420)K^+$†	New	< 2.9				< 2.9
–	$K^{*+}\pi^+K^-$	New	< 11.8				< 11.8
–	$K^{*+}K^+\pi^-$	New	< 6.1				< 6.1
239	$\phi\phi K^+$ §	$2.6^{+1.1}_{-0.9}$	$7.5 \pm 1.0 \pm 0.7$	$3.2^{+0.6}_{-0.5} \pm 0.3$			4.2 ± 0.6
–	$\eta'\eta' K^+$	New	< 25				< 25

†Product BF - daughter BF taken to be 100%; §$M_{\phi\phi} < 2.85$ GeV/c^2

Table 114: Branching Fractions (BF) of charmless mesonic B^+ decays without kaons (in units of 10^{-6}). Upper limits are at 90% CL. Values in red (blue) are new published (preliminary) result since PDG2006 [as of April 15, 2008].

RPP#	Mode	PDG2006 Avg.	BABAR	Belle	CLEO	CDF	New avg.
254	$\pi^+\pi^0$	5.5 ± 0.6	$5.02 \pm 0.46 \pm 0.29$	$6.5 \pm 0.4^{+0.4}_{-0.5}$	$4.6^{+1.8+0.6}_{-1.6-0.7}$		$5.59^{+0.41}_{-0.40}$
255	$\pi^+\pi^-\pi^+$	$16.2 \pm 1.2 \pm 0.9$	$16.2 \pm 1.2 \pm 0.9$				16.2 ± 1.5
256	$\rho^0\pi^+$	8.7 ± 1.1	$8.8 \pm 1.0^{+0.6}_{-0.9}$	$8.0^{+2.3}_{-2.0} \pm 0.7$	$10.4^{+3.3}_{-3.4} \pm 2.1$		$8.7^{+1.0}_{-1.1}$
257	$f_0(980)\pi^+$ †	< 3.0	< 3.0				< 3.0
258	$f_2(1270)\pi^+$	$8.2 \pm 2.1 \pm 1.4$	$8.2 \pm 2.1 \pm 1.4$				8.2 ± 2.5
259	$\rho^0(1450)\pi^+$	< 2.3	< 2.3				< 2.3
260	$f_0(1370)\pi^+$	< 3.0	< 3.0				< 3.0
261	$f_0(600)\pi^+$	< 4.1	< 4.1				< 4.1
262	$\pi^+\pi^-\pi^+(NR)$	< 4.6	< 4.6				< 4.6
264	$\rho^+\pi^0$	12.0 ± 1.9	$10.2 \pm 1.4 \pm 0.9$	$13.2 \pm 2.3^{+1.4}_{-1.9}$	< 43		$10.9^{+1.4}_{-1.5}$
266	$\rho^+\rho^0$	26 ± 6	$16.8 \pm 2.2 \pm 2.3$	$31.7 \pm 7.1^{+3.8}_{-6.7}$			18.2 ± 3.0
–	$f_0(980)\rho^+$ †	New	< 1.9				< 1.9
267	$a_1^+\pi^0$	< 1700	$26.4 \pm 5.4 \pm 4.1$				26.4 ± 6.8
268	$a_1^0\pi^+$	< 900	$20.4 \pm 4.7 \pm 3.4$				20.4 ± 5.8
–	$b_1^0\pi^+$	New	$6.7 \pm 1.7 \pm 1.0$				6.7 ± 2.0
269	$\omega\pi^+$	5.9 ± 1.0	$6.7 \pm 0.5 \pm 0.4$	$6.9 \pm 0.6 \pm 0.5$	$11.3^{+3.3}_{-2.9} \pm 1.4$		6.9 ± 0.5
270	$\omega\rho^+$	$12.6 \pm 3.7^{+3.3}_{-1.6}$	$10.6 \pm 2.1^{+1.6}_{-1.0}$		< 61		$10.6^{+2.6}_{-2.3}$
271	$\eta\pi^+$	4.9 ± 0.5	$5.0 \pm 0.5 \pm 0.3$	$4.2 \pm 0.4 \pm 0.2$	$1.2^{+2.8}_{-1.2}$		4.4 ± 0.4
272	$\eta'\pi^+$	4.0 ± 0.9	$3.9 \pm 0.7 \pm 0.3$	$1.8^{+0.7}_{-0.6} \pm 0.1$	$1.0^{+5.8}_{-1.0}$		$2.7^{+0.6}_{-0.5}$
273	$\eta'\rho^+$	< 22	$8.7^{+3.1+2.3}_{-2.8-1.3}$	< 5.8	$11.2^{+11.9}_{-7.0}$		$9.1^{+3.7}_{-2.8}$
274	$\eta\rho^+$	$8.4 \pm 1.9 \pm 1.1$	$8.4 \pm 1.9 \pm 1.1$	$4.1^{+1.4}_{-1.3} \pm 0.4$	$4.8^{+5.2}_{-3.8}$		5.4 ± 1.2
275	$\phi\pi^+$	< 0.41	< 0.24		< 5		< 0.24
276	$\phi\rho^+$	< 16			< 16		< 16
277	$a_0^0(980)\pi^+$ †	< 5.8	< 5.8				< 5.8
–	$a_0^+(980)\pi^0$ †	New	< 1.4				< 1.4

†Product BF - daughter BF taken to be 100%;

Table 115: Branching fractions of charmless mesonic B^0 decays with kaons (in units of 10^{-6}). Upper limits are at 90% CL. Values in red (blue) are new published (preliminary) result since PDG2006 [as of April 15, 2008].

RPP#	Mode	PDG2006 Avg.	BABAR	Belle	CLEO	CDF	New avg.
168	$K^+\pi^-$	18.2 ± 0.8	$19.1 \pm 0.6 \pm 0.6$	$19.9 \pm 0.4 \pm 0.8$	$18.0^{+2.3+1.2}_{-2.1-0.9}$		19.4 ± 0.6
169	$K^0\pi^0$	11.5 ± 1.0	$10.3 \pm 0.7 \pm 0.6$	$9.2 \pm 0.7^{+0.6}_{-0.7}$	$12.8^{+4.0+1.7}_{-3.3-1.4}$		9.9 ± 0.6
170	$\eta' K^0$	68 ± 4	$66.6 \pm 2.6 \pm 2.8$	$58.9^{+3.6}_{-3.5} \pm 4.3$	$89^{+18}_{-16} \pm 9$		64.9 ± 3.1
171	$\eta' K^{*0}$	< 7.6	$3.8 \pm 1.1 \pm 0.5$	< 2.6	$7.8^{+7.7}_{-5.7}$		3.8 ± 1.2
172	ηK^{*0}	17.7 ± 2.3	$16.5 \pm 1.1 \pm 0.8$	$15.2 \pm 1.2 \pm 1.0$	$13.8^{+5.5}_{-4.6} \pm 1.6$		15.9 ± 1.0
–	$\eta K_0^{*0}(1430)$	New	$9.6 \pm 1.4 \pm 1.3$				9.6 ± 1.9
–	$\eta K_2^{*0}(1430)$	New	$9.6 \pm 1.8 \pm 1.1$				9.6 ± 2.1
173	ηK^0	< 2.0	< 2.9	< 1.9	< 9.3		< 1.9
174	ωK^0	$5.5^{+1.2}_{-1.0}$	$5.4 \pm 0.8 \pm 0.3$	$4.4^{+0.8}_{-0.7} \pm 0.4$	$10.0^{+5.4}_{-4.2} \pm 1.4$		5.0 ± 0.6
175	$a_0^0(980)K^0$ †	< 7.8	< 7.8				< 7.8
176	$a_0^-(980)K^+$ †	< 2.1	< 1.9				< 1.9
–	$a_0^-(1450)K^+$ †	New	< 3.1				< 3.1
178	ωK^{*0}	< 6.0	< 4.2	< 2.7	< 23		< 2.7
179	K^+K^-	< 0.37	$0.04 \pm 0.15 \pm 0.08$	$0.09^{+0.18}_{-0.13} \pm 0.01$	< 0.8	$0.39 \pm 0.16 \pm 0.12$ ‡	$0.15^{+0.11}_{-0.10}$
180	$K^0\overline{K^0}$	$1.13^{+0.38}_{-0.35}$	$1.08 \pm 0.28 \pm 0.11$	$0.87^{+0.25}_{-0.20} \pm 0.09$	< 3.3		$0.96^{+0.21}_{-0.19}$
181	$K_SK_SK_S$	$6.2^{+1.2}_{-1.1}$	$6.9^{+0.9}_{-0.8} \pm 0.6$	$4.2^{+1.6}_{-1.3} \pm 0.8$			6.2 ± 0.9
–	$K_SK_SK_L$	New	< 16[1]				< 16[1]
182	$K^+\pi^-\pi^0$	$36.6^{+4.2}_{-4.3} \pm 3.0$	$35.7^{+2.6}_{-1.5} \pm 2.2$	$36.6^{+4.2}_{-4.3} \pm 3.0$	< 40		$35.9^{+2.9}_{-2.4}$
183	$K^+\rho^-$	8.5 ± 2.8	$8.0^{+0.8}_{-1.3} \pm 0.6$	$15.1^{+3.4+2.4}_{-3.3-2.6}$	$16^{+8}_{-6} \pm 3$		$8.6^{+0.9}_{-1.1}$
–	$f_2(1270)K^0$	New		< 2.5			< 2.5
–	$K^+\rho(1450)^-$	New	< 2.1				< 2.1
–	$K^+\rho(1700)^-$	New	< 1.1				< 1.1
–	$K^+\pi^-\pi^0(NR)$	New	$4.4 \pm 0.9 \pm 0.5$	< 9.4			4.4 ± 1.0
189	$K^{*+}\pi^-$	11.8 ± 1.5	$11.7^{+1.3}_{-1.2}$	$8.4 \pm 1.1^{+1.0}_{-0.9}$	$16^{+6}_{-5} \pm 2$		10.6 ± 0.9
191	$K^{*0}\pi^0$	< 3.5	$3.6 \pm 0.7 \pm 0.4$	$0.4^{+1.9}_{-1.7} \pm 0.1$	$0.0^{+1.3+0.5}_{-0.0-0.0}$		2.4 ± 0.7
–	$K^{*+}(1410)\pi^-$	New		< 86			< 86
–	$K_0^*(1430)^+\pi^-$	New	$25.4^{+3.0+6.1}_{-3.7-5.6}$ [2]	$49.7 \pm 3.8^{+6.8}_{-8.2}$			34.2 ± 5.4
–	$K_0^*(1430)^0\pi^0$	New	$11.7^{+1.4+4.0}_{-1.3-3.6}$ [2]				$11.7^{+4.2}_{-3.8}$
192	$K_2^*(1430)^+\pi^-$	< 18	< 16.2	< 6.3			< 6.3
–	$K_2^*(1430)^0\pi^0$	New	< 4.0				< 4.0
–	$K^*(1680)^+\pi^-$	New	< 25	< 10.1			< 10.1
–	$K^*(1680)^0\pi^0$	New	< 7.5				< 7.5
186	$K^0\pi^+\pi^-$	43.8 ± 2.9	$43.0 \pm 2.3 \pm 2.3$	$47.5 \pm 2.4 \pm 3.7$	$50^{+10}_{-9} \pm 7$		$44.8^{+2.6}_{-2.5}$
187	$K^0\rho^0$	< 39	$4.9 \pm 0.8 \pm 0.9$	$6.1 \pm 1.0^{+1.1}_{-1.2}$	< 39		$5.4^{+0.9}_{-1.0}$
188	$f_0(980)K^0$ †	$5.5 \pm 0.7 \pm 0.6$	$5.5 \pm 0.7 \pm 0.6$	$7.6 \pm 1.7^{+0.9}_{-1.3}$			$5.8^{+0.8}_{-0.9}$
–	$K_1^+(1270)\pi^-$	New	< 25.2				< 25.2
–	$K_1^+(1400)\pi^-$	New	< 21.8				< 21.8
193	$K^0K^-\pi^+$	< 21		< 18	< 21		< 18
194	$K^+K^-\pi^0$	< 19			< 19		< 19
195	$K^+K^-K^0$	24.7 ± 2.3	$23.8 \pm 2.0 \pm 1.6$	$28.3 \pm 3.3 \pm 4.0$			24.7 ± 2.3
196	ϕK^0	$8.6^{+1.3}_{-1.1}$	$8.4^{+1.5}_{-1.3} \pm 0.5$	$9.0^{+2.2}_{-1.8} \pm 0.7$	$5.4^{+3.7}_{-2.7} \pm 0.7$		$8.3^{+1.2}_{-1.0}$
198	$K^{*0}\pi^+\pi^-$	< 1400	$54.5 \pm 2.9 \pm 4.3$				54.5 ± 5.2
199	$K^{*0}\rho^0$	< 34	$5.6 \pm 0.9 \pm 1.3$		< 34		5.6 ± 1.6
200	$f_0(980)K^{*0}$ †	< 170	< 4.3				< 4.3
–	$K^{*+}\rho^-$	New	< 12				< 12
–	$K^{*0}\overline{K^0}$	New	< 1.9				< 1.9
202	$a_1^-K^+$	< 230	$16.3 \pm 2.9 \pm 2.3$				16.3 ± 3.7
–	$b_1^-K^+$	New	$7.4 \pm 1.0 \pm 1.0$				7.4 ± 1.4
203	$K^{*0}K^+K^-$	< 610	$27.5 \pm 1.3 \pm 2.2$				27.5 ± 2.6
204	ϕK^{*0}	9.5 ± 0.9	$9.2 \pm 0.7 \pm 0.6$	$10.0^{+1.6+0.7}_{-1.5-0.8}$	$11.5^{+4.5+1.8}_{-3.7-1.7}$		9.5 ± 0.8
–	$\phi K_0^{*0}(1430)$	New	$4.6 \pm 0.7 \pm 0.6$				4.6 ± 0.9
–	$\phi K_2^{*0}(1430)$	New	$7.8 \pm 1.1 \pm 0.6$				7.8 ± 1.3
–	$\phi K^{*0}(1680)$	New	< 3.5				< 3.5
–	$\phi K_3^{*0}(1780)$	New	< 2.7				< 2.7
–	$\phi K_4^{*0}(2045)$	New	< 15.3				< 15.3
–	$\phi\phi K^0$ §	New	$4.1^{+1.7}_{-1.4} \pm 0.4$	$2.3^{+1.0}_{-0.7} \pm 0.2$			$2.8^{+0.9}_{-0.7}$
–	$K^{*0}\pi^+K^-$	New	$4.6 \pm 1.1 \pm 0.8$				4.6 ± 1.4
–	$K^{*0}K^+\pi^-$	New	< 2.2				< 2.2
205	$K^{*0}\overline{K^{*0}}$	< 22	$1.28^{+0.35}_{-0.30} \pm 0.11$		< 22		$1.28^{+0.37}_{-0.32}$
206	$K^{*0}K^{*0}$	< 37	< 0.41		< 37		< 0.41
207	$K^{*+}K^{*-}$	< 141			< 141		< 141
–	$\eta'\eta' K^0$	New	< 31				< 31

†Product BF - daughter BF taken to be 100%, ‡Relative BF converted to absolute BF §$M_{\phi\phi} < 2.85$ GeV/c^2 [1]Excludes $M(K_SK_S)$ regions [3.400,3.429] and [3.540,3.585] and $M(K_SK_L) <$ 1.049 GeV/c^2 [2]Includes $K_0^*(1430)$ contributions and uses measured $K^*(1430)$ BF

Table 116: Branching fractions of charmless mesonic B^0 decays without kaons (in units of 10^{-6}). Upper limits are at 90% CL. Values in red (blue) are new published (preliminary) result since PDG2006 [as of April 15, 2008].

RPP#	Mode	PDG2006 Avg.	BABAR	Belle	CLEO	CDF	New avg.
229	$\pi^+\pi^-$	4.6 ± 0.4	$5.5 \pm 0.4 \pm 0.3$	$5.1 \pm 0.2 \pm 0.2$	$4.5^{+1.4+0.5}_{-1.2-0.4}$	$5.10 \pm 0.33 \pm 0.36$ ‡	5.16 ± 0.22
230	$\pi^0\pi^0$	1.5 ± 0.5	$1.47 \pm 0.25 \pm 0.12$	$1.1 \pm 0.3 \pm 0.1$	< 4.4		1.31 ± 0.21
231	$\eta\pi^0$	< 2.5	< 1.3	< 2.5	< 2.9		< 1.3
232	$\eta\eta$	< 2.0	< 1.8	< 2.0	< 18		< 1.8
233	$\eta'\pi^0$	< 3.7	$0.8^{+0.8}_{-0.6} \pm 0.1$	$2.8 \pm 1.0 \pm 0.3$	$0.0^{+1.8}_{-0.0}$		$1.5^{+0.7}_{-0.6}$
234	$\eta'\eta'$	< 10	< 2.4	< 6.5	< 47		< 2.4
235	$\eta'\eta$	< 4.6	< 1.7	< 4.5	< 27		< 1.7
236	$\eta'\rho^0$	< 4.3	< 3.7	< 1.3	< 12		< 1.3
–	$f_0(980)\eta'$ †	New	< 1.5				< 1.5
237	$\eta\rho^0$	< 1.5	< 1.5	< 1.9	< 10		< 1.5
–	$f_0(980)\eta$ †	New	< 0.4				< 0.4
238	$\omega\eta$	< 1.9	< 1.9		< 12		< 1.9
239	$\omega\eta'$	< 2.8	< 2.8	< 2.2	< 60		< 2.2
240	$\omega\rho^0$	< 3.3	< 1.5		< 11		< 1.5
–	$f_0(980)\omega$ †	New	< 1.5				< 1.5
241	$\omega\omega$	< 19	< 4.0		< 19		< 4.0
242	$\phi\pi^0$	< 1	< 0.28		< 5		< 0.28
243	$\phi\eta$	< 1	< 0.6		< 9		< 0.6
244	$\phi\eta'$	< 4.5	< 1.0	< 0.5	< 31		< 0.5
245	$\phi\rho^0$	< 13			< 13		< 13
246	$\omega\phi$	< 21	< 1.2		< 21		< 1.2
247	$\phi\phi$	< 1.5	< 1.5		< 12		< 1.5
248	$a_0^\mp(980)\pi^\pm$ †	< 5.1	< 3.1				< 3.1
–	$a_0^\mp(1450)\pi^\pm$ †	New	< 2.3				< 2.3
250	$\rho^0\pi^0$	1.8 ± 0.8	$1.4 \pm 0.6 \pm 0.3$	$3.0 \pm 0.5 \pm 0.7$	$1.6^{+2.0}_{-1.4} \pm 0.8$		2.0 ± 0.5
251	$\rho^\mp\pi^\pm$	22.8 ± 2.5	$22.6 \pm 1.8 \pm 2.2$	$22.6 \pm 1.1 \pm 4.4$	$27.6^{+8.4}_{-7.4} \pm 4.2$		23.0 ± 2.3
252	$\pi^+\pi^-\pi^+\pi^-$	< 230		< 19.0			< 19.0
253	$\rho^0\rho^0$	< 1.1	$0.84 \pm 0.29 \pm 0.17$	$0.4 \pm 0.4 \pm 0.2$	< 18		0.68 ± 0.27
–	$\rho^0\pi^+\pi^-(NR)$	New		< 11.9			< 11.9
–	$f_0(980)\pi^+\pi^-(NR)$	New		< 7.3			< 7.3
–	$f_0(980)\rho^0$ †	New	< 0.53	< 0.6			< 0.53
–	$f_0(980)f_0(980)$ †	New	< 0.16	< 0.4			< 0.16
254	$a_1^\mp\pi^\pm$	< 490	$33.2 \pm 3.8 \pm 3.0$	$29.8 \pm 3.2 \pm 4.6$			31.7 ± 3.7
–	$b_1^\mp\pi^\pm$	New	$10.9 \pm 1.2 \pm 0.9$				10.9 ± 1.5
257	$\rho^+\rho^-$	25 ± 4	$25.5 \pm 2.1^{+3.6}_{-3.9}$	$22.8 \pm 3.8^{+2.3}_{-2.6}$			$24.2^{+3.1}_{-3.2}$
259	$\omega\pi^0$	< 1.2	< 1.2	< 2.0	< 5.5		< 1.2
261	$a_1^\pm\rho^\mp$	< 3400	< 61				< 61

†Product BF - daughter BF taken to be 100%, ‡Relative BF converted to absolute BF

Table 117: Relative branching fractions of $B^0 \to K^+K^-, K^+\pi^-, \pi^+\pi^-$. Values in red (blue) are new published (preliminary) result since PDG2006 [as of March 15, 2007].

RPP#	Mode	PDG2006 Avg.	CDF	DØ	New avg.
179	$\mathcal{B}(B^0 \to K^+K^-)/\mathcal{B}(B^0 \to K^+\pi^-)$		$0.020 \pm 0.008 \pm 0.006$		0.020 ± 0.010
229	$\mathcal{B}(B^0 \to \pi^+\pi^-)/\mathcal{B}(B^0 \to K^+\pi^-)$		$0.259 \pm 0.017 \pm 0.016$		0.259 ± 0.023

7.2 Radiative and leptonic decays

Table 118: Branching fractions of semileptonic and radiative B^+ decays (in units of 10^{-6}). Upper limits are at 90% CL. Values in red (blue) are new published (preliminary) result since PDG2006 [as of April 15, 2008].

RPP#	Mode	PDG2006 Avg.	BABAR	Belle	CLEO	CDF	New Avg.
240	$K^{*+}\gamma$	40.3 ± 2.6	$38.7 \pm 2.8 \pm 2.6$	$42.5 \pm 3.1 \pm 2.4$	$37.6^{+8.9}_{-8.3} \pm 2.8$		40.3 ± 2.6
241	$K_1^+(1270)\gamma$	$43 \pm 9 \pm 9$		$43 \pm 9 \pm 9$			43 ± 12
242	$K^+\eta\gamma$	$8.4^{+1.5}_{-1.2} \pm 0.9$	$10.0 \pm 1.3 \pm 0.5$	$8.4^{+1.5}_{-1.2} \pm 0.9$			9.4 ± 1.1
–	$K^+\eta'\gamma$	New	< 4.2				< 4.2
243	$K^+\phi\gamma$	$3.4 \pm 0.9 \pm 0.4$	$3.5 \pm 0.6 \pm 0.4$	$3.4 \pm 0.9 \pm 0.4$			3.5 ± 0.6
244	$K^+\pi^-\pi^+\gamma$	$25.0 \pm 1.8 \pm 2.2$	$29.5 \pm 1.3 \pm 2.0$ †	$25.0 \pm 1.8 \pm 2.2$ ‡			27.6 ± 1.8
–	$K^0\pi^+\pi^0\gamma$	New	$45.6 \pm 4.2 \pm 3.1$ †				45.6 ± 5.2
245	$K^{*0}\pi^+\gamma$ §	20^{+7}_{-6}		$20^{+7}_{-6} \pm 2$			20^{+7}_{-6}
246	$K^+\rho^0\gamma$ §	< 20		< 20			< 20
247	$K^+\pi^-\pi^+\gamma$ (N.R.) §	< 9.2		< 9.2			< 9.2
248	$K_1^+(1400)\gamma$	< 50		< 15			< 15
249	$K_2^{*+}(1430)\gamma$	$14.5 \pm 4.0 \pm 1.5$	$14.5 \pm 4.0 \pm 1.5$				14.5 ± 4.3
251	$K_3^{*+}(1780)\gamma$	< 39		< 39			< 39
253	$\rho^+\gamma$	< 1.8	$1.10^{+0.37}_{-0.33} \pm 0.09$	$0.86^{+0.30+0.07}_{-0.28-0.08}$	< 13		$0.96^{+0.24}_{-0.22}$
296	$p\overline{\Lambda}\gamma$	$2.16^{+0.58}_{-0.53} \pm 0.20$		$2.45^{+0.44}_{-0.38} \pm 0.22$			$2.45^{+0.49}_{-0.44}$
297	$p\overline{\Sigma^0}\gamma$	< 4.6		< 4.6			< 4.6
315	$\pi^+e^+e^-$	< 3900	< 0.18	< 0.055			< 0.055
316	$\pi^+\mu^+\mu^-$	< 9100	< 0.28	< 0.051			< 0.051
–	$\pi^+\ell^+\ell^-$	New	< 0.12	< 0.037			< 0.037
317	$\pi^+\nu\overline{\nu}$	< 100	< 100	< 170			< 100
318	$K^+e^+e^-$	$0.80^{+0.22}_{-0.19}$	$0.42^{+0.12}_{-0.11} \pm 0.02$	$0.63^{+0.19}_{-0.17} \pm 0.03$	< 2.4		0.49 ± 0.10
319	$K^+\mu^+\mu^-$	$0.34^{+0.19}_{-0.14}$	$0.31^{+0.15}_{-0.12} \pm 0.03$	$0.45^{+0.14}_{-0.12} \pm 0.03$	< 3.68	$0.60 \pm 0.15 \pm 0.04$	$0.45^{+0.09}_{-0.08}$
320	$K^+\ell^+\ell^-$	$0.53^{+0.11}_{-0.10} \pm 0.3$	$0.38^{+0.09}_{-0.08} \pm 0.02$				$0.38^{+0.09}_{-0.08}$
321	$K^+\nu\overline{\nu}$	< 52	< 52	< 14	< 240		< 14
–	$\rho^+\nu\overline{\nu}$	New		< 150			< 150
322	$K^{*+}e^+e^-$	< 4.6	$0.75^{+0.76}_{-0.65} \pm 0.38$	$2.02^{+1.27+0.23}_{-1.01-0.24}$			$1.23^{+0.69}_{-0.62}$
323	$K^{*+}\mu^+\mu^-$	< 2.2	$0.97^{+0.94}_{-0.69} \pm 0.14$	$0.65^{+0.69+0.14}_{-0.53-0.15}$			$0.78^{+0.56}_{-0.44}$
324	$K^{*+}\ell^+\ell^-$	< 2.2	$0.73^{+0.50}_{-0.42} \pm 0.21$				$0.73^{+0.54}_{-0.47}$
–	$K^{*+}\nu\overline{\nu}$	New		< 140			< 140
327	$K^+e^+\mu^-$	< 0.8	< 0.09				< 0.09
328	$K^+e^-\mu^+$	< 6400	< 0.13				< 0.13
–	$K^+\tau^\pm\mu^\mp$	New	< 77				< 77
329	$K^{*+}e^\pm\mu^\mp$	< 7.9	< 1.4				< 1.4
330	$\pi^-e^+e^+$	< 1.6			< 1.6		< 1.6
331	$\pi^-\mu^+\mu^+$	< 1.4			< 1.4		< 1.4
332	$\pi^-e^+\mu^+$	< 1.3			< 1.3		< 1.3
333	$\rho^-e^+e^+$	< 2.6			< 2.6		< 2.6
334	$\rho^-\mu^+\mu^+$	< 5.0			< 5.0		< 5.0
335	$\rho^-e^+\mu^+$	< 3.3			< 3.3		< 3.3
336	$K^-e^+e^+$	< 1.0			< 1.0		< 1.0
337	$K^-\mu^+\mu^+$	< 1.8			< 1.8		< 1.8
338	$K^-e^+\mu^+$	< 2.0			< 2.0		< 2.0
339	$K^{*-}e^+e^+$	< 2.8			< 2.8		< 2.8
340	$K^{*-}\mu^+\mu^+$	< 8.3			< 8.3		< 8.3
341	$K^{*-}e^+\mu^+$	< 4.4			< 4.4		< 4.4
–	$\pi^+e^\pm\mu^\mp$	New	< 0.17				< 0.17

†$M_{K\pi\pi} < 1.8$ GeV/c^2; ‡ $1.0 < M_{K\pi\pi} < 2.0$ GeV/c^2; § $M_{K\pi\pi} < 2.4$ GeV/c^2

Table 119: Branching fractions of semileptonic and radiative B^0 decays (in units of 10^{-6}). Upper limits are at 90% CL. Values in red (blue) are new published (preliminary) result since PDG2006 [as of April 15, 2008].

RPP#	Mode	PDG2006 Avg.	BABAR	Belle	CLEO	CDF	New Avg.
213	$K^{*0}\gamma$	40.1 ± 2.0	$39.2 \pm 2.0 \pm 2.4$	$40.1 \pm 2.1 \pm 1.7$	$45.5^{+7.2}_{-6.8} \pm 3.4$		40.1 ± 2.0
214	$K^0\eta\gamma$	$8.7^{+3.1+1.9}_{-2.7-1.6}$	$11.3^{+2.8}_{-2.6} \pm 0.6$	$8.7^{+3.1+1.9}_{-2.7-1.6}$			$10.3^{+2.3}_{-2.1}$
–	$K^0\eta'\gamma$	New	< 6.6				< 6.6
215	$K^0\phi\gamma$	< 8.3	< 2.7	< 8.3			< 2.7
216	$K^+\pi^-\gamma$ §	4.6 ± 1.4		$4.6^{+1.3+0.5}_{-1.2-0.7}$			4.6 ± 1.4
217	$K^{*0}(1410)\gamma$	< 130		< 130			< 130
218	$K^+\pi^-\gamma$ (N.R.) §	< 2.6		< 2.6			< 2.6
219	$K^0\pi^+\pi^-\gamma$	$24 \pm 4 \pm 3$	$18.5 \pm 2.1 \pm 1.2$ †	$24 \pm 4 \pm 3$ ‡			19.5 ± 2.2
–	$K^+\pi^-\pi^0\gamma$	New	$40.7 \pm 2.2 \pm 3.1$ †				40.7 ± 3.8
220	$K_1^0(1270)\gamma$	< 58		< 58			< 58
221	$K_1^0(1400)\gamma$	< 15		< 15			< 15
222	$K_2^{*0}(1430)\gamma$	12.4 ± 2.4	$12.2 \pm 2.5 \pm 1.0$	$13 \pm 5 \pm 1$			12.4 ± 2.4
224	$K_3^{*0}(1780)\gamma$	< 83		< 83			< 83
226	$\rho^0\gamma$	< 0.4	$0.79^{+0.22}_{-0.20} \pm 0.06$	$0.76 \pm 0.17 \pm 0.06$	< 17		0.77 ± 0.14
227	$\omega\gamma$	< 0.8	$0.40^{+0.24}_{-0.20} \pm 0.05$	$0.42^{+0.20}_{-0.18} \pm 0.04$	< 9.2		$0.41^{+0.16}_{-0.14}$
228	$\phi\gamma$	< 0.85	< 0.85		< 3.3		< 0.85
–	$\pi^0 e^+ e^-$	New	< 0.14	< 0.143			< 0.14
–	$\pi^0 \mu^+ \mu^-$	New	< 0.51	< 0.154			< 0.154
–	$\pi^0 \ell^+ \ell^-$	New	< 0.12	< 0.133			< 0.12
–	$\pi^0 \nu\overline{\nu}$	New		< 220			< 220
293	$K^0 e^+ e^-$	< 0.54	$0.13^{+0.16}_{-0.11} \pm 0.02$	$0.00^{+0.20+0.02}_{-0.12-0.05}$	< 8.45		$0.09^{+0.12}_{-0.09}$
294	$K^0 \mu^+ \mu^-$	$0.20^{+0.13}_{-0.10}$	$0.59^{+0.33}_{-0.26} \pm 0.07$	$0.56^{+0.29}_{-0.23} \pm 0.05$	< 6.64		$0.57^{+0.22}_{-0.18}$
295	$K^0 \ell^+ \ell^-$	< 0.68	$0.29^{+0.16}_{-0.13} \pm 0.03$				$0.29^{+0.16}_{-0.13}$
–	$K^0 \nu\overline{\nu}$	New		< 160			< 160
–	$\rho^0 \nu\overline{\nu}$	New		< 440			< 440
296	$K^{*0} e^+ e^-$	< 2.4	$1.04^{+0.33}_{-0.29} \pm 0.11$	$1.29^{+0.57+0.13}_{-0.49-0.10}$			$1.11^{+0.30}_{-0.26}$
297	$K^{*0} \mu^+ \mu^-$	$1.22^{+0.38}_{-0.32}$	$0.87^{+0.38}_{-0.33} \pm 0.12$	$1.33^{+0.42}_{-0.37} \pm 0.11$		$0.82 \pm 0.31 \pm 0.10$	$0.98^{+0.22}_{-0.21}$
298	$K^{*0} \nu\overline{\nu}$	< 1000		< 340			< 340
299	$K^{*0} \ell^+ \ell^-$	1.17 ± 0.30	$0.81^{+0.21}_{-0.19} \pm 0.09$				$0.81^{+0.23}_{-0.21}$
–	$\phi \nu\overline{\nu}$	New		< 58			< 58
–	$\pi^0 e^\pm \mu^\mp$	New	< 0.14				< 0.14
301	$K^0 e^\pm \mu^\pm$	< 4.0	< 0.27				< 0.27
302	$K^{*0} e^\pm \mu^\pm$	< 3.4	< 0.58				< 0.58

†$M_{K\pi\pi} < 1.8$ GeV/c^2; ‡ $1.0 < M_{K\pi\pi} < 2.0$ GeV/c^2; § 1.25 GeV/$c^2 < M_{K\pi} < 1.6$ GeV/c^2

7.3 $B \to X_s\gamma$

The decay $B \to X_s\gamma$ proceeds through a process of flavor changing neutral current. Since the charged Higgs or SUSY particles may contribute in the penguin loop, the branching fraction is sensitive to physics beyond the Standard Model. Experimentally, the branching fraction is measured using either a semi-inclusive or an inclusive approach. A minimum photon energy requirement is applied in the analysis and the branching fraction is corrected based on the theoretical model for the photon energy spectrum (shape function). In this average of the $B \to X_s\gamma$ branching fraction, we still use the extrapolation factors [392] obtained by O. Buchmüller and H. Flächer and listed in Table 123. The extrapolation factors are defined as the ratios of the $B \to X_s\gamma$ branching fractions with minimum photon energies above and at 1.6 GeV. The appropriate approach to average the experimental results is to first convert them according to the average extrapolation factors and then perform the average, assuming that the errors of the extrapolation factors are 100% correlated.

After releasing our average for 2006 [4], two more measurements on the $B \to X_s\gamma$ branching fraction were available: the BaBar result [393] using full hadronic tags and the Belle inclusive

Table 120: Branching fractions of semileptonic and radiative B decays (in units of 10^{-6}). Upper limits are at 90% CL. Values in red (blue) are new published (preliminary) result since PDG2006 [as of April 15, 2008].

RPP#	Mode	PDG2006 Avg.	BABAR	Belle	CLEO	New Avg.
61	$K_2^*(1430)\gamma$	$1.7 \pm 0.6 \pm 0.1$			$1.7 \pm 0.6 \pm 0.1$	1.7 ± 0.6
63	$K_3^*(1780)\gamma$	< 37		< 2.8		< 2.8
70	$s\gamma$	343 ± 29	$327 \pm 18^{+55}_{-41}$	$325 \pm 16 \pm 24$	$321 \pm 43^{+32}_{-29}$	$352 \pm 23 \pm 9$
–	$s\gamma$ with baryons	New			< 38 †	< 38 †
74	$\rho\gamma$	< 1.9	$1.36^{+0.29}_{-0.27} \pm 0.10$	$1.19 \pm 0.24 \pm 0.12$	< 14	$1.27^{+0.20}_{-0.19}$
75	$\rho/\omega\gamma$	< 1.2	$1.25 \pm 0.25 \pm 0.09$	$1.13 \pm 0.20 \pm 0.11$	< 14	1.18 ± 0.17
–	$K\eta\gamma$	New		$8.5^{+1.3}_{-1.2} \pm 0.9$		$8.5^{+1.6}_{-1.5}$
105	se^+e^- ‡	4.7 ± 1.3	$6.0 \pm 1.7 \pm 1.3$	$4.0 \pm 1.3^{+0.9}_{-0.8}$	< 57	4.7 ± 1.3
106	$s\mu^+\mu^-$	4.3 ± 1.2	$5.0 \pm 2.8 \pm 1.2$	$4.1 \pm 1.1^{+0.9}_{-0.8}$	< 58	$4.3^{+1.3}_{-1.2}$
107	$s\ell^+\ell^-$ ‡	4.5 ± 1.0	$5.6 \pm 1.5 \pm 1.3$	$4.11 \pm 0.83^{+0.85}_{-0.81}$	< 42	$4.50^{+1.03}_{-1.01}$
–	$\pi\ell^+\ell^-$	New	< 0.091	< 0.051		< 0.051
108	Ke^+e^-	$0.60^{+0.14}_{-0.12}$	$0.33^{+0.09}_{-0.08} \pm 0.02$	$0.48^{+0.15}_{-0.13} \pm 0.03$		$0.38^{+0.08}_{-0.07}$
109	$K^*e^+e^-$	$1.24^{+0.37}_{-0.32}$	$0.97^{+0.30}_{-0.27} \pm 0.14$	$1.49^{+0.52+0.11}_{-0.46-0.13}$		$1.13^{+0.28}_{-0.26}$
110	$K\mu^+\mu^-$	$0.47^{+0.11}_{-0.10}$	$0.35^{+0.13}_{-0.11} \pm 0.03$	$0.48^{+0.13}_{-0.11} \pm 0.04$		$0.42^{+0.09}_{-0.08}$
111	$K^*\mu^+\mu^-$	$1.19^{+0.34}_{-0.29}$	$0.88^{+0.35}_{-0.30} \pm 0.12$	$1.17^{+0.36}_{-0.31} \pm 0.10$		$1.03^{+0.26}_{-0.23}$
112	$K\ell^+\ell^-$	0.54 ± 0.08	$0.34 \pm 0.07 \pm 0.02$	$0.48^{+0.10}_{-0.09} \pm 0.03$	< 1.7	0.39 ± 0.06
113	$K^*\ell^+\ell^-$	1.05 ± 0.20	$0.78^{+0.19}_{-0.17} \pm 0.11$	$1.15^{+0.26}_{-0.24} \pm 0.08$	< 3.3	$0.94^{+0.17}_{-0.16}$
115	$\pi e^\pm\mu^\mp$	< 1.6	< 0.092		< 1.6	< 0.092
116	$\rho e^\pm\mu^\mp$	< 3.2			< 3.2	< 3.2
117	$Ke^\pm\mu^\mp$	< 1.6	< 0.038		< 1.6	< 0.038
118	$K^*e^\pm\mu^\mp$	< 6.2	< 0.51		< 6.2	< 0.51

†$E_\gamma > 2.0$ GeV; ‡$M(\ell^+\ell^-) > 0.2$ GeV/c^2

Table 121: Branching fractions of inclusive B decays (in units of 10^{-6}). Values in red (blue) are new published (preliminary) result since PDG2006 [as of April 15, 2008].

RPP#	Mode	PDG2006 Avg.	BABAR	Belle	CLEO	New Avg.
–	K^+X	New	196^{+37+31}_{-34-30}†			196^{+48}_{-45}
–	K^0X	New	154^{+55+55}_{-48-41}†			154^{+77}_{-63}

† $p^* > 2.34$ GeV

result [394] with a factor of five more data than the previous measurement. The former used a data sample orthogonal to the lepton tag sample for the early inclusive measurement. Therefore, the new BaBar result is included in the average while the Belle measurement supersedes their previous one. In the Belle new measurement, the $B \to X_s\gamma$ branching fraction was obtained with various minimum photon energy requirement, 1.7 to 2.1 GeV. The study shows that there are clearly signal events with photon energy between 1.7 and 1.8 GeV. Although lowering E_γ to 1.7 GeV causes larger systematic error from the background, it will encourage a deeper understanding of the theory uncertainties, especially on those related to the extrapolation. Therefore, we choose the Belle measurement with the minimum photon energy at 1.7 GeV to compute the average.

The six experimental measurements selected for the average are shown in Table 124. They have provided in their papers either the $B \to X_s\gamma$ branching fraction at a certain photon energy cut or the extrapolation factor used. Therefore we are able to convert them to the values at $E_{\rm min} = 1.6$ GeV using the information in Table 123. The errors are, in order, statistical, systematic and shape-function systematic, except for the *BABAR* inclusive where there is a second systematic error (third quoted error) due to theoretical uncertainties. Moreover, in the

Table 122: Branching fractions of leptonic B decays (in units of 10^{-6}). Upper limits are at 90% CL. Values in red (blue) are new published (preliminary) result since PDG2006 [as of April 15, 2008].

RPP#	Mode	PDG2006 Avg.	BABAR	Belle	CLEO	CDF	DØ	New Avg.
15	$e^+\nu$	< 15	< 5.2	< 1.0	< 15			< 1.0
16	$\mu^+\nu$	< 6.6	< 5.6	< 1.7	< 21			< 1.7
17	$\tau^+\nu$	< 260	$120 \pm 40 \pm 36$	179^{+56+46}_{-49-51}	< 840			141^{+43}_{-42}
18	$e^+\nu_e\gamma$	< 200			< 200			< 200
19	$\mu^+\nu_\mu\gamma$	< 52			< 52			< 52
290	$\gamma\gamma$	< 0.62	< 1.7	< 0.62				< 0.62
291	e^+e^-	< 0.061	< 0.113	< 0.19	< 0.83			< 0.113
–	$e^+e^-\gamma$	New	< 0.12					< 0.12
292	$\mu^+\mu^-$	< 0.039	< 0.052	< 0.16	< 0.61	< 0.023		< 0.023
–	$\mu^+\mu^-\gamma$	New	< 0.16					< 0.16
–	$\tau^+\tau^-$	New	< 4100					< 4100
300	$e^\pm\mu^\mp$	< 0.17	< 0.092	< 0.17	< 1.5			< 0.092
303	$e^\pm\tau^\mp$	< 110	< 28		< 110			< 28
304	$\mu^\pm\tau^\mp$	< 38	< 22		< 38			< 22
305	$\nu\overline{\nu}$	< 220	< 220					< 220
306	$\nu\overline{\nu}\gamma$	< 47	< 47					< 47

Table 123: Extrapolation factor in various scheme with various minimum photon energy requirement (in GeV).

Scheme	$E_\gamma < 1.7$	$E_\gamma < 1.8$	$E_\gamma < 1.9$	$E_\gamma < 2.0$	$E_\gamma < 2.242$
Kinetic	0.986 ± 0.001	0.968 ± 0.002	0.939 ± 0.005	0.903 ± 0.009	0.656 ± 0.031
Neubert SF	0.982 ± 0.002	0.962 ± 0.004	0.930 ± 0.008	0.888 ± 0.014	0.665 ± 0.035
Kagan-Neubert	0.988 ± 0.002	0.970 ± 0.005	0.940 ± 0.009	0.892 ± 0.014	0.643 ± 0.033
Average	0.985 ± 0.004	0.967 ± 0.006	0.936 ± 0.010	0.894 ± 0.016	0.655 ± 0.037

four inclusive analyses a possible $B \to X_d\gamma$ contamination has been considered according to the expectation of $(4.0 \pm 0.4)\%$. The central value is the same as used in our 2006 average but the uncertainty shrinks by a factor of four, due to better understanding of $|V_{td}/V_{ts}|$ from the B_S-$\overline{B}_S$ mixing and $B \to \rho/\omega\ \gamma$ measurements. Compared to the other systematic uncertainties, the error that arises from the $B \to X_d\gamma$ fraction is too small to be considered. We perform the average assuming that the systematic errors of the shape function are correlated, and the other systematic errors and the statistical errors are Gaussian and uncorrelated. The obtained average is $\mathcal{B}(B \to X_s\gamma) = (352 \pm 23 \pm 9) \times 10^{-6}$ with a χ^2/DOF= 1.00/5, where the errors are combined statistical and systematic and systematic due to the shape function. The second error is estimated to be the difference of the average after simultaneously varying the central value of each experimental result by $\pm 1\sigma$. Although a small fraction of events was used in both the semi-inclusive and inclusive analyses in the same experiment, we neglect their statistical correlations. Some other correlated systematic errors, such as photon detection and

the background suppression, are not considered in our new average.

Table 124: Reported branching fraction, minimum photon energy, branching fraction at minimum photon energy and converted branching fraction for the decay $b \to s\gamma$. All the branching fractions are in units of 10^{-6}. See text for an explanation of the errors. The CLEO measurment on the branching fraction at E_{rmmin} includes $B \to X_d\gamma$ events. The last error of the Belle reported branching fraction in their inclusive analysis is the systematic uncertainty due to the boost of the γ energy from the center of mass frame to the B meson rest frame.

Mode	Reported $\mathcal{B}$	$E_{\rm min}$	$\mathcal{B}$ at $E_{\rm min}$	Modified $\mathcal{B}$ ($E_{\rm min} = 1.6$)
CLEO Inc. [395]	$321 \pm 43 \pm 27^{+18}_{-10}$	2.0	$306 \pm 41 \pm 26$	$329 \pm 44 \pm 28 \pm 6$
Belle Semi. [396]	$336 \pm 53 \pm 42^{+50}_{-54}$	2.24	–	$369 \pm 58 \pm 46^{+56}_{-60}$
BABAR Semi. [397]	$327 \pm 18^{+55+4}_{-40-9}$	1.9	$327 \pm 18^{+55+4}_{-40-9}$	$349 \pm 20^{+59+4}_{-46-3}$
BABAR Inc. [398]	–	1.9	$367 \pm 29 \pm 34 \pm 29$	$392 \pm 31 \pm 36 \pm 30 \pm 4$
BABAR Full [393]	$366 \pm 85 \pm 60$	1.9	$366 \pm 85 \pm 60$	$391 \pm 91 \pm 64 \pm 4$
Belle Inc. [394]	$332 \pm 16 \pm 37 \pm 1$	1.7	$332 \pm 16 \pm 37 \pm 1$	$337 \pm 16 \pm 38 \pm 1$

7.4 Baryonic decays

Table 125: Branching fractions of baryonic B^+ decays (in units of 10^{-6}). Upper limits are at 90% CL. values in red (blue) are new published (preliminary) result since PDG2006 [as of April 15, 2008].

RPP#	Mode	PDG2006 Avg.	BABAR	Belle	CLEO	New Avg.
286	$p\overline{p}\pi^+$	$3.1^{+0.8}_{-0.7}$	$1.69 \pm 0.29 \pm 0.26$ †	$1.68^{+0.26}_{-0.22} \pm 0.12$ ‡	< 160	$1.68^{+0.23}_{-0.21}$
289	$p\overline{p}K^+$	5.6 ± 1.0	$6.7 \pm 0.5 \pm 0.4$ †	$5.98^{+0.29}_{-0.27} \pm 0.39$ ‡		$6.24^{+0.39}_{-0.38}$
290	$\Theta^{++}\overline{p}$ *	< 0.091	< 0.09	< 0.091		< 0.09
291	$f_J(2221)K^+$ *	< 0.41		< 0.41		< 0.41
292	$p\overline{\Lambda}(1520)$	< 1.5	< 1.5			< 1.5
294	$p\overline{p}K^{*+}$	$10.3^{+3.6+1.3}_{-2.8-1.7}$	$5.3 \pm 1.5 \pm 1.3$ †	$3.38^{+0.73}_{-0.60} \pm 0.39$ ‡		$3.64^{+0.79}_{-0.70}$
–	$f_J(2221)K^{*+}$ *	New	< 0.77			< 0.77
295	$p\overline{\Lambda}$	< 0.49		< 0.32	< 1.5	< 0.32
–	$p\overline{\Lambda}\pi^0$	New		$3.00^{+0.61}_{-0.53} \pm 0.33$		$3.00^{+0.69}_{-0.62}$
–	$p\overline{\Sigma}(1385)^0$	New		< 0.47		< 0.47
–	$\Delta^+\overline{\Lambda}$	New		< 0.82		< 0.82
299	$\Lambda\overline{\Lambda}\pi^+$	< 2.8		< 2.8 ‡		< 2.8 ‡
300	$\Lambda\overline{\Lambda}K^+$	$2.9^{+0.9}_{-0.7} \pm 0.4$		$2.9^{+0.9}_{-0.7} \pm 0.4$ ‡		$2.9^{+1.0}_{-0.8}$
301	$\overline{\Delta}^0 p$	< 380		< 1.42	< 380	< 1.42
302	$\Delta^{++}\overline{p}$	< 150		< 0.14	< 150	< 0.14

§Di-baryon mass is less than 2.85 GeV/c^2; † Charmonium decays to $p\overline{p}$ have been statistically subtracted.
‡ The charmonium mass region has been vetoed.
* Product BF - daughter BF taken to be 100%: $\Theta(1540)^{++} \to K^+p$ (pentaquark candidate).

Table 126: Branching fractions of baryonic B^0 decays (in units of 10^{-6}). Upper limits are at 90% CL. values in red (blue) are new published (preliminary) result since PDG2006 [as of April 15, 2008].

RPP#	Mode	PDG2006 Avg.	BABAR	Belle	CLEO	New Avg.
266	$p\overline{p}$	< 0.27	< 0.27	< 0.11	< 1.4	< 0.11
268	$p\overline{p}K^0$	$2.1^{+0.6}_{-0.4}$	$3.0 \pm 0.5 \pm 0.3$ †	$2.51^{+0.35}_{-0.29} \pm 0.21$ ‡		$2.66^{+0.34}_{-0.32}$
269	$\Theta^+\overline{p}$ *	< 0.23	< 0.05	< 0.23		< 0.05
–	$f_J(2221)K^0$ *	New	< 0.45			< 0.45
270	$p\overline{p}K^{*0}$	< 7.6	$1.47 \pm 0.45 \pm 0.40$ †	$1.18^{+0.29}_{-0.25} \pm 0.11$ ‡		$1.24^{+0.28}_{-0.25}$
–	$f_J(2221)K^{*0}$ *	New	< 0.15			< 0.15
271	$p\overline{\Lambda}\pi^-$	2.6 ± 0.5	$3.30 \pm 0.53 \pm 0.31$	$3.23^{+0.33}_{-0.29} \pm 0.29$	< 13	$3.25^{+0.36}_{-0.34}$
–	$p\overline{\Sigma}(1385)^-$	New		< 0.26		< 0.26
–	$\Delta^0\overline{\Lambda}$	New		< 0.93		< 0.93
272	$p\overline{\Lambda}K^-$	< 0.82		< 0.82		< 0.82
273	$p\overline{\Sigma}^0\pi^-$	< 3.8		< 3.8		< 3.8
274	$\Lambda\overline{\Lambda}$	< 0.69		< 0.32	< 1.2	< 0.32

§Di-baryon mass is less than 2.85 GeV/c^2; † Charmonium decays to $p\overline{p}$ have been statistically subtracted. ‡ The charmonium mass region has been vetoed. * Product BF - daughter BF taken to be 100%; $\Theta(1540)^+ \to pK^0$ (pentaquark candidate).

7.5 B_s decays

Table 127: B_s branching fractions (in units of 10^{-6}). Upper limits are at 90% CL. Values in red (blue) are new published (preliminary) result since PDG2006 [as of March 15, 2007].

RPP#	Mode	PDG2006 Avg.	Belle	CDF	D0	New Avg.
9	$\pi^+\pi^-$	< 170		$0.53 \pm 0.31 \pm 0.40$		0.53 ± 0.51
15	$\phi\phi$	14 ± 8		$14^{+6}_{-5} \pm 6$ †		14^{+8}_{-7}
16	π^+K^-	< 210		$5.0 \pm 0.75 \pm 1.0$		5.00 ± 1.25
17	K^+K^-	< 59	< 310	$24.4 \pm 1.4 \pm 4.6$		24.4 ± 4.8
22	$\gamma\gamma$	< 148	< 8.7			< 8.7
23	$\phi\gamma$	< 120	57^{+18+12}_{-15-11}			57^{+21}_{-18}
24	$\mu^+\mu^-$	< 0.15		< 0.047	< 0.075	< 0.047
26	$e^\pm\mu^\mp$	< 6.1		< 6.1		< 6.1
27	$\mu^+\mu^-\phi$	< 47		< 2.3	< 3.2 †	< 2.3

†Relative BF converted to absolute BF

Table 128: B_s rare relative branching fractions. Values in red (blue) are new published (preliminary) result since PDG2006 [as of April 15, 2008].

RPP#	Mode	PDG2006 Avg.	CDF	D0	New Avg.
9	$f_s\mathcal{B}(B_s^0 \to \pi^+\pi^-)/f_d\mathcal{B}(B^0 \to K^+\pi-)$		$0.007 \pm 0.004 \pm 0.005$		0.007 ± 0.006
15	$\mathcal{B}(B_s^0 \to \phi\phi)/\mathcal{B}(B_s^0 \to J/\psi\phi)$		$(10^{+5}_{-4} \pm 1) \times 10^{-3}$		10^{+7}_{-6}
16	$f_s\mathcal{B}(B_s^0 \to K^+\pi^-)/f_d\mathcal{B}(B_d^0 \to K^+\pi^-)$		$0.066 \pm 0.010 \pm 0.010$		0.066 ± 0.014
17	$f_s\mathcal{B}(B_s^0 \to K^+K^-)/f_d\mathcal{B}(B_d^0 \to K^+\pi^-)$		$0.324 \pm 0.019 \pm 0.041$		0.324 ± 0.045
27	$\mathcal{B}(B_s^0 \to \mu^+\mu^-\phi)/\mathcal{B}(B_s^0 \to J/\psi\phi)$		$1.24 \pm 0.60 \pm 0.15$	$< 3.5 \times 10^{-3}$	1.24 ± 0.62

7.6 Charge asymmetries

Table 129: CP asymmetries for charmless hadronic charged B decays (part I). Values in red (blue) are new published (preliminary) result since PDG2006 [as of April 15, 2008].

RPP#	Mode	PDG2006 Avg.	BABAR	Belle	CLEO	CDF	New Avg.
182	$K^0\pi^+$	-0.02 ± 0.07	$-0.029 \pm 0.039 \pm 0.010$	$0.03 \pm 0.03 \pm 0.01$	$0.18 \pm 0.24 \pm 0.02$		0.009 ± 0.025
183	$K^+\pi^0$	0.04 ± 0.04	$0.030 \pm 0.039 \pm 0.010$	$0.07 \pm 0.03 \pm 0.01$	$-0.29 \pm 0.23 \pm 0.02$		0.050 ± 0.025
184	$\eta' K^+$	0.020 ± 0.025	$0.010 \pm 0.022 \pm 0.006$	$0.028 \pm 0.028 \pm 0.021$	$0.03 \pm 0.12 \pm 0.02$		0.016 ± 0.019
185	$\eta' K^{*+}$	New	$0.30^{+0.33}_{-0.37} \pm 0.02$				$0.30^{+0.33}_{-0.37}$
186	ηK^+	-0.25 ± 0.14	$-0.22 \pm 0.11 \pm 0.01$	$-0.39 \pm 0.16 \pm 0.03$			-0.27 ± 0.09
187	ηK^{*+}	0.13 ± 0.14	$0.01 \pm 0.08 \pm 0.02$	$0.03 \pm 0.10 \pm 0.01$			0.02 ± 0.06
–	$\eta K_0^{*+}(1430)$	New	$0.05 \pm 0.13 \pm 0.02$				0.05 ± 0.13
–	$\eta K_2^{*+}(1430)$	New	$-0.45 \pm 0.30 \pm 0.02$				-0.45 ± 0.30
188	ωK^+	-0.02 ± 0.13	$-0.01 \pm 0.07 \pm 0.01$	$0.05^{+0.08}_{-0.07} \pm 0.01$			0.02 ± 0.05
192	$K^{*0}\pi^+$	0.07 ± 0.11	$0.032 \pm 0.052^{+0.16}_{-0.13}$	$-0.149 \pm 0.064 \pm 0.022$			-0.114 ± 0.061
193	$K^{*+}\pi^0$	New	$0.04 \pm 0.29 \pm 0.05$				0.04 ± 0.29
194	$K^+\pi^+\pi^-$	-0.013 ± 0.039	$0.028 \pm 0.020 \pm 0.023$	$0.049 \pm 0.026 \pm 0.020$			0.038 ± 0.022
196	$f_0(980)K^+$	$0.09^{+0.14}_{-0.12}$	$-0.106 \pm 0.050^{+0.036}_{-0.015}$	$-0.077 \pm 0.065^{+0.046}_{-0.026}$			$-0.095^{+0.049}_{-0.042}$
197	$f_2(1270)K^+$	New	$-0.85 \pm 0.22^{+0.26}_{-0.13}$	$-0.59 \pm 0.22 \pm 0.04$			$-0.68^{+0.20}_{-0.18}$
200	$f_0(1500)K^+$ †	New	$0.28 \pm 0.26^{+0.15}_{-0.14}$				$0.28^{+0.30}_{-0.29}$
202	$K^+\rho^0$	$0.32^{+0.16}_{-0.15}$	$0.44 \pm 0.10^{+0.06}_{-0.14}$	$0.30 \pm 0.11^{+0.11}_{-0.05}$			0.37 ± 0.11
203	$K_0^{*0}(1430)\pi^+$	$-0.064^{+0.039}_{-0.041}$	$0.032 \pm 0.035^{+0.034}_{-0.028}$	$0.076 \pm 0.038^{+0.028}_{-0.022}$			$0.055^{+0.034}_{-0.032}$
204	$K_2^{*0}(1430)\pi^+$	New	$0.05 \pm 0.23^{+0.18}_{-0.08}$				$0.05^{+0.29}_{-0.24}$
211	$K^0\rho^+$	New	$-0.12 \pm 0.17 \pm 0.02$				-0.12 ± 0.17
213	$K^{*+}\rho^0$	$0.20^{+0.32}_{-0.29}$	$0.20^{+0.32}_{-0.29} \pm 0.04$				$0.20^{+0.32}_{-0.29}$
214	$K^{*0}\rho^+$	New	$-0.01 \pm 0.16 \pm 0.02$				-0.01 ± 0.16
–	$f_0 K^{*+}$	New	$-0.34 \pm 0.21 \pm 0.03$				-0.34 ± 0.21
218	$K^+\overline{K^0}$	0.15 ± 0.33	$0.10 \pm 0.26 \pm 0.03$	$0.13^{+0.23}_{-0.24} \pm 0.02$			$0.12^{+0.17}_{-0.18}$
220	$K^+K_SK_S$	-0.04 ± 0.11	$-0.04 \pm 0.11 \pm 0.02$				-0.04 ± 0.11
222	$K^+K^-\pi^+$	New	$0.00 \pm 0.10 \pm 0.03$				0.00 ± 0.10
228	$K^+K^-K^+$	-0.02 ± 0.08	$-0.02 \pm 0.03 \pm 0.02$				-0.02 ± 0.04
229	ϕK^+	0.01 ± 0.07	$0.046 \pm 0.046 \pm 0.017$	$0.01 \pm 0.12 \pm 0.05$		$-0.07 \pm 0.17^{+0.03}_{-0.02}$	0.034 ± 0.044
–	$a_1^+ K^0$	New	$0.12 \pm 0.11 \pm 0.02$				0.12 ± 0.11
–	$b_1^0 K^+$	New	$-0.46 \pm 0.20 \pm 0.02$				-0.46 ± 0.20
–	$K^{*+}\pi^+\pi^-$	New	$0.07 \pm 0.07 \pm 0.04$				0.07 ± 0.08
235	$K^{*+}K^+K^-$	New	$0.11 \pm 0.08 \pm 0.03$				0.11 ± 0.09
236	ϕK^{*+}	0.05 ± 0.11	$0.00 \pm 0.09 \pm 0.04$	$-0.02 \pm 0.14 \pm 0.03$			-0.01 ± 0.08
239	$\phi\phi K^+$	New		$0.01^{+0.19}_{-0.16} \pm 0.02$			$0.01^{+0.19}_{-0.16}$
242	$K^+\eta\gamma$	-0.16 ± 0.10	$-0.09 \pm 0.12 \pm 0.01$	$-0.16 \pm 0.09 \pm 0.06$			-0.13 ± 0.08
243	$K^+\phi\gamma$	New	$-0.26 \pm 0.14 \pm 0.05$				-0.26 ± 0.15
254	$\pi^+\pi^0$	-0.02 ± 0.07	$0.03 \pm 0.08 \pm 0.01$	$0.07 \pm 0.06 \pm 0.01$			0.06 ± 0.05
255	$\pi^+\pi^-\pi^+$	-0.01 ± 0.09	$-0.01 \pm 0.08 \pm 0.03$				-0.01 ± 0.09
256	$\rho^0\pi^+$	-0.07 ± 0.13	$-0.07 \pm 0.12^{+0.03}_{-0.06}$				$-0.07^{+0.12}_{-0.13}$
257	$f_0(980)\pi^+$	New	$-0.50 \pm 0.54 \pm 0.06$				-0.50 ± 0.54
258	$f_2(1270)\pi^+$	New	$-0.01 \pm 0.25^{+0.28}_{-0.32}$				$-0.01^{+0.38}_{-0.41}$
264	$\rho^+\pi^0$	0.15 ± 0.12	$-0.01 \pm 0.13 \pm 0.02$	$0.06 \pm 0.17^{+0.04}_{-0.05}$			0.02 ± 0.11
266	$\rho^+\rho^0$	-0.09 ± 0.16	$-0.12 \pm 0.13 \pm 0.10$	$0.00 \pm 0.22 \pm 0.03$			-0.08 ± 0.13
–	$b_1^0\pi^+$	New	$0.05 \pm 0.16 \pm 0.02$				0.05 ± 0.16
269	$\omega\pi^+$	0.10 ± 0.22	$-0.02 \pm 0.08 \pm 0.01$	$-0.02 \pm 0.09 \pm 0.01$	$-0.34 \pm 0.25 \pm 0.02$		-0.04 ± 0.06
270	$\omega\rho^+$	0.05 ± 0.26	$0.04 \pm 0.18 \pm 0.02$				0.04 ± 0.18
271	$\eta\pi^+$	-0.05 ± 0.10	$-0.08 \pm 0.10 \pm 0.01$	$-0.23 \pm 0.09 \pm 0.02$			-0.16 ± 0.07
272	$\eta'\pi^+$	0.14 ± 0.16	$0.21 \pm 0.17 \pm 0.01$	$0.20^{+0.37}_{-0.36} \pm 0.04$			0.21 ± 0.15
273	$\eta'\rho^+$	New	$-0.04 \pm 0.28 \pm 0.02$				-0.04 ± 0.28
274	$\eta\rho^+$	New	$0.02 \pm 0.18 \pm 0.02$	$-0.04^{+0.34}_{-0.32} \pm 0.01$			0.01 ± 0.16

Table 130: CP asymmetries for charmless hadronic charged B decays (part II). Values in red (blue) are new published (preliminary) result since PDG2006 [as of April 15, 2008].

RPP#	Mode	PDG2006 Avg.	BABAR	Belle	CLEO	CDF	New Avg.
286	$p\bar{p}\pi^+$	-0.16 ± 0.22	$0.04 \pm 0.07 \pm 0.04$	$-0.17 \pm 0.10 \pm 0.02$			-0.04 ± 0.06
289	$p\bar{p}K^+$	-0.05 ± 0.11	$-0.16 \pm 0.08 \pm 0.04$	$-0.02 \pm 0.05 \pm 0.02$			-0.06 ± 0.05
294	$p\bar{p}K^{*+}$	New	$0.32 \pm 0.13 \pm 0.05$	$-0.01 \pm 0.19 \pm 0.02$			0.21 ± 0.11
296	$p\bar{\Lambda}\gamma$	New		$0.17 \pm 0.16 \pm 0.05$			0.17 ± 0.17
–	$p\bar{\Lambda}\pi^0$	New		$0.01 \pm 0.17 \pm 0.04$			0.01 ± 0.17
320	$K^+\ell\ell$	New	$-0.07 \pm 0.22 \pm 0.02$				-0.07 ± 0.22

Table 131: CP asymmetries for charmless hadronic neutral B decays. Values in red (blue) are new published (preliminary) result since PDG2006 [as of April 15, 2008].

RPP#	Mode	PDG2006 Avg.	BABAR	Belle	CLEO	CDF	New Avg.
168	$K^+\pi^-$	-0.113 ± 0.020	$-0.107 \pm 0.018^{+0.007}_{-0.004}$	$-0.094 \pm 0.018 \pm 0.008$	$-0.04 \pm 0.16 \pm 0.02$	$-0.086 \pm 0.023 \pm 0.009$	-0.097 ± 0.012
171	$\eta' K^{*0}$	New	$-0.08 \pm 0.25 \pm 0.02$				-0.08 ± 0.25
172	ηK^{*0}	0.02 ± 0.11	$0.21 \pm 0.06 \pm 0.02$	$0.17 \pm 0.08 \pm 0.01$			0.19 ± 0.05
–	$\eta K_0^{*0}(1430)$	New	$0.06 \pm 0.13 \pm 0.02$				0.06 ± 0.13
–	$\eta K_2^{*0}(1430)$	New	$-0.07 \pm 0.19 \pm 0.02$				-0.07 ± 0.19
180	$K^0\overline{K^0}$	New		$-0.58^{+0.73}_{-0.66} \pm 0.04$			$-0.58^{+0.73}_{-0.66}$
182	$K^+\pi^-\pi^0$	0.07 ± 0.11	$0.030^{+0.045}_{-0.051} \pm 0.055$	$0.07 \pm 0.11 \pm 0.01$			$0.042^{+0.059}_{-0.061}$
183	$K^+\rho^-$	0.26 ± 0.15	$0.11^{+0.14}_{-0.15} \pm 0.07$	$0.22^{+0.22+0.06}_{-0.23-0.02}$			0.15 ± 0.13
–	$K^+\pi^-\pi^0(NR)$	New	$0.23^{+0.19+0.11}_{-0.27-0.10}$				$0.23^{+0.22}_{-0.29}$
189	$K^{*+}\pi^-$	-0.05 $\pm$ 0.14	-0.14 ± 0.12		$0.26^{+0.33+0.10}_{-0.34-0.08}$		-0.10 ± 0.11
191	$K^{*0}\pi^0$	New	$-0.09 \pm 0.21^{+0.24}_{-0.09}$				$-0.09^{+0.32}_{-0.23}$
–	$K_0^*(1430)^+\pi^-$	New	$0.17^{+0.11}_{-0.16} \pm 0.22$				$0.17^{+0.25}_{-0.27}$
–	$K_0^*(1430)^0\pi^0$	New	$-0.22 \pm 0.12^{+0.30}_{-0.29}$				$-0.22^{+0.32}_{-0.31}$
198	$K^{*0}\pi^+\pi^-$	New	$0.07 \pm 0.04 \pm 0.03$				0.07 ± 0.05
199	$K^{*0}\rho^0$	New	$0.09 \pm 0.19 \pm 0.02$				0.09 ± 0.19
200	$f_0(980)K^{*0}$	New	$-0.17 \pm 0.28 \pm 0.02$				-0.17 ± 0.28
202	$a_1^+ K^-$	New	$-0.16 \pm 0.12 \pm 0.01$				-0.16 ± 0.12
–	$b_1^- K^+$	New	$0.07 \pm 0.12 \pm 0.02$				0.07 ± 0.12
204	ϕK^{*0}	0.01 ± 0.07	$-0.03 \pm 0.07 \pm 0.03$	$0.02 \pm 0.09 \pm 0.02$			-0.01 ± 0.06
–	$\phi K_0^{*0}(1430)$	New	$0.17 \pm 0.15 \pm 0.03$				0.17 ± 0.15
–	$\phi K_2^{*0}(1430)$	New	$-0.12 \pm 0.14 \pm 0.04$				-0.12 ± 0.15
203	$K^{*0}K^+K^-$	New	$0.01 \pm 0.05 \pm 0.02$				0.01 ± 0.05
–	$K^{*0}\pi^+K^-$	New	$0.22 \pm 0.33 \pm 0.20$				0.22 ± 0.39
230	$\pi^0\pi^0$	0.3 ± 0.4	$0.49 \pm 0.35 \pm 0.05$	$0.44^{+0.73+0.04}_{-0.62-0.06}$			$0.48^{+0.32}_{-0.31}$
–	$b_1^\mp \pi^\pm$	New	$-0.05 \pm 0.10 \pm 0.02$				-0.05 ± 0.10
270	$p\bar{p}K^{*0}$	New	$0.11 \pm 0.13 \pm 0.06$	$-0.08 \pm 0.20 \pm 0.02$			0.05 ± 0.12
271	$p\bar{\Lambda}\pi^-$	New		$-0.02 \pm 0.10 \pm 0.03$			-0.02 ± 0.10

† Measurements of time-dependent CP asymmetries are listed in the section of the Unitarity Triangle.

Table 132: Charmless hadronic CP asymmetries for $B^{\pm}/B^0$ admixtures. Values in red (blue) are new published (preliminary) result since PDG2006 [as of April 15, 2008].

RPP#	Mode	PDG2006 Avg.	BABAR	Belle	CLEO	CDF	New Avg.
58	$K^*\gamma$	-0.01 ± 0.07	$-0.013 \pm 0.036 \pm 0.010$	$-0.015 \pm 0.044 \pm 0.012$	$0.08 \pm 0.13 \pm 0.03$		-0.010 ± 0.028
70	$s\gamma$	0.00 ± 0.04	$0.025 \pm 0.050 \pm 0.015$	$0.002 \pm 0.050 \pm 0.030$	$-0.079 \pm 0.108 \pm 0.022$		0.004 ± 0.037
–	$(s+d)\gamma$	New	$-0.11 \pm 0.12 \pm 0.02$				-0.11 ± 0.12
107	$s\ell\ell$	-0.22 ± 0.26	$-0.22 \pm 0.26 \pm 0.02$				-0.22 ± 0.26
113	$K^*\ell\ell$	New	$0.03 \pm 0.23 \pm 0.03$				0.03 ± 0.23

Table 133: CP asymmetries for charmless hadronic neutral B^0_S decays. Values in red (blue) are new published (preliminary) result since PDG2006 [as of April, 2008].

RPP#	Mode	PDG2006 Avg.	BABAR	Belle	CLEO	CDF	New Avg.
16	$K^+\pi^-$	New				$0.39 \pm 0.15 \pm 0.08$	0.39 ± 0.17

7.7 Polarization measurements

Table 134: Longitudinal polarization fraction f_L for B^+ decays. Values in red (blue) are new published (preliminary) result since PDG2006 [as of April 15, 2008].

RPP#	Mode	PDG2006 Avg.	BABAR	Belle	New Avg.
213	$K^{*+}\rho^0$	$0.96^{+0.04}_{-0.15} \pm 0.04$	$0.96^{+0.04}_{-0.15} \pm 0.05$		$0.96^{+0.06}_{-0.16}$
214	$K^{*0}\rho^+$	$0.43 \pm 0.11^{+0.05}_{-0.02}$	$0.52 \pm 0.10 \pm 0.04$	$0.43 \pm 0.11^{+0.05}_{-0.02}$	0.48 ± 0.08
236	ϕK^{*+}	0.50 ± 0.07	$0.49 \pm 0.05 \pm 0.03$	$0.52 \pm 0.08 \pm 0.03$	0.50 ± 0.05
266	$\rho^+\rho^0$	0.96 ± 0.06	$0.905 \pm 0.042^{+0.023}_{-0.027}$	$0.95 \pm 0.11 \pm 0.02$	$0.912^{+0.044}_{-0.045}$
270	$\omega\rho^+$	$0.88^{+0.12}_{-0.15} \pm 0.03$	$0.82 \pm 0.11 \pm 0.02$		0.82 ± 0.11

Table 135: Full angular analysis of $B^+ \to \phi K^{*+}$. Values in red (blue) are new published (preliminary) result since PDG2006 [as of April 15, 2008].

Parameter	PDG2006 Avg.	BABAR	Belle	New Avg.
$f_\perp = \Lambda_{\perp\perp}$	$0.19 \pm 0.08 \pm 0.02$	$0.21 \pm 0.05 \pm 0.02$	$0.19 \pm 0.08 \pm 0.02$	0.20 ± 0.05
$\phi_\parallel$	$2.10 \pm 0.28 \pm 0.04$	$2.47 \pm 0.20 \pm 0.07$	$2.10 \pm 0.28 \pm 0.04$	2.34 ± 0.17
$\phi_\perp$	$2.31 \pm 0.30 \pm 0.07$	$2.69 \pm 0.20 \pm 0.03$	$2.31 \pm 0.30 \pm 0.07$	2.58 ± 0.17
A^0_{CP}	New	$0.17 \pm 0.11 \pm 0.02$		0.17 ± 0.11
$A^\perp_{CP}$	New	$0.22 \pm 0.24 \pm 0.08$		0.22 ± 0.25
$\Delta\phi_\parallel$	New	$0.07 \pm 0.20 \pm 0.05$		0.07 ± 0.21
$\Delta\phi_\perp$	New	$0.19 \pm 0.20 \pm 0.07$		0.19 ± 0.21

BR, f_L and A_{CP} are tabulated separately.

Table 136: Longitudinal polarization fraction f_L for B^0 decays. Values in red (blue) are new published (preliminary) result since PDG2006 [as of April 15, 2008].

RPP#	Mode	PDG2006 Avg.	BABAR	Belle	New Avg.
199	$K^{*0}\rho^0$	New	$0.57 \pm 0.09 \pm 0.08$		0.57 ± 0.12
204	ϕK^{*0}	0.48 ± 0.04	$0.506 \pm 0.040 \pm 0.015$	$0.45 \pm 0.05 \pm 0.02$	0.484 ± 0.034
–	$\phi K_2^{*0}(1430)$	New	$0.85 \pm 0.07 \pm 0.04$		0.85 ± 0.08
205	$K^{*0}\overline{K^{*0}}$	New	$0.80^{+0.10}_{-0.12} \pm 0.06$		$0.80^{+0.12}_{-0.13}$
253	$\rho^0\rho^0$	New	$0.70 \pm 0.14 \pm 0.05$		0.70 ± 0.15
257	$\rho^+\rho^-$	$0.967^{+0.022}_{-0.027}$	$0.992 \pm 0.024^{+0.026}_{-0.013}$	$0.941^{+0.034}_{-0.040} \pm 0.030$	$0.978^{+0.025}_{-0.022}$

Table 137: Full angular analysis of $B^0 \to \phi K^{*0}$. Values in red (blue) are new published (preliminary) result since PDG2006 [as of April 15, 2008].

Parameter	PDG2006 Avg.	BABAR	Belle	New Avg.
$f_\perp = A_{\perp\perp}$	0.26 ± 0.04	$0.227 \pm 0.038 \pm 0.013$	$0.31^{+0.06}_{-0.05} \pm 0.02$	0.256 ± 0.032
$\phi_\parallel$	$2.36^{+0.18}_{-0.16}$	$2.31 \pm 0.14 \pm 0.08$	$2.40^{+0.28}_{-0.24} \pm 0.07$	$2.33^{+0.14}_{-0.13}$
$\phi_\perp$	2.49 ± 0.18	$2.24 \pm 0.15 \pm 0.09$	$2.51 \pm 0.25 \pm 0.06$	2.33 ± 0.14
A^0_{CP}	0.01 ± 0.09	$-0.03 \pm 0.08 \pm 0.02$	$0.13 \pm 0.12 \pm 0.04$	0.02 ± 0.07
$A^\perp_{CP}$	-0.16 ± 0.15	$-0.03 \pm 0.16 \pm 0.05$	$-0.20 \pm 0.18 \pm 0.04$	-0.11 ± 0.12
$\Delta\phi_\parallel$	0.02 ± 0.28	$0.24 \pm 0.14 \pm 0.08$	$-0.32 \pm 0.27 \pm 0.07$	0.10 ± 0.14
$\Delta\phi_\perp$	0.03 ± 0.33	$0.19 \pm 0.15 \pm 0.08$	$-0.30 \pm 0.25 \pm 0.06$	0.04 ± 0.14

BR, f_L and A_{CP} are tabulated separately.

Table 138: Full angular analysis of $B^0 \to \phi K_2^*(1430)^0$. Values in red (blue) are new published (preliminary) result since PDG2006 [as of April 15, 2008].

Parameter	PDG2006 Avg.	BABAR	Belle	New Avg.
$f_\perp = A_{\perp\perp}$	New	$0.045^{+0.049}_{-0.040} \pm 0.013$		$0.045^{+0.051}_{-0.042}$
$\phi_\parallel$	New	$2.90 \pm 0.39 \pm 0.06$		2.90 ± 0.40
$\phi_\perp$	New	$5.7^{+0.6}_{-0.9} \pm 0.1$		$5.7^{+0.6}_{-0.9}$

BR, f_L and A_{CP} are tabulated separately.

8 D decays

8.1 D^0-$\overline{D}{}^0$ Mixing and CP Violation

8.1.1 Introduction

Mixing in the D^0-$\overline{D}{}^0$ system has been searched for for more than two decades without success — until last year. Three experiments – Belle [399], Babar [400], and CDF [401] – have now observed evidence for this phenomenon. The measurements can be combined with others to yield World Average (WA) values for the mixing parameters $x \equiv (m_1 - m_2)/\Gamma$ and $y \equiv (\Gamma_1 - \Gamma_2)/(2\Gamma)$, where m_1, m_2 and Γ_1, Γ_2 are the masses and decay widths for the mass eigenstates $D_1 \equiv p|D^0\rangle - q|\overline{D}{}^0\rangle$ and $D_2 \equiv p|D^0\rangle + q|\overline{D}{}^0\rangle$, and $\Gamma = (\Gamma_1 + \Gamma_2)/2$. Here we use the phase convention $CP|D^0\rangle = -|\overline{D}{}^0\rangle$ and $CP|\overline{D}{}^0\rangle = -|D^0\rangle$. In the absence of CP violation (CPV), $p = q = 1/\sqrt{2}$ and D_1 is CP-even, D_2 is CP-odd.

Such WA values are calculated by the Heavy Flavor Averaging Group (HFAG) [402] by performing a global fit to measured observables for parameters x, y, δ (the strong phase difference between amplitudes $\mathcal{A}(\overline{D}{}^0 \to K^+\pi^-)$ and $\mathcal{A}(D^0 \to K^+\pi^-)$), an additional strong phase $\delta_{K\pi\pi}$ entering $D^0 \to K^+\pi^-\pi^0$ decays, and $R_D \equiv \left|\mathcal{A}(D^0 \to K^+\pi^-)/\mathcal{A}(\overline{D}{}^0 \to K^+\pi^-)\right|^2$. For this fit, correlations among observables are accounted for by using covariance matrices provided by the experimental collaborations. Systematic errors among different experiments are assumed uncorrelated as, after some study, no significant correlations were identified. The observables used are from measurements of $D^0 \to K^+\ell^-\nu$, $D^0 \to K^+K^-/\pi^+\pi^-$, $D^0 \to K^+\pi^-$, $D^0 \to K^+\pi^-\pi^0$, and $D^0 \to K^0_S\,\pi^+\pi^-$ decays, and from double-tagged branching fractions measured at the $\psi(3770)$ resonance. We have checked this method with a second method that adds together three-dimensional log-likelihood functions for x, y, and δ obtained from various analyses; this combination accounts for non-Gaussian errors. When both methods are applied to the same set of observables, essentially identical results are obtained. The global fitting method is easily expanded to allow for CPV. In this case three additional parameters are included in the fit: $|q/p|$, $\phi \equiv \mathrm{Arg}(q/p)$, and $A_D \equiv (R_D^+ - R_D^-)/(R_D^+ + R_D^-)$, where the $+$ $(-)$ superscript corresponds to D^0 $(\overline{D}{}^0)$ decays.

Mixing in heavy flavor systems such as those of B^0 and B^0_s is governed by the short-distance box diagram. In the D^0 system, however, this diagram is doubly-Cabibbo-suppressed relative to amplitudes dominating the decay width, and it is also GIM-suppressed. Thus the short-distance mixing rate is tiny, and D^0-$\overline{D}{}^0$ mixing is expected to be dominated by long-distance processes. These are difficult to calculate reliably, and theoretical estimates for x and y range over two-three orders of magnitude [403–405].

With the exception of $\psi(3770) \to DD$ measurements, all methods identify the flavor of the D^0 or $\overline{D}{}^0$ when produced by reconstructing the decay $D^{*+} \to D^0\pi^+$ or $D^{*-} \to \overline{D}{}^0\pi^-$; the charge of the pion identifies the D flavor. For signal decays, $M_{D^*} - M_{D^0} - M_{\pi^+} \equiv Q \approx 6$ MeV, which is close to the threshold; thus analyses typically require that the reconstructed Q be small to suppress backgrounds. For time-dependent measurements, the D^0 decay time is calculated as $(d/p) \times M_{D^0}$, where d is the distance between the D^* and D^0 decay vertices and p is the D^0 momentum. The D^* vertex position is taken to be at the primary vertex [401] ($\overline{p}p$) or is calculated from the intersection of the D^0 momentum vector with the beamspot profile (e^+e^-).

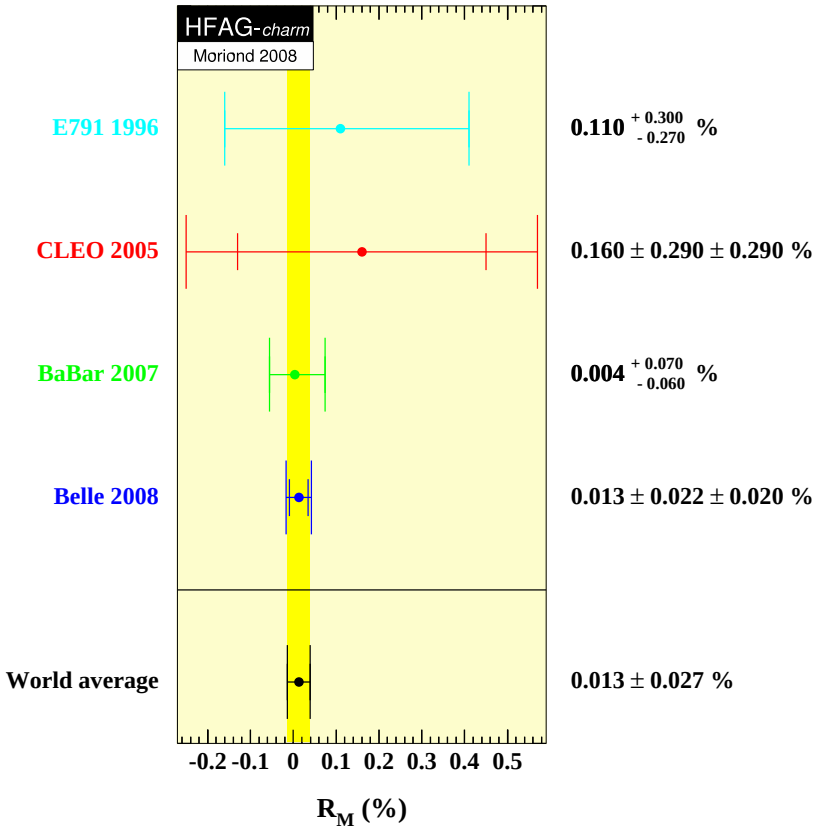

Figure 55: WA value of R_M from Ref. [402], as calculated from $D^0 \to K^+\ell^-\nu$ measurements [406].

8.1.2 Input Observables

The global fit determines central values and errors for eight underlying parameters using a χ^2 statistic constructed from 28 observables. The underlying parameters are x, y, δ, R_D, A_D, $|q/p|$, ϕ, and $\delta_{K\pi\pi}$. The parameters x and y govern mixing, and the parameters A_D, $|q/p|$, and ϕ govern CPV. The parameter $\delta_{K\pi\pi}$ is the strong phase difference between the amplitudes $\mathcal{A}(\overline{D}^0 \to K^+\pi^-\pi^0)$ and $\mathcal{A}(D^0 \to K^+\pi^-\pi^0)$ evaluated at the point $M_{K^+\pi^-} = M_{K^*(890)}$.

All input values are listed in Table 139. The observable $R_M = (x^2 + y^2)/2$ measured in $D^0 \to K^+\ell^-\nu$ decays [406] is taken to be the WA value [402] calculated by HFAG (see Fig. 55). The observables y_{CP} and A_Γ measured in $D^0 \to K^+K^-/\pi^+\pi^-$ decays [399, 407–409] are also taken to be WA values [402] (see Fig. 56). The observables from $D^0 \to K^0_S\,\pi^+\pi^-$ decays [410] for no-CPV are HFAG WA values [402], but for the CPV-allowed case only Belle measurements are available. The $D^0 \to K^+\pi^-$ observables used are from Belle [411], Babar [400], and CDF [401] (these measurements have much greater precision than earlier measurements). The $D^0 \to K^+\pi^-\pi^0$ results are from Babar [412], and the $\psi(3770) \to DD$ results are from CLEOc [413].

The relationships between the observables and the fitted parameters are listed in Table 140. For each set of correlated observables, we construct the difference vector $\vec{V}$, e.g., for $D^0 \to K^0_S\,\pi^+\pi^-$ decays $\vec{V} = (\Delta x, \Delta y, \Delta|q/p|, \Delta\phi)$, where Δ represents the difference between the measured value and the fitted parameter value. The contribution of a set of measured observables to the overall χ^2 is calculated as $\vec{V} \cdot (M^{-1}) \cdot \vec{V}^T$, where M^{-1} is the inverse of the

covariance matrix for the measurement. All covariance matrices used are listed in Table 139.

8.1.3 Fit results

The global fit uses MINUIT with the MIGRAD minimizer, and all errors are obtained from MINOS [414]. Three separate fits are performed: *(a)* assuming CP conservation (A_D and ϕ are fixed to zero, $|q/p|$ is fixed to one); *(b)* assuming no direct CPV (A_D is fixed to zero); and *(c)* allowing full CPV (all parameters floated). The results are listed in Table 141. For the CPV-allowed fit, individual contributions to the χ^2 are listed in Table 142. The total χ^2 is 23.5 for $28 - 8 = 20$ degrees of freedom; this corresponds to a confidence level of 0.26, which is satisfactory.

Confidence contours in the two dimensions (x, y) or in $(|q/p|, \phi)$ are obtained by letting, for any point in the two-dimensional plane, all other fitted parameters take their preferred values. The resulting 1σ-5σ contours are shown in Fig. 57 for the CP-conserving case, and in Fig. 58 for the CPV-allowed case. The contours are determined from the increase of the χ^2 above the minimum value. One observes that the (x, y) contours for the no-CPV fit are almost identical to those for the CPV-allowed fit. In both cases the χ^2 at the no-mixing point $(x, y) = (0, 0)$ is 91 units above the minimum value; for two degrees of freedom this has a confidence level corresponding to 9.2σ. Thus, no mixing is excluded at this high level. In the $(|q/p|, \phi)$ plot, the point $(1, 0)$ is within the 1σ contour; thus the data is consistent with CP conservation.

One-dimensional confidence curves for individual parameters are obtained by letting, for any value of the parameter, all other fitted parameters take their preferred values. The resulting functions $\Delta\chi^2 = \chi^2 - \chi^2_{\rm min}$ ($\chi^2_{\rm min}$ is the minimum value) are shown in Fig. 59. The points where $\Delta\chi^2 = 3.84$ determine 95% C.L. intervals for the parameters; these intervals are listed in Table 141.

8.1.4 Conclusions

From the fit results listed in Table 141 and shown in Figs. 58 and 59, we conclude the following:

- the experimental data consistently indicate that D^0 mesons undergo mixing. The no-mixing point $x = y = 0$ is excluded at 9.2σ. The parameter x differs from zero by 3.0σ, and y differs from zero by 4.0σ. This mixing is presumably dominated by long-distance processes, which are difficult to calculate. Thus it may be difficult to identify new physics from mixing alone (unless $|x| \gg |y|$ – see Ref. [403]).

- Since $y_{\rm CP}$ is positive, the CP-even state is shorter-lived, as in the K^0-$\overline{K}{}^0$ system. However, since x also appears to be positive, the CP-even state is heavier, unlike in the K^0-$\overline{K}{}^0$ system.

- It appears difficult to accomodate a strong phase difference δ larger than 45°.

- There is no evidence yet for CPV in the D^0-$\overline{D}{}^0$ system. Observing CPV at the current level of sensitivity would indicate new physics.

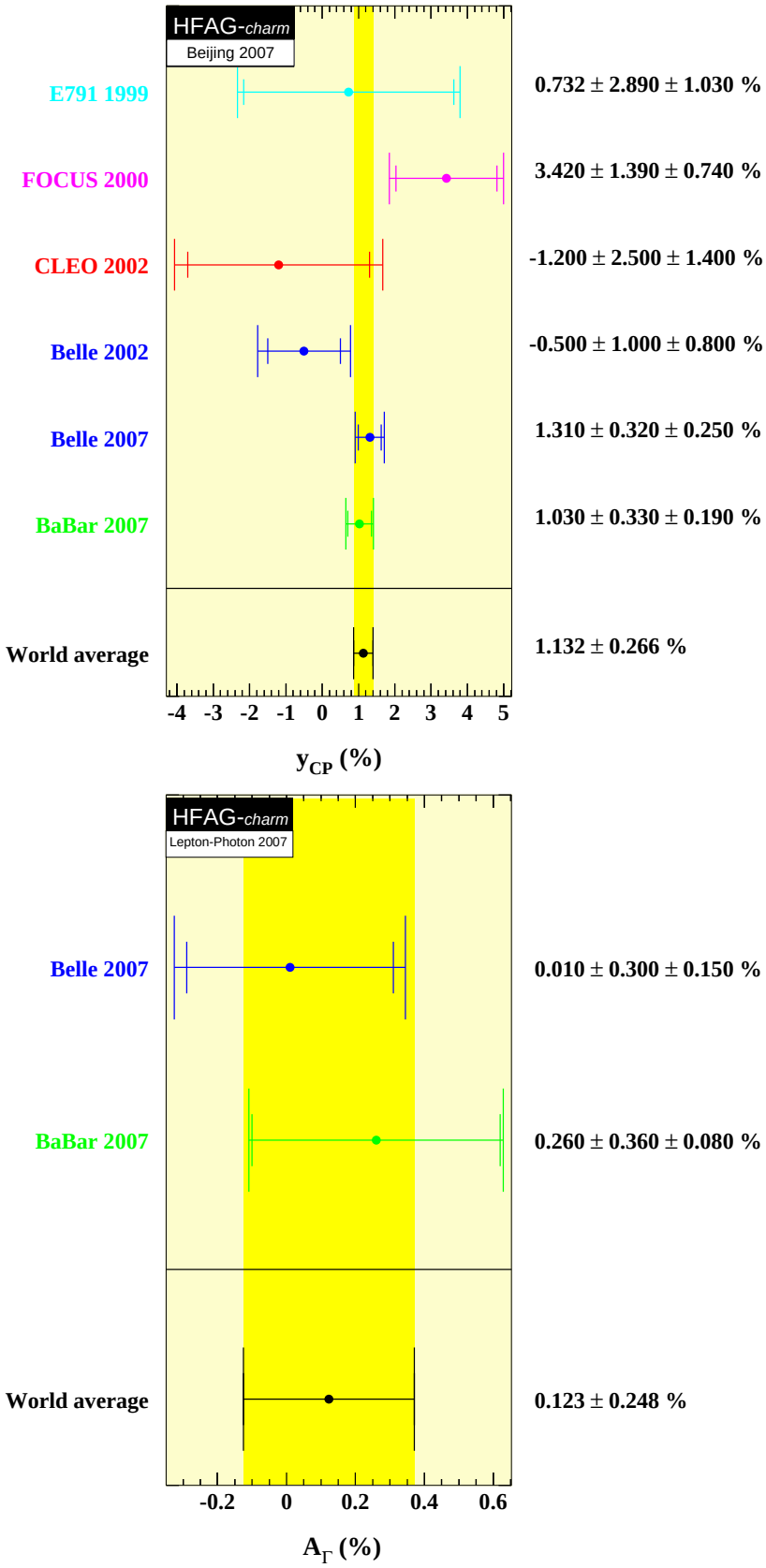

Figure 56: WA values of y_{CP} (top) and A_Γ (bottom) from Ref. [402], as calculated from $D^0 \to K^+K^-/\pi^+\pi^-$ measurements [399, 407–409].

Table 139: Observables used for the global fit, from Refs. [399–401, 406–413].

Mode	Observable	Values	Correlation coefficients
$D^0 \to K^+K^-$, $\pi^+\pi^-$ [402]	y_{CP}	$(1.132 \pm 0.266)\%$	
	A_Γ	$(0.123 \pm 0.248)\%$	
$D^0 \to K^0_S\,\pi^+\pi^-$ [402] (No CPV or no direct CPV)	x	$(0.811 \pm 0.334)\%$	
	y	$(0.309 \pm 0.281)\%$	
	$\lvert q/p\rvert$	$0.95 \pm 0.22^{+0.10}_{-0.09}$	
	ϕ	$(-0.035 \pm 0.19 \pm 0.09)$ rad	
$D^0 \to K^0_S\,\pi^+\pi^-$ [402] (CPV-allowed)	x	$(0.81 \pm 0.30^{+0.13}_{-0.17})\%$	$\begin{pmatrix} 1 & -0.007 & -0.255\alpha & 0.216 \\ -0.007 & 1 & -0.019\alpha & -0.280 \\ -0.255\alpha & -0.019\alpha & 1 & -0.128\alpha \\ 0.216 & -0.280 & -0.128\alpha & 1 \end{pmatrix}$
	y	$(0.37 \pm 0.25^{+0.10}_{-0.15})\%$	
	$\lvert q/p\rvert$	$0.86 \pm 0.30^{+0.10}_{-0.09}$	
	ϕ	$(-0.244 \pm 0.31 \pm 0.09)$ rad	($\alpha = (\lvert q/p\rvert + 1)^2/2$ is a transformation factor)
$D^0 \to K^+\ell^-\nu$ [402]	R_M	$(0.0173 \pm 0.0387)\%$	
$D^0 \to K^+\pi^-\pi^0$	x''	$(2.39 \pm 0.61 \pm 0.32)\%$	-0.34
	y''	$(-0.14 \pm 0.60 \pm 0.40)\%$	
$\psi(3770) \to \overline{D}D$ (CLEOc)	R_M	$(0.199 \pm 0.173 \pm 0.0)\%$	$\begin{pmatrix} 1 & -0.0644 & 0.0072 & 0.0607 \\ -0.0644 & 1 & -0.3172 & -0.8331 \\ 0.0072 & -0.3172 & 1 & 0.3893 \\ 0.0607 & -0.8331 & 0.3893 & 1 \end{pmatrix}$
	y	$(-5.207 \pm 5.571 \pm 2.737)\%$	
	R_D	$(-2.395 \pm 1.739 \pm 0.938)\%$	
	$\sqrt{R_D}\cos\delta$	$(8.878 \pm 3.369 \pm 1.579)\%$	
$D^0 \to K^+\pi^-$ (Babar)	R_D	$(0.303 \pm 0.0189)\%$	$\begin{pmatrix} 1 & 0.77 & -0.87 \\ 0.77 & 1 & -0.94 \\ -0.87 & -0.94 & 1 \end{pmatrix}$
	x'^{2+}	$(-0.024 \pm 0.052)\%$	
	y'^{+}	$(0.98 \pm 0.78)\%$	
$\overline{D}{}^0 \to K^-\pi^+$ (Babar)	A_D	$(-2.1 \pm 5.4)\%$	same as above
	x'^{2-}	$(-0.020 \pm 0.050)\%$	
	y'^{-}	$(0.96 \pm 0.75)\%$	
$D^0 \to K^+\pi^-$ (Belle)	R_D	$(0.364 \pm 0.018)\%$	$\begin{pmatrix} 1 & 0.655 & -0.834 \\ 0.655 & 1 & -0.909 \\ -0.834 & -0.909 & 1 \end{pmatrix}$
	x'^{2+}	$(0.032 \pm 0.037)\%$	
	y'^{+}	$(-0.12 \pm 0.58)\%$	
$\overline{D}{}^0 \to K^-\pi^+$ (Belle)	A_D	$(2.3 \pm 4.7)\%$	same as above
	x'^{2-}	$(0.006 \pm 0.034)\%$	
	y'^{-}	$(0.20 \pm 0.54)\%$	
$D^0 \to K^+\pi^-$ + c.c. (CDF)	R_D	$(0.304 \pm 0.055)\%$	$\begin{pmatrix} 1 & 0.923 & -0.971 \\ 0.923 & 1 & -0.984 \\ -0.971 & -0.984 & 1 \end{pmatrix}$
	x'^{2}	$(-0.012 \pm 0.035)\%$	
	y'	$(0.85 \pm 0.76)\%$	

Table 140: Left: decay modes used to determine fitted parameters x, y, δ, $\delta_{K\pi\pi}$, R_D, A_D, $|q/p|$, and ϕ. Middle: the observables measured for each decay mode. Right: the relationships between the observables measured and the fitted parameters.

Decay Mode	**Observables**	**Relationship**
$D^0 \to K^+K^-/\pi^+\pi^-$	y_{CP} A_Γ	$2y_{CP} = (\lvert q/p\rvert + \lvert p/q\rvert)\, y\cos\phi \;-\; (\lvert q/p\rvert - \lvert p/q\rvert)\, x\sin\phi$ $2A_\Gamma = (\lvert q/p\rvert - \lvert p/q\rvert)\, y\cos\phi \;-\; (\lvert q/p\rvert + \lvert p/q\rvert)\, x\sin\phi$
$D^0 \to K^0_S\,\pi^+\pi^-$	x y $\lvert q/p\rvert$ ϕ	
$D^0 \to K^+\ell^-\nu$	R_M	$R_M = (x^2+y^2)/2$
$D^0 \to K^+\pi^-\pi^0$ (Dalitz plot analysis)	x'' y''	$x'' = x\cos\delta_{K\pi\pi} + y\sin\delta_{K\pi\pi}$ $y'' = y\cos\delta_{K\pi\pi} - x\sin\delta_{K\pi\pi}$
"Double-tagged" branching fractions measured in $\psi(3770)\to DD$ decays	R_M y R_D $\sqrt{R_D}\cos\delta$	$R_M = (x^2+y^2)/2$
$D^0 \to K^+\pi^-$	$R_D^+,\ R_D^-$ $x'^{2+},\ x'^{2-}$ $y'^{+},\ y'^{-}$	$R_D = (R_D^+ + R_D^-)/2$ $A_D = (R_D^+ - R_D^-)/(R_D^+ + R_D^-)$ $x' = x\cos\delta + y\sin\delta$ $y' = y\cos\delta - x\sin\delta$ $A_M \equiv (\lvert q/p\rvert^4 - 1)/(\lvert q/p\rvert^4 + 1)$ $x'^{\pm} = [(1\pm A_M)/(1\mp A_M)]^{1/4}(x'\cos\phi \pm y'\sin\phi)$ $y'^{\pm} = [(1\pm A_M)/(1\mp A_M)]^{1/4}(y'\cos\phi \mp x'\sin\phi)$

Table 141: Results of the global fit for different assumptions concerning CPV.

Parameter	**No CPV**	**No direct CPV**	**CPV-allowed**	**CPV-allowed 95% C.L.**
x (%)	$0.91\,^{+0.25}_{-0.26}$	$0.89\,^{+0.26}_{-0.27}$	$0.89\,^{+0.26}_{-0.27}$	[0.34, 1.39]
y (%)	0.73 ± 0.18	0.76 ± 0.18	$0.75\,^{+0.17}_{-0.18}$	[0.39, 1.09]
δ (°)	$20.6\,^{+11.4}_{-12.4}$	$22.7\,^{+11.4}_{-12.3}$	$21.9\,^{+11.3}_{-12.4}$	[−5.7, 44.3]
R_D (%)	0.3342 ± 0.0084	0.3343 ± 0.0085	0.3348 ± 0.0086	[0.318, 0.352]
A_D (%)	–	–	-2.0 ± 2.4	[−6.7, 2.7]
$\lvert q/p\rvert$	–	$0.95\,^{+0.15}_{-0.14}$	$0.87\,^{+0.18}_{-0.15}$	[0.59, 1.24]
ϕ (°)	–	$-2.7\,^{+5.6}_{-5.8}$	$-9.1\,^{+8.1}_{-7.8}$	[−24.7, 7.0]
$\delta_{K\pi\pi}$ (°)	$31.5\,^{+25.8}_{-26.6}$	$33.4\,^{+25.8}_{-26.5}$	$33.0\,^{+25.9}_{-26.6}$	[−21.2, 85.0]

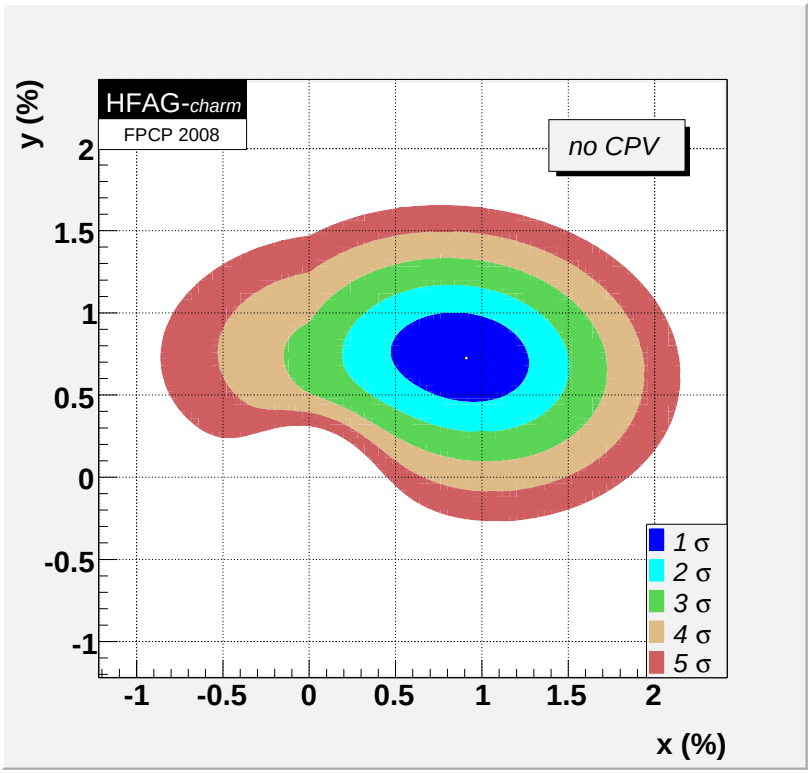

Figure 57: Two-dimensional contours for mixing parameters (x, y), for no CPV.

Table 142: Individual contributions to the χ^2 for the CPV-allowed fit.

Observable	χ^2	$\sum\chi^2$
y_{CP}	2.32	2.32
A_Γ	0.12	2.44
$x_{K^0\pi^+\pi^-}$	0.06	2.49
$y_{K^0\pi^+\pi^-}$	1.68	4.18
$\lvert q/p\rvert_{K^0\pi^+\pi^-}$	0.00	4.18
$\phi_{K^0\pi^+\pi^-}$	0.47	4.64
$R_M(K^+\ell^-\nu)$	0.05	4.70
$x_{K^+\pi^-\pi^0}$	1.73	6.43
$y_{K^+\pi^-\pi^0}$	1.52	7.95
$R_M/y/R_D/\sqrt{R_D}\cos\delta$ (CLEOc)	5.60	13.55
$R_D^+/x'^{2+}/y'^+$ (Babar)	2.59	16.14
$R_D^-/x'^{2-}/y'^-$ (Babar)	1.79	17.93
$R_D^+/x'^{2+}/y'^+$ (Belle)	3.84	21.77
$R_D^-/x'^{2-}/y'^-$ (Belle)	1.22	22.99
$R_D/x'^2/y'$ (CDF)	0.54	23.53

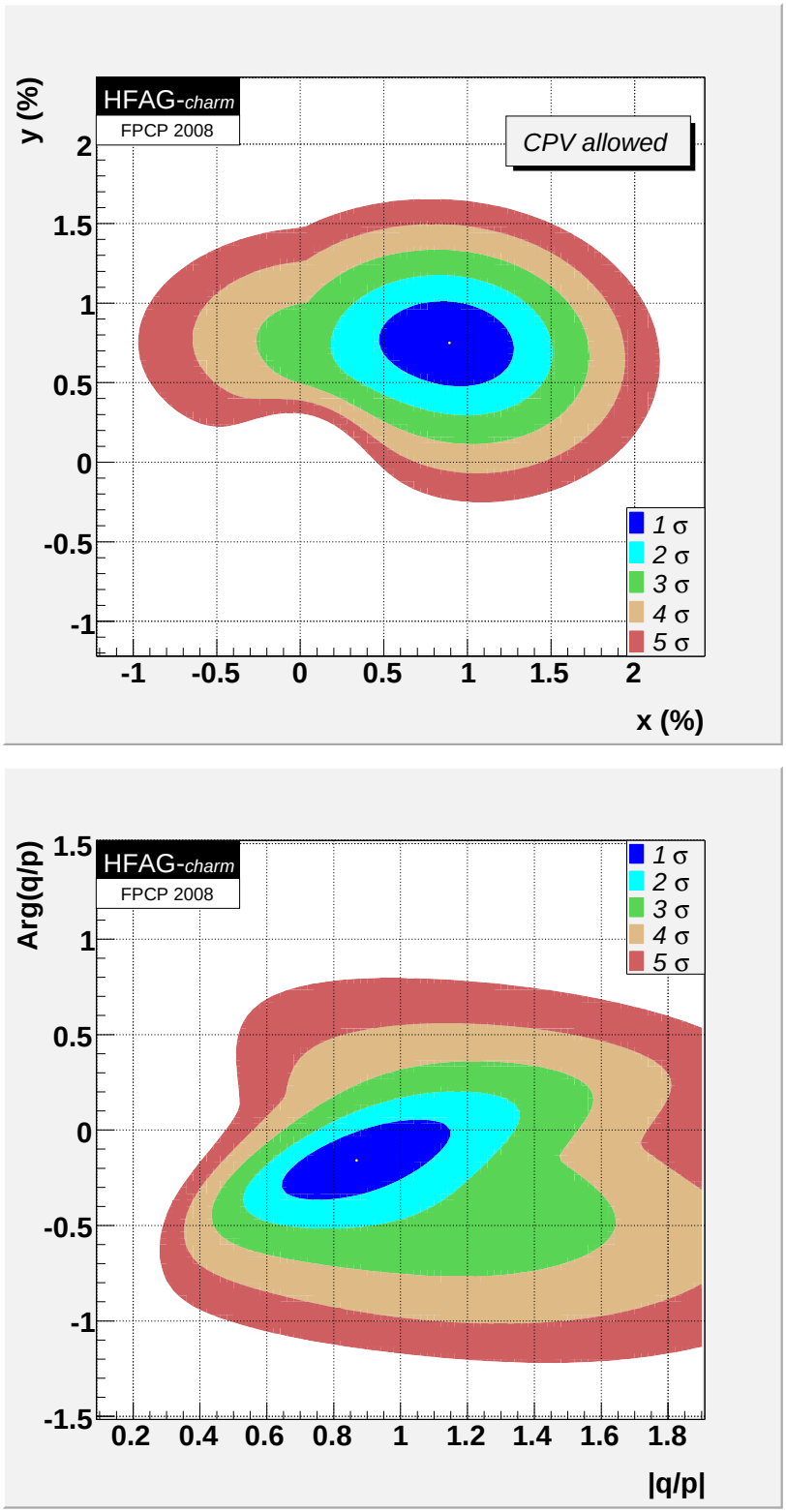

Figure 58: Two-dimensional contours for parameters (x, y) (top) and $(|q/p|, \phi)$ (bottom), allowing for CPV.

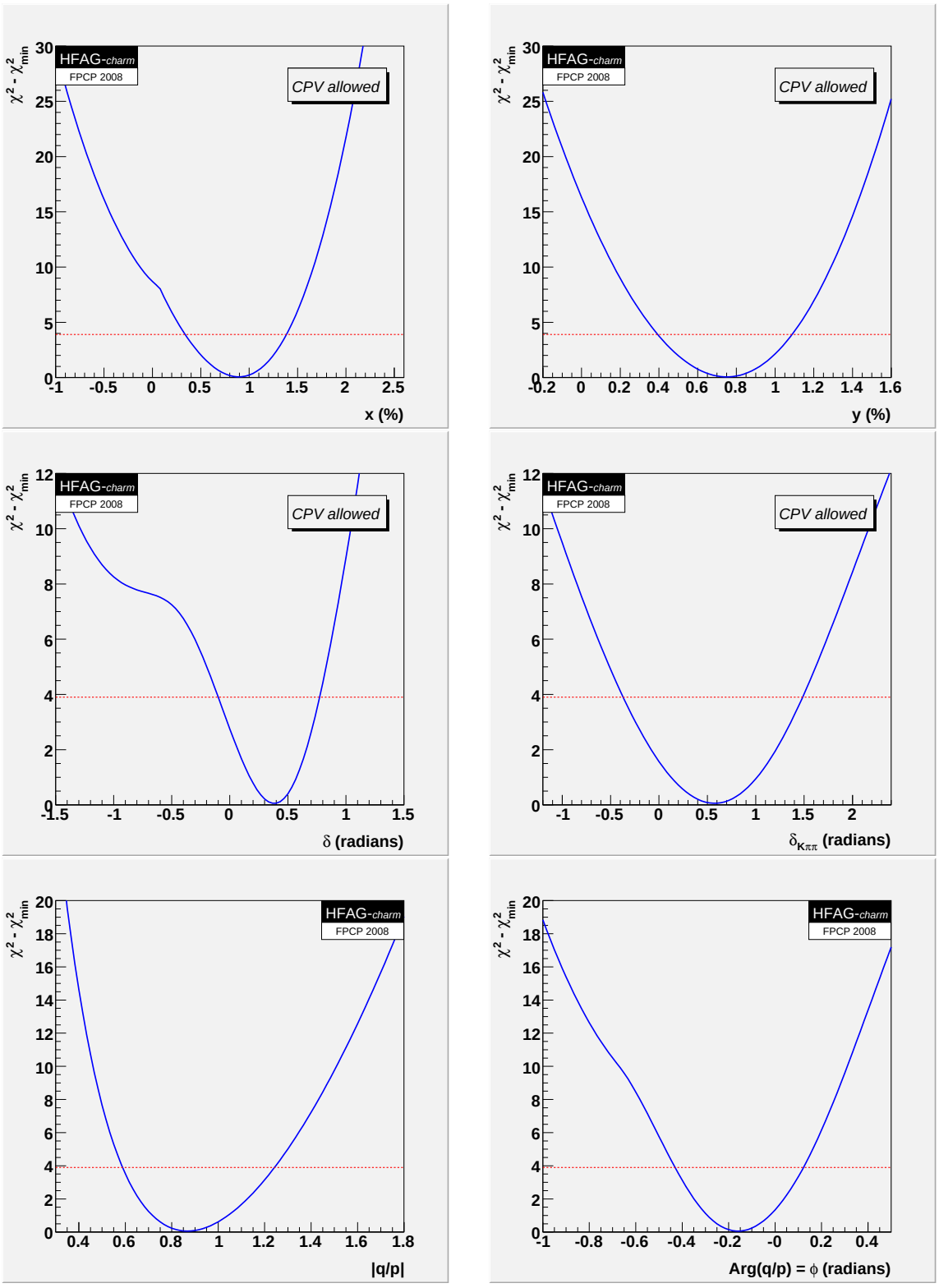

Figure 59: The function $\Delta\chi^2 = \chi^2 - \chi^2_{\rm min}$ for fitted parameters x, y, δ, $\delta_{K\pi\pi}$, $|q/p|$, and ϕ. The points where $\Delta\chi^2 = 3.84$ (denoted by the dashed horizontal line) determine a 95% C.L. interval.

8.2 Excited $D_{(s)}$ Mesons

Tables 143–145 represent a summary of recent results with an emphasis on information not provided in Ref. [3]. For a complete list of related publications, see Ref. [3]. All upper limits (U.L.) correspond to 90% confidence (C.L.) unless otherwise noted. The significances listed are approximate; they are calculated as either $\sqrt{-2\Delta \log \mathcal{L}}$ or $\sqrt{\Delta\chi^2}$, where Δ represents the change in the corresponding minimized function between two hypotheses, e.g., those for different spin states.

The broad charged $J^P = 1^+$ $c\overline{d}$ state is denoted $D_1(2430)^+$, although it has not yet been observed. The masses of narrow states $D_1(2420)^\pm$, $D_1(2420)^0$, $D_2^*(2460)^0$, $D_2^*(2460)^\pm$ and $D_{s0}^*(2317)^\pm$, $D_{s1}(2460)^\pm$, $D_{s1}(2536)^\pm$, $D_{s2}(2573)^\pm$ are well-measured, and thus only their averages are given [3]. The first observations of $D_{s1}(2460)^\pm$ and $D_{s0}^*(2317)^\pm$ states are described in Refs. [415] and [416], respectively.

The masses and widths of narrow ($\Gamma \sim$ 20–40 MeV) orbitally excited D mesons (denoted D^{**}), both neutral and charged, are well established. Measurements of broad states ($\Gamma \sim$ 200–400 MeV) are less abundant, as identifying the signal is more challenging. There is a slight discrepancy between the $D_0^*(2400)^0$ masses measured by the Belle [417] and FOCUS [418] experiments. No data exists yet for the $D_1(2430)^\pm$ state. Dalitz plot analyses of $B \to D^{(*)}\pi\pi$ decays strongly favor the assignments 0^+ and 1^+ for the spin-parity quantum numbers of the $D_0^*(2400)^0/D_0^*(2400)^\pm$ and $D_1(2430)^0$ states, respectively. The measured masses and widths, as well as the J^P values, are in agreement with theoretical predictions based on potential models [419]. While the branching fractions for B mesons decaying to a narrow D^{**} state and a pion are similar for charged and neutral B initial states, the branching fractions to a broad D^{**} state and π^+ are much larger for B^+ than for B^0. This may be due to the fact that color-suppressed amplitudes contribute only to the B^+ decay and not to the B^0 decay (for a theoretical discussion, see Ref. [420]).

The discoveries of the $D_{s0}^*(2317)^\pm$ and $D_{s1}(2460)^\pm$ have triggered increased interest in properties of, and searches for, excited D_s mesons (here generically denoted D_s^{**}). While the masses and widths of $D_{s1}(2536)^\pm$ and $D_{s2}(2573)^\pm$ states are in relatively good agreement with potential model predictions, the masses of $D_{s0}^*(2317)^\pm$ and $D_{s1}(2460)^\pm$ states (and consequently their widths, less than around 5 MeV) are significantly lower than expected (see Ref. [421] for a discussion of $c\overline{s}$ models). Moreover, the mass splitting between these two states greatly exceeds that between the $D_{s1}(2536)^\pm$ and $D_{s2}(2573)^\pm$. These unexpected properties have led to interpretations of the $D_{s0}^*(2317)^\pm$ and $D_{s1}(2460)^\pm$ as exotic four-quark states.

While there are few measurements with respect to the J^P values of $D_{s0}^*(2317)^\pm$ and $D_{s1}(2460)^\pm$, the available data favors 0^+ and 1^+, respectively. A molecule-like (DK) interpretation of the $D_{s0}^*(2317)^\pm$ and $D_{s1}(2460)^\pm$ [422] that can account for their low masses and isospin-breaking decay modes is tested by searching for charged and neutral isospin partners of these states; thus far such searches have yielded negative results. Hence the subset of models that predict equal production rates for different charged states is nominally excluded. The molecular picture can also be tested by measuring the rates for the radiative processes $D_{s0}^*(2317)^\pm/D_{s1}(2460)^\pm \to D_s^{(*)}\gamma$ and comparing to theoretical predictions. The predicted rates, however, are below the sensitivity of current experiments. Another model successful in explaining the total widths and the $D_{s0}^*(2317)^\pm$-$D_{s1}(2460)^\pm$ mass splitting is based on the assumption that these states are chiral partners of the ground states D_s^+ and $D_s^{*\pm}$ [423]. While some measured branching fraction ratios agree with predicted values, further experimental tests with better sensitivity are needed

to confirm or refute this scenario.

In addition to the $D_{s0}^{*}(2317)^{\pm}$ and $D_{s1}(2460)^{\pm}$ states, other excited D_s states may have been observed. SELEX has reported a $D_{sJ}(2632)^{\pm}$ candidate, but this has not been confirmed by other experiments. Recently, Belle and BaBar have observed $D_{sJ}(2700)^{\pm}$ and $D_{sJ}(2860)^{\pm}$ states, which may be radial excitations of the $D_s^{*\pm}$ and $D_{s0}^{*}(2317)^{\pm}$, respectively. However, the $D_{sJ}(2860)^{\pm}$ has been searched for in B decays and not observed, which may indicate that this state has higher spin.

Table 143: Recent results for properties of D^{**} mesons.

Main results		Reference	Comments
Masses [MeV/c^2], widths [MeV]	$M(D_2^*(2460)^0) : 2461.1 \pm 1.6$; $\Gamma(D_2^*(2460)^0) : 43 \pm 4$ $M(D_2^*(2460)^\pm) : 2459 \pm 4$; $\Gamma(D_2^*(2460)^\pm) : 29 \pm 5$ $M(D_1(2420)^0) : 2422.3 \pm 1.3$; $\Gamma(D_1(2420)^0) : 20.4 \pm 1.7$ $M(D_1(2420)^\pm) : 2423.4 \pm 3.1$; $\Gamma(D_1(2420)^\pm) : 25 \pm 6$	[3]	PDG average
	$M(D_0^*(2400)^0) : 2308 \pm 17 \pm 15 \pm 28$ $\Gamma(D_0^*(2400)^0) : 276 \pm 21 \pm 18 \pm 60$ $\Gamma(D_2^*(2460)^0) : 45.6 \pm 4.4 \pm 6.5 \pm 1.6$ $\Gamma(D_1(2420)^0) : 23.7 \pm 2.7 \pm 0.2 \pm 4.0$ $M(D_1(2430)^0) : 2427 \pm 26 \pm 20 \pm 15$ $\Gamma(D_1(2430)^0) : 384 \pm {}^{107}_{75} \pm 24 \pm 70$	[417]	last error due to Dalitz model
	$\Gamma(D_2^*(2460)^\pm) : 49.7 \pm 3.8 \pm 4.1 \pm 4.9$	[424]	
	$\Gamma(D_2^*(2460)^0) : 38.7 \pm 5.3 \pm 2.9$ $\Gamma(D_2^*(2460)^\pm) : 34.1 \pm 6.5 \pm 4.2$	[418]	
	$M(D_0^*(2400)^0/D_1(2430)^0) : 2407 \pm 21 \pm 35$ $\Gamma(D_0^*(2400)^0/D_1(2430)^0) : 240 \pm 55 \pm 59$ $M(D_0^*(2400)^\pm/D_1(2430)^\pm) : 2403 \pm 14 \pm 35$ $\Gamma(D_0^*(2400)^\pm/D_1(2430)^\pm) : 283 \pm 24 \pm 34$		$D_0^*(2400)^0/D_1(2430)^0$ and $D_0^*(2400)^\pm/D_1(2430)^\pm$ may contribute to signal
	$\Gamma(D_2^*(2460)^0) : 49.2 \pm 2.3 \pm 1.2$ $\Gamma(D_1(2420)^0) : 20.0 \pm 1.7 \pm 1.3$	[425]	
Branching fractions [10^{-4}]	$B^- \to D_0^*(2400)^0\pi^-$, $D_0^*(2400)^0 \to D^+\pi^- : 6.1 \pm 0.6 \pm 0.9 \pm 1.6$ $B^- \to D_2^*(2460)^0\pi^-$, $D_2^*(2460)^0 \to D^+\pi^- : 3.4 \pm 0.3 \pm 0.6 \pm 0.4$ $B^- \to D_1(2420)^0\pi^-$, $D_1(2420)^0 \to D^{*+}\pi^- : 6.8 \pm 0.7 \pm 1.3 \pm 0.3$ $B^- \to D_2^*(2460)^0\pi^-$, $D_2^*(2460)^0 \to D^{*+}\pi^- : 1.8 \pm 0.3 \pm 0.3 \pm 0.2$ $B^- \to D_1(2430)^0\pi^-$ $D_1(2430)^0 \to D^{*+}\pi^- : 5.0 \pm 0.4 \pm 1.0 \pm 0.4$	[417]	
	$\overline{B}^0 \to D_2^*(2460)^+\pi^-$, $D_2^*(2460)^+ \to D^0\pi^+ : 2.15 \pm 0.17 \pm 0.29 \pm 0.12$ $\overline{B}^0 \to D_0^*(2400)^+\pi^-$ $D_0^*(2400)^+ \to D^0\pi^+ : 0.60 \pm 0.13 \pm 0.15 \pm 0.22$	[424]	last error due to Dalitz model; $M(D_0^*(2400)^\pm) = M(D_0^*(2400)^0)$, $\Gamma(D_0^*(2400)^\pm) = \Gamma(D_0^*(2400)^0)$ assumed
	$B^- \to D_1(2420)^0\pi^-$, $D_1(2420)^0 \to D^0\pi^+\pi^- : 1.85 \pm 0.29 \pm 0.35 \pm {}^{0.00}_{0.43}$ $\overline{B}^0 \to D_1(2420)^+\pi^-$, $D_1(2420)^+ \to D^+\pi^+\pi^- : 0.89 \pm 0.15 \pm 0.17 \pm {}^{0.00}_{0.27}$	[426]	last error due to possible $D_2^*(2460)^0$, $D_2^*(2460)^\pm$ contr.
Quantum numbers (J^P)	$D_0^*(2400)^0 : 0^+$	[417]	0^+ preferred over $1^-,\ 2^+$ with sign. $> 10\sigma$
	$D_1(2430)^0 : 1^+$		1^+ preferred over $0^-,\ 1^-,\ 2^+$ with sign. $> 10\sigma$
	$D_0^*(2400)^\pm : 0^+$	[424]	0^+ preferred over $1^-,\ 2^+$ with sign. $\sim 5\sigma$

Table 144: Recent results for masses and branching fractions of excited D_s mesons.

Main results		Reference	Comments
Masses [MeV/c^2], widths [MeV]	$M(D^*_{s0}(2317)^\pm) : 2317.8 \pm 0.6$ $M(D_{s1}(2460)^\pm) : 2459.6 \pm 0.6$ $M(D_{s1}(2536)^\pm) : 2535.24 \pm 0.29$ $M(D_{s2}(2573)^\pm) : 2572.6 \pm 0.9$	[3]	PDG average
	$\Gamma(D^*_{s0}(2317)^\pm) :< 4.6$ $\Gamma(D_{s1}(2460)^\pm) :< 5.5$	[427]	
	$\Gamma(D^*_{s0}(2317)^\pm) :< 3.8$ $\Gamma(D_{s1}(2460)^\pm) :< 3.5$	[428]	95% C.L. U.L.
	$M(D_{sJ}(2700)^\pm) : 2708 \pm 9 \pm {}^{11}_{10}$; $\Gamma(D_{sJ}(2700)^\pm) : \ 108 \pm 23 \pm {}^{36}_{31}$	[429]	
	$M(D_{sJ}(2860)^\pm) : 2856.6 \pm 1.5 \pm 5.0$; $\Gamma(D_{sJ}(2860)^\pm) : \ 48 \pm 7 \pm 10$	[430]	
	$M(D_{sJ}(2632)^\pm) : 2632.5 \pm 1.7$; $\Gamma(D_{sJ}(2632)^\pm) :< 17$	[431]	not seen by other exp's; sys. err. not given
Branching fractions [10^{-4}]	$B^0 \to D^- D_{s0}(2317)^+, D_{s0}(2317)^+ \to D_s^+\pi^0 : \ 8.6 \pm {}^{3.3}_{2.6} \pm 2.6$ $B^0 \to D^- D_{s1}(2460)^+, D_{s1}(2460)^+ \to D_s^{*+}\pi^0 : \ 22.7 \pm {}^{7.3}_{6.2} \pm 6.8$ $B^0 \to D^- D_{s1}(2460)^+, D_{s1}(2460)^+ \to D_s^+\gamma : \ 8.2 \pm {}^{2.2}_{1.9} \pm 2.5$	[432]	further br. frac. for $B^0,\ B^\pm$ in paper
	$B^0 \to D^- D_{s0}(2317)^+, D_{s0}(2317)^+ \to D_s^+\pi^0 : \ 18 \pm 4 \pm 3 \pm {}^{6}_{4}$ $B^0 \to D^- D_{s1}(2460)^+, D_{s1}(2460)^+ \to D_s^{*+}\pi^0 : \ 28 \pm 8 \pm 5 \pm {}^{10}_{6}$ $B^0 \to D^- D_{s1}(2460)^+, D_{s1}(2460)^+ \to D_s^+\gamma : \ 8 \pm 2 \pm 1 \pm {}^{3}_{2}$	[433]	further br. frac. for $B^0,\ B^\pm$ in paper; last error from $B(D, D_s^+)$
	$\frac{B(D_{s1}(2460)^\pm \to D_s^+\gamma)}{B(D_{s1}(2460)^\pm \to D_s^{*\pm}\pi^0)} = 0.55 \pm 0.13 \pm 0.08$ $\frac{B(D_{s1}(2460)^\pm \to D_s^+\pi^+\pi^-)}{B(D_{s1}(2460)^\pm \to D_s^{*\pm}\pi^0)} = 0.14 \pm 0.04 \pm 0.02$ $\frac{\sigma(D_{s1}(2536)^\pm)B(D_{s1}(2536)^\pm \to D_s^+\pi^+\pi^-)}{\sigma(D_{s1}(2460)^\pm)B(D_{s1}(2460)^\pm \to D_s^+\pi^+\pi^-)} = 1.05 \pm 0.32 \pm 0.06$	[427]	
	$B \to D^*_{s0}(2317)^\mp K^\mp,\ D^*_{s0}(2317)^\pm \to D_s^+\pi^0 :$ $0.53 \pm {}^{0.15}_{0.13} \pm 0.07 \pm 0.14$ $B \to D_{s1}(2460)^\pm K^\mp,\ D_{s1}(2460)^\pm \to D_s^+\gamma : \ < 0.094$	[434]	last error due to $B(D_s^+)$
	$\frac{\sigma(D^*_{s0}(2317)^\pm)B(D^*_{s0}(2317)^\pm \to D_s^+\pi^0)}{\sigma(D_s^+)} = (7.9 \pm 1.2 \pm 0.4) \cdot 10^{-2}$ $\frac{\sigma(D_{s1}(2460)^\pm)B(D_{s1}(2460)^\pm \to D_s^{*\pm}\pi^0)}{\sigma(D_s^+)} = (3.5 \pm 0.9 \pm 0.2) \cdot 10^{-2}$	[416]	
	$\frac{B(D_{s1}(2536)^\pm \to D^\pm\pi^+K^\pm)}{B(D_{s1}(2536)^\pm \to D^{*\pm}K^0)} = (3.27 \pm 0.18 \pm 0.37)\%$	[435]	
	$B \to D_{s1}(2536)^\pm D^\mp : 1.71 \pm 0.48 \pm 0.32$ $B \to D_{s1}(2536)^\pm D^{*\mp} : 3.32 \pm 0.88 \pm 0.66$ $B^+ \to D_{s1}(2536)^+ \overline{D}^0 : 2.16 \pm 0.52 \pm 0.45$ $B^+ \to D_{s1}(2536)^+ \overline{D}^{*0} : 5.46 \pm 1.17 \pm 1.04$	[436]	$D_{s1}(2536)^+ \to D^{*0}K^+$ used; br. frac. with $D_{s1}(2536)^+ \to D^{*+}K^0$ in paper
	$\frac{B(D_{s1}(2536)^+ \to D^{*0}K^+)}{B(D_{s1}(2536)^+ \to D^{*+}K^0)} = 1.32 \pm 0.47 \pm 0.23$	[437]	
	$B^+ \to D_{sJ}(2700)^+ \overline{D}^0, D_{sJ}(2700)^+ \to D^0K^+ : 11.3 \pm 2.2 \pm {}^{1.4}_{2.8}$	[429]	
	$\frac{B(D_{s1}(2460)^\pm \to D_s^+\gamma)}{B(D_{s1}(2460)^\pm \to D_s^+\pi^0\gamma)} = 0.337 \pm 0.036 \pm 0.038$ $\frac{B(D_{s1}(2460)^\pm \to D_s^+\pi^+\pi^-)}{B(D_{s1}(2460)^\pm \to D_s^+\pi^0\gamma)} = 0.077 \pm 0.013 \pm 0.008$	[428]	95% C.L. U.L.
	$B(D_{s1}(2460)^\pm \to D_s^{*\pm}\pi^0) = (56 \pm 13 \pm 9)\%$ $B(D_{s1}(2460)^\pm \to D_s^+\gamma) = (16 \pm 4 \pm 3)\%$	[438]	
	$\frac{B(D_{sJ}(2632)^+ \to D^0K^+)}{B(D_{sJ}(2632)^+ \to D_s^+\eta)} = 0.14 \pm 0.06$	[431]	not seen by other exp's; sys. err. not given

Table 145: Recent results for quantum numbers of excited D_s mesons.

Main results		Reference	Comments
Quantum numbers (J^P)	$\frac{\mathcal{A}_{L=2}(D_{s1}(2536)^{\pm}\to D^{*\pm}K_S)}{\mathcal{A}_{L=0}(D_{s1}(2536)^{\pm}\to D^{*\pm}K_S)} =$ $= (0.63 \pm 0.07 \pm 0.02) Exp[\pm i(0.76 \pm 0.03 \pm 0.01)]$	[434]	D-/S-wave amp. ratio
	$D^*_{s0}(2317)^{\pm} : 0^+, 1^-, 2^+, \ldots$	[415]	natural J^P based on J^P conserv.
	$D_{s1}(2536)^{\pm} : 1^+, 1^-$	[436]	1^- preferred over 2^+ with sign. $\sim 4\sigma$; 1^+ preferred over 2^- with sign. $\sim 3\sigma$;
	$D_{sJ}(2700)^{\pm} : 1^-$	[429]	1^- preferred over $0^+, 2^+$ with sign. $> 10\sigma$
	$D_{sJ}(2860)^{\pm} : 0^+, 1^-, 2^+, \ldots$	[430]	natural J^P based on J^P conserv.
	$D_{s1}(2460)^{\pm} : 1^+$	[432]	1^+ preferred over 2^- with sign. $\sim 6\sigma$
	$D_{s1}(2460)^{\pm} : J \neq 0$	[428]	0^- disfavored with sign. $\sim 5\sigma$; assuming decay $D_{s1}(2460)^{\pm} \to D_s^{*\pm}\pi^0$ $\to D_s^+\gamma\pi^0$

8.3 Semileptonic Decays

8.3.1 Introduction

Semileptonic decays of D mesons involve the interaction of a leptonic current with a hadronic current. The latter is nonperturbative and cannot be calculated from first principles; thus it is usually parameterized in terms of form factors. The transition matrix element is written

$$\mathcal{M} \;=\; -i\,\frac{G_F}{\sqrt{2}}\,V_{cq}\,L^\mu H_\mu\,, \tag{160}$$

where G_F is the Fermi constant and V_{cq} is a CKM matrix element. The leptonic current L_μ is evaluated directly from the lepton spinors and has a simple structure; this allows one to extract information about the form factors (in H_μ) from data on semileptonic decays [439]. Conversely, because there are no final-state interactions between the leptonic and hadronic systems, semileptonic decays for which the form factors can be calculated allow one to determine V_{cq} [440].

8.3.2 $D \to P\ell\nu$ Decays

When the final state hadron is a pseudoscalar, the hadronic current is given by

$$H_\mu \;=\; \langle P(p)|\overline{q}\gamma^\mu c|D(p')\rangle \;=\; f_+(q^2)\left[(p'+p)^\mu - \frac{M_D^2-m_P^2}{q^2}q^\mu\right] + f_0(q^2)\frac{M_D^2-m_P^2}{q^2}q^\mu, \tag{161}$$

where M_D and p' are the mass and four momentum of the parent D meson, m_P and p are those of the daughter meson, $f_+(q^2)$ and $f_0(q^2)$ are form factors, and $q = p' - p$. Kinematics require that $f_+(0) = f_0(0)$. The contraction $q^\mu L_\mu$ results in terms proportional to m_ℓ [441], and thus for $\ell = e, \mu$ the last two terms in Eq. (161) are negligible. Thus, only the $f_+(q^2)$ form factor is relevant. The differential partial width is

$$\frac{d\Gamma(D \to P\ell\overline{\nu}_\ell)}{dq^2\,d\cos\theta_\ell} \;=\; \frac{G_F^2|V_{cq}|^2}{32\pi^3}p^{*\,3}|f_+(q^2)|^2\sin\theta_\ell^2\,, \tag{162}$$

where p^* is the magnitude of the momentum of the final state hadron in the D rest frame.

The form factor is traditionally parametrized with an explicit pole and a sum of effective poles:

$$f_+(q^2) \;=\; \frac{f(0)}{1-\alpha}\left(\frac{1}{1-q^2/m_{\rm pole}^2}\right) \;+\; \sum_{k=1}^{N}\frac{\rho_k}{1-q^2/(\gamma_k\,m_{\rm pole}^2)}\,, \tag{163}$$

where ρ_k and γ_k are expansion parameters. The parameter $m_{\rm pole}$ is the mass of the lowest-lying $c\overline{q}$ resonance with the appropriate quantum numbers; this is expected to provide the largest contribution to the form factor for the $c \to q$ transition. For example, for $D \to \pi$ transitions the dominant resonance is expected to be D^*, and thus $m_{\rm pole} = m_{D^*}$.

8.3.3 Simple Pole

Equation (163) can be simplified by neglecting the sum over effective poles, leaving only the explicit vector meson pole. This approximation is referred to as "nearest pole dominance" or

"vector-meson dominance." The resulting parameterization is

$$f_+(q^2) \;=\; \frac{f_+(0)}{(1-q^2/m^2_{\rm pole})}\,. \tag{164}$$

However, values of $m_{\rm pole}$ that give a good fit to the data do not agree with the expected vector meson masses [443]. To address this problem, the "modified pole" or Becirevic-Kaidalov (BK) parameterization [444] was introduced. This parametrization assumes that gluon hard-scattering contributions (δ) are near zero, and scaling violations (β) are near unity [443]:

$$1+1/\beta-\delta \;\equiv\; \frac{(M_D^2-m_P^2)}{f_+(0)}\;\left.\frac{df_+}{dq^2}\right|_{q^2=0} \;\approx\; 2\,. \tag{165}$$

The parameterization takes the form

$$f_+(q^2) \;=\; \frac{f_+(0)}{(1-q^2/m^2_{\rm pole})}\left(1-\alpha_{\rm BK}\frac{q^2}{m^2_{\rm pole}}\right)\,. \tag{166}$$

To be consistent with $1+1/\beta-\delta\approx 2$, the parameter $\alpha_{\rm BK}$ should be near the value 1.75.

This parameterization has been used by several experiments to determine form factor parameters. Measured values of $m_{\rm pole}$ and $\alpha_{\rm BK}$ are listed Tables 146 and 147 for $D\to K\ell\nu$ and $D\to\pi\ell\nu$ decays, respectively. Both tables show α_{BK} to be substantially lower than the expected value of ~ 1.75.

Table 146: Results for $m_{\rm pole}$ and $\alpha_{\rm BK}$ from various experiments for $D^0\to K^-\ell^+\nu$ and $D^+\to K_S\ell^+\nu$ decays. The last entry is a lattice QCD prediction.

$D\to K\ell\nu$ Expt.	Ref.	$m_{\rm pole}$ (GeV/c^2)	$\alpha_{\rm BK}$
CLEO III	[445]	$1.89\pm0.05^{+0.04}_{-0.03}$	$0.36\pm0.10^{+0.03}_{-0.07}$
FOCUS	[446]	$1.93\pm0.05\pm0.03$	$0.28\pm0.08\pm0.07$
BELLE	[447]	$1.82\pm0.04\pm0.03$	$0.52\pm0.08\pm0.06$
BaBar	[448]	$1.884\pm0.012\pm0.016$	$0.377\pm0.023\pm0.031$
CLEO-c ($D^0\to K^+$)	[449]	$1.943^{+0.037}_{-0.033}\pm0.011$	$0.258^{+0.063}_{-0.065}\pm0.020$
CLEO-c ($D^0\to K^+$)	[450]	$1.97\pm0.03\pm0.01$	$0.21\pm0.05\pm0.03$
CLEO-c ($D^+\to K_S$)	[449]	$2.02^{+0.07}_{-0.06}\pm0.02$	$0.127^{+0.099}_{-0.104}\pm0.031$
CLEO-c ($D^+\to K_S$)	[450]	$1.96\pm0.04\pm0.02$	$0.22\pm0.08\pm0.03$
Fermilab lattice/MILC/HPQCD	[451]	–	0.50 ± 0.04

8.3.4 z Expansion

Several groups have advocated an alternative series expansion around some value $q^2=t_0$ to parameterize f_+ [439, 442, 452, 453]. This expansion is given in terms of a complex parameter z, which is the analytic continuation of q^2 into the complex plane:

$$z(q^2,t_0) \;=\; \frac{\sqrt{t_+-q^2}-\sqrt{t_+-t_0}}{\sqrt{t_+-q^2}+\sqrt{t_+-t_0}}\,, \tag{167}$$

Table 147: Results for $m_{\rm pole}$ and $\alpha_{\rm BK}$ from various experiments for $D^0 \to \pi^-\ell^+\nu$ and $D^+ \to \pi^0\ell^+\nu$ decays. The last entry is a lattice QCD prediction.

$D \to \pi\ell\nu$ Expt.	Ref.	$m_{\rm pole}$ (GeV/c^2)	$\alpha_{\rm BK}$
CLEO III	[445]	$1.86^{+0.10+0.07}_{-0.06-0.03}$	$0.37^{+0.20}_{-0.31} \pm 0.15$
FOCUS	[446]	$1.91^{+0.30}_{-0.15} \pm 0.07$	–
BELLE	[447]	$1.97 \pm 0.08 \pm 0.04$	$0.10 \pm 0.21 \pm 0.10$
CLEO-c ($D^0 \to \pi^+$)	[449]	$1.941^{+0.042}_{-0.034} \pm 0.009$	$0.20^{+0.10}_{-0.11} \pm 0.03$
CLEO-c ($D^0 \to \pi^+$)	[450]	$1.87 \pm 0.03 \pm 0.01$	$0.37 \pm 0.08 \pm 0.03$
CLEO-c ($D^+ \to \pi^0$)	[449]	$1.99^{+0.11}_{-0.08} \pm 0.06$	$0.05^{+0.19}_{-0.22} \pm 0.13$
CLEO-c ($D^+ \to \pi^0$)	[450]	$1.97 \pm 0.07 \pm 0.02$	$0.14 \pm 0.16 \pm 0.04$
Fermilab lattice/MILC/HPQCD	[451]	–	0.44 ± 0.04

where $t_\pm \equiv (M_D \pm m_h)^2$ and t_0 is the (arbitrary) q^2 value corresponding to $z = 0$. The physical region corresponds to $|z| < 1$.

The form factor is expressed as

$$f_+(q^2) \;=\; \frac{1}{P(q^2)\,\phi(q^2,t_0)} \sum_{k=0}^{\infty} a_k(t_0)[z(q^2,t_0)]^k\,, \tag{168}$$

where the $P(q^2)$ factor accommodates sub-threshold resonances via

$$P(q^2) \;\equiv\; \begin{cases} 1 & (D \to \pi) \\ z(q^2, M^2_{D_s^*}) & (D \to K)\,. \end{cases} \tag{169}$$

The "outer" function $\phi(t,t_0)$ can be any analytic function, but a preferred choice (see, *e.g.* Refs. [442, 452, 454]) obtained from the Operator Product Expansion (OPE) is

$$\begin{aligned} \phi(q^2,t_0) \;=\; & \alpha\left(\sqrt{t_+ - q^2} + \sqrt{t_+ - t_0}\right) \times \\ & \frac{t_+ - q^2}{(t_+ - t_0)^{1/4}}\, \frac{(\sqrt{t_+ - q^2} \;+\; \sqrt{t_+ - t_-})^{3/2}}{(\sqrt{t_+ - q^2} + \sqrt{t_+})^5}\,, \end{aligned} \tag{170}$$

with $\alpha = \sqrt{\pi m_c^2/3}$. The OPE analysis provides a constraint upon the expansion coefficients, $\sum_{k=0}^{N} a_k^2 \le 1$. These coefficients receive $1/M$ corrections, and thus the constraint is only approximate. However, the expansion is expected to converge rapidly since $|z| < 0.051$ (0.17) for $D \to K$ ($D \to \pi$) over the entire physical q^2 range, and Eq. (168) remains a useful parameterization.

The z-expansion formalism has been used by BaBar [448] and CLEO-c [450]. Their fits used the first three terms of the expansion, and the results for the ratios $r_1 \equiv a_1/a_0$ and $r_2 \equiv a_2/a_0$ are listed in Table 148. The CLEO III [445] results listed are obtained by refitting their data using the full covariance matrix. The BaBar correlation coefficient listed is obtained by refitting their published branching fraction using their published covariance matrix. These measurements correspond to using the standard outer function $\phi(q^2,t_0)$ of Eq. (170) and $t_0 =$

$t_+\left(1-\sqrt{1-t_-/t_+}\right)$. This choice of t_0 constrains $|z|$ to be below a maximum value within the physical region.

Table 148: Results for r_1 and r_2 from various experiments, for $D \to \pi K \ell\nu$. The correlation coefficient listed is for the total uncertainties (statistical $\oplus$ systematic) on r_1 and r_2.

Expt.	mode	Ref.	r_1	r_2	ρ
CLEO III	$D^0 \to K^+$	[445]	$0.2^{+3.6}_{-3.0}$	-89^{+104}_{-120}	-0.99
BaBar		[448]	$-2.5 \pm 0.2 \pm 0.2$	$0.6 \pm 6. \pm 5.$	-0.64
CLEO-c		[450]	$-2.4 \pm 0.4 \pm 0.1$	$21 \pm 11 \pm 2$	-0.81
Average			-2.3 ± 0.23	5.9 ± 6.3	-0.74
CLEO-c	$D^+ \to K_S$	[450]	$-2.8 \pm 6 \pm 2$	$32 \pm 18 \pm 4$	-0.84
CLEO-c	$D^0 \to \pi^+$	[450]	$-2.1 \pm 7 \pm 3$	$-1.2 \pm 4.8 \pm 1.7$	-0.96
CLEO-c	$D^+ \to \pi^0$	[450]	$-0.2 \pm 1.5 \pm 4$	$-9.8 \pm 9.1 \pm 2.1$	-0.97

Table 148 also lists average values for r_1 and r_2 obtained from a simultaneous fit to CLEO III, BaBar, and CLEO-c branching fraction measurements. To account for final-state radiation in the BaBar measurement, we allow a bias shift between the fit parameters for the BaBar data and those for the other measurements (a χ^2 penalty is added to the fit for any deviation from BaBar's central value). Table 148 shows satisfactory agreement between the parameters measured for D^0 and D^+ decays.

8.3.5 $D \to V\ell\nu$ Decays

When the final state hadron is a vector meson, the decay can proceed through both vector and axial vector currents, and four form factors are needed. The hadronic current is $H_\mu = V_\mu + A_\mu$, where [441]

$$V_\mu \;=\; \langle V(p,\varepsilon)|\overline{q}\gamma^\mu c|D(p')\rangle \;=\; \frac{2V(q^2)}{M_D+m_h}\varepsilon_{\mu\nu\rho\sigma}\varepsilon^{*\nu}p'^{\rho}p^{\sigma} \tag{171}$$

$$\begin{aligned} A_\mu \;=\; \left\langle V(p,\varepsilon)\right|-\overline{q}\gamma^\mu\gamma^5 c|D(p')\rangle \;&=\; -i\,(M_D+m_h)A_1(q^2)\varepsilon^*_\mu \\ &\quad + i\frac{A_2(q^2)}{M_D+m_h}(\varepsilon^*\cdot q)(p'+p)_\mu \\ &\quad + i\,\frac{2m_h}{q^2}\left(A_3(q^2)-A_0(q^2)\right)[\varepsilon^*\cdot(p'+p)]q_\mu\,. \end{aligned} \tag{172}$$

In this expression, m_h is the daughter meson mass and

$$A_3(q^2) \;=\; \frac{M_D+m_h}{2m_h}A_1(q^2) \;-\; \frac{M_D-m_h}{2m_h}A_2(q^2)\,. \tag{173}$$

Kinematics require that $A_3(0) = A_0(0)$. The differential partial width is

$$\begin{aligned} \frac{d\Gamma(D\to V\ell\overline{\nu}_\ell)}{dq^2\,d\cos\theta_\ell} \;&=\; \frac{G_F^2\,|V_{cq}|^2}{128\pi^3 M_D^2}\,p^*\,q^2\,\times \\ &\quad \left[\frac{(1-\cos\theta_\ell)^2}{2}|H_-|^2 \;+\; \frac{(1+\cos\theta_\ell)^2}{2}|H_+|^2 \;+\; \sin^2\theta_\ell|H_0|^2\right], \end{aligned} \tag{174}$$

where $H_\pm$ and H_0 are helicity amplitudes given by

$$H_\pm = \frac{1}{M_D + m_h}\left[(M_B + m_h)^2 A_1(q^2) \mp 2M_D\, p^* V(q^2)\right] \tag{175}$$

$$H_0 = \frac{1}{|q|}\frac{M_B^2}{2m_h(M_D + m_h)} \times \left[\left(1 - \frac{m_h^2 - q^2}{M_D^2}\right)(M_D^2 + m_h^2)A_1(q^2) - 4p^{*2}A_2(q^2)\right]. \tag{176}$$

The left-handed nature of the quark current manifests itself as $|H_-| > |H_+|$. The differential decay rate for $D \to V\ell\nu$ followed by the vector meson decaying into two pseudoscalars is

$$\begin{aligned}\frac{d\Gamma(D \to V\ell\nu, V \to P_1P_2)}{dq^2 d\cos\theta_V d\cos\theta_\ell d\chi} = {} & \frac{3G_F^2}{2048\pi^4}|V_{cq}|^2 \frac{p^*(q^2)q^2}{M_D^2}\mathcal{B}(V \to P_1P_2) \times \\ & \{(1+\cos\theta_\ell)^2 \sin^2\theta_V |H_+(q^2)|^2 \\ & + (1-\cos\theta_\ell)^2 \sin^2\theta_V |H_-(q^2)|^2 \\ & + 4\sin^2\theta_\ell \cos^2\theta_V |H_0(q^2)|^2 \\ & + 4\sin\theta_\ell(1+\cos\theta_\ell)\sin\theta_V\cos\theta_V\cos\chi H_+(q^2)H_0(q^2) \\ & - 4\sin\theta_\ell(1-\cos\theta_\ell)\sin\theta_V\cos\theta_V\cos\chi H_-(q^2)H_0(q^2) \\ & - 2\sin^2\theta_\ell\sin^2\theta_V\cos 2\chi H_+(q^2)H_-(q^2)\},\end{aligned} \tag{177}$$

where the angles θ_ℓ, θ_V, and χ are defined in Fig. 60.

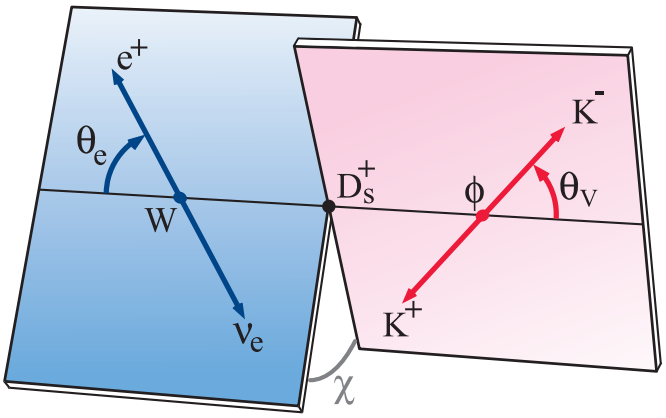

Figure 60: Decay angles θ_V, θ_ℓ and χ. Note that the angle χ between the decay planes is defined in the D-meson reference frame, whereas the angles θ_V and θ_ℓ are defined in the V meson and W reference frames, respectively.

Assuming that the simple pole form of Eq. (164) describes the q^2-dependence of the form factors, the distribution of Eq. (177) will depend only on the parameters

$$r_V \equiv V(0)/A_1(0), \qquad r_2 \equiv A_2(0)/A_1(0)\,. \tag{178}$$

Table 149 lists measurements of r_V and r_2 from several experiments. The average results from $D^+ \to \overline{K}^{*0}\ell^+\nu$ decays are also given. The measurements are plotted in Figs. 61 and 62, which show that the measurements are consistent with one another.

Table 149: Results for r_V and r_2 from various experiments.

Experiment	Ref.	r_V	r_2
$D^+ \to \overline{K}^{*0} l^+ \nu$			
E691	[455]	2.0± 0.6± 0.3	0.0± 0.5± 0.2
E653	[456]	2.00± 0.33± 0.16	0.82± 0.22± 0.11
E687	[457]	1.74± 0.27± 0.28	0.78± 0.18± 0.11
E791 (e)	[458]	1.90± 0.11± 0.09	0.71± 0.08± 0.09
E791 (μ)	[459]	1.84±0.11±0.09	0.75±0.08±0.09
Beatrice	[460]	1.45± 0.23± 0.07	1.00± 0.15± 0.03
FOCUS	[461]	1.504±0.057±0.039	0.875±0.049±0.064
Average		1.62±0.055	0.83±0.054
$D^0 \to \overline{K}^0 \pi^- \mu^+ \nu$			
FOCUS	[462]	1.706±0.677±0.342	0.912±0.370±0.104
$D_s^+ \to \phi\, e^+ \nu$			
BaBar	[463]	1.636±0.067±0.038	0.705±0.056±0.029
$D^0, D^+ \to \rho\, e \nu$			
CLEO	[464]	1.40±0.25±0.03	0.57±0.18±0.06

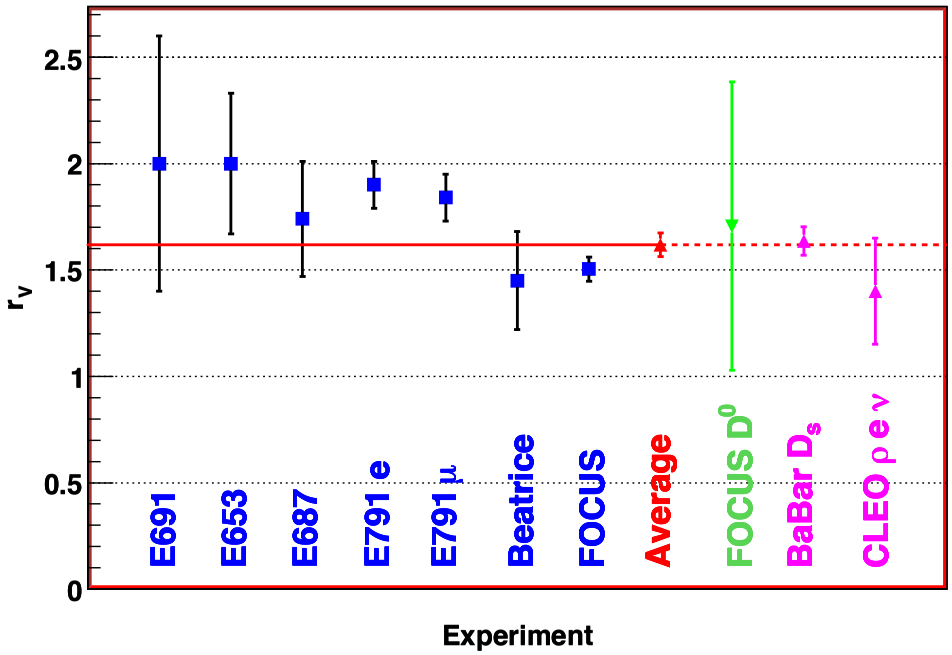

Figure 61: A comparison of r_V values from various experiments. The first set of measurements are for $D^+ \to K^- \pi^+ l^+ \nu_l$ decays. Plotted next is the average of these measurements, followed by measurements in D^0 decays, D_s^+ decays and Cabibbo-suppressed D decays.

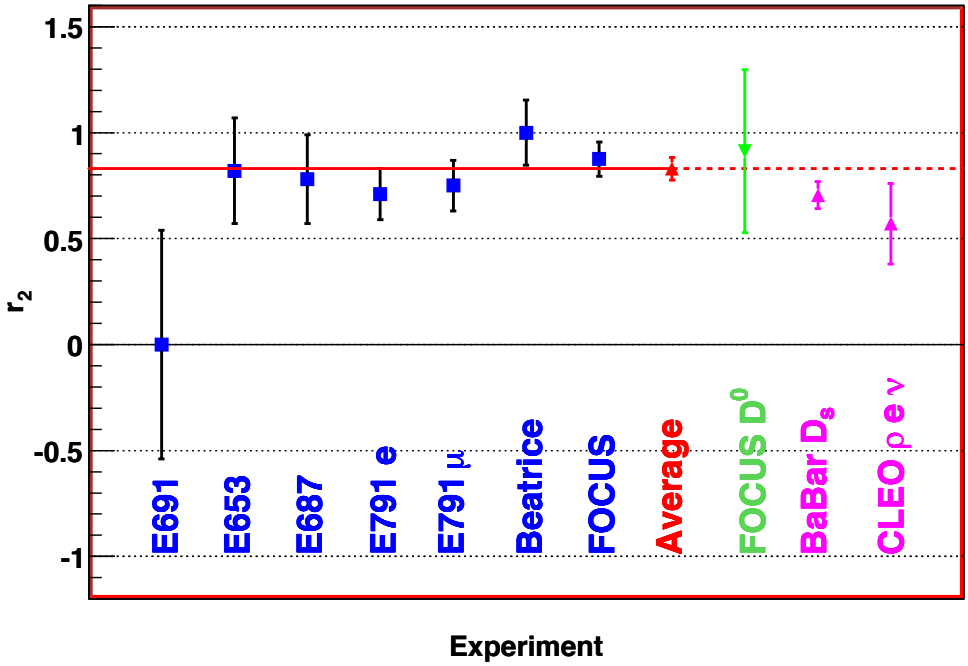

Figure 62: A comparison of r_2 values from various experiments. The first set of measurements are for $D^+ \to K^-\pi^+l^+\nu_l$ decays. Plotted next is the average of these measurements, followed by measurements in D^0 decays, D_s^+ decays and Cabibbo-suppressed D decays.

8.3.6 S-Wave Component

In 2002 FOCUS reported [465] an asymmetry in the observed $\cos(\theta_V)$ distribution. This is interpreted as evidence for an S-wave component in the decay amplitude as follows. Since H_0 typically dominates over $H_\pm$, the distribution given by Eq. (177) is, after integration over χ, roughly proportional to $\cos^2\theta_V$. Inclusion of a constant S-wave amplitude of the form $A\,e^{i\delta}$ leads to an interference term proportional to $|AH_0 \sin\theta_\ell \cos\theta_V|$; this term causes an asymmetry in $\cos(\theta_V)$. When FOCUS fits their data including this S-wave amplitude, they obtain $A = 0.330 \pm 0.022 \pm 0.015$ GeV^{-1} and $\delta = 0.68 \pm 0.07 \pm 0.05$ [461].

8.3.7 Model-independent Form Factor Measurement

The CLEO-c collaboration has recently extracted model-independent form factors, i.e., H_+, H_-, and H_0 directly as functions of q^2 [466]. The results are plotted in Fig. 63. The figure shows that $H_0(q^2)$ dominates, especially at low q^2. CLEO-c also determined the S-wave form factor $h_0(q^2)$ via the interference term, despite the fact that the $K\pi$ mass distribution appears dominated by the vector $K^*(890)$ state. The product $H_0 \times h_0$ is also plotted in Fig. 63.

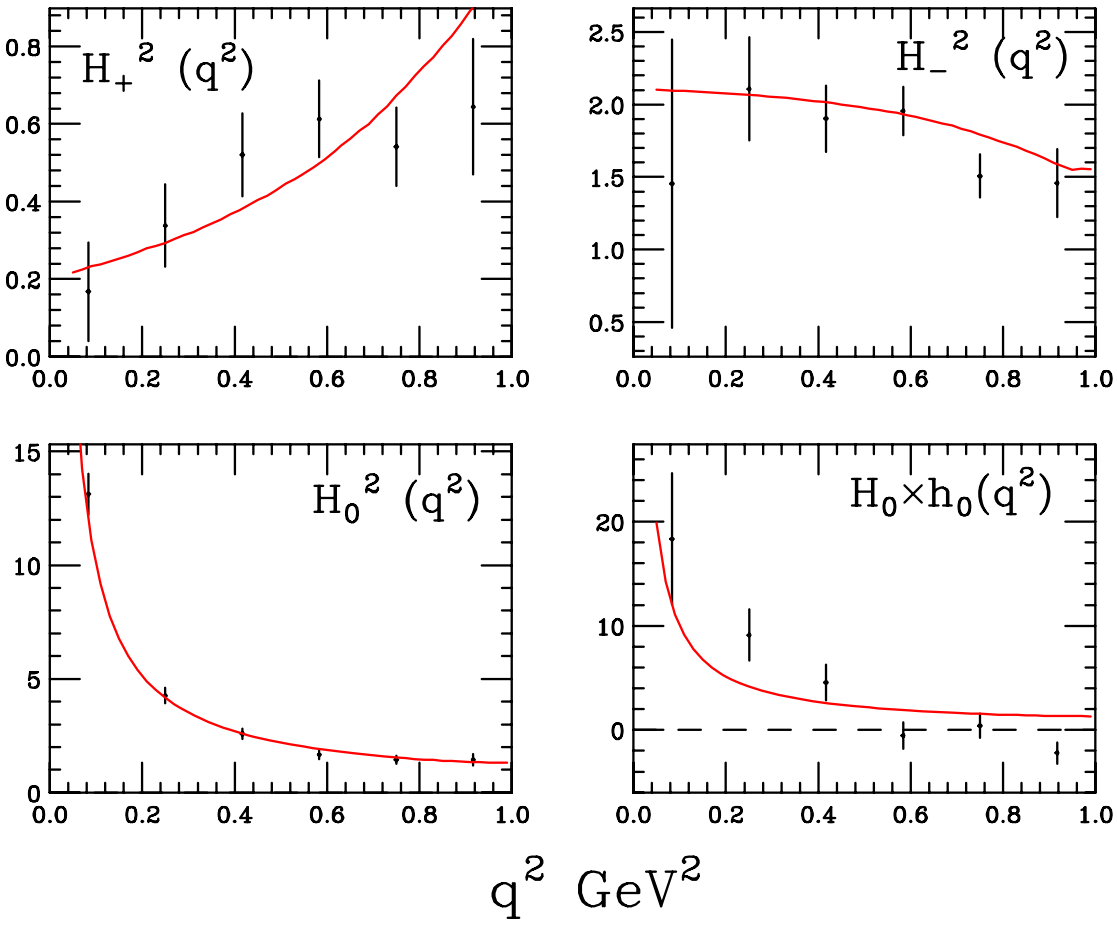

Figure 63: Model-independent form factors measured by CLEO-c [466].

8.4 *CP* Asymmetries

CP violation occurs if the decay rate for a particle differs from that of its *CP*-conjugate [467]. In general there are two classes of *CP* violation, termed *indirect* and *direct* [468]. Indirect *CP* violation refers to $\Delta C = 2$ processes and arises in D^0 decays due to D^0-$\overline{D}^0$ mixing. It can occur as an asymmetry in the mixing itself, or it can result from interference between a decay amplitude arising via mixing and a non-mixed amplitude. Direct *CP* violation refers to $\Delta C = 1$ processes and occurs in both charged and neutral D decays. It results from interference between two different decay amplitudes (e.g., a penguin and tree amplitude) that have different weak (CKM) and strong phases[25]. A difference in strong phases typically arises due to final-state interactions (FSI) [469]. A difference in weak phases arises from different CKM vertex couplings, as is often the case for spectator and penguin diagrams.

The *CP* asymmetry is defined as the difference between D and $\overline{D}$ partial widths divided by their sum:

$$A_{CP} \;=\; \frac{\Gamma(D) - \Gamma(\overline{D})}{\Gamma(D) + \Gamma(\overline{D})}\,. \tag{179}$$

However, to take into account differences in production rates between D and $\overline{D}$ (which would affect the number of respective decays observed), experiments usually normalize to a Cabibbo-favored mode. In this case there is the additional benefit that most corrections due to inefficiencies cancel out, reducing systematic uncertainties. An implicit assumption is that there is no measurable *CP* violation in the Cabibbo-favored normalizing mode. The *CP* asymmetry is calculated as

$$A_{CP} \;=\; \frac{\eta(D) - \eta(\overline{D})}{\eta(D) + \eta(\overline{D})}\,, \tag{180}$$

where (considering, for example, $D^0 \to K^-K^+$)

$$\eta(D) \;=\; \frac{N(D^0 \to K^-K^+)}{N(D^0 \to K^-\pi^+)}\,, \tag{181}$$

$$\eta(\overline{D}) \;=\; \frac{N(\overline{D}^0 \to K^-K^+)}{N(\overline{D}^0 \to K^+\pi^-)}\,. \tag{182}$$

In the case of D^+ and D_s^+ decays, A_{CP} measures direct *CP* violation; in the case of D^0 decays, A_{CP} measures direct and indirect *CP* violation combined. Values of A_{CP} for D^+ and D^0 decays are listed in Tables 150 and 151, respectively.

The *CP* lifetime asymmetry is the parameter A_Γ discussed in the D^0-$\overline{D}^0$ mixing section:

$$A_\Gamma \;=\; \frac{\tau(\overline{D}^0) - \tau(D^0)}{\tau(\overline{D}^0) + \tau(D^0)}\,. \tag{183}$$

[25]The weak phase difference will have opposite signs for $D \to f$ and $\overline{D} \to \overline{f}$ decays, while the strong phase difference will have the same sign. As a result, squaring the total amplitudes to obtain the decay rates gives interference terms having opposite sign, i.e., non-identical decay rates.

Table 150: CP asymmetries $A_{CP} = [\Gamma(D^+) - \Gamma(D^-)]/[\Gamma(D^+) + \Gamma(D^-)]$ for $D^\pm$ decays.

Mode	Year	Collaboration	A_{CP}
$D^+ \to K^0_S \pi^+$	2007	CLEOc [480]	$-0.006 \pm 0.010 \pm 0.003$
	2002	FOCUS [486]	$-0.016 \pm 0.015 \pm 0.009$
		COMBOS average	-0.0086 ± 0.0090
$D^+ \to K^0_S K^+$	2002	FOCUS [486]	$+0.071 \pm 0.061 \pm 0.012$
$D^+ \to \pi^+\pi^-\pi^+$	1997	E791 [487]	-0.017 ± 0.042 (stat.)
$D^+ \to K^-\pi^+\pi^+$	2007	CLEOc [480]	$-0.005 \pm 0.004 \pm 0.009$
$D^+ \to K^0_S \pi^+\pi^0$	2007	CLEO-c [480]	$+0.003 \pm 0.009 \pm 0.003$
$D^+ \to K^+K^-\pi^+$	2007	CLEO-c [480]	$-0.001 \pm 0.015 \pm 0.008$
	2005	BABAR [488]	$+0.014 \pm 0.010 \pm 0.008$
	2000	FOCUS [472]	$+0.006 \pm 0.011 \pm 0.005$
	1997	E791 [487]	-0.014 ± 0.029 (stat.)
	1994	E687 [475]	-0.031 ± 0.068 (stat.)
		COMBOS average	$+0.0059 \pm 0.0075$
$D^+ \to K^-\pi^+\pi^+\pi^0$	2007	CLEOc [480]	$+0.010 \pm 0.009 \pm 0.009$
$D^+ \to K^0_S \pi^+\pi^+\pi^-$	2007	CLEOc [480]	$+0.001 \pm 0.011 \pm 0.006$
$D^+ \to K^0_S K^+\pi^+\pi^-$	2005	FOCUS [485]	$-0.042 \pm 0.064 \pm 0.022$

It is analogous to A_{CP} except that the asymmetry pertains to the *full* width rather than a partial width, and it is calculated in terms of the reciprocal of the widths. The asymmetry A_Γ is measured by fitting decay time distributions, and thus it is insensitive to a production asymmetry between D and $\overline{D}$. Values of A_Γ for some D^0 decays are listed in Table 152.

8.5 T-violating Asymmetries

T-violating asymmetries are measured using triple-product correlations and assuming the validity of the CPT theorem. Triple-product correlations of the form $\vec{a} \cdot (\vec{b} \times \vec{c})$, where a, b, and c are spins or momenta, are odd under time reversal (T). For example, for $D^0 \to K^+K^-\pi^+\pi^-$ decays, $C_T \equiv \vec{p}_{K^+} \cdot (\vec{p}_{\pi^+} \times \vec{p}_{\pi^-})$ is odd under a T transformation. The corresponding quantity for $\overline{D}{}^0$ is $\overline{C}_T \equiv \vec{p}_{K^-} \cdot (\vec{p}_{\pi^-} \times \vec{p}_{\pi^+})$. Defining

$$A_T = \frac{\Gamma(C_T > 0) - \Gamma(C_T < 0)}{\Gamma(C_T > 0) + \Gamma(C_T < 0)} \tag{184}$$

for D^0 decay and

$$\overline{A}_T = \frac{\Gamma(-\overline{C}_T > 0) - \Gamma(-\overline{C}_T < 0)}{\Gamma(-\overline{C}_T > 0) + \Gamma(-\overline{C}_T < 0)} \tag{185}$$

Table 151: CP asymmetries $A_{CP} = [\Gamma(D^0) - \Gamma(\overline{D}{}^0)]/[\Gamma(D^0) + \Gamma(\overline{D}{}^0)]$ for $D^0, \overline{D}{}^0$ decays.

Mode	**Year**	**Collaboration**	$\boldsymbol{A_{CP}}$
$\boldsymbol{D^0 \to \pi^+\pi^-}$	2008	BABAR [470]	$-0.0024 \pm 0.0052 \pm 0.0022$
	2005	CDF [471]	$+0.010 \pm 0.013 \pm 0.006$
	2002	CLEO [408]	$+0.019 \pm 0.032 \pm 0.008$
	2000	FOCUS [472]	$+0.048 \pm 0.039 \pm 0.025$
	1998	E791 [473]	$-0.049 \pm 0.078 \pm 0.030$
		COMBOS average	$+0.0002 \pm 0.0051$
$\boldsymbol{D^0 \to \pi^0\pi^0}$	2001	CLEO [476]	$+0.001 \pm 0.048$ (stat. and syst. combined)
$\boldsymbol{D^0 \to K_s^0\pi^0}$	2001	CLEO [476]	$+0.001 \pm 0.013$ (stat. and syst. combined)
$\boldsymbol{D^0 \to K^+K^-}$	2008	BABAR [470]	$+0.0000 \pm 0.0034 \pm 0.0013$
	2005	CDF [471]	$+0.020 \pm 0.012 \pm 0.006$
	2002	CLEO [408]	$+0.000 \pm 0.022 \pm 0.008$
	2000	FOCUS [472]	$-0.001 \pm 0.022 \pm 0.015$
	1998	E791 [473]	$-0.010 \pm 0.049 \pm 0.012$
	1995	CLEO [474]	$+0.080 \pm 0.061$ (stat.)
	1994	E687 [475]	$+0.024 \pm 0.084$ (stat.)
		COMBOS average	$+0.0015 \pm 0.0034$
$\boldsymbol{D^0 \to K_s^0K_s^0}$	2001	CLEO [476]	-0.23 ± 0.19 (stat. and syst. combined)
$\boldsymbol{D^0 \to \pi^+\pi^-\pi^0}$	2008	BABAR [477]	$-0.0031 \pm 0.0041 \pm 0.0017$
	2008	Belle [478]	$+0.0043 \pm 0.0130$
	2005	CLEO [479]	$+0.001^{+0.09}_{-0.07} \pm 0.05$
		COMBOS average	-0.0023 ± 0.0042
$\boldsymbol{D^0 \to K^+K^-\pi^0}$	2008	BABAR [477]	$0.0100 \pm 0.0167 \pm 0.0025$
$\boldsymbol{D^0 \to K^-\pi^+\pi^0}$	2007	CLEOc [480]	$+0.002 \pm 0.004 \pm 0.008$
	2001	CLEO [481]	-0.031 ± 0.086 (stat.)
		COMBOS average	$+0.0016 \pm 0.0089$
$\boldsymbol{D^0 \to K^+\pi^-\pi^0}$	2005	BELLE [482]	-0.006 ± 0.053 (stat.)
	2001	CLEO [483]	$+0.09^{+0.25}_{-0.22}$ (stat.)
		COMBOS average	-0.0014 ± 0.0517
$\boldsymbol{D^0 \to K_s^0\pi^+\pi^-}$	2004	CLEO [484]	$-0.009 \pm 0.021^{+0.016}_{-0.057}$
$\boldsymbol{D^0 \to K^+\pi^-\pi^+\pi^-}$	2005	BELLE [482]	-0.018 ± 0.044 (stat.)
$\boldsymbol{D^0 \to K^+K^-\pi^+\pi^-}$	2005	FOCUS [485]	$-0.082 \pm 0.056 \pm .047$

Table 152: Lifetime asymmetries $A_\Gamma = [\tau(\overline{D}{}^0) - \tau(D^0)]/[\tau(\overline{D}{}^0) + \tau(D^0)]$ for $D^0, \overline{D}{}^0$ decays.

Mode	Year	Collaboration	A_Γ
$D^0 \to K^+K^-/\pi^+\pi^-$	2007	BELLE [399]	$+0.00010 \pm 0.00300 \pm 0.00150$
	2007	BABAR [409]	$+0.00260 \pm 0.00360 \pm 0.00080$
		COMBOS average	$+0.00123 \pm 0.00248$

for $\overline{D}{}^0$ decay, in the absence of strong phases either $A_T \neq 0$ or $\overline{A}_T \neq 0$ indicates T violation. The asymmetry

$$A_{T\,\mathrm{viol}} \;=\; \frac{A_T - \overline{A}_T}{2} \tag{186}$$

tests for T violation even with nonzero strong phases (see Refs. [489–492]). Values of $A_{T\,\mathrm{viol}}$ for some D^+, D_s^+, and D^0 decay modes are listed in Table 153.

Table 153: T-violating asymmetries $A_{T\,\mathrm{viol}} = (A_T - \overline{A}_T)/2$.

Mode	Year	Collaboration	$A_{T\,\mathrm{viol}}$
$D^0 \to K^+K^-\pi^+\pi^-$	2005	FOCUS [485]	$+0.010 \pm 0.057 \pm 0.037$
$D^+ \to K^0_S K^+\pi^+\pi^-$	2005	FOCUS [485]	$+0.023 \pm 0.062 \pm 0.022$
$D_s^+ \to K^0_S K^+\pi^+\pi^-$	2005	FOCUS [485]	$-0.036 \pm 0.067 \pm 0.023$

In summary, Tables 150–153 show that there is no evidence yet for CP or T violation in the charm sector. The most sensitive searches for CP violation have reached a level of sensitivity well below 1%.

9 Summary

This article provides updated world averages for b-hadron properties as of the end of 2007. Some results that appeared at the beginning of 2008 are also included. A small selection of highlights of the results described in Sections 3-8 is given in Table 154.

Concerning lifetime and mixing averages, the most significant changes since the end of 2006 [4] are due to new measurements from the Tevatron experiments, mainly in the areas of heavy B meson (B_s^0 and B_c^+) lifetimes and B_s^0 mixing parameters. After the direct observation of B_s^0 oscillations by CDF in 2006, DØ has now obtained an independent measurement of this phenomenon. Taking advantage of their increased data sample sizes, both experiments also performed new analyses of $B_s^0 \to J/\psi\phi$ untagged and tagged decays, leading to improvements in the measurement of the decay width difference in the B_s^0 system. Most notably, these analyses investigate mixing-induced CP violation in $B_s^0 \to J/\psi\phi$ decays and determine the corresponding weak phase, although with large uncertainties and with a two-fold ambiguity. The CDF and DØ results are consistent, and the combined result differs from the Standard Model expectation by $2.2\,\sigma$. We also present for the first time a combination of these results with searches for CP violation in B_s^0 mixing, under the hypothesis of a significant New Physics phase.

Measurements by Babar and Belle of the time-dependent CP violation parameter $S_{b\to c\bar{c}s}$ in B decays to charmonium and a neutral kaon have established CP violation in B decays, and they allow a precise extraction of the Unitarity Triangle parameter $\sin 2\beta \equiv \sin 2\phi_1$. Recent studies of $B \to J/\psi K^*$ (Sec. 4.4.2), $B \to D^{(*)}h^0$ where $h^0 = \pi^0$, *etc.* (Sec. 4.5), and $B \to D^{*+}D^{*-}K_S^0$ (Sec. 4.4.3) allow one to resolve the ambiguity for $\beta \equiv \phi_1$ from the measurement of $\sin 2\beta \equiv \sin 2\phi_1$. Measurements of time-dependent CP asymmetries in hadronic $b \to s$ penguin decays continue to provide insight into possible new physics. In this area, results from both Babar and Belle have been updated. A particularly notable change is that the CP violation effect in $B \to \eta' K^0$ is now established with more than 5σ significance in both experiments. First results from time-dependent Dalitz plot analyses of both $B \to K^+K^-K^0$ and $B \to \pi^+\pi^-K^0$ decays are now available. Compared to the previous round of averages, the consistency with the Standard Model expectation remains at about the same level in terms of significance. Results from time-dependent analyses of the decays $B^0 \to \pi^+\pi^-$, $\rho^\pm\pi^\mp$ and $\rho^+\rho^-$ provide constraints on the Unitarity Triangle angle $\alpha \equiv \phi_2$ (Sec. 4.11). Both Babar and Belle have now observed CP violation in $B^0 \to \pi^+\pi^-$ with more than 5σ significance, and both experiments have performed time-dependent Dalitz plot analyses of $B^0 \to (\rho\pi)^0 \to \pi^+\pi^-\pi^0$. Progress continues to constrain the third Unitarity Triangle angle $\gamma \equiv \phi_3$. Both Babar and Belle are using $B^- \to D^{(*)}K^-$ decays (Sec. 4.13), with $D^{(*)}$ decays to final states accessible from both $D^{(*)0}$ and $\overline{D}{}^{(*)0}$. At present, the most constraining results arise from the Dalitz plot analysis of the $D \to K_S^0\pi^+\pi^-$ channel.

Progress in the determination of properties of semileptonic B decays has been steady over the last year. To match the increasing number of results coming from Babar and Belle, several new averages have been added for decays with a $D^{(*)}$ in the final state. Regarding inclusive $B \to X_c\ell^+\nu_\ell$ decays, updated values of the b–quark mass from the kinetic and 1S schemes were obtained. Regarding charmless semileptonic decays, two new calculations (GGOU and ADFR) presented in 2007 were used (together with the already existing calculations BLNP, DGE and BLL) to extract the value of $|V_{ub}|$. All this information contributes to the current effort by theorists and experimentalists to understand the current differences between values of $|V_{ub}|$ extracted from inclusive and exclusive decays. Finally, the $B \to \pi\ell^+\nu_\ell$ branching fraction was

Table 154: Brief summary of the world averages at the end of 2007.

b-hadron lifetimes	
$\tau(B^0)$	1.530 ± 0.008 ps
$\tau(B^+)$	1.639 ± 0.009 ps
$\tau(B_s^0 \to$ flavour specific)	1.456 ± 0.030 ps
$\overline{\tau}(B_s^0) = 1/\Gamma_s$	$1.478^{+0.020}_{-0.022}$ ps
$\tau(B_c^+)$	0.461 ± 0.036 ps
$\tau(\Lambda_b^0)$	1.379 ± 0.051 ps
b-hadron fractions	
f^{+-}/f^{00} in $\Upsilon(4S)$ decays	1.064 ± 0.029
f_s in $\Upsilon(5S)$ decays	0.194 ± 0.029
$f_d = f_u$ at high energy	0.401 ± 0.011
f_s at high energy	0.106 ± 0.012
$f_{\rm baryon}$ at high energy	0.093 ± 0.019
B^0 and B_s^0 mixing/CPV parameters	
Δm_d	0.507 ± 0.004 ps^{-1}
$\lvert q/p\rvert_d$	1.0024 ± 0.0023
Δm_s	17.78 ± 0.12 ps^{-1}
$\Delta\Gamma_s = \Gamma_{\rm L} - \Gamma_{\rm H}$	$+0.067^{+0.031}_{-0.035}$ ps^{-1}
$\lvert q/p\rvert_s$	0.9992 ± 0.0042
$\phi_s = -2\beta_s$ (90% CL range)	$[-1.26, -0.13] \cup [-3.00, -1.88]$
Measurements related to Unitarity Triangle angles	
$\sin 2\beta \equiv \sin 2\phi_1$	0.681 ± 0.025
$\beta \equiv \phi_1$	$(21.5 \pm 1.0)^\circ$
$-\eta S_{\eta' K^0}$	0.61 ± 0.07
$S_{\pi^+\pi^-}$	-0.61 ± 0.08
$C_{\pi^+\pi^-}$	-0.38 ± 0.07
Semileptonic B decay parameters	
$\mathcal{B}(\overline{B} \to X\ell\overline{\nu})$	$(10.74 \pm 0.16)\%$
$\lvert V_{cb}\rvert F(1)$ $(\overline{B}^0 \to D^{*+}\ell^-\overline{\nu})$	$(36.14 \pm 0.55) \times 10^{-3}$
$\lvert V_{cb}\rvert G(1)$ $(\overline{B}^0 \to D^+\ell^-\overline{\nu})$	$(42.3 \pm 4.5) \times 10^{-3}$
$\mathcal{B}(\overline{B} \to \pi\ell\overline{\nu})$	$(1.40 \pm 0.06) \times 10^{-4}$
D^0 mixing/CPV parameters	
x	$(0.89\,^{+0.26}_{-0.27})\%$
y	$(0.75\,^{+0.17}_{-0.18})\%$
R_D	$(0.3348 \pm 0.0086)\%$
A_D	$(-2.0 \pm 2.4)\%$
$\lvert q/p\rvert$	$0.87\,^{+0.18}_{-0.15}$
ϕ	$(-9.1\,^{+8.1}_{-7.8})^\circ$

updated with published (instead of preliminary) results, and for the first time the $B \to \rho \ell^+ \nu_\ell$ average was added.

For rare B decays, branching fractions and charge asymmetries of new decay modes continue to be measured, mostly by Babar and Belle. There are several hundred measurements in the tables in Sec. 7. Particularly noteworthy is the measurement of $B^\pm \to \tau^\pm \nu$; Belle sees evidence for this decay, while Babar reports a somewhat smaller branching fraction.

In the sector of B decays to charmed particles, reductions in uncertainties and new measurements continue to be made. Branching fractions for rare B-meson decays or decay chains of a few 10^{-7} are being measured with statistical uncertainties typically below 30%. Results for more common decay chains, with branching fractions around 10^{-4}, are becoming precision measurements, with uncertainties typically at the 3% level. Branching fractions for several B decays to $D_{sJ}^{*-}(2317)$ and $D_{sJ}^{-}(2460)$ have been measured.

Mixing in the D^0-$\overline{D}{}^0$ system was finally observed last year. Three experiments – Belle [399], Babar [400], and CDF [401] – now observe evidence for this effect. The measurements are combined with others to yield World Average (WA) values for mixing parameters x and y, and for CPV parameters $|q/p|$ and ϕ. From this fit, the no-mixing point $x = y = 0$ is excluded at 9.2σ. The parameter x differs from zero by 3.0σ, and y differs from zero by 4.0σ. This mixing is presumably dominated by long-distance processes, which are difficult to calculate. Thus, it may be difficult to identify new physics from mixing alone. The WA value for the observable $y_{\rm CP}$ is positive, which indicates that the CP-even state is shorter-lived as in the K^0-$\overline{K}{}^0$ system. However, x also appears to be positive, which implies that the CP-even state is heavier; this is unlike in the K^0-$\overline{K}{}^0$ system. It appears difficult to accomodate a strong phase difference δ between amplitudes $A(D^0 \to K^+\pi^-)$ and $A(\overline{D}{}^0 \to K^+\pi^-)$ larger than 45°, and there is no evidence yet for CPV (either direct or indirect) in the D^0-$\overline{D}{}^0$ system.

10 Acknowledgments

We are grateful to the Babar, Belle, CDF, CLEO, DØ, LEP, and SLD collaborations, who have provided experimental results on b-hadron and c-hadron properties and have given assistance to HFAG when needed for averaging. These results would not be possible without the excellent operations of the PEP-II, KEKB, CESR, Tevatron, LEP, and SLC accelerators, and fruitful collaborations between the accelerator groups and the experimental collaborations.

References

[1] N. Cabibbo, Phys. Rev. Lett. 10, 531 (1963); M. Kobayashi and T. Maskawa, Prog. Theor. Phys. **49**, 652 (1973).

[2] ALEPH, CDF, DELPHI, L3, OPAL, and SLD collaborations, "Combined results on b-hadron production rates and decay properties", CERN-EP-2000-096, hep-ex/0009052 (2000); updated in CERN-EP-2001-050, hep-ex/0112028 (2001).

[3] W.-M. Yao et al., Journal of Physics, G 33, 1 (2006); see also 2007 update at `http://pdg.lbl.gov/`.

[4] Heavy Flavor Averaging Group (HFAG), "Averages of b-hadron Properties at the End of 2006" arXiv:0704.3575 (2007).

[5] J.P. Alexander *et al.* (CLEO Collaboration), Phys. Rev. Lett. **86**, 2737 (2001).

[6] B. Aubert *et al.* (Babar Collaboration), Phys. Rev. D **65**, 032001 (2002).

[7] S.B. Athar *et al.* (CLEO Collaboration), Phys. Rev. D **66**, 052003 (2002).

[8] N.C. Hastings *et al.* (Belle Collaboration), Phys. Rev. D **67**, 052004 (2003).

[9] B. Aubert *et al.* (Babar Collaboration), Phys. Rev. D **69**, 071101 (2004).

[10] B. Aubert *et al.* (Babar Collaboration), Phys. Rev. Lett. **94**, 141801 (2005).

[11] B. Aubert *et al.* (Babar Collaboration), Phys. Rev. Lett. **95**, 042001 (2005).

[12] B. Aubert *et al.* (Babar Collaboration), Phys. Rev. Lett. **96**, 232001 (2006);
A. Sokolov, M. Shapkin *et al.* (Belle Collaboration), Phys. Rev. D **75**, 071103 (2007);
B. Aubert *et al.* (Babar Collaboration), arXiv:0807.2014v1 [hep-ex], 13 July 2008, submitted to Phys. Rev. D.

[13] B. Barish *et al.* (CLEO Collaboration), Phys. Rev. Lett. **76**, 1570 (1996).

[14] G.S. Huang *et al.* (CLEO Collaboration), Phys. Rev. D **75**, 012002 (2007); this supersedes the results of Ref. [16].

[15] A. Drutskoy *et al.* (Belle Collaboration), Phys. Rev. Lett. **98**, 052001 (2007).

[16] M. Artuso *et al.* (CLEO Collaboration), Phys. Rev. Lett. **95**, 261801 (2005).

[17] G. Bonvicini *et al.* (CLEO Collaboration), Phys. Rev. Lett. **96**, 022002 (2006).

[18] A. Drutskoy *et al.* (Belle Collaboration), Phys. Rev. Lett. **76**, 012002 (2007).

[19] P. Abreu *et al.* (DELPHI Collaboration), Phys. Lett. B **289**, 199 (1992);
P.D. Acton *et al.* (OPAL Collaboration), Phys. Lett. B **295**, 357 (1992);
D. Buskulic *et al.* (ALEPH Collaboration), Phys. Lett. B **361**, 221 (1995).

[20] P. Abreu *et al.* (DELPHI Collaboration), Z. Phys. C **68**, 375 (1995).

[21] R. Barate *et al.* (ALEPH Collaboration), Eur. Phys. J. C **2**, 197 (1998).

[22] D. Buskulic *et al.* (ALEPH Collaboration), Phys. Lett. B **384**, 449 (1996).

[23] J. Abdallah *et al.* (DELPHI Collaboration), Eur. Phys. J. C **44**, 299 (2005).

[24] P. Abreu *et al.* (DELPHI Collaboration), Z. Phys. C **68**, 541 (1995).

[25] R. Barate *et al.* (ALEPH Collaboration), Eur. Phys. J. C **5**, 205 (1998).

[26] J. Abdallah *et al.* (DELPHI Collaboration), Phys. Lett. B **576**, 29 (2003).

[27] T. Affolder *et al.* (CDF Collaboration), Phys. Rev. Lett. **84**, 1663 (2000).

[28] F. Abe *et al.* (CDF Collaboration), Phys. Rev. D **60**, 092005 (1999).

[29] T. Aaltonen *et al.* (CDF Collaboration), Phys. Rev. D **77**, 072003 (2008).

[30] LEP collaborations ALEPH, CDF, DELPHI, L3, OPAL, LEP Electroweak Working Group, SLD Electroweak and Heavy Flavour Working Groups, "Precision electroweak measurements on the Z resonance", Phys. Reports **427**, 257 (2006); we use the average given in Eq. 5.39 of this paper, obtained from a 10-parameter global fit of all electroweak data where the asymmetry measurements have been excluded.

[31] D. Acosta *et al.* (CDF Collaboration), Phys. Rev. D **69**, 012002 (2004).

[32] V.M. Abazov *et al.* (DØ Collaboration), Phys. Rev. D **74**, 092001 (2006).

[33] M.A. Shifman and M.B. Voloshin, Sov. Phys. JETP **64**, 698 (1986);
J. Chay, H. Georgi and B. Grinstein, Phys. Lett. B **247**, 399 (1990);
I.I. Bigi, N.G. Uraltsev and A.I. Vainshtein, Phys. Lett. B **293**, 430 (1992), erratum ibid. B **297**, 477 (1993).

[34] I. Bigi, UND-HEP-95-BIG02 (1995);
G. Bellini, I. Bigi and P. Dornan, Phys. Reports **289**, 1 (1997).

[35] M. Ciuchini, E. Franco, V. Lubicz and F. Mescia, Nucl. Phys. B **625**, 211 (2002);
M. Beneke, G. Buchalla, C. Greub, A. Lenz and U. Nierste, Nucl. Phys. B **639**, 389 (2002);
E. Franco, V. Lubicz, F. Mescia and C. Tarantino, Nucl. Phys. B **633**, 212 (2002).

[36] C. Tarantino, Eur. Phys. J. C **33**, S895 (2004) [hep-ph/0310241];
F. Gabbiani, A. Onishchenko and A. Petrov, Phys. Rev. D **68**, 114006 (2003).

[37] F. Gabbiani, A. Onischenko and A. Petrov, Phys. Rev. D **70**, 094031 (2004).

[38] L. Di Ciaccio *et al.*, internal note by former B lifetime working group (1996), `http://lepbosc.web.cern.ch/LEPBOSC/lifetimes/ps/final_blife.ps`

[39] D. Buskulic *et al.* (ALEPH Collaboration), Phys. Lett. B **314**, 459 (1993).

[40] P. Abreu *et al.* (DELPHI Collaboration), Z. Phys. C **63**, 3 (1994).

[41] P. Abreu *et al.* (DELPHI Collaboration), Phys. Lett. B **377**, 195 (1996).

[42] J. Abdallah *et al.* (DELPHI Collaboration), Eur. Phys. J. C **33**, 307 (2004).

[43] M. Acciarri *et al.* (L3 Collaboration), Phys. Lett. B **416**, 220 (1998).

[44] K. Ackerstaff *et al.* (OPAL Collaboration), Z. Phys. C **73**, 397 (1997).

[45] K. Abe *et al.* (SLD Collaboration), Phys. Rev. Lett. **75**, 3624 (1995).

[46] D. Buskulic *et al.* (ALEPH Collaboration), Phys. Lett. B **369**, 151 (1996).

[47] P.D. Acton *et al.* (OPAL Collaboration), Z. Phys. C **60**, 217 (1993).

[48] F. Abe *et al.* (CDF Collaboration), Phys. Rev. D **57**, 5382 (1998).

[49] R. Barate *et al.* (ALEPH Collaboration), Phys. Lett. B **492**, 275 (2000).

[50] D. Buskulic *et al.* (ALEPH Collaboration), Z. Phys. C **71**, 31 (1996).

[51] P. Abreu *et al.* (DELPHI Collaboration), Z. Phys. C **68**, 13 (1995).

[52] W. Adam *et al.* (DELPHI Collaboration), Z. Phys. C **68**, 363 (1995).

[53] P. Abreu *et al.* (DELPHI Collaboration), Z. Phys. C **74**, 19 (1997).

[54] M. Acciari *et al.* (L3 Collaboration), Phys. Lett. B **438**, 417 (1998).

[55] R. Akers *et al.* (OPAL Collaboration), Z. Phys. C **67**, 379 (1995).

[56] G. Abbiendi *et al.* (OPAL Collaboration), Eur. Phys. J. C **12**, 609 (2000).

[57] G. Abbiendi *et al.* (OPAL Collaboration), Phys. Lett. B **493**, 266 (2000).

[58] K. Abe *et al.* (SLD Collaboration), Phys. Rev. Lett. **79**, 590 (1997).

[59] F. Abe *et al.* (CDF Collaboration), Phys. Rev. D **58**, 092002 (1998).

[60] D. Acosta *et al.* (CDF Collaboration), Phys. Rev. D **65**, 092009 (2003).

[61] CDF Collaboration, CDF note 7514, 1 March 2005,
`http://www-cdf.fnal.gov/physics/new/bottom/050224.blessed-bsemi-life/`

[62] CDF Collaboration, CDF note 7386, 23 March 2005,
`http://www-cdf.fnal.gov/physics/new/bottom/050303.blessed-bhadlife/`

[63] CDF Collaboration, CDF note 8524, 7 March 2007,
`http://www-cdf.fnal.gov/physics/new/bottom/061130.blessed-bh-lifetime_v2/`;
these preliminary results replace the $\Lambda_b \to J/\psi\Lambda$ and $B^0 \to J/\psi K_S$ lifetime measurements of A. Abulencia *et al.* (CDF Collaboration), Phys. Rev. Lett. **98**, 122001 (2007), as well as the $B^0 \to J/\psi K^{*0}$ lifetime measurement of D. Acosta *et al.* (CDF Collaboration), Phys. Rev. Lett. **94**, 101803 (2005).

[64] V.M. Abazov *et al.* (DØ Collaboration), Phys. Rev. Lett. **95**, 171801 (2005).

[65] V.M. Abazov *et al.* (DØ Collaboration), Phys. Rev. Lett. **94**, 042001 (2005).

[66] V.M. Abazov *et al.* (DØ Collaboration), Phys. Rev. Lett. **99**, 142001 (2007).

[67] B. Aubert *et al.* (Babar Collaboration), Phys. Rev. Lett. **87**, 201803 (2001).

[68] B. Aubert *et al.* (Babar Collaboration), Phys. Rev. Lett. **89**, 011802 (2002), erratum ibid. **89**, 169903 (2002).

[69] B. Aubert *et al.* (Babar Collaboration), Phys. Rev. D **67**, 072002 (2003).

[70] B. Aubert *et al.* (Babar Collaboration), Phys. Rev. D **67**, 091101 (2003).

[71] B. Aubert *et al.* (Babar Collaboration), Phys. Rev. D **73**, 012004 (2006).

[72] K. Abe *et al.* (Belle Collaboration), Phys. Rev. D **71**, 072003 (2005).

[73] V.M. Abazov *et al.* (DØ Collaboration), Phys. Rev. Lett. **94**, 182001 (2005).

[74] A. Lenz and U. Nierste, hep-ph/0612167, JHEP06 (2007) 072;
M. Beneke *et al.*, Phys. Lett. B **459**, 631 (1999).

[75] K. Hartkorn and H.-G. Moser, Eur. Phys. J. C **8**, 381 (1999).

[76] D. Buskulic *et al.* (ALEPH Collaboration), Phys. Lett. B **377**, 205 (1996).

[77] F. Abe *et al.* (CDF Collaboration), Phys. Rev. D **59**, 032004 (1999).

[78] P. Abreu *et al.* (DELPHI Collaboration), Eur. Phys. J. C **16**, 555 (2000).

[79] K. Ackerstaff *et al.* (OPAL Collaboration), Phys. Lett. B **426**, 161 (1998).

[80] V.M. Abazov *et al.* (DØ Collaboration), Phys. Rev. Lett. **97**, 241801 (2006).

[81] CDF Collaboration, CDF note 9203, 15 February 2008, submitted to the Winter 2008 conferences; we consider that these new results supersede the ones from the 3-year old CDF note 7386 [62], although the lifetime analysis of one of the modes ($B_s \to D_s\pi\pi\pi$) has not been updated.

[82] CDF Collaboration, CDF note 7757, 13 August 2005.

[83] D. Buskulic *et al.* (ALEPH Collaboration), Eur. Phys. J. C **4**, 367 (1998).

[84] P. Abreu *et al.* (DELPHI Collaboration), Eur. Phys. J. C **18**, 229 (2000).

[85] K. Ackerstaff *et al.* (OPAL Collaboration), Eur. Phys. J. C **2**, 407 (1998).

[86] CDF Collaboration, D. Tonelli, FPCP 2006 proceedings, FPCP06_112, hep-ex/0605038.

[87] F. Abe *et al.* (CDF Collaboration), Phys. Rev. Lett. **81**, 2432 (1998).

[88] CDF Collaboration, CDF note 9294, 28 April 2008,
http://www-cdf.fnal.gov/physics/new/bottom/080327.blessed-BC_LT_SemiLeptonic/;
this result replaces A. Abulencia *et al.* (CDF Collaboration), Phys. Rev. Lett. **97**, 012002 (2006).

[89] V.M. Abazov *et al.* (DØ Collaboration), arXiv:0805.2614v1 [hep-ex], 16 May 2008, submited to Phys. Rev. Lett.

[90] A. Abulencia *et al.* (CDF Collaboration), Phys. Rev. Lett. **96**, 082002 (2006).

[91] T. Aaltonen *et al.* (CDF Collaboration), Phys. Rev. Lett. **100**, 182002 (2008).

[92] D. Acosta *et al.* (CDF Collaboration), Phys. Rev. Lett. **96**, 202001 (2006).

[93] D. Buskulic *et al.* (ALEPH Collaboration), Phys. Lett. B **365**, 437 (1996).

[94] F. Abe *et al.* (CDF Collaboration), Phys. Rev. Lett. **77**, 1439 (1996).

[95] V.M. Abazov *et al.* (DØ Collaboration), Phys. Rev. Lett. **99**, 182001 (2007).

[96] P. Abreu *et al.* (DELPHI Collaboration), Eur. Phys. J. C **10**, 185 (1999).

[97] P. Abreu *et al.* (DELPHI Collaboration), Z. Phys. C **71**, 199 (1996).

[98] R. Akers *et al.* (OPAL Collaboration), Z. Phys. C **69**, 195 (1996).

[99] M. Beneke, G. Buchalla and I. Dunietz, Phys. Rev. D **54**, 4419 (1996);
Y. Keum and U. Nierste, Phys. Rev. D **57**, 4282 (1998).

[100] M.B. Voloshin, Phys. Rep. **320**, 275 (1999);
B. Guberina, B. Melic and H. Stefancic, Phys. Lett. B **469**, 253 (1999);
M. Neubert and C.T. Sachrajda, Nucl. Phys. B **483**, 339 (1997).

[101] N. Uraltsev, Phys. Lett. B **376**, 303 (1996);
D. Pirjol and N. Uraltsev, Phys. Rev. D **59**, 034012 (1999);
P. Colangelo and F. De Fazio, Phys. Lett. B **387**, 371 (1996);
M. Di Pierro, C. Sachrajda, C. Michael, Phys. Lett. B **468**, 143 (1999).

[102] J. Bartelt *et al.* (CLEO Collaboration), Phys. Rev. Lett. **71**, 1680 (1993).

[103] B.H. Behrens *et al.* (CLEO Collaboration), Phys. Lett. B **490**, 36 (2000).

[104] D.E. Jaffe *et al.* (CLEO Collaboration), Phys. Rev. Lett. **86**, 5000 (2001).

[105] F. Abe *et al.* (CDF Collaboration), Phys. Rev. D **55**, 2546 (1997).

[106] CDF Collaboration, CDF note 9015, 16 October 2007,
http://www-cdf.fnal.gov/physics/new/bottom/070816.blessed-acp-bsemil/

[107] K. Ackerstaff *et al.* (OPAL Collaboration), Z. Phys. C **76**, 401 (1997).

[108] R. Barate *et al.* (ALEPH Collaboration), Eur. Phys. J. C **20**, 431 (2001).

[109] B. Aubert *et al.* (Babar Collaboration), Phys. Rev. Lett. **92**, 181801 (2004) and Phys. Rev. D **70**, 012007 (2004).

[110] B. Aubert *et al.* (Babar Collaboration), Phys. Rev. Lett. **88**, 231801 (2002).

[111] B. Aubert *et al.* (Babar Collaboration), Phys. Rev. Lett. **96**, 251802 (2006).

[112] B. Aubert *et al.* (Babar Collaboration), BABAR-CONF-06/013, hep-ex/0607091, submitted to ICHEP06.

[113] E. Nakano *et al.* (Belle Collaboration), Phys. Rev. D **73**, 112002 (2006).

[114] G. Abbiendi *et al.* (OPAL Collaboration), Eur. Phys. J. C **12**, 609 (2000).

[115] M. Beneke, G. Buchalla and I. Dunietz, Phys. Lett. B **393**, 132 (1997);
I. Dunietz, Eur. Phys. J. C **7**, 197 (1999).

[116] D. Buskulic *et al.* (ALEPH Collaboration), Z. Phys. C **75**, 397 (1997).

[117] P. Abreu *et al.* (DELPHI Collaboration), Z. Phys. C **76**, 579 (1997).

[118] J. Abdallah *et al.* (DELPHI Collaboration), Eur. Phys. J. C **28**, 155 (2003).

[119] M. Acciarri *et al.* (L3 Collaboration), Eur. Phys. J. C **5**, 195 (1998).

[120] K. Ackerstaff *et al.* (OPAL Collaboration), Z. Phys. C **76**, 417 (1997).

[121] K. Ackerstaff *et al.* (OPAL Collaboration), Z. Phys. C **76**, 401 (1997).

[122] G. Alexander *et al.* (OPAL Collaboration), Z. Phys. C **72**, 377 (1996).

[123] G. Abbiendi *et al.* (OPAL Collaboration), Phys. Lett. B **493**, 266 (2000).

[124] F. Abe *et al.* (CDF Collaboration), Phys. Rev. Lett. **80**, 2057 (1998) and Phys. Rev. D **59**, 032001 (1999).

[125] F. Abe *et al.* (CDF Collaboration), Phys. Rev. D **60**, 051101 (1999).

[126] F. Abe *et al.* (CDF Collaboration), Phys. Rev. D **60**, 072003 (1999).

[127] T. Affolder *et al.* (CDF Collaboration), Phys. Rev. D **60**, 112004 (1999).

[128] CDF Collaboration, CDF note 8235, April 26, 2006,
`http://www-cdf.fnal.gov/physics/new/bottom/060406.blessed-semi_B0mix/`

[129] CDF Collaboration, CDF note 7920, November 15, 2005,
`http://www-cdf.fnal.gov/physics/new/bottom/050804.hadr_B0mix/`

[130] V.M. Abazov *et al.* (DØ Collaboration), Phys. Rev. D **74**, 112002 (2006).

[131] B. Aubert *et al.* (Babar Collaboration), Phys. Rev. Lett. **88**, 221802 (2002) and Phys. Rev. D **66**, 032003 (2002).

[132] B. Aubert *et al.* (Babar Collaboration), Phys. Rev. Lett. **88**, 221803 (2002).

[133] Y. Zheng *et al.* (Belle Collaboration), Phys. Rev. D **67**, 092004 (2003).

[134] H. Albrecht *et al.* (ARGUS Collaboration), Z. Phys. C **55**, 357 (1992); Phys. Lett. B **324**, 249 (1994).

[135] V.M. Abazov *et al.* (DØ Collaboration), Phys. Rev. D **76**, 057101 (2007).

[136] V.M. Abazov *et al.* (DØ Collaboration), Phys. Rev. Lett. **98**, 151801 (2007).

[137] R. Aleksan, Phys. Lett. B **316**, 567 (1993).

[138] D. Acosta *et al.* (CDF Collaboration), arXiv:0712.234v2 [hep-ex], 14 Dec. 2007, submitted to Phys. Rev. Lett.

[139] D. Acosta *et al.* (CDF Collaboration), arXiv:0712.2397v1 [hep-ex], 14 Dec. 2007, submitted to Phys. Rev. Lett.

[140] V.M. Abazov *et al.* (DØ Collaboration), arXiv:0802.2255v1 [hep-ex], 15 Feb. 2008, submitted to Phys. Rev. Lett.

[141] U. Nierste, private communication, September 2006.

[142] R. Barate *et al.* (ALEPH Collaboration), Phys. Lett. B **486**, 286 (2000).

[143] V.M. Abazov *et al.* (DØ Collaboration), Phys. Rev. Lett. **99**, 241801 (2007).

[144] T. Aaltonen *et al.* (CDF Collaboration), Phys. Rev. Lett. **100**, 021803 (2008).

[145] A. Lenz and U. Nierste, J. High Energy Physics **0706** 072 (2007) [arXiV:hep-ph/0612167].

[146] As determined before direct experimental inputs of $2\beta_s^{J/\psi\phi} = -\phi_s^{J/\psi\phi}$: CKMfitter Group (J. Charles *et al.*), Eur. Phys. J. C **41**, 1 (2005) [hep-ph/0406184], updated results and plots available at: `http://ckmfitter.in2p3.fr`, Summer 2007 result; M. Bona *et al.* [UTfit Collaboration], arXiv:hep-ph/0606167.

[147] M. Bona *et al.* [UTfit Collaboration], arXiv:0803.0659 [hep-ph].

[148] DØ Collaboration, additional online information with Ref. [140], likelihood scans for fits with floating strong constraints, δ_i.
`http://www-d0.fnal.gov/Run2Physics/WWW/results/final/B/B08A/`

[149] M. Beneke, G. Buchalla, A. Lenz, and U. Nierste, Phys. Lett. B **576**, 173 (2003).

[150] A. Abulencia *et al.* (CDF Collaboration), Phys. Rev. Lett. **97**, 242003 (2006); this result supersedes A. Abulencia *et al.* (CDF Collaboration), Phys. Rev. Lett. **97**, 062003 (2006).

[151] DØ Collaboration, DØ note 5474-CONF, August 2007, and DØ note 5254-CONF, October 2006; these two notes supersede any previous preliminary results from DØ and replace V.M. Abazov *et al.* (DØ Collaboration), Phys. Rev. Lett. **97**, 021802 (2006).

[152] DØ Collaboration, DØ note 5618-CONF v1.1, 10 March 2008.

[153] M. Okamoto, plenary talk at the XXIIIth International Symposium on Lattice Field Theory, Dublin, July 2005, hep-lat/0510113; this estimate is obtained by combining the unquenched lattice QCD calculations from A. Gray *et al.* (HPQCD Collaboration), Phys. Rev. Lett. **95**, 212001 (2005) and S. Aoki *et al.* (JLQCD Collaboration), Phys. Rev. Lett. **91**, 212001 (2003).

[154] H.-G. Moser and A. Roussarie, Nucl. Instrum. Methods A **384**, 491 (1997).

[155] A. Heister *et al.* (ALEPH Collaboration), Eur. Phys. J. C **29**, 143 (2003).

[156] F. Abe *et al.* (CDF Collaboration), Phys. Rev. Lett. **82**, 3576 (1999).

[157] J. Abdallah *et al.* (DELPHI Collaboration), Eur. Phys. J. C **35**, 35 (2004).

[158] G. Abbiendi *et al.* (OPAL Collaboration), Eur. Phys. J. C **11**, 587 (1999).

[159] G. Abbiendi *et al.* (OPAL Collaboration), Eur. Phys. J. C **19**, 241 (2001).

[160] K. Abe *et al.* (SLD Collaboration), Phys. Rev. D **67**, 012006 (2003).

[161] K. Abe *et al.* (SLD Collaboration), Phys. Rev. D **66**, 032009 (2002).

[162] SLD Collaboration, SLAC-PUB-8568, contrib. to 30th Int. Conf. on High-Energy Physics, Osaka, Japan (2000).

[163] CDF Collaboration, CDF notes 7907 and 7941, October and November 2005, submitted to fall 2005 conferences.

[164] DØ Collaboration, DØ notes 4878 and 4881, July 2005, submitted to summer 2005 conferences.

[165] D. Buskulic *et al.* [ALEPH Collaboration], Phys. Lett. B **395**, 373 (1997).

[166] J. Bartelt *et al.* (CLEO Collaboration), Phys. Rev. Lett. **82**, 3746 (1999) [arXiv:hep-ex/9811042].

[167] K. Abe *et al.* (Belle Collaboration), Phys. Lett. B **526**, 258 (2002) [arXiv:hep-ex/0111082].

[168] B. Aubert *et al.* [BABAR Collaboration], Phys. Rev. Lett. **100**, 151802 (2008) [arXiv:0712.3503 [hep-ex]].

[169] R. Fulton *et al.* [CLEO Collaboration], Phys. Rev. D **43**, 651 (1991).

[170] G. Abbiendi *et al.* (OPAL Collaboration), Phys. Lett. B **482**, 15 (2000) [arXiv:hep-ex/0003013].

[171] P. Abreu *et al.* (DELPHI Collaboration), Phys. Lett. B **510**, 55 (2001) [arXiv:hep-ex/0104026].

[172] K. Abe *et al.* (Belle Collaboration), Phys. Lett. B **526**, 247 (2002) [arXiv:hep-ex/0111060].

[173] N. E. Adam *et al.* (CLEO collaboration), Phys. Rev. D **67**, 032001 (2003) [arXiv:hep-ex/0210040].

[174] J. Abdallah *et al.* (DELPHI Collaboration), Eur. Phys. J. C **33**, 213 (2004) [arXiv:hep-ex/0401023].

[175] B. Aubert [BABAR Collaboration], Phys. Rev. D **77**, 032002 (2008).

[176] H. Albrecht *et al.* [ARGUS Collaboration], Phys. Lett. B **275**, 195 (1992).

[177] M. Okamoto *et al.*, Nucl. Phys. Proc. Suppl. **140**, 461 (2005) [arXiv:hep-lat/0409116].

[178] I. Caprini, L. Lellouch and M. Neubert, Nucl. Phys. B **530** (1998) 153 [arXiv:hep-ph/9712417].

[179] J. E. Duboscq *et al.* [CLEO Collaboration], Phys. Rev. Lett. **76**, 3898 (1996).

[180] J. Laiho [Fermilab Lattice and MILC Collaborations], PoS **LATTICE2007**, 358 (2007) [arXiv:0710.1111 [hep-lat]].

[181] D. Liventsev *et al.* [Belle Collaboration], arXiv:0711.3252 [hep-ex].

[182] D. Buskulic *et al.* [ALEPH Collaboration], Z. Phys. C **73**, 601 (1997).

[183] G. Abbiendi *et al.* [OPAL Collaboration], Eur. Phys. J. C **30**, 467 (2003) [arXiv:hep-ex/0301018].

[184] A. Anastassov *et al.* [CLEO Collaboration], Phys. Rev. Lett. **80**, 4127 (1998) [arXiv:hep-ex/9708035].

[185] V. M. Abazov *et al.* [D0 Collaboration], Phys. Rev. Lett. **95**, 171803 (2005) [arXiv:hep-ex/0507046].

[186] H. Albrecht *et al.* [ARGUS Collaboration], Phys. Lett. B **318**, 397 (1993).

[187] K. Abe *et al.* [Belle Collaboration], Phys. Lett. B **547**, 181 (2002) [arXiv:hep-ex/0208033].

[188] A. H. Mahmood *et al.* [CLEO Collaboration], Phys. Rev. D **70**, 032003 (2004) [arXiv:hep-ex/0403053].

[189] B. Aubert *et al.* [BABAR Collaboration], Phys. Rev. D **69**, 111104 (2004) [arXiv:hep-ex/0403030].

[190] B. Aubert *et al.* [BABAR Collaboration], Phys. Rev. D **74**, 091105 (2006) [arXiv:hep-ex/0607111].

[191] P. Urquijo *et al.* [Belle Collaboration], Phys. Rev. D **75**, 032001 (2007) [arXiv:hep-ex/0610012].

[192] O. Buchmuller and H. Flacher, Phys. Rev. D **73**, 073008 (2006) [arXiv:hep-ph/0507253].

[193] P. Gambino and N. Uraltsev, Eur. Phys. J. C **34**, 181 (2004) [arXiv:hep-ph/0401063].

[194] D. Benson, I. I. Bigi and N. Uraltsev, Nucl. Phys. B **710** (2005) 371 [arXiv:hep-ph/0410080].

[195] D. Benson, I. I. Bigi, T. Mannel and N. Uraltsev, Nucl. Phys. B **665** (2003) 367 [arXiv:hep-ph/0302262].

[196] M. Artuso *et al.* [CLEO Collaboration], Phys. Lett. B **399**, 321 (1997) [arXiv:hep-ex/9702007].

[197] S. Henderson *et al.* [CLEO Collaboration], Phys. Rev. D **45**, 2212 (1992).

[198] H. Albrecht *et al.* [ARGUS Collaboration], Phys. Lett. B **324**, 249 (1994).

[199] See, for example, I. I. Y. Bigi, M. A. Shifman and N. Uraltsev, Ann. Rev. Nucl. Part. Sci. **47**, 591 (1997) [arXiv:hep-ph/9703290]; M. Neubert, Nucl. Phys. Proc. Suppl. **59**, 101 (1997) [arXiv:hep-ph/9702310]; A. H. Hoang, Z. Ligeti and A. V. Manohar, Phys. Rev. D **59**, 074017 (1999) [arXiv:hep-ph/9811239], and references therein.

[200] N. Uraltsev, Int. J. Mod. Phys. A **20** (2005) 2099 [arXiv:hep-ph/0403166].

[201] M. Trott, Phys. Rev. D **70** (2004) 073003 [arXiv:hep-ph/0402120].

[202] V. Aquila, P. Gambino, G. Ridolfi and N. Uraltsev, Nucl. Phys. B **719** (2005) 77 [arXiv:hep-ph/0503083].

[203] B. Aubert *et al.* [BABAR Collaboration], Phys. Rev. D **69** (2004) 111103 [arXiv:hep-ex/0403031].

[204] B. Aubert *et al.* [BABAR Collaboration], Phys. Rev. D **72** (2005) 052004 [arXiv:hep-ex/0508004].

[205] B. Aubert *et al.* [BABAR Collaboration], arXiv:hep-ex/0507001.

[206] C. Schwanda *et al.* [BELLE Collaboration], Phys. Rev. D **75** (2007) 032005 [arXiv:hep-ex/0611044].

[207] P. Urquijo *et al.*, Phys. Rev. D **75** (2007) 032001 [arXiv:hep-ex/0610012].

[208] K. Abe *et al.* [Belle Collaboration], arXiv:hep-ex/0508005.

[209] D. E. Acosta *et al.* [CDF Collaboration], Phys. Rev. D **71** (2005) 051103 [arXiv:hep-ex/0502003].

[210] S. E. Csorna *et al.* [CLEO Collaboration], Phys. Rev. D **70** (2004) 032002 [arXiv:hep-ex/0403052].

[211] S. Chen *et al.* [CLEO Collaboration], Phys. Rev. Lett. **87** (2001) 251807 [arXiv:hep-ex/0108032].

[212] J. Abdallah *et al.* [DELPHI Collaboration], Eur. Phys. J. C **45** (2006) 35 [arXiv:hep-ex/0510024].

[213] D. Cronin-Hennessy *et al.* [CLEO Collab.], Phys. Rev. Lett. **87**, 251808 (2001).

[214] C. W. Bauer, Z. Ligeti, M. Luke, A. V. Manohar and M. Trott, Phys. Rev. D **70**, 094017 (2004) [arXiv:hep-ph/0408002].

[215] K. Abe *et al.* [BELLE Collaboration], arXiv:hep-ex/0611047.

[216] N. E. Adam *et al.* (CLEO Collab.), Phys. Rev. Lett. **99**:041802 (2007) [hep-ex/0703041].

[217] B. Aubert *et al.* (BABAR Collaboration), Phys. Rev. Lett. **98** (2007) 091801 [arXiv:hep-ex/0612020].

[218] T. Hokuue *et al.* [Belle Collaboration], Phys. Lett. B **648** (2007) 139 [arXiv:hep-ex/0604024].

[219] B. Aubert *et al.* [BABAR Collaboration], Phys. Rev. Lett. **97** (2006) 211801 [arXiv:hep-ex/0607089].

[220] K. Abe [Belle Collaboration], arXiv:hep-ex/0610054.

[221] P. Ball and R. Zwicky, Phys. Rev. D **71**, 014029 (2005) [arXiv:hep-ph/0412079].

[222] J. Shigemitsu *et al.*, Nucl. Phys. Proc. Suppl. **140**, 464 (2005) [arXiv:hep-lat/0408019].

[223] A. Abada, D. Becirevic, P. Boucaud, J. P. Leroy, V. Lubicz and F. Mescia, Nucl. Phys. B **619**, 565 (2001) [arXiv:hep-lat/0011065].

[224] B. Aubert *et al.* [BABAR Collaboration], Phys. Rev. D **72**, 051102 (2005) [arXiv:hep-ex/0507003].

[225] C. Schwanda *et al.* [Belle Collaboration], Phys. Rev. Lett. **93**, 131803 (2004) [arXiv:hep-ex/0402023].

[226] B. Aubert *et al.* [BABAR Collaboration], arXiv:hep-ex/0607066.

[227] B. Aubert *et al.* [BABAR Collaboration], arXiv:0708.3702 [hep-ex].

[228] I. Bizjak *et al.* (Belle Collaboration), Phys. Rev. Lett. **95** (2005) 241801 [arXiv:hep-ex/0505088].

[229] C. W. Bauer, Z. Ligeti and M. E. Luke, Phys. Rev. D **64**, 113004 (2001) [arXiv:hep-ph/0107074].

[230] M. Neubert, Phys. Rev. D **49** (1994) 4623 [arXiv:hep-ph/9312311].

[231] A. K. Leibovich, I. Low and I. Z. Rothstein, Phys. Rev. D **61**, 053006 (2000) [arXiv:hep-ph/9909404].

[232] B. O. Lange, M. Neubert and G. Paz, JHEP **0510**, 084 (2005) [arXiv:hep-ph/0508178].

[233] B. Aubert *et al.* [BABAR Collaboration], Phys. Rev. Lett. **96**, 221801 (2006) [arXiv:hep-ex/0601046].

[234] V. B. Golubev, Y. I. Skovpen and V. G. Luth, Phys. Rev. D **76** (2007) 114003 [arXiv:hep-ph/0702072].

[235] B. Aubert *et al.* [BABAR Collaboration], Phys. Rev. D **73**, 012006 (2006) [arXiv:hep-ex/0509040].

[236] A. Bornheim *et al.* [CLEO Collaboration], Phys. Rev. Lett. **88**, 231803 (2002) [arXiv:hep-ex/0202019].

[237] R. Kowalewski and S. Menke, Phys. Lett. B **541**:29 (2002).

[238] B. Aubert *et al.* [BABAR Collaboration], Phys. Rev. Lett. **95**, 111801 (2005) [Erratum-ibid. **97**, 019903 (2006)] [arXiv:hep-ex/0506036].

[239] A. Limosani *et al.* [Belle Collaboration], Phys. Lett. B **621**, 28 (2005) [arXiv:hep-ex/0504046].

[240] H. Kakuno *et al.* [BELLE Collaboration], Phys. Rev. Lett. **92**, 101801 (2004) [arXiv:hep-ex/0311048].

[241] B. O. Lange, M. Neubert and G. Paz, Phys. Rev. D **72**, 073006 (2005) [arXiv:hep-ph/0504071].

[242] S. W. Bosch, B. O. Lange, M. Neubert and G. Paz, Nucl. Phys. B **699**, 335 (2004) [arXiv:hep-ph/0402094].

[243] S. W. Bosch, M. Neubert and G. Paz, JHEP **0411**, 073 (2004) [arXiv:hep-ph/0409115].

[244] M. Neubert, Eur. Phys. J. C **44**, 205 (2005) [arXiv:hep-ph/0411027].

[245] M. Neubert, Phys. Lett. B **612**, 13 (2005) [arXiv:hep-ph/0412241].

[246] J. R. Andersen and E. Gardi, JHEP **0601**, 097 (2006) [arXiv:hep-ph/0509360].

[247] P. Gambino, P. Giordano, G. Ossola and N. Uraltsev, JHEP **0710** (2007) 058 [arXiv:0707.2493 [hep-ph]].

[248] U. Aglietti, F. Di Lodovico, G. Ferrera and G. Ricciardi, arXiv:0711.0860 [hep-ph].

[249] U. Aglietti, G. Ferrera and G. Ricciardi, Nucl. Phys. B **768** (2007) 85 [arXiv:hep-ph/0608047].

[250] U. Aglietti, G. Ricciardi and G. Ferrera, Phys. Rev. D **74** (2006) 034004 [arXiv:hep-ph/0507285].

[251] U. Aglietti, G. Ricciardi and G. Ferrera, Phys. Rev. D **74** (2006) 034005 [arXiv:hep-ph/0509095].

[252] U. Aglietti, G. Ricciardi and G. Ferrera, Phys. Rev. D **74** (2006) 034006 [arXiv:hep-ph/0509271].

[253] L. L. Chau and W. Y. Keung, Phys. Rev. Lett. **53** (1984) 1802.

[254] L. Wolfenstein, Phys. Rev. Lett. **51** (1983) 1945.

[255] A. J. Buras, M. E. Lautenbacher and G. Ostermaier, Phys. Rev. D **50** (1994) 3433 [arXiv:hep-ph/9403384].

[256] C. Jarlskog, Phys. Rev. Lett. **55** (1985) 1039.

[257] C. Jarlskog, Phys. Lett. B **615** (2005) 207 [arXiv:hep-ph/0503199].

[258] J. D. Bjorken, P. F. Harrison and W. G. Scott, Phys. Rev. D **74** (2006) 073012 [arXiv:hep-ph/0511201].

[259] A. B. Carter and A. I. Sanda, Phys. Rev. D **23** (1981) 1567.

[260] I. I. Y. Bigi and A. I. Sanda, Nucl. Phys. B **193** (1981) 85.

[261] B. Aubert *et al.* [Babar Collaboration], Phys. Rev. Lett. **86** (2001) 2515 [arXiv:hep-ex/0102030].

[262] K. Abe *et al.* [Belle Collaboration], Phys. Rev. Lett. **87** (2001) 091802 [arXiv:hep-ex/0107061].

[263] B. Aubert *et al.* [Babar Collaboration], Phys. Rev. D **76** (2007) 031102 [arXiv:0704.0522 [hep-ex]].

[264] R. Itoh *et al.* [Belle Collaboration], Phys. Rev. Lett. **95** (2005) 091601 [arXiv:hep-ex/0504030].

[265] B. Aubert *et al.* [Babar Collaboration], Phys. Rev. Lett. **99** (2007) 171803 [arXiv:hep-ex/0703021].

[266] K. F. Chen *et al.* [Belle Collaboration], Phys. Rev. Lett. **98** (2007) 031802 [arXiv:hep-ex/0608039].

[267] H. Sahoo *et al.* [Belle Collaboration], Phys. Rev. D **77** (2008) 091103.

[268] R. Barate *et al.* [ALEPH Collaboration], Phys. Lett. B **492** (2000) 259 [arXiv:hep-ex/0009058].

[269] K. Ackerstaff *et al.* [OPAL collaboration], Eur. Phys. J. C **5** (1998) 379 [arXiv:hep-ex/9801022].

[270] A. A. Affolder *et al.* [CDF Collaboration], Phys. Rev. D **61** (2000) 072005 [arXiv:hep-ex/9909003].

[271] J. Charles *et al.* [CKMfitter Group], Eur. Phys. J. C **41** (2005) 1 [arXiv:hep-ph/0406184]. Updated results available at `http://www.slac.stanford.edu/xorg/ckmfitter/`

[272] M. Bona *et al.* [UTfit Collaboration], JHEP **0507** (2005) 028 [arXiv:hep-ph/0501199]. Updated results available at `http://www.utfit.org/`

[273] I. Dunietz, H. R. Quinn, A. Snyder, W. Toki and H. J. Lipkin, Phys. Rev. D **43** (1991) 2193.

[274] D. Aston *et al.*, Nucl. Phys. B **296** (1988) 493.

[275] M. Suzuki, Phys. Rev. D **64** (2001) 117503 [arXiv:hep-ph/0106354].

[276] B. Aubert *et al.* [Babar Collaboration], Phys. Rev. D **71** (2005) 032005 [arXiv:hep-ex/0411016].

[277] T. E. Browder, A. Datta, P. J. O'Donnell and S. Pakvasa, Phys. Rev. D **61** (2000) 054009 [arXiv:hep-ph/9905425].

[278] B. Aubert *et al.* [Babar Collaboration], Phys. Rev. D **74** (2006) 091101 [arXiv:hep-ex/0608016].

[279] J. Dalseno *et al.* [Belle Collaboration], Phys. Rev. D **76** (2007) 072004 [arXiv:0706.2045 [hep-ex]].

[280] I. Dunietz, R. Fleischer and U. Nierste, Phys. Rev. D **63** (2001) 114015 [arXiv:hep-ph/0012219].

[281] A. Lenz and U. Nierste, JHEP **0706** (2007) 072 [arXiv:hep-ph/0612167].

[282] T. Aaltonen *et al.* [CDF Collaboration], Phys. Rev. Lett. **100** (2008) 161802 [arXiv:0712.2397 [hep-ex]].

[283] V. M. Abazov *et al.* [D0 Collaboration], arXiv:0802.2255 [hep-ex].

[284] T. Aaltonen *et al.* [CDF collaboration], Phys. Rev. Lett. **100** (2008) 121803 [arXiv:0712.2348 [hep-ex]].

[285] V. M. Abazov *et al.* [D0 Collaboration], Phys. Rev. Lett. **98** (2007) 121801 [arXiv:hep-ex/0701012].

[286] Y. Grossman and M. P. Worah, Phys. Lett. B **395** (1997) 241 [arXiv:hep-ph/9612269].

[287] R. Fleischer, Phys. Lett. B **562** (2003) 234 [arXiv:hep-ph/0301255].

[288] R. Fleischer, Nucl. Phys. B **659** (2003) 321 [arXiv:hep-ph/0301256].

[289] B. Aubert *et al.* [Babar Collaboration], Phys. Rev. Lett. **99** (2007) 081801 [arXiv:hep-ex/0703019].

[290] A. Bondar, T. Gershon and P. Krokovny, Phys. Lett. B **624** (2005) 1 [arXiv:hep-ph/0503174].

[291] P. Krokovny *et al.* [Belle Collaboration], Phys. Rev. Lett. **97** (2006) 081801 [arXiv:hep-ex/0605023].

[292] B. Aubert *et al.* [Babar Collaboration], Phys. Rev. Lett. **99** (2007) 231802 [arXiv:0708.1544 [hep-ex]].

[293] R. Fleischer, Int. J. Mod. Phys. A **12** (1997) 2459 [arXiv:hep-ph/9612446].

[294] D. London and A. Soni, Phys. Lett. B **407** (1997) 61 [arXiv:hep-ph/9704277].

[295] M. Ciuchini, E. Franco, G. Martinelli, A. Masiero and L. Silvestrini, Phys. Rev. Lett. **79** (1997) 978 [arXiv:hep-ph/9704274].

[296] T. Gershon and M. Hazumi, Phys. Lett. B **596** (2004) 163 [arXiv:hep-ph/0402097].

[297] Y. Grossman, Z. Ligeti, Y. Nir and H. Quinn, Phys. Rev. D **68** (2003) 015004 [arXiv:hep-ph/0303171].

[298] M. Gronau and J. L. Rosner, Phys. Lett. B **564** (2003) 90 [arXiv:hep-ph/0304178].

[299] M. Gronau, Y. Grossman and J. L. Rosner, Phys. Lett. B **579** (2004) 331 [arXiv:hep-ph/0310020].

[300] M. Gronau, J. L. Rosner and J. Zupan, Phys. Lett. B **596** (2004) 107 [arXiv:hep-ph/0403287].

[301] H. Y. Cheng, C. K. Chua and A. Soni, Phys. Rev. D **72** (2005) 014006 [arXiv:hep-ph/0502235].

[302] M. Gronau and J. L. Rosner, Phys. Rev. D **71** (2005) 074019 [arXiv:hep-ph/0503131].

[303] G. Buchalla, G. Hiller, Y. Nir and G. Raz, JHEP **0509** (2005) 074 [arXiv:hep-ph/0503151].

[304] M. Beneke, Phys. Lett. B **620** (2005) 143 [arXiv:hep-ph/0505075].

[305] G. Engelhard, Y. Nir and G. Raz, Phys. Rev. D **72** (2005) 075013 [arXiv:hep-ph/0505194].

[306] H. Y. Cheng, C. K. Chua and A. Soni, Phys. Rev. D **72** (2005) 094003 [arXiv:hep-ph/0506268].

[307] G. Engelhard and G. Raz, Phys. Rev. D **72** (2005) 114017 [arXiv:hep-ph/0508046].

[308] M. Gronau, J. L. Rosner and J. Zupan, Phys. Rev. D **74** (2006) 093003 [arXiv:hep-ph/0608085].

[309] L. Silvestrini, Ann. Rev. Nucl. Part. Sci. **57**, 405 (2007) [arXiv:0705.1624 [hep-ph]].

[310] R. Dutta and S. Gardner, arXiv:0805.1963 [hep-ph].

[311] B. Aubert *et al.* [Babar Collaboration], Phys. Rev. Lett. **99** (2007) 161802 [arXiv:0706.3885 [hep-ex]].

[312] B. Aubert *et al.* [Babar Collaboration], Phys. Rev. Lett. **98** (2007) 031801 [arXiv:hep-ex/0609052].

[313] B. Aubert *et al.* [Babar Collaboration], Phys. Rev. D **76** (2007) 091101 [arXiv:hep-ex/0702046].

[314] B. Aubert *et al.* [Babar Collaboration], Phys. Rev. D **77** (2008) 012003 [arXiv:0707.2980 [hep-ex]].

[315] K. Abe *et al.* [Belle Collaboration], Phys. Rev. D **76** (2007) 091103 [arXiv:hep-ex/0609006].

[316] B. Aubert *et al.* [Babar Collaboration], arXiv:0708.2097 [hep-ex].

[317] B. Aubert *et al.* [Babar Collaboration], arXiv:hep-ex/0607101.

[318] B. Aubert *et al.* [Babar Collaboration], Phys. Rev. D **76** (2007) 071101 [arXiv:hep-ex/0702010].

[319] K. Abe *et al.* [Belle Collaboration], arXiv:0708.1845 [hep-ex].

[320] B. Aubert *et al.* [Babar Collaboration], Phys. Rev. D **71** (2005) 091102 [arXiv:hep-ex/0502019].

[321] A. Garmash *et al.* [Belle Collaboration], Phys. Rev. D **71** (2005) 092003 [arXiv:hep-ex/0412066].

[322] B. Aubert *et al.* [Babar Collaboration], Phys. Rev. D **74** (2006) 032003 [arXiv:hep-ex/0605003].

[323] A. Garmash *et al.* [Belle Collaboration], Phys. Rev. D **75** (2007) 012006 [arXiv:hep-ex/0610081].

[324] B. Aubert *et al.* [Babar Collaboration], arXiv:0803.4451 [hep-ex].

[325] B. Aubert *et al.* [Babar Collaboration], Phys. Rev. D **74** (2006) 011101 [arXiv:hep-ex/0603012].

[326] S. E. Lee *et al.* [Belle Collaboration], Phys. Rev. D **77** (2008) 071101 [arXiv:0708.0304 [hep-ex]].

[327] B. Aubert *et al.* [Babar Collaboration], Phys. Rev. Lett. **99** (2007) 071801 [arXiv:0705.1190 [hep-ex]].

[328] S. Fratina *et al.*, Phys. Rev. Lett. **98** (2007) 221802 [arXiv:hep-ex/0702031].

[329] B. Aubert *et al.* [Babar Collaboration], Phys. Rev. D **76** (2007) 111102 [arXiv:0708.1549 [hep-ex]].

[330] H. Miyake *et al.* [Belle Collaboration], Phys. Lett. B **618** (2005) 34 [arXiv:hep-ex/0501037].

[331] T. Aushev *et al.* [Belle Collaboration], Phys. Rev. Lett. **93** (2004) 201802 [arXiv:hep-ex/0408051].

[332] B. Aubert *et al.* [Babar Collaboration], Phys. Rev. Lett. **97** (2006) 171805 [arXiv:hep-ex/0608036].

[333] Y. Nakahama *et al.* [Belle Collaboration], Phys. Rev. Lett. **100** (2008) 121601 [arXiv:0712.4234 [hep-ex]].

[334] D. Atwood, M. Gronau and A. Soni, Phys. Rev. Lett. **79** (1997) 185 [arXiv:hep-ph/9704272].

[335] D. Atwood, T. Gershon, M. Hazumi and A. Soni, Phys. Rev. D **71** (2005) 076003 [arXiv:hep-ph/0410036].

[336] B. Grinstein, Y. Grossman, Z. Ligeti and D. Pirjol, Phys. Rev. D **71** (2005) 011504 [arXiv:hep-ph/0412019].

[337] B. Grinstein and D. Pirjol, Phys. Rev. D **73** (2006) 014013 [arXiv:hep-ph/0510104].

[338] M. Matsumori and A. I. Sanda, Phys. Rev. D **73** (2006) 114022 [arXiv:hep-ph/0512175].

[339] P. Ball and R. Zwicky, Phys. Lett. B **642** (2006) 478 [arXiv:hep-ph/0609037].

[340] B. Aubert *et al.* [Babar Collaboration], arXiv:0708.1614 [hep-ex].

[341] Y. Ushiroda *et al.* [Belle Collaboration], Phys. Rev. D **74** (2006) 111104 [arXiv:hep-ex/0608017].

[342] B. Aubert *et al.* [Babar Collaboration], Phys. Rev. D **72** (2005) 051103 [arXiv:hep-ex/0507038].

[343] Y. Ushiroda *et al.* [BELLE Collaboration], Phys. Rev. Lett. **100** (2008) 021602 [arXiv:0709.2769 [hep-ex]].

[344] A. E. Snyder and H. R. Quinn, Phys. Rev. D **48** (1993) 2139.

[345] H. R. Quinn and J. P. Silva, Phys. Rev. D **62** (2000) 054002 [arXiv:hep-ph/0001290].

[346] B. Aubert *et al.* [Babar Collaboration], Phys. Rev. Lett. **99** (2007) 021603 [arXiv:hep-ex/0703016].

[347] H. Ishino *et al.* [Belle Collaboration], Phys. Rev. Lett. **98** (2007) 211801 [arXiv:hep-ex/0608035].

[348] B. Aubert *et al.* [Babar Collaboration], Phys. Rev. D **76** (2007) 052007 [arXiv:0705.2157 [hep-ex]].

[349] A. Somov *et al.*, Phys. Rev. Lett. **96** (2006) 171801 [arXiv:hep-ex/0601024].

[350] K. Abe *et al.* [Belle Collaboration], Phys. Rev. D **76** (2007) 011104 [arXiv:hep-ex/0702009].

[351] B. Aubert *et al.* [Babar Collaboration], arXiv:0708.1630 [hep-ex].

[352] B. Aubert *et al.* [Babar Collaboration], Phys. Rev. Lett. **91** (2003) 201802 [arXiv:hep-ex/0306030].

[353] C. C. Wang *et al.* [Belle Collaboration], Phys. Rev. Lett. **94** (2005) 121801 [arXiv:hep-ex/0408003].

[354] B. Aubert *et al.* [Babar Collaboration], Phys. Rev. D **76** (2007) 012004 [arXiv:hep-ex/0703008].

[355] A. Kusaka *et al.* [Belle Collaboration], Phys. Rev. Lett. **98** (2007) 221602 [arXiv:hep-ex/0701015].

[356] A. Kusaka *et al.* [Belle Collaboration], Phys. Rev. D **77** (2008) 072001 [arXiv:0710.4974 [hep-ex]].

[357] B. Aubert *et al.* [Babar Collaboration], Phys. Rev. Lett. **98** (2007) 181803 [arXiv:hep-ex/0612050].

[358] M. Gronau and D. London, Phys. Rev. Lett. **65** (1990) 3381.

[359] H. J. Lipkin, Y. Nir, H. R. Quinn and A. Snyder, Phys. Rev. D **44** (1991) 1454.

[360] B. Aubert *et al.* [Babar Collaboration], Phys. Rev. D **76** (2007) 091102 [arXiv:0707.2798 [hep-ex]].

[361] B. Aubert *et al.* [Babar Collaboration], Phys. Rev. D **73** (2006) 111101 [arXiv:hep-ex/0602049].

[362] F. J. Ronga *et al.* [Belle Collaboration], Phys. Rev. D **73** (2006) 092003 [arXiv:hep-ex/0604013].

[363] B. Aubert *et al.* [Babar Collaboration], Phys. Rev. D **71** (2005) 112003 [arXiv:hep-ex/0504035].

[364] K. Abe *et al.* [Belle Collaboration], Phys. Lett. B **624** (2005) 11 [arXiv:hep-ex/0408106].

[365] K. Abe *et al.* [Belle Collaboration], Phys. Rev. Lett. **93** (2004) 031802 [Erratum-ibid. **93** (2004) 059901] [arXiv:hep-ex/0308048].

[366] O. Long, M. Baak, R. N. Cahn and D. Kirkby, Phys. Rev. D **68** (2003) 034010 [arXiv:hep-ex/0303030].

[367] R. Fleischer, Nucl. Phys. B **671** (2003) 459 [arXiv:hep-ph/0304027].

[368] I. I. Y. Bigi and A. I. Sanda, Phys. Lett. B **211** (1988) 213.

[369] M. Gronau and D. London., Phys. Lett. B **253** (1991) 483.

[370] M. Gronau and D. Wyler, Phys. Lett. B **265** (1991) 172.

[371] D. Atwood, I. Dunietz and A. Soni, Phys. Rev. Lett. **78** (1997) 3257 [arXiv:hep-ph/9612433].

[372] D. Atwood, I. Dunietz and A. Soni, Phys. Rev. D **63** (2001) 036005 [arXiv:hep-ph/0008090].

[373] A. Giri, Y. Grossman, A. Soffer and J. Zupan, Phys. Rev. D **68** (2003) 054018 [arXiv:hep-ph/0303187].

[374] A. Poluektov *et al.* [Belle Collaboration], Phys. Rev. D **70** (2004) 072003 [arXiv:hep-ex/0406067].

[375] A. Bondar and A. Poluektov, Eur. Phys. J. C **47** (2006) 347 [arXiv:hep-ph/0510246].

[376] A. Bondar and A. Poluektov, arXiv:0801.0840 [hep-ex].

[377] D. Atwood and A. Soni, Phys. Rev. D **68** (2003) 033003 [arXiv:hep-ph/0304085].

[378] A. Bondar and T. Gershon, Phys. Rev. D **70** (2004) 091503 [arXiv:hep-ph/0409281].

[379] B. Aubert *et al.* [Babar Collaboration], arXiv:0708.1534 [hep-ex].

[380] K. Abe *et al.* [Belle Collaboration], Phys. Rev. D **73** (2006) 051106 [arXiv:hep-ex/0601032].

[381] B. Aubert *et al.* [Babar Collaboration], Phys. Rev. D **71** (2005) 031102 [arXiv:hep-ex/0411091].

[382] B. Aubert *et al.* [Babar Collaboration], Phys. Rev. D **72** (2005) 071103 [arXiv:hep-ex/0507002].

[383] B. Aubert *et al.* [Babar Collaboration], Phys. Rev. D **72** (2005) 032004 [arXiv:hep-ex/0504047].

[384] K. Abe *et al.* [Belle Collaboration], arXiv:hep-ex/0508048.

[385] B. Aubert *et al.* [Babar Collaboration], Phys. Rev. D **72** (2005) 071104 [arXiv:hep-ex/0508001].

[386] B. Aubert *et al.* [Babar Collaboration], Phys. Rev. D **76** (2007) 111101 [arXiv:0708.0182 [hep-ex]].

[387] M. Gronau, Phys. Lett. B **557** (2003) 198 [arXiv:hep-ph/0211282].

[388] B. Aubert *et al.* [Babar Collaboration], arXiv:hep-ex/0607104.

[389] A. Poluektov *et al.* [Belle Collaboration], Phys. Rev. D **73** (2006) 112009 [arXiv:hep-ex/0604054].

[390] B. Aubert *et al.* [Babar Collaboration], arXiv:hep-ex/0507101.

[391] B. Aubert *et al.* [Babar Collaboration], Phys. Rev. Lett. **99** (2007) 251801 [arXiv:hep-ex/0703037].

[392] O. Buchmüller and H. Flächer, hep-ph/0507253.

[393] BaBar Collaboration (B. Aubert *et al.*), Phys. Rev. D **77**, 051103 (2008).

[394] Results presented by Antonio Limosani in Moriond EW 2008.

[395] S. Chen *et al.* (CLEO Collaboration), Phys. Rev. Lett. **87**, 251807 (2001).

[396] K. Abe *et al.* (Belle Collaboration), Phys. Lett. B **511**, 151 (2001).

[397] B. Aubert *et al.* (Babar Collaboration), Phys. Rev. D **72**, 052004 (2005).

[398] B. Aubert *et al.* (Babar Collaboration), Phys. Rev. Lett. **97**, 171803 (2006).

[399] M. Staric *et al.* (Belle Collab.), Phys. Rev. Lett. **98**, 211803 (2007).

[400] B. Aubert *et al.* (BaBar Collab.), Phys. Rev. Lett. **98**, 211802 (2007).

[401] T. Aaltonen *et al.* (CDF Collab.), Phys. Rev. Lett. **100**, 121802 (2008).

[402] http://www.slac.stanford.edu/xorg/hfag/charm/index.html

[403] I. Bigi and N. Uraltsev, Nucl. Phys. B **592**, 92 (2001).

[404] For a survey of predictions see: A. A. Petrov, eConf **C030603** (2003), arXiv:hep-ph/0311371; Nucl. Phys. Proc. Suppl. **142**, 333 (2005).

[405] A. F. Falk *et al.*, Phys. Rev. D **69**, 114021 (2004).

[406] E. M. Aitala *et al.* (E791 Collab.), Phys. Rev. Lett. **77**, 2384 (1996);
C. Cawlfield *et al.* (CLEO Collab.), Phys. Rev. D **71**, 071101 (2005);
B. Aubert *et al.* (BaBar Collab.), Phys. Rev. D **76**, 014018 (2007);
U. Bitenc *et al.* (Belle Collab.), Phys. Rev. D **77**, 112003 (2008).

[407] E. M. Aitala *et al.* (E791 Collab.), Phys. Rev. Lett. **83**, 32 (1999);
J. M. Link *et al.* (FOCUS Collab.), Phys. Lett. B **485**, 62 (2000);

[408] S. E. Csorna *et al.* (CLEO Collab.), Phys. Rev. D **65**, 092001 (2002);

[409] B. Aubert *et al.* (BaBar Collab.), arXiv:0712.2249 (submitted to Phys. Rev. D).

[410] D. M. Asner *et al.* (CLEO Collab.), Phys. Rev. D **72**, 012001 (2005); arXiv:hep-ex/0503045 (revised April 2007);
L. M. Zhang *et al.* (Belle Collab.), Phys. Rev. Lett. **99**, 131803 (2007).

[411] L. M. Zhang *et al.* (Belle Collab.), Phys. Rev. Lett. **96**, 151801 (2006).

[412] W. Lockman (Belle Collab.), presented at LP'07, Daegu, S. Korea (13 August 2007);
See also: X. C. Tian *et al.* (Belle Collab.), Phys. Rev. Lett. **95**, 231801 (2005).

[413] D. M. Asner *et al.* (CLEOc Collab.), arXiv:0802.2268 (submitted to Phys. Rev. D).

[414] See `http://wwwasdoc.web.cern.ch/wwwasdoc/minuit/minmain.html`

[415] B. Aubert *et al.* (BaBar Collab.), Phys. Rev. Lett. **90**, 242001 (2003).

[416] D. Besson *et al.* (CLEO Collab.), Phys. Rev. D **68**, 032002 (2003).

[417] K. Abe *et al.* (Belle Collab.), Phys. Rev. D **69**, 112002 (2004).

[418] J. M. Link *et al.* (Focus Collab.), Phys. Lett. B **586**, 11 (2004).

[419] S. Godfrey, N. Isgur, Phys. Rev. D **32**, 189 (1985); J. L. Rosner, Comm. Nucl. Part. Phys. **16**, 109 (1986); S. Godfrey, R. Kokoski, Phys. Rev. D **43**, 1679 (1991); N. Isgur, B. Wise, Phys. Rev. Lett. **66**, 1130 (1991); M. Di Pierro, E. Eichten, Phys. Rev. D **64**, 114004 (2001).

[420] P. Colangelo, F. De Fazio, R. Ferrandes, Mod. Phys. Lett. A **19**, 2083 (2004); F. Jugeau *et al.*, Phys. Rev. D **72**, 094010 (2005).

[421] R. N. Cahn, J. D. Jackson, Phys. Rev. D **68**, 037502 (2003).

[422] T. Barnes, F. E. Close, H. J. Lipkin, Phys. Rev. D **68**, 054065 (2003); H. J. Lipkin, Phys. Lett. B **580**, 50 (2004).

[423] W. A. Bardeen, E. J. Eichten, C. T. Hill, Phys. Rev. D **68**, 054024 (2003).

[424] A. Kuzmin *et al.* (Belle Collab.), Phys. Rev. D **76**, 012006 (2007).

[425] A. Abulencia *et al.* (CDF Collab.), Phys. Rev. D **73**, 051104 (2006).

[426] K. Abe *et al.* (Belle Collab.), Phys. Rev. Lett. **94**, 221805 (2005).

[427] Y. Mikami *et al.* (Belle Collab.), Phys. Rev. Lett. **92**, 012002 (2004).

[428] B. Aubert *et al.* (BaBar Collab.), Phys. Rev. D **74**, 032007 (2006).

[429] J. Brodzicka *et al.* (Belle Collab.), Phys. Rev. Lett. **100**, 092001 (2008).

[430] B. Aubert *et al.* (BaBar Collab.), Phys. Rev. Lett. **97**, 222001 (2006).

[431] A. V. Evdkimov *et al.* (Selex Collab.), Phys. Rev. Lett. **93**, 242001 (2004).

[432] P. Krokovny *et al.* (Belle Collab.), Phys. Rev. Lett. **91**, 262002 (2003).

[433] B. Aubert *et al.* (BaBar Collab.), Phys. Rev. Lett. **93**, 181801 (2004).

[434] A. Drutskoy *et al.* (Belle Collab.), Phys. Rev. Lett. **94**, 061802 (2005).

[435] V. Balagura *et al.* (Belle Collab.), Phys. Rev. D **77**, 032001 (2008).

[436] B. Aubert *et al.* (BaBar Collab.), Phys. Rev. D **77**, 011102(R) (2008).

[437] A. Heister *et al.* (ALEPH Collab.), Phys. Lett. B **526**, 34 (2002).

[438] B. Aubert *et al.* (BaBar Collab.), Phys. Rev. D **74**, 031103(R) (2006).

[439] T. Becher and R. J. Hill, Phys. Lett. B **633**, 61 (2006).

[440] M. Kobayashi and T. Maskawa, Prog. Theor. Phys. **49**, 652 (1973).

[441] F. J. Gilman and R. L. Singleton, Phys. Rev. D **41**, 142 (1990).

[442] C. G. Boyd, B. Grinstein, and R. F. Lebed, Phys. Rev. Lett. **74**, 4603 (1995).

[443] R. J. Hill, arXiv:hep-ph/0606023 (2006).

[444] D. Becirevic and A. B. Kaidalov, Phys. Lett. B **478**, 417 (2000).

[445] G. S. Huang *et al.*, Phys. Rev. Lett. **94**, 011802 (2005).

[446] J. M. Link *et al.*, Phys. Lett. B **607**, 233 (2005).

[447] L. Widhalm *et al.*, Phys. Rev. Lett. **97**, 061804 (2006).

[448] B. Aubert *et al.*, Phys. Rev. D **76**, 052005 (2007).

[449] Y. Gao, Talk presented at the XXXIII International Conference on High Energy Physics (ICHEP'06), Moscow, the Russian Federation, August 2006.

[450] S. Dobbs *et al.*, arXiv:0712.1020 (2007).

[451] C. Aubin *et al.*, Phys. Rev. Lett. **94**, 011601 (2005).

[452] C. G. Boyd and M. J. Savage, Phys. Rev. D **56**, 303 (1997).

[453] M. C. Arnesen, B. Grinstein, I. Z. Rothstein, and I. W. Stewart, Phys. Rev. Lett. **95**, 071802 (2005).

[454] C. Bourrely, B. Machet, and E. de Rafael, Nucl. Phys. B **189**, 157 (1981).

[455] J. C. Anjos *et al.*, Phys. Rev. Lett. **65**, 2630 (1990).

[456] K. Kodama *et al.*, Phys. Lett. B **274**, 246 (1992).

[457] P. L. Frabetti *et al.*, Phys. Lett. B **307**, 262 (1993).

[458] E. M. Aitala *et al.*, Phys. Rev. Lett. **80**, 1393 (1998).

[459] E. M. Aitala *et al.*, Phys. Lett. B **440**, 435 (1998).

[460] M. Adamovich *et al.*, Eur. Phys. J. C **6**, 35 (1999).

[461] J. M. Link *et al.*, Phys. Lett. B **544**, 89 (2002).

[462] J. M. Link *et al.*, Phys. Lett. B **607**, 67 (2005).

[463] B. Aubert *et al.*, arXiv:hep-ex/0607085 (2006).

[464] H. Mahlke, arXiv:hep-ex/0702014 (2007).

[465] J. M. Link *et al.*, Phys. Lett. B **535**, 43 (2002).

[466] J. Wiss, arXiv:0709.3247 (2007).

[467] I. I. Bigi and A. I. Sanda, *CP Violation*, Cambridge University Press (2000).

[468] Y. Nir, arXiv:hep-ph/9911321 (1999).

[469] F. Buccella *et al.*, Phys. Rev. D **51**, 3478 (1995).

[470] B. Aubert *et al.* (BaBar Collab.), Phys. Rev. Lett. **100**, 061803 (2008).

[471] D. Acosta *et al.* (CDF Collab.), Phys. Rev. Lett. **94**, 122001 (2005).

[472] J. M. Link *et al.* (FOCUS Collab.), Phys. Lett. B **491**, 232 (2000); Err., Phys. Lett. B **495**, 443 (2000).

[473] E. M. Aitala *et al.* (E791 Collab.), Phys. Lett. B **421**, 405 (1998).

[474] J. E. Bartelt *et al.* (CLEO Collab.), Phys. Rev. D **52**, 4860 (1995).

[475] P. L. Frabetti *et al.* (E687 Collab.), Phys. Rev. D **50**, 2953 (1994).

[476] G. Bonvicini *et al.* (CLEO Collab.), Phys. Rev. D **63**, 071101 (2001).

[477] B. Aubert *et al.* (BaBar Collab.), arXiv:0802.4035 (2008).

[478] K. Arinstein *et al.* (Belle Collab.), Phys. Lett. B **662**, 102 (2008).

[479] D. Cronin-Hennessy *et al.* (CLEO Collab.), Phys. Rev. D **72**, 031102 (2005).

[480] S. Dobbs *et al.* (CLEOc Collab.), Phys. Rev. D **76**, 112001 (2007).

[481] S. Kopp *et al.* (CLEO Collab.), Phys. Rev. D **63**, 092001 (2001).

[482] X. C. Tian *et al.* (Belle Collab.), Phys. Rev. Lett. **95**, 231801 (2005).

[483] G. Brandenburg *et al.* (CLEO Collab.), Phys. Rev. Lett. **87**, 071802 (2001).

[484] D. M. Asner *et al.* (CLEO Collab.), Phys. Rev. D **70**, 091101 (2004).

[485] J. M. Link *et al.* (FOCUS Collab.), Phys. Lett. B **622**, 239 (2005).

[486] J. M. Link *et al.* (FOCUS Collab.), Phys. Rev. Lett. **88**, 041602 (2002); Err., Phys. Rev. Lett. **88**, 159903 (2002).

[487] E. M. Aitala *et al.* (E791 Collab.), Phys. Lett. B **403**, 377 (1997).

[488] B. Aubert *et al.* (BaBar Collab.), Phys. Rev. D **71**, 091101 (2005).

[489] E. Golowich and G. Valencia, Phys. Rev. D **40**, 112 (1989).

[490] I. I. Bigi, in Proceedings of KAON2001: Inter. Conf. on CP Violation, Pisa, Italy, 12-17 Jun 2001, p.417 (arXiv:hep-ph/0107102).

[491] W. Bensalem, A. Datta and D. London, Phys. Rev. D **66**, 094004 (2002); W. Bensalem and D. London, Phys. Rev. D **64**, 116003 (2001).

[492] W. Bensalem, A. Datta and D. London, Phys. Lett. B **538**, 309 (2002).